

Lecture Notes in Civil Engineering

Andrey A. Radionov · Dmitrii V. Ulrikh ·
Svetlana S. Timofeeva ·
Vladimir N. Alekhin ·
Vadim R. Gasiyarov *Editors*

Proceedings of the 7th International Conference on Construction, Architecture and Technosphere Safety

ICCATS 2023

 Springer

Series Editors

Marco di Prisco, *Politecnico di Milano, Milano, Italy*

Sheng-Hong Chen, *School of Water Resources and Hydropower Engineering, Wuhan University, Wuhan, China*

Ioannis Vayas, *Institute of Steel Structures, National Technical University of Athens, Athens, Greece*

Sanjay Kumar Shukla, *School of Engineering, Edith Cowan University, Joondalup, WA, Australia*

Anuj Sharma, *Iowa State University, Ames, IA, USA*

Nagesh Kumar, *Department of Civil Engineering, Indian Institute of Science Bangalore, Bengaluru, Karnataka, India*

Chien Ming Wang, *School of Civil Engineering, The University of Queensland, Brisbane, QLD, Australia*

Zhen-Dong Cui, *China University of Mining and Technology, Xuzhou, China*

Lecture Notes in Civil Engineering (LNCE) publishes the latest developments in Civil Engineering—quickly, informally and in top quality. Though original research reported in proceedings and post-proceedings represents the core of LNCE, edited volumes of exceptionally high quality and interest may also be considered for publication. Volumes published in LNCE embrace all aspects and subfields of, as well as new challenges in, Civil Engineering. Topics in the series include:

- Construction and Structural Mechanics
- Building Materials
- Concrete, Steel and Timber Structures
- Geotechnical Engineering
- Earthquake Engineering
- Coastal Engineering
- Ocean and Offshore Engineering; Ships and Floating Structures
- Hydraulics, Hydrology and Water Resources Engineering
- Environmental Engineering and Sustainability
- Structural Health and Monitoring
- Surveying and Geographical Information Systems
- Indoor Environments
- Transportation and Traffic
- Risk Analysis
- Safety and Security

To submit a proposal or request further information, please contact the appropriate Springer Editor:

- Pierpaolo Riva at pierpaolo.riva@springer.com (Europe and Americas);
- Swati Meherishi at swati.meherishi@springer.com (Asia—except China, Australia, and New Zealand);
- Wayne Hu at wayne.hu@springer.com (China).

All books in the series now indexed by Scopus and EI Compendex database!

Andrey A. Radionov · Dmitrii V. Ulrikh ·
Svetlana S. Timofeeva · Vladimir N. Alekhin ·
Vadim R. Gasiyarov
Editors

Proceedings of the 7th International Conference on Construction, Architecture and Technosphere Safety

ICCATS 2023

 Springer

Editors

Andrey A. Radionov
Moscow Polytechnic University
Moscow, Russia

Dmitrii V. Ulrikh
South Ural State University
Chelyabinsk, Russia

Svetlana S. Timofeeva
Irkutsk National Research State Technical
University
Irkutsk, Russia

Vladimir N. Alekhin
Ural Federal University named after the first
President of Russia B. N. Yeltsin
Ekaterinburg, Russia

Vadim R. Gasiyarov
Moscow Polytechnic University
Moscow, Russia

ISSN 2366-2557

ISSN 2366-2565 (electronic)

Lecture Notes in Civil Engineering

ISBN 978-3-031-47809-3

ISBN 978-3-031-47810-9 (eBook)

<https://doi.org/10.1007/978-3-031-47810-9>

© The Editor(s) (if applicable) and The Author(s), under exclusive license to Springer Nature Switzerland AG 2024

This work is subject to copyright. All rights are solely and exclusively licensed by the Publisher, whether the whole or part of the material is concerned, specifically the rights of translation, reprinting, reuse of illustrations, recitation, broadcasting, reproduction on microfilms or in any other physical way, and transmission or information storage and retrieval, electronic adaptation, computer software, or by similar or dissimilar methodology now known or hereafter developed.

The use of general descriptive names, registered names, trademarks, service marks, etc. in this publication does not imply, even in the absence of a specific statement, that such names are exempt from the relevant protective laws and regulations and therefore free for general use.

The publisher, the authors, and the editors are safe to assume that the advice and information in this book are believed to be true and accurate at the date of publication. Neither the publisher nor the authors or the editors give a warranty, expressed or implied, with respect to the material contained herein or for any errors or omissions that may have been made. The publisher remains neutral with regard to jurisdictional claims in published maps and institutional affiliations.

This Springer imprint is published by the registered company Springer Nature Switzerland AG
The registered company address is: Gewerbestrasse 11, 6330 Cham, Switzerland

Paper in this product is recyclable.

Preface

The International Conference on Construction, Architecture and Technosphere Safety (ICCATS-2023) was organized by Moscow Polytechnic University, Moscow; Irkutsk National Research Technical University, Irkutsk; and Ural Federal University named after the first President of Russia B. N. Yeltsin, Yekaterinburg, on 10–16 September 2023.

The conference program encompassed a wide range of topics and was divided into 4 sections: Industrial and Civil Engineering; Special and Unique Structures Construction; Urban Engineering and Planning; and Engineering Structure Safety, Environmental Engineering and Environmental Protection.

Participants could take part in the conference as in a traditional face-to-face format and as format of video conference remotely.

The international program committee has selected totally 54 papers for publishing in Lecture Notes in Civil Engineering (Springer International Publishing AG).

On behalf of the organizing committee, we express appreciation to our colleagues who participated in the review procedure of the papers and especially thank members of international program committee, who helped us to organize this conference.

We express our gratitude to the participants for the active work at the conference sections and look forward to meeting at ICCATS-2024 next September in Sochi, Russia.

Moscow, Russia
Chelyabinsk, Russia
Irkutsk, Russia
Ekaterinburg, Russia
Moscow, Russia

Prof. Andrey A. Radionov
Prof. Dmitrii V. Ulrikh
Prof. Svetlana S. Timofeeva
Prof. Vladimir N. Alekhin
Prof. Vadim R. Gasiyarov

Contents

Industrial and Civil Engineering

Method for Calculating the Number of Transitions Through Zero Degrees in the Outer Layers of Enclosing Structures	3
<i>N. P. Umnyakova</i>	
Application of the Method of Digital Image Processing for Evaluation of Crack Formation of Paint Coatings	13
<i>V. I. Loganina, K. V. Zhegera, and I. Yu. Lavrov</i>	
Mechanical Behaviour Feature of 3D-Printed Reinforced Composites	22
<i>G. Slavcheva, A. Levchenko, D. Karakchi-Ogli, and D. Babenko</i>	
BIM Technology for Creating Digital Doubles of Buildings: Implementation Analysis of Functional Complexity	32
<i>M. Filonova, S. Shirobokova, and M. Shutova</i>	
Accounting for Changes of Silty-Clay Soils Characteristics in the Ground Base of Buildings and Structures in the Process of Flooding of Territories	44
<i>M. A. Stepanov and A. P. Shestakova</i>	
Creation of Indicators of a Qualitative Component of a Construction Object at Operational Phases	55
<i>M. Zh. Yeskaliyev, Z. R. Mukhametzyanov, A. S. Salov, A. A. Yudin, and A. R. Biktasheva</i>	
Calculation Methodology for Constituent Wooden Rods on Discrete Shear Bonds	67
<i>S. A. Isupov</i>	
Probabilistic Organizational and Technological Model of Engineering and Technical Preparation of the Construction of an Industrial Facility	78
<i>Z. Y. Mukhambetzhana, D. A. Sinitsin, A. N. Pudovkin, A. K. Raschepkin, and O. N. Rakhimova</i>	
The Efficiency of Self-Healing Cementing Materials	90
<i>Wang Mingyuan, V. S. Rudnov, Tang Dongyang, Xiao Xinyuan, and Liu Zhenzhi</i>	

Influence of Preliminary Decompression on Soil Swelling Pressure	102
<i>M. S. Kim and V. Kh. Kim</i>	
Computer Simulation of a Prefabricated Spatial Framework	112
<i>N. Tsaritova, A. Kurbanov, A. Kurbanova, and A. Shtankevich</i>	
The Analysis of the Strength Characteristics of Rubber Concrete as Compared with Ordinary Cement Concrete	122
<i>A. V. Levchenko and M. V. Shitikova</i>	
Modification of Fine Concrete with Carbon Nanotubes	132
<i>D. A. Lyashenko, V. A. Perfilov, M. E. Nikolaev, and E. Yu. Kozlovceva</i>	
Specific Energy Absorbed by Fiber-Reinforced Concrete Under Static and Dynamic Loading	143
<i>S. Savin and M. Sharipov</i>	
Modification of Fine Multicomponent Concrete with Activated Component-Based Additive	152
<i>A. Kogai, A. Puzatova, and M. Dmitrieva</i>	
Large Panel Reinforced Concrete Buildings Inelastic Behavior Modeling Approach for Nonlinear Seismic Analysis	162
<i>Z. Abaev, A. Valiev, and M. Kodzaev</i>	
Recycling of Waste from the Woodworking Industry into Eco-friendly Materials for Construction	175
<i>A. Yu. Lopatin, V. D. Eskin, A. I. Krivorotova, and A. E. Tyumentseva</i>	
Optimization of Plane Frames with Variable Cross-Section	185
<i>Pham Van Trung and Nguyen Vu Thiem</i>	
Reducing the Metal Consumption of the Formwork Profile for Monolithic Construction	196
<i>D. V. Gromov, L. V. Radionova, I. N. Erdakov, L. A. Glebov, and A. S. Lunegova</i>	

Special and Unique Structures Construction

Designs and Technologies for Creating Impervious Screens at Reclamation Facilities	211
<i>O. A. Baev, A. V. Kolganov, and V. F. Talalaeva</i>	

Development of Single-Node Finite Elements for the Calculation of Systems with Unilateral Constraints by FEM in the Form of the Classical Mixed Method	222
<i>M. I. Bochkov and V. A. Ignatyev</i>	
Technique for Solving Finite Element Systems of High-Order Linear Algebraic Equations Describing the Stress–Strain State of One-Dimensional and Two-Dimensional Structures	232
<i>A. V. Ignatyev and I. S. Zavyalov</i>	
Experimental Studies of Reinforced Concrete Beams, Taking into Account the Reaction of Thrust on Compliant Supports Under Short-Term Dynamic Loading	244
<i>O. Kumpyak, Z. Galyautdinov, D. Galyautdinov, and N. Zboykova</i>	
Freeform Surfaces in Architectural and Structural Design	256
<i>V. A. Korotkiy, E. A. Usmanova, and L. I. Khmarova</i>	
Transformation of Vectors the Formation of Unique Architectural Objects When the Frame of the Situation Changes	268
<i>N. A. Saprykina</i>	
The Process of Progressive Limiting State and Determination of the Residual Strain Energy of a Structure Based on the Force Method	280
<i>L. Yu Stupishin, K. E. Nikitin, and M. L. Moshkevich</i>	
Historic Building Information Modeling in the Context of Architectural Education	290
<i>G. Zakharova</i>	
Urban Engineering and Planning	
The Rationale and Principles of “Smart Urban Planning”	303
<i>V. Yu Spiridonov, V. A. Kolyasnikov, and S. G. Shabiev</i>	
Concept Project for the Comprehensive Renovation of the Urban Area of the Microdistrict	315
<i>Arthur Manko, Valeria Vinogradova, Maria Voropaeva, Alina Ganshina, and Olga Matyukhova</i>	
Contextual Approach in the Process of Integrating Modern Buildings into the Architectural and Spatial Environment of Historical Centers in Large Cities	325
<i>I. N. Maltseva and N. N. Kaganovich</i>	

Dynamics of Development of Public Green Spaces in the City of Simferopol ...	336
<i>O. O. Korenkova</i>	
Long-Term Risks of Urban Landscape Transformation	346
<i>A. Gushchin and M. Divakova</i>	
Hydropower System of the Ural Factory City as a Unique Object of Industrial Heritage	356
<i>T. Bystrova, E. Alekseeva, and V. Litovskiy</i>	
Forming the Coherence of the Cultural and Social Framework in the Arctic Settlements Using GIS-Technologies	372
<i>A. Korobeynikova, N. Danilina, and I. Teplova</i>	
Ecopositive Environment at a Preschool Educational Institution	384
<i>N. V. Lamekhova</i>	
Use of Water Resources and the Irrigation Network of the Chui Valley	396
<i>M. T. Abylgazieva and T. A. Ableshov</i>	
Engineering Structure Safety, Environmental Engineering and Environmental Protection	
Reagent Treatment of Domestic Wastewater in Arctic Settlements from Ammonium Ions	407
<i>A. M. Fugaeva and E. I. Vialkova</i>	
Use of Non-magnetic Fraction of Metallurgical Slags in Carbon Dioxide Sequestration Technology	422
<i>E. V. Kolodezhnaya, M. S. Garkavi, I. V. Shadrnova, O. E. Gorlova, and K. A. Vorobyev</i>	
Study of the Composition of the Activating Mixture for the Production of Foamed Geopolymer Materials	433
<i>A. V. Ryabova, A. I. Izvarin, A. A. Timofeeva, L. A. Yatsenko, and P. O. Orlovsky</i>	
Changes in Runoff During the Growing Season in the Upper Reaches of the Naryn River in the Context of Global Climate Change	443
<i>R. T. Akmatov, O. A. Karymshakov, Zh. O. Karamoldoev, and T. M. Choduraev</i>	

Subject-Economic Groups for the Information-Measuring System for Determining the Ecological Well-Being of a Person	452
<i>D. V. Martynov, O. E. Bezborodova, O. N. Bodin, M. Yu Rudyk, and A. A. Trofimov</i>	
Removing Biogenic Elements from Urban Sewage: Technology Review	463
<i>M. Dyagelev</i>	
Environmental and Economic Balance in the Refurbishment of the Sewage Treatment Plant	474
<i>N. G. Vurdova</i>	
Evaluation of the Effectiveness of the Occupational Health and Safety Management System Using Fuzzy Logic Methods (Harrington Desirability Function)	487
<i>A. Yu Semeykin, E. V. Klimova, O. N. Tomarovschenko, V. A. Petrova, and I. A. Kochetkova</i>	
Prospects for the Use of Drilling Sludge from the Oil Fields of the Southern Federal District as Raw Materials for the Production of Ceramic Building Bricks	497
<i>V. S. Romanyuk, T. A. Bondareva, V. M. Kurdashov, N. A. Vilbitskaya, and A. A. Yakovenko</i>	
Study of the Effect of Zirconium Dioxide on the Physical and Mechanical Properties of Foamed Geopolymer Materials for Construction Purposes Based on Coal Combustion Waste at Arctic Thermal Power Plants	508
<i>B. M. Goltsman, V. A. Smoliy, Yu. V. Novikov, V. S. Yatsenko, and D. A. Golovko</i>	
Evaluation of the Physical and Performance Properties of Porous Polymers Depending on the Curing Mode	518
<i>E. A. Yatsenko, S. V. Trofimov, A. A. Chumakov, S. A. Vilbitsky, and N. S. Goltsman</i>	
Conceptual Foundations of Methodology in the Creation and Development of a Class of Natural-Technical Systems	529
<i>E. D. KHetsuriani, V. L. Bondarenko, O. A. Surzhko, T. E. KHetsuriani, and A. A. Asatryan</i>	
Study of Primary Graphite Separation Products for the Creation of Petroleum Product Sorbents on Their Basis	539
<i>N. Orekhova, N. Fadeeva, E. Musatkina, and L. Isaeva</i>	

Methodology for Predicting Work on the Maintenance and Repair of Urban Facilities Using Machine Learning	549
<i>L. Adamtsevich and A. Adamtsevich</i>	
The Carbon Dioxide Capture Potential of Ash and Slag from Waste Incineration Plants	558
<i>K. A. Vorobyev, I. V. Shadrinova, and T. V. Chekushina</i>	
Penicillin Antibiotics and Their Phytotoxicity	569
<i>S. S. Timofeeva and O. V. Tyukalova</i>	
Using Constructed Wetlands to Clean Wastewater from Various Sources	578
<i>O. A. Samodolova, A. P. Samodolov, D. V. Ulrikh, and M. N. Bryukhov</i>	
Digital Platform for Construction of Environmental and Economic Water Resource Maps	585
<i>A. I. Semyachkov, Yu. O. Slavikovskaya, and V. A. Pochechun</i>	

Industrial and Civil Engineering



Method for Calculating the Number of Transitions Through Zero Degrees in the Outer Layers of Enclosing Structures

N. P. Umnyakova^{1,2}(✉)

¹ Research Institute of Building Physics of the Russian Academy of Architecture and Building Sciences, 21, Lokomotivnyi Pr., Moscow 127238, Russia

n.umnyakova@mail.ru

² Moscow State University of Civil Engineering (National Research University), 26, Yaroslavskoye Shosse, Moscow 129337, Russia

Abstract. The article presents a new method for determining the required frost resistance of finishing and front facing materials of external walls. In the extension of a theory of thermal stability O. E. Vlasova, M. A. Shklover, B. F. Vasiliev a new method for calculating the temperature on the surface of external wall structures and in their thickness is developed. It considers hourly fluctuations in the temperature of the outside air, hourly changes in the incident direct and scattered solar incident on vertical surfaces of various orientations, as well as the thermal insulation of wall and the heat capacity of the materials of the separate layers. The developed technique made it possible to calculate the temperature on the outer surface of external wall and at the boundary of layers in multilayer walls of various design solutions. The performed calculations made it possible to determine the number of cycles of transitions through the temperature of zero degrees both on the surface and in the thickness of the structure. This method makes it is possible to develop requirements for frost resistance of external finishing and front layers of wall of various designs, oriented to the south, southeast, east, northeast, north, northwest, west and southwest under the influence of hourly changes temperature and hourly changes in diffuse and direct solar radiation incident on vertical surfaces, heat protection qualities of wall materials, their thermal inertia, attenuation of temperature fluctuations of outdoor temperature fluctuations in the thickness of the walls.

Keywords: Temperature · Solar radiation · Thermal inertia · Temperature amplitude · Temperature fluctuations attenuation · Brick wall · Hollow brick

1 Introduction

Russia is one of the largest countries in the world, with a total area of 17,075 million km², with a length of about 10,000 km from west to east and 4000 km from north to south. Russia is simultaneously located on the European and northern parts of the Asian

continents and is washed by the Arctic, Atlantic and Pacific Oceans [1]. The huge size of the Russian Federation causes a wide variety of climatic conditions on its territory. At the same time, it should be taken into account that winter temperatures drop below $0\text{ }^{\circ}\text{C}$ practically throughout Russia.

On a large territory of the Russian Federation, in winter and in the autumn-spring period, thaws and transitions of the outside air temperature through $0\text{ }^{\circ}\text{C}$ are often observed. The number of temperature transitions through zero degrees is up to 70–80 days a year, and in some areas 90–100 days a year [2, 3]. Such temperature transitions through zero degrees negatively affect the frost resistance of the finishing layers of building walls and the durability of external building envelopes. It should be taken into account that climate change towards warming is currently taking place throughout the territory of the Russian Federation [4–9]. This leads to an increase in the number of thaws in regions with a cold climate and the number of temperature transitions through zero degrees also increases.

It is known that when the temperature drops below zero degrees, water turns into ice and increases in volume by about 10%. Such an increase in the size of frozen water particles leads to the destruction of inter-pore partitions in building materials (plaster, brick, especially with a porous shard, etc.) and negatively affects the durability of building structures [10, 11]. First, this applies to the materials of external walls, the plaster layer, the cladding of ventilated facades, the basement of the building, etc. [12]. Therefore, when choosing materials for such types of fences, one should take into account the frost resistance of materials that largely determine the durability of building envelopes (Fig. 1).



Fig. 1 Map of climatic zones of the Russian Federation with temperatures: 1—less than $-45.5\text{ }^{\circ}\text{C}$; 2— (-45.5) — $(-40.1)\text{ }^{\circ}\text{C}$; 3— (-40.0) — $(-34.5)\text{ }^{\circ}\text{C}$; 4— (-34.4) — $(-28.9)\text{ }^{\circ}\text{C}$; 5— (-28.8) — $(-23.4)\text{ }^{\circ}\text{C}$; 6— (-23.3) — $(-17.8)\text{ }^{\circ}\text{C}$; 7— (-17.7) — $(-12.3)\text{ }^{\circ}\text{C}$; 8— (-12.2) — $(-6.7)\text{ }^{\circ}\text{C}$

As shown by the analysis of regulatory documentation [13–17] it contains the requirements for frost resistance of the front layer of external walls, depending on the location

on the structural elements of the building, which is F50–F100 for parapets and plinth, F75–F100 for walls. The requirements for frost resistance of revetment products, taking into account the class of responsibility and the height of the building, according to [16] are the following: F35 for reduced responsibility class, F50–F75 for a normal responsibility class, F75–F100 for an increased responsibility class F75–F100, as well as the requirements for frost resistance of facing products used in facades of external walls F35–F75. However, on the base of what studies and calculations the requirements for frost resistance of materials for finishing and front layers of building envelope are presented it is not clear. Practically nothing is mentioned how the level of thermal protection effects on the requirements for frost resistance of external finishing layers. In addition, as already noted, climatic conditions across the territory of the Russian Federation vary greatly. Therefore, when assigning the required durability of materials for external wall structures, it is necessary to proceed from the climatic conditions in which they will be operated, taking into account the constructive solution of the building envelope.

2 Problem Formulation

Due to the lack of a scientifically based approach to the assignment of requirements for frost resistance of materials for the finishing layers of external fences, the problem arose of developing a methodology for determining the number of temperature transitions through zero degrees on the surface and in the skin of external walls.

It is known that the temperature on the outer surface of the wall depends on its heat-protection properties of the wall and on external climatic parameters. In our work, as climatic factors, we chose the temperature of the outside air and solar radiation—direct and diffuse, incident on a vertical surface of various orientations. It should be noted that during the day the temperature of the outside air changes constantly, as well as the amount of solar radiation falling on the walls. Therefore, to solve this problem, non-stationary conditions for heat transfer through external wall were studied. To consider the climatic impact, it was expedient to select the data of a typical climatic year. This form of presentation of climate information is widely used in Scandinavian and European countries, in America. The traditional purpose of a model year is to estimate the energy consumption of a building in an annual cycle. However, the author proposes to use a standard year with an hourly change in parameters to determine the required frost resistance of finishing and facing materials on the outer surface of wall enclosures. For this, the effect of hourly changes in both the outdoor temperature and the amount of incident solar radiation (direct and diffuse) on vertical surfaces oriented to different cardinal points (based on data from a typical year) on the temperature distribution over the wall thickness and on the amount of temperature transitions through temperatures of zero degrees for various constructions of external walls was studied.

Climatic data on temperatures and the amount of solar radiation (direct and diffuse) incident on horizontal and vertical surfaces of various orientations were taken from the typical year developed by the Research Institute of Building Physics of the Russian Academy of Construction Sciences for the city of Moscow with an hourly change in parameters. In this typical year for each day of the year both the values of outdoor temperature and solar radiation (direct and diffuse) with an interval of one hour, incident

on horizontal and vertical surfaces of various orientations, are given. This set of climate data made it possible to calculate for each day of the year:

- the average temperature of the outside air per day, as well as the magnitude of the amplitude of temperature fluctuations above the average daily temperature value A_{\max} and below the average daily value A_{\min} ;
- the maximum and average daily value of the total solar radiation incident on each of the vertical surfaces oriented to the south, southeast, east, northeast, north, northwest, west and southwest.

Also, when assessing the impact of the above climatic factors, the heat-protection properties of the enclosing structure were taken into account—the heat transfer resistance of the wall and the thermal resistance of its individual layers, as well as the heat absorption coefficients of materials, the thermal inertia of the structure and temperature fluctuations attenuation.

3 Development of Calculation Method

In the development of the theory of heat resistance by O. E. Vlasov, the works of K. F. Fokin, A. M. Shklover, B. F. Vasiliev [18–20], a new method for calculating the temperature on the surface and in the thickness of the wall structure under the influence of changing outdoor temperatures and the amount of solar radiation incident on vertical surfaces of various orientations was developed. The temperature on the surface of the outer wall depends on the outdoor temperature and solar radiation. As a result of exposure to solar radiation the temperature increase on the outer surface of the wall. The temperature of the outside air depends on the heat transfer from the wall surface to the outside due to convective and radiant heat transfer. For this A. M. Shklover proposed the use of the conventional temperature of the outside air [20]. Based on the data of a typical climatic year, the conventional outdoor temperature $t_{\text{exti}}^{\text{rad}}$, taking into account hourly changes in temperature t_{exti} and solar radiation $Q_{\text{rad},i}$, falling on a vertical surface, determined by the formula

$$t_{\text{exti}}^{\text{rad}} = t_{\text{exti}} + \frac{pQ_{\text{sum},i}}{\alpha_{\text{ext}}} \quad (1)$$

where $\frac{pQ_{\text{sum},i}}{\alpha_{\text{ext}}}$ —hourly value of the equivalent temperature of solar irradiation, °C; α_{ext} —coefficient of heat exchange of external surface of the wall, $\text{Wt/m}^2 \text{ } ^\circ\text{C}$.

Based on the data of a typical climatic year with an hourly change in parameters, the amount of solar radiation incoming on the outer surface of the wall Q_i , changes periodically, and its fluctuations can be considered close to harmonic fluctuations [19]. The hourly value of the amplitude of solar radiation fluctuations A_{radi} is calculated as the difference between the hourly value of solar radiation, falling on the surface of the wall Q_i , and its average daily value Q_{av} :

$$A_{\text{radi}} = Q_i - Q_{\text{av}} \quad (2)$$

Substituting the amplitude of solar radiation fluctuations into the expression for calculating the amplitude of the equivalent value of solar irradiation, we obtain the formula

$$A_{\text{eqi}} = \frac{pA_{\text{radi}}}{\alpha_{\text{ext}}} = \frac{p(Q_i - Q_{\text{av}})}{\alpha_{\text{ext}}} \quad (3)$$

Taking into account the hourly fluctuations in the outdoor temperature with a period of 24 h and its amplitude $A_{\text{ttext}} = (t_{\text{texti}} - t_{\text{av}})$, the hourly amplitude of the conventional outdoor temperature fluctuations will be calculated by the formula $A_{\text{sum}} = (A_{\text{eqi}} - A_{\text{ttext}})$.

To determine the average daily outdoor temperature, the average daily total solar radiation, which includes direct and diffuse solar radiation, should be taken into account. Their influence can be estimated by the average daily conventional temperature of the outside air $t_{\text{ext.av}}^{\text{rad}}$, taking into account solar radiation, which is the sum [21] consisting of the average daily temperature of the outside air $t_{\text{ext.av}}$ and the equivalent temperature of solar irradiation $t_{\text{eq}} = p(Q_{\text{rad}}^{\text{max}} - Q_{\text{rad}}^{\text{av}})$ [18, 19], which is calculated by the formula

$$t_{\text{ext.av}}^{\text{rad}} = t_{\text{ext.av}} + \frac{p(Q_{\text{rad}}^{\text{max}} - Q_{\text{rad}}^{\text{av}})}{\alpha_{\text{ext}}} \quad (4)$$

where p —the coefficient of heat absorption from solar radiation by the surface of the wall material; $Q_{\text{rad}}^{\text{max}}$ —the maximum amount of solar radiation incident on the wall surface during the day, Wt/m^2 ; $Q_{\text{rad}}^{\text{av}}$ —the average amount of solar radiation falling on the wall surface per day, Wt/m^2 .

The amplitude of temperature fluctuations on the surface A_{ttext} will be determined by the value of attenuation of the amplitude of fluctuations in the outdoor air temperature A_{ttext} depending on the value of attenuation of temperature fluctuations ϑ_{ext} on the surface of the wall structure:

$$A_{\tau\text{ext}} = \frac{A_{\text{ttext}}}{\vartheta_{\text{ext}}}, \quad (5)$$

Attenuation of temperature fluctuations on the outer surface of the wall with thermal inertia of the layer of the finishing layer $D > 1$ will be calculated by the formula $\vartheta_{\text{ext}} = 1 + Y_{\text{ext}}R_{\text{ext}} = 1 + s_{\text{ext}}R_{\text{ext}}$, where s_{ext} —heat absorption of the outer layer material of the external construction, $\text{Wt}/(\text{m}^2 \text{ } ^\circ\text{C})$; $R_{\text{ext}} = \frac{1}{\alpha_{\text{ext}}}$, $\text{m}^2 \text{ } ^\circ\text{C}/\text{Wt}$.

Then the temperature value on the outer surface of the wall, taking into account the solar radiation incident on the wall and the temperature attenuation, is calculated by the formula

$$\tau_{\text{ext}} = t_{\text{ext.av}}^{\text{rad}} + \frac{A_{\text{ttext}}}{\vartheta_{\text{ext}}} \quad (6)$$

It is known that the temperature on the outer surface of the outer wall can be calculated by the formula

$$\tau_{\text{ext}} = t_{\text{ext}} + \frac{t_{\text{int}} - t_{\text{ext}}}{R_0} R_{\text{ext}} \quad (7)$$

where t_{int} —the temperature of the internal air in the room, $^\circ\text{C}$; t_{ext} —outdoor air temperature, $^\circ\text{C}$; R_0 —resistance to heat transfer of the outer wall, $\text{m}^2 \text{ } ^\circ\text{C}/\text{Wt}$.

Substituting expressions (4), (5) and (6) into (7) and making a number of transformations, we obtain a formula for calculating the temperature on the outer surface of the wall, taking into account the effect of solar radiation:

$$\tau_{\text{ext}} = \left(t_{\text{ext}} + \frac{pQ_{\text{sum}}}{\alpha_{\text{ext}}} \right) + \left[\frac{t_{\text{int}} - \left(t_{\text{ext}} + \frac{pQ_{\text{sum}}}{\alpha_{\text{ext}}} \right)}{R_0} \right] R_{\text{ext}} + \frac{(t_{\text{int}} - t_{\text{ext}}^{\text{av}}) + \frac{p(Q_{\text{sum}} - Q_i)}{\alpha_{\text{ext}}}}{\vartheta_{\text{ext}}} \quad (8)$$

where Q_{sum} —total solar radiation, including diffuse and direct solar radiation incident on vertical walls oriented to the cardinal points (north, northeast, east, southeast, south, southwest, west, northwest), Wt/m^2 .

Taking into account that the amplitude of temperature fluctuations in the thickness of the wall $A_{\tau_{\text{ext1}}}$ will be also determined by the value of attenuation of the amplitude of fluctuations in the outdoor air temperature $A_{t_{\text{ext}}}$ depending on the value of attenuation of temperature fluctuations ϑ_{ext1} in the thickness of the wall structure:

$$A_{\tau_{\text{ext1}}} = \frac{A_{t_{\text{ext}}}}{\vartheta_{\text{ext1}}} \quad (9)$$

where ϑ_{ext1} —the attenuation of temperature fluctuations in the outer facing layer (layers) of the wall structure

It is known that the temperature onto the thickness of the outer lay of the external wall can be calculated by the formula

$$\tau_{\text{ext1}} = t_{\text{ext}} + \frac{t_{\text{int}} - t_{\text{ext}}}{R_0} (R_{\text{ext}} + R_{\text{ext1}}) \quad (10)$$

where R_{ext1} —thermal resistance of the facing layer or outer layers of the wall, $\text{m}^2 \text{ } ^\circ\text{C/Wt}$.

Carrying out similar transformations, taking into account (4), (11), (6) and (10) we obtain a formula for calculating the temperature in the thickness of the structure, taking into account the hourly change in the temperature of the outside air, the hourly changes in solar radiation incident on the wall, oriented to the cardinal points, and the attenuation of temperature fluctuations in the thickness of the structure

$$\tau_{\text{ext1}} = \left(t_{\text{ext}} + \frac{pQ_{\text{sum}}}{\alpha_{\text{ext}}} \right) + \left[\frac{t_{\text{int}} - \left(t_{\text{ext1}} + \frac{pQ_{\text{sum}}}{\alpha_{\text{ext}}} \right)}{R_0} \right] (R_{\text{ext}} + R_f) + \frac{(t_{\text{ext1}} - t_{\text{ext}}^{\text{av}}) + \frac{p(Q_{\text{sum1}} - Q_{\text{av}})}{\alpha_{\text{ext}}}}{\vartheta_{\text{ext1}}} \quad (11)$$

where R_f —thermal resistance of the facing layer or outer layers of the wall, $\text{m}^2 \text{ } ^\circ\text{C/Wt}$.

Thus, based on the presentation of climatic information in the form of a typical year with hourly change in parameters, a new methodological approach has been developed to determine the range of temperature fluctuations and their amplitudes in the outer facing layer of multilayer building envelopes, taking into account the impact of solar radiation. This takes into account the orientation of the walls to the cardinal points (north, northeast, east, southeast, south, southwest, west, northwest) and the amount of total solar radiation falling on the wall of each orientation.

4 Main Results

This method can be used for thermotechnical calculations to determine the required frost resistance and durability of materials for finishing and facing layers of external walls, depending on the climatic conditions of construction and the constructive solution of the wall.

On the basis of this technique, according to the obtained dependences, calculations of temperatures in the thickness of walls of various designs were carried out:

- a three-layer brick wall with mineral wool insulation 50, 100, 150 mm thick and facing hollow face brick 0.12 m thick (Fig. 2a, b);

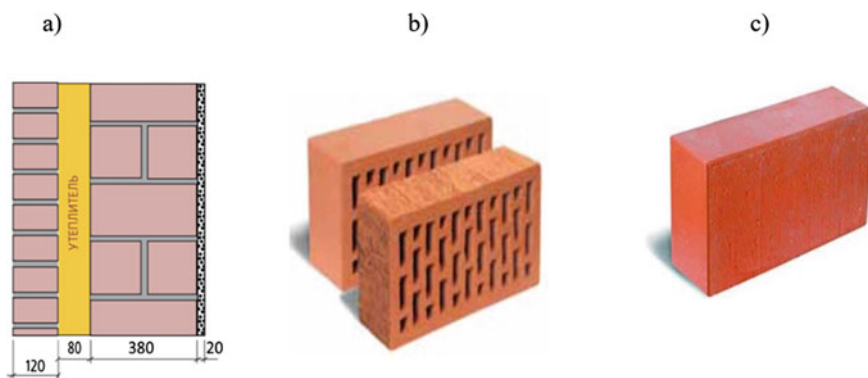


Fig. 2 Scheme of a three-layer wall structure made of ordinary clay brick 380 mm thick with mineral wool insulation and a facing outer layer 120 mm thick (a) made of hollow face brick (b) and ordinary clay brick (c)

- a three-layer brick wall with mineral wool insulation 50, 100, 150 mm thick and facing solid brick 0.12 m thick (Fig. 2a, c).

When calculating the temperature on the surface and in the thickness of the wall according to the developed method, each outer wall was divided along its thickness by sections parallel to the outer surface of the wall. For each section of the wall, the thermal inertia D_i and the attenuation of temperature fluctuations on the outdoor wall surface ϑ_{ext} in the building envelope were calculated. This made it possible to carry out calculations using formulas (8) and (11) and obtain patterns of temperature distribution over the wall thickness under the influence of changing both outdoor temperature and total solar radiation on the surface of walls oriented to 8 cardinal points (Fig. 3).

Based on these calculations, the number of cycles of transitions of the temperature in the thickness of the wall through the temperature of 0 °C was determined. The calculations for walls with different orientation of the external surface were fulfilled. Figure 3 shows diagrams with the results of calculating the number of zero-crossing cycles on the surface of a hollow brick lining of a three-layer brick wall with mineral wool insulation, and Fig. 4 shows the number of zero-crossing cycles in the thickness of a facing hollow brick at a distance of 15 mm from the outer surface. The value of 15 mm, taken in the

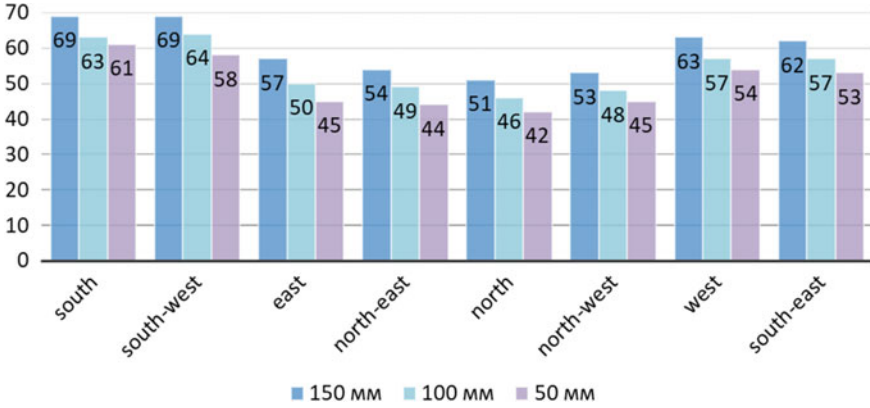


Fig. 3 The number of transitions through 0 °C on the outer surface of a 3-layer brick wall with mineral wool insulation 50, 100, 150 mm thick and facing with hollow brick 0.12 m thick

calculations, corresponds to the thickness of the shard from the outer surface of the brick to the first row of voids.

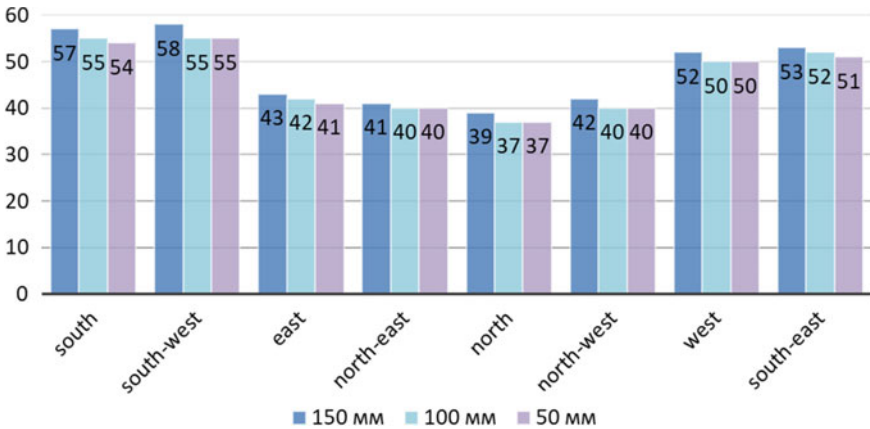


Fig. 4 The number of transitions through 0 °C in the thickness of hollow brick at a distance of 15 mm from the outer surface of a 3-layer brick wall with mineral wool insulation 50, 100, 150 mm thick and facing with hollow brick 0.12 m thick

Thus, based on the analysis of the results of calculations for three-layer structures of brick walls with mineral wool insulation and an outer facing layer of hollow bricks, it was established:

- the largest number of cycles of temperature transitions through 0 degrees is observed on the walls of the southern, southwestern and southeastern orientation; the minimum number on the walls of the northern orientation;
- the thickening of layer of the thermal insulation leads to increasing of the number of cycles of temperature transitions through 0 °C on the wall surfaces;

- the amount of cycles of temperature transitions through 0 °C in the thickness of the front hollow brick depends on the thickness of thermal insulation of the wall and its orientation to cardinal points. The maximum number of cycles of temperature transitions through 0 °C occurs in a three-layer brick wall, oriented to the south and southwest with thermal insulation thickness of 150 mm and is 30 cycles; the minimum is 14 cycles on the wall with 50 mm of thermal insulation, oriented to north and north-east.
- the outer shard of the front hollow brick 15 mm thick is subjected to the greatest number of freezing cycles: on the walls of the southern and south-western orientation—54–57 cycles, on the walls of the northern and north-eastern orientation—37–41 cycles.

5 Conclusions

Based on the study and analysis of the calculation results of the number of temperature transitions through zero degrees on the surface and in the thickness of the wall structure in climatic conditions of Moscow (Russian Federation) the following conclusions can be formulated:

1. The calculations carried out according to the developed method once again confirmed that increase in the level of thermal protection of three-layer brick walls with outer layer of facing hollow brick leads to expansion in the number of cycles of temperature transitions through 0 degrees on the surface and in the thickness of the facing brick.
2. The shard of the outer hollow brick 15 mm thick of three-layer brick walls is subjected to the greatest number of transition cycles, which causes its rapid destruction.
3. When designing the exterior brick walls of buildings, it should be taken into account that, by increasing the thermal protection of the wall, the outer brick shard is subject to more temperature transitions through zero than the outer shard of a poorly insulated wall.
4. In assessing the economic efficiency of higher thermal insulation of walls with brick cladding, it is necessary to repair the external walls more frequent or use materials that are more expensive with higher frost resistance and durability or with more durable clinker tiles. Also, when assessing the life cycle cost of a building with walls with an higher thermal protection, it is necessary to take into account an increase in the number of repairs to the facing hollow brick, or to use more expensive facing bricks or clinker tiles with increased frost resistance in the walls.

References

1. Grishina EA (2019) Features of the geographical position of the Russian Federation. Theory and practice of solving complex tasks of the GIA in geography. Bull Sci Educ 6(60):38–42
2. SP 131.13330.2020 (2021) Building climatology. Moscow, p 146
3. Umnyakova NP, Shubin IL (2021) On the problem of revising SP 131.13330 “Construction climatology” in a changing climate. Zhilishchnoe Stroitel'stvo (Hous Constr) 6:3–10
4. Report on climate features in the territory of the Russian Federation for 2020 (2021) Roshydromet, Moscow, p 104

5. Report on climate features in the territory of the Russian Federation for 2021 (2022) Roshydromet, Moscow, p 110
6. Report on climate features in the territory of the Russian Federation for 2017 (2018) Roshydromet, Moscow, p 69
7. Abakumova GM, Gorbarenko EV (2008) Atmospheric transparency in Moscow over the past 50 years and its changes in Russia. Moscow, p 192
8. Chernokulsky AV, Mokhov II (2010) Comparative analysis of global cloudiness characteristics based on various satellite and ground-based observations. *Res Earth Space* 3:12–29
9. Bartnicki J, Lövblad GE (eds) (2004) European monitoring and evaluation programme, EMEP assessment, part II: national contributions. The Norwegian Meteorological Institute, p 244
10. Hansen J, Lebedeff S (1987) Global trends of measured surface air temperature. *J Geophys Res*, pp 13345–13372
11. Aleksandrovsky SV (2004) Durability of external enclosing structures. Moscow
12. Ananiev AI, Ananiev AA (2010) Durability and energy efficiency of exterior walls made of lightweight brickwork. *Acad Arch Constr* 3:352–356
13. Lobov OI, Ananiev AI (2008) Durability of the facing layers of the outer walls of multi-storey buildings with an increased level of thermal insulation. *Walls Facades Mag* 3(52)
14. GOST 7025-91 (2006) Ceramic and calcium silicate bricks and stones. Methods for water absorption and density determination and frost resistance control. Moscow, p 10
15. GOST 10060-2012 (2018) Concretes. Methods for determination of frost-resistance. Moscow, p 18
16. GOST 25192-2012 (2013) Concretes. Classification and general technical requirements. Moscow, p 8
17. Methodological recommendations for the selection of facing products for external walls (general provisions. nomenclature of indicators. basic requirements) (2017). Moscow, p 96
18. STO 36554501-013-2008 (2008) Method of calculation of thermal expansion of brick veneer. Moscow, p 13
19. Vlasov OE (1927) Plane thermal waves. *Izvestia Therm Eng Inst (Izvestiya Teplotekhnicheskogo Instituta)* 3(26)
20. Fokin KF (2006) Building heat engineering of enclosing parts of buildings. Moscow, p 256
21. Shklover AM, Vasiliev BF, Ushkov FV (1956) Fundamentals of building heat engineering for residential and public buildings. Stroyizdat, Moscow, p 350



Application of the Method of Digital Image Processing for Evaluation of Crack Formation of Paint Coatings

V. I. Loganina^(✉), K. V. Zhegera, and I. Yu. Lavrov

Penza State University of Architecture and Construction, 28, Street Titova, Penza 440028, Russia
loganin@mail.ru

Abstract. Information is given on the application of the method of digital processing of images to assess the cracking of paint coatings. As a paint composition, white water-dispersion paint VA-17 was used. To create a texture, spray paint was applied discretely to the surface of the film. Data processing, calculation of shear fields, volumetric deformations and other additional operations, as well as graphical presentation of the results, were carried out in the MatLab program. The development of a transverse crack, which is the cause of film destruction, was considered. The process of crack formation proceeds from the middle of the film in its narrow part. It has been established that shear bands are observed already at the first stage of loading. It has been established that the appearance of microcracks was detected at a load of 0.01 kgf with transverse strain values of 0.01 mm. As the crack propagates, the isofield of the deformed state of the film changes, the deformations and the fraction of deformation at the crack mouth increase. The application of the digital image processing method will make it possible to develop recommendations for improving the crack resistance of paint and varnish coatings.

Keywords: Paintwork · Deformation · Cracking · Digital image processing method

1 Introduction

One of the most common defects in protective and decorative coatings of building facades is cracking [1–3]. Cracks in the coating can be of technological origin or nucleate and grow during operation. In this regard, the study of crack formation processes and the development of recommendations for improving crack resistance is an important scientific and technical task [4, 5]. Indirect methods evaluate crack resistance by coefficients that take into account a combination of physical and mechanical properties, or the properties themselves: modulus of elasticity, ultimate tensile strength, ultimate elongation, shrinkage deformation and other properties. This approach was proposed by Orentlicher and Novikova [6]. In [7], crack propagation was studied by computer graphics. Gobron S., Tiba N. modeled the structure of cracks on a 3D object. The authors present an initial

stress spectrum model, followed by a description of the interaction between cracks and stresses. In [8], the authors used the holography method to assess the stress state and the possibility of crack formation in the paint coating.

It is known that one of the factors of destruction of protective and decorative coatings of the outer walls of buildings is thermal stresses arising in the coatings due to the difference in the coefficients of linear thermal expansion of the CTE of the coatings and the substrate. Cracks can either appear directly on the coating surface or grow from the lower zones of the coating layer. To study the stress state of coatings and evaluate cracking, the paper [9] considers the case of a coating applied to concrete and bonded to it by cohesive forces. The coating layer is in a plane stress state. The calculation was performed using the SCAD Office software module. The authors found that one of the ways to increase the crack resistance of coatings is the creation of such a pore structure on the surface of the cement substrate, which would contribute to their more complete filling with a paint composition.

Currently, many methods for crack detection based on sensors or detectors have been developed. Fiber optic sensors [10–13], flexible strain sensors [14], piezoelectric ceramic sensors [15, 16], and acoustic emission sensors [17, 18] are used to detect the development of cracks.

The Finite Element Model (FEM) is often used to simulate crack formation [19].

Shneiderova [20] proposed a method for assessing the crack resistance of protective and decorative coatings. The technique consists in modeling the process of crack formation in a reinforced concrete element, during which cracks are created in the concrete under the coating. The state of the coating above the crack of the measured width is assessed by its continuity at a 20–30-fold increase through an optical device. The crack resistance index is taken as the width of the crack opening preceding the one when the formation of the first defect in the coating above the crack was noticed.

In [4], it is proposed to use a technique based on the ratio between the crack length, the Vickers indenter imprint, and the fracture toughness to assess the formation of cracks in polymer coatings. In this method, the value of the stress intensity factor K_{Ic} is determined from the length of radial cracks formed in brittle materials from the corners of the Vickers indentation. The authors found that when assessing crack resistance using the proposed method, there is a small spread in the obtained values of the stress intensity factor.

Recently, a new scientific direction has been widely developed—fracture mechanics. The application of the concepts of fracture mechanics makes it possible to obtain qualitative and quantitative characteristics of crack resistance. The English scientist Griffiths formulated an energy approach to the quantitative assessment of crack resistance precisely from the standpoint of modern fracture mechanics. The main idea was that the potential energy of the body, accumulated by it in the process of elastic deformation, at the beginning of destruction is completely spent on the formation of new surfaces [21].

The method of acoustic emission has become widely used in the field of coating fracture mechanics [22]. The authors obtained a comprehensive assessment of the influence of the quality of the substrate on the crack resistance of coatings using the Vickers indentation method and the AE acoustic emission method.

In work [23], a program was proposed that allows, by analyzing the digital surface of images, to numerically estimate the area of peeling from the base layer of samples

and calculate its adhesion at points. To create a program that allows you to calculate the peel area on a painted surface plate, the authors used the Visual Studio development environment on the resulting image.

The digital image correlation method is used in many areas of mechanical engineering and materials science [24]. This method was used to assess the impact strength of materials [25], to characterize refractories [26], as well as to detect the initiation and propagation of a crack [27].

In [28–33], the digital image processing (PIV) method is used to determine the displacements and the presence of cracks in the sample. PIV is the international name for the digital tracer imaging method. Particle Image Velocimetry (PIV) belongs to the class of non-contact measurement methods. By processing digital images, the fields of particle displacements, shear and volume deformations, etc. can be obtained. Good convergence of the processing results and an increase in the accuracy of the results obtained is achieved by processing the same area several times, using the result of the previous iteration as an estimate for the processing parameters at the next iteration.

The scope of the PIV method is quite extensive. It includes both fundamental and applied scientific research. Among them, we can single out the tasks of optimizing the flow around aircraft and ships in the aircraft industry, shipbuilding, structures of industrial units in the energy and oil and gas industries, studying processes in internal combustion engines, physical modeling of the operation of artificial vessels and valves in medicine, etc.

It is of scientific and practical interest to use the method of digital image processing in the study of crack propagation in a paint coating, since the patterns obtained will make it possible to develop recommendations for improving the quality of coatings.

2 Materials and Research Methods

The experiment is carried out in order to study the process of deformation of films under plane deformation conditions. The PIV method procedure is shown in Fig. 1.

As a paint composition, white water-dispersion paint VA-17 was used. The film was obtained by applying paint to a non-adhered substrate. After the film had cured, specimens of size $h = 51.02$ mm and width $l = 7.67$ mm were cut from it. The measurement of the displacement field in a given plane is based on the measurement of the displacement of individual particles, for which the surface must have some texture. To create a texture, spray paint was applied discretely to the surface of the film.

The standard algorithm for digital processing of PIV images for determining particle displacements included the following procedures:

- splitting each pair of images into elementary equal computational areas;
- calculation of the cross-correlation function for each region;
- calculation of the maximum of the correlation function;
- pixel-by-pixel interpolation of the maximum of the correlation function.

Particle images are recorded on a digital video camera. The shooting mode was selected manually. Lighting was chosen so that the subject was evenly lit, there were no glare and shadows. Video recording was carried out at certain intervals at a speed of 60

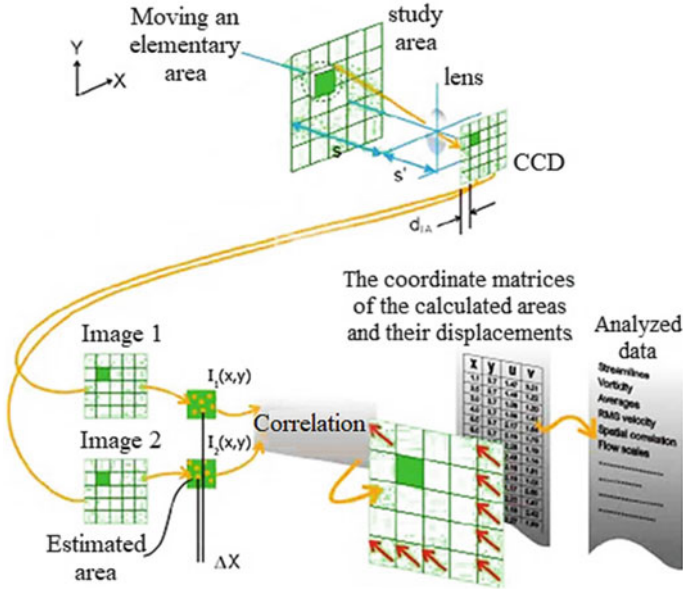


Fig. 1 Procedure of the PIV method

frames/s. Subsequent image processing made it possible to calculate particle displacements over time and construct a two-component displacement field. To reduce geometric distortions, the video camera was focused on the plane of the coating surface. The focal length of the camera lens and the aperture value were selected to provide maximum positioning ability and minimize optical distortion.

A cross-correlation algorithm was used in the work, when the initial and final positions of the particles are recorded on different images. Each image was divided into elementary regions (computational regions) of size X by X pixels, so that at least a few particles fell into each computational region.

The tensile rate of the specimen during testing was 10 mm/min. The tests were carried out on an IR 5057-50 tensile tester. Film samples were fixed in the clamps of a tensile testing machine so that its longitudinal axis was located in the direction of tension, and the applied forces acted uniformly over the entire cross section of the sample.

The tests were carried out at air temperature $t = (20 \pm 2)^\circ\text{C}$ and relative air humidity $\varphi = 65\%$. Data processing, calculation of shear fields, volumetric deformations and other additional operations, as well as graphical presentation of the results, were carried out in the MatLab program.

3 Research Results

On Fig. 2 shows the load-strain diagram. The maximum tensile load was 0.46 kgf, relative deformations—0.234 mm/mm. Figures 3, 4, 5 and 6 show the characteristic features of crack development from the beginning of nucleation.

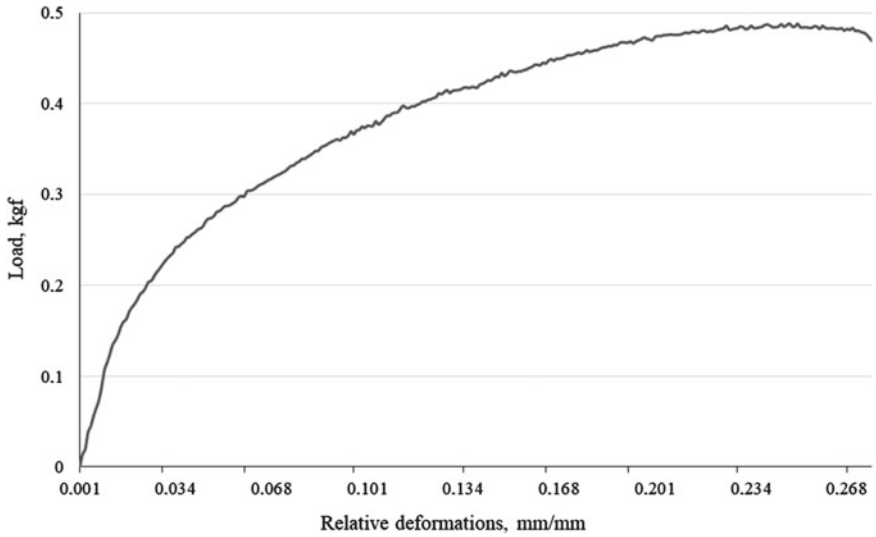


Fig. 2 Load-strain diagram

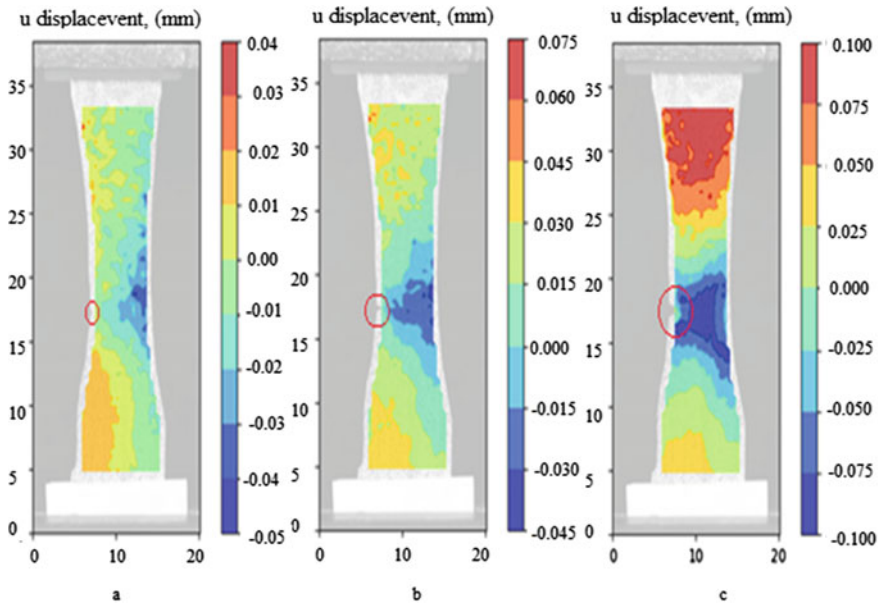


Fig. 3 Isofields of transverse strains of the film: **a**—beginning of crack initiation; **b**, **c**—crack propagation

On Fig. 3 shows the transverse deformations along the x-axis over the entire surface of the paint film. To the right of each image of the deformed surface of the coating, a scale of deformation values in mm is given in accordance with the color scheme. Figure 4

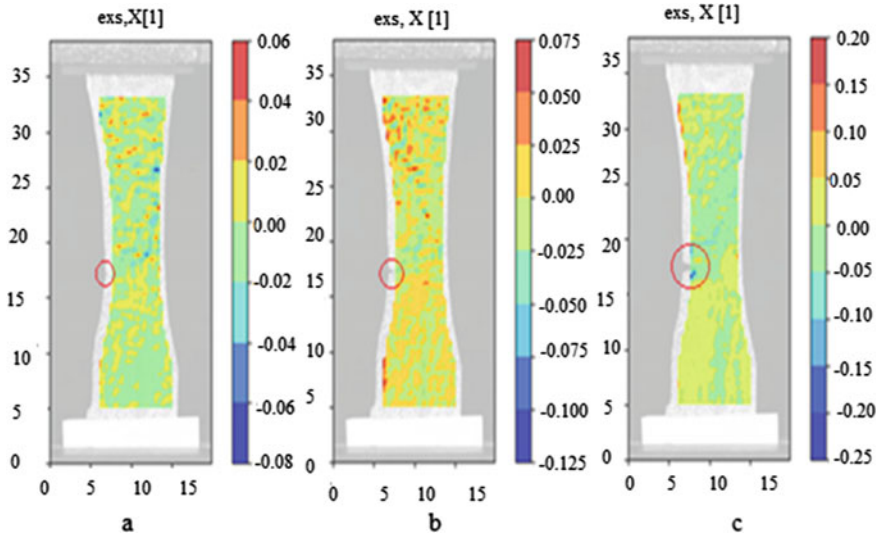


Fig. 4 Film strain isofields (strains along the x axis in fractions of a unit): **a**—beginning of crack initiation; **b, c**—crack propagation

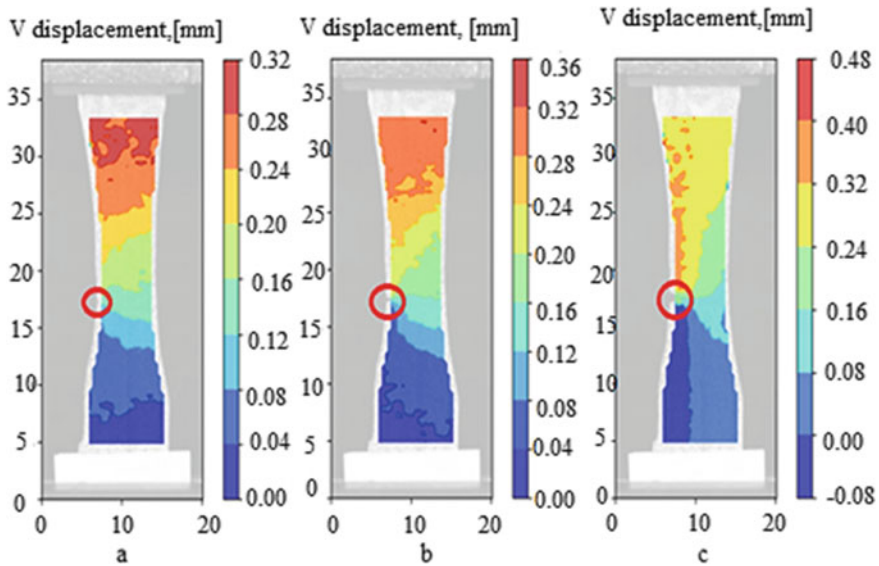


Fig. 5 Isofields of longitudinal deformations of the film: **a**—beginning of crack initiation; **b, c**—crack propagation

shows transverse deformations over the entire surface of the paint film in fractions of units. To the right of each image of the deformed surface of the coating is a scale of values of transverse deformations in fractions in accordance with the color scheme.

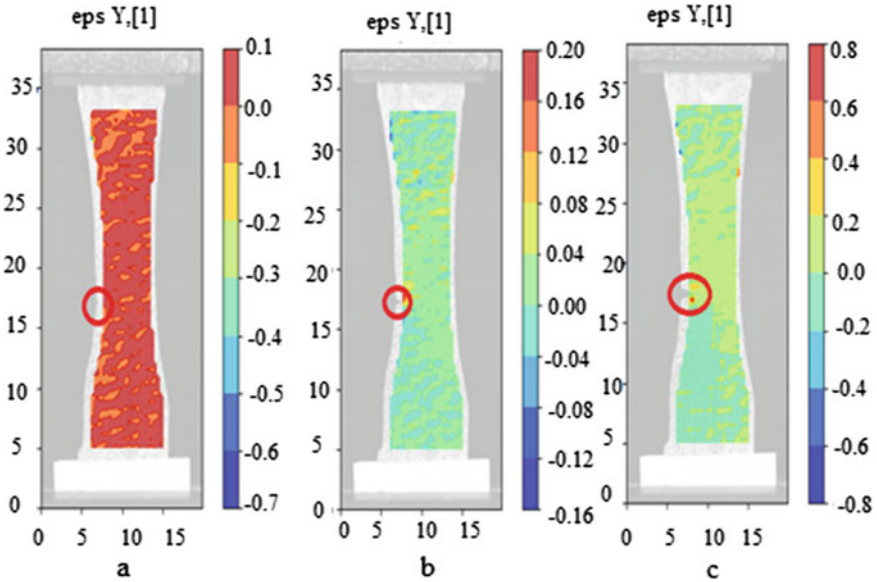


Fig. 6 Isofields of longitudinal deformations of the film (strains along the y axis in fractions of a unit): **a**—beginning of crack initiation; **b, c**—crack propagation

The development of a transverse crack, which is the cause of film destruction, was considered.

On Figs. 3, 4, 5 and 6 recorded the beginning of crack formation and crack development. It has been established that shear bands are observed already at the first stage of loading (Fig. 3a). The process of crack formation proceeds from the middle of the film in its narrow part. Deformations at the time of the appearance of a crack were 0.01 mm (Fig. 3a). The appearance of microcracks was found at a load of 0.01 kgf.

As the crack propagates, the isofield of the deformed state of the film changes. The transverse deformations at the mouth of the crack increase and become equal to 0.025 mm (Fig. 3c).

The proportion of transverse deformation also increases. If at the stage of crack initiation, the fraction of transverse strain was 0.02 (Fig. 4a), then as the crack develops, the fraction of transverse strain increases and becomes equal to 0.1 (Fig. 4c).

Figures 5 and 6 show the values of the longitudinal deformations of the film.

It was found that the longitudinal deformations by the time the crack appeared amounted to 0.12 mm (Fig. 5a). As the crack propagates, the longitudinal deformations at the mouth of the crack increase and become equal to 0.16 mm (Fig. 5c). The proportion of longitudinal strain at the stage of crack initiation was 0.1 (Fig. 6a).

4 Conclusion

Thus, the conducted studies have confirmed the effectiveness of the digital image processing method for studying the cracking of paint films. The development of distribution fields of longitudinal and transverse displacements under the influence of a tensile load

on a paint film has been established. The value of displacements at the moment of formation and development of a crack in the VA-17 coating is established. The results of research and subsequent processing using the method of digital image processing will allow developing recommendations for improving the crack resistance of paint coatings, depending on the method of application, surface preparation before painting.

References

1. Uchaeva TV, Loganina VI (2018) Analysis of the risk at the finishing of the building products and construction of paint compositions. *Case Stud Constr Mater* 8:213–216
2. Loganina VI, Kislitsyna SN, Makarova LV, Khristolyubov VG (2004) Assessment of the degree of destruction of protective and decorative coatings. *Lacquer-and-Lacquer Mater* 9:14–18
3. Loganina VI (2014) Maintenance of quality of paint and varnish coverings of building products and designs. *Contemp Eng Sci* 7(33–36):1943–1947
4. Loganina VI, Makarova LV (2003) On the methodology for assessing the crack resistance of protective and decorative coatings. *Plastic Masses* 4:43
5. Loganina VI, Ariskin MV, Svetalkina MA (2022) Estimation of the temperature effect on the stress state of protective and decorative coatings, taking into account the porosity of the cement substrate. *Constr Geotechn* 13(2):67–76
6. Gorchakov GI, Orentlicher LP, Savin VI, Voronin VV, Alimov LA, Novikova IP (1976) Composition, structure and properties of cement concretes. *Stroyizdat, Moscow*
7. Gobron S, Chiba N (2001) Crack pattern simulation based on 3D surface cellular automata. *Vis Comput* 17(5):287–309
8. Loganina VI, Skachkov YuP (2016) The Application of the holographic method for evaluation of a stress deformation state of cement paint coatings. *Int J Appl Eng Res* 11(14):8377–8378
9. Loganina VI, Svetalkina MA, Ariskin MV (2022) Effect of surface roughness of the cement substrate on the stress state of paint and varnish coatings. *Reg Arch Constr* 4(53):12–17
10. Berrocal CG, Fernandez I, Rempling R (2020) Crack monitoring in reinforced concrete beams by distributed optical fiber sensors. *Struct Infrastruct Eng* 17:124–139
11. Luo D, Yue Y, Li P, Ma J, Zhang L, Ibrahim Z, Ismail Z (2016) Concrete beam crack detection using tapered polymer optical fiber sensors. *Measurement* 88:96–103
12. Leung CKY, Wan KT, Inaudi D, Bao X, Habel W, Zhou Z, Ou J, Ghandehari M, Wu HC, Imai M (2015) Review: optical fiber sensors for civil engineering applications. *Mater Struct* 48:871–906
13. Imai M, Nakano R, Kono T, Ichinomiya T, Miura S, Mure M (2010) Crack detection application for fiber reinforced concrete using BOFDA-based optical fiber strain sensor. *J Struct Eng* 136:1001–1008
14. Yan T, Wang Z, Pan Z (2018) Flexible strain sensors fabricated using carbon-based nanomaterials: a review. *Curr Opin Solid State Mater Sci* 22:213–228
15. Morichika S, Sekiya H, Maruyama O, Hirano S, Miki C (2020) Fatigue crack detection using a piezoelectric ceramic sensor. *Weld World* 64:141–149
16. Song G, Olmi C, Gu H (2007) An overheight vehicle-bridge collision monitoring system using piezoelectric transducers. *Smart Mater Struct* 16:462–468
17. Williams CRS, Hutchinson MN, Hart JD, Merrill MH, Finkel P, Pogue WR, Cranch GA (2020) Multichannel fiber laser acoustic emission sensor system for crack detection and location in accelerated fatigue testing of aluminum panels. *APL Photon* 5:030803
18. Li W, Jiang Z, Yu Q (2020) Multiple damaging and self-healing properties of cement paste incorporating microcapsules. *Constr Build Mater* 255:119302

19. Bansal P, Shipway PH, Leen SB (2006) Finite element modelling of the fracture behaviour of brittle coatings. *Surf Coat Technol* 200:5318–5327
20. Shneiderova VV (1982) *Anti-corrosion coatings*. Stroyizdat, Moscow
21. Leonovich SN (2013) Strength and crack resistance of structural building materials under complex stress state. BNTU, Minsk
22. Loganina VI, Makridin NI, Makarova LV, Karpov VN (2003) Evaluation of crack formation in coatings using the acoustic emission method. *Construction* 6(534):35–38
23. Antonova NM, Khaustova EYu, Nebrat AA, Puzanova AS (2020) Rapid assessment of adhesion of paint coatings by digital image. *IOP Conf Ser Mater Sci Eng* 971(2):022043
24. McNeill S, Peters W, Sutton M (1987) Estimation of stress intensity factor by digital image correlation. *Eng Fract Mech* 28(1):101–112
25. Abanto-Bueno J, Lambros J (2002) Investigation of crack growth in functionally graded materials using digital image correlation. *Eng Fract Mech* 69:1695–1711
26. Robert L, Nazaret F, Cutard T, Orteu J (2007) Use of 3D digital image correlation to characterize the mechanical behavior of a fiber reinforced refractory castable. *Exp Mech* 47(6):761–773
27. Rupil J, Roux S, Hild F, Vincent L (2011) Fatigue microcrack detection with digital image correlation. *J Strain Anal Eng Des* 46(6):492–509
28. Boldyreva OV (2019) Determination of displacements of a reinforced concrete beam by digital image processing. *Struct Mech Calcul Co-ruzheny* 1:23–28
29. Zihnioglu ISNÖ, Hosseini A (2015) Particle image velocimetry (PIV) to evaluate fresh and hardened state properties of self compacting fiber+reinforced cementitious composites (SC+FRCCs). *Constr Build Mater* 78:450–463
30. Trivedi N, Singh RK, Chattopadhyay J (2015) Investigation on fracture parameters of concrete through optical crack profile and size effect studies. *Eng Fract Mech* 10:119–140
31. Boldyrev G, Guskov I, Lavrov S, Sidorchuk V, Skopintsev D (2015) Comparison of soil test data, obtained with different probes. In: *Proceedings 8 of the 3-d international conference on the flat dilatometer 3*
32. Boldyrev GG, Melnikov AV, Barvashov VA (2012) Particle image velocimetry and numeric analysis of sand deformations under a test plate. In: *Proceedings of the 5-th European geosynthetics congress, vol 1, pp 685–691*
33. Melnikov AV, Novichkov GA, Boldyrev GG (2012) The study of the deformed state of the sandy base using the method of digital image processing. *Int J Geotechn* 1:28–41



Mechanical Behaviour Feature of 3D-Printed Reinforced Composites

G. Slavcheva[✉], A. Levchenko, D. Karakchi-Ogli, and D. Babenko

Voronezh State Technical University, 84, 20-Letiya Oktyabrya Street, Voronezh 394006, Russia
gslavcheva@yandex.ru

Abstract. This paper presents the investigation of mechanical properties of 3D-printed composites. The effects of reinforcing on its tensile, flexural and splitting strength are presented together. It has been established that reinforcing changes mechanical behaviour of 3d-printed reinforced composites compared to non-reinforced references. The strength of 3d-printed reinforced composites increases by 2–2.5 times by using steel wire for their reinforcing. The 3d-printed reinforced composites had flexural strength 8–13 MPa, tensile strength 5.8–3.3 MPa. That is defined by the number of reinforcing steel wire in a layer. The greatest reinforcing effect is achieved in bending test. In this case it is possible to increase the strength of reinforced samples by 2.5–3 times compared to non-reinforced ones. Significant differences in the mechanical behaviour of 3D printed reinforced composites as compared to non-reinforced analogues were explained by the fact that reinforcing fibres were put to work. The tensile and flexural strength of 3DPRC samples increased in proportion to the increase in the number of fibres in the layer. The greatest increase in flexural strength up to 13 MPa was achieved for 3DPRC samples reinforced with 5 fibres when a force was applied across the boundary surface in the sample.

Keywords: Additive manufacturing · 3D-printed composite · Reinforcing · Strength · Mechanical behaviour

1 Introduction

In world science and practice 3D build printing has been qualified as a technology for the developing markets of the future. This technology can potentially provide a significant potential of the consumption volume at the building market [1, 2]. However, at this stage of development, the prospects of practical implementation of the technology in construction are not yet obvious as engineering solutions are only being formed [3].

Despite a great number of studies and research, today 3D printing is used in building only for construction of shells of vertical structures, mainly walls that are reinforced and finished in a traditional manual way. Apart from walls, other structures of these objects (floor structures, beams, stairs, etc.) are usually also produced using the traditional concrete casting technology. As a result of implementation of this scientific and practical

approach, labour and time efforts as well as the cost of 3D printed objects remain on the same level with traditional building technologies.

The way out of this situation is associated with the implementation of two strategies. The first one involves the improvement of the process of reinforcement of printed structures with traditional reinforcing elements (grids, bars) along or across the layer [4–6]. There are also options for 3D printing of steel reinforcement using gas arc welding [7] and printing plastic moulding with ribbed structures as replacement for steel reinforcement [8]. However, the implementation of this strategy requires a great deal of manual labour, which contradicts the idea of 3D printing as a robot-assisted building technology. The second strategy is related to the increase of tensile strength and decrease of crack resistance of printing composites themselves due to an introduction of continuous reinforcing fibres in the course of extrusion and layering of concrete [9–20]. Steel [9, 10, 13, 14, 20], nylon [12], carbon [11, 16–18, 20], aramid, and polyethylene fibres have also been used [19]. The introduction of a steel wire and carbon fibre provides the best results, allowing to increase the bending tension up to 150–250%. The obtained results are rather promising. It can be forecasted that the implementation of this technology is the most promising for the development and introduction of 3D printing in building practice. It fully complies with the technological possibilities of extrusion 3D build printing and does not require a significant complexity.

The authors' idea of creating 3D printed reinforced composites (3DPRC) is that in the course of printing the rigid cement-concrete matrix will be reinforced with fibres with high tensile strength. It is planned to ensure the formation of the specified set of physical and mechanical properties due to a rational balance of strength and deformation characteristics of the matrix and fibres, the regulation of material composition and geometry of the matrix layer; type, diameter, quantity, and location of reinforcing fibres, and creation of a strong adhesive matrix—fibre connection [21].

The goal of this work was to experimentally establish the patterns of changes in the strength of 3D printed reinforced composites (3DPRC) depending on the number of reinforcing steel wire in a layer based on the study of their mechanical behaviour feature.

2 Materials and Methods

The studies were performed on sand-based 3D-printable mix [patent RU 2729085 C1 [22], (Table 1)], the compositions of which were optimised by the authors in previous studies regarding extrudability, buildability, and strength of the layer material.

Table 1 Concrete mix design

Components, mass %					W/C
cement	Plasticizer	Metakaolin	Polypropylene fiber	Sand	
100	1.2	2	0.5	125	0.29

The initial components were used of the mix:

- portland cement CEM I 42.5 R (EN 197-1: 2011),
- the plasticiser of Sika trademark based on polycarboxylate ethers,
- viscosity modifying additive—metakaolin ($\text{Al}_2\text{O}_3 \cdot \text{SiO}_2$ content $\sim 98\%$, a particle size distribution ranging from 1 to 5 μm),
- polypropylene fiber ($l = 12 \text{ mm}$, $d = 0.022 - 0.034 \text{ mm}$).

Steel wire with the diameter 230 μm and tensile strength 2769–2950 MPa of a single fiber was used for the reinforcing of 3d-printed composites.

To study and assess the mechanical properties of 3d-printed reinforced composites (3DPRC), an element $\sim 50 \text{ cm}$ long, 4 cm wide, and 16 cm high was printed on a laboratory printer. The cross section of the layer was $4 \times 1.5 \text{ cm}$, and the number of printed layers was 11. The reinforcing fibers were placed between layers by hand. The following printing modes were used in the course of the studies:

- constant print speed 20 mm/s.
- constant distance between the nozzle and the layer 20 mm.
- printing time gap $\Delta t \leq 0.5 \text{ min}$.

After printing, the 3D-printed samples were stored for 28 days in a standardised environment ($T = 20 \pm 2 \text{ }^\circ\text{C}$, $\text{RH} = 100\%$). After curing, the model element was sawn into samples with the different sizes. The cutting layout of a 3D-printed model element is presented in Fig. 1.

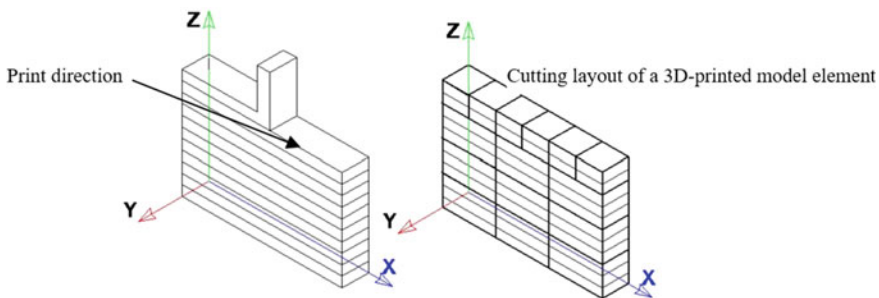


Fig. 1 Schematic of 3DPRC-sample preparation for strength tests

Mechanical properties of casted composite were assessed as a reference. In order to do this, mould reference samples were made from each batch sand-based mixtures in the course of the studies simultaneously with the printing of model fragments. The mould samples were stored for 28 days in a standardised environment ($T = 20 \pm 2 \text{ }^\circ\text{C}$, $\text{RH} = 100\%$).

3DPRC-samples were tested as follows:

- tensile test upon load application along to the printed direction (X-axes)—3 prism samples in a series;
- flexural test with point force across the boundary surface in the sample across to the printed direction (Z-axes)—3 prism samples in a series;

- flexural test with point force along the boundary surface in the sample across to the printed direction (Y-axes)—3 cube samples in a series;
- splitting test to assess the interlayer bond strength with point force along the boundary surface in the sample along to the printed direction (X-axes)—3 prism samples in a series.

Test patterns for 3DPRC-samples are presented in Fig. 2.

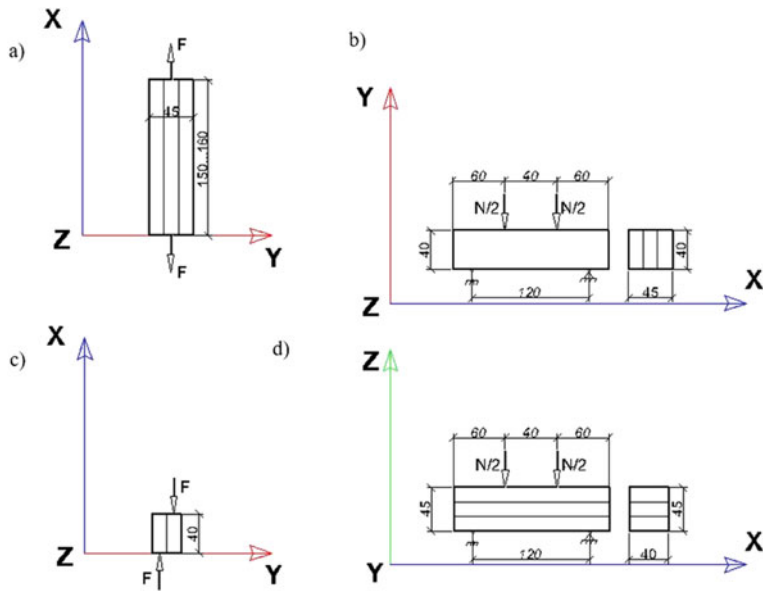


Fig. 2 Schemes of strength test for 3DPRC-samples: **a** tensile test (X-axes), **b** four-point bending test (Y-axes), **c** splitting test (X-axes), **d** four-point bending test (Z-axes)

The mould CC-samples were tested according to GOST 10180 “Concretes. Methods for strength determination using reference specimens”. Summary of tests is presented in Table 2.

3 Experimental Results and Discussion

The test results allowed establishing significant differences in the mechanical behaviour of 3D printed reinforced composites as compared to non-reinforced analogues (Figs. 3, 4, 5 and 6).

Upon central tension (see Figs. 3a and 4), the appearance of a macrocrack in the samples was recorded with similar values of the breaking load of 2.5–2.8 MPa (Table 3). Non-reinforced samples were destroyed, while in the reinforced samples tensions increased, as steel wires were intensively put into operation. Due to putting into work reinforcing steel wires the load increase is fixed on the tensile test diagrams.

Table 2 Test matrix

Strength parameter (MPa)	Schemes of strength test	Samples type	Number of reinforcing steel wire in a layer			
			0	1	3	5
Tensile strength R_x^t	Tensile test (X-axes), scheme (a)	Prism $4.5 \times 4 \times 16$ cm, layer's number—3	0	1	3	5
Flexural strength R_y^f	Four-point bending test (Y-axes), scheme (b)	Prism $4 \times 4, 5 \times 16$ cm, layer's number—3	0	1	3	5
Flexural strength R_z^f	Four-point bending test (Z-axes), scheme (d)	Prism $4.5 \times 4 \times 16$ cm, layer's number—3	0	1	3	5
Splitting strength R_x^{sp}	Splitting test (X-axes), scheme (c)	Cube $4 \times 3 \times 4$ cm, layer's number—2	0	1	3	5

As a result, the tensile strength of 3DPRC samples increased up to 3.3 MPa in comparison with tensile strength 2.8 MPa of non-reinforced samples. When the number of fibres in the layer grew from 1 to 5, the tensile strength increased by 25%.

When testing the samples in flexural strength, the nature of the four-point bending test diagram was similar for the Z-axes and Y-axes load directions (see Fig. 3a, b). The main difference in the nature of operation under the load of the reinforced samples was an expressed compression region and smoother destruction as compared to non-reinforced samples. At the same time, an increase in stiffness was typical for 3DPRC samples. Therefore, the destruction of the samples occurred along the compression region upon the reinforcement with 5 fibres.

When testing the tension of the samples in the course of bending, the appearance of the first crack and, accordingly, the destruction of concrete in layered printed samples was recorded with similar values of the breaking load of 4.8–5.5 MPa. After that, reinforcing fibres put to work and, as a result, the flexural strength of 3DPRC samples increased in proportion to the increase in the number of fibres in the layer. The greatest increase in strength up to 13 MPa was achieved for 3DPRC samples reinforced with 5 fibres when the force was applied across the boundary surface in the sample (Z-axes direction). When the force was applied along the boundary surface in the sample (Y-axes direction), the strength of the samples reinforced with 3 or 5 fibres was practically the same, approximately 8.4–8.6 MPa. This was due to the fact that when loading along the Z-axes direction, 5 reinforcing fibres were put to work at the same time, while when bending along the Y-axes direction, the fibres were put to work one by one. The samples were destroyed when the outermost fibre achieved the strength limit. Thus, it was established that the layered reinforced composite had greater strength when bending across the layer along the Z-axes direction. In this case, it was possible to ensure the increased strength of reinforced samples by 2.5–3 times as compared to non-reinforced ones. The nature of the reinforced samples destruction (see Figs. 5b and 6b) allows to state that the reinforcing fibers are able to take the load because they are not pulled out of the samples. Destruction of the reinforced samples is fixed at the moment of fiber break.

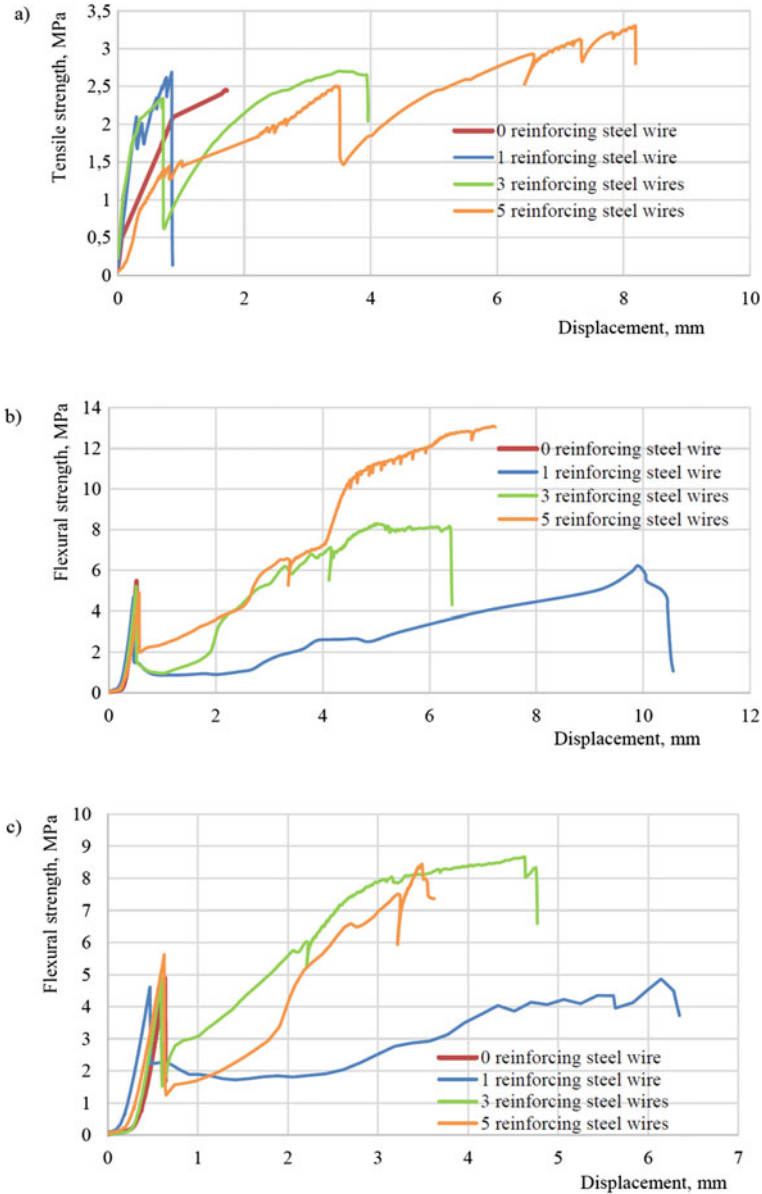


Fig. 3 a tensile test diagram (X-axes); b four-point bending test diagram (Z-axes), c four-point bending test diagram (Y-axes)

It should be noted that the tensile strength and bending strength values of the non-reinforced 3D printed samples were higher than the reference casting samples (see Table 3). This can be explained by the inhibition of cracks at the interfaces and the corresponding increase in the fracture work.

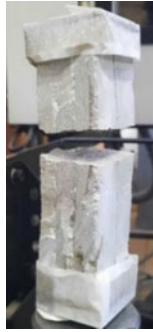


Fig. 4 Destruction of samples with 1 wire as a result of tensile test (X-axes)

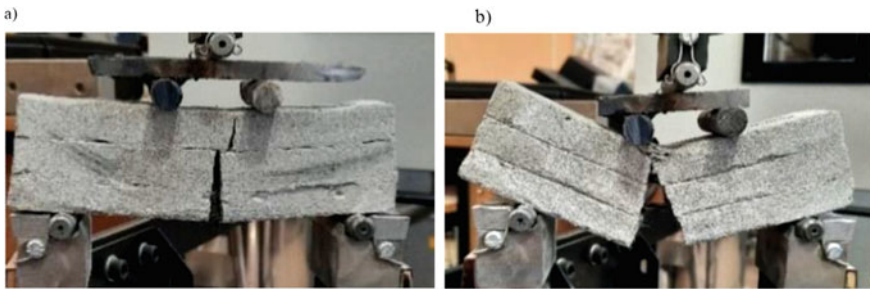


Fig. 5 Destruction of samples as a result of four-point bending test (Z-axes) **a** without wire; **b** with 3 wires

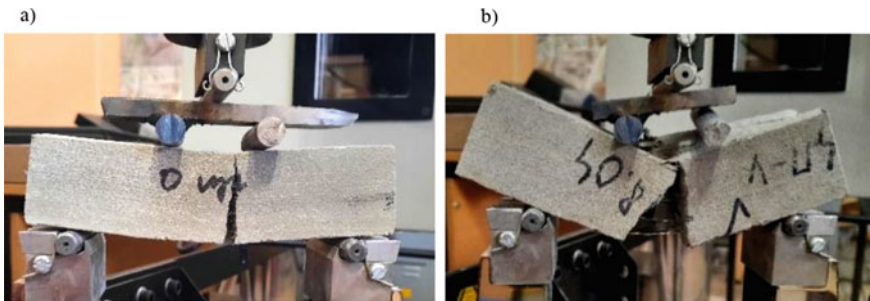


Fig. 6 Destruction of samples as a result of four-point bending test (Y-axes) **a** without wire; **b** with 5 wires

According to the results of shear testing when applying the load along the surface of the layers, we established the following. The splitting strength of non-reinforced and reinforced 3D printed samples was naturally lower than the splitting strength of reference casting samples. Also, reinforcement had practically no effect on this parameter due to the small cross-sectional area of the applied ropes 0.2 mm^2 .

Table 3 Test result

Strength parameter (MPa)	CC-samples	3DPRC-samples, number of reinforcing steel wire in a layer ^a			
		0	1	3	5
Tensile strength R_x^t	2.45	2.86	2.1/2.69	2.38/2.82	2.5/3.3
Flexural strength R_z^{fl}	4.45	5.46	4.68/6.22	5.19/8.28	4.88/13.10
Flexural strength R_y^{fl}	4.45	4.90	4.61/4.86	4.89/8.67	5.62/8.43
Splitting strength R_x^{sp}	4.04	2.64	2.6	2.55	2.6

^a The strength of the samples before the crack appearance is above the line, the final strength of the samples is below the line

In general, a significant change in the values of strength of 3D printed reinforced composites as compared to non-reinforced analogues could be achieved with 3-fibre reinforcement. The strength did not grow considerably with a further increase of the reinforcing fibres number in a layer up to 5. Based on this, it can be concluded that the further increase of the reinforcing fibres number is not reasonable.

A new class of building composites will be created based on cement matrices reinforced with high-strength fibers. The possibility of their production can be provided by using the extrusion technology of 3D-build printing. The complex of specified mechanical properties layered reinforced composites will be achieved due to the rational combination and adhesive bonding in their structure of inorganic aluminosilicate (cement) matrices with high density, compressive strength, low deformability and high tensile strength reinforcing fibers.

Steel fiber has an inhomogeneous structure (ferritic and cementite areas). Due to that, the adhesive bond between the cement matrix and the steel fiber will be determined by mechanical adhesion because «rivets» are formed between the fiber and the cement matrix. On the other hand, adhesive bond can be may be related to the interaction ϕ_{TB} intermolecular forces of components.

4 Conclusion

1. Tensile strength for 3D printed reinforced composites (3DPRC) increased by 1.5 times as compared to non-reinforced analogues. As the number of fibres in a layer grew from 1 to 5, tensile strength increased by 25%.
2. The greatest reinforcement effect was achieved when 3D printed reinforced composites were put to work in bending conditions, as in this case the strength of reinforced samples could be increased by 2.5–3 times as compared to non-reinforced samples.

3. Significant differences in the mechanical behaviour of 3D printed reinforced composites as compared to non-reinforced analogues were explained by the fact that reinforcing fibres were put to work. As a result, the tensile and flexural strength of 3DPRC samples increased in proportion to the increase in the number of fibres in the layer. The greatest increase in flexural strength up to 13 MPa was achieved for 3DPRC samples reinforced with 5 fibres when a force was applied across the boundary surface in the sample.

Acknowledgements. This research was supported by the Russian Science Foundation, No. 22-19-00280, <https://rscf.ru/en/project/22-19-00280/>. The experimental studies have been carried out using the facilities of the Collective Research Center named after Professor Yu. M. Borisov, Voronezh State Technical University, which is partly supported by the Ministry of Science and Education of the Russian Federation, Project No. 075-15-2021-662.

References

1. Lu B, Weng Y, Li M et al (2019) A systematical review of 3D printable cementitious materials. *Constr Build Mater* 207:477–490. <https://doi.org/10.1016/j.conbuildmat.2019.02.144>
2. Rehman AU, Kim JH (2021) 3d concrete printing: A systematic review of rheology, mix designs, mechanical, microstructural, and durability characteristics. *Materials* 14(14):3800. <https://doi.org/10.3390/ma14143800>
3. Salet T, Bos F, Wolfs RJM, Ahmed Z (2017) 3D concrete printing- a structural engineering perspective. In: High tech concrete: where technology and engineering meet. Published online. <https://doi.org/10.1007/978-3-319-59471-2>
4. Marchment T, Sanjayan J (2020) Bond properties of reinforcing bar penetrations in 3D concrete printing. *Autom Constr* 120:3394. <https://doi.org/10.1016/j.autcon.2020.103394>
5. Marchment T, Sanjayan J (2020) Mesh reinforcing method for 3D concrete printing. *Autom Constr* 109:2992. <https://doi.org/10.1016/j.autcon.2019.102992>
6. Classen M, Ungermann J, Sharma R (2020) Additive manufacturing of reinforced concrete-development of a 3D printing technology for cementitious composites with metallic reinforcement. *Appl Sci* 10(11):3791. <https://doi.org/10.3390/app10113791>
7. Mechtcherine V, Grafe J, Nerella VN, Spaniol E, Hertel M, Füssel U (2018) 3D-printed steel reinforcement for digital concrete construction—manufacture, mechanical properties and bond behaviour. *Constr Build Mater* 179:125–137. <https://doi.org/10.1016/j.conbuildmat.2018.05.202>
8. Kutzer J, Szatkiewicz T (2019) Properties of concrete elements with 3-D printed formworks which substitute steel reinforcement. *Constr Build Mater* 210:157–161. <https://doi.org/10.1016/j.conbuildmat.2019.03.204>
9. Lim JH, Panda B, Pham QC (2018) Improving flexural characteristics of 3D printed geopolymer composites with in-process steel cable reinforcement. *Constr Build Mater* 178:32–41. <https://doi.org/10.1016/j.conbuildmat.2018.05.010>
10. Ducoulombier N, Demont L, Chateau C, Bornert M, Caron JF (2020) Additive manufacturing of anisotropic concrete: A flow-based pultrusion of continuous fibers in a cementitious matrix. *Procedia Manufacturing*. 47:1070–1077. <https://doi.org/10.1016/j.promfg.2020.04.117>
11. Mechtcherine V, Michel A, Liebscher M, Schmeier T (2020) Extrusion-based additive manufacturing with carbon reinforced concrete: concept and feasibility study. *Materials* 13(11):2568. <https://doi.org/10.3390/ma13112568>

12. Marchment T, Sanjayan J (2020) Penetration reinforcing method for 3D concrete printing. In: Bos F (ed) Concrete and digital fabrication. 2nd Second RILEM international conference, Eindhoven, pp 680–690. https://doi.org/10.1007/978-3-030-49916-7_68
13. Weger D, Baier D, Straßer A et al (2020) Reinforced particle-bed printing by combination of the selective paste intrusion method with wire and arc additive manufacturing—A first feasibility study. In Bos F (ed) Concrete and digital fabrication. 2nd Second RILEM international conference, Eindhoven, pp 978–987. https://doi.org/10.1007/978-3-030-49916-7_95
14. Bos FP, Ahmed ZY, Jutinov ER, Salet TAJM (2017) Experimental exploration of metal cable as reinforcement in 3D printed concrete. *Materials* 10:1314. <https://doi.org/10.3390/ma10111314>
15. Asprone D, Menna C, Bos FP, Salet TA, Mata-Falcón J, Kaufmann W (2018) Rethinking reinforcement for digital fabrication with concrete. *Cem Concr Res* 112:111–121
16. Zhu B, Pan J et al (2019) Development of 3D printable engineered cementitious composites with ultra-high tensile ductility for digital construction. *Mater Des* 181:108088
17. F et al (2015) Additive manufacturing of carbon fiber reinforced thermoplastic composites using fused deposition modeling. *Compos Part B Eng* 80:369–378
18. Hambach M, Möller H, Neumann T, Volkmer D (2017) Portland cement paste with aligned carbon fibres exhibiting exceptionally high flexural strength (>100 MPa). *Cem Concr Res* 89:80–86
19. Curosu I et al (2017) Tensile behaviour of high-strength strain-hardening cement-based composites (HS-SHCC) made with high-performance polyethylene, aramid and PBO fibres. *Cem Concr Res* 98:71–81
20. Li Z, Wang L, Ma G (2020) Mechanical improvement of continuous steel microcable reinforced geopolymer composites for 3D printing subjected to different loading conditions. *Compos Part B Eng* 187:107796
21. Slavcheva GS, Artamonova OV (2020) Development of principles for creating reinforced composites for building 3D additive technologies. *Constr Mater* 12:52–58. <https://doi.org/10.31659/0585-430X-2022-809-12-52-58>
22. Slavcheva GS, Artamonova OV, Britvina EA, Babenko DS, Ibryaeva A (2020) Two-phase cement-based mixture for 3D building printable composites. Patent RF 2729085 C1



BIM Technology for Creating Digital Doubles of Buildings: Implementation Analysis of Functional Complexity

M. Filonova^(✉), S. Shirobokova, and M. Shutova

Platov South-Russian State Polytechnic University (NPI), 132, Prosveshcheniya,
Novocheerkassk 346428, Russia
filonovamaryana@yandex.ru

Abstract. The buildings life cycle management is the actual problem of construction industry digitalization process. BIM-software is widely used on the new construction design stage. At the same time, the Russian market has no full-fledged software tools for life-cycle and re-enactment modelling. Existing software tools can be applied to this problem with significant constraint. To solve the whole problem, it should be created new specialized program modules. In this article, seven CAD systems were analyzed by their functions, such as BIM integration, availability of their own application program interface (API) and dealing with temporary loads for steel structures and were defined the optimal BIM-systems for users.

Keywords: Life cycle of buildings · Digital twin · Point cloud · Building information modeling · BIM

1 Introduction

The increasing digitization of the economy means that a new digital resource—a digital twin of an organization—required for a complete description of the life cycle of the building [1].

In many countries, the transition to digital twins of buildings is underway. So, for example, the development of Level 3 BIM Strategy is carried out in Great Britain. This system is known as “Digital Built Britain” (DBB) [2].

Two main questions of this theme are: how to define a right digital twin, and how to build a right digital twin. The answer of this question may be the evolutionary concurrent modeling method for DT (ECoM4DT) [3].

Digital twins of buildings are developed on the basis of design data and monitoring information. In article [4] more than 25,000 sensor reading instances were collected, analyzed, and utilized to create and test a limited digital twin of an office building facade element.

Digital doubles are created for specific purposes. In the study [5], both technical and financial viability of Net Zero Energy Buildings (NZEB) for ‘existing’ buildings will be

highlighted. Modeling of the building applies renewable technologies to the building by aiming to identify ultimate benefit of the building especially in terms of effectiveness and efficiency in energy consumption [6].

The problem of creating digital doubles based on the Architecture, Engineering, Construction, and Facility Management (AEC-FM) [7].

BIM technologies are used to create digital twins. At the same time, there are significant problems in the complexity of the use of one or another BIM application.

Building Information Modeling (BIM) is the foundation for the construction industry digitalization. BIM is used to create the state information system for urban-planning activity in the Russian Federation [8].

The building digital twin is created on the basis of researches into the current features constructions and the high-level determination of sizes and position in the space [9]. In the current economic conditions, BIM-designing is used in various software tools [10]. They also allow to develop new program modules that solve reliability loss problems for specific structures [11].

Augmented and virtual reality technology allows to combine the BIM-model directly with the real-world object for determination of collisions [12, 13].

Different BIM software types implement different features [14] and ways of spatial and temporal parameters variations [15].

At present, most of the construction fund has no progress information [16]. BIM application and advanced information and communication technologies can solve the problem of re-enactment [17] and restoration [18] projects. In the construction industry, the demand for digital innovation is growing rapidly [19]. The BIM-technologies development and the creation linear capital construction object stimulate the development of methods of working with the accumulated data set [20]. For existing buildings and structures, the information model is a digital twin of buildings [21]. The development and improving digital twin can solve forecasting problem of construction properties degradation and technical condition deterioration [22]. However, it is impossible to do that using existing software tools due to their functional constraints [23]. Thus, for implementation of the tasks, it is necessary to analyze the software for information modelling of construction objects by functional completeness [24–33].

2 Preliminary Analysis of Existing Systems

In this article, seven CAD systems were analyzed by their functions, such as BIM integration, availability of their own application program interface (API) and dealing with temporary loads for steel structures.

The software programs under study are listed in Table 1. Let $S = \{S_i\}$, ($i = 1..7$) be a set of systems.

The analyzed systems functions are given in Table 2. Let $R = \{R_j\}$, ($j = 1..89$) be a set of system functions.

On the basis of S and R sets we define X_{ij} matrix as:

$$X_{ij} = \begin{cases} 1, & \text{if the function } R_i \text{ is implemented in the system } S_j \\ 0 & \text{if the function } R_i \text{ is not implemented in the system } S_j \end{cases};$$

Table 1 The list of studied CAD systems

Designation	Name	Information source
S_1	LIRA SOFT [18, 19]	https://lira-soft.com/
S_2	SCAD [20]	https://scadsoft.com/
S_3	Robot Autodesk [21, 22]	https://www.autodesk.com/
S_4	SAP2000 [23]	https://steel-concrete.ru/
S_5	ETABS [24]	https://etabsmate.com/etabsmate_en
S_6	DLUBAL [25]	https://www.dlubal.com/ru
S_7	SciaEneer [26]	https://www.scia.net/

Table 2 The list of analyzed CAD systems functions (a fragment)

Designation	Name	Designation	Name
R_1	Commercial license	R_{12}	Format support <i>DXF</i>
R_2	Open Source license
R_3	Russian SNIP compliance	R_{81}	Automatisation of recurring solves
R_4	Presence of russified interface	R_{82}	Creating and updating models
R_5	<i>BIM integration</i> formats	R_{83}	Creating loads on constructions
R_6	Format support <i>MSH</i>	R_{84}	Control constructions following SNIP requirements
R_7	Format support <i>STL</i>	R_{85}	Graphical representation calculations
R_8	Format support <i>OBJ</i>	R_{86}	Import and export of models
R_9	Format support <i>MESH</i>	R_{87}	Temporary loads support
R_{10}	Format support <i>OFF</i>	R_{88}	Steel constructions
R_{11}	Format support <i>POLY</i>	R_{89}	Specification of loads parameters as function of time

The fragment of \mathbf{X}_{ij} matrix is given in Table 3.

In the beginning, we calculated P_{ik}^{11} matrix (a number of operations that are implemented by both S_i and S_k systems):

$$P_{ik}^{11} = \{S_i \cap S_k\}.$$

Then we built P_{ik}^{10} matrix (a number of operations that are implemented by S_i system, not by S_k system):

$$P_{ik}^{10} = \{S_i/S_k\}.$$

Table 3 The matrix X

Functions	Systems						
	S_1	S_2	S_3	S_4	S_5	S_6	S_7
R_1	1	1	1	1	1	0	1
R_2	0	0	0	0	0	1	0
R_3	1	1	0	0	1	1	0
R_4	1	1	0	1	1	0	0
R_5	0	0	0	0	0	0	0
R_6	1	0	0	0	0	0	0
R_7	1	0	0	0	0	0	0
R_8	1	0	0	0	0	0	0
R_9	1	1	0	0	0	0	0
R_{10}	1	0	0	0	0	0	0
...
R_{81}	0	1	1	1	1	1	0
R_{82}	1	1	1	1	1	1	0
R_{83}	1	1	0	1	1	1	0
R_{84}	0	0	1	1	0	1	0
R_{85}	1	0	0	0	0	1	0
R_{86}	0	1	1	0	0	1	0
R_{87}	1	1	0	0	0	1	1
R_{88}	1	1	1	1	1	1	1
R_{89}	0	0	1	1	0	0	0

After that, we calculated P_{ik}^{01} matrix (a number of operations that are implemented by S_k system, not by S_i system):

$$P_{ik}^{01} = \{S_k/S_i\}.$$

The matrices specified earlier become the base of P superiority matrix calculated by formula:

$$P_{ik} = \frac{P_{ik}^{01}}{P_{ik}^{11} + P_{ik}^{10}}.$$

The result is a matrix presented below:

$$P_{ik} = \begin{bmatrix} 0 & 16 & 15 & 12 & 7 & 18 & 4 \\ 25 & 0 & 15 & 12 & 8 & 17 & 2 \\ 30 & 21 & 0 & 8 & 6 & 18 & 7 \\ 26 & 17 & 7 & 0 & 4 & 18 & 5 \\ 29 & 21 & 13 & 12 & 0 & 23 & 8 \\ 25 & 15 & 10 & 11 & 8 & 0 & 3 \\ 32 & 21 & 20 & 19 & 14 & 24 & 0 \end{bmatrix}.$$

The G_{ik} system similarity is calculated by Jaccard similarity formula:

$$G_{ik} = \frac{P_{ik}^{11}}{P_{ik}^{11} + P_{ik}^{10} + P_{ik}^{01}}.$$

The result is a matrix presented below:

$$G_{ik} = \begin{bmatrix} 1.000 & 0.281 & 0.196 & 0.283 & 0.250 & 0.271 & 0.200 \\ 0.281 & 1.000 & 0.234 & 0.341 & 0.275 & 0.347 & 0.324 \\ 0.196 & 0.234 & 1.000 & 0.559 & 0.406 & 0.364 & 0.182 \\ 0.283 & 0.341 & 0.559 & 1.000 & 0.484 & 0.356 & 0.250 \\ 0.250 & 0.275 & 0.406 & 0.484 & 1.000 & 0.262 & 0.185 \\ 0.271 & 0.347 & 0.364 & 0.356 & 0.262 & 1.000 & 0.270 \\ 0.200 & 0.324 & 0.182 & 0.250 & 0.185 & 0.270 & 1.000 \end{bmatrix}.$$

The H_{ik} value allows us to evaluate the functional part of S_i system, that is also implemented by S_k system. Thus we obtain the matrix below:

$$H_{ik} = \begin{bmatrix} 1.000 & 0.390 & 0.268 & 0.366 & 0.293 & 0.390 & 0.220 \\ 0.500 & 1.000 & 0.344 & 0.469 & 0.344 & 0.531 & 0.344 \\ 0.423 & 0.423 & 1.000 & 0.731 & 0.500 & 0.615 & 0.231 \\ 0.556 & 0.556 & 0.704 & 1.000 & 0.556 & 0.593 & 0.296 \\ 0.632 & 0.579 & 0.684 & 0.789 & 1.000 & 0.579 & 0.263 \\ 0.471 & 0.500 & 0.471 & 0.471 & 0.324 & 1.000 & 0.294 \\ 0.692 & 0.846 & 0.462 & 0.462 & 0.385 & 0.769 & 1.000 \end{bmatrix}.$$

All matrices obtain should be transformed into logic forms. In this regard, threshold values are defined:

$$\varepsilon_P = 20, \varepsilon_H = 0.7, \varepsilon_G = 0.4.$$

According to threshold values we generate P_0 , H_0 , G_0 logic matrices:

$$P_0 = \begin{bmatrix} 0 & 1 & 1 & 1 & 1 & 1 & 1 \\ 0 & 0 & 1 & 1 & 1 & 1 & 1 \\ 0 & 0 & 0 & 1 & 1 & 1 & 1 \\ 0 & 1 & 1 & 0 & 1 & 1 & 1 \\ 0 & 0 & 1 & 1 & 0 & 0 & 1 \\ 0 & 1 & 1 & 1 & 1 & 0 & 1 \\ 0 & 0 & 1 & 1 & 1 & 0 & 0 \end{bmatrix}, H_0 = \begin{bmatrix} 0 & 0 & 0 & 0 & 0 & 0 & 0 \\ 0 & 0 & 0 & 0 & 0 & 0 & 0 \\ 0 & 0 & 0 & 1 & 0 & 0 & 0 \\ 0 & 0 & 1 & 0 & 0 & 0 & 0 \\ 0 & 0 & 0 & 1 & 0 & 0 & 0 \\ 0 & 0 & 0 & 0 & 0 & 0 & 0 \\ 0 & 1 & 0 & 0 & 0 & 0 & 0 \end{bmatrix}, G_0 = \begin{bmatrix} 0 & 0 & 0 & 0 & 0 & 0 & 0 \\ 0 & 0 & 0 & 0 & 0 & 0 & 0 \\ 0 & 0 & 0 & 1 & 1 & 0 & 0 \\ 0 & 0 & 1 & 0 & 2 & 0 & 0 \\ 0 & 0 & 1 & 1 & 0 & 0 & 0 \\ 0 & 0 & 0 & 0 & 0 & 0 & 0 \\ 0 & 0 & 0 & 0 & 0 & 0 & 0 \end{bmatrix}.$$

Based on P_0, H_0, G_0 logic matrices we create three related graphs.

From the superiority graph (Fig. 1) it is clear that S_1 (LIRA SOFT) exceeds all systems. For example, the function number implemented in the S_1 system, but absent in the S_7 system is 32.

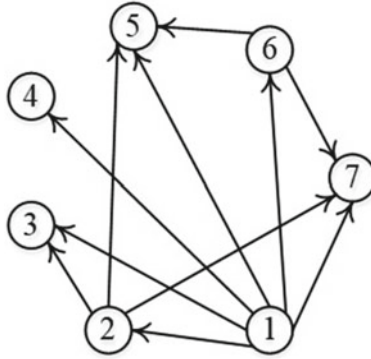


Fig. 1 Superiority graph in preliminary analysis

S_1 (SCAD) also exceeds S_3, S_5, S_7 systems.

Figure 2 shows the similarity graph, that demonstrates CAD systems similarity with threshold values $\varepsilon_G = 0.4$. The similarity between S_3 and S_4 systems is 55.9%, between and S_5 is 40.6% and between S_4 and S_5 is 48.4%.

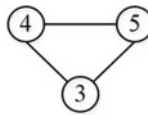


Fig. 2 Similarity graph in preliminary analysis

Using the H matrix we build the absorption graph (Fig. 3). The graph shows, that S_7 system is absorbed by S_2 systems and S_6 over 70%. Functional of S_3, S_4 and S_5 systems is absorbed serially that demonstrates their high level of consistency.

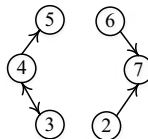


Fig. 3 Absorption graph in preliminary analysis

As a result of this study, it was established that S_1 и S_2 systems are the most functionally complete. Their significant advantage is complying with Russia’s normative requirements, federal laws and Russian interface available.

However, these systems do not support the most important functions for the problem of calculating the residual operation life. S_3 and S_4 systems have necessary functions, but do not meet Russian SNIPs and are not available to Russian customers.

Therefore, to make an optimal choice of a CAD system we should analyze its compliance with a reference system, including all necessary customer functions.

3 Comparison of Existing Solutions with an Ideal System

To assess whether the functions of analyzed systems meet customer requirements, we create the S_8 reference system. The fragment of functions implemented by a new system is presented in Table 4.

Similarly P , G and H matrices are calculated, their contents are given below:

$$P_{ij} = \begin{bmatrix} 0 & 16 & 15 & 12 & 7 & 18 & 4 & 18 \\ 25 & 0 & 15 & 12 & 8 & 17 & 2 & 20 \\ 30 & 21 & 0 & 8 & 6 & 18 & 7 & 20 \\ 26 & 17 & 7 & 0 & 4 & 18 & 5 & 20 \\ 29 & 21 & 13 & 12 & 0 & 23 & 8 & 23 \\ 25 & 15 & 10 & 11 & 8 & 0 & 3 & 14 \\ 32 & 21 & 20 & 19 & 14 & 24 & 0 & 30 \\ 23 & 16 & 10 & 11 & 6 & 12 & 7 & 0 \end{bmatrix}$$

$$H_{ij} = \begin{bmatrix} 1.000 & 0.390 & 0.268 & 0.366 & 0.293 & 0.390 & 0.220 & 0.439 \\ 0.500 & 1.000 & 0.344 & 0.469 & 0.344 & 0.531 & 0.344 & 0.500 \\ 0.423 & 0.423 & 1.000 & 0.731 & 0.500 & 0.615 & 0.231 & 0.615 \\ 0.556 & 0.556 & 0.704 & 1.000 & 0.556 & 0.593 & 0.296 & 0.593 \\ 0.632 & 0.579 & 0.684 & 0.789 & 1.000 & 0.579 & 0.263 & 0.684 \\ 0.471 & 0.500 & 0.471 & 0.471 & 0.324 & 1.000 & 0.294 & 0.647 \\ 0.692 & 0.846 & 0.462 & 0.615 & 0.385 & 0.769 & 1.000 & 0.462 \\ 0.500 & 0.444 & 0.444 & 0.444 & 0.444 & 0.361 & 0.167 & 1.000 \end{bmatrix}$$

$$G_{ij} = \begin{bmatrix} 1.000 & 0.281 & 0.196 & 0.283 & 0.250 & 0.271 & 0.200 & 0.305 \\ 0.281 & 1.000 & 0.234 & 0.341 & 0.275 & 0.347 & 0.324 & 0.308 \\ 0.196 & 0.234 & 1.000 & 0.559 & 0.406 & 0.364 & 0.182 & 0.348 \\ 0.283 & 0.341 & 0.559 & 1.000 & 0.484 & 0.356 & 0.250 & 0.340 \\ 0.250 & 0.275 & 0.406 & 0.484 & 1.000 & 0.262 & 0.185 & 0.310 \\ 0.271 & 0.347 & 0.364 & 0.356 & 0.262 & 1.000 & 0.270 & 0.458 \\ 0.200 & 0.324 & 0.182 & 0.250 & 0.185 & 0.270 & 1.000 & 0.140 \\ 0.305 & 0.308 & 0.348 & 0.340 & 0.310 & 0.458 & 0.140 & 1.000 \end{bmatrix}$$

We determine the number of functions realized in the S_1 – S_7 systems but absent in the S_8 system (Table 5). We also find the number of functions implemented in S_8 system, but absent in other systems (Table 6).

Having calculated the P_0 , H_0 , G_0 matrices for the threshold values chosen ($\varepsilon_P = 22$, $\varepsilon_H = 0.68$, $\varepsilon_G = 0.4$), we construct three graphs.

Table 4 Compliance of systems' functions with the reference system

Function name	CAD system identification						
	S_1	S_2	S_3	S_4	S_5	S_6	S_7
1	2	3	4	5	6	7	8
Commercial license	1	1	1	1	1	0	1
Open Source license	0	0	0	0	0	1	0
Russian SNIP compliance	1	1	0	0	1	1	0
Presence of russified interface	1	1	0	1	1	0	0
Format support <i>MSH</i>	1	0	0	0	0	0	0
Commercial license	1	1	1	1	1	0	1
...
Format support BYU	1	0	0	0	0	0	0
Format support IFC 2.3	1	1	1	1	1	1	1
Format support IFC4	1	1	1	1	1	1	0
...
Format support Renga Structure	1	0	0	0	0	0	0
Format support PLAXIS 3D	1	0	0	0	0	0	0
...
Format support ConED	0	0	0	0	0	1	0
Support Microsoft Access	0	0	1	1	0	0	0
Support Python	0	0	1	0	1	1	0
Support C#	1	0	1	1	1	1	0
...
Support Matlab	0	0	1	0	1	0	0
Automatisation of recurring solves	0	1	1	1	1	1	0
Creating and updating models	1	1	1	1	1	1	0
Creating loads on constructions	1	1	0	1	1	1	0
Control constructions following SNIP requirements	0	0	1	1	0	1	0
Graphical representation calculations	1	0	0	0	0	1	0
Import and export of models	0	1	1	0	0	1	0
Temporary loads support	1	1	0	0	0	1	1
Steel constructions	1	1	1	1	1	1	1
Specification of loads parameters as function of time	0	0	1	1	0	1	0
Determination of the structure relative reliability	0	0	0	0	0	0	0

(continued)

Table 4 (continued)

Function name	CAD system identification						
	S_1	S_2	S_3	S_4	S_5	S_6	S_7
Efforts redistribution with the failure of elements	0	0	0	0	0	0	0
Support PILOT BIM	0	0	0	0	0	0	0
Support BIM NanoCAD	0	0	0	0	0	0	0

Table 5 The Number of functions realized in the S_1 – S_7 systems

CAD system identification	System name	Number of functions
S_1	LIRA SOFT	24
S_2	SCAD	18
S_3	Robot Autodesk	10
S_4	SAP2000	13
S_5	ETABS	7
S_6	DLUBAL	13
S_7	SciaEngeneer	7

Table 6 The Number of functions realized in the S_8 system

CAD system identification	System name	Number of functions
S_1	LIRA SOFT	10
S_2	SCAD	13
S_3	Robot Autodesk	11
S_4	SAP2000	13
S_5	ETABS	15
S_6	DLUBAL	6
S_7	SciaEngeneer	21

The superiority graph shows that the S_1 (LIRA SOFT) system is superior to all other systems by over 22%. The reference system has over 22% unique functions than S_5 and S_7 systems. S_7 is the weakest system (Fig. 4).

The similarity graph shows that S_6 (DLUBAL) system is the closest analogue of the reference system (Fig. 5).

By analyzing absorption graph it is clear that S_1 , S_2 and S_6 systems absorb over 68% of all system functions (Fig. 6).

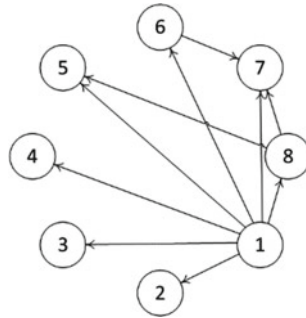


Fig. 4 Superiority graph including ideal system

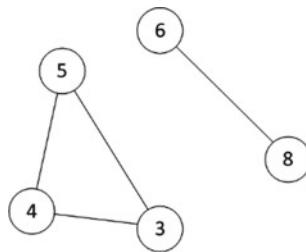


Fig. 5 Similarity graph including ideal system

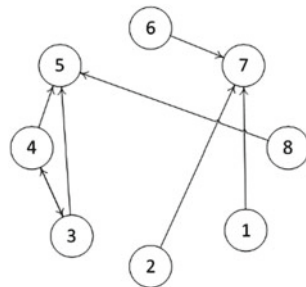


Fig. 6 Absorption graph including ideal system

4 Conclusions

As a result of CAD systems analysis some conclusions were made. It may be noted that S_1 , S_2 , S_6 systems have the most functional completeness. However, they do not meet requirements that are necessary to calculate the residual life of a building. Therefore, it is suggested that S_1 system should be improved with its own API.

References

1. Parmar R, Leiponen A, Thomas LDW (2020) Building an organizational digital twin. *J Bus Horiz* 63:725–736. <https://doi.org/10.1016/j.bushor.2020.08.001>
2. Lu Q et al (2020) Developing a digital twin at building and city levels: case study of West Cambridge campus. *J Manage Eng* 36:05020004
3. Zhang L, Zhou L, Horn BKP (2021) Building a right digital twin with model engineering. *J Manuf Syst* 59:151–164. <https://doi.org/10.1016/j.jmsy.2021.02.009>
4. Khajavi SH, Motlahg NH, Jaribon A et al (2019) Digital twin: vision, benefits, boundaries, and creation for buildings. *J IEEE Access* 7:147406–147419. <https://doi.org/10.1109/ACC ESS.2019.2946515>
5. Kaewunruen S, Rungskunroch P, Welsh J (2018) A digital-twin evaluation of net zero energy building for existing buildings. *Sustainability* 11:159. <https://doi.org/10.3390/su11010159>
6. Qiuchen Lu V et al (2019) Developing a dynamic digital twin at a building level: using Cambridge campus as case study. In: *J International conference on smart infrastructure and construction 2019 (ICSIC) driving data-informed decision-making*, pp 67–75
7. Hosamo HH et al (2022) A review of the digital twin technology in the AEC-FM industry. *J Adv Civ Eng*. <https://doi.org/10.1155/2022/2185170>
8. Badenko VL, Bolshakov NS, Tishchenko EB et al (2020) Integration of digital twin and BIM technologies within factories of the future. *J Mag Civ Eng*, p 10114. <https://doi.org/10.34910/MCE.101.14>
9. Krinitskiy YN (2010) Building information model (BIM). *J Mag Civ Eng* 12:16–18. <https://doi.org/10.18720/MCE.12.2>
10. Akinradewo O, Aigbavboa C, Oke A (2022) Key requirements for effective implementation of building information modelling for maintenance management. *J Int J Constr Manage*. <https://doi.org/10.1080/15623599.2021.2023724>
11. AliFH BS (2022) Correlation between BIM data creation and big data attributes in construction. *Int J Constr Manage*. <https://doi.org/10.1080/15623599.2022.2119071>
12. Mayer M, Bechtold M (2020) Data refinement for urban scale life cycle modeling. *J Architectural Sci Rev* 63(3–4):351–360. <https://doi.org/10.1080/00038628.2019.1689914>
13. Kurkela M, Maksimainen M, Julin A (2022) Applying photogrammetry to reconstruct 3D luminance point clouds of indoor environments. *J Architectural Eng Des Manage* 18:56–72. <https://doi.org/10.1080/17452007.2020.1862041>
14. Skrzypczak I, Oleniacz G, Leśniak G (2022) Scan-to-BIM method in construction: assessment of the 3D buildings model accuracy in terms inventory measurements. *J Build Res Inf* 50:859–880. <https://doi.org/10.1080/09613218.2021.2011703>
15. Rodríguez-Moreno C, Reinoso-Gordo JF, Rivas-López E (2016) From point cloud to BIM: an integrated workflow for documentation, research and modelling of architectural heritage. *J Surv Rev* 50(360):212–231. <https://doi.org/10.1080/00396265.2016.1259719>
16. Boland RJ Jr, Lyytinen K, Yoo Y (2007) Wakes of innovation in project networks: The case of digital 3-D representations in architecture, engineering, and construction. *Organ Sci* 18(4):631–647
17. Martínez-Carricondo P, Carvajal-Ramírez F, Yero-Paneque L (2020) Combination of nadir and oblique UAV photogrammetry and HBIM for the virtual reconstruction of cultural heritage. Case study of CortijodelFraile in Níjar, Almería (Spain). *J Build Res Inf* 48(2):140–159. <https://doi.org/10.1080/09613218.2019.1626213>
18. Migilinskas D, Pavlovskis M, Urba I (2017) Analysis of problems, consequences and solutions for BIM application in reconstruction projects. *J Civ Eng Manage* 23(8):1082–1090. <https://doi.org/10.3846/13923730.2017.1374304>

19. Pustovgar AP, Zhunzhun C, Vensen Y (2020) Application of BIM-technology in the restoration of buildings. *J Ind Civ Eng* 6:42–48. <https://doi.org/10.33622/0869-7019.2020.06>
20. Gruen A, Behnischand M, Kohler N (2009) Perspectives in the reality-based generation, modelling, and operation of buildings and building stocks. *J Build Res Inf* 37(5–6):503–519. <https://doi.org/10.1080/09613210903189509>
21. Shibeikaand A, Harty C (2015) Diffusion of digital innovation in construction: a case study of a UK engineering firm. *J Constr Manage Econ* 33(5–6):453–466. <https://doi.org/10.1080/01446193.2015.1077982>
22. Wikberg F, Olofsson T, Ekholm A (2014) Design configuration with architectural objects: linking customer requirements with system capabilities in industrialized house-building platforms. *J Constr Manage Econ* 32(1–2):196–207. <https://doi.org/10.1080/01446193.2013.864780>
23. Aleksanin AV, Zharov YV (2022) The potential of using digital information models in the framework of construction management. *J Ind Civ Eng* 1:52–55. <https://doi.org/10.33622/0869-7019.2022.01.52-55>
24. Khubaev GN (1998) Comparison of complex software systems by functional completeness criterion. *J Softw Syst* 2:6–9
25. SP LIRA Soft. Multifunctional analysis and calculation system, LIRA Soft. <https://lira-soft.com/lira-10/>. Accessed 29 Oct 2022
26. Geraimovich YD, Evzerov ID, Kirichok VV et al (2022) Software package lira 10.12. User manual, LIRA SOFT
27. ScadSoft, SCAD Office. <https://scadsoft.com/products/scad>. Accessed 29 Oct 2022
28. Robot Structural Analysis, Autodesk. <https://www.autodesk.com/>. Accessed 29 Oct 2022
29. Autodesk® Robot™ Structural analysis professional getting started guide robot API, Autodesk, Inc. (2020)
30. SAP2000, Steel-concrete.ru. <https://steel-concrete.ru/products/csi/sap2000/>. Accessed 29 Oct 2022
31. ETABS MATE Software, ETABS MATE. https://etabsmate.com/etabsmate_en.htm. Accessed 29 Oct 2022
32. Programs for calculation and design of structures. Dlubal. <https://www.dlubal.com/ru> Accessed 29 Oct 2022
33. Imagination Calculated, SCIA. <https://www.scia.net/en> Accessed 29 Oct 2022



Accounting for Changes of Silty-Clay Soils Characteristics in the Ground Base of Buildings and Structures in the Process of Flooding of Territories

M. A. Stepanov^(✉) and A. P. Shestakova

Industrial University of Tyumen, Volodarskogo Street, 38, Tyumen 625001, Russia
maxim_stepanov@inbox.ru

Abstract. The article considers the problem of flooding of territories both in Russia and abroad. The authors give the diagram of the main sources and causes of flooding, as well as a classification of the consequences of flooding areas. They present the laboratory test results of physical soil properties changes and of mechanical soil properties changes, such as: oedometric modulus of deformation; the angle of internal friction and intercept cohesion. Analysis of the results show the negative effect of soil water saturation on the soils mechanical characteristics. The laboratory tests allowed the authors of the article to get the results of numerical modeling of forecasting the development of the geotechnical situation during the construction of a multi-storied residential building with an underground floor. This was done in the conditions of a possible increase of groundwater levels, which has calculated additionally. The article gives the forecast of the development area flooding considering two types of foundation (slab and strip).

Keywords: Foundation · Flooding · Silty-clay soils · Laboratory tests · Numerical modeling · Stress–strain state

1 Introduction

In recent years, the problem of interaction between the ground base, foundations and building structures with the geological environment has become relevant within urban areas and large industrial enterprises. At the same time, more and more territories are exposed to influence of dangerous geological processes. The flooding of territories is one of the most unfavorable of them [1–14]. The development of these processes violates the operating conditions of buildings and structures and, as a result, it affects the occurrence of social, economic and environmental problems [1].

The huge scale and pace of industrial, hydrotechnical, meliorative and urban construction often cause a high rise of the groundwater level.

To date, only in Russia, about 960 cities and large areas of agricultural land have been flooded to varying degrees. Such cities as Moscow, St. Petersburg, Novosibirsk, Omsk,

Rostov-on-Don, Saratov, Samara, Tyumen and many others are exposed to flooding. Thus, almost all natural zones of Russia are covered by this process.

The causes of flooding can appear both separately and in combination [4, 15]. Figure 1 shows a diagram of the main sources and causes of flooding.

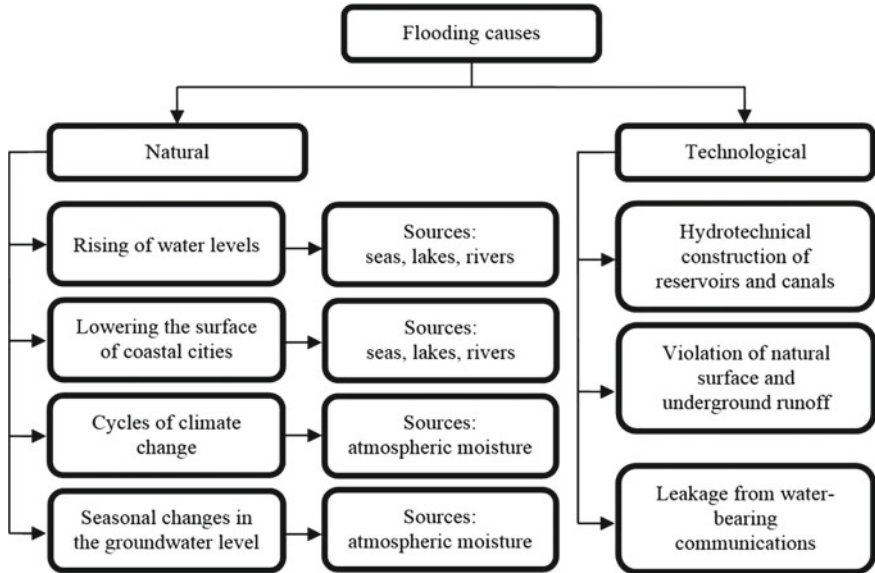


Fig. 1 Diagram of the main sources and causes of flooding

The mechanical impact of groundwater on ground base soils is mainly in the water saturation of soils and in a simultaneous change of their stress state. It leads to a change in the soil properties, which causes additional deformations of the foundation constructions and, consequently, the building structures themselves [15]. The damage from flooding, according to the latest data, is about 5–6 billion dollars per year [2, 16–28]. Flooding often causes activation of karst processes, landslides, swelling of clay soils, collapsing of loess soils and changes in the microseismic characteristics of territories. In addition, the intensity of the seismic effect on water-saturated soils increases by 1 point [17]. Figure 2 shows the classification of consequences of flooding of territories.

The consequences of flooding are always interconnected. First, the phenomenon of flooding itself occurs, which causes capillary moistening and water saturation of the ground base soils and building materials. Long-term moisture influences on physical and mechanical characteristics of soils and the stress–strain state of the ground base. It provides a violation of the operational suitability of structures and buildings, which can lead to their additional settlements and deformations. Besides of it, possible flooding of underground floors accelerates corrosion of concrete structures, which reduce the service life of buildings and not provide the sanitary standards for their operation [1].

The purpose of this issue was to identify the dependence of changes in the characteristics of silty clay soils due to flooding of the built-up area on the basis of experimental

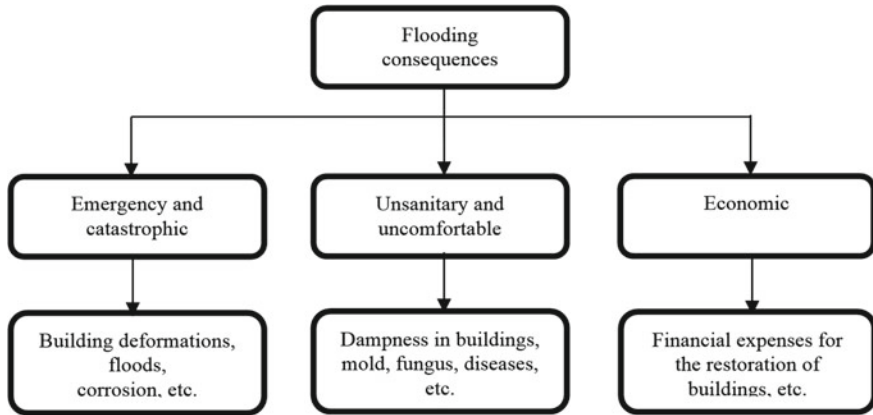


Fig. 2 Classification of consequences of territories flooding

and theoretical studies. It will help us to forecast this effect on the mechanical safety of buildings and structures.

At the same time, it was necessary to establish the dependence of the change of silty-clay soils characteristics during flooding on the basis of laboratory studies. And the obtained data should be used to analyze the change in the stress–strain state of the ground base soil during flooding of the territory of a residential building under construction in Tyumen.

2 Laboratory Studies of the Flooding Process Influence on the Physical and Mechanical Characteristics of the Soil

During watering, a change in the physical state of soils is primarily expressed in an increase of their moisture content, and, as a result, of their liquidity index and unit weight. At the same time, we can assume that the mechanical properties of soils, such as: oedometric modulus of deformation; the angle of internal friction, intercept cohesion—change too.

This paper presents the results of a study of changes in the physical and mechanical properties of the soil when it is moistened for samples of silty clay soils, the most common in the south of the Tyumen region. To identify the qualitative and quantitative effect of water saturation, shear and compressive tests of loams were carried out (in the amount of up to 50 tests of soil samples with natural water content and 50 samples of saturated soil) (Table 1). The tests were carried out in accordance with GOST 12248 “Soils. Laboratory methods for determining the strength and strain characteristics”.

Statistical processing of the results of a series of oedometer and shear soil tests and their analysis make it possible to draw conclusions about the overall negative effect of soil water saturation on the mechanical characteristics of silty-clay soils:

- the value of the oedometric modulus of deformation during water saturation decreases to 55.4%;

Table 1 Results of laboratory studies

Characteristic name	Symbol	Units	Soil with natural water content	Water saturated soil
<i>Physical soil characteristics</i>				
Water content	W	%	22.47	25.80
Plastic limit	W _p	%	16.38	
Liquid limit	W _L	%	32.94	
Plasticity index	I _p	%	16.56	
Liquidity index	I _L	Unit fraction	0.37	0.57
Unit weight	γ	kN/m ³	18.23	20.78
<i>Mechanical soil characteristics</i>				
Modulus of deformation	E	MPa	11.9	5.3
Intercept cohesion	c	kPa	12.9	11.3
Angle of internal friction	φ	degree	22	10.5

- the angle of internal friction decreases to 12.4%,
- intercept cohesion decreases to 52%.

3 Numerical Modeling of the “Foundation—Ground Base” System Interaction During Flooding

The results of laboratory studies were used to forecast the development of the geotechnical situation during the construction of a multi-storey residential building with an underground floor in Tyumen. According to the technical task, two types of foundation were considered: slab and strip with width of 2.4 m.

At the time of investigations, the construction site was surrounded by numerous water-bearing communications, leaks from which contribute to the saturation of the aeration zone with technogenic waters and, as a result, to increase of groundwater levels.

Maps of the distribution of the level surface of groundwater at the construction site in different periods of time are shown in Fig. 3.

The forecast of flooding of this area was carried out to take into account the possible increase of the groundwater level with unfavorable climatic, hydrogeological and technogenic factors (Fig. 4).

Groundwater level rise for an unrestricted water level:

$$\Delta h = \frac{\omega \cdot t}{\pi \cdot n} \cdot \left(\operatorname{arctg} \frac{\xi_1}{\tau} + \operatorname{arctg} \frac{\xi_2}{\tau} - \frac{\xi_1}{2 \cdot \tau} \cdot \ln \frac{\xi_1^2}{\xi_1^2 + \tau^2} - \frac{\xi_2}{2 \cdot \tau} \cdot \ln \frac{\xi_2^2}{\xi_1^2 + \tau^2} \right) \quad (1)$$

ω—additional infiltration; t—the period from the start of additional infiltration on the free surface (t = 30 days); n—lack of saturation; τ—value equal to $\tau = (k \cdot t)/(n \cdot L)$;

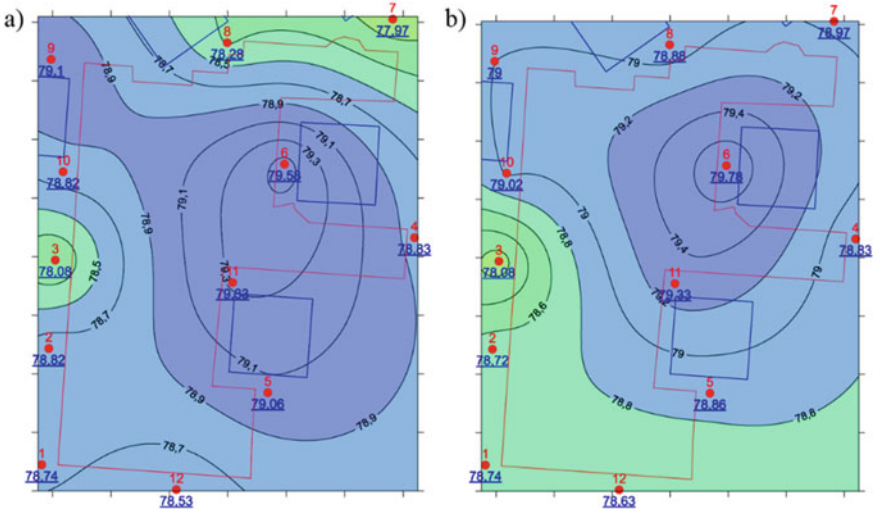


Fig. 3 Map of absolute marks of the groundwater level: **a** in April 24, 2019; **b** in May 25, 2019

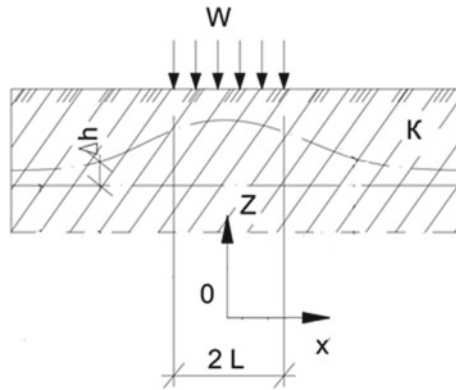


Fig. 4 Calculation scheme for determining additional infiltration

k —layer filtration coefficient ($k = 0.06$ m/day); L —the source width; $\xi_{1,2}$ —value equal to $\xi = \pm 1x$.

$$\omega = (1 - \alpha) \cdot \omega_g - \Delta u + \beta \cdot \frac{W}{F} \tag{2}$$

α —the coefficient of surface runoff; ω_g —the intensity of precipitation, m/day; Δu —the change in the amount of evaporation from the groundwater surface, m/day; $\beta = 0.063$ —coefficient of water loss from water-bearing communications; W —daily water consumption, m^3 /day; F —buildings area, m^2 .

Table 2 shows the average monthly daily intensity of precipitation according to observations in Tyumen.

The groundwater level increase Δh was—2.05 m.

Table 2 The average monthly daily intensity of precipitation according to observations in Tyumen

Month	I	II	II	IV	V	VI	VII	VIII	IX	X	XI	XII	For a year
Precipitation, mm	36	16	21	30	37	43	108	91	56	64	30	41	569

The calculation scheme for determining additional infiltration is shown in Fig. 4.

In the situation under consideration, a layer of silty-clay soil (loam) is subject to possible flooding. Initially, the groundwater level was at a depth of 5 m, after the flooding of the territory—at a depth of 3 m. The depth of the foundation was 4 m.

There were two options for the construction of foundations: strip foundation and solid slab foundation. Building has a reinforced concrete frame with ceilings in the form of a single stiffening disk.

Calculations to determine the deformations of the ground base were carried out both without taking into account the influence of groundwater, and taking into account the flooding of the territory (Fig. 5). The calculation modeling took into account the staged construction of the building.

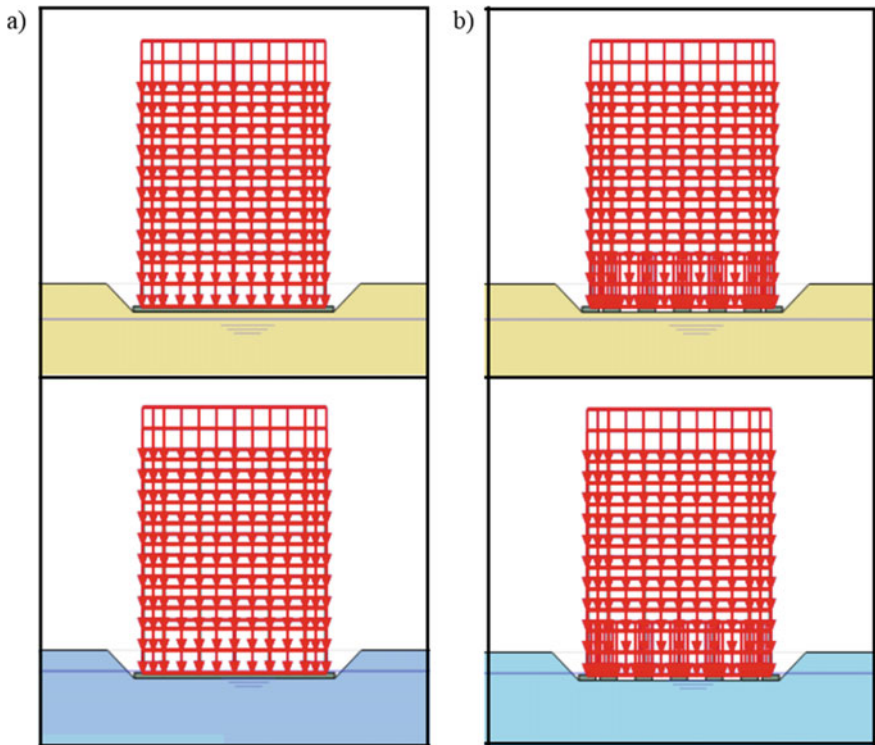


Fig. 5 Calculation schemes of the building in Plaxis program: **a** for slab foundation; **b** for strip foundation

Points for considering deformations are shown in Fig. 6.

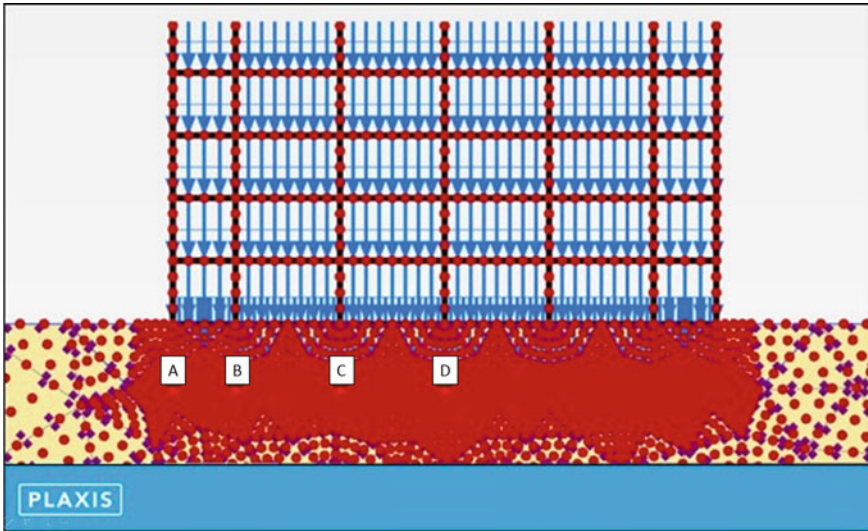


Fig. 6 Points for considering deformations

The numerical modeling shows us that slab foundation, which has a higher rigidity in relation to a strip foundation, has a relative differential settlement value of up to 60% lower (Table 3). And this values are acceptable in accordance with the requirements of regulatory documents.

But, in general, as a result of flooding, taking into account changes in the characteristics of soils, deformations of the ground base increase significantly, exceeding the required standard values. According to the results of the numerical modeling, it was found that, in accordance with the negative scenario, water saturation of soils can lead to an increase in the deformation of the base, on average, up to 77% (Fig. 7).

Table 3 Numerical modeling results

Comparable indicators	Point	Strip foundation	Slab foundation
Settlements before water-saturation from flooding, sm	A	10.39	10.46
	B	11.23	10.91
	C	12.30	11.59
	D	12.89	11.93
Settlements after water-saturation from flooding, sm	A	20.36	17.85
	B	21.30	18.32
	C	22.49	19.05
	D	23.50	19.43
Relative differential settlements before water-saturation from flooding	A and B	0.0028	0.0015
	B and C	0.0021	0.0014
	C and D	0.0012	0.0007
Relative differential settlements after water-saturation from flooding	A and B	0.0031	0.0016
	B and C	0.0024	0.0015
	C and D	0.0020	0.0008

Bold indicates more than the limit value

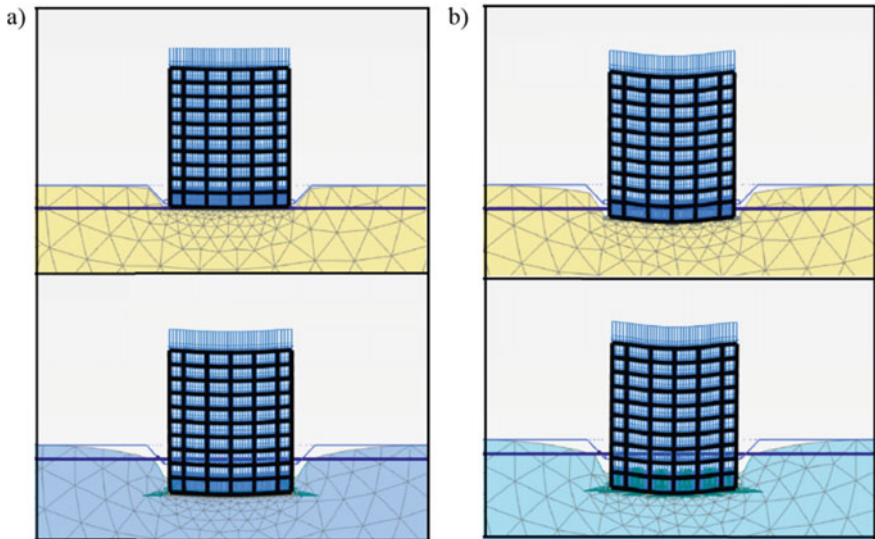


Fig. 7 Deformation schemes before (top) and after (bottom) flooding: **a** for a slab foundation; **b** for strip foundation

4 Conclusion

Thus, the flooding of territories has a negative impact on ground base characteristics and can lead to the most complex accident-catastrophic, anti-sanitary-discomfort and economic consequences.

According to the results of the analysis of oedometer and shear soil tests, the dependence of the change in the mechanical characteristics of silty-clay soils during water saturation was established: the value of the oedometric modulus of deformation during water saturation decreases to 55.4%; the angle of internal friction decreases to 12.4%, intercept cohesion decreases to 52%.

The numerical modeling of the geotechnical situation during the construction of a multi-storied residential building with an underground part in the conditions of a possible increase of groundwater levels shows us a change in the stress-strain state of a ground base. To assess the impact of changes in physical and mechanical characteristics of soils on the bearing capacity of ground base, a calculation of a residential building on slab and strip foundations was carried out. It has been established that when the soil is water saturated, the deformations will increase to an average of 77%, exceeding the maximum allowable deformations of this type of buildings, in accordance with the requirements of regulatory documents.

Forecasting the influence of the area flooding process on the buildings ground base characteristics can make it possible to prevent negative consequences associated with the possibility of excess settlement, more than ultimately-allowable, and their relative difference.

References

1. Kaloshina SV, Salimgariyeva NI (2013) Vliyaniye podtopleniya na polucheniye dopolnitel'nykh osadok zdaniy i sooruzheniy (Influence of flooding on the increment settlements of buildings and constructions). Vestnik PNIPU. Stroitel'stvo i arkhitektura 1:104–113
2. Averin IV, Rakitina NN, Bukreyev DS (2010) Potentsial'naya podtoplyayemost' i prognoz izmeneniya urovnya gruntovykh vod zastraivayemykh ploshchadok stroitel'stva (Potential underflooding and prognosis of ground water level change at sites being under development). Promyshlennoye i grazhdanskoye stroitel'stvo 1:41–42
3. Sologayev VI (1990) Zashchita ot podtopleniya v gorodskom stroitel'stve. Ustroystvo i rabota. Konspekty lektsiy (Protection against flooding in urban construction. Design and operation. Lecture notes). SiBADI, Omsk
4. Razumov GA, Khasin MF (1991) Tonushchiye goroda (Sinking cities). Stroyizdat, Moscow
5. Klorina GI, Osin VA, Shumilov VS (1984) Inzhenernaya podgotovka gorodskikh territoriy (Land development of urban areas). Vysshaya shkola, Moscow
6. Gavshina ZP, Dzintser YS (1982) Usloviya podtopleniya gruntovymi vodami (Groundwater flooding conditions). Stroyizdat, Moscow
7. Averin IV et al (2009) Opredeleniye stepeni potentsial'noy podtoplyayemosti i prognoznaya otsenka vozmozhnogo izmeneniya urovnya gruntovykh vod zastraivayemykh territoriy (Determination of the degree of potential flooding and predictive assessment of a possible change in the groundwater level of the built-up territories). Vestnik MGSU, pp 235–237
8. Retkhati L (1989) Gruntovyye vody i stroitel'stvo (Groundwater in civil engineering). Stroyizdat, Moscow

9. Simonov AV (1976) Osusheniye i regulirovaniye vodno-teplovogo rezhima zastraivayemykh territoriy v nefte dobyvayushchikh rayonakh Zapadnoy Sibiri (Desaturation and regulation of the water-and-thermal regime of the built-up territories in the oil producing zones of Western Siberia). VNIIOENG, Moscow
10. Slinko OV (1988) Zadachi gidrogeologicheskikh izyskaniy po stadiyam proyektirovaniya dlya prognoza urovennogo rezhima gruntovykh vod na gorodskikh territoriyakh (Concerns of hydrogeological surveyings at the design stages for predicting the level regime of groundwater in urban areas). Gidrogeologicheskiye issledovaniya na zastraivayemykh territoriyakh, pp 87–93
11. Velikina GM, Bruskova VV, Koyda AN (1987) Gidrogeologicheskoye i matematicheskoye obosnovaniye vosproizvedeniya na EVM protsessa podtopleniya gorodskikh territoriy (Hydrogeological and mathematical justification of reproduction on a computer of the urban areas flooding process). Voprosy inzhenerno-gidrogeologicheskikh issledovaniy na zastraivayemykh territoriyakh, pp 18–21
12. Vedernikov VV, Tikhonova NI (1988) Kolichestvennaya otsenka tekhnogennykh faktorov podtopleniya zastroyennykh territoriy (Quantitative assessment of technogenic factors of flooding of built-up territories). Gidrogeologicheskiye issledovaniya na zastraivayemykh territoriyakh, pp 15–21
13. Zinov'yev ML (1988) Vliyaniye glubiny promerzaniya gruntov na formirovaniye protsessa podtopleniya (The influence of soil freezing depth on the formation of the flooding process). Gidrogeologicheskiye issledovaniya na zastraivayemykh territoriyakh, p 25–31
14. Nekrasova YL (1988) Metodicheskiye osnovy rayonirovaniya zastraivayemykh territoriy po izmeneniyu khimicheskogo sostava gruntovykh vod pri podtoplenii (Methodological foundations for zoning of built-up territories to change the chemical composition of groundwater during flooding). Gidrogeologicheskiye issledovaniya na zastraivayemykh territoriyakh, pp 43–48
15. Degtyarev BM, Dzehtser YS, Muftakhov AZ (1985) Zashchita osnovaniy zdaniy i sooruzheniy ot vozdeystviya podzemnykh vod (Protection of the foundations of buildings and structures from the exposure of groundwater). Stroyizdat, Moscow
16. Aref'yeva YV (2007) Podtopleniye obyektov i zastroyennykh territoriy kak potentsial'nyy istochnik chrezvychaynykh situatsiy (Inundation of building projects and built-up territories as a potential cause of emergency situations). Promyshlennoye i grazhdanskoye stroitel'stvo 10:33–34
17. Aref'yeva YV (2007) Regulirovaniye rezhima gruntovykh vod pri podtoplenii obyektov i zastroyennykh territoriy (Regulation of ground water conditions in case of project and built-up area inundation). Promyshlennoye i grazhdanskoye stroitel'stvo 11:47
18. Aref'yeva YV, Samoylov SV (2009) Otsenka effektivnosti preventivnykh meropriyatiy po preduprezhdeniyu avari i chrezvychaynykh situatsiy, svyazannykh s navodneniyem i podtopleniyem zastroyennykh territoriy (Assessment of efficiency of preventive measures aimed at prevention of damages and extreme situations as a result of flooding and underflooding of building territories). Promyshlennoye i grazhdanskoye stroitel'stvo 11:7–10
19. Aref'yeva YV, Mukhin VI, Shimitilo VL (2010) Otsenka parametrov empiricheskikh raspredeleniy zatopleniya i podtopleniya zastroyennykh territoriy (Estimation of parameters of empirical distributions of flooding and inundation of the built-up territories). Promyshlennoye i grazhdanskoye stroitel'stvo 2:35–37
20. Kozlovskiy SV, Sheshenya NL (2009) Monitoring opasnykh inzhenerno-geologicheskikh protsessov (Monitoring of dangerous engineering and geological processes). Promyshlennoye i grazhdanskoye stroitel'stvo 11:7–10
21. Rubinato M et al (2019) Urban and river flooding: comparison of flood risk management approaches in the UK and China and an assessment of future knowledge needs. Water Sci Eng 12(4):274–283

22. Pregolato M et al (2017) The impact of flooding on road transport: A depth-disruption function. *Transp Res Part D Transp Environ* 55:67–81
23. Khaing ZM et al (2019) Flood hazard mapping and assessment in data-scarce Nyaungdon area. Myanmar
24. Booth DB (1991) Urbanization and the natural drainage system: Impacts, solutions and prognosis. *Northwest Environ* 7(1):93–118
25. Environment Agency (2014) Flood and coastal erosion risk management long-term investment scenarios (LTIS)
26. Hofmann J, Schüttrumpf H (2020) Risk-based and hydrodynamic pluvial flood forecasts in real time
27. Environment Agency (2017) Flooding in England: a national assessment of flood risk
28. Dawson RJ et al (2008) Attribution of flood risk in urban areas. *Hydroinf* 10(4):275–288



Creation of Indicators of a Qualitative Component of a Construction Object at Operational Phases

M. Zh. Yeskaliyev^(✉), Z. R. Mukhametzyanov, A. S. Salov, A. A. Yudin,
and A. R. Biktasheva

Ufa State Oil Technical University, 1, Kosmonavtov Str, Ufa 450062, Russia
eskaliev-1991@mail.ru

Abstract. Quality of construction—one of the key factors defining solvency and the prospects of development of this field of practical activities (production of goods). Indicators of quality characterize degree of compliance of suitability of a construction object of a certain functional purpose to the required parameters of operational conditions, efficiency and reliability of functioning. Development of the rational decisions directed to achievement of indicators of quality of construction production and their implementation is constantly relevant problem of architectural and construction and production activity, demands development and improvement of the corresponding methods of researches. The purpose of researches to this article is identifications of conditions and development of methodical justification for management of processes of formation of indicators of quality of construction objects at various stages (periods) of life cycle. The main result of a research is development of provisions of a scientific hypothesis of assessment of possible decisions with use of an integrated indicator of functional quality of a construction object. This indicator is accepted on the basis of the main result of the system analysis of decisions on formation and realization of functional quality of a construction object at various stages (obligatory and possible) life cycle. The offered concept can be considered how the direction of expansion of opportunities concerning management of the productions providing achievement of indicators of quality of construction subjects to various functional and technological appointment.

Keywords: Construction objects · Functional quality · System analysis · Life cycle · Analytical indicators · Integrated indicator · Technical and economic indicators

1 Introduction

Construction objects (buildings and constructions) represent the material structures, systems and educations created by means of construction technologies for the purpose of satisfaction of certain consumer functions. Specific features of the organization of space in a format of construction objects define the corresponding features and functional quality of buildings and constructions.

The corresponding set of requirements is imposed to the modern construction objects intended for satisfaction of various and numerous vital and public needs of the population: social, economic, functional, engineering, technical, fire-prevention, sanitary and hygienic, ecological, architectural and art and others.

For this reason of a condition and a possibility of ensuring functional quality are, at the same time, a subject and subject to scientific research and also constantly relevant problem of development of construction branch, the equipment and technologies.

For example, in scientific works [1, 2] the functional quality of a construction subject to inhabited appointment contacts conditions of ensuring comfort (microclimate) of internal space.

In works [3, 4] providing functional the quality of construction production (buildings and constructions) is connected with development and improvement of the organizational and technological sequence of performance of the corresponding construction processes.

The functional quality of construction objects is considered in works [5, 6] as the considerable structural element defining "quality of life" of modern society. Formation of functional quality is considered as social and cultural inquiry to the organization and functioning of the environment of activity as a part of the existing and perspective formats of town-planning educations.

The carried-out literary review indicates a wide range of the aspects which are taken cognizance and confirms "sketchiness" of the approaches connected with the analysis only of certain (selective) factors of influence.

This circumstance staticizes such statement of the purposes and research problems which are focused on the complete and multiple-factor analysis of features of formation of functional quality of construction production, and some quantitative measuring instrument, in a format of an integrated indicator of functional quality becomes result of such analysis.

2 Research Methods

The considered structure of scientific works and researches points that formation of functional quality of modern construction objects of different function is result of education and functioning of difficult, complex and dynamic education—the system of construction production. The system of construction production accompanying development and implementation of productions of a concrete construction object, equally as well as construction branch in general, it is possible to characterize as a way of the organization of interaction of the elements forming structural and functional integrity [7, 8].

The most rational and logical method (tool) of studying of features of processes, the phenomena and conditions of system educations is the system analysis. The system analysis is meant as formation of an algorithm for the purpose of receiving the most complete and complete idea of features and regularities of formation of properties and conditions of an object of researches. The basis of development of an algorithm is made by methodology of scientific knowledge of an object of researches as system or a complete complex of the interacting parts and elements [9, 10].

System approach gives opportunities of the annex of the theory of knowledge and the general dialectics to a research of certain subject processes and the phenomena on the

basis of the following basic principles of integrity, hierarchy, the structural organization, goal-setting and plurality.

One of practical applications of a methodical basis of the system analysis to a research of properties and conditions of construction production is the concept of management of life cycle of a construction object (Fig. 1) [11, 12].

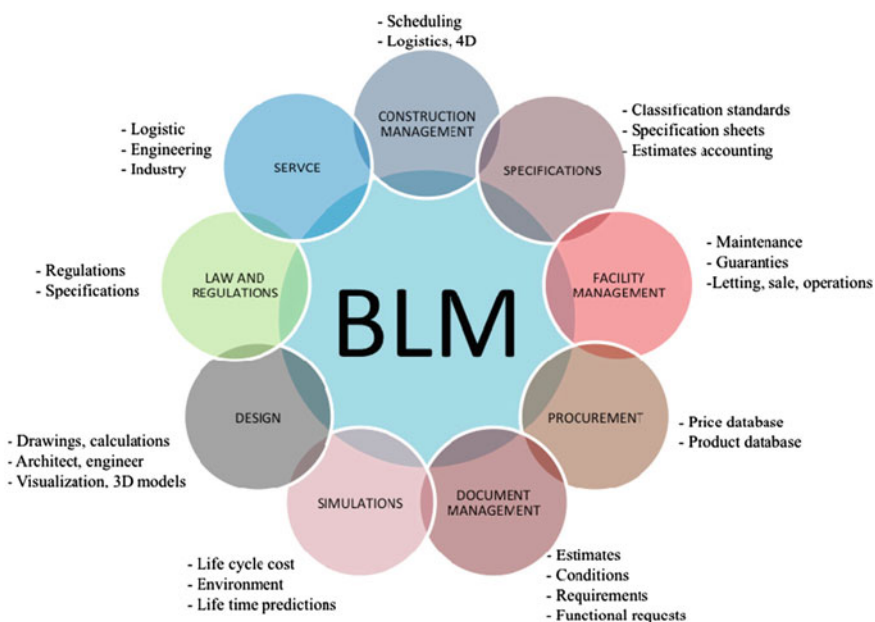


Fig. 1 Concept of a control system of life cycle of a construction object (“Building life cycle management” system, “BLM”)

Display of features of life cycle of a construction object of any functional purpose can be carried out in the form of the hierarchical and strictly focused structure (system) of properties and states and also communications between them (Fig. 2).

The hierarchical subordination and progressive relationship of individual life cycle periods (both mandatory and possible, see Fig. 2) allows us to put forward a scientific hypothesis regarding the dependence of the characteristics of the properties and conditions of the current period on the conditions, composition, efficiency and quality of solutions in the previous (earlier) life cycle periods under consideration [13, 14].

For example, the performance indicators of the operation of a low-rise residential building (for example, before the first scheduled repair) are directly dependent on the quality of solutions implemented at the previous stages: design (development of quality indicators of the corresponding structural system) and construction (implementation of construction processes aimed at implementing previously developed quality indicators of the corresponding construction system) [15, 16].

Thus, an objective assessment of the functional quality of a construction object is possible only at the end of all, but above all, mandatory periods of its life cycle.

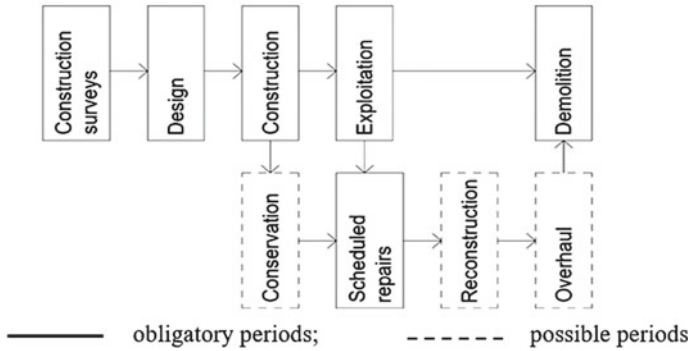


Fig. 2 The system of properties and conditions of a construction object at the stages (periods) of the life cycle

The functional quality of construction objects (for example, low-rise residential buildings) is usually assessed by a certain number of indicators: absolute (single) and relative. The types of indicators under consideration are called technical and economic indicators (TEP) of construction [17–19].

For example, the absolute TEP of a low-rise residential building includes:

- full (general) area, S_{full} ;
- useful (inhabited) area, S_{useful} ;
- building volume of the building, $V_{building}$;
- built-up area, $S_{built-up}$;

Absolute (single) indicators fix the result of the development of design solutions and characterize the quantitative parameters of the construction object.

The functional efficiency of a building is characterized by relative indicators (relative efficiency coefficients) of functional quality, for example, in the form:

- coefficient of relative efficiency of space-planning solution:

$$\mathcal{K}_1 = \frac{S_{useful}}{V_{building}}. \tag{1}$$

An increase in the \mathcal{K}_1 parameter means an increase in the functional quality of the building (an indicator of the effectiveness of the corresponding space-planning solution).

- coefficient of relative efficiency of the planning solution:

$$\mathcal{K}_2 = \frac{S_{useful}}{S_{full}}. \tag{2}$$

An increase in the \mathcal{K}_2 parameter means an increase in the functional quality of the building (an indicator of the effectiveness of the corresponding planning solution).

- coefficient of relative efficiency of use of the territory available for development:

$$\mathcal{K}_3 = \frac{V_{building}}{S_{built-up}}. \tag{3}$$

An increase in the K_3 parameter means an increase in the functional quality of the building (an indicator of the effectiveness of the corresponding volumetric solution or structural scheme).

The modern practice of developing and implementing solutions in relation to the formation of the functional quality of construction products is characterized by the division of TEP to assess the effectiveness of architectural and construction and constructive (the “design” period of the life cycle), construction (the “construction” period of the life cycle) and operational (the “operation” period of the life cycle) systems of the capital construction object.

With this approach, the achievement of the required indicators of the functional quality of construction objects is practically confined to the spatio-temporal characteristics of each separately from the considered periods and is practically not subject to optimization and system management. Moreover, possible deviations from the established TEP values can lead not only to a partial loss of functional quality at the considered stage (period) of the life cycle, but also provoke problematic production situations and construction risks for subsequent periods [20].

A systematic research approach related to the analysis of the formation of the functional quality of construction objects at all stages of the life cycle is able to solve the problem of separating the assessment of the functional quality of a separate stage and organize the conditions for quality management in the dynamic context of changes in the properties and states of the construction production system.

When developing design (architectural, structural, functional, organizational and technological) solutions for a construction object, the method of variant design is widely used. The essence of this method is to offer several possible solutions. Options for design decisions (which are accepted for competitive comparison) are characterized by a certain number of single (absolute) and relative indicators, and the assessment of the proposed options is possible using a rating system of analysis [21].

For example, Table 1 shows the data of absolute and relative indicators characterizing the functional quality of a low-rise residential building (for 6 apartments) for four options for design solutions:

The rating assessment of design solutions, for example, according to the absolute indicator of the type “Full (total) area” includes the following algorithm (see Table 1):

1. The highest quality indicator for the indicator under consideration corresponds to the variant of design decisions No. 3 (the smallest of the possible values, which is: 84.16 m²). Accordingly, the considered version of the design solution is assigned the highest (minimum in absolute value) rating: 1.
2. The next, after the option of design decisions No. 3, is option No. 1 (the value is: 88.77 m²). Accordingly, the considered version of the design solution is assigned a rating: 2.
3. The next, after design options No. 1 and 3, is option No. 2 (the value is: 93.44 m²). Accordingly, the considered version of the design solution is assigned a rating: 3.
4. The worst quality indicator for the considered indicator corresponds to the variant of design solutions No. 4 (the smallest of the possible values, which is: 102.3 m²). Accordingly, the considered version of the design solution is assigned the worst (maximum in absolute value) rating: 4.

Table 1 Absolute and relative indicators characterizing the functional quality of a low-rise residential building (living area 33.29 m²) for four design options

No	Name of indicator	Unit	Design options			
			No. 1	No. 2	No. 3	No. 4
<i>Single (absolute) indicators</i>						
1	Full (total) area	m ²	88.77	93.44	84.16	102.3
2	Useful (residential) area	m ²	33.29	33.29	33.29	33.29
3	Structural volume of the building	m ³	420.23	400.80	440.14	450.66
4	Built-up area	m ²	160.87	177.12	95.38	102.34
<i>Relative indicators</i>						
5	Coefficient of relative efficiency of space-planning solution	m ² /m ³	0.079	0.083	0.075	0.073
6	Coefficient of relative efficiency of planning solution	m ² /m ²	0.375	0.356	0.396	0.325
7	Coefficient of relative efficiency of building	m ³ /m ²	2.612	2.262	4.614	4.403

Thus, the rating system for the indicators given in Table 1 is reduced to the form shown in Table 2.

An analysis of the ratings of design options given in Table 2 shows:

- the best design solution in terms of the sum of single indicators corresponds to option No. 3 (the lowest quantitative rating, equal to 6);
- the best design solution in terms of the sum of relative indicators corresponds to option No. 3 (the smallest quantitative rating equal to 5);
- the best design solution in terms of the sum of relative and relative indicators corresponds to option No. 3 (the smallest quantitative rating, equal to 11).

The coincidence (as in the considered design situation) of the rating of options by the sum of absolute and relative is not at all necessary.

3 Results and Discussions

In order to apply a systematic approach to the analysis of the properties and states of the research object, as well as to develop a methodological justification for the effectiveness of decisions and production processes necessary to achieve established or prospective indicators of the functional quality of construction objects (construction products), the concept of an **integral indicator of the functional quality** of a construction object (constructive part) is proposed. or separate design). The integral indicator of functional

Table 2 Rating of absolute and relative indicators characterizing the functional quality of a low-rise residential building (living area 33.29 m²) for four design options

No	Name of indicator	Unit	Design options			
			No. 1	No. 2	No. 3	No. 4
<i>Single (absolute) indicators</i>						
1	Full (total) area	m ²	2 (88.77)	3 (93.44)	1 (84.16)	4 (102.3)
2	Useful (residential) area	m ²	1 (33.29)	1 (33.29)	1 (33.29)	1 (33.29)
3	Structural volume of the building	m ³	2 (420.23)	1 (400.80)	3 (440.14)	4 (450.66)
4	Built-up area	m ²	3 (160.87)	4 (177.12)	1 (95.38)	2 (102.34)
	Sum of ratings		8	9	6	11
<i>Relative indicators</i>						
5	Coefficient of relative efficiency of space-planning solution	m ² / m ³	2 (0.079)	1 (0.083)	3 (0.075)	4 (0.073)
6	Coefficient of relative efficiency of planning solution	m ² / m ²	2 (0.375)	3 (0.356)	1 (0.396)	4 (0.325)
7	Coefficient of relative efficiency of building	m ³ / m ²	3 (2.612)	4 (2.262)	1 (4.614)	2 (4.403)
	Sum of ratings		7	8	5	10
	Total for all ratings		15	17	11	21

quality is a quantitative characteristic of the properties and states of a building object and is determined in the context of relationships between successive periods of the life cycle (see Fig. 2).

The concept under consideration makes it possible to analyze the features of a specific period of the life cycle (mandatory and possible) through the corresponding quality indicator:

- for the mandatory period “construction surveys”, in the form:

$$P_1 = f \left(\sum_{i=1}^n m_i q_i; \sum_{j=1}^k M_j \cdot Q_j \right). \quad (4)$$

here P_1 —indicator of the quality of the development of the composition and the effectiveness of construction surveys; m_i —a single indicator of the quality and effectiveness of solutions; q_i —significance (share) of a single indicator; n —number of single indicators considered; M_j —relative indicator of the quality and effectiveness of solutions; Q_j —significance (specific weight) of the relative indicator; k —number of relative indicators considered.

- for the mandatory period “design”, in the form:

$$P_2 = f \left(\sum_{i=1}^n m_i q_i; \sum_{j=1}^k M_j \cdot Q_j \right). \quad (5)$$

here P_2 —indicator of the quality of the development of the composition and the effectiveness of design solutions;

- for the mandatory period “construction”, in the form:

$$P_3 = f \left(\sum_{i=1}^n m_i q_i; \sum_{j=1}^k M_j \cdot Q_j \right). \quad (6)$$

here P_3 —indicator of the quality of the development of the composition and the effectiveness of production decisions (construction).

- for the mandatory period “exploitation”, in the form:

$$P_4 = f \left(\sum_{i=1}^n m_i q_i; \sum_{j=1}^k M_j \cdot Q_j \right). \quad (7)$$

here P_4 —indicator of the quality of the development of the composition and the effectiveness of operational decisions.

- for the mandatory period “scheduled repairs”, in the form:

$$P_5 = f \left(\sum_{i=1}^n m_i q_i; \sum_{j=1}^k M_j \cdot Q_j \right). \quad (8)$$

here P_5 —indicator of the quality of the development of the composition and efficiency of production decisions for the implementation of planned work.

- for the mandatory period “demolition”, in the form:

$$P_6 = f \left(\sum_{i=1}^n m_i q_i; \sum_{j=1}^k M_j \cdot Q_j \right). \quad (9)$$

here P_6 —indicator of the quality of the development of the composition and the effectiveness of production decisions for the demolition of the facility.

- in relation to the possible period of “conservation”, in the form:

$$P_1^0 = f \left(\sum_{i=1}^n m_i q_i; \sum_{j=1}^k M_j \cdot Q_j \right). \quad (10)$$

here P_1^0 —indicator of the quality of the development of the composition and the effectiveness of production solutions for the conservation of the facility.

- in relation to the possible period of “reconstruction” (“renovation”), in the form:

$$P_2^0 = f \left(\sum_{i=1}^n m_i q_i; \sum_{j=1}^k M_j \cdot Q_j \right). \quad (11)$$

here P_2^0 —indicator of the quality of the development of the composition and efficiency of production decisions for the reconstruction (renovation) of the facility.

- in relation to the possible period of “overhaul” (“re-profiling”), in the form:

$$P_3^0 = \left(\sum_{i=1}^n m_i q_i; \sum_{j=1}^k M_j \cdot Q_j \right). \quad (12)$$

here P_3^0 —indicator of the quality of the development of the composition and efficiency of production solutions for the overhaul (re-profiling) of the facility.

Analytical parameters of the form: m_i , q_i , n , M_j , Q_j , k , included in dependences (2) ÷ (9), are characterized by a semantic analytical load similar to the parameters of dependence (4).

The integral indicator of the functional quality of a construction object (part of a building or a separate structural element) is determined by the dependence of the form:

$$P_{\mathcal{K}} = (a_1 \cdot P_1) + (a_2 \cdot P_2) + (a_3 \cdot P_3) + (a_4 \cdot P_4) + (a_5 \cdot P_5) + (a_6 \cdot P_6) + (a_0^1 \cdot P_0^1) + (a_0^2 \cdot P_0^2) + (a_0^3 \cdot P_0^3). \quad (13)$$

here $a_1 \div a_6 \Leftrightarrow$ —levels of significance (specific weight) of quality indicators of mandatory periods; $a_0^1 \div a_0^3$ —levels of significance (specific weight) of quality indicators of possible periods.

The proposed concept of a systemic assessment of the functional quality (an integral indicator of the functional quality of a construction object) is characterized by the following main features:

- believes and allows the use of methodically sound methods for studying the properties and states of complex system elements and formations and, at the same time, is open to integration with analytical techniques and approaches of related scientific and practical fields;
- has an “open structure” that allows optimizing (reducing or expanding) the composition of the stages of states (life cycle periods) taken into consideration, including those that can only be considered at a theoretical level.

Quantitative values of analytical parameters of the form: $a_{_1} \div a_{(6 \Leftrightarrow)}$ and $a_{_0^1} \div a_{_0^3}$ are determined by the following possible methods and techniques:

- statistical processing of data on completed construction projects of the corresponding functional and technical (industry) purpose;

- mathematical (analytical, digital, informational) modeling of processes, phenomena and states, including various scenarios (forecasts) of development for the corresponding system formations;
- directive (normative) approval of design values justified by technical, technological, economic, social or other factors;
- using algorithms and peer review tools.

Table 3 (as an example of adapting the considered methodology to solving practical problems) presents the results of the analysis of the functional quality of a construction object using single and relative indicators for six options for design solutions.

Table 3 Data on the quality of design solutions taken for analysis

No	Design stage		Construction stage		Operational phase		All main stages	
	Single indicators	Relative indicators	Single indicators	Relative indicators	Single indicators	Relative indicators	Single indicators	Relative indicators
1	5	5	3	2	3	4	11	11
2	1	1	4	4	1	1	6	6
3	5	6	5	6	4	6	14	18
4	2	3	6	5	2	2	10	10
5	3	2	1	1	5	3	9	6
6	4	4	2	2	6	4	12	10

Figure 3 shows the result of the analysis of the effectiveness of design solutions in the format of an integral indicator of the functional quality of construction products.

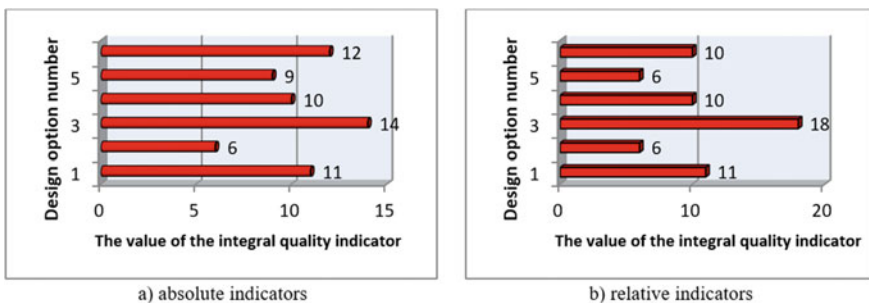


Fig. 3 Integral indicator of the functional quality of a construction object

To conduct the analysis, some of the mandatory life cycle stages were considered, but having a direct impact on the functional quality of construction products. To simplify the analysis procedure, all indicators (single and relative) are assigned an equal weight (value equal to: 1.0). It can be noted that according to the results of the research, the best

rating (the minimum value for single and relative indicators) turned out to be in option No. 2, respectively, the worst rating indicators for option No. 3 of the considered design solutions.

Depending on the formulation of a specific research problem, an arbitrary (limited only by the complexity of calculations and modeling) quantitative and qualitative composition of parameters of the form: m_i , q_i , n , M_j , Q_j , k can be accepted for analysis. As single and relative indicators, it is possible to use both existing TEPs (for example, construction volume, construction duration, prefabrication factor, coefficient of combination of construction processes), and other indicators (for example, manufacturability factor or level of organizational and technological reliability), which are the closest and accurately reflect the nature of processes, events and phenomena specifically for the analyzed object and the characteristics of the composition and duration of the stages of the life cycle.

4 Conclusions

Based on the results of the research, the following main conclusions were obtained:

1. The system approach remains the basic methods for studying properties and states, as well as the conditions for the formation of indicators of the functional quality of construction objects.
2. The developed concept "integral indicator of the functional quality of a construction object" opens up additional opportunities for the analysis of a construction object as a complex system formation and is presented as a tool for managing the functional quality of construction products for various stages of the life cycle.
3. The concept of forming a quantitative assessment of the functional quality of a construction object is an open analytical structure that is available for solving practical problems using (algorithmization) modern information platforms.

References

1. Novikova KE (2020) A microclimate—the main consumer quality of the building. *Messenger Magistracy* 1–3(100):26–29
2. Ignashchenko OO, Chernukhina SA (2019) Village of Chernukhino. A. Ensuring quality of a microclimate in rooms of modern residential buildings. Current problems of construction, housing and public utilities and technosphere safety. *Materials VI All-Russian (with the international participation) a scientific and technical conference of young researchers, Volgograd*, pp 359–361
3. Bayburin AH, Nikonorov SV (2015) About improvement of standards of quality of construction of residential buildings. *Hous Constr* 8:8–9
4. Petrova AA, Mikhaylov DA (2022) Prospects of construction of low frame buildings and improvement of quality of their construction. *Sci Heritage* 103:4–6
5. Yefimova NV (2008) Formation of system of consumer qualities of the building as conditions of implementation of the national project “affordable and comfortable housing”—to citizens of Russia. *Top Issues Econ Sci* 1:124–128

6. Generalov VP, Generalova EM (2021) Way of life, architecture, and quality of the urban environment/*Accusative*. *Town Plan Arch* 1(42):160–168
7. Haruna M, Tasaka R (1982) A study on systems analysis of construction planning and scheduling method. *Proc Jpn Soc Civ Eng* 3:318–322
8. Ian Faulconbridge R, Ryan M (2021) *Applied systems engineering*. Argos Press Pty Ltd., Yarralumla, Australia, pp 119–121
9. Rebentisch E (2017) *Integrating program management and systems engineering: methods, tools, and organizational systems for improving performance*. Wiley, New York, USA, pp 25–29
10. Mironenko IN (2022) Systems theory and system engineering as modern applied tools of system analysis. *Econ Manage Challenges Solut* 6(126):134–142
11. Mukhametzyanov ZR, Oleinik PP (2019) Formation of organizational and technological solutions in the construction of industry complexes. *Ind Civ Constr* 11:35–41. <https://doi.org/10.33622/0869-7019.2019.11.35-41>
12. Ustinovičius L, Rasiulis R, Nazarko L, Vilutienė T, Reizgevičius M (2015) Innovative research projects in the field of building lifecycle management. *Procedia Eng* 122:166–171
13. Ylmén P, Berlin J, Mjörnell K, Arfvidsson J (2020) Managing choice uncertainties in life-cycle assessment as a decision-support tool for building design: a case study on building framework. *Sustainability* 12:130–138
14. Eisner H (2011) *Systems engineering. Building successful systems*. Morgan & Claypool Publishers, London, Great Britain, pp 94–98
15. Islam H, Bhuiyan M, Tushar Q, Navaratnam S, Zhang G (2022) Effect of star rating improvement of residential buildings on life cycle environmental impacts and costs. *Buildings* 12:1605–1612
16. Myers D (2022) *construction economics. A new approach*. Routledge, New York, USA, pp 17–21
17. Abel C (2004) *Architecture, technology and process*. Architectural Press, London, Great Britain, pp 126–133
18. Mukhametzyanov Z, Oleinik P (2021) Sustainability method organizational and technological decisions in the construction of industrial complexes. In: *E3S web of conferences. Ural environmental science forum “Sustainable Development of Industrial Region UESF 2021”*, Chelyabinsk, Russia
19. Mukhametzyanov ZR, Mogucheva TA (2022) Conditions for achieving sustainability of organizational and process solutions in the facilities construction. *AIP Conf Proc* 2559:22–27
20. Bogachev SN, Shkolnikov AA, Rozentel RA, Klimova NA (2015) Construction risks and opportunities for their minimization. *Acad Architecture Constr* 1:88–92
21. Tabunshchikov YA, Granev VV, Naumov AL (2010) The rating system of assessment of quality of the building in Russia. *AVOK* 6:16–21



Calculation Methodology for Constituent Wooden Rods on Discrete Shear Bonds

S. A. Isupov^(✉)

Vyatka State University, 36, Moskovskaya Str, Kirov 610000, Russia
deka_1958@mail.ru

Abstract. Almost all methods for calculating constituent rods are based, as a rule, on a uniform, rather frequent arrangement of shear bonds along the length of the bar. Calculations based on the solution of differential equations, even for simple cases of a symmetrical section without taking into account the vertical stiffness of the bonds, turn out to be rather complicated. Approximate calculations obtain good convergence also only in the case of a sufficiently large number of connections. The proposed work presents a fairly simple approach to the calculation of composite bending rods on discrete shear bonds. The technique makes it possible to take into account the nonlinear dependence of deformations on the forces in the bonds; take into account the positions of shear forces in the bonds along the height of the beam cross section, which leads to a significant increase in the accuracy of calculations. Additional features of the technique include: taking into account the transverse stiffness of the bonds; the possibility of calculating with different stiffness of the elements that make up the rod; the possibility of taking into account an arbitrary arrangement of discrete bonds along the length of the beam, depending on the type of loading. As a result, according to the proposed method, on the basis of numerical analysis, an assessment was made of the significance concerning these factors in the calculations of bending constituent rods.

Keywords: Constituent rod · Discrete ties · Nagel plates · Stress–strain state · Rigidity of ties · Nonlinear calculation · Deformation diagram

1 Introduction

The first works on the calculation of constituent rods, taking into account the compliance of bonds, appeared as early as the 30s...50s of the twentieth century, the founders of which were Soviet scientists Rzhantsyn [1, 2], Pleshkov [3], Kochenov [4]. All further studies of this issue, including contemporary studies [5–18], are based mainly on their work.

Almost all methods for calculating constituent rods are based, as a rule, on a uniform, rather frequent arrangement of bonds along the length of the rod (or along its sections). Calculations based on the solution of differential equations, even for simple cases of a symmetrical section without taking into account the vertical stiffness of the bonds, turn out to be rather complicated. Approximate calculations get good convergence also

only in the case of a sufficiently large number of connections, and in the solutions of Kochenov [4] did not take into account a number of practically significant factors: the nature of the distribution of the external load, possible differences in the size and stiffness of the constituent elements of the rod, and some others.

Piskunov [19] proposed a technical theory for calculating constituent rods, in which discrete shear bonds are considered as a single set. The distribution of the load over the elements that make up the rod is dependent on the rigidity of the bonds. The coordinates of the resultant shear forces are determined in the course of an iterative process. This approach makes it possible to take into account the nonlinear nature of the connection means, as well as the position of the shear forces in the height of the cross section relative to the plane of the beams connection.

Mechanical means of connecting wooden structures, including shear joints of the nail type, are characterized by rather specific deformation patterns.

With regard to rods of a constituent section with joints on mechanical shear bonds, two main deformation patterns can be distinguished:

- for the first of them, it is typical that during the period of the initial and any subsequent loading cycle, the mechanism for the perception of shear forces along the planes of connection of its individual constituent elements at all loading levels is characterized by constant contact between the shear bonds and the connected elements; the diagram of deformation of the joints corresponding to this is shown in the diagram in Fig. 1a;

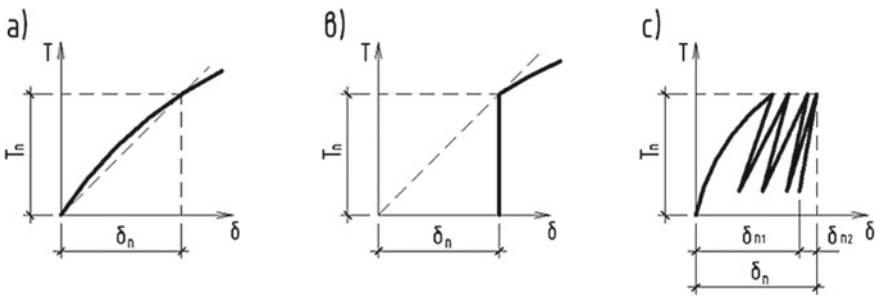


Fig. 1 Diagrams of deformation of connections

- the second type of deformation is characterized by the fact that during the initial and all subsequent cycles of loading the rod, carried out after full or partial unloading, there is no contact between the connection elements at the initial loading levels and therefore the shear bonds come into operation with some delay; The fundamental nature of such deformation is shown in the scheme of Fig. 1b.

The most common “mixed” type of deformation in real load-bearing structures—its “idealized” version, which reflects the final state of the connection and connected elements with a sufficiently large number of cycles, is shown schematically in Fig. 1c.

Both models of deformation of mechanical joints of wooden structures were previously used as fundamental for various options for engineering calculation of constituent wooden rods [20], which were further used in the current design standards. For the first

of these theoretical approaches, the base model is the deformative shear bonds operating in contact with the constituent elements of the rod at all stages of its loading; in the second—a model of yielding bonds, which allows for the possibility of separate deformation of the constituent elements at the initial levels of loading of the rod.

Since in real connections of load-bearing wooden structures, including on the currently quite common—TGc nagel plates (developed at Vyatka State University [21, 22]), these models of deformation of the connecting elements do not exclude, but complement each other, there is a need to develop sufficiently simple calculation methods, which take into account the presence of these two components of the deformation of shear bonds at the stage of engineering design. At the same time, the nonlinear dependence of deformations on forces in discrete bonds is taken into account, the positions of shear forces in the bonds along the height of the beam cross section are taken into account, and additional possibilities are created—taking into account the transverse stiffness of the bonds; the possibility of calculating with different stiffness of the elements that make up the rod; the possibility of arbitrary arrangement of connections along the length of the beam.

2 Methods

Summarizing what has been said, it follows that at present there are two main approaches to the calculation of constituent rods and a procedure for using numerical methods.

The first approach is based on solving differential equations, when a constituent rod is represented by a single deformable system, in which the elements that make up the rod and the means of their connection work together at all stages of loading [1, 2]. Discrete ties are replaced by continuum shear ties with linear stiffness K_c and transverse ties endowed with the ability to distribute the external load between the elastic constituent elements with bending stiffness $E_i J_i$.

The second approach is an approximate solution, which is based on the representation of the connection means as compliant bonds [4]. Since at the first stage of loading, shear bonds have zero stiffness, it is therefore possible to separate the external load into components that are perceived by the constituent elements during separate, relative to their own axes, and joint deformation.

In the case of a small number of discrete bonds installed with a variable step along the length of the seam, if their arrangement does not correspond to the nature of the distribution of shear forces, the calculation of a constituent rod can only be performed by numerical methods. In this case, the force on each shear bond, as well as the force in each transverse bond, is considered to be unknown. The general view and design scheme of a constituent rod loaded with a transverse load is shown in Fig. 2.

To determine the forces in the bonds, various numerical methods can be used, in particular, the most common is the finite element method [23]. The accuracy of the finite element method largely depends on a number of parameters, in particular, on the ratio of the sizes of the finite elements. It is quite difficult to take into account the position of the resultant of shear forces in the method. In order to achieve the set tasks, the most acceptable in this case is the method of forces [24].

Let us consider the use of this method for the calculation of constituent rods on deformable bonds using the example of a bending element loaded with a transverse load.

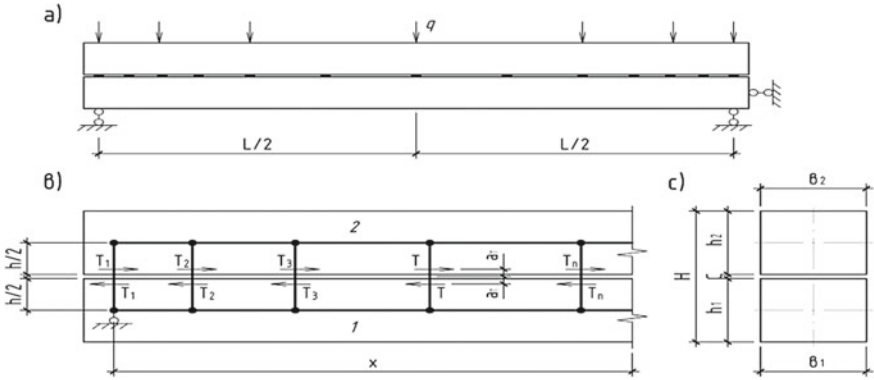


Fig. 2 General view, fragment of the design scheme and cross section of the constituent element

To solve the problem the following assumptions are considered acceptable:

1. the rods that make up the rod obey Hooke’s law;
2. the work of the bonds is considered to be nonlinearly elastic, i.e. unloading effects are not taken into account, and is expressed by piecewise linear diagrams $T - \Delta$, given in tabular form, i.e. intermediate values of Δ are determined by interpolation;
3. the hypothesis of plane sections is considered valid.

The basic system of a beam with the number of ties— n and the number of sections between the ties— m , $m = n - 1$ is shown in Fig. 3. Unknown forces in shear bonds are marked as T_{xn} , forces in transverse bonds— T_{yn} .

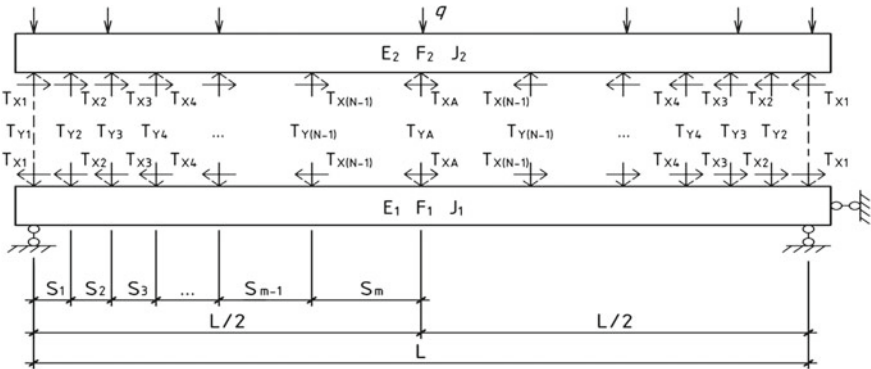


Fig. 3 The main system for calculating a constituent element on discrete bonds

The system of linear canonical equations is obtained from the condition of compatibility of deformations in horizontal and vertical directions.

$$[\Delta]\{T\} + \{\Delta_p\} = 0 \tag{1}$$

where $[\Delta]$ is the matrix of unit displacements, taking into account the deformability of the bonds; $\{\Delta_p\}$ —column vector of freight movements.

Matrix $[\Delta]$ is calculated by summing 2 matrices: single displacements and deformability of bonds.

$$[\Delta] = [\Delta_{un}] + [\Delta_c] \quad (2)$$

The bond deformability matrix $[\Delta_c]$ is diagonal and is formed as follows: in the upper left part, the cross-link stiffness K_y to the power of -1 is located diagonally, in the lower right part, similarly to the shear bond stiffness K_x to the power of -1 , the remaining cells of the matrix are equal to zero.

The rigidity of the shear bonds in the general case is determined by the ratio of the force attributable to the bond to the displacement caused by this force, or as the tangent of the slope of the bond deformation diagram $T - \Delta$ at the design point. Such an approach to the formation of a matrix creates the possibility of calculating a constituent rod having bonds of different stiffness. The matrix of unit displacements $[\Delta_{un}]$ is determined by adding unit displacements in the constituent elements δ_{uni} along the edges of the seam under consideration

$$[\Delta_{un}] = \sum [\delta_{un}] \quad (3)$$

The unit and load terms of Eqs. (1–3) are determined by the methods of structural mechanics, so we write their calculation in matrix form

$$[\delta_{un}] = [M_{un}]^T [D] [M_{un}] + [N_{un}]^T [D_f] [N_{un}] \quad (4)$$

$$\{\Delta_p\} = [M_{un}]^T [D_p] \{M_{pf}\} \quad (5)$$

where $[M_{un}]$ is the matrix of moments from unit loads; $[N_{un}]$ —matrix of unit longitudinal loads; $[D]$, $[D_f]$, $[D_p]$ —compliance matrices; $\{M_{pf}\}$ —vector of cargo moments.

Let us show the differences in the formation of the main matrices for the seam of a constituent element with n bonds. The matrix $[M_{un}]$ generally has a dimension of $2n$ rows by $2m$ columns and is written as follows

$$[M_{un}] = \begin{bmatrix} M'_{11} & M'_{12} & M'_{12} & M'_{13} & M'_{13} & \cdots & M'_{nm} \\ M'_{21} & M'_{22} & M'_{22} & M'_{23} & M'_{23} & \cdots & M'_{nm} \\ \cdot & \cdot & \cdot & \cdot & \cdot & \cdots & \cdot \\ M'_{n1} & M'_{n2} & M'_{n2} & M'_{n3} & M'_{n3} & \cdots & M'_{nm} \\ M_{11} & M_{12} & M_{12} & M_{13} & M_{13} & \cdots & M_{1m} \\ M_{21} & M_{22} & M_{22} & M_{23} & M_{23} & \cdots & M_{2m} \\ \cdot & \cdot & \cdot & \cdot & \cdot & \cdots & \cdot \\ M_{n1} & M_{n2} & M_{n2} & M_{n3} & M_{n3} & \cdots & M_{nm} \end{bmatrix} \quad (6)$$

where M_{23}' —the moment in the 3rd connection from a unit effort applied to the 2nd connection in the transverse direction; M_{23} —moment in the 3rd connection from a unit force applied to the 2nd connection in the longitudinal direction.

For a symmetrical transverse load with respect to the center of the beam, the matrix turns out to be square, with a dimension of $2m$, because you can remove two zero lines—the first and last, characterizing single transverse displacements on the support and longitudinal ones in the center of the beam. The values of single moments are determined as follows:

$$M'_{xn} = K_n \quad M'_{xn} = 0 \quad \text{at } x = K_n \quad M'_{xn} = \frac{h_i}{2} - \alpha_t \quad \text{at } x > K_n \quad (7)$$

where K_n is a coordinate of n -th bond; h_i —the height of the constituent element for which the single moment is determined; α_t —distance from the neutral line of the seam to the place of application of the resultant shear force in the connection.

The value of α_t is determined from the calculation of the nagel joint [25] as the distance from half the length of the nagel to the resultant of the crushing stresses $\sigma_{cr,n}$ by the depth of the nest.

The matrix $[D]$ for unit elements having a diagram with straight sections has a diagonal form with a dimension of $2m$ with working (non-zero) elements

$$\frac{k_n - k_{n-1}}{6E_i J_i} \begin{bmatrix} 2 & 1 \\ 1 & 2 \end{bmatrix} \quad (8)$$

In the case when the diagram has parabolic sections, for the vector of load moments, the matrix $[D_p]$ has work elements of the form

$$\frac{k_n - k_{n-1}}{6E_i J_i} \begin{bmatrix} 2 & 2 & 1 \\ 1 & 1 & 2 \end{bmatrix} \quad (9)$$

The matrices related to the longitudinal loads N are formed in a similar way, for $[D_f]$ the working elements will be the expressions

$$\frac{k_n - k_{n-1}}{E_i F_i} \begin{bmatrix} 2 & 1 \\ 1 & 2 \end{bmatrix} \quad (10)$$

Determination of unit displacements of compliance matrices by the described method allows one to take into account the real modules of elasticity and the cross-sectional dimensions of the constituent elements in the calculations. The vector of load moments $\{M_{pf}\}$ is also formed also on the sections between the bonds but only for the upper element constituting the rod

$$\{M_{pf}\}^m = \{M_{p0}b_{o1}M_{p1}b_{o2} \dots M_{pn}\} \quad (11)$$

where M_{pn} —are the values of the moments from the transverse load in the section $x = K_n$, determined for a statically determinate system; $b_{n-1,n}$ —is the value of the lifting boom in the middle of the section of the load moment diagram, for a diagram with straight sections $b_{n-1,n} = 0$.

If the diagram of moments is outlined by a square parabola, then the value of $b_{n-1,n}$ is determined as follows:

- for sinusoidal transverse load on the beam

$$b_{n-1,n} = \frac{ql^2}{\pi^2} \sin \frac{\pi \left(\frac{k_{n+1}}{2} + \frac{k_n}{2} \right)}{L} - \frac{M_n + M_{n+1}}{2} \quad (12)$$

- for a uniformly distributed load on the beam

$$b_{n-1,n} = \frac{q(k_{n+1} + k_n)}{4} \left[L - \left(\frac{k_{n+1} + k_n}{2} \right) \right] - \frac{M_n + M_{n+1}}{2} \quad (13)$$

After solving the system of Eq. (1), we obtain the values T_{xn} and T_{yn} , which determine the magnitude of the shear forces in the n-th connection and the magnitude of the vertical forces in the transverse bonds. Further, the main system, devoid of connections, is calculated without difficulty. The bending moments in the constituent elements are determined from the expression

$$\{M\} = [M_{un}] \{T\} + \{M_p\} \quad (14)$$

where $\{M_p\}$ is the vector of bending moments in the characteristic sections of the upper element in the main system.

The displacements at the points $x = K_n$ of the constituent elements in the vertical and horizontal directions are determined by the Mohr formula, in matrix notation

$$\{f\} = [M_{un}]^m [D_p] \{M\} \quad (15)$$

In the form of expressions (14) and (15), internal force factors and displacements of the constituent elements are determined for the j-th type of loading. Under the combined action of a number of force factors, the column vectors for T, M, f are replaced by matrices of size $2n \times j$. The stress at the point with coordinate y relative to its own neutral axis of the i-th constituent element for the j-th type of loading is determined from the expression

$$\sigma_{ij} = \frac{M_{ij}}{I_i} y + \frac{\sum T_x}{F_i} \quad (16)$$

here M_{ij} is the moment in the i-th element, determined taking into account the moment from $\sum T_x$ forces in n bonds preceding the considered section.

The deformation of the majority of joints of wooden structures, in particular, on the TGc nagel plates, according to the load has a clearly pronounced non-linear character [26], which should be taken into account when calculating constituent rods. The most accurate account of the nonlinear work of bonds in a constituent rod is the introduction into the calculation of the diagrams of deformation of the bonds under load directly and the determination of the stiffness of each bond according to the calculated forces $T_{x(y)}$.

The iterative scheme of the solution is constructed on the basis of the method of variable elasticity parameters. At the first stage of calculations, the stiffness of the links K_c is set according to the first section of the diagram assuming the linear operation of all the links, then the stiffness for each link is calculated using the determined $T_{x(y)n}$ and

a new matrix (3) is formed. The exit from the iterative cycle is carried out on the basis of a check on the most significant calculation parameter— f .

$$\frac{|f_i - f_{i-1}|}{|f_i|} < \varepsilon_\alpha \tag{17}$$

where f_i, f_{i-1} is the maximum value of the deflection of the constituent element for $i-1$ and i -th approximation; ε_α is a small value taken equal to 0.001.

After the fulfillment of inequality (17), the calculation can be completed if it was built in the form of checking the accepted design parameters of the constituent element.

3 Results and Discussion

1. To assess the significance of the influence of the main factors on the results of the calculation, a theoretical analysis was carried out, which allows determining the stress–strain state of a constituent beam with the introduction of the transverse stiffness of the bonds and the value of α_t , taking into account the position of the shifting force, into the calculation. The influence of different arrangement of shear bonds will be considered in further studies.

The results of the calculations are summarized in Table 1, which shows the main parameters of the stress–strain state of the beam (deflection in the middle of the span, maximum edge stresses and total shear force) when loaded with a concentrated force in the middle of the span and a uniform arrangement of bonds.

Table 1 The results of the calculation of a constituent beam, taking into account the transverse stiffness and correction α_t

Number of bonds	Diagram T—Δ	Y = 0 α _T = 0			Y = 0 α _T = 0.85 cm			Y ≠ 0 α _T = 0		
		f cm	MPa	ΣT kN	f cm	MPa	ΣT kN	f cm	MPa	ΣT kN
4	Linear	3.44	13.2	47.87	3.69	13.9	53.96	3.44	13.4	47.87
	Non-linear	3.93	13.7	44.23	4.32	14.7	48.96	3.94	13.9	44.22
9	Linear	2.96	12.2	54.21	3.37	13.2	60.01	2.97	12.7	54.21
	Non-linear	2.93	12.0	55.10	3.37	13.1	60.54	2.94	12.4	55.16
14	Linear	2.81	11.8	56.53	3.27	12.9	62.10	2.81	12.4	56.53
	Non-linear	2.73	11.5	58.19	3.27	12.7	63.67	2.73	11.9	58.59

In the table: $Y = 0$ —the absolute of the cross-links stiffness; $Y \neq 0$ —stiffness of cross-links in the range of the strain diagram.

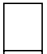

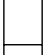


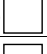

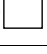
The calculations were made for a single-span constituent wooden beam with a span of 6 m and a cross section of $2 \times 100 \times 125$ mm. Estimated bending moment—10.845 kN cm. TGc nagel plates with 7 nagels 5 mm in diameter and 60 mm long were used

as shear bonds. The stiffness characteristics of the bonds are taken from the table [26] for short-term loading, the elastic modulus of the rods $E_i = 1000$ MPa. All calculations were performed in two versions: with a linear and non-linear shear bond deformation diagram. The linear diagram is constructed from the conditions $T_c = 7$ kN, $\Delta_c = 0.06$ sm.

These tables confirm the conclusion of A. R. Rzhnitsyn about a slight effect on the results of the calculation of the transverse stiffness of the bonds in the range under consideration. Taking into account the actual position of the shifting force in the constituent element increases the deflection by 7...18%, stresses by 5...10% and the total shear force by 9...13% compared with the application along the the edges of the seam of the joint. Similar results were obtained for other types of loading of a constituent beam.

- When designing load-bearing wooden structures from constituent rods, it is possible to use component beams of different heights and different types of wood, i.e. different bending stiffness $E_i J_i$. As an illustration, in Table 2 we present the calculation of a similar beam with a span of 6 m, loaded with a concentrated load in the middle of the span with $M = 10.84$ kN sm. Calculations were made for 4 types of beam cross section with a change in the height of the component beams and their modulus of elasticity by 1.5 times, which corresponds to the transition from the 2nd to the 3rd grade of wood.

Table 2 Results of calculating a constituent beam with different cross sections

No	Beam section	Calculation Method	f cm	G_v MPa	G_n MPa	ΣT kN
1	125  E=3900	Rulebook	8.54	11.57	11.57	
		Recommendations	8.59	11.60	11.60	57.67
	125  E=3900	Suggested Solution	7.89	12.36	12.36	52.86
2	125  E = 2550	Rulebook	10.57	10.53	12.82	
		Recommendations	10.10	10.57	12.86	58.96
	125  E = 3900	Suggested Solution	9.51	10.65	13.84	53.30
3	100  E = 3900	Rulebook	8.54	11.57	11.57	
		Recommendations	8.50	10.98	11.92	56.79
	150  E = 3900	Suggested Solution	7.77	11.35	12.69	50.33
4	100  E = 2550	Rulebook	10.62	10.31	13.00	
		Recommendations	10.80	9.55	12.89	57.44
	150  E = 3900	Suggested Solution	9.21	9.51	13.94	48.17

For comparison, the table shows the results of calculating a constituent beam with a width of 100 mm using 3 methods with the same number of uniformly installed shear bonds ($n = 9$) with equal bearing capacity $T_c = 7$ kN with a linear deformation diagram $T - \Delta$.

The deflection in the table is conditional, determined by the first limit state for the design load at $E_i = 300 R_c$.

Calculations show that the result is mainly influenced by the change in the elastic modulus E_i and the rods that make up the rod, while changing the heights of the rods at a constant total height does not significantly affect the final result.

4 Conclusion

The proposed approach to the calculation of constituent rods allows with sufficient accuracy to perform calculations of constituent wooden elements on discrete bonds with an arbitrary arrangement of bonds along the length of the rod and creates new opportunities for improvement in design.

1. The calculation program created on the basis of the proposed methodology makes it possible to take into account the nonlinear dependence of deformations on the forces in the shear bonds and the position of the shear forces in the bonds along the height of the cross section.
2. The proposed approach to the formation of the matrix creates the possibility of calculating a constituent rod having bonds of different stiffness along the length, taking into account their transverse stiffness.
3. Determination of unit displacements of compliance matrices by the described method allows considering the real elastic modules and cross-sectional dimensions of the constituent elements in the calculations.
4. The technique makes it possible to abandon several simplifying prerequisites and refines the operation of constituent rods with discrete bonds, installed with an arbitrary length step.

References

1. Rzhantsyn AR (1986) Constituent rods and plates. Stroyizdat, Moscow
2. Rzhantsyn AR (1948) Theory of constituent rods of building structures. Stroyizdat, Moscow
3. Pleshkov AF (1952) Theory of calculation of wooden constituent rods. Stroyizdat, Leningrad
4. Kochenov VM (1953) Bearing capacity of elements and connections of wooden structures. Gosstroyizdat, Moscow
5. Popov E, Sopilov W, Bardin I, Ljanagel D (2021) Calculation of vertical deformations of constituent bending wooden structures with non-linear behavior of shear bonds. In: Lecture notes in civil engineering, vol 160, pp 109–116. https://doi.org/10.1007/978-3-030-75182-1_15
6. Chen S, Wei Y, Zhu J, Lin Y, Du H (2023) Experimental investigation of the shear performance of bamboo scrimber beams reinforced with bamboo nails. *Constr Build Mater* 365:950–618. <https://doi.org/10.1016/j.conbuildmat.2022.130044>
7. Bilinski T, Socha T (2015) Numerical analysis of deflections of multi-layered beams. *Civil and environmental engineering reports* 15(4):33–42. <https://doi.org/10.1515/ceer-2014-0033>
8. Filatov VV (2013) Calculation of through beams according to the theory of constituent rods A.R. Rzhantsyn. *Vestnik MGSU* 9:23–31
9. Gabbasov RF, Filatov VV (2014) Numerical method for calculating constituent rods and plates with absolutely rigid cross braces. ASB Publishing House, Moscow

10. Filatov V, Ryasny N (2018) A numerical algorithm for solving a two-layered constituent beam subjected to vibrational loads. In: IOP Conference Series: Materials Science and Engineering 365:042065. doi:<https://doi.org/10.1088/1757-899X/365/4/042065>
11. Shevchenko A, Hapovalov S (2017) Calculation of constituent wood beams is based on variational method. In: Bulletin Belgorod state technological university named after V G Shukhov 1(2):88–91. doi:<https://doi.org/10.12737/23928>
12. Smorchkov AA, Shevelev AS (2009) Studies of the work of constituent rods on discrete bonds. *Industrial and Civil Engineering* 1:16–17
13. Olifer VI, Podolsky IYa, (1989) To the calculation of constituent rods. *Structural mechanics and structural design* 4:1–3
14. Stolyanagel (dowel) AA, Goldin YaG, Korobitsyna (2018) Refinement of the methodology for calculating the cross-links of constituent wooden beams. In: Proceedings of the international scientific and practical conference, Scientific Center “Dispute”, Vologda, December 12:33–35
15. Linkov NV (2013) Calculation of wooden beams of constituent section on joints using a constituent material according to the theory of constituent rods by A. R. Rzhantsyna. *Industrial and Civil Engineering* 4:20–22
16. Čas B, Planinc I, Schnabl S (2018) Analytical solution of three-dimensional two-layer constituent beam with interlayer slips. *Eng Struct* 173:269–282. <https://doi.org/10.1016/j.engstruct.2018.06.108>
17. Monetto I, Campi F (2017) Numerical analysis of two-layer beams with interlayer slip and step-wise linear interface law. *Eng Struct* 144:201–209. <https://doi.org/10.1016/j.engstruct.2017.04.010>
18. Roche S, Robeller C, Humbert L, Weinand Y (2015) On the semi-rigidity of dovetail joint for the joinery of LVL panels. *Eur. J. Wood Prod* 73:667–675. <https://doi.org/10.1007/s00107-015-0932-y>
19. Piskunov YuV (1989) Calculation of constituent rods on deformative shear bonds. VNITPI, Moscow, p 9976
20. Dmitriev PA (1975) Experimental studies of joints of wooden structure elements on metal and plastic nagels and the theory of their calculation taking into account elastic-viscous and plastic deformations. Thesis. Novosibirsk Engineering and Construction Institute
21. Recommendations for the design and manufacture of wood structures with connections on plates with cylindrical nagels of the TsNIISK-KirPI system (1988) TsNIISK, Moscow
22. Isupov SA (2020) Experimental substantiation by choosing basic variant of plates with cylindrical nagels. In: IOP Conference Series. Materials Science and Engineering 962:022047. doi:<https://doi.org/10.1088/1757-899X/962/2/022047>
23. Zienkiewicz OC (1978) The finite element method in engineering science. World, Moscow
24. Shaposhnikov NN, Darkov AV, Kristalinsky RI (2022) Structural mechanics. Lan, Moscow
25. Piskunov YuV, Burov EV, Zvorygin AV (1986) Determination of the stress-strain state of the nagel in the composition of the nagel plate, taking into account physically nonlinear behavior of materials. Moscow, VNIIS 6948:9
26. Isupov SA (2022) Bearing capacity and deformability of connections of wooden structures on TGc nagel plates. *Lecture Notes in Civil Engineering* 308:167–167. https://doi.org/10.1007/978-3-031-21120-1_16



Probabilistic Organizational and Technological Model of Engineering and Technical Preparation of the Construction of an Industrial Facility

Z. Y. Mukhambetzhani¹ (✉), D. A. Sinitsin¹, A. N. Pudovkin¹, A. K. Raschepkin¹,
and O. N. Rakhimova²

¹ Ufa State Oil Technical University, 1, Kosmonavtov Str., Ufa 450062, Russia
zerek-wkau@yandex.ru

² Kumertau Branch of the Federal State Budgetary Educational Institution of Higher Education
“Orenburg State University”, 3B, 2nd lane, Sovetskiy Str., Kumertau 453300, Russia

Abstract. Timeliness, quality and volume of engineering and technical preparation measures are one of the significant, key factors determining the consistency of design (organizational and technological) solutions with regard to sustainability and efficiency of main stages of industrial facility construction. Development of adequate organizational and technological solutions taking into account actual conditions of construction area or expected conditions of construction production and, simultaneously, including the forecast of displays of possible negative factors is an actual task of increasing quality of preparation for erection of an industrial facility. The purpose of the research in this article is to reveal conditions and to develop a methodical justification for improving methods and techniques of forming and management of building production procedures in the preparation of the construction area. The main result of the research is development of scientific and practical hypothesis provisions about expediency of applying probabilistic models when developing organizational and technological solutions—concerning quality and efficiency assurance of engineering and technical preparation of construction production. The proposed approach appears as an actual direction of expansion of possibilities at organization and management of construction processes which are produced under conditions of dynamically changing states of production environment of building production, and also practical application of the tool of predictive account of risks of consequences of negative factors manifestation.

Keywords: Industrial facilities · System analysis · Probabilistic model · Construction processes · Random factors

1 Introduction

Development of organizational and technological solutions in relation to engineering and technical preparation of industrial facility construction is an independent, complex and responsible type of design activity. Moreover, some aspects of preparatory period works cannot be solved and implemented by means and methods of solving similar problems, means of designing and implementing works of the main and final construction periods.

The influence of quality of engineering-technical preparation on the conditions of stability and effectiveness of carrying out the following main, special and final stages of construction production is viewed in scientific papers [1–3] as a significant factor of providing (increasing) functional quality of construction production.

Directions for increasing the effectiveness of organizational and technological solutions aimed at the preparation and practical implementation of the established technical and economic indicators of construction processes are considered in the works [4–6].

Analysis of the conditions of stability, organizational and technological reliability and minimization of risks of construction production is considered in scientific papers [7–9], as a significant tool of investment and construction activities. For example, the indicator of the duration of construction production, and, accordingly, the timely completion of construction, is recognized as one of the most significant target indicators of organizational and technological solutions [10–12].

Construction process modeling is considered as a modern format for developing technological, managerial and organizational solutions for construction production [5, 13, 14]. Particular attention in scientific and practical studies is paid to the application of information (digital) models of organizational and technological solutions for construction production [15–17].

Organizational and technological model of engineering training reflects the results of the analysis of initial data (specific features of properties and states) of the corresponding elements of the construction system [18–20]:

- digital (information) model of an industrial facility;
- the organizational and technological sequence of the main, special and final stages of construction;
- the natural and artificial environment in the area of the proposed location of the construction site (temporary construction camp);
- needs in material, technical and other types of ensuring of construction production.

At the same time, the existing practice of developing organizational and technological solutions is focused on the use of “hard” information models in a deterministic format that makes it impossible to predict and consider manifestations of negative random factors of construction production [21, 22].

It is for this reason, the relevance of the development of opportunities to improve the quality of organizational and technological solutions in relation to engineering and technical preparation of construction production of industrial facilities seems to be associated with the development of methodological foundations for the application of predictive, probabilistic models of construction production.

2 Research Methods

The quality of the development of design, organizational and technological solutions, it is customary to evaluate some number of indicators.

The structure (system) of quality assessment includes a number of indicators, which can be displayed by analytical dependence of the form:

$$K_{lev} = f \sum_{i=1}^n r_i q_i; \sum_{j=1}^m R_j Q_j; \quad (1)$$

where K_{lev} —the level of quality of development of organizational and technological solutions; r_i —a single indicator of the quality and effectiveness of solutions; q_i —significance (specific weight) of a single indicator; n —the number of absolute indicators under consideration; R_j —relative indicator of quality and effectiveness of solutions; Q_j —significance (specific weight) of the relative indicator; m —the number of relative indicators under consideration.

The use of technical and economic indicators is the main modern tool for assessing the quality of development of design solutions in relation to engineering and technical preparation of the construction of an industrial facility [4, 6].

Table 1 shows quantitative characteristics (technical and economic indicators) of the quality of organizational and technological solutions, characterizing the results of design solutions for one of the possible options of engineering and technical preparation of construction of an industrial facility.

The qualitative and quantitative composition of the indicators given in Table 1 is not exhaustive. Depending on the specific design situation, this list may be supplemented by other indicators (absolute and relative), which affect the formation of the assessment of the quality level of design solutions.

Analyzing the data in Table 1 using the analytical relationship (1) we can note the following:

- to assess the level of quality of development of organizational and technological solutions for consideration adopted 7 indicators. Three indicators (No. 1, 3, 5) are absolute, and four indicators (No. 2, 4, 6, 7) are relative;
- each of the adopted indicators (both absolute and relative) are characterized by the same significance in relation to the assessment of the level of quality.

The features discussed above are common and generally accepted practice for assessing the quality of design, organizational and technological solutions.

Accepting in general this approach, we can note the following:

- each of the indicators accepted for consideration (see Table 1) can be accepted as an object or a subject of researches at the analysis of a condition or conditions of optimization of a level of quality of development of organizational-technological decisions;
- optimization of even one, separately taken indicator, can lead to an overall increase in the quality level of development of organizational and technological solutions [see dependence (1)].

The parameters of the type q_i and Q_j [see dependence (1)] are able to establish the priority order of consideration of the indicators adopted for the analysis, in order to identify the most effective approaches to solving the design problems.

Table 1 Technical and economic indicators of the variant of organizational and technological solutions of engineering and technical preparation of construction (example)

No.	Indicator name	Indicator characteristic	Unit of measure	Indicator
1	2	3	4	5
1	Duration of construction (Π_p)	By organizational and technological model	Days	23
2	Reducing the standard duration of construction (D_w)	By organizational and technological model: $\mathcal{K}_{d.} = P_{d.f.} / P_{d.norm}$ $\mathcal{K}_{d.} = 23/25 = 0.92$	–	0.92
3	Total labor input (T_{ii})	By organizational and technological model	Man-days	178
4	Labor input per 1 m ³ of the building, man-days/1 m ³ , ($T_p/1m^3$)	$T_p/1 m^3 = T_p/V_3$ $T_p/1 m^3 = 178/75816 = 0.115$	Man-days/1 m ³	0.0023
5	Maximum number of workers	By organizational and technological model	Man	16
6	The coefficient of irregularity of movement of workers	$N_{av.} = T_p/\Pi_p = 178/23 = 7.74$ $N_{irreg.} = N_{max}/N_{av.} = 16/7.74 = 2.067$	–	2.067
7	Coefficient of combination of construction processes	By organizational and technological model: $\mathcal{K}_{com.} = \Pi_{d.norm.}/\Pi_{d.f.}\mathcal{K}_{d.} = 35/23 = 1.52$	–	1.52

The proposed methodological approach is considered on the example of the analysis of the indicator of the “duration of construction” (“Pr”, see Table 1).

The indicator of duration is a quantitative characteristic of the measure of time (time estimate or time estimate) required to perform a simple (complex) construction process (work). Accordingly, the sum of the durations of production of all the works included in the organizational and technological model forms the total duration of the engineering preparation of construction.

The duration of execution (time estimate) of each simple (complex) construction process (work) is a mandatory and significant structural element of the organizational and technological model of engineering preparation of construction of an industrial facility. All types of modern organizational and technological models of construction production (schedules, network schedules, cyclograms) are focused exactly on the analysis of duration of construction processes (works), separate stages (including the cycle of engineering preparation of construction) and the total duration of construction.

The organizational and technological model is a conventional image and a characteristic of the anticipated properties and states of a construction object which reflect the sequence and terms of implementation of simple and complex construction processes (works) and specify their composition and technological sequence of implementation. Peculiarities of formation and supposed implementation of organizational and technological solutions of construction production are displayed through the development and presentation of an appropriate topology of organizational and technological model.

By the topology of organizational and technological model of construction production we mean a formalized (using a system of symbolic signs) representation of physical processes (simple and complex construction works) and representation of states of objects of organization, management and control. In general, the topology of organizational and technological model includes the following structural (graphic and symbolic) elements: representations of events corresponding to certain system states, relations determining the conditions of organizational and technological sequence (hierarchical dependencies) of simple and complex construction processes (works), information and calculation data.

Organizational and technological solutions with regard to the formation and functioning of the construction production system are focused on creating the optimal (for example, according to the indicator of the total duration or the critical path of construction) technological sequence of simple and complex construction processes. The algorithm, established by the provisions of the normative and technical documents, leads to the formation of the organizational and technological model of construction production of a constant or deterministic kind (format).

For organizational and technological models of deterministic type the main, characteristic features are: fixed (constant, rigid, unchangeable) schedule topology and constant quantitative values of duration (time estimates) of simple and complex construction processes included in the organizational and technological model [18].

Deterministic format of organizational and technological solutions (model) allows to provide conditions of construction stability and reliability (e.g., timely completion) only in the absence of manifestation of negative factors. The fixed topology of the deterministic format of the organizational-technological model, combined with the fixed values of the time evaluation of construction processes (works) leaves no room for preventive account of the possibilities of negative factors' consequences manifestation (for example, the increase of actual duration of works). This circumstance is especially obvious with regard to the construction processes (works) constituting the critical path of construction (the values of general and partial time reserves of such works being equal to zero).

The format of the probabilistic (stochastic) model of organizational and technological solutions differs from the deterministic format by the presence in its composition of structural elements that are random (probabilistic) in nature.

The main formats of probabilistic (stochastic) model of organizational and technological solutions for engineering and technical preparation of construction include:

- stochastic organizational-technological models, which include structural elements that characterize the random or (probabilistic) nature of the quantitative values of the duration of execution (time evaluation) of simple and complex construction processes

(works) included in the organizational-technological model of construction production—with a deterministic format of the topology of the organizational-technological model;

- stochastic organizational and technological models, which include structural elements, characterizing a random or (probabilistic) nature of the topology of the organizational and technological model with a deterministic format of the quantitative values of the duration (time evaluation) of simple and complex construction processes (works), included into the organizational and technological model of the construction production
- stochastic organizational and technological models, which include structural elements that characterize the random or (probabilistic) nature of the quantitative values of the duration of the execution (time evaluation) of simple and complex construction processes (works) included in the organizational and technological model of construction production—in the probabilistic format of the topology of the organizational and technological model.

Application of the probabilistic format of organizational and technological models is focused on the analysis of possible (probable) manifestations of negative factors and assessment of their impact on the level of reliability of the construction production system that accompanies the engineering and technical preparation of construction of an industrial facility.

3 Results and Discussions

Formation of the topology of the organizational and technological model of engineering and technical preparation of the construction of an industrial facility implies a system analysis, determination of quantitative characteristics and organization of the conditions of the following main types (groups) of simple and complex construction processes (works):

- Complex of activities carried out outside the construction site (temporary construction camp), information index **CM_TC**:
 - protection of the area from flooding or inflow of surface water (information index **TC1**);
 - protection of the territory against waterlogging or groundwater infiltration (information index **TC2**);
 - connection to external (city) engineering networks (water supply, wastewater disposal, heat supply, gas supply, air supply, steam supply, electricity supply) of resource supply (information index **TC3**);
 - organization of access to elements of transport (road, rail, water, air, pipeline) infrastructure (information index **TC4**).
- A set of activities carried out on (inside) the construction site (temporary construction camp), information index **CM_Ins**:

- *Geodetic support for the construction of the preparatory period (information index **GS**):*
 - determination of the required level of the geodetic network reference points (information index **GS1**);
 - restoration of existing geodetic network reference points (information index **GS2**);
 - development of new geodetic network reference points (information index **GS3**);
 - taking the project (temporary construction site) into the ground (information index **GS4**).

- *Cleaning the construction site (information index **CA**):*
 - clearing the area from natural (trees, bushes, boulders) formations (information index **CA1**);
 - clearing the area of large debris and man-made waste (information index **CA2**);
 - demolition or relocation of capital construction facilities located in the construction area (information index **CA3**);
 - dismantling of transport infrastructure (roads, tracks, overpasses) located on the construction site (information index **CA4**);
 - demolition or relocation of elements of technological equipment located on the construction site (information index **CA5**);
 - disassembly or re-laying of elements of underground utility networks (water supply, sewage, heating, gas, electricity supply) located in the construction area (information index **CA6**).

- *Protection against possible manifestations of adverse natural and climatic factors (information index **PP**):*
 - dewatering of the ground (ground water level (information index **PP1**);
 - drainage of wetlands (information index **PP2**);
 - protection of the territory against possible landslides (information index **PP3**);
 - increasing the bearing capacity of weak (subsident) soils (information index **PP4**);
 - elimination of karst manifestations (information index **PP5**).

- *Vertical planning of the construction site area (information index **VP**):*
 - removal of the vegetative (fertile) layer of soil to its full capacity (information index **VP1**);
 - rough surface leveling for surface drainage (information index **VP2**).

- *Installation (erection) of temporary facilities (buildings and structures) of various functional and technological purposes (information index **TF**):*

installation (erection) of temporary residential (household) facilities (information index **TF1**);
 installation (erection) of temporary administrative facilities (information index **TF2**);
 construction (erection) of temporary facilities for household purposes (information index **TF3**);
 device (erection) of temporary facilities for production purposes (information index **TF4**).

- *Construction of temporary transport and pedestrian routes, engineering networks, technological platforms and structures (information index TP):*

arrangement of temporary elements of transport infrastructure (roads, unloading areas, parking lots and means of mechanization) (information index **TP1**);
 arrangement of temporary elements of production infrastructure (stands for enlarging or conveyor assembly, warehouses, concrete and mortar units, tower crane tracks, fencing of work areas) (information index **TP2**);
 installation of temporary elements of engineering networks of water supply, wastewater disposal, heat supply, air supply, steam supply, gas supply, power supply (information index **TP3**);
 construction of pedestrian paths and passageways to work areas (information index **TP4**).

- *Ensuring the safe operation and performance of production processes (information index SO):*

installation of elements of physical protection (fencing) of the perimeter area (information index **SO1**);
 arrangement of checkpoints (admission) to the construction site (information index **SO2**);
 information aids (posters, stands, boards) (information index **SO3**);
 lightning protection components (information index **SO4**).

- *Ensuring environmental protection (information index OC):*

Arrangement of points for cleaning and washing vehicles (information index **OC1**);
 arrangement of places for collection, processing, temporary storage of garbage and construction waste (information index **OC2**);
 installation of technological devices for collection, processing and temporary maintenance of liquid technological media, sewage (information index **OC3**).

- *Ensuring environmental protection (information index EP):*

arrangement of fire extinguishing facilities (information index **EP1**);
 smoking areas (information index **EP2**);

the construction of elements and systems of fire alarm systems (information index **EP3**);
 fire hydrants (information index **EP4**).

The above-mentioned composition of measures for engineering and technical preparation of industrial facility construction is aimed at forming necessary or sufficient conditions for the planned deployment and timely start of production and technological procedures of the subsequent (main) stage of construction production.

Probabilistic format of organizational-technological model topology is intended for prediction of consequences of negative factor manifestation in construction production and its influence on the considered indicator of organizational-technological solutions quality (indicator “duration”, see Table 1).

Suppose the manifestation of such (negative) factor by the example of one of the construction processes, included in the complex of measures **CM_TC**.

Figure 1 shows a fragment of the decomposition of the topology of the deterministic model format, which presents the state of the construction process due to a possible negative factor in the implementation of the construction process, denoted by the information index **TC1**.

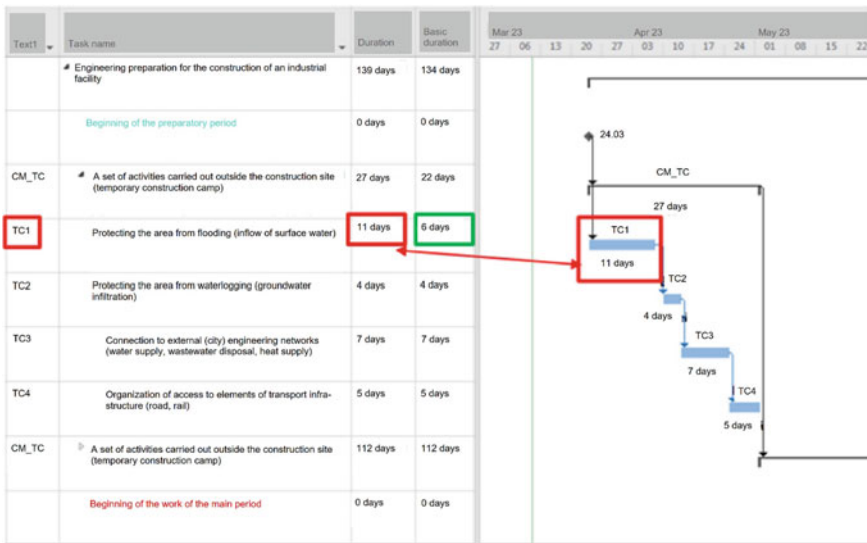


Fig. 1 State of the construction industry due to the manifestation of the negative factor. The complex of measures of **CM_TC**

From the data shown in Fig. 1, it follows that the manifestation of the negative factor in the production of the complex construction process BH2 increases the originally established (baseline) duration from 6 to 11 days. Thus, the negative consequences of the manifestation of a random factor add “+5 days” to the duration of the process BH1 and, together with it, lead to a delay in the implementation of a set of measures **CM_TC**

(by five days, from the base value of 22 days to the actual value of 27 days), as well as the total composition of “Engineering and technical preparation of construction of an industrial facility” (by five days, from the base value of 134 days to the actual value of 139 days).

“Hard”, deterministic format of organizational-technological model topology does not allow to carry out planning of measures to parry negative consequences of accidental factor manifestation—without involving additional resources.

The solution of the problem seems possible with the use of probabilistic format of organizational-technological model topology (Fig. 2). The solution of the problem seems possible with the use of probabilistic format of organizational-technological model topology (Fig. 2).

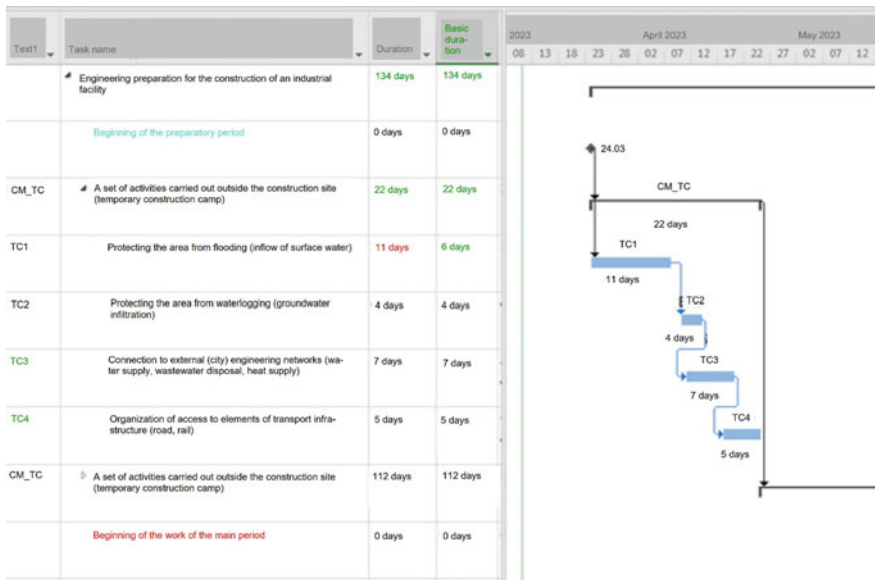


Fig. 2 Probabilistic format of the model topology. Variant with changing links for two construction processes (works): TC3 and TC4

From the data in Fig. 2 it follows that the manifestation of the negative factor, which occurs in the production of the complex construction process TC2, is to be countered by changing the links (probabilistic format of model topology) for the two construction processes (works): TC3 and TC4.

This approach allows to parry the negative effects of a random factor (“+5 days” to the duration of the process TC1) on the total duration of the complex of CM_TC activities and the overall composition of “Engineering preparation of construction of an industrial facility”. The actual duration returned to the base or pre-set values (respectively, 122 and 134 days).

It is important to note that the measures proposed for implementation to change (optimize) the topology of the organizational and technological model do not require

additional resources: the duration of the optimized processes TC3 and TC4 is equal to their pre-established values.

4 Conclusions

According to the results of the research the following main conclusions are obtained:

1. Analysis (definition, calculation) of organizational and technological solutions indicators using the above considered probabilistic model formats is a significantly more complex design procedure compared to the deterministic format of a similar organizational and technological model.
2. The considered methodical approach with the use of probabilistic format of organizational-technological model can be applied for development of forecast and analysis of consequences of negative factors manifestation for various construction processes included in the model.
3. Methodical approach with the use of probabilistic format of organizational-technological model topology contributes to improving the quality of the development of design (organizational-technological) solutions aimed at taking into account the consequences of manifestations of negative factors of construction production during engineering and technical preparation of the construction of an industrial facility.

References

1. Oleinik PP (2017) Organizational and technological support for the construction of modern industrial enterprises. *Mech Constr* 7:9–13
2. Belov AV (2012) Tasks of ensuring the quality of construction processes. *Bull Saratov State Socio-Econ Univ* 2:98–100
3. Mukhametzyanov ZR, Razyapov RV (2017) Classification of combinations of technologically interrelated construction processes used in the construction of the object. *Ind Civ Eng* 10:72–77
4. Weinstein MS et al (2015) Evaluation of the effectiveness of organizational and technological solutions in the selection of means of mechanization of construction and installation works. *Sci Rev* 13:123–128
5. Kabanov VN et al (2017) Variant designing of building processes as a way of making a rational decision on the timing and cost of construction. *Bull Volgograd State Architectural Constr Univ Ser Constr Architecture* 50(69):37–45
6. Organization of construction production in the engineering preparation of the territory of construction (2018). Ministry of Construction and Housing and Communal Services of the Russian Federation, Moscow, p 166
7. Abdullaev GI (2010) Main directions of increasing the reliability of construction processes. *Eng Constr J* 4:59–60
8. Bogachev SN et al (2015) Construction risks and opportunities of their minimization. *Acad Architecture Constr* 1:88–92
9. Nedavny OI et al (2013) Estimation of organizational and technological reliability of object construction. *Syst Methods Technol* 2(18):137–141

10. Dementieva VV (2018) Characteristics of the concept of timing of construction and analysis of the main directions of reducing the timing of construction. *Sci Pract Electron J Alley Sci* 5(21):71–77
11. Velichko VV (2019) Construction project risk management. Hot Line-Telecom, Moscow, p 214
12. Mukhametzyanov ZR, Oleynik PP (2019) Formation of organizational and technological solutions in the construction of industrial complexes. *Ind Civ Eng* 11:35–41. <https://doi.org/10.33622/0869-7019.2019.11.35-41>
13. Kostyuchenko VV, Kudinov DO (2012) Organizational and technical modeling of design and construction systems. *Eng Vestnik Don* 1:731–734
14. Smirnov OL (2018) Composition and optimization of models of complex systems. LAP LAMBERT Academic Publishing, Moscow, p 144
15. Abakumov RG et al (2017) Advantages, tools and effectiveness of the introduction of information modeling technologies in construction. *Bull BSTU Named After V.G. Shukhov* 05:171–181
16. Zheleznov MM, Adamtsevich LA (2021) Information modeling at the construction stage. MISI-MGSU, Moscow, p 116
17. Dmitriev AN, Vladimirova IL (2019) Technologies of information modeling in the management of construction projects in Russia. *Ind Civ Eng* 10:48–59
18. Bogomolov YM (2002) Information technologies in the organization of construction. BELFORT, Minsk, p 158
19. Gusev EV, Mukhametzyanov ZR, Razyapov RV (2017) Methodology for determining the rational limits of the alignment of construction and assembly processes on the basis of quantitative assessment of technological links. *IOP Conf Ser Mater Sci Eng (MSE)* 262:012140. <https://doi.org/10.1088/1757-899X/262/1/012140>
20. Vladykin VN, Abakumov RG (2017) Information Modeling in modern construction. *Innov Sci* 03–1:20–22
21. Kurchenko NS (2018) The choice of organizational and technological solutions for construction projects, taking into account random factors. *Syst Technol* 27:64–68
22. Lebedev VM (2008) Organizational and technological reliability of control systems of construction. *MSCU Bull* 4:191–194



The Efficiency of Self-Healing Cementing Materials

Wang Mingyuan¹(✉), V. S. Rudnov¹, Tang Dongyang², Xiao Xinyuan³,
and Liu Zhenzhi³

¹ Ural Federal University Named After the First President of Russia B.N.Yeltsin, 19, Mira Str.,
Ekaterinburg 620002, Russia

wmy_hitcq@163.com

² Belarussian National Technical University, 65, Nezavisimosti Avenue, 220002 Minsk, Belarus

³ Ural Science and Technology Development (Chongqing) Co. Ltd, 98, Yumin Road,
Chongqing 401120, Yubei District, China

Abstract. To meet the special requirements (for the strength and conductivity of concrete structures) that arise during the transmission of electricity to remote areas of the Russian Federation, a variant of using self-healing concrete is proposed. In this material, it is proposed to use microcapsules obtained by the physical method, consisting of sodium silicate and bentonite clay coated with ethyl cellulose with graphene. The mechanism of action of the capsule is as follows: after external mechanical destruction, access to graphene appears and it acts as a conductive medium, resulting in the cementing properties of the capsule core. In the course of the work, the optimal ratio of graphene and the capsule core was established, which was determined during several experiments and microstructure studies. The dependences of the compressive strength and conductivity of the composite on the graphene content in the capsule, the number of microcapsules in concrete, and the time of strength gain were also revealed. In the experiments, the average size of microcapsules was 1.25 mm, and the grain shape is predominantly spherical with a rough surface and dense structure. The optimal microcapsule content was 2% of the cement binder weight, which corresponds to 0.1% graphene oxide. With an increase in the graphene content, the conductivity of the concrete composite monotonically increases, and the compressive strength increases to a certain limit and then decreases. After partial destruction of the samples (discontinuity) at the micro level, the composite material recovered, while the recovery coefficient was 81%, and the recovery coefficient of compressive strength was 57%.

Keywords: Graphene · Microcapsules · Self-healing cementing materials · Compressive strength · Conductivity

1 Introduction

Currently, the number of energy consumers throughout the Russian Federation is rapidly increasing, which in turn stimulates the active growth of electricity transmission and conversion lines, including in remote areas of the country (see Fig. 1) with harsh climatic conditions.

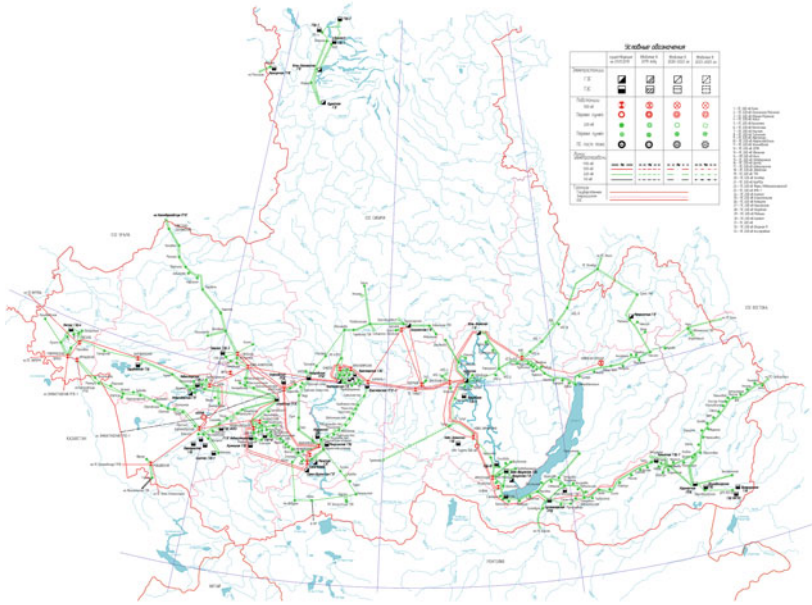


Fig. 1 Schematic diagram of transmission and conversion lines of electricity in the Russian Federation

At the same time, the foundations of power transmission towers are affected by both weather conditions (large amounts of rain, extreme temperatures) and difficult geological conditions (saline or weak soils), which leads to the destruction of the concrete structure, frost heaving, uneven precipitation, cracks, and other damage. At the same time, the foundations are "hidden works", which makes it difficult to identify the resulting defects and cracks, and reduces the durability and terms of safe operation of structures. Also, the fundamentals must have a certain electrical conductivity to ensure the safety of people and equipment and to improve the reliability of the power system. Ordinary heavy concrete has a resistivity of $10^4 10^9 \text{ OM} \times \text{M}$ and for its use in the construction of power line foundations, it must be reduced. All of these factors determine the requirements for concrete foundations.

Created by a team of authors, intelligent self-healing concrete is developed based on bionic theory. The repair material in the manufacture of the mixture is located inside the monolith and when the structure is damaged, trigger mechanisms (temperature, change in pH of the medium or cracks) start the restoration of the damaged area, which prolongs the life of the structure and increases its durability. Microcapsule technology of self-healing materials based on Portland cement has the advantages of the possibility of mass use, low cost (compared to repair work), ease of process control, and excellent dispersibility over the body of concrete [1–3]. Currently, similar materials consist of urea–formaldehyde resins/epoxy microcapsules [4–7], phenolic resin/dicyclopentadiene microcapsules [2, 8, 9], which have lower adhesion and slight expansion of the core material in combination with insufficient strength of the capsule wall, which significantly limits the possibility of their use in cement compositions [10]. Methods for manufacturing such capsules are

based on physical [11–13], chemical [14], physicochemical [14–19] and other methods (see Table 1). Yang [20], Zhang [21], Wang [22], and others conducted experimental research and mathematical modeling in the field of petrochemistry, road engineering, bridge construction, polymer materials, coatings and other fields. However, for the foundations of power lines operating in difficult geological and meteorological conditions of remote areas of the Far North, such studies have not been carried out, despite the high demand.

Table 1 Preparation method of microcapsule [11–19]

Method of preparation	Method of production	Core material	Wall material	Material properties
Physics	Spray drying method	CSA	PVA	$E_d(\uparrow)$
Chemistry	Microfluidics/photopolymerization	CS, SS	AE	$\sigma_{bc}(\downarrow)$, $C_r(\uparrow)$
	Chemically activated emulsion polymerization	SF	PS	$C_r(\uparrow)$, $E(\downarrow)$, $pH(\uparrow)$
	Radiation aggregation	BS	MA	$\sigma_{bc}(\downarrow)$, $\sigma(\downarrow)$
Synthesis of physics and chemistry	Extrusion method	CH, MFP, Ag+	EC, MA	$pH(\uparrow)$, $C_r(\downarrow)$
	Sol gel	BS	SiO ₂ , M	$\sigma_{bc}(\downarrow)$, $\sigma(\downarrow)$, $f_{cf}(\downarrow)$, $K(\uparrow)$
	Melting and dispersing method	SS	G	$\sigma_{bc}(\downarrow)$, $f_{cf}(\uparrow)$, $K(\uparrow)$
	Complex emulsion method	PER, SS, DCPD, MMA, CS	UF, PU, PUF, PS, PF, MF	$\sigma_{bc}(\downarrow)$, $f_{cf}(\downarrow)$, $E(\uparrow)$, $K(\uparrow)$

Note The abbreviations in the table have the following meanings: *E*: modulus of elasticity, *Ed*: dynamic modulus of elasticity, *Cr*: corrosion rate, *K*: crack healing rate, *BS*: bacterial spores, *MA*: alginate, *G*: gelatin, *PER*: epoxy resin, *AE*: acrylate, *CH*: calcium hydroxide, *CS*: silica gel, *CSA*: calcium thioaluminum, *DCPD*: dicyclopentadiene, *EC*: ethylene cellulose, *M*: melamine, *MF*: melamine, *MF*: monofluorophosphate, *F*: phenol formaldehyde, *PS*: polystyrene, *PU*: polyurethane, *PVA*: polyvinyl alcohol, *SF*: sodium fluorophosphate, *SS*: sodium silicate, *UF*: urea–formaldehyde

At the same time, special design requirements for the foundations of power transmission towers complicate requests for concrete material. Most often in practice, additional components of the mixture, such as graphite, carbon fiber, steel slag, steel fiber and carbon black, are used to improve the conductive properties of concrete. The use of graphene (with high conductivity and a large specific surface area) can significantly improve the electrical conductivity of cement compositions, but reduces the strength characteristics of the material and increases its cost, which limits its use. At the same time, it should be noted that other conductive components adversely affect the technological properties of concrete mixtures. Therefore, the use of microcapsules as a solution to this technical

and technological issue is very important in the design and construction of power lines in Russia and northwest China.

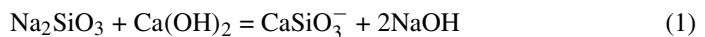
In the presented study, the authors made the core of a microcapsule based on sodium silicate and bentonite by physical methods, and the shell was based on ethylcellulose and xylene with the addition of graphene. In the course of the work, the dependence of the strength characteristics of cement composites on the content of microcapsules in concrete, graphene in microcapsules and hardening time was studied. At the micro level, the process of restoring defects (cracks) of concrete was investigated by optical microscopy and X-ray diffraction analysis.

2 Production of Samples of Cement Composite, Microcapsules, and Their Mechanism of Action

For the manufacture of cement composite samples, the composition cement: sand = 1: 3 with a water-cement ratio of 06 was adopted. The content in the composition varied and it was 1, 2, 3, 4 and 5%, sodium fluorosilicate was introduced in an amount of 15% by weight of microcapsules and a solution of graphene oxide in an amount of 0.025; 0.05; 0.1; 0.25 and 0.5% by the weight of the concrete. From the control and experimental compositions of cement compositions, cube samples with a size of 70 × 70 × 70 mm were made and after 7, 14 and 28 days of hardening, they were tested to determine the compressive strength and the rate of restoration of the structure was determined as the ratio of strength after restoration to the strength of control samples.

Initially, the core of the microcapsule is made, for which sodium silicate, microcrystalline cellulose, bentonite and methylcellulose are taken in a ratio of 25, 30, 10 and 2%, respectively, and mixed until homogeneous in the dry state (see Fig. 2). Then 29% distilled water and 4% Tween 80 are added and stirred at a temperature of 40 °C. Particles are obtained from the resulting mass by extrusion followed by granulation. The shell material of ethyl cellulose, ethyl alcohol and xylene (10, 18 and 72%, respectively) is applied to the surface of the capsules after thorough mixing. The capsules themselves are dried in an air stream with simultaneous dispersion. For further experiments, particles with a size of 1–1.25 mm are selected by screening. When soaking a random number of capsules with distilled water, only a few capsules dissolved, and most of them remained intact, which indicates the integrity of the composite structure of the capsules.

Microcapsules are mixed with other components of the cement composition in conventional forced mixers, closed and formed samples, which, after hardening, are ready for further experiments. When the sample is exposed to external influences, a microcrack occurs in its structure, which ruptures the shell of the microcapsules, moisture from the surrounding concrete stone penetrates to the core and triggers chemical reactions with sodium silicate (see formula 1). As a result, a gel-like silicon hydroxide $\text{Si}(\text{OH})_4$ is formed, which in turn fills the free space, binds to the walls of the crack and the neoplasms have a certain strength.



As water is absorbed, bentonite expands in the cement composite and fills cracks, which prevents further penetration of corrosive substances from the environment. A

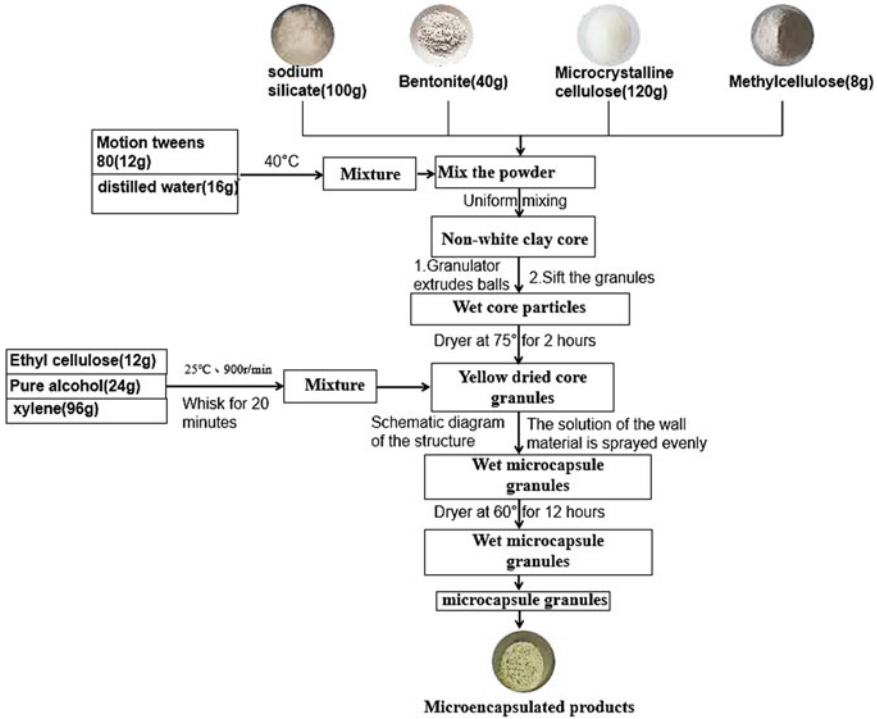


Fig. 2 Microcapsule production process

chemical reaction occurs (see formula 2) and the cracks are glued together by the products of the neoplasm, the rigidity, and impermeability of the cement matrix are restored (see Fig. 3).



3 Methods of Experiments and Results of Work

In the first stage, the strength of samples with sand (control) was determined only and recorded as K_0 . Then the samples are loaded without destruction to a force of 60% of the destructive force (K_1), after which they harden and restore the structure under conditions of heat and humidity treatment. Determination of the strength of the structure and strength (maintainability) was carried out after determination after additional hardening (K_2) for the estimated amount of time and was determined by the formulas (3) and (4):

$$K_x = \frac{K_2 - K_1}{K_0 - K_1} \times 100\% \quad (3)$$

$$K_h = \frac{K_2}{K_0} \times 100\% \quad (4)$$

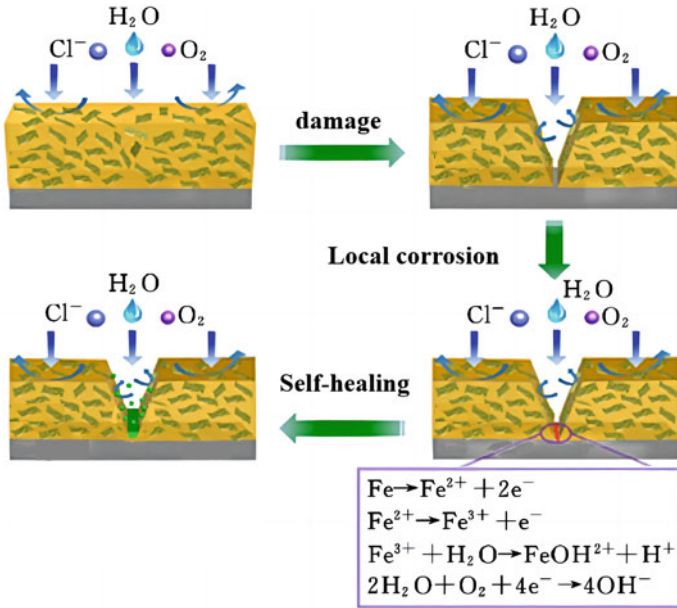


Fig. 3 Schematic diagram of microcapsule self-healing mechanism

Four-electrode voltammetry was used, which eliminates the contact resistance between the electrode sheet and the cement base, and reduces the polarization effect. Stainless steel electrodes were evenly placed on the sample at a distance of 20 mm from each other (see Fig. 4), and a DC source, an ammeter (I) and a voltmeter (U) were connected.

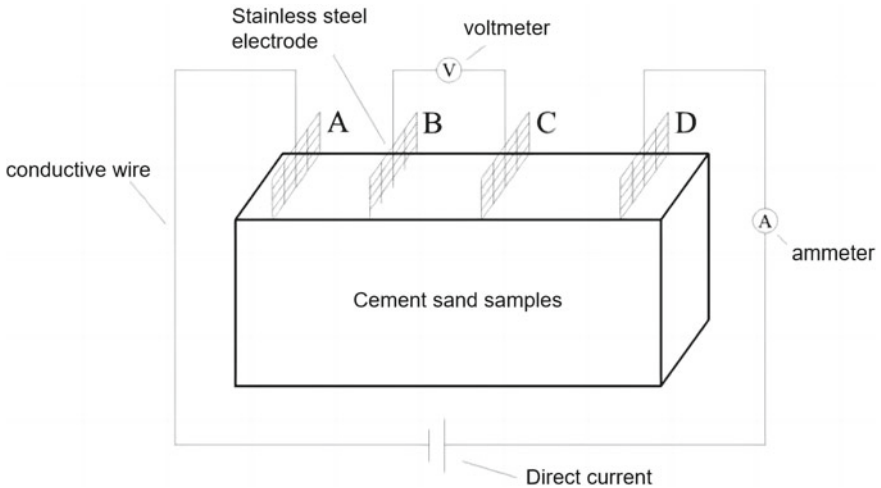


Fig. 4 Working mechanism of resistance method

The cross-sectional area through the BC segment was S , and the distance between the electrodes was L . The resistivity ρ was calculated by the formula 5:

$$\rho = \frac{US}{IL} \quad (5)$$

X-ray phase analysis of cement composites with microcapsules showed the presence of the following minerals: albite, arcade, quartz (19%), calcium hydroxide, calcium thioaluminate, aluminates, and clinker minerals (73%). In them, the content of quartz, albite and albite increased by 2.22 and 23%, respectively, compared with the control composition. This proves that the core material is released after the “opening” of the microcapsules and forms an additional amount of calcium hydro silicates (the main hydration products of Portland cement).

In addition to X-ray phase analysis, micrographs of microcapsules and cementing reaction products were also taken (see Fig. 5). The shape of the microcapsules is predominantly spherical, and the intact shell completely covers the smooth surface of the core (see Fig. 5a). At higher magnification, it appears that the surface of the microcapsule shell is uneven, which contributes to increased adhesion to the cement matrix (Fig. 5b). When a microcrack forms in the composite due to the adhesive forces, the capsule will also open and release access to the core material, the hydration products of which will then fill the space of the microcrack. After the sample is preloaded, a pressurized microcapsule releases the base material (see Fig. 5c), which reacts with water and carries out the recovery work. The color of the composition with graphene and microcapsules is darker and at the same time graphene conglomeration is not detected (see Fig. 5d). At the same time, the structure of the material becomes denser (see Fig. 5e). Graphene intensifies hydration reactions, combines hydration products and increases strength.

Excellent dispersibility, combined with hydrophilicity, accelerates the release and hydration of the main components of the microcapsule core, increases the content of calcium ions, and mineral formations fill microcracks. With a small dielectric constant (55%) and high specific strength, the resistivity of the cement composite is reduced and the need for a low resistivity for the power transmission network is realized.

The compressive strength of samples of cement compositions hardened for 28 days, with an increase in the content of microcapsules, gradually decreases to 1% with 5% of microcapsules (see Fig. 6), which cannot meet the needs. Alleged reasons for the decline: low strength of the microsphere (at the level of the pore of concrete) violates the original strength of the composite; The addition of microcapsules reduces the content of other components (including Portland cement) and weakens the concrete. However, a small content of microcapsules (up to 2%) leads to a slight increase in strength compared to the control composition. This happens for the following reasons: sodium fluorosilicate added to the samples slows down the kinetics of hardening; microcrystalline cellulose and ethyl cellulose slow down coagulation and increase strength at low contents; When preparing a cement composite, a small part of the capsules are destroyed and the core material begins to interact, filling the shrinkage cracks.

Microcapsules reduce the rate of strength gain of the composite, which is manifested in strength after 7 days of hardening: with microcapsules, the strength is 70% of the control composition. However, in the future, the strength of the activity increases and after 28 days exceeds the control samples. Therefore, for further experiments, samples

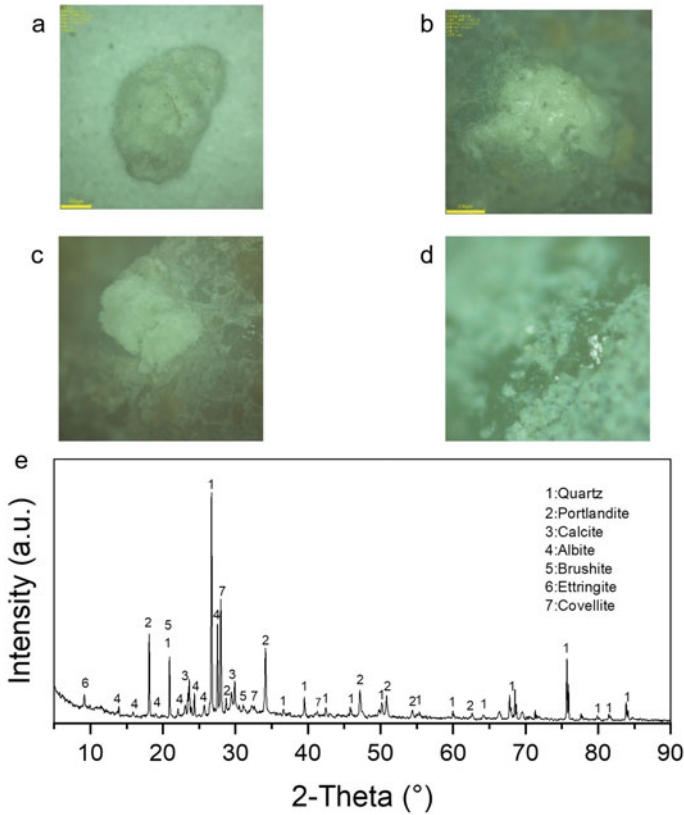


Fig. 5 SEM photos and XRD analysis of self-healing mortar matrix: **a** Morphology of microcapsules; **b** Morphology of the wall; **c** Crushing of microcapsules to eliminate gaps; **d** Morphology of grapheme; **e** Composition of cementing material: graphene-microcapsule

were taken that hardened for 28 days, after which the sample was subjected to an aqueous hardening test for 10, 20 and 30 days, after which the compressive strength was determined and the rate and recovery rate was calculated.

The rate of recovery of compressive strength K_x gradually increases with an increase in the content of microcapsules (see Fig. 7). It has been established that sodium silicate in the cement matrix interacts with water and sodium fluorosilicate to form cementitious substances, the amount of which increases with an increase in the content of microcapsules, which explains the increase in strength (self-healing effect). However, it should be borne in mind that with an increase in the content of microcapsules, the number of stress concentration points and the likelihood of defects—cracks—also increase. But at the same time, the number of microcapsules involved in self-healing also increases.

It has been established that the rate of strength recovery in samples that have additionally hardened for 30 days under heat and humidity conditions is the highest, and for hardened 10 days, it is the lowest. The reason for this increase in the self-healing effect can be explained by the limited reaction rate of sodium silicate in the microcapsule core

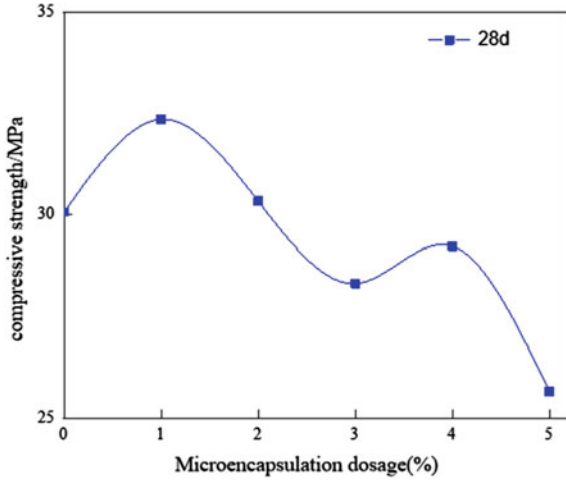


Fig. 6 Compressive strength of specimens cured for 28 days

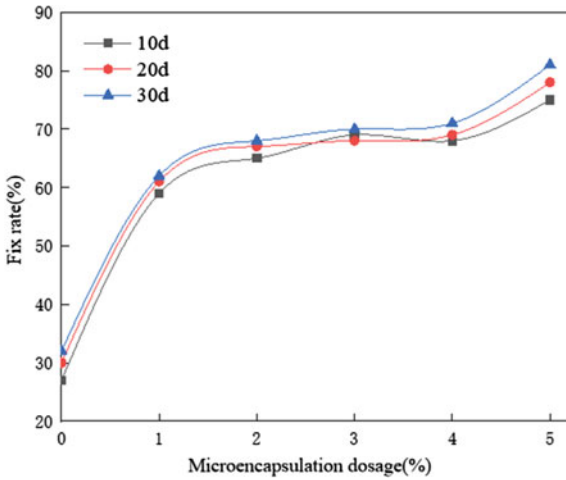


Fig. 7 Compressive strength recovery rate

material, and the fewer particles of fully hydrated cement, the greater the recovery rate. The slowdown in the growth of K_x is explained by the limitations of the microcapsules that have not reacted, and an increase in the duration of recovery does not give the desired effect. In parallel with this, the expansion of bentonite, which has already entered into reactions, leads to the filling of cracks with neoplasms and a decrease in the flow of water from the outside.

The compressive strength and recovery rate of concrete are more influenced by microcapsules, and graphene serves as an additive that improves the conductive properties of the cement composition. Therefore, the effect of graphene was studied under other

constant conditions: the content of microcapsules was 2%, and the cement composite hardened for 28 days.

With an increase in the graphene content in the composite, the strength of concrete steadily increases to a composition of 0.1% graphene and reaches a value of 121.6% of the control (see Fig. 8). A further increase in the proportion of graphene leads to a decrease in strength and with a content of 0.5%, concrete has a compressive strength of only 92%. The results obtained are explained by the fact that graphene, with a low content, accelerates the processes of cement hydration, fills voids at the micro level, and also changes the structure of hydration products.

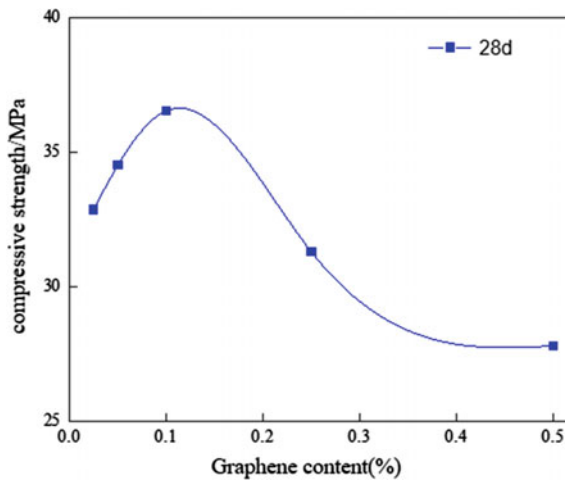


Fig. 8 Compressive strength of a 28-day specimen

Another mechanism of action of graphene can be explained by its high specific surface area, which contributes to the binding of water, distributing it evenly throughout the cement matrix. With a further increase in the content, graphene oxide particles aggregate and form microcells with zero strength, which creates points with increased internal resistance.

Surface resistance was also determined on samples that hardened for 28 days. It was found that the minimum graphene content does not significantly affect the resistance, and the composition with 0.1% graphene has a resistance of only 48% of the control (see Fig. 9). A further increase in the proportion of graphene does not significantly affect the resistance and it even increases slightly, which is also explained by the aggregation of dispersed particles and a simultaneous decrease in the plasticity of the cement mixture, which leads to a decrease in the quality of molding and the formation of air voids with high resistance.

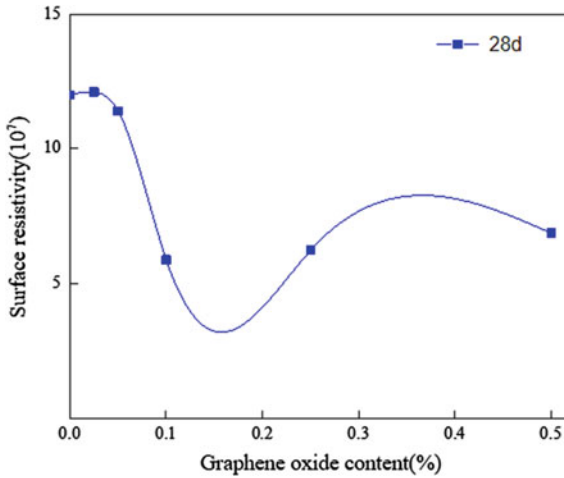


Fig. 9 Surface resistance distribution of specimens

4 Conclusions from the Results of Experiments

1. The developed microcapsules containing sodium silicate and bentonite and obtained by the physical method can improve the self-healing efficiency of the cement composition (the recovery rate of compressive strength is higher than that of ordinary samples). Methods of microscopy and X-ray diffraction analysis have established that the microcapsules have a spherical shape with a high-quality shell of a rough surface. After the shell cracks, the capsule core material is released and its reaction products are deposited in the cracks, filling them and thereby repairing them.
2. The introduction of microcapsules up to 1% increases the compressive strength, however, with a further increase in the proportion of microcapsules, the strength gradually decreases and at a content of 3.0% it is lower than the control composition. The recommended content of microcapsules is 2%, which gives optimal compressive strength and self-healing effect.
3. The introduction of graphene oxide into the composition first increases the strength of the concrete, and then decreases. The optimal content of graphene oxide in the concrete composition is from 0.05 to 0.15%, which allows the most complete use of this advantage.
4. The addition of graphene oxide improves the conductivity of cement concrete, the optimal content is 0.1%: below this, graphene improves conductivity less, and exceeding it does not improve this characteristic, and taking into account the cost of the material, it is not economically feasible.

References

1. Dry C, Mcmillan W (1999) Three-part methylmethacrylate adhesive system as an internal delivery system for smart responsive concrete. *J Smart Mater Struct* 5(3):297

2. Mao Q, Wu W, Liang P et al (2018) Self-healing effect of calcium alginate/epoxy microcapsules in cement-based materials. *J Mater Rep* 32(22):4016–4021
3. Li VC, Robust EH (2012) Self-healing concrete for sustainable infrastructure. *J ACT* 10(6):207–218
4. Dong BQ, Fang GH, Wang YH et al (2017) Performance recovery concerning the permeability of concrete by means of a microcapsule based self-healing system. *J Cem Concr Compos* 78:84–96
5. Wang X, Xia L, Fu X, Xu W, Wang X (2020) Particle characteristics and sustained release properties of epoxy resin/ethyl cellulose microcapsule. *J Build Mater* 23:396–400
6. Zhang P, Feng J, Chen W et al (2018) Research and progress of self-repair technology for concrete damage. *J Mater Rep* 32(19):3375–3386
7. Lv L, Yang Z, Chen G et al (2016) Synthesis and characterization of a new polymeric microcapsule and feasibility investigation in self-healing cementitious materials. *J Constr Build Mater* 105(15):487–495
8. Dong X, Guan X, Ou J et al (2010) Effect of particle size distribution on properties of resin-based magnetostrictive composites. *J AMCS* 27(02):1–8
9. Ou J, Guan X, Li H (2006) Research progress of stress self-sensing cementitious composites and their sensors. *J Compos* 4(04):1–8
10. Bergman SD, Wudl F (2007) Mendable polymers. *J Mater Chem* 18(1):41–62
11. Kan L, Shi H, Qu G et al (2011) Self-healing process and products of engineering cementitious composites. *J Tongji Univ (Natural Science Edition)* 39(10):1517–1523
12. Zhang M, Chen L, Xing F et al (2014) Properties of percolation structure of self-healing cementitious composites based on UF/E microcapsule. *J Build Mater* 17(4):706–710
13. Wang R, Hu H, Liu W et al (2012) The effect of synthesis condition on physical properties of epoxy-containing microcapsules. *J Appl Polym Sci* 124(3):1866–1879
14. Duan T, Huang G, Ma L et al (2020) Preparation and corrosion resistance of Q235/Ni-Co-based self-healing coating. *Chin J Mater Res* 34(10):777–783
15. Xing R, Zhang Q, AII Q et al (2009) Preparation of reactive vinyl silicone oil/polyurea formaldehyde self-healing microcapsule. *Mater Rep* 23(10):87–89
16. Lyu Z, Chen H (2014) Research progress on autonomous healing of cracks in cement-based materials. *J Chin Ceram Soc* 42(02):156–168
17. Dang X, Zhang H, He Y (2005) Research on capsule-type self-healing intelligent composites. *Mater Rep* 4(01):30–32
18. Yan Y, Luo Y, Zhang H (2011) Preparation and performance of self-healing microcapsules. *J Chem Eng Chin Univ* 25(03):513–518
19. Zhu K, Qian C, Li M et al (2020) Effects of size and content of microcapsule repair agent on release rate of microbial self-healing concrete. *Mater Rep* 34(S2):1212–1216
20. Yang G, Jiang G, Liu T et al (2021) Preparation of temperature-controlled self-healing microcapsules and their application in cementing cement slurry in hydrate formation. *Mater Rep* 35(02):2032–2038
21. Zhang M (2013) Research on self-healing technology and principle of microcapsules for cement-based materials. Central South University
22. Wang R (2014) Preparation and properties of microcapsules for waterborne self-healing coatings. Beijing University of Technology



Influence of Preliminary Decompression on Soil Swelling Pressure

M. S. Kim^(✉) and V. Kh. Kim

Voronezh State Technical University, 84, 20 Years of October St., Voronezh 394006, Russia
marskim@yandex.ru

Abstract. The article describes the results of experimental studies of the influence of preliminary decompaction on the magnitude of the swelling pressure of soils of natural and disturbed structure. The determination of the swelling pressure at various degrees of preliminary decompaction was carried out in laboratory conditions for clays of natural and disturbed structure. The conducted researches made it possible to reveal the features of the patterns of influence on the process of swelling of the mineralogical composition of the soil from its initial density and moisture content. In montmorillonite clays, decompaction reduces the swelling pressure as more, as more montmorillonite is included in their composition. In the soil of a disturbed structure, the initial density and moisture do not affect the dependence of the relative magnitude of the swelling pressure on the degree of preliminary decompaction of the soil. In a soil of natural structure, an increase in the initial density contributes to a more significant decrease in the swelling pressure from preliminary decompaction compared to the pressure developed by the soil in the complete absence of swelling deformations. Structural cohesion in soils of natural composition prevents the decrease in swelling pressure during decompaction. It was revealed that the relationship between the relative magnitude of the swelling pressure and the degree of preliminary decompaction of the soil can be described by an exponential function. The values of the coefficients of this function are determined.

Keywords: Swelling soil · Swelling pressure · Laboratory tests

1 Introduction

The foundations of structures based on swelling soils, and any structures buried in this soil, receive additional pressure from swelling when there is a soaking of the soil mass adjacent to the structure [1, 2]. This is a significant problem in construction both in Russia [1–3] and in many countries of the world [4–7].

Preliminary soil decompaction reduces the magnitude of the swelling pressure the more, the higher the specified decompaction [1, 8, 9].

Features of the development of soil swelling and the influence of various factors on this process are the subject of study by many scientists [4–14].

This article is devoted to experimental studies of the effect of preliminary soil decompaction on the magnitude of the swelling pressure.

2 Materials and Methods

The swelling pressure was determined in the laboratory at various degrees of preliminary decompaction of the soil for Khvalyn chocolate clay (Volgograd) and overburden clay (Sergiev Posad, Moscow region) of natural and disturbed structure in accordance with the requirements of regulatory documents [15].

The physical properties of soils are presented in Table 1.

Table 1 Physical characteristics of the studied soils

Name of soil	Soil moisture W , %	Liquid limit w_L , %	Plastic limit w_p , %	Plasticity index	Density, g/cm^3			Porosity factor e	Degree of humidity S_r
					ρ	ρ_s	ρ_d		
Khvalyn chocolate clay of natural structure	5–20	58.2	24.8	33.4	1.35–1.65	2.76	1.28–1.38	1.0–1.15	0.12–0.51
Khvalyn chocolate clay of disturbed structure	20–35	59.5	26.7	32.8	1.8–1.9	2.76	1.33–1.45	0.89–1.05	0.78–1.0
Overburden clay of disturbed structure	10–15	34.2	15.2	19	1.52–1.79	2.7	1.38–1.55	0.74–0.96	0.30–0.40

The mineralogical composition of the Khvalyn chocolate clay includes illite—71%, kaolinite—28%, and a small amount of montmorillonite and Halloysite.

The mineralogical composition of overburden clay includes montmorillonite—23%, illite—6% and kaolinite—14%.

The studies were carried out in a consolidometer. The swelling pressure was determined by consolidation test. Preliminary soil decompaction was created by lifting locking device by a predetermined value.

Several samples of the same density and soil moisture were prepared simultaneously. A part of the samples was soaked from the prepared batch, without preload to determine the amount of free swelling. The other part of the samples was tested with a fully twisted ring of the locking device, and the rest of the samples were tested with raising the ring of the locking device to a height equal to 2, 4, 6, 8% of their original height, which, as a result of swelling during soaking, created a preliminary decompaction of the soil by the appropriate size. All these preliminary soil decompaction samples were tested by the same procedure as natural ones.

The swelling of the samples was determined according to the readings of the dial gauge with an accuracy of 0.01 mm. The time of preliminary soaking of the samples under the locking device was set according to the stabilization time of the free swelling of identical samples. The results of determining the swelling pressure at various degrees

of preliminary decompaction for the Khvalyn chocolate clay and overburden clays of a disturbed structure are shown in Figs. 1 and 2.

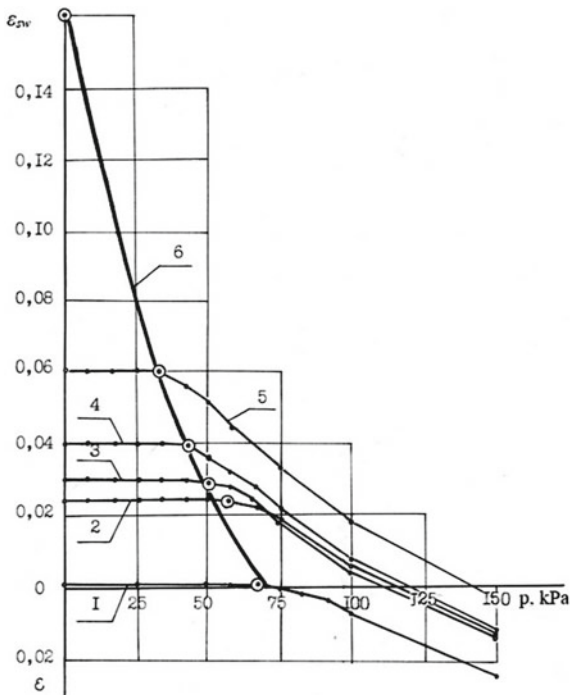


Fig. 1 Relationship between the relative swelling ε_{sw} of the Khvalyn chocolate clay of the disturbed structure and the pressure p at various preliminary decompaction η ($W = 10\%$; $\rho_d = 1.32 \text{ g/cm}^3$; $S_r = 0.274$) (1) $\eta = 0.001$; (2) $\eta = 0.025$; (3) $\eta = 0.041$; (4) $\eta = 0.051$; (5) $\eta = 0.061$; (6) curve $P_{sw} = f(\eta)$

The application of a load to soil with a disturbed structure leads to a sharp increase in compressive deformations when the load slightly exceeds the swelling pressure. A well-defined break in the graph curve appears, corresponding to the swelling pressure when testing the soil under the locking device (Figs. 1 and 2). The soil of natural structure has other patterns when a load is applied above the swelling pressure, so its deformations change slowly under the influence of an increasing load. The graph $\varepsilon_{sw} = f(p)$ has the form of a smooth curve without a break when testing such soil under a locking device (Fig. 3). The magnitude of the swelling pressure in this case corresponded to such a pressure at which the subsequent stage of loading caused the soil compression deformation to be twice as large as the deformation at the previous stage. Differences in the nature of the compression curve of natural soil and soil of a disturbed structure indicate a significant effect on the process of decompaction during moisture and on the occurrence of swelling pressure of structural bonds, which are completely absent in the latter.

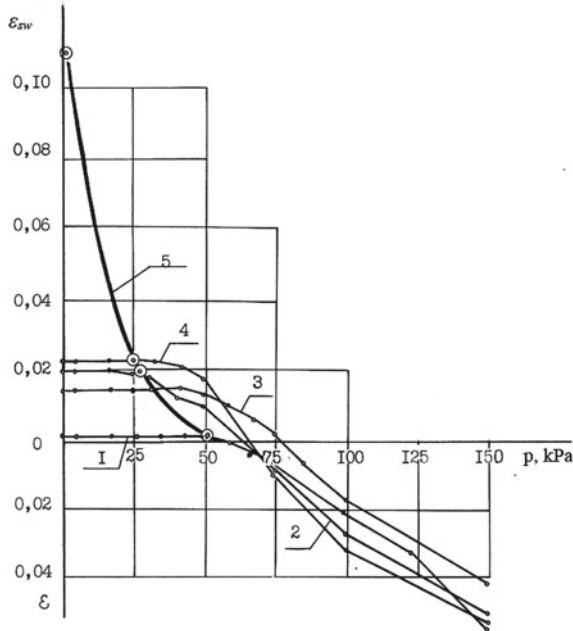


Fig. 2 Relationship between the relative swelling ε_{sw} of the disturbed structure overburden clay and the pressure p at various preliminary decompaction η ($W = 10\%$; $\rho_d = 1.55 \text{ g/cm}^3$; $S_r = 0.364$) (1) $\eta = 0.001$; (2) $\eta = 0.015$; (3) $\eta = 0.02$; (4) $\eta = 0.023$; (5) curve $P_{sw} = f(\eta)$

3 Results

The degree of preliminary decompaction of the soil ($\eta = \Delta h/h$) is equal to the ratio of the absolute value of decompaction (raising the ring of the locking device) Δh to the height of the soil sample h . Studies of the dependence of the swelling pressure on the degree of preliminary decompaction η showed that it is influenced by the initial state, the structure of the soil and its mineralogical composition.

In the soil of a disturbed structure, which is in a state of preliminary decompaction during swelling by a given value η , the magnitude of the swelling pressure is determined by the initial state of the soil. An increase in the initial moisture content of soil of the same density reduces the swelling pressure at the same pre-swelling. An increase in the initial density of the soil at constant humidity leads to an increase in the corresponding pressure values.

The swelling pressure depends linearly on the initial density and initial soil moisture. This linear dependence is preserved under the preliminary decompaction of η . Figure 4a shows a plot of swelling pressure versus initial density ($W = 10\%$) for different pre-decompaction. It can be seen that the slope of the straight lines decreases with increasing η .

Figure 4b shows the dependence of the swelling pressure of a preliminarily decompaction soil on the initial moisture content. The given graphs correspond to the initial soil density $\rho_d = 1.38 \text{ g/cm}^3$.

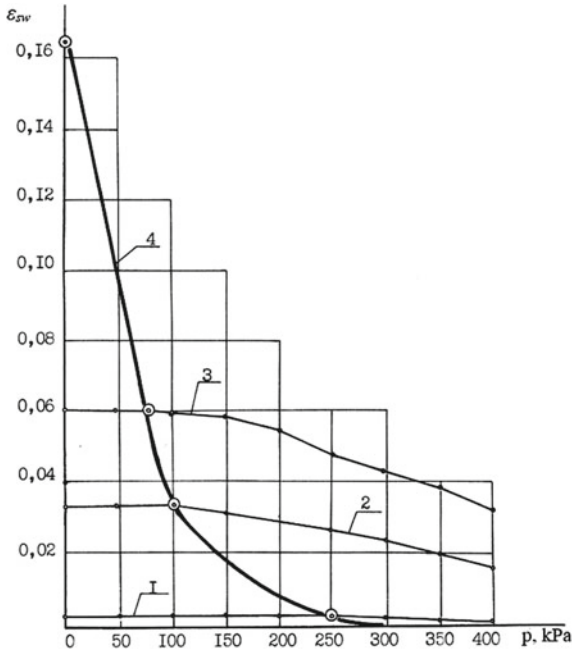


Fig. 3 Relationship between relative swelling ϵ_{sw} of Khvalyn chocolate clay of natural structure and pressure p at various preliminary decompaction η ($W = 32\%$; $\rho_d = 1.455 \text{ g/cm}^3$; $Sr = 0.993$) (I)— $\eta = 0.003$; (2)— $\eta = 0.034$; (3)— $\eta = 0.061$; (4)—curve $P_{sw} = f(\eta)$

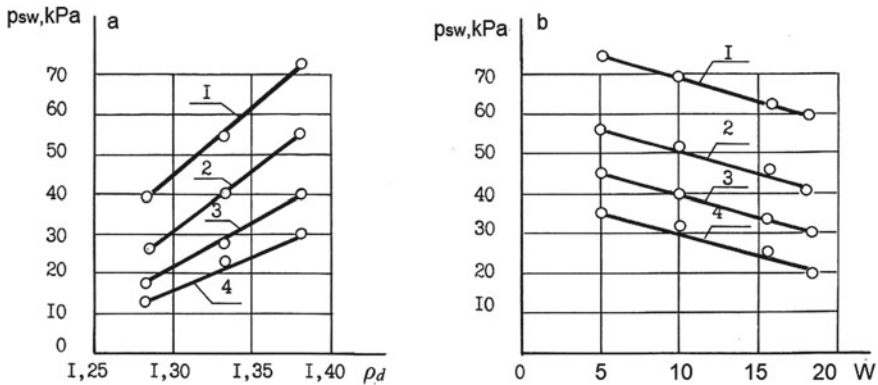


Fig. 4 Relationship between swelling pressure and soil density ($W = 10\%$) (a) and swelling pressure and soil moisture ($\rho_d = 1.38 \text{ g/cm}^3$) (b) at preliminary decompaction η (I) $\eta = 0$; (2) $\eta = 0.02$; (3) $\eta = 0.04$; (4) $\eta = 0.06$

The initial density of the soil has a great influence on the relationship between the swelling pressure and the degree of preliminary decompaction in the soil of natural structure.

The mineralogical composition of the soil also significantly affects the process of reducing the swelling pressure during decompression (Fig. 5).

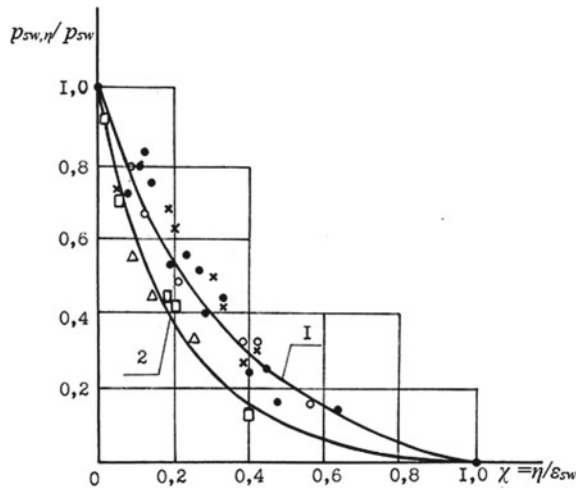


Fig. 5 The relationship between the decrease in the swelling pressure of soil of a disturbed structure and the relative decompression Khvalyn chocolate clay (•— $\rho_d = 1.28 \text{ g/cm}^3$; ○— $\rho_d = 1.33 \text{ g/cm}^3$; x— $\rho_d = 1.28 \text{ g/cm}^3$) cover clay (□— $\rho_d = 1.38 \text{ g/cm}^3$; Δ— $\rho_d = 1.55 \text{ g/cm}^3$)

Decompression reduces the swelling pressure of overburden clays more than for the Khvalyn chocolate clay. The first contains 23% montmorillonite, while the second contains a small amount. As can be seen from Fig. 4, the relative decompression by 20% of the value of free swelling ε_{sw} in overburden clay reduces the swelling pressure by 60%, and in Khvalyn chocolate clay it decreases by 46%.

The graphs presented in Fig. 5 show that in the soil of a disturbed structure, the initial state has little effect on the nature of the relationship between the decrease in swelling pressure and relative decompression. Here are the results of experiments with Khvalyn chocolate clay of a disturbed structure, which has an initial density of dry soil $\rho_d = 1.28, 1.33, \text{ and } 1.38 \text{ g/cm}^3$ (curve 1). The experimental points are located quite closely near one curve, regardless of the corresponding values of the initial density-humidity. The same character of the arrangement of experimental points is also observed for overburden clay-paste with a density of dry soil of $\rho_d = 1.38 \text{ and } 1.55 \text{ g/cm}^3$ (curve 2).

The initial density of the soil significantly affects the decrease in swelling pressure during decompression in the soil of natural structure. This decrease is more noticeable in a soil with a high density than in a soil of a lower density (Fig. 6).

It can be seen from the graphs that the preliminary swelling of the soil by 5% of its free swelling value reduces the pressure value compared to the swelling pressure in the absence of decompression by 60% for clay $\rho_d = 1.60 \text{ g/cm}^3$, by 20% for clay $\rho_d = 1.45 \text{ g/cm}^3$ and by 8% for clay $\rho_d = 1.33 \text{ g/cm}^3$.

The decrease in the swelling pressure of preliminary decompression is associated with the action of adsorption, capillary and osmotic forces, which lead to thickening of

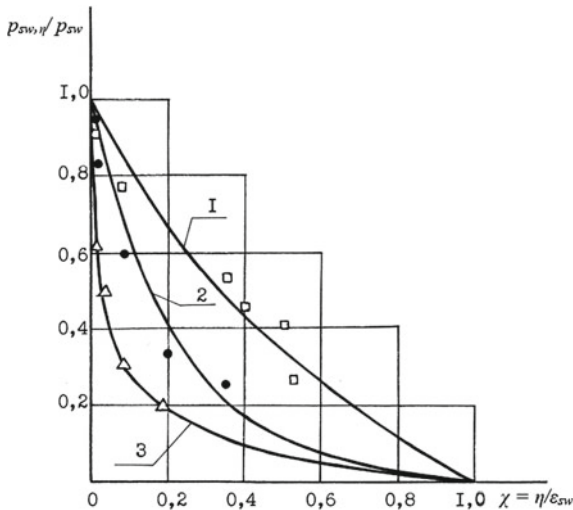


Fig. 6 Relationship between swelling pressure reduction of Khvalyn chocolate clay of natural structure and relative decompaction (1) $\rho_d = 1.33 \text{ g/cm}^3$; (2) $\rho_d = 1.45 \text{ g/cm}^3$; (3) $\rho_d = 1.60 \text{ g/cm}^3$

the hydrate shells, wedging and weakening of the action of molecular cohesive forces between clay particles.

The state of the wetted soil without the possibility of increasing its volume ($\epsilon_{sw} = 0$) corresponds to the smallest thickness of water films and the highest disjoining pressure that occurs at the points of particle contacts, which is balanced by the external pressure taken as the swelling pressure. Preliminary decompaction of the soil increases the thickness of the hydrated shell due to weakly bound water and thereby reduces the disjoining pressure. Less external pressure is required to balance it in this case, i.e. swelling pressure is reduced.

As the soil density increases, the number of contacts between particles increases. Decompaction reduces their number, and the more, the higher the initial density of the soil. Therefore, the relative decrease in swelling pressure is related to the initial density of the soil and is more pronounced in dense soils.

Structural cohesion prevents decompaction for natural soil at the same time. The relative decrease in swelling pressure is less in soil of natural structure than in soil of disturbed structure at the same density. This can be seen from a comparison of curve I in Fig. 5, constructed for natural soil, the density of which $\rho_d = 1.33 \text{ g/cm}^3$ is in the range of densities of the investigated soil of disturbed structure, with curve I in Fig. 4, expressing the decrease in swelling pressure during decompaction of soil of a disturbed structure of different density-humidity. If a relative decompaction of 5% reduces the swelling pressure by 8% in the first case, then in the second case the same decompaction leads to a decrease in the swelling pressure by 15%.

The mineralogical composition of the soil affects the decrease in swelling pressure during decompaction, and this is due to the different nature of the interaction of clay minerals with water. Thus, montmorillonite has the property of intracrystalline swelling, in contrast to kaolinite. The penetration of water molecules weakens the molecular

cohesive forces between clay particles in the interpackage space of this mineral and helps to reduce the density of the soil and, accordingly, the swelling pressure. This explains the fact that the effect of preliminary decompression on the swelling pressure of cover clay is more significant than that of Khvalyn chocolate clay. Obviously, the effect of preliminary decompression will be the stronger on the magnitude of the swelling pressure in montmorillonite clays, the more montmorillonite is included in their composition.

4 Discussion

The experiments made it possible to establish the relationship between the relative value of the swelling pressure on the degree of preliminary decompression of the disturbed and natural soil structure, which can be represented as an exponential function. The swelling pressure can be determined by the formula in the case of the possibility of preliminary decompression of the soil.

$$p_{sw,\eta} = (A \cdot e^{-B\chi} - C)p_{sw}, \quad (1)$$

where $p_{sw,\eta}$ —swelling pressure at decompression η , p_{sw} —swelling pressure at constant sample volume ($\eta = 0$);

$\chi = \eta/\varepsilon_{sw}$ —the ratio of decompression η to the amount of free swelling ε_{sw} ; A , B , C —parameters determined empirically.

The parameters of Eq. (1) A , B , C were selected by statistical analysis using the least squares method. The values of the coefficients of Eq. (1) are presented in Table 2 for the studied soils.

Table 2 The values of the coefficients of Eq. (1) according to the results of statistical processing

Soil type	Coefficients of the Eq. (1)		
	A	B	C
Khvalyn chocolate clay of disturbed structure	1.08	2.63	0.08
Overburden clay of disturbed structure	1.013	4.44	0.013
Khvalyn chocolate clay of natural structure			
$\rho_d = 1.33 \text{ g/cm}^3$	1.39	1.25	0.39
$\rho_d = 1.45 \text{ g/cm}^3$	1.014	4.24	0.014
$\rho_d = 1.60 \text{ g/cm}^3$	1.001	10.80	0.001

5 Conclusions

1. The study of the regularities of swelling pressure reduction due to preliminary decompression of the soil due to its swelling showed that the relative decrease in swelling pressure during preliminary decompression depends on the structure of the soil and its mineralogical composition.

2. The initial density and humidity do not affect the nature of the dependence of the relative magnitude of the swelling pressure on the degree of preliminary decompaction of the soil in the soil of a disturbed structure. An increase in the initial density contributes to a more significant decrease in the swelling pressure from preliminary decompaction in the soil of a natural structure compared to the pressure developed by the soil in the complete absence of swelling deformations.
3. Structural cohesion for soils of natural composition prevents the decrease in swelling pressure during decompaction. The relative decrease in swelling pressure in soil of natural structure is less than in soil of disturbed structure at the same density.
4. The effect of preliminary decompaction on the magnitude of the swelling pressure is the stronger in montmorillonite clays, the more montmorillonite is included in their composition.
5. The dependence of the relative magnitude of the swelling pressure on the degree of preliminary decompaction of the soil can be described by an exponential function. The coefficients included in the equation of the approximating curve are constant for soil of a disturbed structure of the same mineralogical composition, and for soil of a natural structure they change with a change in the initial density.

References

1. Sorochan EA (1989) Construction of structures on swelling soils. Moscow
2. Golli OR (2004) Use of the patterns of swelling of clay soils in construction. *J Reconstr Cities Geotechn Constr* 8:132–141
3. Olyansky YI, Trokhimchuk MV (1998) On the issue of swelling clay pounds in the Volgograd region Tez. report. In: International scientific and practical conference Türkiye-Kemer, pp 77–78
4. Olyansky YI, Bogdevich OP et al (1991) Relationship between swelling of Sarmatian clays of Northern Moldova and the degree of their aggregation. *News Acad Sci MSSR Phys Technol* 1(4):61–66
5. Ashram Mahmoud Nihad (1999) Swelling pressure depending on the physical properties of dusty clay soils. *J Municipal Serv Cities Rel* 19-K:120–122
6. Lates EM, El Monshid BEP, Abbo SH (1983) Review of problems generated by expansive soils in Sudan. In: Proceedings of the seminar on expansive clay soil problems in the Sudan, Wad Medani, 29–30 Jan 1983, pp 11–20
7. Liang WY, Yan RT, Xu YF, Zhang Q, Tian HH, Wei CF (2021) Swelling pressure of compacted expansive soil over a wide suction range. *J Appl Clay Sci* 203:106018
8. Sorochan EA, Ryabova MS (1988) Swelling soil pressure on retaining walls. *J Soil Mech Found Eng* 3:9–11
9. Dashko RE, Shidlovskaya AV (2013) Physico-chemical nature of swelling and osmotic shrinkage of clayey rocks at the base of structures according to the results of experimental studies. *Notes Min Inst* 200:193–200
10. Franklin JA (1984) A ring swell test for measuring swelling and shrinkage characteristics of rock. *Int J Rock Mech Min Sci Geom Abstr* 21(3):113–121
11. Ruan K, Wang H, Komine H, Ito D (2022) Experimental study for temperature effect on swelling pressures during saturation of bentonites. *J Soils Found* 62:101245
12. Ghalamzan F, De Rosa J, Gajo A, Di Maio C (2022) Swelling and swelling pressure of a clayey soil: experimental data, model simulations and effects on slope stability. *J Eng Geol* 297:106512

13. Yang Y, Qiao R, Wang Y, Sun S (2021) Swelling pressure of montmorillonite with multiple water layers at elevated temperatures and water pressures: a molecular dynamics study. *J Appl Clay Sci* 201:105924
14. Kaufhold S, Baille W, Schanz T, Dohrmann R (2015) About differences of swelling pressure—dry density relations of compacted bentonites. *J Appl Clay Sci* 107:52–61
15. STST 12248.6-2020 (2020) Soils. Method for determining swelling and shrinkage. Moscow



Computer Simulation of a Prefabricated Spatial Framework

N. Tsaritova^(✉), A. Kurbanov, A. Kurbanova, and A. Shtankevich

Platov South-Russian State Polytechnic University (NPI), 132, Prosveshcheniya,
Novocherkassk 346428, Russia
ncaritova@yandex.ru

Abstract. The object of the study is a spatial hinge-rod structure. The research method—the analysis of the wide variability of the forms of hinge-rod joints, the economical installation process using the principle of “self-expansion” allow us to speak about the relevance of research in this direction. The article gives an overview of spatial structures and shows the pros and cons of such structures. Examples of popular nodal connections of rod structures are given. Results: development of general principles for the formation of a spatial rod structure, development of a hinge joint, a finite element coating model. As a result of the analysis of existing prefabricated buildings, the authors of the article present their surfaces main shapes. A variant of the swivel joint developed by the authors in the COMPASS-3D software package is presented, and a model of the frame is obtained. The introduction of new types of spatial architectural and structural systems into the practice of construction is the historical objectivity of the interaction of architecture and scientific and technological progress.

Keywords: Computer simulation · Spatial structures · A prefabricated spatial framework

1 Introduction

The use of spatial skeleton is widespread both in civil and industrial construction [1–5]. The main advantages of spatial skeleton is the ability to overlap large space without internal supports, which allows the use of space without restrictions [6–8].

The disadvantages include a large number of nodal connections and core elements and the complexity of installation.

Currently, spatial frameworks are widely used; an example is the Biotechnopark of the Novosibirsk region (Fig. 1). The glass facade flows into the dome above the atrium. The facade is a mesh structure using the “SpaceStructure” technology: a cylindrical nodal system, a single-layer structure in a triangular geometric surface.

In construction practice, spatial metal structures of tubular cross-section are widely used, due to the elegance of forms. An example is a tower built in 2011 in Cincinnati, USA, on top of which there is a steel structure consisting of 15 arches and hundreds of other steel elements, which looks like a tiara (Fig. 2). The main arches are made of pipes



Fig. 1 Biotechnopark, Novosibirsk region

with a diameter of 16 inches, the remaining arches are made of pipes with a diameter of 4 to 8625 inches.



Fig. 2 The Great American Tower, Cincinnati, USA

Steel tubular rods with proper protection are more resistant to corrosion and fire. However, the manufacture of tubular rod assemblies is quite time-consuming and expensive, since it requires a large amount of cutting, drilling and welding, which increases the cost of the project [9–13].

The development of new prefabricated buildings and structures based on a metal frame is an urgent topic of modern research. Frames of this type can be used both for energy-efficient buildings in the conditions of the north, and in emergency situations for temporary accommodation of people.

2 Methods and Materials

The authors examined examples of patented frames of prefabricated buildings, analyzed their pros and cons, and also proposed their own version of a metal frame that meets all modern requirement.

The invention, patented in 1995, presented in Fig. 3, is a metal frame, including a two-pitched crossbar, inclined posts, vertical tightening and inclined braces, forming a symmetrical structure relative to the vertical axis when connected [14].

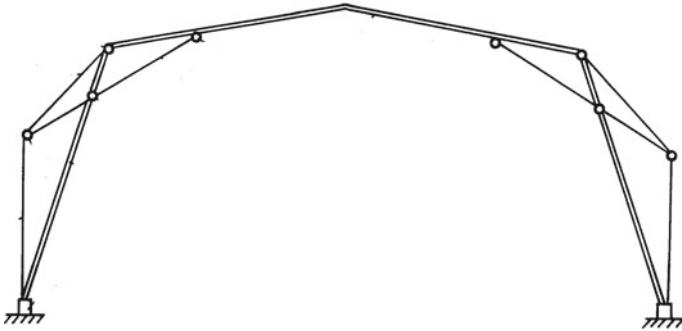


Fig. 3 Metal frame of the building

The advantages of this frame include: a combination of cross bars, braces, struts and tightens provide multiple triangular rigidity; accelerated assembly and design development.

And the disadvantages: the complexity of the connection nodes of its elements; the impossibility of quick installation and dismantling of structures due to the presence of a tightening built into the foundation.

Another invention patented in 2009, shown in Fig. 4, is a folding hinged metal frame for mobile structures and shelters, containing transverse struts connected pivotally to form transverse bearing arches, and longitudinal struts pivotally connected to transverse struts to form longitudinal bearing belts [15].

The advantages include: the radius of the arc on which the vertices of the trapezoids are located is able to provide a large height of the trapezoid; the spacers connecting the transverse arches serve to determine the length of the frame and increase the strength of the structure.

The disadvantages include: the complexity of the installation and dismantling of the metal frame; low strength characteristics.

The invention, patented in 2015, presented in Fig. 5 the frame of a collapsible structure, including pivotally connected elements of an arch-frame structure in the form of belts with brackets forming cells of four-link mechanisms, support hinges [16].

The advantages include the assembly of the frame by alternately attaching one element of the upper belt and the ascending brace to the mounted part of the frame; the ability to perform installation work mainly on the ground, there is no need for work at

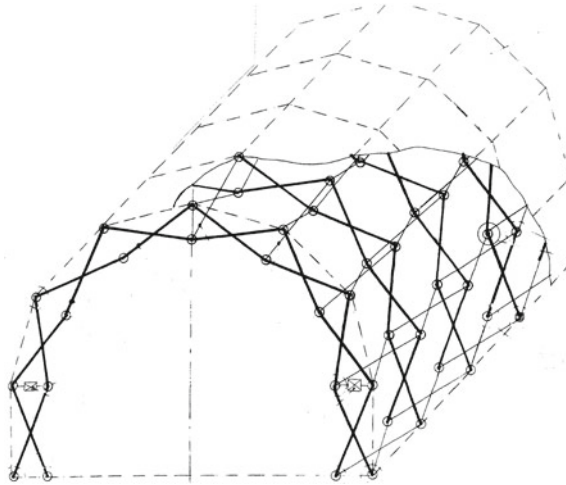


Fig. 4 Folding hinged metal frame for mobile structures and shelters

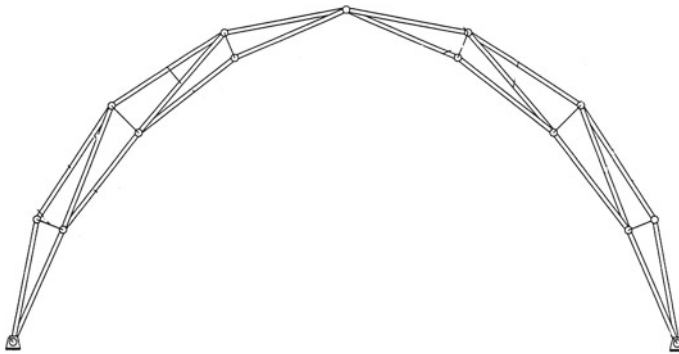


Fig. 5 The frame of a prefabricated structure

height, which increases the safety of construction; if necessary, during the pre-assembly process, elements of roofing fencing can be attached to the frame.

The disadvantages include: limited use with an increase in span, because at the same time it is necessary to increase the length of the elements and, as a consequence, weighting the structure. In addition, it is difficult to rest on the ground part of the intermediate nodes of the frame, which complicates the installation.

A pre-fabricated dome, patented in 2017, shown in Fig. 6, is made in the form of a combination of pentahedrons and hexahedrons [17].

The advantages include: good fire resistance, high service life, good corrosion resistance and good earthquake resistance.

Disadvantages: limited use when increasing the span, because at the same time, the structure is weighted.

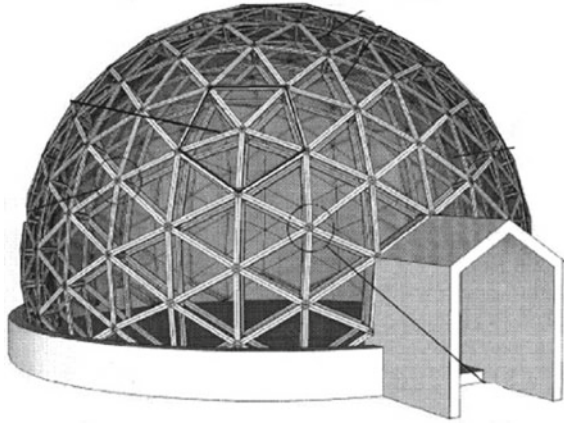


Fig. 6 The frame of a prefabricated dome

With the development of spatial structures, the design of nodal connections also began to develop. Currently, a large number of compounds that have been developed by domestic and foreign developers are known. Work on the creation of a nodal connection of spatial rod structures with an ideal price-reliability ratio continues at the present time.

One of the most popular systems with an Odebolt connection is the “Mero” system (Fig. 7), it is considered one of the most accessible for creating spatial lattice structures. Round tubular elements are connected at the nodes with cast “balls” using one hidden bolt for each tube. This concept was developed on the basis of studies of natural structures conducted in the 1930s by the creator of the system, Dr. Max Mengerinhausen [18].

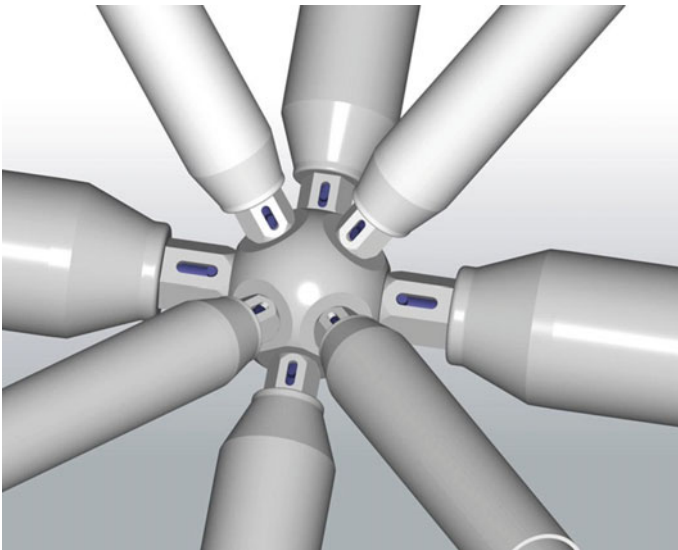


Fig. 7 Node connection “Mero”

The British corporation has developed a hollow spherical node of the Nodus system (Fig. 8). The node consists of two half cross-shaped shapes connected using a single high-strength friction bolt, nut and washer.

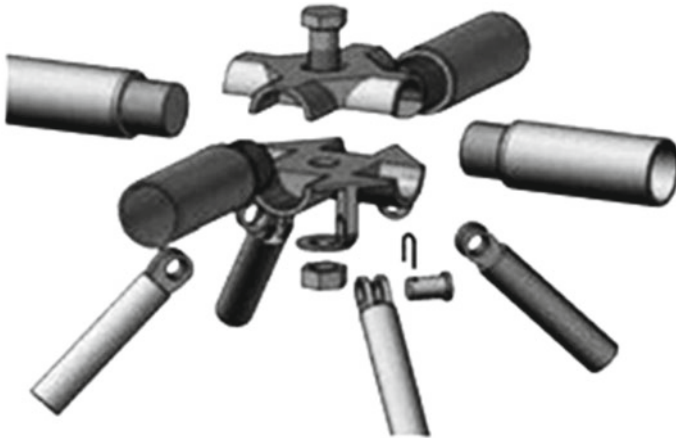


Fig. 8 Node connection

The disadvantage of the system is the complexity of manufacturing complex shaped parts.

The designers of large-span rod structures are currently engaged in the development of new material-intensive, compact, easy-to-assemble nodal joints.

3 Results

As a result of the analysis of existing prefabricated buildings, the authors of the article in Table 1 present their main surface shapes, they are divided into cylindrical (mesh arches), spherical (mesh domes), conical shells and transfer shells, and the latter two types of shells are used relatively rarely, examples are given.

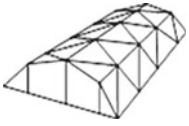


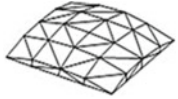
Currently, the authors are developing a prefabricated frame of a temporary building based on a mesh dome, which can be quickly disassembled and assembled, used in seismic areas. The design scheme in the plan is shown in Fig. 9.

The uniqueness of this design lies in the nodal connection of the rods this type of node makes compact packaging and delivery to the construction site possible.

The nodal element for this type of construction is a patented hinge assembly of a spatial rod structure [19, 20], shown in Fig. 10.

The nodal consists of rod elements of different lengths, Fig. 11, in the diagram in Fig. 9 they are marked with different colors for ease of assembly of the frame.

Table 1 The main forms of the surface of prefabricated buildings

Surface Shapes	Title
	Cylindrical (mesh arches)
	Spherical (mesh domes)
	Conical shells
	Transfer shells

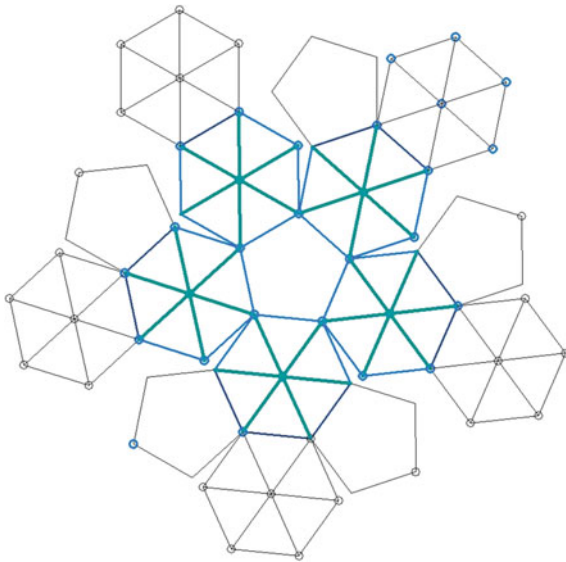


Fig. 9 The design scheme in the plan

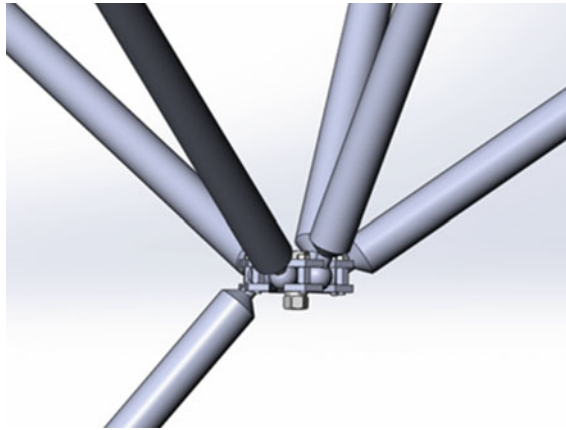


Fig. 10 The hinge assembly of a spatial rod structure

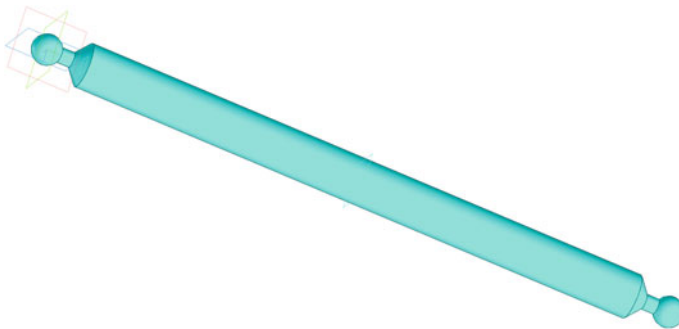


Fig. 11 Rod elements of different lengths

4 Conclusion

The obvious advantages of this system in low material consumption, mobility, unification and standardization allow it to be used in the organization of various temporary, quick-mounted coatings of buildings used in the liquidation of natural and man-made emergencies. The possibility of using various types of energy-efficient coatings makes such a design relevant in the modern world.

As a result of the work, a computer model of the frame was obtained (Fig. 12).

The use of the proposed spatial coating has a number of advantages compared to known structures, thanks to the new nodal connection, stability is ensured without additional structural elements (braces, puffs, etc.), which on average account for about 25% of the material consumption of the entire volume, this can significantly reduce the metal consumption.

The purpose of the invention is to increase reliability, reduce transportation costs and reduce installation time.

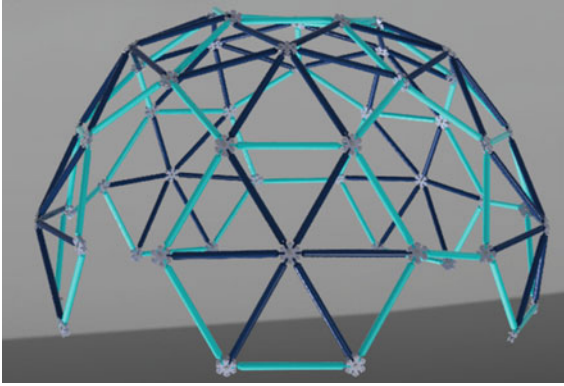


Fig. 12 A computer model

The introduction into the practice of construction of new types of spatial architectural and structural systems capable of solving the problems of socio-functional, technological and aesthetic formation of the architectural environment based on industrial methods is the historical objectivity of the interaction of architecture and scientific and technological progress.

References

1. Gómez-López M, Miguel V, Martínez A, Coello J, Calatayud A (2013) Simulation and modeling of single point incremental forming processes within a solidworks environment. *Procedia Eng* 63:632–641. <https://doi.org/10.1016/j.proeng.2013.08.253>
2. Mackevičius J, Tomašević V (2011) Model for evaluating the economic efficiency of investment projects: architecture and main aspects of application. *Ekonomika* 90(4):133–149. <https://doi.org/10.15388/Ekon.2011.0.920>
3. Arayici Y, Aouad G (2010) Building information modelling (BIM) for construction life-cycle management: design, materials, and techniques. Nova Science Publishers, NY, USA, *Construction and Building*, pp 99–118
4. Chengshuang S, Shaohua J, Mirosław S, Qingpeng M, Liyin S (2015) A literature review of the factors limiting the application of BIM in the construction industry. *Technol Econ Dev Econ* 23:1–14. <https://doi.org/10.3846/20294913.2015.1087071>
5. Azhar S (2011) Building information modeling (BIM): trends, benefits, risks, and challenges for the AEC industry. *Leadersh Manag Eng* 11:241–252. [https://doi.org/10.1061/\(ASCE\)LM.1943-5630.0000127](https://doi.org/10.1061/(ASCE)LM.1943-5630.0000127)
6. Hart F, Henn V, Sontag H (1977) Atlas of steel structures. Multi-storey buildings. Stroyizdat, Moscow
7. Knyazkov VV, Fazlulin EM (2014) Geometric modeling in SolidWorks. In: Proceedings of the Moscow State Technical University MAMI 5, no 1(19), pp 170–176
8. Liu LJ, Ren JP (2005) Application of the secondary development in SolidWorks. *Mecha Manage Dev* 1:74–75
9. Duarte HPCSG, de Lima LRO, da PCG, Vellasco S, da Silva AT (2017) Structural behaviour of stainless steel tubular columns. In: Tubular structures XVI: proceedings of the 16th international symposium for tubular structures, ISTS 2017, 4–6 Dec 2017. <https://doi.org/10.1201/9781351210843-66>

10. Kanyilmaz A (2019) The problematic nature of steel hollow section joint fabrication, and a remedy using laser cutting technology: a review of research, applications, opportunities. *Eng Struct* 183:1027–1048
11. Clean Air Task Force (2009) About EOR. Archived March 13, 2012, at the Wayback Machine
12. Zhao X-L, Tong L (2011) New development in steel tubular joints. *Adv Struct Eng* 14:699–716. <https://doi.org/10.1260/1369-4332.14.4.699>
13. De Oliveira C (2015) Steel castings in structural design—case studies. SEAOC convention proceedings. Bellevue, Washington, DC, pp 427–439
14. Baranov SM, Moskalev NS (1995) Metal frame of the building frame. Patent No. 2040645 C1 Russian Federation, IPC E04B 1/24. No. 5051741/33
15. Artemov AV, Nikolaev NN, Ryabov AN (2009) Folding hinged metal frame for mobile structures and shelters. Utility model Patent No. 87735 U1 Russian Federation, IPC E04H 15/00. No. 2009121351/22
16. Mukhin BG (2015) The frame of a prefabricated structure and the method of its installation. Patent No. 2564292 C1 Russian Federation, IPC E04B 1/343, E04B 1/32. No. 2014113473/03
17. Lii YH (2020) Prefabricated dome. Patent No. 2725192 C2 Russian Federation, IPC E04B 1/32. No. 2017114605
18. Ramaswamy GS, Eekhout M, Suresh GR (2002) Steel space frames, analysis, design and construction. Thomas Telford Publishing, London
19. Tumasov A, Tsaritova N, Kurbanov A, Kalinina A (2017) Geometric parameters of rod transformable arch systems. *Constr Archit* 5:135–140
20. Buzalo NA, Alekseev S, Tsaritova N (2016) Numerical analysis of spatial structural node bearing capacity in the view of the geometrical and physical nonlinearity. *Procedia Eng* 150:1748–1753



The Analysis of the Strength Characteristics of Rubber Concrete as Compared with Ordinary Cement Concrete

A. V. Levchenko¹ and M. V. Shitikova²(✉)

¹ Voronezh State Technical University, 84, 20 Let Oktyabrya St., Voronezh 394006, Russia

² Moscow State Research University of Civil Engineering, 26, Yaroslavskoye Shosse, Moscow 129337, Russia
mvs@vgasu.vrn.ru

Abstract. Increasing the strength of cement concrete could significantly improve the technical and economic performance of structures. However, an increase in strength also entails an increase in the brittleness of the material, as a result of which there is a faster (almost instantaneous) destruction of concrete, and in the case of its destruction in a compressed zone, reinforced concrete elements when they reach the limit state. Thus, the actual problem of modern materials science is to increase the plastic-deformation properties of concrete and resistance to cracking. Polymer concretes obtained on the basis of liquid rubber are usually called Rubcons. Rubber concrete is a more plastic material, the ratio of its compressive strength to tensile strength is 8, while this indicator for ordinary concrete is equal to 18–19, while the modulus of elasticity, of course, is somewhat inferior to the modulus of elasticity of ordinary cement concrete, and is within the level of 25–26 GPa. At the same time, due to the high tensile strength of Rubcon, in the case of the manufacture of reinforced structures, better protection of reinforcing bars from an aggressive environment is provided than in traditional reinforced concrete structures.

Keywords: Polymer concrete · Rubber concrete · Rubcon · Strength · Efficiency

1 Introduction

Elements of structures often operate under the influence of various aggressive environments, while the use of traditional materials (reinforced concrete and steel) without additional protection measures is ineffective. A promising way to solve this problem is to make such structures from composite materials, for example, polymer concrete—materials in which polymers of various nature are used as a binder.

In civil engineering practice, polymer concretes based on polyurethanes, epoxy, polyester and other resins are widely used. However, the industrial production of some of these resins in Russia has been significantly decreased in recent years, as a result of which their cost has risen sharply. In this situation, the solution of issues related to the protection of structures from the aggressive effects of the environment is possible

with the use of alternative types of industrially produced polymers, for example, diene oligomers belonging to the class of liquid rubbers. Polymer concretes obtained on the basis of liquid rubber are called Rubcons [1–6]. It should be noted that rubbers are readily available and widespread, which makes them promising in comparison with the resins used in the production of polymer concrete and cheaper raw materials.

As a result of the research by Potapov and his collaborators [1–8] the quantitative content of the components of the vulcanizing system for the rubber concrete matrix was determined, and the optimal content of the vulcanizer, accelerator and activator were found. At the level of the rubber binder, the qualitative influence of the type of filler on the properties of rubber concrete was revealed, and the boundaries of the amount of filler in the rubber binder and its effect on the physical and mechanical characteristics of the rubber binder were established. Chemical resistance studies have been carried out on Rubcon, which have shown that Rubcon has almost universal chemical resistance. The main technological parameters, modes of manufacturing products and structures from rubber are determined. Solving the problem of expanding the range of low molecular weight rubbers used in the production of high-strength and chemically resistant products and structures, effective composites based on a polybutadiene oligomer of a mixed microstructure of the PBN brand were developed and studied. For composites based on PBN rubber, a rubber matrix has been developed and studied. The influence of the amount of rubber introduced into the composition has been studied. It has been established that the effective limits of its content are within (8–11)% by weight.

Rubber concretes are characterized by favorable deformation and strength characteristics due to the high filling of the mixture [1, 2], high electrical insulating and damping performance, high adhesion to metal surfaces and other properties, which were studied in [1–9]. The main property of rubber concrete, which distinguishes it favorably from analogues, is its high chemical resistance [5, 6] (Table 1).

Table 1 Chemical resistance of rubber concrete [6]

Kind of aggressive environment	Coefficient of chemical resistance calculated due to experimental measurements after	
	1 year	10 years
20% H ₂ SO ₄	0.95	0.95
3% HNO ₃	0.8	0.7
10% C ₆ H ₈ O ₇	0.9	0.8
20% NaOH	0.95	0.95
10% KOH	0.8	0.65
NaCl	0.9	0.8
Gasoline	0.95	0.95
Water	1.0	0.99

Oligodienes (diene hydrocarbons of various microstructures), which belong to the class of liquid rubbers and are capable of forming spatially crosslinked polymers under the influence of specially selected curing systems, are used as a binder in rubbers [3, 4]. Increasing the strength of concrete could significantly improve the technical and economic performance of structures. However, an increase in strength also entails an increase in the brittleness of the material, as a result of which there is a faster (almost instantaneous) destruction of concrete and reinforced concrete elements (in the case of destruction in a compressed zone) when they reach the limit state. Thus, the actual problem of modern materials science is to increase the plastic-deformation properties of concrete and resistance to cracking. The possibility of using reinforced rubber concrete bending elements of various cross-sections was proved in [7, 8], and it was found [8] that reinforced rubber concrete elements undergo 3 stages of the stress–strain state similar to traditional reinforced concrete elements. The fractional parameter for Rubcon, which characterizes the level of its viscoelasticity, was determined in [9] analytically using the fractional derivative standard linear solid model and was identified experimentally by the impulse excitation technique [10].

At the moment, the most accessible liquid rubber in the territory of the Russian Federation is SKDN-N rubber. Rubber SKDN-N has a higher reactivity, that is why it has a lower vulcanization temperature (110–120 °C), which allows one to reduce the amount of hardening group components used and, as a result, to reduce the cost of the composition and labor costs.

2 Materials and Methods

Purpose of this study is to conduct a comparative analysis of the strength characteristics of conventional cement concrete and rubber concrete.

In order to obtain the best strength characteristics, it was decided to use cement instead of fly ash as a first-class material, since the size of the cement fraction ranges from 5 to 40 μm , while the size of the fraction of the ash used is in the range from 5 to 100 μm , namely, the size of the fraction of fine filler is one of the important factors in the formation of crystallization centers during the polymerization of the binder. Table 2 shows the composition of cement concrete, Table 3 presents the composition of rubber concrete with cement, and Table 4 demonstrates the characteristics of the fine and coarse aggregates used.

Table 2 Component composition of ordinary cement concrete

Name of components	Content of components, kg/m^3
Water	180
Cement	360
Sand	681
Crushed stone	1190

Table 3 Component composition of Rubcon SKDN-N with cement

Name of components	Content of components, mass %
Low molecular weight rubber SKDN-N	8.2
Sulphur technical	4.0
Tiuram-D	0.4
zinc oxide	1.2
calcium oxide	0.4
Cement	7.8
Quartz sand	24.2
Crushed stone	53.8

Table 4 Physical properties of sand and gravel

Aggregate	Fraction size, mm	Density, g/cm ³	Bulk density, g/cm ³	Specific surface, cm ² /g	Voidage, %
Granite crushed stone	5.0–10.0	2.67	1.50	5.4	41.4
Quartz sand	1.25–2.50	2.65	1.61	33.0	39.1
	0.63–1.25				
	0.315–0.630				

To determine the deformation-strength characteristics, tests for central compression and axial tensile were carried out. Due to the frequent formation and destruction of beams along an inclined crack of the second type [11], i.e. when the crack does not cross the longitudinal reinforcement, a test was carried out for splitting a cube sample mounted on an edge, the experimental scheme of which corresponds to [12]. The general views of rubber concrete samples and ordinary concrete samples are shown in Figs. 1 and 2, respectively. Geometric parameters of experimental samples for each type of testing are given in Table 5.

According to [12], the tensile strength σ_{st} during splitting is determined by the following formula:

$$\sigma_{st} = 0.5187P/S^2 \quad (1)$$

where P is shear load, and S is the length of the cube edge.

Before testing, the samples were carefully prepared. It was checked that the surface of the samples was even, smooth, without cavities, cracks and other defects, and the ends of the samples were perpendicular to their longitudinal axis. The load was applied at a constant speed. The tests were carried out on certified Instron equipment at the VSTU Collective Research Center. Compressive and tensile deformations were measured by strain gauges, sensor readings were taken using an MGSplus amplifier.

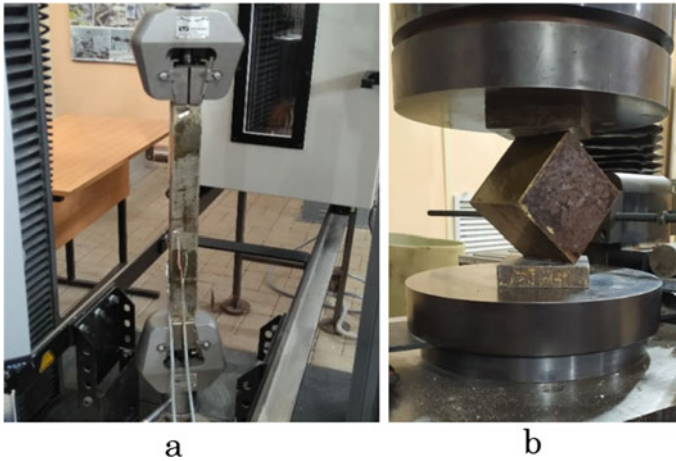


Fig. 1 Rubber concrete: **a** tensile strength sample during testing; **b** sample cube during testing

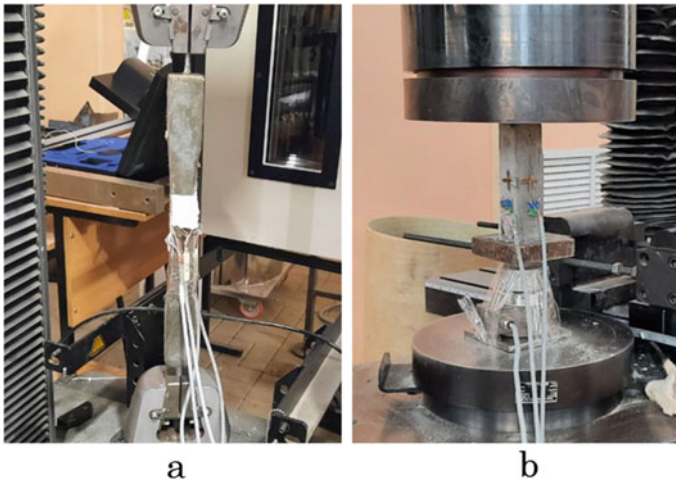


Fig. 2 Ordinary cement concrete: **a** tensile strength sample during testing; **b** sample prism during testing

3 Results

Based on the diagram shown in Fig. 3, equations were obtained for the rubber concrete that describe the relationship between normal stresses σ_r and relative strains ε_r during compression.

$$\sigma_r = 29212\varepsilon_r - 2.5 \times 10^6 \varepsilon_r^2 \quad (2)$$

where subindex r refers to rubber concrete, i.e. Rubcon.

Table 5 Parameters of samples

Type of sample	No.	Width, mm	Thickness, mm	Height, mm	Width, mm	Thickness, mm	Height, mm
Rubber concrete				Cement concrete			
Prism	1	40	41	160	40	40	160
	2	40	40.5	160	40	40	159
	3	40	40.5	159.8	40	40.5	160
	4	40	40	159.8	40	40.5	160
	5	40	39.5	160	40.5	40.5	160
Tensile strength sample	1	28	41	295	29	40	300
	2	29	41	295	29	40	300
	3	28	40.5	301	28	41	295
	4	29	41	301	29	40.5	300
	5	29	40.5	296	25	41	295
Cube	1	100	100	99			
	2	100	100	99			
	3	101	100	100			
	4	100	100	100			
	5	101	100	100			

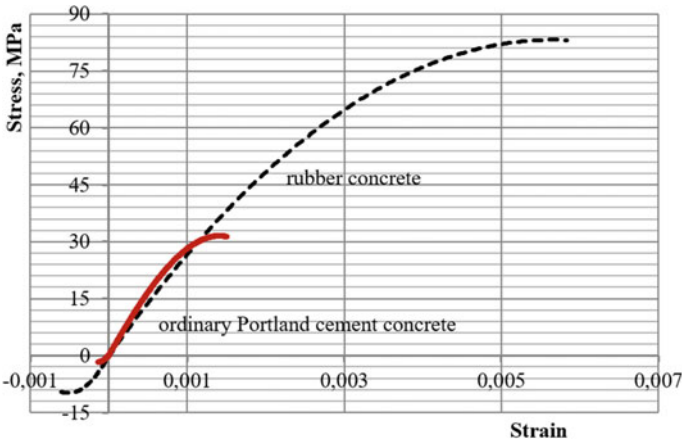


Fig. 3 Deformation diagram of rubber concrete in comparison with B25 concrete: dashed curve—rubber concrete, red curve—ordinary Portland cement concrete

Relationship between tensile stresses σ_{rt} and corresponding relative strains ε_{rt}

$$\sigma_{rt} = 38842\varepsilon_{rt} + 3.35 \times 10^7 \varepsilon_{rt}^2 \tag{3}$$

Tables 6 and 7 show the deformation-strength characteristics obtained as a result of physical testing of samples of ordinary cement concrete B25 and rubber concrete, respectively. In so doing, the following notations have been used: R_b , ε_b and R_{bt} , ε_{bt} are the ultimate strength and strain under compression and tension for ordinary cement concrete, respectively, R_r , ε_r and R_{rt} , ε_{rt} are the ultimate strength and strain under compression and tension for Rubcon, respectively, E_b and E_r are elastic moduli for ordinary cement concrete and Rubcon, respectively, and R_{srt} is the splitting tensile strength of Rubcon.

Table 6 Test results for ordinary cement concrete

R_b , MPa	R_{bt} , MPa	R_b/R_{bt}	ε_b	ε_{bt}	E_b , MPa
31.0	1.65	18.8	0.0015	0.00014	36,000
30.0	1.6	18.8	0.0014	0.00013	35,000
31.2	1.6	19.5	0.0015	0.00014	36,200
29.0	1.6	18.1	0.0014	0.00012	35,300
29.0	1.6	18.1	0.0015	0.00013	35,300

Table 7 Test results for rubber concrete

R_r , MPa	R_{rt} , MPa	R_r/R_{rt}	ε_r	ε_{rt}	E_r , MPa	R_{srt} , MPa
84.0	10.9	7.7	0.0057	0.00054	25,200	8.9
83.0	10.9	7.6	0.0056	0.00054	24,800	8.9
86.0	11.8	7.3	0.0058	0.00056	26,600	9.3
86.0	11.8	7.3	0.0058	0.00054	25,500	9.3
83.0	10.4	8.0	0.0053	0.00053	24,700	8.8

From Table 7 it follows that the average compressive strength and the tensile strength of Rubcon are 84.4 MPa and 11.2 MPa, respectively. A comparative histogram of the characteristics of cement concrete and rubber concrete is shown in Fig. 4.

Also, from Table 7 it is seen that the tests of a cube of concrete for splitting have a lower strength value than with central tension and make up around 81% of the axial tension, a similar ratio also corresponds to the results of testing cement concrete with a cubic strength of 74.6 MPa [13]. The tensile strength of rubber concrete is 7 times greater than the strength of cement concrete. Figure 3 shows that rubber concrete is a more plastic material than ordinary cement concrete, the ratio of compressive strength to tensile strength is 8, while the modulus of elasticity, of course, is somewhat inferior to the modulus of elasticity of conventional cement concrete (Fig. 4), and is at the level of 25–26 GPa. However, in this case, the increase in strength does not lead to an increase in the brittleness of the material, and, consequently, the opening of cracks and destruction will not occur so rapidly, in particular, in comparison with high-strength concretes. It is

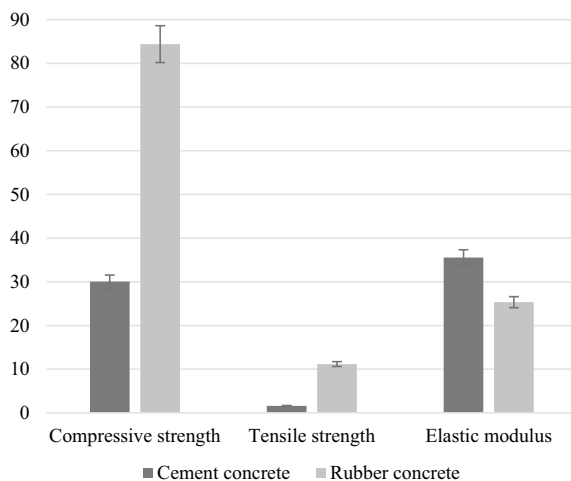


Fig. 4 Comparative histogram of the characteristics of cement concrete and rubber concrete

important to note that high tensile strength has a positive effect on structures working in bending, in addition to increasing the load before cracking, it also increases the rigidity of structures due to the longer period of joint work of rubber concrete and rebar [14].

4 Discussion

It should be noted that rubber concrete has a high fullness of the mixture. This indicates the possibility of adding second-rate materials to the Rubcon composition (instead of crushed stone, you can use waste from concrete breakage, or ground glass instead of sand. Thus, its high strength gives one the opportunity to use recycled materials in the mixture. This means that up to 89.8% of the Rubcon mixture could consist of various production wastes. In view of the fact that one of the trends in the modern technological development of the construction industry is the focus on energy efficiency, the important criteria of which are to ensure the durability of structures, their environmental safety, as well as the possibility of using recycled industrial waste and by-products of other industries [15], rubber concretes can be among those materials that will have waste in their composition and at the same time be used in the production of durable structures and products. For example, in [16], crushed stone was replaced with secondary crushed stone after the demolition of a hydroelectric power plant, and in [17], crumb rubber was added to the concrete. It is common practice to combine fly ash with cement in the production of so-called “Green concrete” [18, 19]. Moreover, due to the high tensile strength of Rubcon, in the case of the manufacture of reinforced products, better protection of reinforcing bars from an aggressive environment is provided as compared with traditional reinforced concrete products.

5 Conclusion

The following conclusion could be made based on the results obtained:

- The mechanical properties of rubber concrete are much higher than those of the traditional cement concrete. Thus, compressive strength of Rubcon with the use of cement is 84.4 MPa, while the tensile strength is 8 times less than the compressive strength, while this indicator for conventional concrete is 18–19.
- The tensile strength of Rubcon is 7 times greater than the strength of cement concrete B25.
- Due to the high strength of rubber, its use in load-bearing structures leads to a reduction in material consumption and weight of structures. This helps to reduce the cost of manufacturing and operating of structures.
- Rubber concrete has the potential to utilize industrial waste in its composition.

Acknowledgements. This research has been supported by the Ministry of Science and High Education of the Russian Federation, Project No 075-03-2023-132 (FZGM-2023-0006). The experimental studies have been carried out using the facilities of the Collective Research Center named after Professor Yu.M. Borisov, Voronezh State Technical University, which is partly supported by the Ministry of Science and Education of the Russian Federation, Project No 075-15-2021-662.

References

1. Figovsky O, Potapov Y, Makarova T, Beilin D (2002) Load-carrying capacity of polymer concrete with polybutadiene matrix. *Sci Israel Technol Adv* 4(1–2):21
2. Figovsky O, Potapov Yu, Borisov Yu, Beilin D (2002) RubCon-technology of high filled composite materials. In: The 3D international rubber chemicals, compounding and mixing conference proceedings, Munich, 11–12 July 2002
3. Potapov YuB et al (2003) Research of polymer concrete based on low molecular polybutadiene influence of temperature on physical-mechanical characteristics. *Sci Israel Technol Adv* 5(1–2):11–13
4. Potapov Yu, Figovsky O, Borisov Yu (2002) Rubber concretes with decreased hardening temperature. In: Ninth annual international conference on composites engineering. University of New Orleans, San Diego, California
5. Potapov YuB, Chmykhov VA, Borisov YuM (2013) Resistance of a polymer concrete based on polybutadiene binder to organic and inorganic acids. *Sci Israel Technol Adv* 15(4):7–10
6. Makarova TV (2000) Effective building composites based on liquid stereoregular polybutadiene rubber. Dissertation, Voronezh State Academy of Architecture and Civil Engineering
7. Potapov Y, Polikutin A, Panfilov D, Okunev M (2016) Comparative analysis of strength and crack resistance of normal sections of bending elements of T-sections made of rubber concrete, Rubcon reinforcement and concrete. *MATEC Web of Conf* 73:04018. <https://doi.org/10.1051/mateconf/20167304018>
8. Polikutin A, Potapov Y, Levchenko A, Perekal'skiy O (2019) The stress-strain state of normal sections Rubcon bending elements with mixed reinforcement. *Adv Intell Syst Comput* 983:586–599. https://doi.org/10.1007/978-3-030-19868-8_56
9. Popov II, Shitikova MV, Levchenko AV, Zhukov AD (2023) Experimental identification of the fractional parameter of the fractional derivative standard linear solid model for fiber-reinforced rubber concrete. *Mech Adv Mat Struct*. <https://doi.org/10.1080/15376494.2023.2191600>
10. Popov II, Shitikova MV (2020) Impulse excitation technique and its application for identification of material damping: an overview. *IOP Conf Ser Mat Sci Eng* 962:022025. <https://doi.org/10.1080/15376494.2023.2191600>

11. Dem'yanov A, Kolchunov VI I (2018) To the approximation of rectangular and complex cross-sections of reinforced concrete structures under the action torsion with bending. IOP Conf Ser: Mat Sci Eng 456(1):012104. <https://doi.org/10.1088/1757-899X/456/1/012104>
12. Gambhir M (2013) Concrete technology: theory and practice. Tata McGraw-Hill Education
13. Hansen E (1995) Determination of the tensile strength of concrete. NORDIC Concr Res Publ 17:1–17. <https://www.danskbetonforening.dk/media/ncr/publication-no-17-01.pdf>. Accessed 25 May 2023
14. Polikutin AE, Potapov YuB, Levchenko AV (2019) Deformability of rubcon and fibrorubcon beams. Arch Tech Sci 20(1):25–32. <https://doi.org/10.7251/afts.2019.1121.025P>
15. Zhukov AD et al (2019) Ecological and energy efficiency of insulating systems. E3S Web of Conf 135:03070. <https://doi.org/10.1051/e3sconf/201913503070>
16. Dosho Y (2007) Development of a sustainable concrete waste recycling system: application of recycled aggregate concrete produced by aggregate replacing method. J Adv Concrete Tech 5(1):27–42. <https://doi.org/10.3151/jact.5.27>
17. Gesoğlu M et al (2014) Investigating properties of pervious concretes containing waste tire rubbers. Constr Building Mat 63:206–213. <https://doi.org/10.1016/j.conbuildmat.2014.04.046>
18. Suhendro B (2014) Toward green concrete for better sustainable environment. Procedia Eng 95:305–320. <https://doi.org/10.1016/j.proeng.2014.12.190>
19. Berry M, Cross D, Stephens J (2009) Changing the environment: an alternative “Green” concrete produced without Portland cement. In: Proceedings. World of coal ash conference, Lexington, KY, USA



Modification of Fine Concrete with Carbon Nanotubes

D. A. Lyashenko^(✉), V. A. Perfilov, M. E. Nikolaev, and E. Yu. Kozlovceva

Volgograd State Technical University, 1, Akademicheskaya Str., Volgograd 400074, Russia
dmitiry.lyashenko@yandex.ru

Abstract. The priority direction of construction materials science is the production of materials with increased performance characteristics. The most common building material is concrete, of various functional purposes. The development of the construction complex leads to the design of increasingly complex structures, the construction of which requires highly efficient concrete with increased operational reliability. In this article, the application of a modifying complex additive to concrete of carbon nanotubes “Taunit-M” and plasticizer SP-3 is considered. Two methods of introducing nanoscale additives into the composition of fine concrete are considered. The results of two series of tests of beam samples at the age of 28 days using different methods of nanotube injection, namely, the use of an ultrasonic dispersant and the use of a linear induction apparatus (LIA), are presented. The positive effect of the introduction of nanotubes on the strength characteristics of concrete has been established. It is determined that the use of LIA provides a greater increase in strength due to the double effect of activation of the cement binder and the distribution of the nano-additive by active mixing due to vortex action.

Keywords: Carbon nanotubes · Ultrasonic dispersion · Vortex layer apparatus · Plasticizer · Nanoconcrete

1 Introduction

Nanotechnology is widely used in all fields of research, including the construction industry. There are many papers studying the introduction of various kinds of nanoscale components into a concrete mixture. The introduction of a small amount of additives such as nanosilicon, carbon nanotubes (CNTs), titanium nanoxide, etc. can significantly increase the 28-day strength of concrete with the introduction of their optimal amount [1].

In modern construction, concrete is one of the most widely used building materials, with the greatest use in the history of mankind. With the continuous development of the construction industry, the use of concrete structures and their operating conditions are becoming more and more complicated [2]. In this regard, to ensure the safety and reliability of building structures, it is necessary to adapt building materials to more severe engineering conditions. It can be noted that in recent years, a promising technology is

high-strength concrete (high performance concrete), such concretes provide compressive strength from 80 to 120 MPa. One of the possible directions for improving the performance characteristics of concrete is the use of complex additives and the selection of the optimal composition of the mixture.

The improvement of functional materials is an actual direction of materials science today. This approach is focused on determining the mechanisms, phenomena and processes of the formation of the structure of the material at the nanoscale. Nanoscale additives are new modifying additives for concrete, providing a significant increase in strength characteristics [3]. In this regard, the study of the technology of application of nano-additives is a promising direction in the field of building materials science. Carbon nanostructures are one of the promising nanomodifiers. Carbon has abnormally high strength characteristics and a powerful dispersion effect, these properties can significantly affect the performance characteristics of the material even when using a small concentration of such additives. Nevertheless, there are difficulties in their application, since nanomaterials are prone to the formation of aggregates, based on this, the methods and technologies for the synthesis and introduction of nanomodifiers should take into account the possibility of the most uniform distribution of the nano-additive in the matrix of the material. It is compliance with these conditions that will allow to obtain the maximum effect of the interaction of the additive with the matrix of the composite material at the phase boundaries, this will effectively distribute the load from the matrix to the nanotubes, which will ultimately increase the physical and mechanical characteristics of the material [4].

2 The Theoretical Part

Research in the field of materials science is aimed at the development of building materials, as well as technologies for their preparation, providing the required operational properties. Based on the possibility of increasing durability, as well as on economic feasibility, the actual direction of research in building materials science is to reduce costs by simplifying production technology, or the use of composite additives that increase the performance characteristics of concrete. To obtain the required characteristics, the most effective is to determine the optimal formulation of the concrete mixture [5]. One of the promising technologies for improving the strength characteristics of concrete is the use of nanomodifying additives.

In the last twenty years, there has been an increase in the number of studies in the field of nanomodification of concrete. Nanoscale particles can be used as modifiers of various materials [6]. Two types of building materials can be distinguished: a class of materials consisting of nanoscale structural elements and a class of materials including nanostructured elements as part of their structure [7]. Multicomponent mixtures with a nanomodifier introduced into the composition are the most common and belong to the second class.

When introduced into the mixture, nanoscale particles play the role of nuclei of structure formation, nanoarming element, centers of zoning of neoplasms in the matrix.

Concretes are a complex structure that can be considered not only at the macro and micro levels, but also at the nanoscale, since concrete includes cement grains with a size

of 10–100 nm and hydrate phases of cement with a particle size of 1–100 nm. Many well-known processes can also be explained at the nanoscale [8, 9].

Currently, there are many studies aimed at studying the effect of nanoscale additives on the performance properties of concrete [10, 11]. Additives such as carbon nanotubes (CNTs) of various modifications, fullerenes, nanoscale SiO_2 (or Fe_2O_3), microsilicon are used. Their use dramatically improves a number of mechanical properties of materials [12, 13]. The addition of CNT makes it possible to improve the adhesion of the cement binder, as well as to increase the durability and toughness of the resulting composite with increased mechanical strength. The effectiveness of nanotubes also lies in preventing cracking. This is due to the fact that the modification of such concretes occurs at the nanoscale. The mechanism of concrete destruction consists in the formation of cracks at the nanoscale, the accumulation of which leads to the appearance of larger areas of cracking, up to the complete destruction of the structure [14].

Numerous studies in the field of nanomodification of concrete carried out by research organizations show that the introduction of modifying nanoadditives in the manufacture of concrete provides:

- increased compressive and bending strength.
- improvement of the physical properties of concrete: frost resistance, water resistance and thermal conductivity.
- improving the structure of concrete [15].

Assessing the mechanism of the effect of nanomodifying additives on concrete, the authors identify signs that significantly affect the structure of the composite material. The high sorption activity of nano-additives can influence the formation of additional micelle formations, which act as active centers of compounds [16].

The main three hypotheses of the influence of nanomaterials on the composite structure are formulated.

1. Nanomaterials, having high surface energy, affect the structure formation of the matrix material, which contributes to the formation of a dense, durable substance.
2. Primary nano-additives act as crystallization centers.
3. Nanostructures are formed at the boundaries of the crystal interface, which excludes the possibility of their enlargement, which reduces the formation of bulk defects [17].

Carbon nanomodifiers have an effective effect on the formation of the cement stone matrix. Carbon modifiers with a geometry (length, diameter, etc.) close to the thickness of the layers of calcium hydrosilicates reduces the number of cracks. This is due to a decrease in the possibility of the propagation of main cracks in the material, since these processes are hindered by carbon fibers, which prevents the further spread of damage. This reduces the effect of material fracture and promotes adhesion between planes. In addition, carbon nanotubes allow you to distribute the energy of cracking to increase the propagation paths, since they interfere with their initial trajectory and speed of advancement.

As many studies show, reducing the particle size of the material significantly increases its characteristics. For example, Portland cement has a specific grain surface of approximately $3000 \text{ cm}^2/\text{g}$. In this case, about a quarter of the cement volume enters into a chemical reaction. To achieve complete hydration of cement, grinding of

materials to the smallest possible sizes is used. For this purpose, so-called activation methods are used. When activated, cement binders have an increase in reactivity, which is due not only to a decrease in particle size, but also to an increase in the concentration of defects, as well as the formation of active surface centers, which leads to a change in the crystal structure. In addition, during mechanical activation, the sorption properties of solid surfaces change, due to the active centers formed in it, which have a radical nature. The disadvantage of this technology is the high energy consumption of the process. For mechanical activation of solids, it is necessary to transfer a large amount of energy capable of deforming the crystal lattice of the material. In this regard, such devices have high energy intensity. It is known that the most effective way to transfer energy for mechanical activation is impact, due to the fact that this method allows you to direct energy to certain areas of the processed material. For mechanical activation of binders, various types of mills are used. In such installations, the working element is grinding bodies, which can be balls, cylinders or segments made of solid, dense material. The grinding mechanism can be based on driving grinding bodies due to an electric motor and gravity, as well as due to a magnetic field.

Another direction of microstructure modification is the introduction of nanomodifying additives into the cement mixture. The most well-known modifier is microsilicon, a by-product of the production of ferrosilicon and metallic silicon, the size of the colloidal parts 10^{-5} – 10^{-3} m. Nanocrete is a building material that includes nanoscale additives in its composition. It is known that the introduction of a small amount of nanomodifying additives (particles with sizes from 1 to 100 nm) into the composition of concrete makes it possible to acquire completely new properties. This is due to the modification of the structure of the resulting composite material at the nanoscale. It is known that nanoscale particles are present in chrysolite asbestos in the form of nanotubes. It is possible that the presence of nanotubes provides an increase in the strength of the cement matrix when using asbestos. In addition, nanotubes are contained in serpentinite. Repair and restoration compositions are made on this mineral. Special attention can be paid to fulleroids (single- or multilayer nanotubes). Various materials of both natural and artificial origin are used as nanomodifying components. The following additives can be distinguished: nanofibers of various modifications, carbon black, astralenes, carbon nanotubes, fullerenes, microsilicon, minerals, nanoscale rocks, etc. The choice of nanomodifying additives depends on the required parameters, as well as the technical and functional properties of the material structure. Carbon nanomodifying additives, sols and fullerenes are the most widespread. In this work, it was decided to use carbon nanotubes. The key parameters were CNT length (3–5 microns), outer diameter (10–60 nm) and inner diameter (10–20 nm). Based on the literature data considered, such values are the most effective.

An important role is played by the method of introducing nano-additives, since often their amount in the composition is very small (from 0.0001% by weight of the binder). To achieve the best effect, a uniform distribution of nanoparticles over the entire volume of the finished mixture is required [18].

In this paper, two methods of introducing nanomodifying additives are compared: ultrasonic dispersion and the use of a vortex layer apparatus.

Ultrasonic dispersion: The technology consists in the use of ultrasonic dispersants. These devices can be used for grinding various kinds of solid particles in liquids or for the preparation of emulsions by intensive stirring of all components in water. Ultrasonic dispersants generate ultrasound in excess of 20 kHz, which makes it possible to obtain a highly dispersed, homogeneous mixture with both soluble and insoluble additives.

Plasticizing additives can be used to prevent agglomeration of the additives used when they are introduced into the mixing water and, as a result, for a more uniform distribution of particles. Many studies indicate a positive effect for the introduction of nanoscale additives into the composition of concrete [19, 20].

The second method considered in this paper is the technology of using a linear induction apparatus (LIA). Such installations, due to the generated magnetic field, set in motion grinding bodies made of ferrimagnetic materials. Due to this, active stirring and activation of the cement binder by domol takes place in the chamber. Thus, the use of LIA has a double effect, namely, mixing of the introduced additives in the cement binder and its mechanical activation [21].

Cement activation studies were carried out using vortex layer apparatuses. The resulting samples showed an increase in strength, frost resistance and water resistance. This technology has the following sequence: The binder used is processed in the installation for a set time, after which cement is mixed with coarse and fine aggregate with further introduction of mixing water [22, 23].

3 The Experimental Part

The following materials were used for the research: «Eurocement» cement, sand, plasticizer SP-3 of “Polyplast Novomoskovsk” LLC, carbon nanotubes of the Taunit-M series.

Plasticizer SP-3 is a mixture of sodium poly-naphthalene methylene sulfonate, technical lignosulfonates, an industrial mixture of sodium thiosulfate and rhodanide and, if necessary, an anti-foaming agent based on higher fatty acids and oligomeric lapromol. According to state standard 24211, this additive refers to superplasticizers of a plasticizing-water-reducing type. Polyplast SP-3 is intended for:

- to increase workability without reducing strength with a constant water-cement ratio;
- to increase the physical and mechanical properties (strength) of concrete by reducing water with constant workability;
- to reduce cement consumption without reducing the workability and physical and mechanical properties of concrete [24].

Carbon nanotubes (CNTs) of the Taunit-M series are quasi-one-dimensional, nanoscale, filamentous formations of polycrystalline graphite of predominantly cylindrical shape with an internal channel. These tubes have a length of 2 or more microns and a diameter of 10–30 nm. Carbon has a strength of up to several Gpa. In this regard, the concentration of nanotubes is hundredths, thousandths and ten thousandths of a percent by weight of the binder.

For the study, it was decided to produce 4 compositions using two CNT injection technologies. As the studied compositions, the following were used: a control composition, without the inclusion of a nano-additive and 3 compositions with the addition

of CNT 0.004; 0.005; 0.006% by weight of the binder, respectively. The introduction of a nano-additive in such an amount is due to the tests carried out earlier [25, 26]. To determine the optimal amount of the injected plasticizer, tests were performed to determine the mobility of the mixture. Thus, the use of a plasticizer made it possible to reduce the water-cement ratio from 0.5 to 0.42 without loss of mobility. Table 1 shows the compositions of the manufactured samples.

Table 1 Compositions of the studied mixtures of fine-grained concrete

Structure	S-1	S-2	S-3	S-4
Cement, g	500	500	500	500
CNT, %/g	–	0.004/0.02	0.005/0.025	0.006/0.03
Sand, g	1500	1500	1500	1500
Water, g	210	210	210	210
SP-3, g	3.5	3.5	3.5	3.5

According to the compositions indicated in Table 1. Two series of samples were produced using ultrasonic dispersion and linear induction apparatus. For each composition, three samples were made-beams, according to state standard 18105. The compressive strength was determined as the main characteristic. The compressive strength limit was determined for each sample using the Pulsar-1.2 device at the age of 28 days.

This device made it possible to record the propagation time of the ultrasonic pulse in the samples under study during the through sounding from the emitter to the receiver. The distance between the emitter and the receiver divided by the measured time is the value of the ultrasound velocity. In order to increase the level of reliability of research, measurements are divided into cycles consisting of six sounds, the final result of which is formed by statistical processing of the data obtained. The speed of propagation of the ultrasonic wave in the sample is influenced by the mechanical characteristics of the material, such as density and elasticity, as well as the presence of defects.

The management of CNT with the help of a dispersant was as follows:

Nanotubes and a plasticizer SP-3 were injected into a predetermined amount of sealing water. After that, the working chamber of the dispersant, which generates ultrasound, was placed in a container with water. Then the ultrasonic treatment was carried out for 5 min until the uniform distribution of all components. The resulting aqueous suspension was added to pre-mixed dry components for further mixing and molding;

Introduction of nano-additives using LIA:

Nanotubes were introduced into the set amount of cement, after which the mixture was placed in the installation chamber, in which grinding bodies in the form of anisotropic ferromagnetic bodies with a diameter of 1.5 mm and a length of 5–15 mm were also placed. After loading the chamber, the mixture was processed for two minutes. The resulting activated cement mixture was mixed with the remaining components for further forming of the samples.

Below are tables with the obtained strength characteristics of the studied samples.

For greater clarity, a diagram was constructed based on tabular data, Fig. 1.

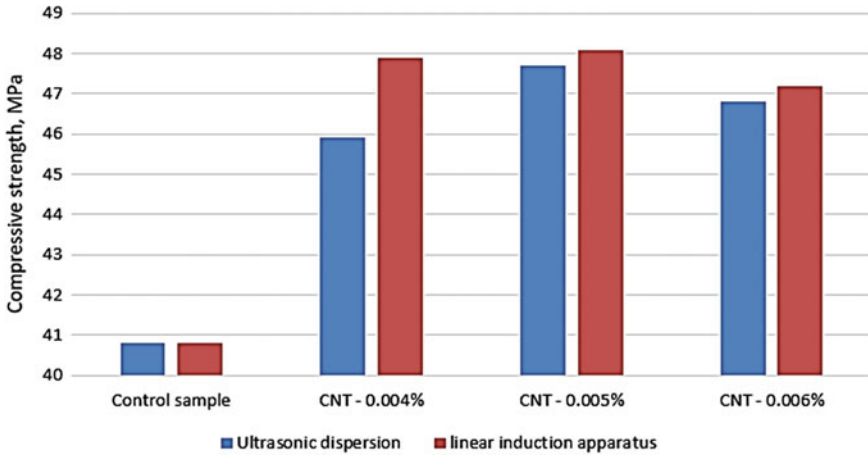


Fig. 1 Diagram of comparison of strength characteristics of the studied samples

According to Tables 2 and 3, it can be seen that the maximum strength is achieved when 0.005% of the nano-additive by weight of the binder is introduced into the composition. The increase in strength was 14.5% and 15.2%, respectively, with the first and second methods of CNT administration.

Table 2 Strength characteristics of samples prepared using ultrasonic dispersion technology

Structure	R_{com} , MPa	R_{com} , MPa	R_{com} , MPa	Average
S-1.1	41.3	40.2	40.8	40.8
S-1.2	45.5	44.1	48	45.9
S-1.3	46.7	49.2	47.2	47.7
S-1.4	45.1	48.1	47.1	46.8

Table 3 Strength characteristics of samples prepared using vortex layer technology

Structure	R_{com} , MPa	R_{com} , MPa	R_{com} , MPa	Average
S-2.1	41.3	40.2	40.8	40.8
S-2.2	48.5	47.3	47.9	47.9
S-2.3	48.8	46.9	48.6	48.1
S-2.4	46.4	47.8	47.5	47.2

Thus, the increase in strength characteristics occurred equally for each cooking technology. However, the samples prepared using LIA had slightly higher strength. This can be explained by the double effect of vortex action, namely stirring and activation of the cement binder.

In order to understand the structure formation of nanomodified concrete, samples were prepared for research on the electronic double-beam microscope “Versa 3D”. Samples were taken from the obtained samples by grinding fine-grained concrete to a powdery state. The resulting powder was sieved through a sieve with a cell of 0.315 mm. The selected samples were loaded into the microscope chamber for further analysis. Below are micrographs with different magnification multiplicities.

Based on the analysis of micrographs of Figs. 2 and 3, the nanomodified structure of concrete is characterized by the presence of areas with the inclusion of carbon nanotubes. The obtained micrographs show that the inclusion of the nano-additive acts as a reinforcing material, as well as additional crystallization centers. In this regard, as many authors confirm, there is a decrease in the porosity of the material during the formation of gel-like hydration products that fill the interstitial space. Carbon nanomodifiers have a structure-forming effect on the matrix of the material with the formation of an additional amount of hydrosilicates. Carbon nanotubes recorded in microphotographs have a stable diameter value along the entire length of the fibers, which provides stable conditions for the growth of cement stone. There are neoplasm particles on the nanotubes, which indicates a modification of the structure of fine-grained concrete. The structure of the modified material has a dense arrangement of particles, due to which there is an increase in strength characteristics. Minerals together with nanotubes produce discrete reinforcement of the cement matrix, which makes it possible to combine the neoplasm into a single structure.

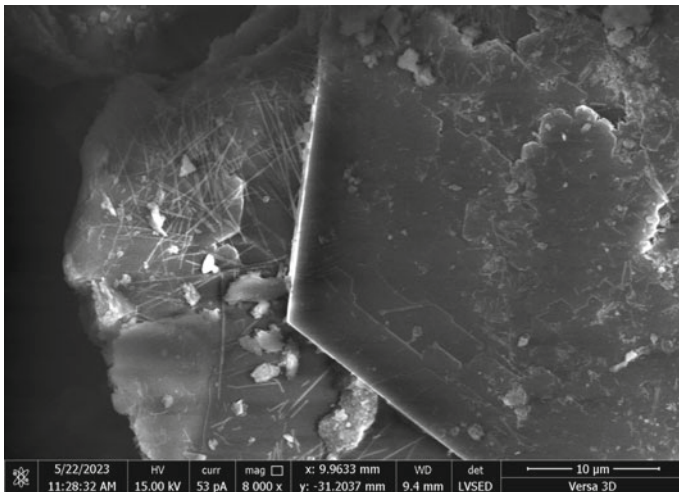


Fig. 2 Micrograph of nanomodified concrete at 8000× magnification

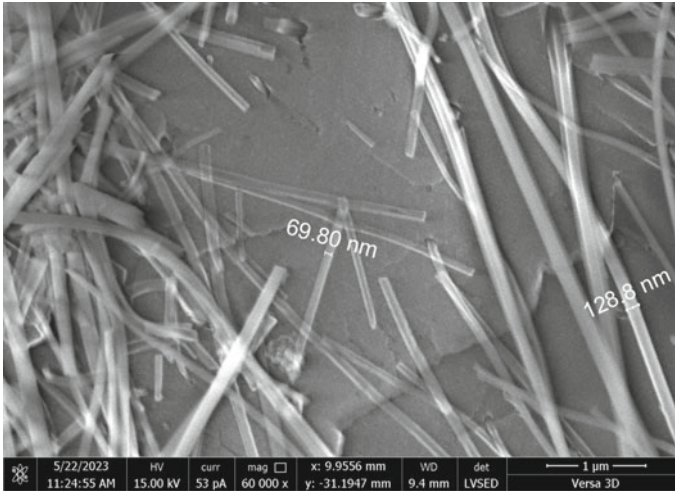


Fig. 3 Micrograph of nanomodified concrete at 60,000× magnification

4 Conclusions

The results of studies of the effect of a complex additive and methods of introducing CNT on the strength of the concrete mixture are presented. As a result of the studies carried out, a positive effect of the introduction of carbon nanotubes on the strength of fine-grained concrete was found.

Thus, the use of the CNT additive in conjunction with the plasticizer SP-3 using two methods of administration contributed to an increase in the compressive strength. Both technologies showed an increase in strength of over 14%. However, the use of LIA made it possible to obtain greater strength due to the additional grinding cement.

Studies using an electron microscope show the presence of modified sections of fine-grained concrete with carbon nanotubes. The increase in strength is due to the modification of the concrete structure. The introduced nanotubes act as crystallization centers, which leads to matrix hardening and increased crack resistance. However, the nanomodifying additive is not distributed over the entire volume of the mixture, in this regard, additional measures for the distribution of the components of the mixture should be taken into account. The use of mixers of various types can have a positive effect on the dispersion of CNTs.

References

1. Ashwini RM, Potharaju M, Srinivas V, Kanaka Durga S, Rathnamala, Anish Paudel GV (2023) Compressive and flexural strength of concrete with different nanomaterials: a critical review. *J Nanomater* 1:15
2. Palamarchuk AA, Shishakina OA, Kochurov DV, Arakelyan AG (2018) Polymer concretes—promising building materials. *Int Student Scientific Bull* 6:105
3. Fakhratov MA, Evdokimov VO, Borodin AS (2018) Prospects for the use of nanostructured concrete in construction. *Inzhenernyy vestnik Dona* 3(50):124

4. Korolev EV, Bazhenov YuM, Beregovoy VA (2006) Modification of building materials with nanocarbon tubes and fullerenes. *Build Mater* 8:1–4
5. Gabidullin MG, Khuzin AF, Suleymanov NM, Togulev PN (2011) The effect of the addition of a nanomodifier based on carbon nanotubes on the strength of cement stone. *Izvestiya Kazan State Univ Archit Civil Eng* 2(16):185–189
6. Chen SJ (2011) Carbon nanotube–cement composites: a retrospect. *IES J A Civil Struct Eng* 4(44):254–265
7. Tolchkov YuN, Mikhaleva ZA, Tkachev AG, Popov AI (2012) Modification of building materials with carbon nanotubes: current trends in the development of industrial technologies. *Nanotechnol Constr Sci Online J* 4:57–67
8. Kunadian I, Andrews R, Qian D, Mengus MP (2009) Growth kinetics of MWCNTs synthesized by a continuous-feed CVD method. *Carbon* 47:384–395
9. Tolchkov YuN, Mikhaleva ZA, Tkachev AG (2018) The effect of a carbon nanotubes-based modifier on the formation of the cement stone structure. *Adv Mater Technol* 3:49–56
10. Askari KOA, Singh VP, Dalezios NR, Crusberg TC (2018) Polymer concrete. *Int J Hydro* 2(5):630–635. <https://doi.org/10.15406/ijh.2018.02.00135>
11. Moiseeva VI, YaV P, Tyumentsev ME, Pankov PA (2019) Nanotechnologies in the field of production of building materials. *Innov Investments* 11:293–297
12. Dahlan AS (2021) Impact of nanotechnology on high performance cement and concrete. *J Mol Struct* 1223:128896. <https://doi.org/10.1016/j.molstruc.2020.128896>
13. Bhatta DP, Singla S, Garg R (2021) Microstructural and strength parameters of Nano-SiO₂ based cement composites. *Mater Today Proc* 15(46):6743–6747. <https://doi.org/10.1016/j.matpr.2021.04.276>
14. Pimenov AI, Ibragimov RA, Izotov VS (2014) Influence of carbon nanotubes and the method of their introduction on the properties of cement compositions. *News Higher Educ Inst Constr* 6(666):26–30
15. Tolchkov YuN, Panina TI, Mikhaleva ZA (2017) Influence of surfactants on the distribution of carbon nanomaterials in aqueous dispersions during nanomodification of building composites. *Chem Phys Mesoscopy* 2(19):292–298
16. Artamonova OV, Sergutkina OR (2013) Building nanomaterials: development trends and prospects. *Sci Bull Voronezh State Univ Archit Constr* 1:13–23
17. Korolev EV (2014) Assessment of the concentration of primary nanomaterials for modifying building composites. *Build Mater* 6:31–34
18. Konsta-Gdoutos MS, Metaxa ZS, Shah SP (2010) Multi-scale mechanical and fracture characteristics and early-age strain capacity of high performance carbon nanotube/cement nanocomposites. *Cement Concr Compos* 32:110–115
19. Galinovsky AL, Moiseev VA, Provatorov AS, Osipkov AS, Yakovlev GI (2016) Development of ultra-jet technology for obtaining suspensions with carbon nanotubes. *Hardening Technol Coat* 11(143):37–43
20. Tkachev AG, Mikhaleva ZA, Tolchkov YuN (2012) Investigation of the effect of modifying additives based on gel-like dispersions of carbon nanomaterials on the properties of building composites. *Nanotechnol Constr Sci Online J* 4(14):15–23
21. Monina TA, Antonov II (2021) Modern materials and technologies in prototyping. *Nanotechnologies and nanomaterials. Decorative art and the subject-spatial environment. Bulletin of the MGHPA* 2(2):20–28
22. Pimenov SI, Ibragimov RA (2017) The influence of mechanical activation of cement suspension on the physical and technical properties of cement compositions. *Fundamentals of building materials science. Collection of reports of the International Online Congress. Belgorod State Technological University*, pp 797–805

23. Ibragimov RA, Korolev EV (2017) Intensification of hydration processes during mechanical activation of binder. *Fundamentals of building materials science. Collection of reports of the International Online Congress. Belgorod State Technological University*, pp 806–808
24. Novoselov KS (2011) Graphene: materials of Flatland. *UFN* 181(12):1299–1311
25. Lyashenko DA, Perfilov VA, Vesova LM (2022) Fine-grained nanomodified concrete. *Inzhenernyy Vestnik Dona* 10(94):369–378
26. Lyashenko DA, Perfilov VA, Lukyanitsa SV, Lupinogin VV (2022) Development of the composition of nanomodified cement. *Inzhenernyy Vestnik Dona* 5(89):393–402



Specific Energy Absorbed by Fiber-Reinforced Concrete Under Static and Dynamic Loading

S. Savin^(✉) and M. Sharipov

Moscow State University of Civil Engineering, 26, Yaloslavskoe Shosse, Moscow 129337,
Russia
savinsyu@mgsu.ru

Abstract. Dynamic strength is one of the factors determining the strain of buildings and structures under extreme impacts caused by, among other things, the restructuring when one of the load-bearing elements fails, as well as the dissipation properties of the materials the structure is made of. The purpose of this research is to analyze the dynamic strength parameters and dissipation properties of concrete and fiber-reinforced concrete under loads typical for emergency impacts and failures of one of the load-bearing elements. The results of the dissipation properties comparison for workpieces made of concrete types with different compression strength grades, as well as concrete reinforced with indirect-reinforcement fiber grid in terms of the specific strain energy absorption allowed the authors to recommend fiber-reinforced concrete for effective local reinforcement of structures taking into account their strength against specific emergency impacts. The suggested analytical expression for the specific strain energy absorption can be used to assess the additional dynamic loading of reinforced concrete building frames under specific emergency impacts.

Keywords: Fiber-reinforced concrete · Specific energy absorption · Static loading · Dynamic loading · Resistance

1 Introduction

The current growth of technology-related threats provokes interest in various aspects of building structure durability assurance under specific impacts [1–4]. Dynamic strength is one of the factors determining the strain of buildings and structures under extreme impacts caused by, among other things, the restructuring when one of the load-bearing elements fails, as well as the dissipation properties of the materials the structure is made of. Multiple experiments [5–10] show that the dynamic strength of concrete exceeds its strength under loading that lasts for minutes. The dissipation properties of materials are largely defined by the proportion of the plastic and elastic strain phases that can be accounted for integral structural elements with the damage tolerance (plasticity) factor [11–13].

Considering concrete blends, the authors of [14–16] analyzed the specific strain energy absorption value during one-axis compression of workpieces. Adding 1% of

steel fiber allowed increasing the specific absorbed energy by almost two times [14, 16]. Similar results were obtained while limiting concrete strain by using carbon fiber and fiberglass cloths [15]. The results mentioned above were obtained through the quasi-static testing of workpieces. Apparently, the respective comparison data for static-dynamic loading are absent.

Besides, developing analytical dependencies for the states of concrete, fiber-reinforced concrete, and indirect-reinforcement concrete under the static-dynamic loading for restructuring situations, as well as assessing their adequacy is an important research and practical problem. Experiments on the dynamic strength of concrete, including indirect-reinforcement concrete, under the static-dynamic loading in question were described in [17–20]. However, any respective data for fiber-reinforced concrete were previously absent, and the results have not been compared in terms of the specific strain energy absorption.

The purpose of this research is to analyze the dynamic strength parameters and dissipation properties of concrete and fiber-reinforced concrete under loads typical for emergency impacts and failures of one of the load-bearing elements, as well as the justification of a strain model for the fiber-reinforced concrete of building and structure elements under the static-dynamic loading considered.

2 Materials and Methods

2.1 Research Methodology

The research stipulated researching the strain parameters of fiber-reinforced concrete under three loading modes: quasi-static, dynamic, and dynamic with the initial stress state from the preliminary quasi-static loading. After that, we compared the dissipation properties depending on the loading mode with other concrete blends reviewed in [17–20].

We used specific strain energy absorption as the assessment criterion for the dissipation properties of the material [14–16]. This parameter helps assess how well structures made of different materials can absorb the energy of dynamic impacts and determine the absorbed energy value depending on the initial stress–strain condition. Unlike the expression for the specific strain energy absorption provided in [16], we eliminate the elastic strain energy and obtain the following:

$$SEA = \frac{\left(\int_0^l P dl\right)}{m} = \frac{\left(\int_0^\varepsilon \sigma(\varepsilon) A_b l d\varepsilon\right)}{m} - \frac{(\sigma^2(\varepsilon) A_b \cdot l)}{(2 \cdot E_b \cdot m)} \quad (1)$$

To calculate the specific strain energy, we approximated the experimental diagrams for the state of concrete, fiber-reinforced concrete, and concrete reinforced with indirect-reinforcement fiber in the Table Curve 2D software package using the following expressions:

$$\sigma(\varepsilon) = \frac{(a + c \cdot \varepsilon + e \cdot \varepsilon^2 + g \cdot \varepsilon^3)}{(1 + b \cdot \varepsilon + d \cdot \varepsilon^2 + f \cdot \varepsilon^3 + h \cdot \varepsilon^4)}; E_b = c - a \cdot b \quad (2)$$

where parameters a, b, c, d, e, f, g, h are selected empirically. Note that for singular quasi-static and dynamic loading diagrams parameters f, g, h are zeroed.

2.2 Test Specimens

To identify the specifics of fiber-reinforced concrete strain under singular dynamic impact taking into account the initial stresses caused by previously-applied static load, we produced and tested a series of 6 cubic workpieces sized $10 \times 10 \times 10$ cm (Fig. 1a) and 9 prism workpieces sized $7 \times 7 \times 28$ cm. The materials used in these fiber-reinforced concrete workpieces are listed in Table 1. The selected material proportions without the steel fiber had to comply with concrete compression grade B30.

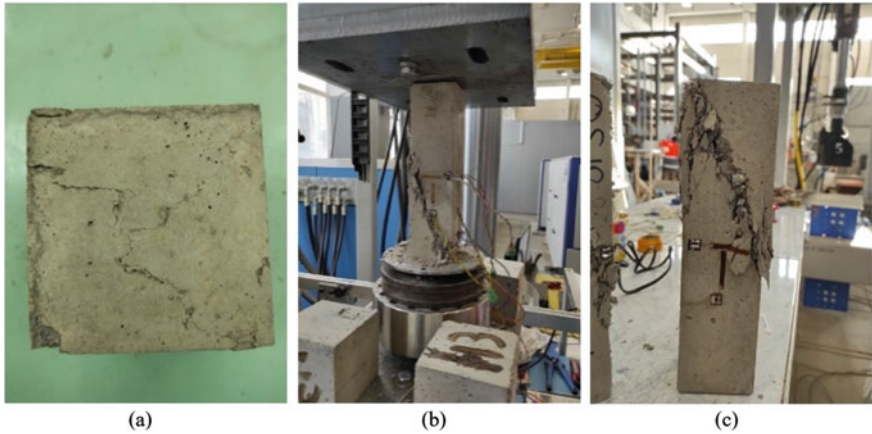


Fig. 1 Close view of the test specimens: cubes (a); prism in the testing machine (b); close view of the prism after testing (c)

Table 1 Materials for fiber concrete specimens

Material	Weight per 1 m ³ , kg
Portland cement 500-D0 GOST 10178-85	360
Washed sand, fraction 2–2.5 mm	950
Crushed granite fraction 5–10 mm	950
Water	190
Steel fiber	47.1

2.3 Loading Modes and Test Equipment

The singular dynamic impact testing for the fiber-reinforced concrete prisms taking into account the initial stresses caused by the previous application of a static load was performed using the universal dynamic testing machine LabTest 6.500H.5.01.1 (Fig. 1b) that can generate a maximum testing load of 500 kN. The values of longitudinal and lateral strains of fiber-reinforced concrete prisms were recorded using BX-120-30AA

strain gauges with a gauge length of 30 mm. Strain gauge readings were recorded using NI PXIe-1082 with a sampling rate up to 10 kHz. Apart from the load sensor built into the LabTest machine, we used an auxiliary load sensor DYLF-102 with a maximum permitted load of 500 kN. The general view of the prism workpiece after the testing is shown in Fig. 1c. The results of fiber-reinforced concrete workpieces were compared to the data for concrete workpieces, including those with indirect reinforcement [17–20].

3 Results and Discussion

3.1 Test Results of Fiber Concrete Under Different Loading Modes

The average results of fiber-reinforced concrete prisms tested according to the methodology set out in Sect. 2.3 are provided as the graph in Fig. 2.

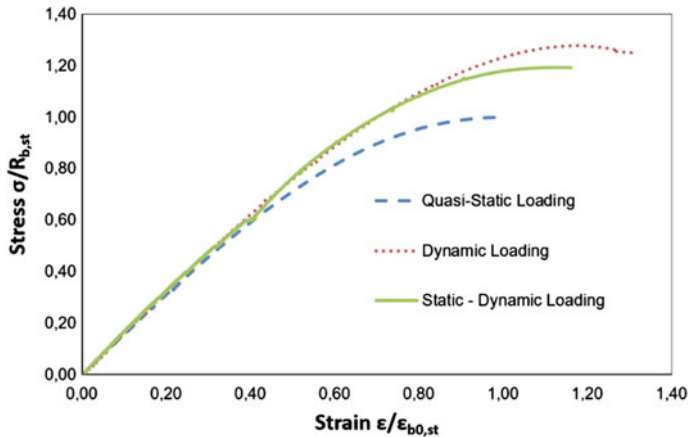


Fig. 2 The diagrams of fiber-reinforced concrete specimen states in dimensionless coordinates according to the results of tests

The analysis of fiber-reinforced concrete state diagrams under different loading modes in Fig. 2 demonstrates the following: the strength limit of fiber-reinforced concrete prisms under singular dynamic loading from the initial static load stress $\sigma = 0$ MPa to 28% exceeds the strength limit obtained in the quasi-static loading tests. The strains corresponding to the dynamic strength limit exceed the respective values for the quasi-static loading by 20%. In the singular dynamic impact tests for fiber-reinforced concrete prisms from initial stress level $\sigma = 0.6 \cdot R_{bn}$ of the expected strength limit for a one-axis quasi-static compression, the strength limit and the respective strain exceeded the respective values for singular quasi-static loading tests by 19 and 13%. The strength limit and the respective strain under singular dynamic impact taking into account the initial stresses $\sigma = 0.6 \cdot R_{bn}$ from the previously-applied static load were 32.1 and 35% lower than for the respective values obtained in dynamic tests without initial stresses.

The values of approximating function coefficients (2) for the stress–strain diagrams are shown in Table 2.

Table 2 Approximating expression parameters of the stress–strain diagrams for fiber-reinforced concrete

Equation (2) parameter	Fiber-reinforced concrete B45, fiber reinforcement mass percentage 1.8%		
	Static	Dynamic	Static–dynamic
a	−0.1393	−0.5450	−0.4581
b	−207.5	−183.3	719.8
c	36,360	43,880	50,500
d	60,540	5416	−415,200
e	−8,304,000	−11,440,000	4235
f	–	–	3.190e08
g	–	–	1.276e10
h	–	–	−2.613

3.2 The Stress–Strain Diagrams for the Dynamic Loading of Concrete, Fiber-Reinforced Concrete, and Indirect-Reinforcement Concrete

Figure 3 compares the diagrams for fiber-reinforced concrete and regular concrete, including indirect-reinforcement concrete for this research and articles [17–20].

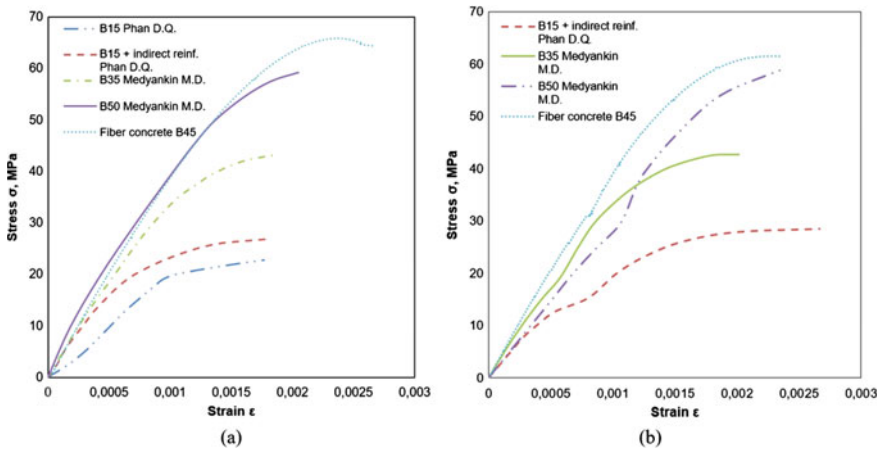


Fig. 3 The stress–strain diagrams under uniaxial dynamic compression: **a** without initial stresses; **b** with initial stresses

3.3 Comparative Analysis Using the Specific Energy Absorption

Figures 4, 5 and 6 show dependencies between the specific energy absorption (SEA) and the strain condition ϵ/ϵ_{b0} .

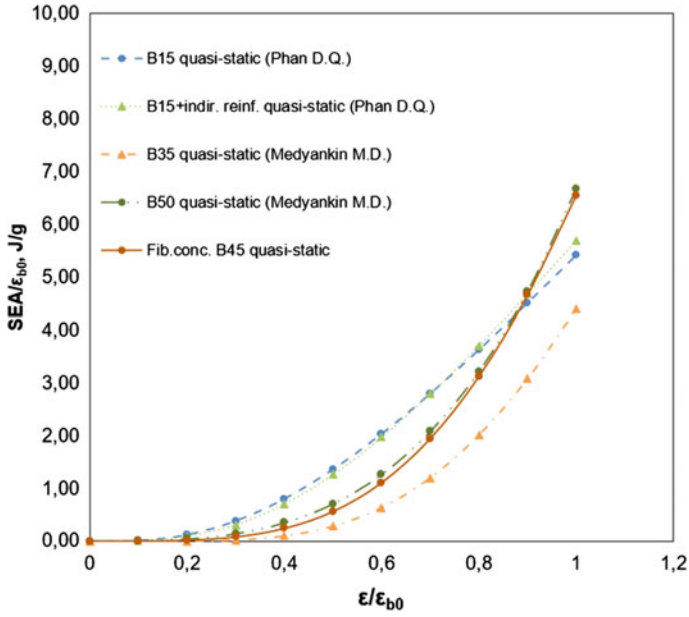


Fig. 4 Specific energy absorption under quasi-static loading

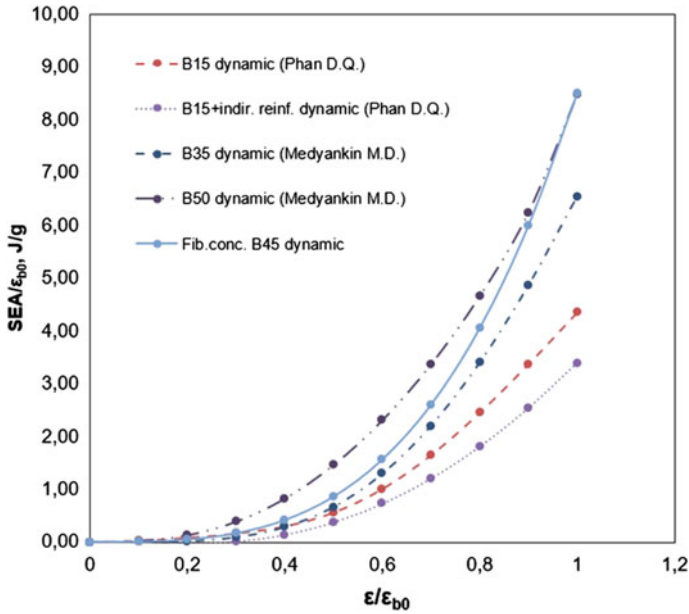


Fig. 5 Specific energy absorption under dynamic loading

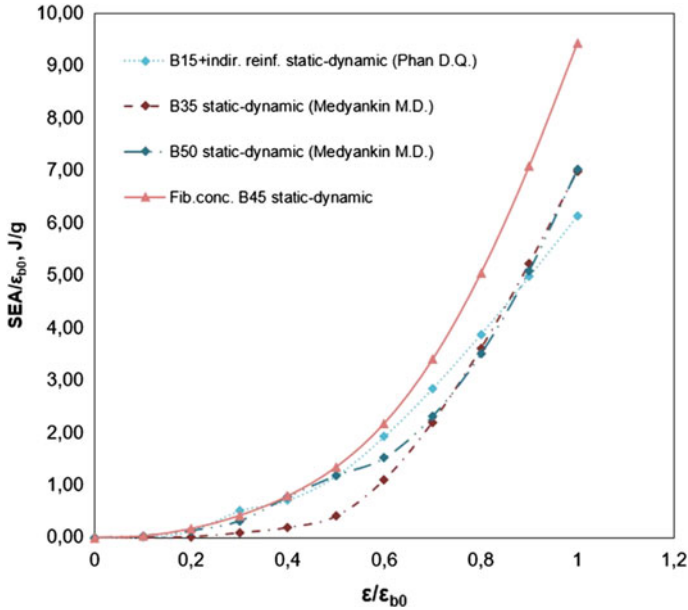


Fig. 6 Specific energy absorption under dynamic loading of the statically preloaded specimens

The analysis of dependency graphs for $SEA/\epsilon_{b0} - \epsilon/\epsilon_{b0}$ shown in Figs. 4, 5 and 6 allows drawing the following conclusions.

The specific strain energy absorption increases with the axial compression strength limit of the concrete both under quasi-static, dynamic, and static-dynamic loading. The greatest increase in the SEA/ϵ_{b0} value was observed when strain exceeded $\epsilon/\epsilon_{b0} = 0.4$, which can be attributed to the intensification of cracking and is in line with the ultrasound examination of workpieces [18].

The specific strain energy absorption corresponding to the compression strength limit under the quasi-static loading varied between 4.4 J/g for B35 concrete workpieces and 6.67 J/g for the B50 concrete workpieces. For dynamic loading, this figure varied between 3.4 J/g for the B15 concrete with indirect grid reinforcement and 8.5 J/g for the B45 fiber-reinforced concrete. The figure for the dynamic loading of prisms taking into account initial stresses from static load (static-dynamic loading) varied between 6.13 J/g for the B15 concrete with indirect grid reinforcement and 9.43 J/g for the B45 fiber-reinforced concrete.

For the B15 concrete, including the indirect grid reinforcement pieces, the $SEA/\epsilon_{b0} - \epsilon/\epsilon_{b0}$ curve was smoother than for workpieces made of higher compression-strength grade regular and fiber-reinforced concrete. This can be explained by the fact that the plastic strain for low-strength concrete is evident at low stress levels, while concrete types with higher compression-strength ratings feature nearly-elastic strain under low stresses. Considering the low concrete matrix strength of workpieces with indirect reinforcement, they showed lower absolute specific energy absorption compared to other workpieces.

Nevertheless, this local reinforcement method can be more effective with matrices made of higher-strength-grade concrete.

The highest absolute value of SEA/ϵ_{b0} among the workpieces in question under quasi-static loading was obtained for the B50 concrete. For the dynamic and static-dynamic loading of workpieces, the greatest absolute values of specific energy consumption were observed in the B45 fiber-reinforced concrete prisms. This allows us to recommend fiber-reinforced concrete as a material that can improve the carrying capacity of reinforced concrete structures under emergency impacts through, among other things, their application in structural nodes and sections that can experience the greatest loads during extreme impacts.

The obtained dependencies of $SEA/\epsilon_{b0} - \epsilon/\epsilon_{b0}$ can be used to assess the additional dynamic loading of reinforced concrete elements of buildings and structures.

4 Conclusions

Based on the research results, we made the following key conclusions:

- (a) The results of the dissipation properties comparison for workpieces made of concrete types with different compression strength grades, as well as concrete reinforced with indirect-reinforcement fiber grid in terms of the specific strain energy absorption allowed the authors to recommend fiber-reinforced concrete for effective local reinforcement of structures taking into account their strength against specific emergency impacts.
- (b) The suggested analytical expression for the specific strain energy absorption can be used to assess the additional dynamic loading of reinforced concrete building frames under specific emergency impacts.

Acknowledgements. The authors are grateful to I.M. Khaliullin and M.D. Medyankin for their help with the experimental part of the study. This work was supported by the Russian Science Foundation grant No. 24-49-10010.

References

1. Alekseytsev AV (2021) Mechanical safety of reinforced concrete frames under complex emergency actions. *Mag Civil Eng* 103:10306. <https://doi.org/10.34910/MCE.103.6>
2. Tur AV, Tur VV, Lizahub AA (2023) Experimental and theoretical study of the reinforced concrete flat slabs with the central support loss. *Build Reconstr* 105:77–103. <https://doi.org/10.33979/2073-7416-2023-105-1-77-103>
3. Savin S, Kolchunov V, Fedorova N, Tuyen VuN (2023) Experimental and numerical investigations of RC frame stability failure under a corner column removal scenario. *Buildings* 13. <https://doi.org/10.3390/buildings13040908>
4. Tamrazyan AG (2023) Methodology for the analysis and assessment of the reliability of the state and prediction the service life of reinforced concrete structures. *Reinforced Concr Struct* 1:5–18

5. Habib A, Yildirim U, Eren O (2020) Mechanical and dynamic properties of high strength concrete with well graded coarse and fine tire rubber. *Constr Build Mater* 246:118502. <https://doi.org/10.1016/j.conbuildmat.2020.118502>
6. Alanazi N, Susmel L (2020) Estimating static/dynamic strength of notched unreinforced concrete under mixed-mode I/II loading. *Eng Fract Mech* 240:107329. <https://doi.org/10.1016/j.engfracmech.2020.107329>
7. Zhong W, Pan J, Wang J, Zhang C (2021) Size effect in dynamic splitting tensile strength of concrete: experimental investigation. *Constr Build Mater* 270:121449. <https://doi.org/10.1016/j.conbuildmat.2020.121449>
8. Fu Q, Xu W, He J et al (2021) Dynamic strength criteria for basalt fibre-reinforced coral aggregate concrete. *Compos Commun* 28:100983. <https://doi.org/10.1016/j.coco.2021.100983>
9. Le Minh H, Khatir S, Abdel Wahab M, Cuong-Le T (2021) A concrete damage plasticity model for predicting the effects of compressive high-strength concrete under static and dynamic loads. *J Build Eng* 44:103239. <https://doi.org/10.1016/j.jobe.2021.103239>
10. Kim K-M, Lee S, Cho J-Y (2022) Influence of friction on the dynamic increase factor of concrete compressive strength in a split Hopkinson pressure bar test. *Cem Concr Compos* 129:104517. <https://doi.org/10.1016/j.cemconcomp.2022.104517>
11. Kabantsev O, Mitrovic B (2018) Deformation and power characteristics monolithic reinforced concrete bearing systems in the mode of progressive collapse. *MATEC Web Conf* 251:02047. <https://doi.org/10.1051/mateconf/201825102047>
12. Velesztos AS, Newmark NM, Chelapati CV (1965) Deformation spectra for elastic and elasto-plastic systems subjected to ground shock and earthquake motions. In: *Proceedings of the third world conference on earthquake engineering, Auckland and Wellington*, pp 663–682
13. Kabantsev O, Kovalev M (2022) Failure mechanisms and parameters of elastoplastic deformations of anchorage in a damaged concrete base under seismic loading. *Buildings* 12. <https://doi.org/10.3390/buildings12010078>
14. Libre NA, Shekarchi M, Mahoutian M, Soroushian P (2011) Mechanical properties of hybrid fiber reinforced lightweight aggregate concrete made with natural pumice. *Constr Build Mater* 25:2458–2464. <https://doi.org/10.1016/j.conbuildmat.2010.11.058>
15. Dai J-G, Bai Y-L, Teng JG (2011) Behavior and modeling of concrete confined with FRP composites of large deformability. *J Compos Constr* 15:963–973. [https://doi.org/10.1061/\(ASCE\)CC.1943-5614.0000230](https://doi.org/10.1061/(ASCE)CC.1943-5614.0000230)
16. Poon CS, Shui ZH, Lam L (2004) Compressive behavior of fiber reinforced high-performance concrete subjected to elevated temperatures. *Cem Concr Res* 34:2215–2222. <https://doi.org/10.1016/j.cemconres.2004.02.011>
17. Fedorova NV, Phan DQ, Korenkov PA (2020) Indirect reinforcement of reinforced concrete elements as a means of protecting a constructive system from a progressive collapse. *IOP Conf Ser Mater Sci Eng* 753:032032. <https://doi.org/10.1088/1757-899X/753/3/032032>
18. Fedorova NV, Medyankin MD, Bushova OB (2020) Experimental determination of the parameters of the static-dynamic deformation of concrete under loading modal. *Build Reconstr* 89:72–81. <https://doi.org/10.33979/2073-7416-2020-89-3-72-81>
19. Fedorova N, Medyankin M, Fedorov S, Savin S (2022) Experimental and theoretical studies of the concrete static-dynamic stress–strain curves. In: Akimov P, Vatin N (eds) *Proceedings of FORM 2021. Lecture notes in civil engineering*, vol 170. Springer, Cham. https://doi.org/10.1007/978-3-030-79983-0_14
20. Fedorova NV, Medyankin MD, Bushova OB (2020) Determination of static-dynamic deformation parameters of concrete. *Promyshlennoe i Grazhdanskoe Stroitel'stvo*, 4–11. <https://doi.org/10.33622/0869-7019.2020.01.04-11>



Modification of Fine Multicomponent Concrete with Activated Component-Based Additive

A. Kogai^(✉), A. Puzatova, and M. Dmitrieva

Immanuel Kant Baltic Federal University, 14, Nevskogo Street, Kaliningrad 236041, Russia
ad.kogai@yandex.ru

Abstract. In accordance with modern requirements for building materials, concrete must be of high quality with minimal resource waste. Using the initial components internal potential allows to create high-quality binder systems that contribute to the achievement of the required performance properties of concrete. The optimal mode for the preparation of an activated mixture based on special cement and sand of a certain granulometry was determined in this work by conducting a series of mechanical activation in a planetary mill. The influence of the degree of substitution of the cement-sand mixture with an activated component on the kinetics of the early strength gain of concrete was studied in order to analyze the applicability of the developed composition in 3D construction printing. The qualities of the modifier based on the activated cement-sand mixture were evaluated for the persistence of properties by the method of isothermal calorimetry. A multicomponent concrete with improved physical and mechanical properties was obtained, modified with a finely ground cement-sand composition of optimal content.

Keywords: Cement · Concrete · Mechanical activation · Additive technologies · Modifier · Calorimetric analysis

1 Introduction

The development of additive technologies in construction shifts the criteria for the modern cement concretes applicability to the issues of regulating the kinetics of their hardening. Such requirements are based on the features of the building's construction using 3D printing methods. According to them, each layer applied using an extruder must have dimensional stability, the necessary initial strength and optimal setting time to ensure adhesion between layers and, as a result, the durability of the structure. The requirements for ensuring such characteristics contribute to the development of new technological approaches to the building materials engineering.

Nowadays much attention is paid to nanotechnologies in solving modern issues of building materials science. Composition of concretes is designed taking into account of various nano modifiers, for example, carbon nanotubes, nanodispersed silicon dioxide, nanosilica, halloysite, wollastonite, etc. to ensure the necessary physical and mechanical

characteristics of mixtures [1–3]. However, their widespread use in the creation of concrete is limited by the high cost of such additives, taking into account the logistics costs for remote areas of construction. Therefore, the actual direction is the development of the potential of the base components of the mixture, which form the basis of fine-grained concrete.

Appeal to the aspects and features of the structure formation of the composite, based on the use of the internal potential of the system itself, emphasizes the importance of improving the quality of the initial materials and their reactivity in order to achieve the desired performance characteristics. Therefore, various activation methods are used, consisting in the dispersion of the cement-sand mixture, taking into account the characteristics of the hydration of cement particles and the role of fine aggregate in the formation of structural framework.

The need for additional grinding of dry components is caused by the heterogeneity of cement grains, which prevents the full use of its binding properties. Large particles, like inert aggregate, may not react chemically with water. It leads to the formation of agglomerates of unreacted particles and the impossibility of uniform distribution of grains of one component in another. In addition, fewer internal structural defects will be located in smaller particles.

There are various ways to activate the components of the mixture, among which three main ones can be distinguished: chemical, physical and mechanical methods [4–6]. Chemical activation is carried out by introducing surfactants into the composition, causing spontaneous dispersion of cement grains in the solution. Physical activation implies the influence of physical effects, for example, thermal effects when the hydration temperature of the cement–water system rises or electromagnetic effects when exposed to ferromagnetic particles in the vortex field apparatus. However, the methods described above have significant drawbacks, consisting in the low speed of the process or dependence on external factors. Mechanical activation is often recognized as the most effective method. This method may include wet and dry dispersion of the components.

The mechanical effect during wet grinding [6] is caused by the penetration of water deep into the cement grain, removing the upper layers, thereby increasing the reactive area of the particles. In addition, the uniform distribution of water around the cement grains increases the effectiveness of their interaction with the liquid medium. Ball and vibratory mills with grinding media are mainly used for the purposes of wet grinding. The amount of water is of great importance with this activation method, for the largest grinding efficiency it is necessary to use a high amount of water. In this regard, there are limitations in the application of this method in relation to fine-grained mixtures in additive technologies, where the amount of water required to achieve the optimal molding and plasticity is strictly limited. Therefore, the most optimal is the dry grinding of the components by mechanical activation.

Mechanical activation is an intense mechanical action on the components of the mixture, which helps to reduce the threshold for initiation of reactions. The essence of the mechanical activation method is the dispersion of particles and the accompanying deformation of the crystal structure of the material, which increases the area of contact surfaces and reactivity, thereby providing conditions for the implementation of chemical reactions. The main attention in the issue of mechanical activation of the components is

mainly given to the dispersion of the cement. A direct correlation between the growth of cement activity and the improvement in the strength characteristics of concrete is based on the acceleration of the crystallization of new hydrate formations and their fixation during the hydration of new areas. At the same time, the quality of sand plays an important role in the formation of the strength framework of fine-grained concrete. Its particle size distribution, grain strength and surface layer morphology determine the quality of particle packing into a single array. The formation of active crystallization centers on a freshly formed surface is observed under mechanical action and dispersion of sand. The indicators of physical and chemical activity vary due to a change in internal energy, structural defects and the creation of a surface layer with excess energy [7].

The creation of a finely ground activated component by mutual mechanical activation of cement and sand should combine all the advantages of separate dispersion of the components. The use of such powder mixtures with the effect of nanoparticles should provide an increase in the early strength of concrete, a necessary condition for the applicability of the material for 3D building printing.

2 Materials and Methods

Previous studies [8, 9] and analysis of international experience in designing the composition of fine-grained concrete mixtures suitable for 3D printing [10–12] made it possible to select a composition that meets the necessary requirements for additive technologies. The consumption of components per 1 m³ is shown in Table 1.

Table 1 The consumption of components per 1 m³

Component	Consumption
Cement, kg	545.3
Sand, kg	1168
Silica fume, kg	156
Metakaolin, kg	78
Hyperplasticizer Stachement 1267, l	11.7
Fiberglass, kg	1.09

Portland cement grade M500 and quartz building sand were used to create a cement-sand composition. In order to form the densest structure of the concrete, certain sand fractions were selected based on the results of granulometric analysis: 70%—1.25 mm and 30%—0.315. Characteristics of cement and sand are given in Tables 2 and 3.

Additives such as silica fume and metakaolin were used to improve the properties of the mixture in the control composition. Silica fume is a nanoscale material synthesized as a by-product of the ferrosilicium production. The increased dispersity of metakaolin improves the uniformity of the composite structure, contributing to the acceleration of cement hydration, and, as a result, an increase in the strength of concrete [13].

Table 2 Properties of cement

Characteristic	Meaning
Specific surface area, cm^2/kg	3470
Standard consistency, %	30.8
Initial setting, min	150
Final setting, min	205

Table 3 Properties of sand

Characteristic	Meaning
Fineness modulus	3.2
Bulk density, g/cm^3	1.59
True density, g/cm^3	2.4

In the conditions of modern materials science, chemical modifiers of various effects are also used to control the properties of concrete. A special place among them is occupied by superplasticizers based on polycarboxylates. The experience of their use proves that such additives contribute to an increase in the strength and mobility of concrete, as well as a decrease in the water demand of the concrete mixture [14].

As part of additive technologies, preference is given to alternative methods of reinforcement, for example, dispersed reinforcement with polypropylene fiber. The selection of the geometric characteristics of the fiber used should be based on the possibility of optimal distribution over the concrete matrix.

The original cement-sand mixture (cement/sand = 1/2.14) was subjected to a series of mechanical activation in a Retsch Emax planetary ball mill at 1000 rpm for 5 min. For the study, weighing of cement-sand mixture of 50 and 100 g of grinding corundum balls with diameters of 5 and 10 mm were placed in grinding jars in a ratio of 50/50. Dispersion in ball mills occurs as a result of free impact, in which the destruction of the material occurs along the weakest structural bonds at the junctions of crystals or layers. The product of grinding are grains of isometric shape without internal defects with an increased indicator of structural strength. It is noted [15] that these types of mills are particularly effective in dispersing sands of various fractions.

The grinding efficiency was evaluated by the results of determining the specific surface of the resulting composition, so the non-activated cement-sand mixture was characterized by a specific surface of $1488 \text{ cm}^2/\text{g}$. After activation at 1000 rpm— $3691 \text{ cm}^2/\text{g}$. Thus, dispersion of the cement-sand mixture for 5 min at 1000 rpm can increase the specific surface of the particles by almost 2.5 times. The process of mechanical activation is shown in Fig. 1.

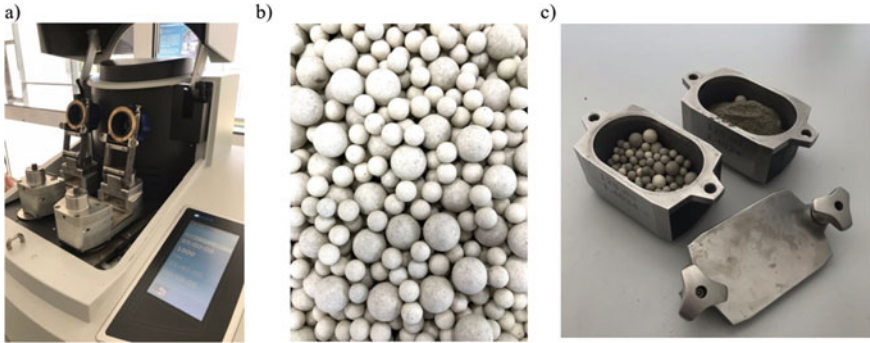


Fig. 1 Mechanical activation process: planetary ball mill (a), corundum balls (b), ground mixture (c)

2.1 Initial Strength Tests

The experimental compositions were formed on the basis of various degrees of replacement of the cement-sand mixture with an activated cement-sand component: 1st composition—control; 2nd composition—50% activated and 50% non-activated mixture; 3rd composition—75% activated and 25% non-activated mixture; 4th composition—100% activated composition.

Concrete mixes were created from prepared components in the indicated proportions with a water/cement ratio of 0.73–1.1, because due to the increase in the specific surface of the particles of the activated composition, there was an increase in the water consumption of dry components and, as a result, in the water-cement ratio (Fig. 2). The resulting concrete mixture was placed in steel molds intended for the manufacture of laboratory samples—cubes $20 \times 20 \times 20$ mm.

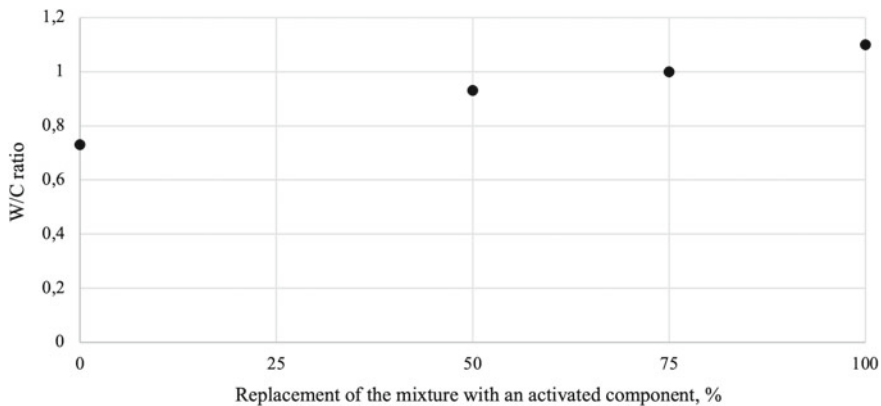


Fig. 2 Changing the water-cement ratio

The initial compressive strength of the samples was determined in the first hour and a half after the production of the concrete mixture, starting from 30 min and with a

step of 15 min. In the case of the development of compositions for 3D construction, the early strength of concrete is of great importance, since it characterizes the ability of the developed concrete to provide the required shape during layer-by-layer printing and adhesion to other layers. The universal testing machine ElectroPuls E100 was used for strength tests.

2.2 Isothermal Calorimetry

It is important to evaluate the shelf life of activated cement-sand composition properties with the possibility of using material as a modifier. A calorimetric analysis of the system was carried out to assess the retention of the activity of the cement-sand mixture at various points in time. This method makes it possible to study the kinetics of the cement hydration reaction by analyzing the thermodynamics of the course of mortar hardening. Calorimetry is a method for real-time prediction of the strength characteristics of cement systems with a proven correlation between heat generation and strength development [16, 17].

Taking into account the exothermic nature of cement hydration, heat release makes it possible to assess the stage of completion of the process, thereby establishing a relationship between the degree of hydration and age. Thus, accounting for the amount of released heat can be used to indirectly compare the strength characteristics of compositions with the same mineralogical composition [17]. In this study, we analyzed the dynamics of heat release of compositions on a cement-sand mixture of various storage times to assess the retention of modifier properties.

An 8-channel TAM Air isothermal calorimeter, designed for measurements of thermal effects with high stability and accuracy, was used for the experimental part. The device is specially optimized for the tasks of studying and developing new compositions in the cement and reinforced concrete industry. A sample of 9 g of the activated mixture was transferred into ampoules with a volume of 20 ml and filled with water, providing a W/C ratio of 0.5. The container was sealed with a lid and directed to the appropriate channel. An ampoule with a reference inert filler was placed in the pair compartment. A constant temperature of 20 °C was maintained inside each channel. The heat release of the samples was studied for a fresh activated mixture, as well as after storage for 7, 14 and 28, 35 and 42 days.

3 Results and Discussion

The effectiveness of the use of modifying components is usually evaluated by the value of the technical effect, which consists in changing the strength of the experimental compositions compared to the control at different points in time. Based on the data presented in Fig. 3, it can be concluded that the introduction of a finely ground cement-sand mixture into the composition contributes to an increase in the initial strength of concrete at any dosage. The trends in the change in strength characteristics can be traced after 60 min of maturation most clearly. The largest increase in strength is typical for composition No. 3 when replacing 75% of the cement-sand mixture with an activated component, which may be due to the formation of the densest packing of particles

in the concrete matrix and the most productive mutual work of all components. The advantage of the dosed input of the activated component in comparison with the complete replacement of the cement-sand mixture by it can be explained by the presence of a certain amount of coarse sand fractions present in the initial mixture and performing the function of a stiffening frame.

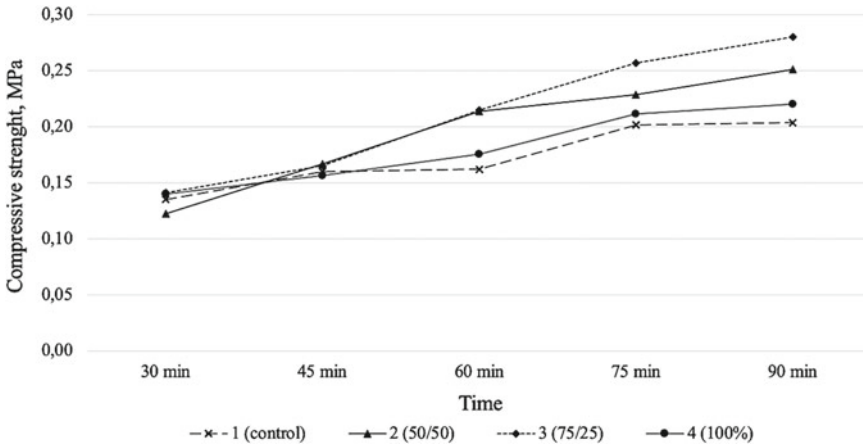


Fig. 3 Compressive strength of concrete samples

Thus, the effectiveness of the modifier introduced at a dosage of 75% was 37.74%, demonstrating an increase in strength at the age of 90 min up to 0.292 MPa, while the control composition reached only 0.212 MPa.

Analysis of the graphs obtained in the study of the preservation of the additives properties makes it possible to evaluate the intensity of heat release of the samples at given points in time (Figs. 4 and 5). The change in the amount of heat released in the process of cement hydration is clearly reflected. Immediately after contact between the particles of cement and water, heat is released, since an active reaction of tricalcium silicate with water begins. In the course of their interaction, membranes are formed around the grains of cement, the destruction of which requires a lot of energy; therefore, the graph shows a decrease in heat release in the first three hours of the reaction. The next stage is determined by self-acceleration and a high intensity of the hydration reaction, which is caused by the coalescence of hydrated particles into a single system. This stage characterizes the heat release schedule from 3 to 10 h. Further, the rate of heat begins to fall and a small amount of heat is released during the curing process.

For compositions based on the activated component of different storage times, there are no noticeable changes in their reactivity that go beyond the errors that would be demonstrated by varying the peak value of the heat flux. Thus, the preservation of the properties of the activated cement-sand mixture during 42 days of storage in a sealed container was proved. This confirms the possibility of using the resulting finely ground composition as an independent modifier for concrete mixtures, subject to storage and operation conditions.

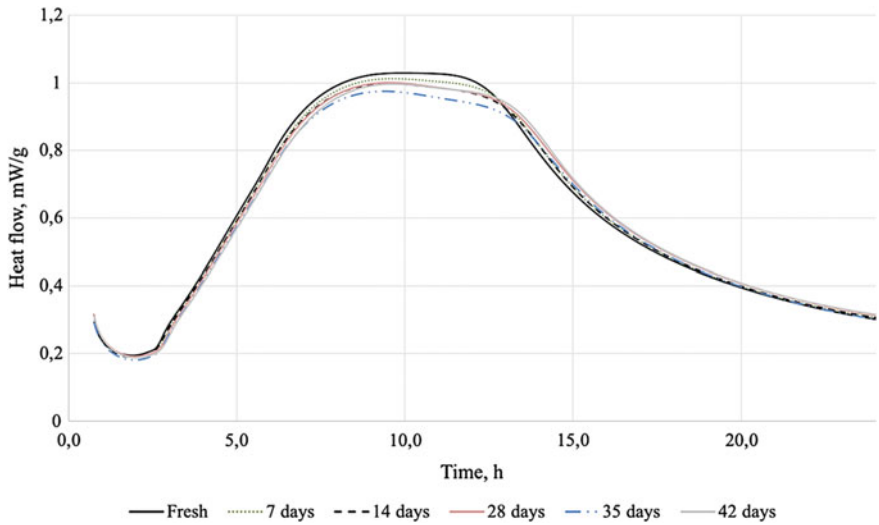


Fig. 4 Heat flow

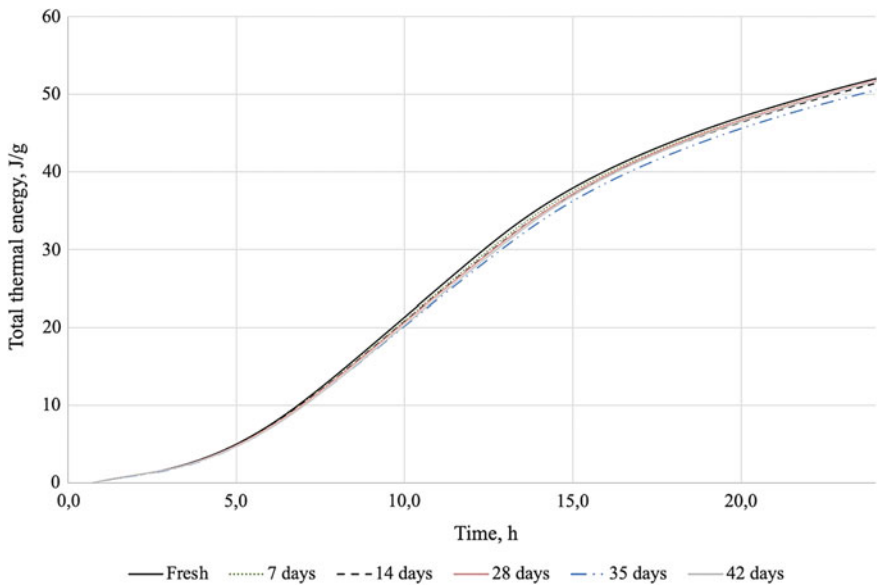


Fig. 5 Total thermal energy

4 Conclusion

A high-quality finely ground cement-sand mixture was obtained, produced by joint mechanical activation of cement and quartz sand of a certain granulometric composition. The effect of this composition on the mechanical properties of cement stone and the

process of structure formation was studied. Based on the results of strength tests at the initial stages of hardening, the optimal dosage of the introduction of the obtained modifier was determined in the amount of 75% by weight of the initial cement-sand mixture. Concrete of this composition has a specific structure, determined both by particles with an increased dispersion index, which contribute to the intensification of structure formation processes, and by coarsened fractions of the original sand, which form a strong frame.

Evaluation of the obtained activated composition properties, carried out by methods of determining the compressive strength and calorimetric analysis of the system, led to the conclusion that the properties of the modifier are fully preserved under long-term storage conditions in a sealed container. The results obtained confirm the possibility of using an activated cement-sand mixture as a modifier for concrete mixtures, which are used, among other things, as a printing material in 3D construction.

References

1. Reales OAM, Filho RDT (2017) A review on the chemical, mechanical and microstructural characterization of carbon nanotubes-cement based composites. *Constr Build Mater* 154:697–710. <https://doi.org/10.1016/j.conbuildmat.2017.07.232>
2. Xiao H, Zhang F, Liu R, Zhang R, Liu Z, Liu H (2019) Effects of pozzolanic and non-pozzolanic nanomaterials on cement-based materials. *Constr Build Mater* 213:1–9. <https://doi.org/10.1016/j.conbuildmat.2019.04.057>
3. Hemalatha P, Ramujee K (2021) Influence of nano material (TiO₂) on self-compacting Geo polymer concrete containing fly ash, GGBS and wollastonite. *Mater Today* 43:2438–2442. <https://doi.org/10.1016/j.matpr.2021.02.279>
4. Sobolev K, Lin Z, Cao Y, Sun H, Flores-Vivian I, Rushing T, Cummins T, Weiss WJ (2016) The influence of mechanical activation by vibro-milling on the early-age hydration and strength development of cement. *Cem Concr Compos* 71:53–62. <https://doi.org/10.1016/j.cemconcomp.2016.04.010>
5. Allahverdi A, Maleki A, Mahinroosta M (2018) Chemical activation of slag-blended Portland cement. *J Build Eng* 18:76–83. <https://doi.org/10.1016/j.jobe.2018.03.004>
6. Li M, Tan H, He X, Jian S, Zheng Z, Su Y, Yang J, Wang Y, Luo Z (2021) Preparation of nano cement particles by wet-grinding and its effect on hydration of cementitious system. *Constr Build Mater* 307:125051. <https://doi.org/10.1016/j.conbuildmat.2021.125051>
7. Mashkin NA, Kosach AF, Obadyanov AV (2013) Effektivnost' razdel'noj kavitacionnoj aktivacii peska pri proizvodstve melkozernistyh betonov (The efficiency of separate cavitation activation of sand in the production of fine-grained concrete). *Izvestiya Vuzov. Stroitel'stvo* 5:23–28
8. Sharanova AV, Panfilova AD, Plahiy AA, Dmitrieva MA (2019) Investigation of viscosity of construction mixtures applied for 3D printing. *IOP Conf Ser: Mater Sci Eng* 525:102055. <https://doi.org/10.1088/1757-899X/525/1/012055>
9. Sharanova A, Dmitrieva M (2019) Selection of compositions for additive technologies in construction. *E3S Web Conf* 97:06018. <https://doi.org/10.1051/e3sconf/20199706018>
10. Paul SC, Tay YWD, Panda B, Tan MJ (2018) Fresh and hardened properties of 3D printable cementitious materials for building and construction. *Arch Civ Mech Eng* 18:311–319. <https://doi.org/10.1016/j.acme.2017.02.008>
11. Khalil N, Aouad G, Cheikh KE, Remond S (2017) Use of calcium sulfoaluminate cements for setting control of 3D-printing mortars. *Constr Build Mater* 157:382–391. <https://doi.org/10.1016/j.conbuildmat.2017.09.109>

12. Panda B, Paul SC, Hui LJ, Tay YWD, Tan MJ (2017) Additive manufacturing of geopolymer for sustainable built environment. *J Clean Prod* 167:281–288. <https://doi.org/10.1016/j.jclepro.2017.08.165>
13. Patil S, Rao HS, Ghorpade VG (2022) The influence of metakaolin, silica fume, glass fiber, and polypropylene fiber on the strength characteristics of high-performance concrete. *Mater Today: Proc.* <https://doi.org/10.1016/j.matpr.2022.11.051>
14. Zhang C, Zhang X, Hou J, Wang J, Duan G (2022) Rheology and early microstructure evolution of fresh ultra-high-performance concrete with polycarboxylate superplasticizer. *Case Stud Constr Mater* 17:01575. <https://doi.org/10.1016/j.cscm.2022.e01575>
15. Andreeva AV, Davydova NN, Byrenina ON (2014) Mekhanoaktivacionnaya obrabotka zapolnitelya dlya povysheniya kachestva melkozernistogo betona (Mechanical activation treatment of aggregates to improve the quality of fine-grained concrete). *Politematicheskii setevoi elektronnyi nauchnyi zhurnal Kubanskogo gosudarstvennogo agrarnogo universiteta* 101:1–11
16. Linderoth O, Wadsö L, Jansen D (2021) Long-term cement hydration studies with isothermal calorimetry. *Cem Concr Res* 141:106344. <https://doi.org/10.1016/j.cemconres.2020.106344>
17. Bensed J (1987) Some applications of conduction calorimetry to cement hydration. *Adv Cem Res* 1:35–44. <https://doi.org/10.1680/adcr.1987.1.1.35>



Large Panel Reinforced Concrete Buildings Inelastic Behavior Modeling Approach for Nonlinear Seismic Analysis

Z. Abaev, A. Valiev^(✉), and M. Kodzaev

North Caucasian Institute of Mining and Metallurgy, 44, Nikolaeva St., Vladikavkaz 362021,
Russia

azamat99valiev@gmail.com

Abstract. This paper presents an in-depth investigation into the inelastic behavior of large panel reinforced concrete buildings, with a focus on developing an accurate modeling approach for nonlinear seismic analysis. The study begins by discussing the modeling assumptions used in the analysis, considering various factors such as material properties and stress distribution along the connection region. To implement the proposed modeling approach, the finite element method is adopted, utilizing the LIRA SAPR software. Nonlinear behavior of the connection region is modeled by a combination of two finite elements: (i) shell elements representing stress distribution in the connection region and (ii) 2-mode link element for modeling shear keys. The paper provides a detailed explanation of the finite element implementation process, highlighting the necessary calculations for stiffness determination for each structural element. The validity and performance of the proposed approach are assessed through both static and dynamic verifications. Overall, this research contributes to the field of structural engineering by offering an improved approach to capture the inelastic behavior of large panel reinforced concrete buildings during seismic events.

Keywords: Large panels · Seismic response · Inelastic behavior · Finite elements

1 Introduction

Large panel precast concrete structures are extensively employed in seismic-prone areas worldwide. The adoption of this construction method poses numerous distinctive challenges regarding aseismic design, primarily due to the inherent presence of connection regions in precast construction [1–5]. These connection regions represent a key contributor to the non-linear and inelastic behavior observed in the seismic response of such structures. Conversely, the concentration of non-linear and inelastic behavior within these connection regions facilitates the non-linear modeling of these structures. The stiffness and strength characteristics of the joints are determined by many factors: the mortar grade, the gap sizes between the panels, the presence, location and parameters of the embedded plates and reinforcement [6, 7].

This paper aims to develop a non-linear modeling approach of horizontal and vertical connections for inelastic seismic analysis of precast concrete walls.

The typical large panel building system denoted as “Seria 1.464s”, widely spread in the Soviet Union republics is taken as an object of this research.

Prefabricated RC large-panel buildings (LPB) are widely spread throughout the territory of Russia because of the industrialization policy implementation in USSR [8–10]. LPBs have experienced the effects of several impactful earthquakes, notably the 1976 Gazli event in Uzbekistan (Soviet Union), the 1977 Vrancea earthquake in Romania, and the 1988 Spitak earthquake in Armenia. Remarkably, the performance of these buildings during these seismic events was deemed satisfactory, as no substantial damage or structural failure was observed. Nevertheless, a notable gap exists in terms of technical resources that comprehensively document the seismic design principles associated with this particular construction technology [7].

The paper begins with the description of precast configurations typical of the USSR construction practice. A proposed approach utilizing a combination of finite elements for representing a nonlinear behavior of the connection regions is described. A parametric study is conducted for verifying the proposed model response. The findings provide valuable insights for engineers and researchers involved in the seismic design and analysis of such structures, facilitating more reliable and efficient assessment of their structural integrity and performance.

2 Large Panel Precast Buildings Modeling Approach

2.1 Description of the Large Panel Precast Building System

Many countries used various precast building systems during the second half of the twentieth century to provide low-income housing for the growing urban population. They were very popular after the Second World War, especially in Eastern European countries and former Soviet Union republics. In the former Soviet Union, different precast buildings systems are denoted as “Seria”.

The designation “large-panel system” refers to multistory structures composed of large wall and floor concrete panels connected in the vertical and horizontal directions so that the wall panels enclose appropriate spaces for the rooms within a building. These panels form a box-like structure. Both vertical and horizontal panels resist gravity load. Wall panels are usually one story high. Horizontal floor and roof panels span either as one-way or two-way slabs. When properly joined together, these horizontal elements act as diaphragms that transfer the lateral loads to the walls.

Thickness of wall panels ranges from 120 mm for interior walls to 300 mm for exterior walls. Floor panel thickness is 160 mm. Wall panel length is equal to the room length, typically on the order of 2.7–3.6 m. In some cases, there are no exterior wall panels and the facade walls are made of lightweight concrete [11, 12].

In this study, the details of the typical buildings system “Seria 1.464s” widely spread in the Soviet Union republics are investigated (see Fig. 1).

Large-panel buildings were increasingly common in mass standard housing in seismic regions of the USSR, their height reaches up to 9 stories in regions with the intensity

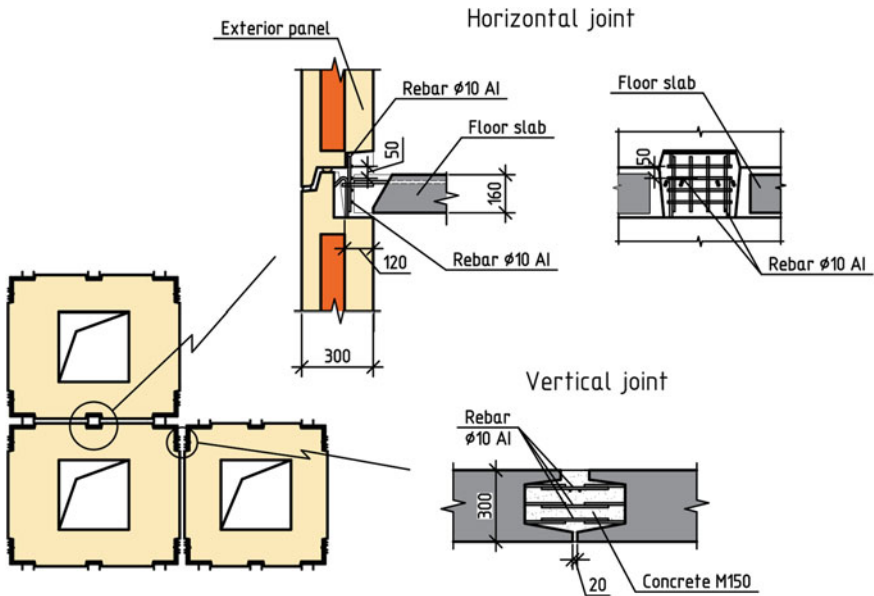


Fig. 1 Details of large panel precast building (building system “Seria 1.464s”)

magnitude 9 (MSK-64 scale) and 14–16 stories—in regions with the intensity magnitude 9. In view of the fact, in order to evaluate properly their reliability and economic efficiency it is necessary to know exactly the types and the extent of possible damages, the nature of non-linear deformations, the limits of the bearing capacity and the failure mechanisms.

2.2 Modeling Assumptions

In the modelling of large panel precast concrete structures, it is typical to assume that solid panels remain linear elastic. This assumption is reasonable in light of the expected role of these elements in the structure’s seismic response. Typical wall panels can be assumed to behave in an elastic-brittle fashion with regard to in-plane normal forces, and whatever non-linear-inelastic behavior that may exist can be effectively lumped into the behavior of the connection regions [13].

The following assumptions are made for the joint element [14]:

- all points of the horizontal section remain in one plane after the force is applied (plane sections remain plane);
- for the tensile zone of the section the tensile strength of concrete is not taken into account;
- normal compressive stresses σ_c distribution along the section is linear or bilinear.

Linear normal stress distribution is taken when the maximum value of compressive stresses σ_{\max} does not exceed the value of compressive strength of concrete R_c . Otherwise a bilinear diagram consisting of two zones is taken, in the first of which the compressive

stresses change linearly from $\sigma_{\min} > 0$ (positive values are taken for the compressive stresses) to $\sigma_{\max} = R_c$, and in the second zone the values are constant and equal to R_c . During the calculation it is assumed that within the length of the linear zone the material of the is elastic, and in the zone where $\sigma_{\max} = R_c$, it is in the plastic state.

The bilinear diagram of compressive stress allows to describe all designed situations and includes linear and rectangular diagrams of normal compressive stresses as special cases (see Fig. 2).

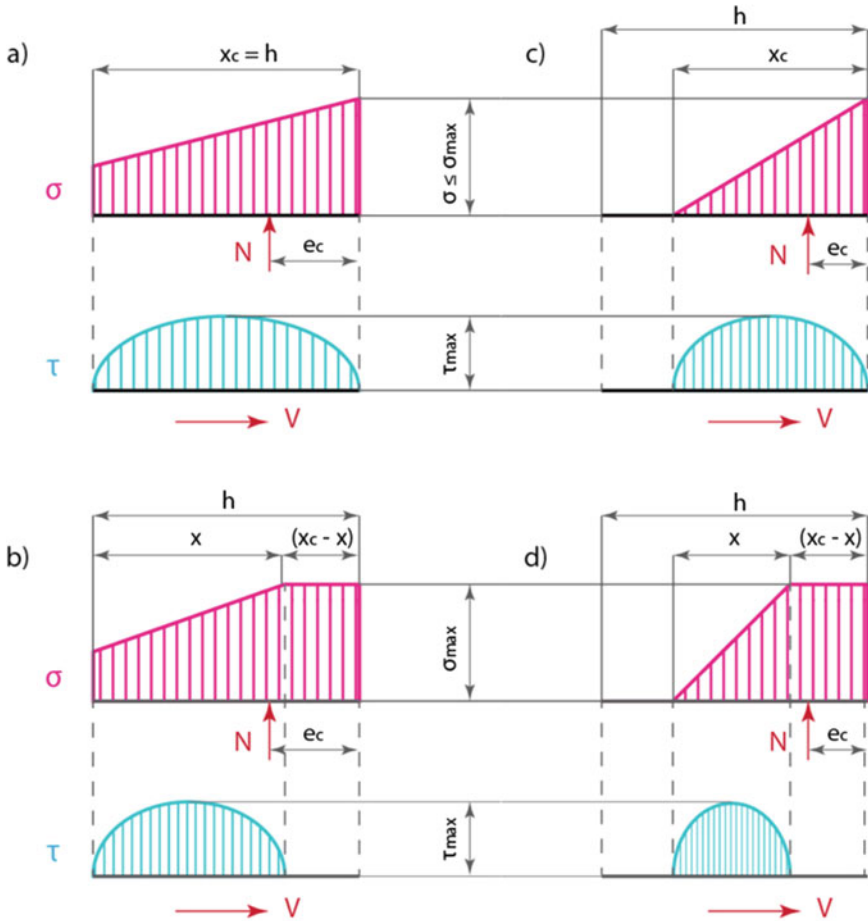


Fig. 2 Normal σ and shear τ stress distribution in the horizontal joint element in the combined shear-compression action: **a, b** compression along the entire length of the section, respectively for linear and bilinear distributions; **c, d** compression in portion of the length of the section (adopted from [14])

The shear key joints are the most practical alternative because they are capable to transfer the shear forces in a mechanical way even if there is no bond between the cast in situ concrete and the prefabricated concrete, therefore the contribution of shear keys

must be considered for both horizontal and vertical connection zones in addition to the joint element behavior described above.

2.3 Finite Element Implementation in LIRA SAPR Software

The finite element method software LIRA SAPR is used for numerical analysis. The software is intended for analysis and design of building and engineering structures of various purposes and contains many analytical modules [15].

Nonlinear behavior of the connection region implementing the stress distribution presented in Fig. 2 is modeled by a combination of two finite elements (FE) (see Fig. 3):

- Shell Elements (FE 259) representing stress distribution in the connection region,
- 2-mode link element (FE 255) for modeling shear keys.

The precast walls are modeled with elastic shell element FE 44.

2.3.1 2-Mode Link Element (FE 255) Stiffness

According to clause B4 of SP 335.1325800.2017 [16], the design shear strength V_{kb} of one shear key of the is taken equal to the smallest of the force values $V_{sh,b}$; $V_{c,b}$; $V_{crc,b}$, corresponding to the destruction of the shear key, respectively, from shear, crushing and shear cracks opening:

$$V_{sh,b} = 1.5R_{bt}A_{sh} \quad (1)$$

$$V_c = R_{b,loc}A_c \quad (2)$$

$$V_{crc,b} = 0.7R_{bt}A_j \quad (3)$$

where R_{bt} —design tensile strength of grouting concrete; $R_{b,loc}$ —crushing strength, taken equal $1.5R_b$ —for single keys, $0.8R_b$ —for multikey connections; A_{sh} —shear area; A_c —crushing area; A_j —cross-sectional area of the connection tributary to each shear key:

$$A_j = s_{bt} \cdot b_{mon} \quad (4)$$

where s_{bt} —distance between shear keys; b_{mon} —wall thickness of the grouting area.

Stiffness along Z-axis is represented by bilinear elastoplastic force–displacement relationship, elastic stiffness is determined by:

$$k_z = EA_s/h \quad (5)$$

where E —elastic modulus of the rebar; A_s —rebar cross-sectional area; h —rebar length (equal to the joint height).

Stiffness along X-axis is represented by bilinear elastoplastic force–displacement relationship, elastic stiffness is determined by:

$$\lambda_x^1 = \frac{l_{loc} \left(\frac{1}{E_{b,\omega}} + \frac{1}{E_{b,mon}} \right)}{A_{loc}} \quad (6)$$

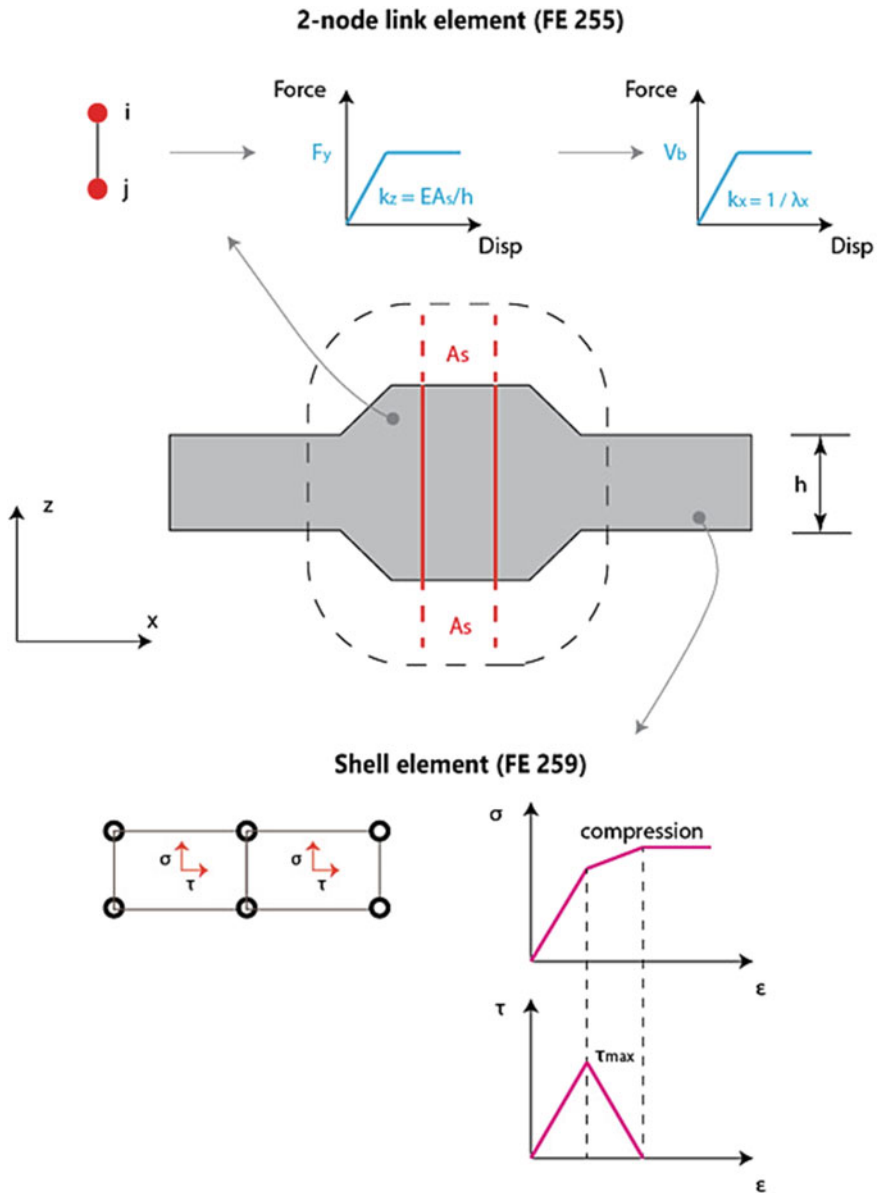


Fig. 3 Finite element implementation of the connection region

where A_{loc} —loaded area; l_{loc} —shear key height (recommended $l_{loc} = 250$ mm); E_b —elastic modulus of concrete precast element; $E_{b,mon}$ —elastic modulus of grouting concrete.

The area after shear cracks occurring (exceeding the shear force $V_{cr,b}$):

$$\lambda_x^2 = \frac{6}{d_s n_s} \left(\frac{1}{E_{B,\omega}} + \frac{1}{E_{b,mon}} \right) \quad (7)$$

where d_s —connection rebars diameter; n_s —number of the connection rebars.

2.3.2 Shell Element (FE 259) Stiffness [17–20]

During short-term compression for a mortar with a compressive strength of 1 MPa or more, with a joint thickness of 10–20 mm, flexibility coefficient of the mortar bed joint λ_T , mm³/N:

$$\text{for } \sigma_m \leq 1.15R_m^{2/3} \quad \lambda_m = 1.5 \times 10^{-3} R_m^{-2/3} t_m \quad (8)$$

$$\text{for } 2R_m^{2/3} \geq \sigma_m \geq 1.15R_m^{2/3} \quad \lambda_m = 5 \times 10^{-3} R_m^{-2/3} t_m \quad (9)$$

Flexibility coefficient of the joint:

$$\lambda_{c,pl} = \left(\lambda_m + \lambda_{m'} + \frac{h_{sl}}{E_b} \right) \frac{B_{pl}}{B_{pl} - h_v} \quad (10)$$

where λ_m' and λ_m —upper and lower mortar bed joint flexibility coefficients; h_{sl} —floor panel height; B_{pl} —contact areas width; h_v —joint width between floor panels.

Strain:

$$\varepsilon = \frac{\lambda_i \sigma_i}{h_v} \quad (11)$$

Stresses:

$$\sigma_m^1 = 1.15R_m^{2/3} \quad (12)$$

$$\sigma_m^2 = 2R_m^{2/3} \quad (13)$$

$$\sigma_m^y = 1.01\sigma_m^2 \quad (14)$$

2.3.3 Model Modification

The proposed model implementation should be sufficient to perform nonlinear static and nonlinear dynamic analyses, but during the preliminary analysis procedures a significant limitation was revealed. LIRA SAPR software couldn't perform nonlinear static analysis with FE 255 elements included in the model. The authors have contacted the developers and informed them about this drawback, so hopefully it will be fixed in the future releases of the software.

In order to overcome this impediment, the proposed model was modified for two different implementations (see Fig. 4):

- Model A (nonlinear time history analysis, NLTHA)
- Model B (nonlinear static analysis, Pushover).

In Model B FE 255 is replaced by a combination of two elements

- 2-node elastic link elements (FE 55) representing the axial stiffness of the original FE 255
- Nonlinear frame element (FE 210) representing the horizontal stiffness of the original FE 255.

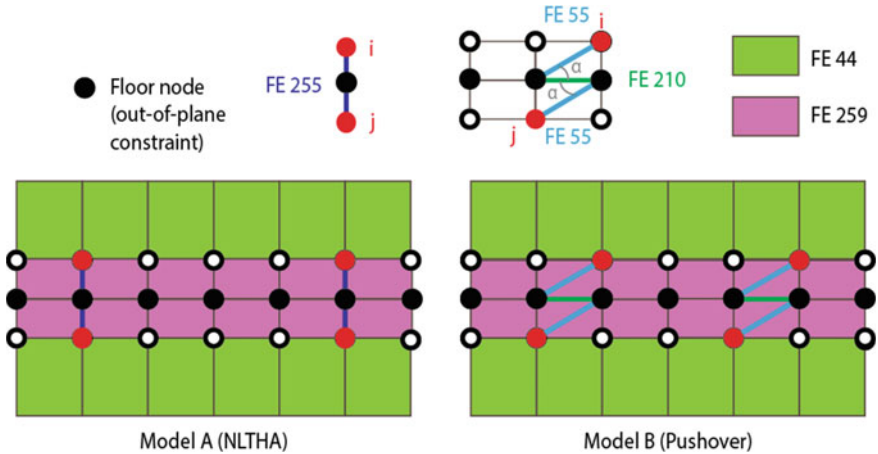


Fig. 4 Model modification

Stiffness of the FE 55 is calculated by:

$$k_z = \frac{k_z^{255} \cdot l^{255}}{2 \cos \alpha \cdot l^{55}} \tag{15}$$

It should be noted that FE 55 is an elastic element, therefore the forces in this element obtained from nonlinear analysis will not be correct. The main purpose of this element is to provide structural stability during the analysis. Its effect on the overall inelastic response is discussed further in the next section of the paper.

The nonlinear frame element FE 210 implemented by piece-wise stress–strain diagram. The dimensions of the element set equal to loaded area of the shear key. Conversion from the original stiffness is made by the following equations:

$$\sigma^{210} = V_{cr,c,b}/A_{loc} \tag{16}$$

$$\varepsilon^{210} = \Delta l/l_{loc} \tag{17}$$

2.4 Models Verification

Wall panels with 3.0 m height and 3.6 m length were analyzed in this study. Connection region height is 0.2 m. Connection details are taken from typical building system “Seria 1.464s”.

Wall panel meshing is 0.2×0.2 m. Connection region meshing is 0.2×0.1 m.

Two model implementations (Model A and Model B) were analyzed with nonlinear properties calculated by equations and assumptions proposed previously in this research.

Materials (Russian standards):

- Panel concrete—B15 ($R_b = 8.5$ MPa, $R_{bt} = 0.75$ MPa);
- Grouting concrete—B15 ($R_b = 8.5$ MPa, $R_{bt} = 0.75$ MPa);
- Reinforcement—A400 ($R_s = 350$ MPa).

Two sets of verification have been conducted:

- static verification
- dynamic verification.

2.4.1 Static Verification

The set of 4 wall models with different values of axial load (1000, 1500 and 2000 kN) and eccentricity (0.2, 0.8, 1.4 m) was analyzed for static verification (see Fig. 5).

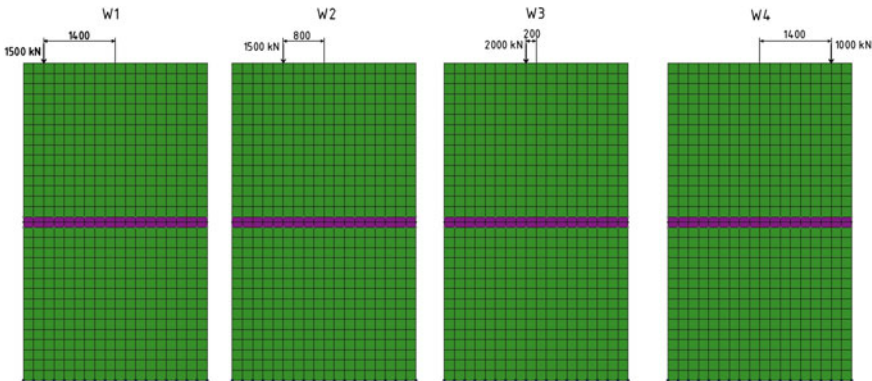


Fig. 5 Wall models for static verification

The results of the analysis presented in Table 1 show fair agreement between values for displacements, maximum axial and shear stresses of the joint. Higher values of shear force of the joint in Model B are caused by elastic stiffness of the FE 55. Analyst must be cautious while interpretation the results for this element and compare the values with design strength calculated for FE 255.

2.4.2 Dynamic Verification

Two models were subjected to the ground motion of the 1988 Spitak, Armenia earthquake (see Fig. 6). An earthquake registering 6.9 on the Richter scale hit the northern part of

Table 1 Static analysis results

Parameter	Model	Wall No			
		W1	W2	W3	W4
Displacement along X-axis, mm	Model A	114	65.6	14.8	-78.3
	Model B	113	67.4	13.9	-73.5
	Δ , %	0.87	2.67	6.08	6.13
Maximum (absolute) axial stress of the joint, kN/m ²	Model A	-4.55	-3.75	-2.28	-3.03
	Model B	-5.01	-4.05	-2.36	-3.13
	Δ , %	9.18	4.93	3.39	3.13
Maximum (absolute) shear force of the joint, kN	Model A	-11.45	-7.42	-6.14	-15
	Model B	-11.67	-7.13	-7.56	-17.83
	Δ , %	1.03	-3.91	18.78	15.87

the Armenian Republic of the Soviet Union on 7 December 1988, resulting in thousands of deaths and injuries. The performance of LPB buildings was satisfactory, without evidence of significant damage or collapse [21].

- Only one wall W1 from static verification (see Fig. 5) was analyzed for each model implementation.
- Modified Newton-Raphson method is used for direct integration of the equations of motion.
- Classical Rayleigh damping proportional to a linear combination of mass and stiffness is applied for damping ratio 2.5%.
- Total integration time is 20 s.
- Integration step is 0.01 s.

The results of nonlinear time history analysis for the W1 are presented in Table 2. The models show similar performance for displacements and axial stress of the joint. Model A has smaller values of velocity and acceleration (relative error between models 8% and 9% respectively) because of the higher dissipative capacity of the original FE 255 element.

The conducted static and dynamic verifications show that proposed modeling approach can be utilized for both nonlinear static and nonlinear dynamic analyses. A special concern must be taken for interpretation stresses and forces of the shear key elements in Model B implementations.

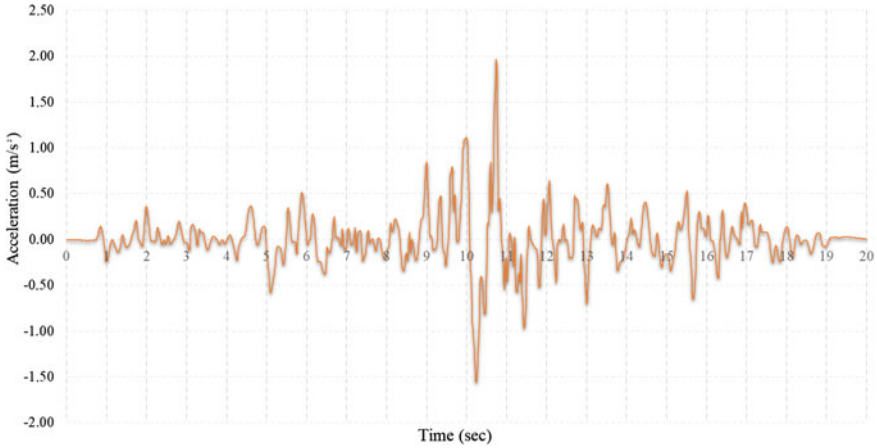


Fig. 6 Ground acceleration record (Spitak, Armenia, 12/7/1988, Gukasian, 0) [22]

Table 2 Dynamic analysis results

Parameter	Model	Wall No.
		W1
Displacement along X-axis, mm	Model A	107
	Model B	108
	Δ , %	0.9
Velocity along X-axis, mm/s	Model A	74
	Model B	80.5
	Δ , %	8.05
Acceleration along X-axis, mm/s ²	Model A	2.5
	Model B	2.75
	Δ , %	9.09
Maximum (absolute) axial stress of the joint, kN/m ²	Model A	-4.55
	Model B	-4.56
	Δ , %	0.22

3 Conclusion

In this study, a comprehensive investigation was conducted to develop an accurate modeling approach for nonlinear seismic analysis of large panel reinforced concrete buildings. The paper addressed important aspects such as modeling assumptions, finite element implementation, and static and dynamic verifications to evaluate the performance of the proposed approach.

By utilizing the finite element method and implementing it within the LIRA SAPR software, the study provided a detailed framework for the numerical analysis. The calculations for stiffness determination for each element were derived, ensuring accurate representation of the building's response to seismic forces. This approach facilitates a more realistic simulation of the structural behavior, enhancing the reliability of the analysis results.

In conclusion, this paper presents a comprehensive and reliable modeling approach for nonlinear seismic analysis of large panel reinforced concrete buildings. The developed methodology, supported by the finite element implementation and verification studies, offers a valuable tool for engineers involved in the design and analysis of these structures. The research contributes to the advancement of seismic engineering practices, providing a solid foundation for future studies and enhancing the resilience of large panel reinforced concrete buildings in seismic-prone regions.

The results obtained from the static and dynamic verifications demonstrated the effectiveness of the proposed modeling approach for seismic analysis of large panel reinforced concrete buildings.

In conclusion, this paper presents a comprehensive and reliable modeling approach for nonlinear seismic analysis of large panel reinforced concrete buildings. The developed methodology, supported by the finite element implementation and verification studies, offers a valuable tool for engineers involved in the design and analysis of these structures. The research contributes to the advancement of seismic engineering practices, providing a solid foundation for future studies and enhancing the resilience of large panel reinforced concrete buildings in seismic-prone regions.

References

1. Clough R, Malhas F, Oliva M (1989) Seismic behavior of large panel precast concrete walls: analysis and experiment. *PCI J* 34:42–66. <https://doi.org/10.15554/pcij.09011989.42.66>
2. Mueller P (1988) Experimental investigation on the seismic performance of precast walls. In: 9th world conference on earthquake engineering IV, pp 755–760
3. Velkov M, Ivkovich M, Perishich Z (1984) Experimental and analytical investigation of prefabricated large panel systems to be constructed in seismic regions. In: Proceedings of the eighth world conference on earthquake engineering
4. Velkov M (1981) Large panel systems in Yugoslavia: design, construction and research for improvement of practice and elaboration of codes. ATC-8 proceedings of a workshop on design of prefabricated concrete buildings for earthquake loads. Applied Technology Council
5. Szulc J, Piekarczyk A (2022) Diagnostics and technical condition assessment of large-panel residential buildings in Poland. *J Build Eng* 50:104144. <https://doi.org/10.1016/j.jobe.2022.104144>
6. Srikanth K, Borghate SB (2023) Review on seismic performance evaluation of precast concrete buildings. *Mater Today Proc.* <https://doi.org/10.1016/j.matpr.2023.04.106>
7. Guri M, Brzev S, Lluca D (2021) Performance of prefabricated large panel reinforced concrete buildings in the November 2019 Albania earthquake. *J Earthquake Eng* 26:5799–5825. <https://doi.org/10.1080/13632469.2021.1887010>
8. Polyakov S, Denisov B, Zhunuzov T et al (1969) Investigations into earthquake resistance of large panel buildings. Proceedings of the 7th world conference on earthquake engineering, vol 5, pp 351–358

9. Shapiro G, Ashkinadze G (1980) Ultimate stresses in large-panel buildings exposed to seismic loads. In: Proceedings of the 7th world conference on earthquake engineering, pp 351–358
10. Makhviladze L (1987) Earthquake-resistant large-panel housing construction. Stroyizdat, Moscow
11. Wardach M, Krentowski JR, Knyziak P (2022) Degradation analyses of systemic large-panel buildings using comparative testing during demolition. *Materials* 15:3770. <https://doi.org/10.3390/ma15113770>
12. Pavel F, Scupin A, Vacareanu R (2022) Analysis of the seismic risk of low-code masonry and large panels structures in Romania. *Iran J Sci Technol Trans Civil Eng* 46:1915–1928. <https://doi.org/10.1007/s40996-021-00736-2>
13. Becker J, Llorente C, Mueller P (1980) Seismic response of precast concrete walls. *Earthq Eng Struct Dyn* 8:545–564. <https://doi.org/10.1002/eqe.4290080605>
14. Ashkinadze G, Sokolov M et al (1988) Reinforced concrete walls of earthquake-resistant buildings: research and fundamentals of design. Stroyizdat, Moscow & University of Athens, Athens
15. LIRA-SAPR structural analysis software. LIRA LAND GROUP. <https://www.liraland.com/lira/>. Accessed 15 June 2023
16. SP 335.1325800.2017 (2017) Large-panel construction systems. Design rules. Ministry of Construction, Moscow
17. Abaev Z, Valiev A, Kodzaev M (2023). Methodology of determination of the platform joint of reinforced concrete large-panel buildings stiffnesses. In: Proceedings of the 6th International conference on construction, architecture and technosphere safety. ICCATS 2022. Lecture notes in civil engineering, vol 308. Springer, Cham. https://doi.org/10.1007/978-3-031-21120-1_27
18. SP 63.13330.2018 (2018) Concrete and reinforced concrete structures. Ministry of Construction, Moscow
19. TsNIIEPzhilishcha (1989) Handbook for the design of residential buildings. Stroyizdat, Moscow
20. TsNIIEPzhilishcha (1985) Recommendations for design of large panel buildings in seismic areas. Stroyizdat, Moscow
21. Noji E (1989) The 1988 earthquake in Soviet Armenia: implications for earthquake preparedness. *Disasters* 13:255–262. <https://doi.org/10.1111/j.1467-7717.1989.tb00715.x>
22. PEER Ground Motion Database. <https://ngawest2.berkeley.edu/>. Accessed 15 June 2023



Recycling of Waste from the Woodworking Industry into Eco-friendly Materials for Construction

A. Yu. Lopatin^(✉), V. D. Eskin, A. I. Krivorotova, and A. E. Tyumentseva

Siberian State University of Science and Technology, 31, Krasnoyarskii Rabochii Av.,
Krasnoyarsk 660037, Russia
aikrivorotova@mail.sibsau.ru

Abstract. The article is devoted to the processing of waste from the woodworking industry into environmentally friendly materials for construction and discussion of the results of the study of their basic physical and mechanical properties. Recycling waste from the woodworking industry into environmentally friendly materials for construction is one of the important steps in the development of an environmentally responsible economy. This paper describes the process of processing wood waste into slab materials. The main physical and mechanical properties of the developed materials, such as static bending strength, water absorption and swelling of samples, are considered in detail. The article also discusses the advantages of using eco-friendly materials for construction, such as environmental friendliness and safety for human health, as well as their economic efficiency.

Keywords: Bark · Waste · Recycling · Slab materials · Environmental friendliness · Building materials · Properties

1 Introduction

The problem of filling the construction industry with environmentally safe structural and thermal insulation materials is quite acute. One of the ways to solve this problem may be the use of waste from the processing of commercial timber.

Recycling of waste from the woodworking industry is also an urgent issue today, which plays an important role in the sustainable development of the economy in general and the issue of environmental friendliness of production on renewable natural resources in particular. Every year, woodworking enterprises produce a significant amount of waste that poses a certain danger to the environment. An effective way to solve this problem is the recycling of waste from the woodworking industry into environmentally friendly materials for construction. Such materials can be used to create various structures, including residential buildings, industrial and administrative buildings, public spaces and other structures.

Currently, there are many technologies and materials that allow the recycling of wood waste into new building materials. Among them are wood-polymer composite (WPC),

wood-cement composite (DCC), cement-chipboard, paper-wood composites and others. Plywood products (plywood, plywood boards, bakelized plywood), wood-fiber plastics, fibrolite, chipboard and fiberboard, OSB, MDF are manufactured on the basis of business wood. Such materials have a number of advantages over traditional building materials such as concrete, steel and brick. They have high strength, resistance to humidity, low thermal conductivity, fire protection and other characteristics, which makes them an attractive option for those who care about environmental safety and construction costs.

A well-thought-out choice of wood waste processing technology at such enterprises of the woodworking industry will not only solve one of the main tasks in the field of environmental protection, but also bring new materials with high physical and mechanical characteristics to the construction market at a relatively low cost, since the cost of raw materials is already incorporated into the production of the main products. This will increase the competitiveness of both woodworking enterprises and expand the choice of construction technologies and contribute to the creation of an environmentally friendly future.

The first in processing technology and the largest-tonnage waste of the woodworking industry is the bark of coniferous and deciduous wood species.

Bark from the point of view of processing or recycling is a rather complex component of wood. It has a more complex structure than wood. The bark is heterogeneous in its composition and consists of two parts: the inner one—which is a bast or phloem, and the outer one—which is a crust or cork. The main purpose of the bark is to perform special functions for carrying out nutrients produced by the leaves of the tree and protecting the tree from adverse external influences. The protective function is performed by the outer part of the crust which protects the tree from mechanical damage, the effects of insects and microorganisms that cause rotting, as well as from atmospheric temperature changes. The main elements of the bast that perform a conductive function are sieve cells (in conifers) and sieve tubes (in hardwoods). They form a thin conductive layer in the bast with a thickness of 0.1–0.3 mm. Outside, the bark is covered with dead tissue with deep cracks and furrows, tears and scales. In some breeds, for example, birch, the smooth surface of cork tissue is preserved throughout life [1].

The amount of bark on the wood depends on the age of the tree, the conditions of its growth, the diameter of the trunk. Its safety and quality during the delivery of harvested wood to the enterprise depends on the method of transportation of raw materials. The bark of driftwood in its properties will differ sharply from the bark of freshly cut wood transported by land transport.

The density of the bark depends not only on the type of tree and the moisture content, but also its location on the trunk [2]. The most important role of the characteristics of the structure and the values of the density of the crust is that they mainly depend on various physical and mechanical properties of the crust [3].

The chemical composition of tree bark also differs significantly from the chemical composition of wood. A characteristic feature of the chemical composition of the bark is the high content of extractive substances. The mass fraction of holocellulose in the bark is about 2 times lower than in wood (on average 30–40%). The main polysaccharide in bark, as in wood, is cellulose, but unlike wood, it is not the predominant component. Its content in the bark is 10–30%. The content of lignin varies widely from 20 to 50%.

Bark is more difficult to delignify than wood. The bark is also rich in minerals. The mass fraction of ash is 5–10%, which is 10 times higher than the ash content of wood [4–17].

It should be noted that significant differences in the chemical composition of wood and bark determine the need for separate processing of these parts of the biomass of the tree. Bark can be used as fuel, in agriculture for the production of bark compost, in the tanning and extraction industry for the extraction of tannins, which are used in the leather industry for tanning leather. Due to the presence of valuable extractive substances in the bark, it can be used in medicine [15, 16].

One of the ways of industrial processing of bark can be called manufacturing technologies of piezothermoplastics and lignocarbon plastics. These technologies provide the processing of woodworking waste without restriction in the composition of bark and rot under the influence of high temperature and pressure [5]. Most often, this is piezothermic treatment of wood waste in a closed space which ensures the production of plastics without binders due to complex physico–chemical processes that determine the quality of plastics. The advantages of such plates are as follows: production does not depend on the availability of binders, their scarcity and cost; there is an almost unlimited raw material base and, as a result, low cost of manufactured products; production is environmentally safe [18].

Another method of industrial processing of bark was proposed by the Kirov Scientific Research Institute of the Forest Industry. KirNIILP has developed a technology for the production of fuel briquettes from bark and small waste of mechanical processing of wood. Briquettes can be used for combustion in a mixture with other fuels or in pure form. The raw materials for briquetting are the waste of debarking and wood that are not used for technological purposes. The density of fuel briquettes is 0.9–1 g/cm³, the calorific value at a humidity of 20% is from 3500 to 4000 J/kg.

In SverdNIIPDrev [6], the use of spruce bark for sheets without binders (wood plastics) was investigated, a technology for producing sheet materials without binders (with cooling during pressing) was developed. Pressing mode of plates for the bark of the alloy spruce: humidity 12%; temperature from 438 to 443 °C; specific pressure 50–105 N/m²; cooling time 1 min per 1 mm of plate thickness.

In the GDR [7, 8], medium-density fibrous plates were made from spruce bark (wet leg waste) with the addition of 6% binder and paraffin. Since the bark had a humidity of 100% before pressing, to accelerate drying during pressing in a hot press, a drainage material containing lignocellulose (sawdust, xylitol, bonfire or waste from debarking of other wood species) was introduced into the filler.

In Poland single-layer sheets from the waste of debarking were pressed without hydrophobic additives on a urea binder. When pressing, three types of raw materials were used: pine bark from the hams with a humidity of 140%; a mixture of pine and birch bark from the dump with a humidity of 220%; a mixture of bark from «Cambio» machines and bark from the heap in a ratio of 1:3.

Most of the above-described bark-based materials have low physical and mechanical properties, and therefore much attention is paid to the development of sheets structures using bark for the middle layer.

In Finland single-layer sheets were pressed from a mixture of bark and sawdust taken in different ratios, with the addition of 18% aminoplast binder. The density of the plates was 0.65 g/cm^3 .

The company “Bizon” in the work [4] proposes a method for the production of bark sheets using air fractionation when gluing wood particles and forming a carpet. The plates obtained by fractionation have a high surface quality and are 20% stronger than the plates obtained by the usual method; they are less susceptible to warping and delamination.

One of the modern directions of wood waste processing which is widely represented in the works of a number of authors, is the mechanical activation of wood particles in cavitation installations operating on the principle of a rotary pulsating apparatus [9, 10, 19]. The grinding of particles to an appropriate state is carried out in an aqueous medium in combination with high angular velocities and hydrodynamic impact. In the produced material the lignocarbon matrix and anatomical elements are destroyed with the simultaneous release of chemicals.

Thus, it should be noted:

- recycling of waste from wood processing industries of hardwood, including waste from debarking of wood raw materials, is a promising direction for the development of new composite materials with high physical and mechanical properties;
- deciduous wood debarking waste has a fairly wide scope of application in the pharmacological and cosmetic industries;
- the chemical composition of the bark of hardwood has differences from the chemical composition of hardwood. The structure of the cells of the bark also differs depending on the type of wood.

2 Experimental Part

The main objective of the research presented in this paper is to conduct a comparative analysis of the properties of sheets made on the basis of the bark of deciduous and coniferous wood species in order to determine possible directions and methods of their application as thermal insulation, finishing or structural materials in the construction industry [20].

The bark of birch and aspen wood was used for the experiments. The bark was harvested in the autumn-spring period in Krasnoyarsk region, crushed and aged for seven days at positive temperatures to acquire equilibrium humidity.

Further preparation of the tree bark and the manufacture of sheets was carried out according to the methods described in the works of the authors [11, 12]. A brief description of the plate manufacturing process is as follows. In laboratory conditions the bark was prepared for mechanical activation in a knife-type crusher after which the crushed bark was sieved on a sieve with a hole diameter of 5 mm. For mechanical activation of the bark a machine of the RGGD–1 brand was used. The device disperses the processed material in an aqueous medium. The main elements of the machine installation are the rotor and stator. The bark treated in a hydrodynamic dispersant with a given concentration was dehydrated in two stages. At the first stage, the suspension, in the amount necessary for the production of samples according to the established procedure,

was placed in a box, the bottom of which was a grid with a certain cell size. Due to the influence of gravity, the water was removed through the grid, thereby reducing the humidity of the mass by 40–60% of the original. The partially dehydrated mass for one sample of the plate is placed in a mold, where the second stage of dehydration takes place and a carpet with the required dimensions is obtained. Next, hot or cold pressing is performed.

To conduct a comparative analysis of the properties of sheet material made on the basis of hardwood bark, birch bark, aspen bark and softwood bark were used as raw materials. Three groups of samples were produced by hot pressing. The first group is based on birch bark, in which the outer part of the bark (birch bark) almost completely prevailed. The second group of samples was made from a mixture of birch bark and aspen, while the birch bark content of birch bark and bast was not controlled. The ratio of birch and aspen bark was maintained approximately equally. The third group of samples was made from a mixture of softwood bark for the purpose of comparative analysis.

3 Discussion of the Results

Figures 1, 2, 3 and 4 present comparative histograms of static bending strength, water absorption and swelling of samples of different densities.

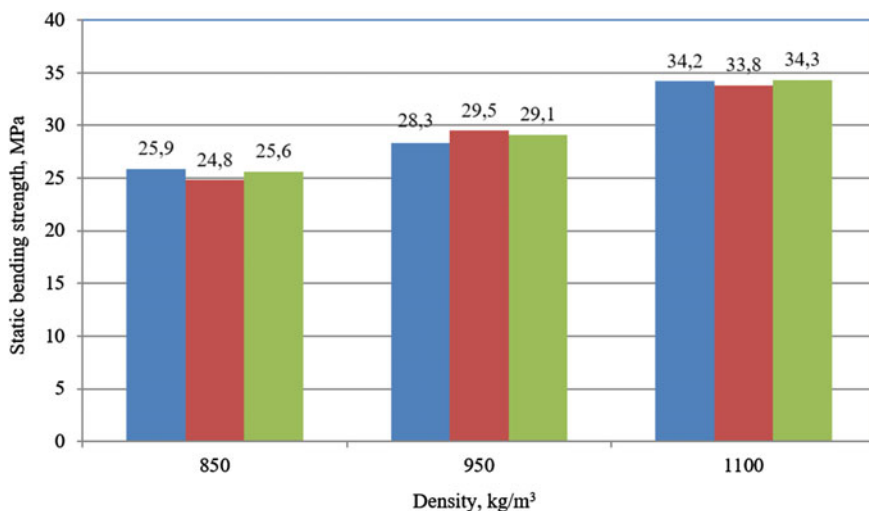


Fig. 1 Comparative histogram of the strength index during static bending of samples based on mechanically activated bark. Bark: 1—coniferous; 2—birch; 3—deciduous (birch, aspen)

As can be seen from Fig. 1, all samples of manufactured plates have similar strength indicators, regardless of the rock composition of the crust. The difference in strength indicators is within the measurement error. The strength under static bending varies more pronounced depending on the density of the samples, which is clearly seen in Fig. 2.

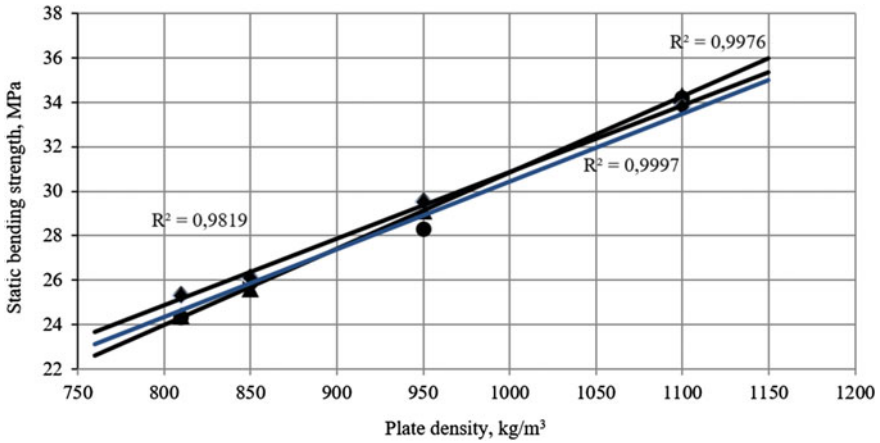


Fig. 2 A graph of the strength dependence during static bending of samples based on mechanically activated bark. Bark: ●—birch; ▲—coniferous; ◆—deciduous (birch, aspen)

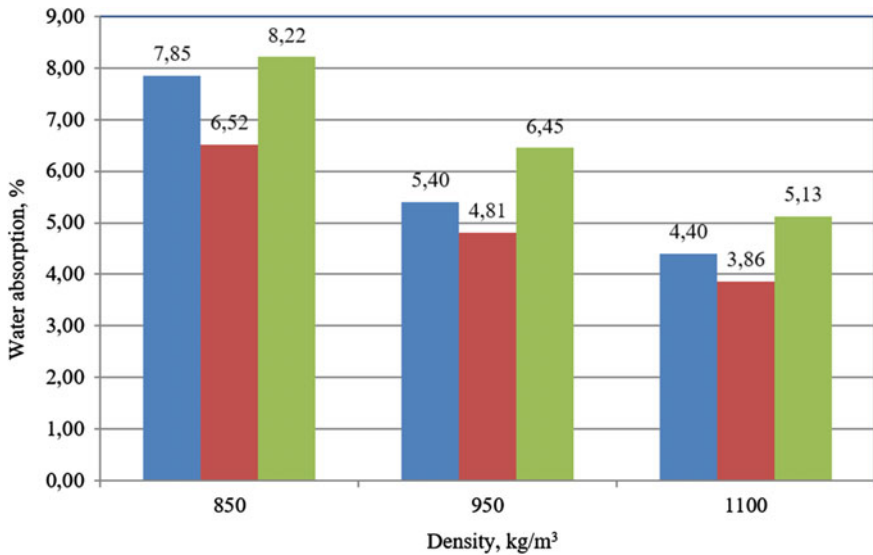


Fig. 3 Comparative histogram of the water absorption index of samples based on mechanically activated bark. Bark: 1—coniferous; 2—birch; 3—deciduous (birch, aspen)

For all samples, an increase in static bending strength is observed with an increase in density. The density was measured from 830 to 1100 kg/m³. At the same time, the linear dependence graphs are located close enough to each other, which also confirms the assumption that the properties of plate materials based on mechanically activated bark depend primarily on the degree of crushing of the bark and the time of its processing, as well as on the pressing conditions and slightly depend on the rock composition of the bark mass.

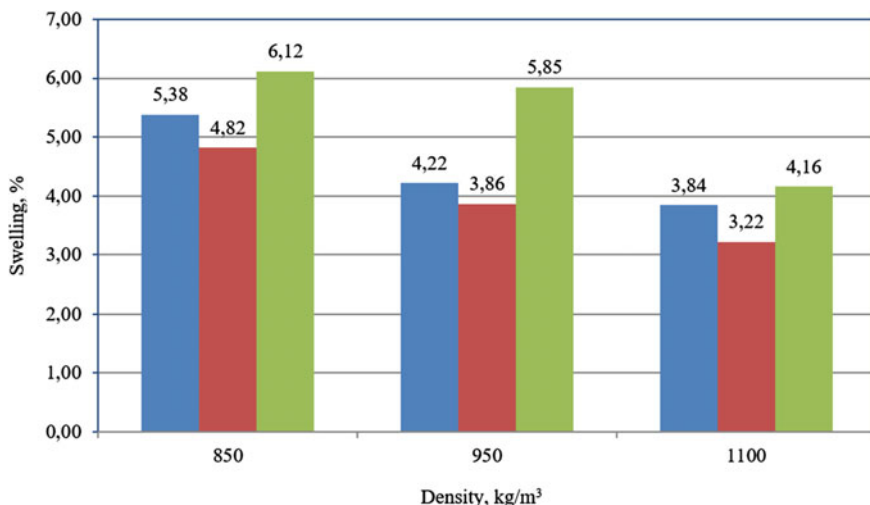


Fig. 4 Comparative histogram of the swelling index of samples based on mechanically activated bark. Bark: 1—coniferous; 2—birch; 3—deciduous (birch, aspen)

As a result of mathematical processing of experimental data, regression equations were obtained expressing the dependence of the strength during static bending of material samples on density.

For samples based on treated birch bark:

$$\sigma_{izg} = -2.826 + 0.033 \cdot \rho \quad (1)$$

based on treated hardwood bark:

$$\sigma_{izg} = 0.914 + 0.029 \cdot \rho \quad (2)$$

based on processed softwood bark:

$$\sigma_{izg} = -3.517 + 0.034 \cdot \rho \quad (3)$$

The regression coefficients were respectively:

- based on birch bark: $R^2 = 0.9990$;
- based on hardwood bark: $R^2 = 0.9973$;
- based on softwood bark: $R^2 = 0.9997$.

Figure 3 shows a comparative histogram of the water absorption index for plates with densities of 850, 950 and 1100 kg/m³. As can be seen from the presented histogram, a plate based on mechanically activated birch bark has the lowest water absorption indicators. Depending on the density, the water absorption varies from 3.86 to 6.52%. The material based on the bark of hardwood has the highest indicators. In the range between the values presented is a material based on mechanoactivated softwood bark.

The difference in the indicators of water absorption of the material based on birch bark can be explained by its physical structure and chemical composition. Birch bark has two clearly distinguishable parts—the outer (birch bark) and the inner (bast), which differ significantly in chemical composition. The outer bark is the most rich in extractive substances. Birch bark bast contains less extractive substances and their composition differs from the composition of substances extracted from birch bark. Birch bark has a denser structure, low wettability of the surface, low absorbency. The club is more porous, less dense. For experimental studies, it was the outer part of the bark (birch bark) that was mostly selected for samples from birch bark, while all parts of birch bark were used in the manufacture of samples of material based on hardwood without prior sorting.

Nevertheless, it should also be noted a rather insignificant difference in the water absorption rates of sheets based on the bark of different types of wood.

Figure 4 shows a comparative histogram of the swelling index of sheets based on birch bark, deciduous and coniferous wood species. As can be seen from the histogram, the trend of changes in the swelling indicators corresponds to the picture of changes in the water absorption index. The lowest swelling rates are observed in samples of plates made of mechanically activated birch bark, the largest from mechanically activated hardwood bark. The minimum index has plates with a density of 1100 kg/m^3 —3.22%, the highest swelling index is a plate based on mechanically activated hardwood bark with a density of 850 kg/m^3 —6.12%.

Table 1 presents the results of a study of the properties of sheets based on deciduous and coniferous wood species.

Table 1 Results of the study of the basic physical and mechanical properties of plates based on mechanoactivated bark of various types of wood

The name of the indicator	Rock composition of mechanoactivated bark		
	Birch tree	A mixture of deciduous	A mixture of conifers
Density, kg/m^3	700	700	730
Compressive strength, MPa	1.91	1.90	2.18
Water absorption, %	17.60	18.00	16.00
Swelling, %	9.00	9.00	7.00

As can be seen from the data presented in Table 1, cold pressing plates with almost the same density have slightly different properties in comparison with hot pressing plates. The compressive strength of cold-pressed plates made from a mixture of softwood bark has higher values in comparison with plates made from mechanically activated birch bark and a mixture of hardwood bark. Indicators of water absorption and swelling also differ for the better in plates made of softwood bark. However, it should also be noted, as in the case of hot pressing plates, a low difference in the values of the properties indicators. Nevertheless, this difference is more significant and amounts to 1.6–2% for the water absorption index, 2% for the swelling index.

4 Summary

As a result of the research work the following main conclusions can be drawn:

1. With an increase in the density of hot pressing plates, the strength during static bending of the plates increases regardless of the rock composition of the processed bark;
2. Plates based on mechanoactivated bark of coniferous and deciduous wood species have similar values of water absorption and swelling indicators, therefore, it should be said that the water resistance of the materials obtained does not depend much on the rock composition of the bark used for mechanoactivation;
3. Plates obtained by cold pressing have a large dependence of properties on the rock composition of the crust, however, these dependencies cannot be called significant or critical for materials based on them;
4. Strength properties, water absorption, swelling of plates based on mechanically activated bark depends more on the density of the plates than on the rock composition of the treated bark;

Thus, it should be noted that for the manufacture of plates based on mechanoactivated bark, it is possible to use the bark of both deciduous and coniferous wood species without a significant deterioration in the physical and mechanical properties of materials. The developed materials obtained by cold and hot pressing methods have high prospects of application in various areas of the construction industry, so they have a wide range of density and high physical and mechanical characteristics combined with complete environmental safety.

References

1. Dendrology (2023). <http://dendrology.ru/books/item/f00/s00/z0000030/st002.shtml>. Accessed 6 June 2023
2. Simonov MN (1984) Mechanization of timber debarking. Moscow
3. Modern Production Technologies (2023). <https://extxe.com/15673/svojtva-kory-opredelja-jushhie-process-okorki/>. Accessed 1 June 2023
4. Russian State Library (2023). <https://viewer.rsl.ru/ru/rsl01005542009?page=17&rotate=0&theme=white>. Accessed 25 May 2023
5. Kazitsin SN, Ermolin VN, Bayandin MA, Namyatov AV (2016) Development of the hot pressing mode of plates without binders from mechanically activated wood particles. Conifers of the boreal zone, no 5–6
6. Korchagov SA (2012) Wood science: an educational and methodological manual. Vologda
7. Musikhina LN (1971) Complex use of spruce bark. Abstracts of the All-Union Conference on the use of tree bark, Sverdlovsk, pp 51–53
8. Dictionaries and encyclopedias. “Academician”. <http://dic.academic.ru/>. Accessed 25 May 2023
9. Namyatov AV, Bayandin MA, Kazitsin SN, Ermolin VN (2018) Investigation of the properties of low-density plates made of mechanically activated wood particles without the use of binders. Wood Structure, Properties and Quality—2018: in honor of B.N. Ugolev. In: Proceedings of the 6th RCCWS international symposium dedicated to the 50th anniversary of the Regional Coordinating Council of Wood Science, Krasnoyarsk, 10–16 Sept 2018, Novosibirsk, SB RAS Publ., pp 149–152

10. Kazitsin SN (2018) Obtaining wood slabs without binders from mechanically activated wood particles. Dissertation, Siberian State University of Science and Technology named after Academician M. F. Reshetnev (Krasnoyarsk), p 132
11. Eskin VD, Krivorotova AI (2021) Investigation of modes and properties of sheet materials from mechanically activated wood particles. Current problems and prospects for the development of the forest industry, Kostroma, 8–11 Sept 2021, pp 109–111
12. Method of manufacturing wood slabs (2013) Russian Federation № 2013156883/04, 20 Dec 2013
13. Pokhilo ND (1988) Isoprenoids of various species of the genus *Betula*. *Chem Nat Compd* 3:325–341
14. Kuznetsov BN et al (1998) Isolation of betulin and suberin from birch bark activated under conditions of “explosive autohydrolysis.” *Chem Plant Raw Mater* 1:5–9
15. Bondarenko SM (1989) Leucoanthocyanidins of the bark of the hanging birch. *Izv SB RAS USSR Ser Chem Sci* 1:86–90
16. Azarov VI et al (1999) Chemistry of wood and synthetic polymers. SPbLTA: St. Petersburg, p 628
17. Goodwin T, Mercer E (1986) Introduction to plant biochemistry. Moscow
18. PROMZN.RU Industrial Portal. <https://promzn.ru/derevoobrabotka/pererabotka-drevesnyh-othodov.html>. Accessed 29 May 2023
19. Promtov MA (2001) Pulsating rotary type apparatuses: theory and practice. Moscow
20. Lopatin AYu, Tyumentseva AE, Eskin VD, Krivorotova AI (2022) Composite materials from waste wood raw materials, pp 826–827



Optimization of Plane Frames with Variable Cross-Section

Pham Van Trung^(✉) and Nguyen Vu Thiem

Hanoi Architectural University, Km 10, Nguyen Trai Street, Thanh Xuan District, Hanoi, Vietnam

pvtrung07@gmail.com, tthvan.hau@gmail.com

Abstract. Nowadays, in structural engineering, many elements in structural systems are selected with variable cross-sections for some purposes. The optimization problem helps to define the suitable dimensions of elements for the optimal weight of the system under given loading and other effects. In the studies of optimization, it is applied many methods depending on the characteristics of the problem. The article uses the Gradient and graphic methods to optimize plane frames with constant and variable cross-sections. The authors established the relationship between internal forces and displacements of the element ends with different boundary conditions using force and displacement methods. With the development of technology, it is allowed to use programming software to avoid mathematical difficulties. The calculation procedure of the considered optimization problem is written in the programming software MATLAB in the article. The obtained results are compared with those of other methods to verify the applied method's accuracy, reliability and effectiveness.

Keywords: Optimization · Gradient method · Variable cross-section · Plane frame

1 Introduction

Recently, in the design process of structural systems, the problems of optimization problem have been increasingly discussed in many studies due to their essential role and saving materials. The optimization problem aims to determine the most suitable dimensions of elements to save the structural weight under the strength, stiffness and stability conditions [1–3]. Determining optimal sizes for structural elements subjected to given loads and other effects could result in the minimum weight of the structure. This allows to reduce the cost of construction and gives the advantageous characteristics of structural elements. Besides that, the problem of optimization helps in determining the cross-section dimensions and the rules of variation of cross-section stiffness. Therefore, with the same weight, the structural systems can be subjected to maximum loads.

The cross-section stiffness of structural elements is often constant for convenient manufacturing and installation works. However, in some instances, the cross-section of elements is selected in the design process with variation because of requirements from

an architectural point of view or the saving of material. In many studies, the elements of plane frames are chosen with variable cross-sections according to linear or step rules in segments along the length of members [4, 5].

In optimization problems, the objective function usually presents the quantities that need to be minimized, such as weight, volume of the structure and cost of materials. Constraint conditions in the form of equality are usually equilibrium conditions and continuous deformation conditions. Constraint conditions in the form of inequality are strength, stiffness and yield conditions. The form of the objective function and constraints depends on the type of structures and applied analysis method. To determine the internal forces of structural elements, the analytical approach can be applied using the programming software MATLAB to avoid mathematical difficulties. The optimization problems could be solved by many methods due to the criteria of the issues and objectives of the studies [2, 3, 5–12]. However, the Gradient method is suitable for applying to problems where gradients of objective and constraint functions can be computed quickly. Besides that, for structural systems with few elements, using Gradient and graphic methods allows for solving problems simply.

2 Static Analysis of Plane Frame Using Analytical Method

2.1 Determination of Internal Forces and Displacements

Consider an indeterminate plane frame (with n redundant constraints) and subjected to m concentrated loads. Getting:

Load vector:

$$P = [P_1 \ P_2 \ P_3 \ \dots \ P_n] \quad (1)$$

Force vector in redundant constraints:

$$R = [R_1 \ R_2 \ R_3 \ \dots \ R_n] \quad (2)$$

The internal forces due to loads and reaction support of redundant constraints:

$$S_0 = B_0 \times P; \quad S_R = B_1 \times R; \quad B_1 = \sum B_i \quad (3)$$

S_0 —Vector of internal forces due to loads in primary system; S_R —Vector of internal forces due to support reaction of redundant constraints in primary system; B_0 —Matrix considers the influence of internal forces due to concentrated load P ; B_i —Matrix considers the influence of internal forces due to support reaction R_i .

Vector of internal forces of the system:

$$S = S_0 + S_R = B_0 \times P + B_1 \times R \quad (4)$$

Vector of strain of the system:

$$U = f \times S = f(B_0 \times P + B_1 \times R) \quad (5)$$

In which: f —flexible matrix of frame structure.

2.2 Compatibility Conditions for Strain

Call X_P —displacement in the direction of the external force P ; X_R —displacement in the direction of the redundant constraints.

In order to find the displacement X_P , it is created a displacement state on the primary system by removing all the forces P and R and adding a virtual load P_k at the point of applied P of any value.

S_{Pk} —internal forces in primary system due to virtual load P_k . According to (3), getting that:

$$\bar{S}_P = B_0 \times \bar{P} \quad (6)$$

Applying the principle of virtual work:

$$\bar{P}' \times X_P = \bar{S}_P \times U \quad (7)$$

In which, the left side of (7) represents the virtual work of external force in virtual state with the virtual displacements in actual state. Whereas, the right side of (7) shows the virtual work of internal forces in virtual state with the virtual displacements in actual state.

However:

$$\bar{S}_P = B_0 \times \bar{P} \rightarrow \bar{P}' \times X_P = \bar{P}' \times B_0' \times U$$

P have any magnitude, so:

$$X_P = B_0' \times U \quad (8)$$

Substitute the vector of displacement from (5):

$$X_P = B_0'(f \times B_0 \times P + f \times B_1 \times R) = B_0' \times f \times B_0 \times P + B_0' \times f \times B_1 \times R \quad (9)$$

Similarly, in order to find displacement X_R , it is created X_R in the primary system by removing all the forces P and R and adding a virtual load R_k at the point of applied load R of any value.

Call S_R —internal forces in primary system due to virtual load R_k . According to (3), getting:

$$X_R = B_1'(f \times B_0 \times P + f \times B_1 \times R) = B_1' \times f \times B_0 \times P + B_1' \times f \times B_1 \times R \quad (10)$$

In the system, the displacement in the direction of constraint R equal to 0 ($X_R = 0$), so:

$$B_1' \times f \times B_0 \times P + B_1' \times f \times B_1 \times R = 0 \quad (11)$$

Equation (11) is called primary equation of forced method, or equation of compatibility conditions for strain. For determinate system, since $R = 0$, getting:

$$S = B_0 \times P; \quad U = f \times S = f \times B_0 \times P; \quad X_P = F \times P \quad (12)$$

In which, F —flexibility matrix of the structure:

$$F = B_1' \times f \times B_0 \quad (13)$$

2.3 Relationship Between Internal Forces and Strain

The relationship between the moment and the rotation angle of *ij*-element with fixed ends can be written:

$$M_i = 4\left(\frac{EI}{L}\right)_{ij}\theta_i + 2\left(\frac{EI}{L}\right)_{ij}\theta_j; \quad M_j = 2\left(\frac{EI}{L}\right)_{ij}\theta_i + 4\left(\frac{EI}{L}\right)_{ij}\theta_j \quad (14)$$

M_i, M_j —Moment of the ends of *ij*-element; θ_i, θ_j —The rotation angle at I, j ends of the *ij*-element (Fig. 1).

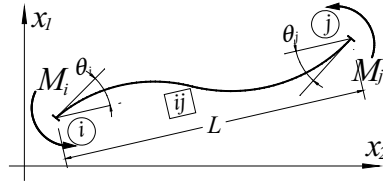


Fig. 1 Deformation scheme of *ij*-element

Solve Eq. (14) with unknowns θ_i, θ_j

$$\theta_i = \frac{1}{3}\left(\frac{L}{EI}\right)_{ij} M_i - \frac{1}{6}\left(\frac{L}{EI}\right)_{ij} M_j; \quad \theta_j = \frac{1}{6}\left(\frac{L}{EI}\right)_{ij} M_i - \frac{1}{3}\left(\frac{L}{EI}\right)_{ij} M_j \quad (15)$$

In the matrix form:

$$U_{ij} = f_{ij} \times S_{ij} \quad (16)$$

U_{ij} —Vector of strain; S_{ij} —Vector of internal forces; f_{ij} —Flexibility matrix of *ij*-element.

$$U_{ij} = \begin{bmatrix} \theta_i \\ \theta_j \end{bmatrix}; \quad S_{ij} = \begin{bmatrix} M_i \\ M_j \end{bmatrix}; \quad f_{ij} = \frac{1}{6}\left(\frac{L}{EI}\right)_{ij} \begin{bmatrix} 2 & -1 \\ -1 & 2 \end{bmatrix} \quad (17)$$

3 Optimization for Plane Frame with Variable Cross-Section

3.1 Flexibility Matrix of Element with Variable Cross-Section

In practical engineering, many different solutions are offered to utilize the working capacity of the structures and reduce the material cost. One of the solutions is making the variable cross-section match the internal force that is often applied.

- Function of area and moment of inertia of cross-section:

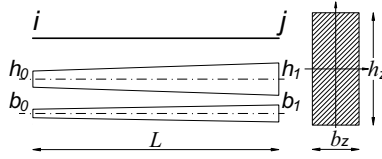


Fig. 2 Element of variable cross-section

Consider ik -element with variable rectangular cross-section along the length of element. The dimensions at the i -end is b_i, h_i and at the j -end is b_k, h_k as shown in Fig. 2.

The area and moment of inertia of cross-section at the element ends.

$$A_i = b_i \times h_i; \quad A_k = b_k \times h_k; \quad I_i = \frac{b_i \times h_i^3}{12}; \quad I_k = \frac{b_k \times h_k^3}{12} \quad (18)$$

Assign: $\xi = \frac{z}{L} \rightarrow z = \xi L \rightarrow dz = Ld\xi \quad (0 \leq \xi \leq 1)$

$$b = \frac{b_k - b_i}{b_i}; \quad h = \frac{h_k - h_i}{h_i}; \quad b_z = b_i(1 + b\xi); \quad h_z = h_i(1 + h\xi) \quad (19)$$

The area and moment of inertia of cross-section at coordinate z are expressed through ξ as follow:

The highest degree of ξ for function of area is two:

$$A_z = b_z h_z = A_i \left[1 + (b + h)\xi + bh\xi^2 \right] = A_i \left[1 + c_1\xi + c_2\xi^2 \right] \quad (20)$$

In which: $c_1 = (b + h); \quad c_2 = bh$.

The highest degree of ξ for function of moment of inertia is four:

$$I_z = \frac{b_z h_z^3}{12} = I_i \left[1 + a_1\xi + a_2\xi^2 + a_3\xi^3 + a_4\xi^4 \right] = I_{if}(\xi) \quad (21)$$

- Relationship between internal forces and displacements of the element ends:

Consider ik -element with two fixed ends subjected to rotation θ_i in the i -end and rotation θ_k in the k -end. Determine the internal forces in the element using forced method. The primary system and unit moment diagram as shown in Fig. 3.

The functions for unit moment according to forced method:

$$M_1(z) = z = \xi L; \quad M_2(z) = 1 \quad (22)$$

Calculate the coefficients of canonical equations:

$$\delta_{11} = \int_0^L \frac{[M_1(z)]^2}{EI_z} dz = \int_0^1 \frac{\xi L \xi L}{EI_{if}(\xi)} L d\xi = \frac{L^3}{EI_i} \int_0^1 \frac{\xi^2}{f(\xi)} d\xi = A \frac{L^3}{EI_i}$$

$$\delta_{22} = \int_0^L \frac{[M_2(z)]^2}{EI_z} dz = \int_0^1 \frac{1 \cdot 1}{EI_{if}(\xi)} L d\xi = \frac{L}{EI_i} \int_0^1 \frac{1}{f(\xi)} d\xi = B \frac{L}{EI_i}$$

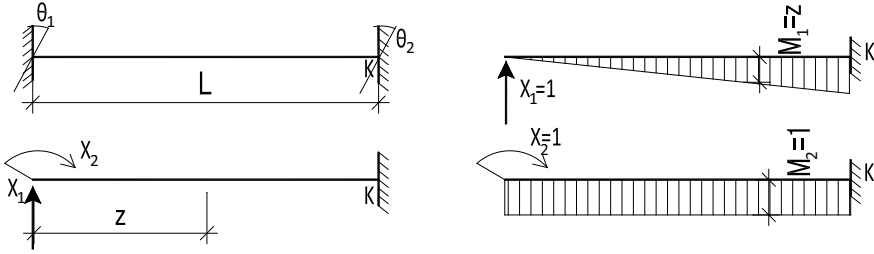


Fig. 3 Primary system and unit moment diagram for fixed-beam

$$\delta_{12} = \delta_{21} = \int_0^L \frac{M_1(z)M_2(z)}{EI_z} dz = \frac{L^2}{EI_i} \int_0^1 \frac{\xi}{f(\xi)} d\xi = C \frac{L^2}{EI_i} \tag{23}$$

In which:

$$A = \int_0^1 \frac{\xi^2}{f(\xi)} d\xi; \quad B = \int_0^1 \frac{1}{f(\xi)} d\xi; \quad C = \int_0^1 \frac{\xi}{f(\xi)} d\xi \tag{24}$$

The free terms of canonical equations:

$$\Delta_{1\theta} = -L\theta_k; \quad \Delta_{2\theta} = \theta_i - \theta_k \tag{25}$$

Substitute the system of canonical equations, solving the system of equation, getting the solution:

$$\begin{cases} X_1 = \frac{EI_i}{L(C^2-AB)} [-C\theta_i + (B-C)\theta_k] \\ X_2 = \frac{EI_i}{L(C^2-AB)} [-A\theta_i + (A-C)\theta_k] \end{cases} \tag{26}$$

Bending moment in the element ends:

$$\begin{cases} M_i = \frac{EI_i}{L(C^2-AB)} [A\theta_i - (A-C)\theta_k] \\ M_k = \frac{EI_i}{L(C^2-AB)} [(A-C)\theta_i - (A+B-2C)\theta_k] \end{cases} \tag{27}$$

In the matrix form:

$$\begin{bmatrix} M_i \\ M_k \end{bmatrix} = \frac{EI_i}{L(C^2-AB)} \begin{bmatrix} A & -(A-C) \\ (A-C) & -(A+B-2C) \end{bmatrix} \begin{bmatrix} \theta_i \\ \theta_k \end{bmatrix} \tag{28}$$

The expression of rotation angle according to bending moment:

$$\begin{bmatrix} \theta_i \\ \theta_k \end{bmatrix} = \begin{bmatrix} -\frac{L(A+B-2C)}{EI_i} & \frac{L(A-C)}{EI_i} \\ -\frac{L(A-C)}{EI_i} & \frac{LA}{EI_i} \end{bmatrix} \begin{bmatrix} M_i \\ M_k \end{bmatrix} \tag{29}$$

Flexibility matrix of element with variable cross-section

$$f_{ik} = \frac{L}{EI_i} \begin{bmatrix} -(A+B-2C) & (A-C) \\ -(A-C) & A \end{bmatrix} \tag{30}$$

3.2 Establishment of Constraint Conditions

Consider a plane frame, the vector of internal forces is determined in Eq. (4).

a. Strength constraint

For the beam element:

$$\sigma_i = \frac{M_i}{W_i} \leq \sigma_i^* \quad (31)$$

In which, M_i —bending moment at the cross-section i ; W_i —section modulus of cross-section i ; σ_i^* —yield strength of materials.

In the matrix formulation, Eq. (31) can be written:

$$W \times S = W(B_0 \times P + B_1 \times R) \leq \sigma_i^* \quad (32)$$

Or:

$$W \times B_0 \times P + W \times B_1 \times R \leq \sigma_i^* \quad (33)$$

In which W —diagonal matrix with number of cross-section k

$$W = \begin{bmatrix} W_1^{-1} & 0 & \dots & 0 \\ 0 & W_2^{-1} & \dots & 0 \\ \vdots & \vdots & \ddots & \vdots \\ 0 & 0 & \dots & W_k^{-1} \end{bmatrix} \quad (34)$$

In the aboved expressions, the parameters W_i with the same index are iterated pairwise on the diagonal of the matrix because for the ij -th element $W_i = W_j$ (for constant cross-section).

At the section of element i , the condition of strength is written as follows:

$$\frac{\left(\frac{D_{ii}}{W_i} + \sum_{k=1}^n e_{tik} R_k \right)}{W_i} \leq \sigma_i^* \quad (35)$$

The first term in brackets is the result of multiplying the k -th row of the matrix W by the matrix $[B_0 P]$. The second term is the result of multiplying the k -row of the matrix W by the matrix $[B_1 R]$.

b. For beam-column elements, the strength constraint takes form

$$\frac{N_i}{A_i} + \frac{\left(\frac{D_{ii}}{W_i} + \sum_{k=1}^n e_{tik} R_k \right)}{W_i} \leq \sigma_i^* \quad (36)$$

In which: N_i —axial force in i -element; A_i —area of cross section of i -element.

c. Stiffness constraint

Assume that Δ_j —displacement vector at the points where the load applied. Using the formula (10), getting the stiffness constraint:

$$X_P = \{y_1 \ y_2 \ \dots \ y_m \} = B'_0 \times f \times B_0 \times P + B'_0 \times f \times B_1 \times R \leq \Delta \quad (37)$$

To check the displacement at the point where the force P_j is applied, it is multiplied the j -th row of the matrix $[B'_0.f.B_0]$ with force vector P and j -th row of matrix $[B'_0.f.B_1]$ with vector R . Based on the multiplication, the constraint condition gets the form:

$$\sum_{i=1}^r \frac{a_{ji}}{I_i} + \sum_{k=1}^n R_k \sum_{i=1}^r \frac{b_{jki}}{I_i} \leq \Delta_j \quad (38)$$

In which: Δ_j —permissible displacement at the point where the load P_j applied.

d. Constraint condition of compatibility

$$B'_0 \times f \times B_0 \times P + B'_0 \times f \times B_1 \times R = 0 \quad (39)$$

From Eq. (39), the constraint condition of compatibility at the points where the reactions of redundant constraints R_s applied ($s = 1, 2, 3 \dots n$):

$$\sum_{i=1}^r \frac{g_{ji}}{I_i} + \sum_{k=1}^n R_k \sum_{i=1}^r \frac{f_{jki}}{I_i} = 0 \quad (40)$$

In which: $\sum_{i=1}^r \frac{g_{ji}}{I_i}$ —the result of multiplying k -th of matrix $[B'_0.f.B_0]$ with P ;
 $\sum_{i=1}^r \frac{f_{jki}}{I_i}$ —the element of the s —row and k -column of matrix $[B'_0.f.B_1]$.

3.3 Establishment of Objective Function

Consider a structure with n element, the i -th element have the length L_i and area A_i . The specific gravity of the element material is γ_i . The mass of the i -th element is G_i .

The objective function in form of weight of structure:

$$G = \sum_{k=1}^n \gamma_i A_i L_i \quad (41)$$

3.4 Calculation Procedure

The optimization problem is performed by following procedure:

- Calculate the internal forces in frames with variable cross-section
- Establish the constraint condition
- Establish the objective function
- Solve the optimization problem:

- Using graphic method:

Draw the constraint of strength and stiffness—determine the solution area;
 Determine the slope of the objective function;
 Draw a line of objective function which tangent to the stiffness constraint line.
 Determine the contact point, coordinates and objective function value

- Using Gradient method:

Calculate the Gradient vectors of the objective function and the constraint conditions;
 Choose the starting point A in the solution area $\{x_0\}$, determine λ and $\{d_0\}$.
 Calculate the coordinates of the point to B $\{x_1\}$, determine $\{d_0\}$ and λ and to calculate the coordinates of the next point C. This step requires to continue until the optimal point is reached.
 Determine the coordinates of optimal point and objective function value.

4 Numerical Examples

Consider a single span frame with the height H , span length L subjected to the load P as shown in Fig. 4. The column with cross-sectional area varies in rectangular shapes at the support $A_0 = b_0.h_0$, at the top of the column $A_1 = b_1.h_1$. The beams have constant cross-sectional area $A_2 = b_2.h_2$. The maximum valuable stress arising in the structure σ^* . The maximum horizontal displacement does not exceed Δ . Find the values of h_1 và h_2 which corresponding to the minimum weight of frame.

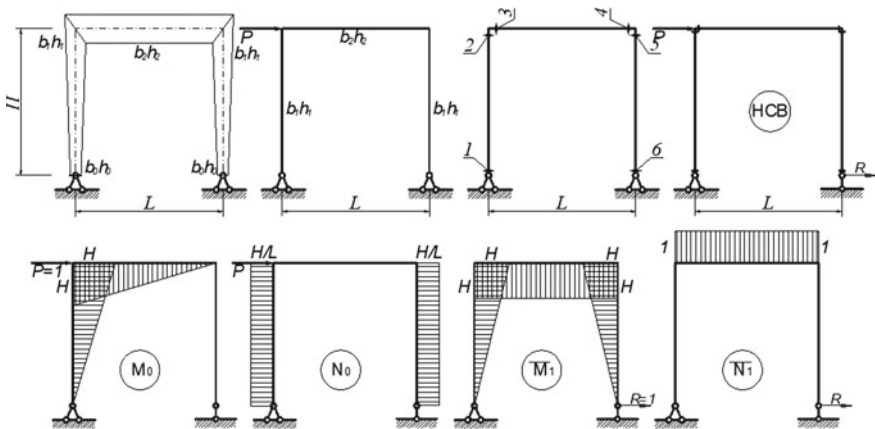


Fig. 4 Calculation diagram of the frame with variable cross-section

Given $H = 9000$ mm; $L = 6000$ mm; $P = 50$ kN; $E = 400$ kN/mm²; according to require of manufacture $b_1 = b_2 = 200$ mm và $h_0 = 0.5h_1$; $\Delta = 8$ mm; $\sigma^* = 0.1$ kN/mm²; $\gamma = 0.000025$ kN/mm³.

The objective function:

$$Z = 67.5h_1 + 30h_2 \tag{42}$$

The constraint condition:

$$g_1 = \frac{513204727500}{343h_1^3} + \frac{303750000}{h_2^3} \leq 8;$$

$$g_2 = \frac{h_2 + 54000}{8h_2^2} \leq 0.1;$$

$$g_3 = \frac{3(h_1 + 18000)}{8h_1^2} \leq 0.1 \tag{43}$$

Applying the programming software MATLAB and using the graphic method, the results are obtained:

- The contact point: $h_1 = 634.4341315765114$; $h_2 = 521.5694055354313$. That is the value of variable
- The value of objective function: $G = 58471.386048$ kN (Fig. 5).

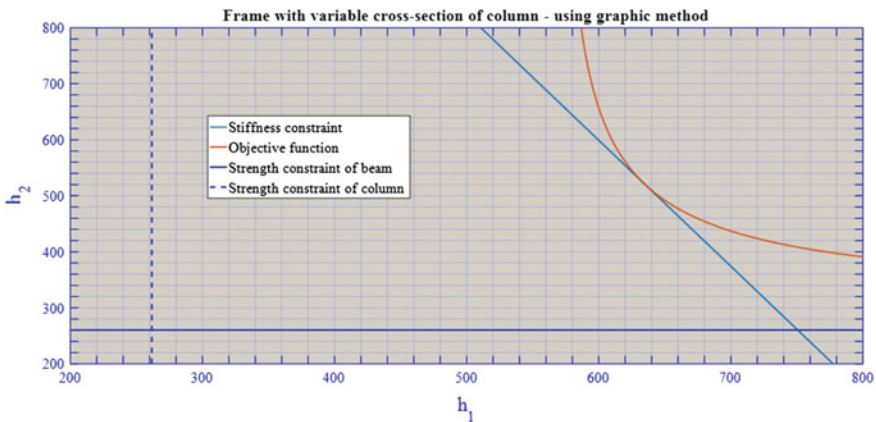


Fig. 5 The result of optimization problem using graphic method

Applying the programming software MATLAB and using the Gradient method, the results are obtained:

The coordinated of optimal point:

$$\{x_2\} = \begin{Bmatrix} x_{2,1} \\ x_{2,2} \end{Bmatrix} = \begin{Bmatrix} 633.360547164 \\ 524.130811846 \end{Bmatrix}$$

That is value of variable.

The value of objective function: $G = 58,475.761289$ kN.

Therefore, the results obtained from two methods (Gradient and graphic) show the clearly convergence. It is verified the accuracy of calculation procedure for the considered optimization problem.

5 Conclusions

The report has established and successfully solved the static analysis for the optimization problem of plane frames with variable cross-sections. The authors have built the algorithm and the calculation procedure and written the routine in MATLAB programming software to determine the displacements and internal forces for the optimization problem of the plane frame with variable cross-section. The comparison between obtained result and the result of the manual calculation and other studies shows good convergence. It verified the accuracy of obtained results of the calculation algorithm.

In the report, the authors successfully solved the optimization problem of plane frames with variable cross-sections using the Gradient and graphic methods. Similarly, it is established the calculation procedure and written the routine in the programming software MATLAB for the optimization problem of the plane frame with variable cross-section. The obtained results are compared with those of other studies and converge well.

References

1. Erbatur F, Hasancebi O, Tutuncil I, Kihc H (2000) Optimal design of planar and structures with genetic algorithms. *Comput Struct* 75:209–224. [https://doi.org/10.1016/S0045-7949\(99\)00084-X](https://doi.org/10.1016/S0045-7949(99)00084-X)
2. Florian M, Sonia C, Florian B, Segonds S, Castanie F, Duysinx P (2021) Topological gradient in structural optimization under stress and buckling constraints. *Appl Math Comput* 409. <https://doi.org/10.1016/j.amc.2021.126032>
3. Pflug L, Bernhardt N, Grieshammer M, Michael Stingl CSG (2020) A new stochastic gradient method for the efficient solution of structural optimization problems with infinitely many states. *Struct Multidiscip Optim*. <https://doi.org/10.1007/s00158-020-02571-x>
4. De Biagi V, Chiaia B, Marano GC, Fiore A, Greco R, Sardone L, Cucuzza R, Cascella GL, Spinelli M, Lagaros ND (2020) Series solutions of beams with variable cross-section. In: 1-st international conference on optimization-driven architectural design. *Procedia Manuf* 44:489–496
5. Van TTT, Kien NT (2020) Non-linear optimization of frames with variable section stiffness of columns using Genetic Algorithm. *IOP Conf Ser Mater Sci Eng* 913. <https://doi.org/10.1088/1757-899X/913/2/022007>
6. Shen W, Ohsaki M (2021) Geometry and topology optimization of plane frames for compliance minimization using force density method for geometry model. *Eng Comput* 37:2029–2046. <https://doi.org/10.1007/s00366-019-00923-w>
7. Zuo W, Zhao C, Zhou L, Guo G (2018) Comparison of gradient and nongradient algorithms in the structural optimization course. *Int J Mech Eng Educ*. <https://doi.org/10.1177/030641901877543>
8. da Rosaa Espath LF, Linn RV, Awruch AM (2010) Structural shape optimization using gradient-based method. *Mecánica Computacional XXIX*:727–745
9. Gythiel W, Schevenels M (2022) Gradient-based size, shape, and topology optimization of single-layer reticulated shells subject to distributed loads. *Struct Multidiscip Optim* 65(501). <https://doi.org/10.1007/s00158-022-03225-w>
10. Vanderplaats Garret N (1984) *Numerical optimization techniques for engineering design*. McGraw-Hill Book Company, New York, USA
11. Niclas A, Anton E, Michael P (2005) *An Introduction to Continuous. Optimization: foundations and fundamental algorithms*
12. Rao SS (2009) *Engineering optimization: theory and practice*. Wiley



Reducing the Metal Consumption of the Formwork Profile for Monolithic Construction

D. V. Gromov¹, L. V. Radionova¹(✉), I. N. Erdakov², L. A. Glebov²,
and A. S. Lunegova³

¹ Moscow Polytechnic University, 38, Bolshaya Semyonovskaya Str., Moscow 107023, Russia
radionovalv@rambler.ru

² South Ural State University, 76, Lenin Avenue, Chelyabinsk 454080, Russia

³ NPP “Uchtekh-Profi” LLC, Chelyabinsk 454080, Russia

Abstract. The article discusses the possibility of reducing the metal consumption of formwork for monolithic construction by reducing the thickness of the profile wall and increasing the mechanical properties of the steel grade from which it is made. Using strength analysis in the SolidWorks program, its operational properties and safety factor were assessed. Strength analysis of the formwork profile confirmed the possibility of moving from steel grade St3 (DIN 17100) with a thickness of 3.00 mm to steel grade 09G2S (DIN 9MnSi5) with a thickness of 2.20 mm. Simulation of profile loading during operation in the SolidWorks program showed that changing the steel grade and thickness leads to an increase in the safety factor. Formwork with a modified profile will not only not lose its strength properties, but may also have an increased service life. To design technologies for roll forming thin-walled profiles from blanks, a model was developed in the QForm program. Checking the adequacy of the developed model by comparing wear areas and contact zones showed its high convergence with the real process. Based on simulation in the QForm program, calibration of stands was developed for the production of profiles from steel grade 09G2S (DIN 9MnSi5) with a wall thickness of 2.20 mm from a workpiece (electric-welded pipe). The effectiveness of the proposed calibration is confirmed by comparing the profile obtained from the simulation with a reference sample.

Keywords: QForm · SolidWorks · Simulation · Roll forming · Strength analysis · Profile · Formwork

1 Introduction

Monolithic construction is the leading technology for the construction of buildings and structures for industrial and civil purposes at the present time [1]. The technology of monolithic construction is increasingly being used not only in the construction of industrial buildings and residential apartment buildings, but also in private construction. This technology makes it possible to build buildings with high-strength walls and ceilings,

implement any designer's ideas, and build complex geometric and rounded elements. When erecting monolithic buildings, a removable reusable formwork is most often used (Fig. 1) [2–5], consisting of wooden, plastic, steel or aluminum elements. The most common steel [6] and aluminum [7] formwork. Steel formwork is the most cost-effective to use. It is made from galvanized [8] and powder-coated steel sheet with a thickness of 0.7 mm or more (depending on the specification of this steel formwork kit). Steel formwork has the highest performance. The resistance of steel to mechanical stress allows the same set to be used more than 500 times. The main disadvantage of steel formwork is its significant weight. The main elements of the formwork are the supporting frame, transverse stiffeners and the formwork slab. The frame design uses a closed hollow profile. Ultimately, the reliability of the entire building structure depends on its quality. The profile is made from steel strip or roll-formed welded pipe [9].

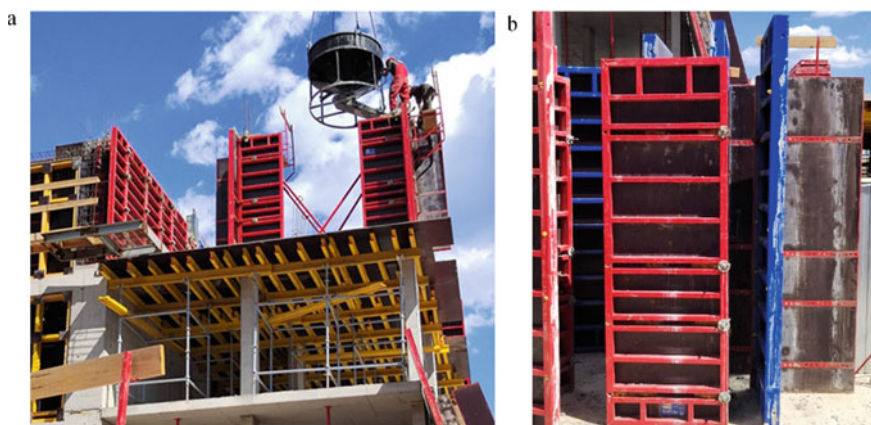


Fig. 1 Panel frame formwork in monolithic construction

In the manufacture of a profile from a steel strip, the metal is first formed, and at the final stage, the seam is already welded.

The first method is the most attractive both from an economic and a technical point of view. For example, to expand the range of manufactured products, it is enough to replace the calibration part or introduce a series of profiling stands into the line.

In the second method, the electric-welded pipe is placed in a rolling mill, where it is deformed and acquires the desired geometry. It is widely used both in Russia and other countries. However, in the production of profiles with many angles and various transitions, it turns out to be inconvenient: a complex shaping scheme may remain unrealized due to the design limitations of the forming equipment, and the cost of the roll tool also increases.

Companies that are engaged in the production of a bent profile (Fig. 2) as a workpiece use electric-welded longitudinal-seam steel pipes according to GOST 10704-91 $\varnothing 120$ mm with a wall thickness of 3.0 mm made of steel grade St3 (DIN 17100) [10].

Currently, the high cost of rolled metal, the significant weight of steel formwork and high competition in the construction market require manufacturers to use innovative

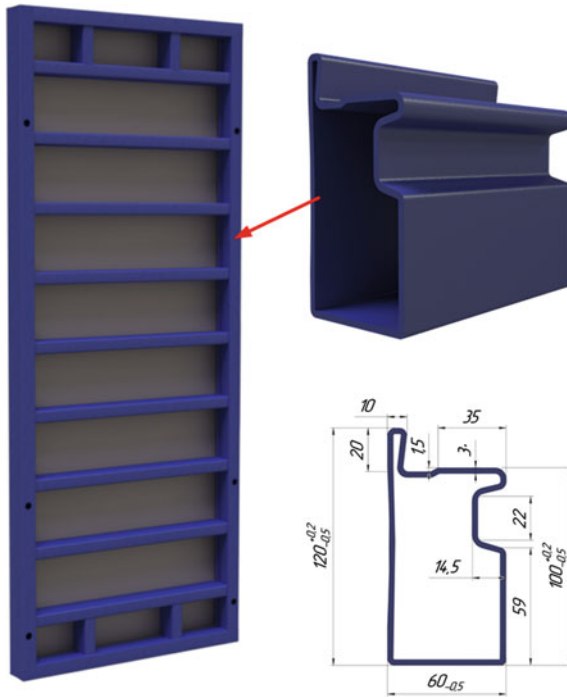


Fig. 2 Formwork profile

technical solutions to reduce costs. One of such solutions may be the transition from the use of St3 (DIN 17100) steel with a thickness of 3.00 mm, which is currently used, to steel with increased strength properties, namely 09G2S (DIN 9MnSi5), but with thickness of 2.20 mm [11]. Reducing the thickness of rolled steel used to obtain a bent profile, without reducing the strength characteristics of the frame, will not only reduce the metal consumption of the formwork profile, but also have lower costs when transporting finished formwork sets to the construction site.

The purpose of this work is to analyze the possibility of using a blank made of steel grade 09G2S (DIN 9MnSi5) with a thickness of 2.20 mm without deteriorating the strength and operational properties of the formwork.

2 Strength Analysis of the Formwork Profile

The formwork is subject to various loads, including during transportation, storage, installation/dismantling, temperature effects, etc. Such loads are experienced by any prefabricated and installation elements, and they are not so significant compared to the loads during concreting. The greatest loads occur when laying the concrete mixture. Significant horizontal loads arise from the lateral pressure of the concrete mixture. It is on them that the formwork is calculated.

To assess the possibility of reducing the wall thickness of a bent profile and changing the steel grade without reducing the operational properties of the formwork, it is

necessary to analyze the strength properties of the main structural elements of the frame panel (Figs. 1 and 2).

There are various methods in the world for determining the pressure of freshly prepared concrete mixture on formwork structures, which take into account various influencing factors [12]. These methods are constantly being improved. This is due to the trend towards a constant reduction in concreting time and the associated increase in the productivity of concrete pumps, which has led to an increase in the speed of concrete placement and the filling height of concrete structures.

In Russia, the calculation of loads during concreting is carried out according to the SP 20.13330.2016 method [13, 14]. In each of the formwork structures there is the most loaded element. As a rule, this is always the longest element of the structure, in our case it is a vertical formwork profile with a length of 3000 mm (see Fig. 2).

To conduct a strength analysis, 3D models of the profiles included in the formwork were created. Load modeling and strength analysis of structural elements were carried out in the SolidWorks program. CAD SolidWorks has a Simulation complex, which allows for strength testing [15].

During the strength analysis, the safety factor was determined when loading a profile with a pipe wall thickness from 3.00 to 2.20 mm and changing the steel grade from St3 (DIN 17100) to 09G2S (DIN 9MnSi5).

During the strength analysis, deformations, stresses, maximum displacement under load and safety factor were determined. The initial data for the strength analysis of the formwork profile are given in Table 1.

Table 1 Initial data for strength analysis

Types of profiles	Steel grade	Pipe wall thickness, mm	Profile length, mm	Yield strength, MPa
1	St3 (DIN 17100)	3.00	3000	221
2		2.20		
3	09G2S (DIN 9MnSi5)	3.00		350
4		2.20		

The strength analysis consisted of a bending calculation, where each sample was in a fixed position (Fig. 3). The applied pressure was 50,000 N/m² of distributed load, this pressure is created by concrete with a specific gravity of 1800 kg/m³ [12]. For each of the four profiles, the same loading and fastening scheme was chosen.

To calculate the profile in the SolidWorks CAD program, the resulting 3D model must be divided into elements. The area under study is divided into finite elements, in each of the elements the type of approximating function is arbitrarily selected and then the values of these functions are found at the boundaries of the elements. The following profile mesh parameters were selected in SolidWorks CAD: mesh element size—19.2 mm; tolerance—1.208 mm; number of grid elements—28,635. Since the grid parameters were set automatically by the program, a comparative analysis of the

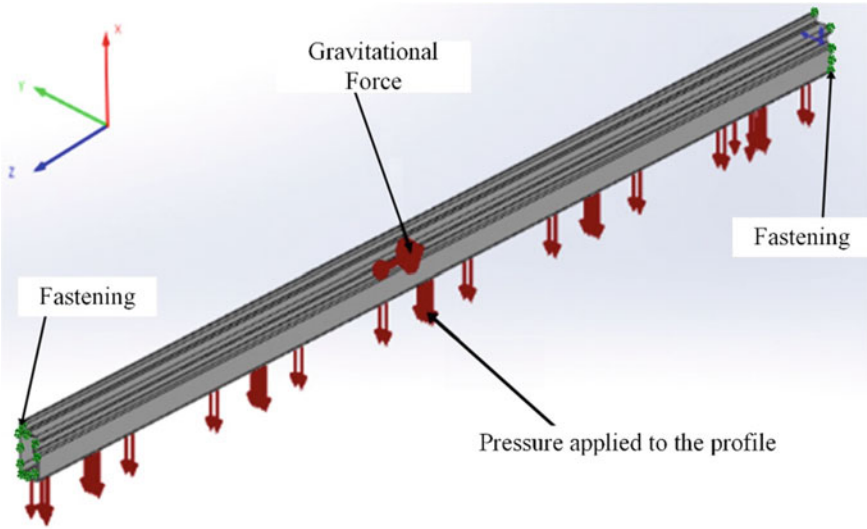


Fig. 3 Scheme of profile fastening and application of loads

dependence of the grid size on the modeling result was carried out. To achieve this, the number of grid elements was increased by 35%. With an increase in the number of elements, it was determined that the results change slightly—3.4%, but at the same time the calculation time increases. Consequently, it is not practical to increase the number of elements and strength calculations can be carried out with the specified parameters. The calculation of four types of profiles (see Table 1) made it possible to determine the equivalent deformation, stress distribution, profile movement and safety factor. The calculation results for a profile made of steel grade St3 (DIN 17100) with a wall thickness of 2.20 mm are shown in Fig. 4. The calculation results for the four studied profiles are given in Table 2.

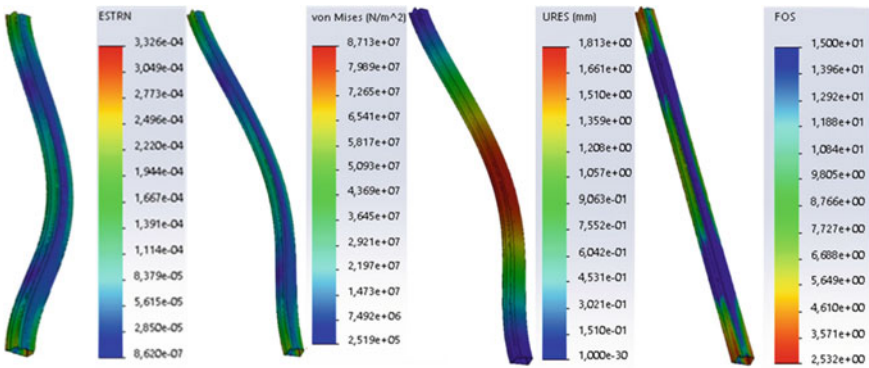


Fig. 4 Strength analysis of a profile made of steel grade St3 (DIN 17100) with a pipe wall thickness of 2.20 mm

Table 2 Results of strength analysis of formwork profiles

Parameter	Types of profiles			
	1	2	3	4
Equivalent deformation (ESTRN), $\times 10^{-4}$	3.33	3.85	3.49	3.97
Maximum stress (von Mises), MPa	87.1	101.0	86.4	101.0
Maximum movement (URES), mm	1.813	2.065	1.903	2.163
Minimum safety factor (FOS)	2.5	2.2	4.0	3.5

Strength analysis showed the possibility of switching to a profile with a smaller pipe wall thickness. At the same time, the use of steel grade 09G2S will make it possible to reduce the thickness of the profile wall not only while maintaining the performance properties, but also to significantly increase them. The profile will have an increased safety factor, which is equal to 3.5, and this will increase the life and frequency of its use. In addition, the analysis showed the possibility of using a thinner pipe wall when using steel grade 09G2S (DIN 9MnSi5).

3 Model of Roller Formation of a Form Profile from a Round Welded Pipe in the QForm Program

To simulate the formation of profiles, specialized packages [16–18] are used, such as Ansys, Nastran, ABAGUS, Ls-dyna, which are based on the finite element method. Recently, a Russian-developed package, QForm, has become widespread and accessible to enterprises and educational institutions [19, 20]. The software product has proven itself quite well in modeling the processes of stamping, extrusion [21], and rolling [22, 23]. At the same time, no experience of using this package for roll forming operations was found in the literature. The first step in the simulation is to create a solid model of the workpiece and forming tool in the CAD program Kompas-3D v19 [24]. When creating solid models of forming tools, calibrations of real equipment of an operating enterprise were used. Profiling of the blank pipe is carried out on an automated profile production line, which includes a feed roller table, a bending and rolling machine, a cutting saw and a receiving table with a dumper. The forming line consists of 24 rolling stands: 20 horizontal and 4 verticals.

The following parameters were specified for the simulation using QForm version 9.0.10.

Workpiece:

- steel grade—St3;
- temperature—20 °C;
- friction coefficient of the workpiece at self-intersection—0.1;
- workpiece length—400 mm;
- external/internal diameter of the workpiece—120/114 mm;
- length of the deformable area—300 mm;

- length of the fine-element mesh zone—25 mm.

Tool:

- steel grade—DIN 1.2510;
- temperature—20 °C;
- friction coefficient according to the Coulomb law—0.1;
- rotation speed—10 rpm;
- the size of the mesh element on the surface is 1.5 mm.

Boundary conditions and calculation parameters:

- pusher: speed—0.1 m/s;
- calculation taking into account elastoplastic deformations;
- re-splitting the workpiece every 100 steps;
- constant time step (deformation)—0.1 ms.

The mesh in the tool is divided into large and small elements; a fine-element mesh with a tetrahedral edge length of 1.5 mm is located on the surface. Figure 5 shows the mesh using the example of the cross section and lower roll of stand No. 6. This method of constructing a mesh will make it possible to more accurately evaluate the contact zones of the workpiece with the tool, comparing not only the resulting geometry of the workpiece, but also the wear areas of the rolls.

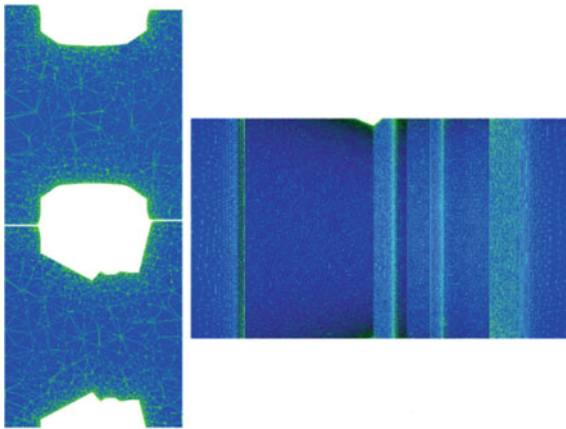


Fig. 5 The mesh of the tool

Using workpiece models, tools and specified parameters, a simulation model consisting of 23 operations was created. The tool drive was specified for horizontal stands No. 1, 2, 19 and 20. For the remaining stands, the rotation speed was not specified. The tools received rotational torque due to friction and pushing the workpiece through the rolls at a speed of 0.1 m/s.

One of the visual methods for analyzing simulation results is the method of analyzing contact zones between the workpiece and the tool. Figure 6 shows the contact zones of

the workpiece and the tool of rolling stand No. 13 in the QForm program and the wear areas of the forming rolls of the real mill. To check the adequacy, stands No. 1, 3, 5, 7, 10, 13, 15, and 19 were examined in detail.

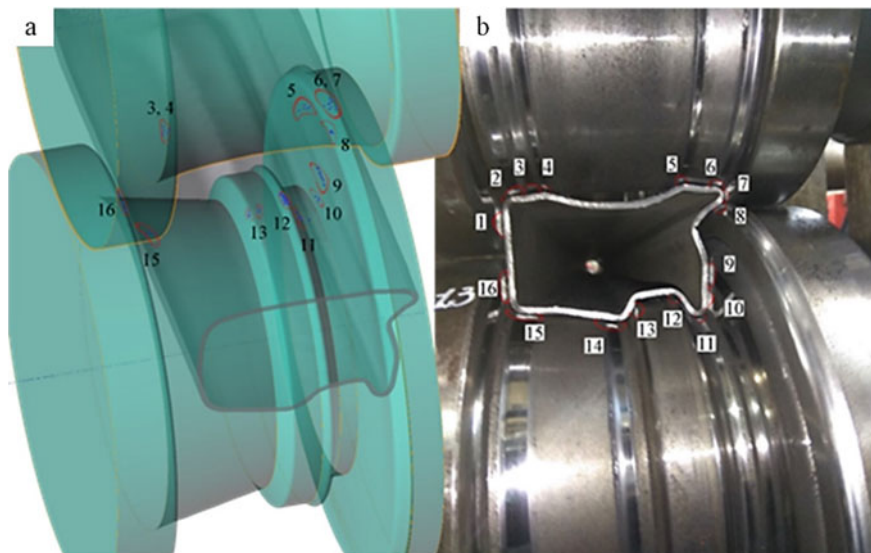


Fig. 6 Contact zones between the tool and the workpiece in the model (a) and wear areas of the forming rolls of stand No. 13 (b)

There are 16 wear zones on the forming rolls of stand No. 13. They coincide with the following contact zones: 3–13 and 15–16. Contact zones 9 and 10 are clearly separated, and 3, 4 and 6, 7 merge into one zone. In contrast to the wear zone 13 of the lower forming roll, the contact zone of the workpiece with the roll 13 is clearly divided into two areas. The formation of a separated zone may indicate a defect in geometric dimensions. The missing contact zones 1, 2 and the geometry of the profile obtained from the simulation indicate the radius of curvature.

The results of comparison of wear zones and tool-workpiece contact confirm the adequacy of the model to the real forming process. The discrepancies that are recorded in certain areas throughout the entire modeling process are the error ($\pm 0.8\%$) of the outer diameter of the welded pipes received for production. The length of the outer circumference at $\text{Ø}120$ mm is 376 mm. With an error of $+0.8\%$, the outer diameter of the pipe is $\text{Ø}121$ mm, which in turn increases the length of the arc to 383 mm, which significantly affects the geometry of the profile (Fig. 7).

For a formwork profile, an important parameter is the geometry, which directly depends on the method of its production, the technological parameters of profiling and the accuracy of the geometry of the workpiece (electric-welded pipe). Therefore, depending on the actual diameter of the welded pipe, it is necessary to adjust the calibration of the rolls or tighten the tolerance requirements for the workpiece. This issue requires

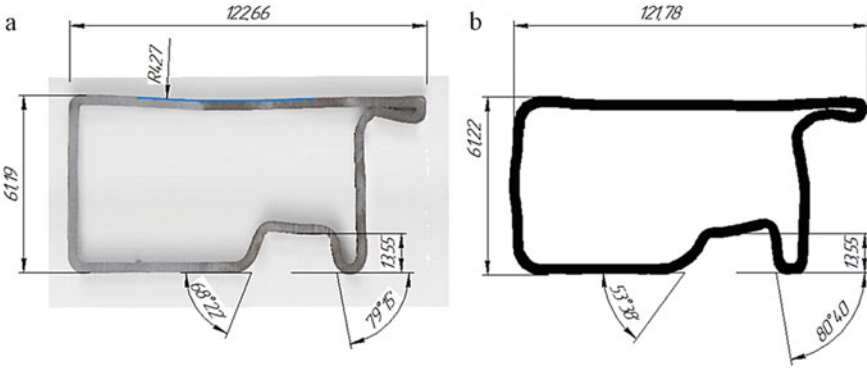


Fig. 7 Basic geometric parameters of the formwork profile: **a** scan of a real sample; **b** cross section of the model

additional simulation research and will be addressed in future publications. The simulation results were used to create a roll forming model of a workpiece with a smaller wall thickness and a changed steel grade. Geometric defects resulting from unsuccessful calibration were taken into account when developing a new model.

4 Modeling of Roller Forming of a Profile from a Round Welded Pipe 120 × 2.20

When changing the wall thickness and steel grade of the workpiece, it is necessary to change some previously used modeling parameters and set the following: the minimum element size is 0.894 mm, the workpiece steel grade is 09G2S (DIN 9MnSi5), the outer/inner diameter of the workpiece is 120/115.6 mm. The remaining simulation parameters remain unchanged. In addition, in order to obtain a more correct geometry, the geometric parameters of the vertical and horizontal forming rolls were taken into account and refined. During modeling, the workpiece was divided into segments of length equal to the sections of the profile (Fig. 8). Thanks to this approach, it became possible to more accurately control the resulting geometry by adjusting the tool.

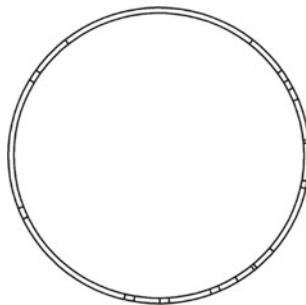


Fig. 8 Workpiece divided into profiling sections

Simulation of the process with a workpiece located in all stands at the same time, that is, a length of 8 m, according to preliminary calculations, would take about 500 h. This option eliminates the possibility of timely debugging of the model in the event of software errors. Therefore, the model was divided into 24 operations, i.e. one operation per forming stand. With this modeling option, machine time is reduced to 94 h per group of stands. During the simulation process, workpiece data was uploaded in two versions in STL format, followed by processing using the Kompas-3D program and a point area with subsequent processing in Excel. To make sure that the adjustment to the geometry of the forming rolls was made correctly, the modeling results with the parameters of a workpiece with a wall thickness of 2.20 mm made of 09G2S steel (Fig. 9b, d, f) were compared with the results obtained when modeling a profile made of St3 steel with a wall thickness of 3.00 mm (Fig. 9a, c, e).

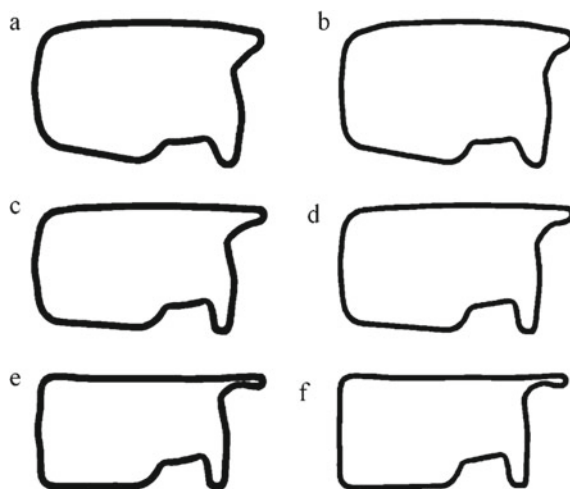


Fig. 9 Sections of workpieces in the forming stand: **a** stand No. 13 St3; **b** stand No. 13 09G2S; **c** stand No. 15 St3; **d** stand No. 15 09G2S; **e** stand No. 20 St3; **f** stand No. 20 09G2S

Comparison of the cross-section of the profile obtained during the simulation using the corrected calibration and the reference sample showed (Fig. 10) that the differences in the cross-sections of the profiles lie in the formed bend. During the simulation, the support pad of the molded workpiece is not extended. We assume that the groove of the supporting surface is not formed due to the contact nodes. Using simulation in QForm, the weld joint location area was determined. To do this, lines were traced in the workpiece section and a field for displaying plastic deformation was selected (Fig. 11).

By studying the profile section, zones with minimal plastic deformation were identified. Four profile elements are less deformed and, as a result, experience less stress during the molding process: the bottom flange, the groove of the vertical post, the support platform and the rear post. Analyzing the geometry of these elements, the recommended location for the seam is the middle of the bottom flange (position 1 in Fig. 11) and the middle of the rear pillar (position 2 in Fig. 11).

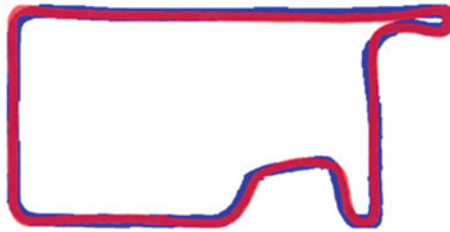


Fig. 10 Profile cross-section: blue—profile, obtained by simulation; red—reference profile

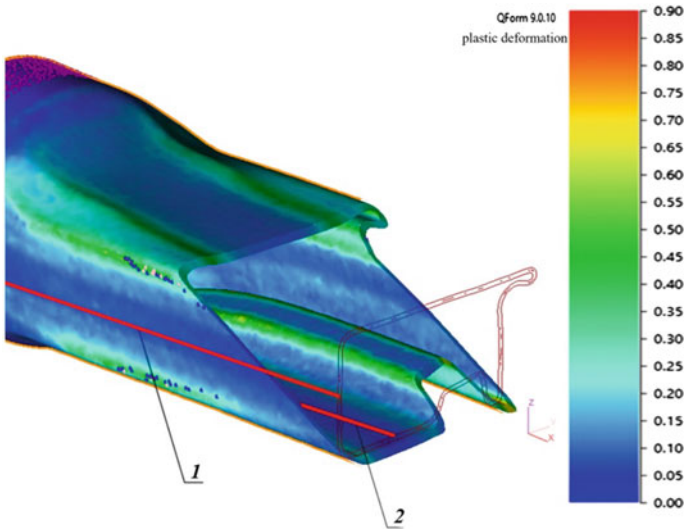


Fig. 11 Recommendations for the location of the welded joint: 1—middle of the bottom shelf; 2—middle of the rear pillar

To follow the recommendations for the location of the seam, it is necessary to correctly set the initial position of the workpiece in the forming stand No. 1. For this purpose, you can use a pipe blank previously divided into sections (elements of the formwork profile) (Fig. 8). The position of the seams during the workpiece task is shown in Fig. 12.

The weld located at $39^{\circ}2'$ is in the middle of the back post and has a position error zone of $\pm 20^{\circ}$, and the weld at $94^{\circ}57'$ is in the middle of the bottom flange with an error zone of $\pm 6^{\circ}$.

To achieve the reference geometry, it is necessary to make changes to the mill design, namely, to move from alternating horizontal and vertical stands to a four-roll calibration. Such a scheme will complicate the design and setup of the mill, but will allow achieving the required geometry.

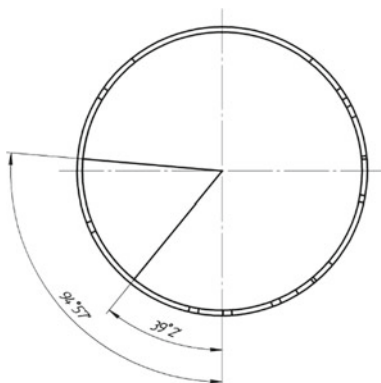


Fig. 12 Location of the welded joint when tasking the workpiece in stand No. 1

5 Conclusion

Strength analysis of the formwork profile confirmed the possibility of moving from steel grade St3 (DIN 17100) with a thickness of 3.00 mm to steel grade 09G2S (DIN 9MnSi5) with a thickness of 2.20 mm. Simulation of profile loading during operation in the SolidWorks program showed that changing the steel grade and thickness leads to an increase in the safety factor. Formwork with a modified profile will not only not lose its strength properties, but may also have an increased service life.

To design technologies for roll forming thin-walled profiles from blanks, a model was developed in the QForm program. Checking the adequacy of the developed model by comparing wear areas and contact zones showed its high convergence with the real process.

Based on simulation in the QForm program, calibration of stands was developed for the production of profiles from steel grade 09G2S (DIN 9MnSi5) with a wall thickness of 2.20 mm from a workpiece (electric-welded pipe). The effectiveness of the proposed calibration is confirmed by comparing the profile obtained from the simulation with a reference sample.

References

1. Farzaliyev SA, Pahomov R (2021) Analysis of the main features of organizational and technological solutions for the construction of high-rise monolithic reinforced concrete buildings. Lecture notes in civil engineering, vol 181, pp 105–114
2. Terzioglu T, Polat G (2022) Formwork system selection in building construction projects using an integrated rough AHP-EDAS approach: a case study. *Buildings* 12(8):1084
3. Rana N (2023) Cost benefit analysis of modern formwork over conventional formwork in mass dwellings. In: Building construction and technology. Lecture notes in civil engineering, vol 360. Springer, Singapore
4. Ansari DS, Kudale PS (2016) Comparative analysis of MIVAN formwork building and conventional formwork building based on cost and duration. *Int J Eng Res* 5(8):672–675

5. Kolekar P, Nigade V, Hajare S, Kamble P, Patade S, Kumavat A (2020) Analysis and comparison of MIVAN formwork system with conventional formwork system. *Int Res J Eng Technol (IRJET)* 07(06). e-ISSN: 2395-0056, p-ISSN: 2395-0072
6. Li S, Jin W, Yu Z, Li Y, Guo H (2023) Study on the bearing capacity of steel formwork concrete columns. *Buildings* 13(3):820. <https://doi.org/10.3390/buildings13030820>
7. Aaditya V, Anandakumar S (2018) Scope of aluminium formwork technology in affordable housing scheme based on cost and duration. *Int J Adv Sci Eng Res* 3(1):150–156
8. Radionova LV, Subbotina YuM (2016) The study of aging cold rolled and hot dip galvanized automotive steel. *MSF*
9. Gromov DV, Radionova LV, Svistun AS, Erdakov IN, Zaramenskikh SE, Lisovskiy RA (2022) Influence of steel pipe billet diameter on formwork profile geometry for monolithic construction. *Russ Internet J Ind Eng* 9(3):3–8. https://zmk.ru/produkcija/stenovaya_opalubka. Accessed 2 Sept 2023
10. Gromov DV, Erdakov IN et al (2021) Computer modeling in the QForm program of roll forming of a profile from a round welded pipe. In: *Industrial engineering. Proceedings of the VII all-Russian scientific and technical conference*, Chelyabinsk, pp 176–179
11. Abramyan SG, Burlachenko OV (2018) *Integrated development of technology for the construction of monolithic structures of high-rise and unique buildings: textbook. Manual*. Ministry of Education and Science of Russia. Federation, Volgogr. State Tech. Univ, VolgSTU Publishing House, Volgograd
12. SP 20.13330.2016 *Loads and impacts*. Updated edition of SNiP 2.01.07-85* (with Amendments No. 1, 2, 3)
13. STO 02494680-0058-2008 *Steel building structures. Loads and impacts (Additions and changes to SNiP 2.01.07-85*)*.
14. Mitin EV, Suldin SP, Ovchinnikov AY et al (2023) Stirrup design using SolidWorks simulation tools. *Russ Eng Res* 43:934–938
15. Ilyushkin MV, Filimonov VI, Markovtseva VV (2014) Modeling of contact interactions of a roller tool with a channel-type profile flange in the manufacture of bent profiles using the method of intense deformation. *News Samara Sci Center Russ Acad Sci* 16(1 (2)):397–400
16. Torgonin KS, Batalov GS et al (2021) Study of the simulation results convergence in various software complexes in the production of stamp welded tee. *Bull South Ural State Univ Ser Metall* 21(2):58–69. <https://doi.org/10.14529/met210206/>
17. Batalov GS, Lunev AA, Radionova LV, Lezin VD (2021) Development of new methods for the production of large-diameter double-seam pipes. *Solid State Phenom* 316:538–548
18. Loginov YuN, Stepanov SI, Khanykova EV (2017) Effect of pore architecture of titanium implants on stress-strain state upon compression. *Solid State Phenom* 265:606–610
19. Radionova LV, Lisovskiy RA, Svistun AS, Gromov DV, Erdakov IN (2023) FEM simulation analysis of wire drawing process at different angles dies on straight-line drawing machines. In: Radionov AA, Gasiyarov VR (eds) *Proceedings of the 8th international conference on industrial engineering. ICIE 2022. Lecture notes in mechanical engineering*. Springer, Cham
20. Faizov S, Sarafanov A et al (2021) On the direct extrusion of solder wire from 52In-48Sn alloy. *Machines* 9(5):93
21. Gasiyarov VR, Bovshik PA, Loginov BM, Karandaev AS, Khramshin VR, Radionov AA (2023) Substantiating and implementing concept of digital twins for virtual commissioning of industrial mechatronic complexes exemplified by rolling mill coilers. *Machines* 11(2):276
22. Radionov AA, Petukhova OI, Erdakov IN, Karandaev AS, Loginov BM, Khramshin VR (2022) Developing an automated system to control the rolled product section for a wire rod mill with multi-roll passes. *J Manuf Mater Process* 6:88
23. Naizabekov A, Lezhnev S, Volokitina I, Panin E (2014) Computer modeling of the rolling process of reinforcing steel. *Adv Mater Res* 1030–1032:1286–1291

Special and Unique Structures Construction



Designs and Technologies for Creating Impervious Screens at Reclamation Facilities

O. A. Baev^(✉), A. V. Kolganov, and V. F. Talalaeva

Russian Scientific-Research Institute of Land Improvement Problems (RosNIIPM), 190,
Baklanovsky Ave, Novocherkassk 346421, Russia
Oleg-Baev1@yandex.ru

Abstract. Reclamation systems hydraulic structures long-term operation lead to some elements significant physical wear, averaging 28% or more for irrigation and principal canals. Concrete and reinforced concrete linings are subject to deformations, cracking, base subsidence and other negative processes over time. Hence, there is a need to develop and apply improved design and process solutions using modern polymer-based composite materials, which will make it possible to most effectively and quickly restore the canals protective coatings and other feeding hydraulic structures. To determine the specific filtration flow rate through damage, the method of calculating the water permeability of the anti-filtration concrete facings taking into account the colmatation of damage. Technical and technological solutions developed at the level of applications and patents for inventions are characterized by increased efficiency and reliability, which consist in eliminating filtration losses and filtration deformations, while increasing the durability of the repaired area due to increased physical and mechanical characteristics of the materials used in the structures. The presented method of calculating the water permeability of the anti-filtration concrete lining, taking into account the colmatation of damage, made it possible to determine the specific filtration flow rate through damage equal to 0.112 m²/day. Based on the performed calculation, it is possible to make a decision on the expediency of reconstructing certain damages to concrete channel linings, including during their colmatation.

Keywords: Canal · Seepage-control lining · Seepage losses · Composite material · Polymer

1 Introduction

The irrigation and drainage canals operation requires protective coatings and seepage-control linings long service life, the hydraulic structures for reclamation purposes operation normative period is 60 years. Water flow continuous impact leads to the concrete and reinforced concrete coatings expansion joints depressurization, reinforcement exposure, concrete cracks, voids form in the under-slab space, slabs individual sections (maps) complete destruction and others.

2 Relevance

The ways to reduce water seepage losses in irrigation canals are the highly effective seepage-control measures and the modern building composite materials usage. Research on usage improved seepage-control structures from geocomposites on canals was carried out by domestic scientists and specialists: Yu. M. Kosichenko, A. V. Ishchenko, S. V. Solsky, O. A. Baev, E. O. Sklyarenko, M. A. Bandurin, F. K. Abdrazakov and others [1–8].

Processes for the installation of seepage-control canal coatings and also the modernization, construction and irrigation systems lining structures operation problems were carried out by following foreign scientists: K. Ding, L. Gao [8], H. Plusquellec [9], X. Han, X. Wang [10, 11], H. F. Abd-Elhamid [12] and others [13–19].

The generally accepted technology for the construction of protective coatings, developed for cladding using a polyethylene film and a protective layer of monolithic concrete (Fig. 1).

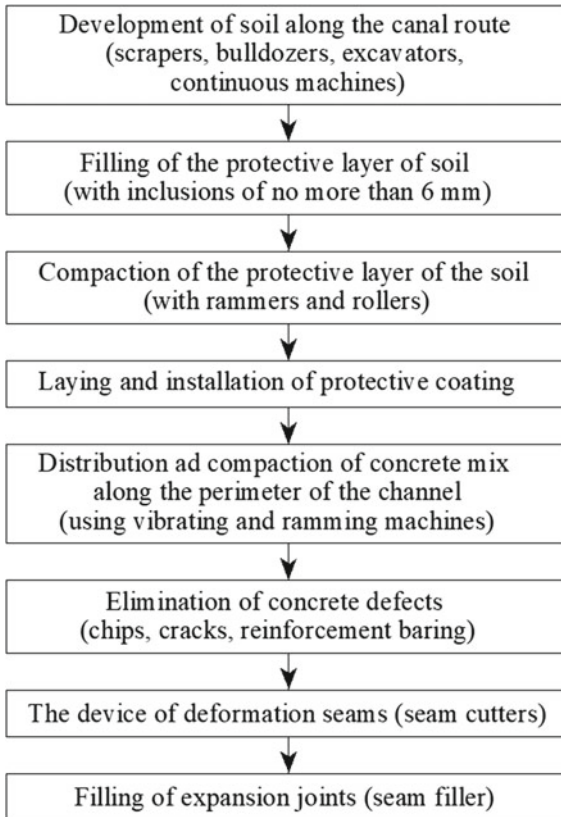


Fig. 1 Diagram of the technology of construction of protective coatings

The use of specialized equipment greatly simplifies the installation of cladding, but along with this, the costs of the entire technological process significantly increase. Due to the high costs of laying protective coatings, the choice of the most effective anti-filtration measures and building materials remains a particularly important issue.

Based on the analysis results of domestic and foreign works, it was revealed that the current technologies for the reclamation canals construction and reconstruction are complex, economically unprofitable, and also require specialized machinery and equipment large amount. Therefore, developing cost-effective and efficient design and process solutions for the reconstruction of existing concrete linings of irrigation canals question remains important. Standard concrete, as a rule, is short-lived (service life on channels is up to 25–28 years), is prone to cracking, and the creation technologies are highly labor-intensive. Geosynthetic materials such as geomembranes and bentonite mats usage is a highly effective seepage-control protection. But, despite this, such materials have a number of disadvantages. For example, geomembranes have low strength, are prone to punctures both during installation and during operation (by plant roots, a protective layer). In addition, the geomembranes usage requires careful base preparation before its layin, which significantly increases the design work cost. The bentonite mats main disadvantages are the need for additional loading of the material, as well as low resistance to freeze–thaw cycles.

To date, large number methods for restoring concrete coatings shall be known; various composite materials shall be used for this (Fig. 2).

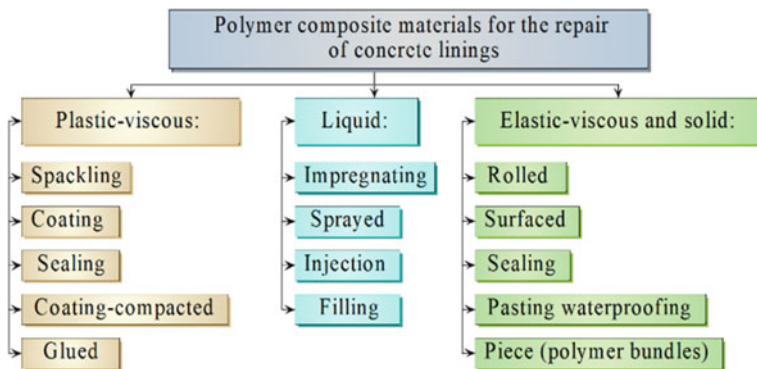


Fig. 2 Polymer composite materials used for the concrete canal linings repairs

Not all existing anti-filtration measures and the construction materials used in them are effective enough and have their drawbacks. Below we will consider some materials and give a comparative description of their physical and mechanical parameters (Table 1).

The use of geosynthetic materials, such as geomembranes and bentonite mats, is a highly effective protection against seepage. But, despite this, such materials have a number of disadvantages. For example, geomembranes have low strength, are prone to punctures both during installation and during operation (plant roots, protective layer). In addition, the use of geomembranes requires careful preparation of the foundation before laying it, which significantly increases the cost of design work. The main disadvantages

Table 1 Comparative characteristics of physical and mechanical parameters of anti-filtration materials

Indicator	Material			
	Concrete canvas	Geomembrane	Concrete cladding	Bentonite mat
Weight (before hydration), kg/m ²	7–20	0.7–3	1800–2500	4–7
Density (before hydration), kg/m ²	1500	910–975	2200–2500	3600–4300
Thickness, mm	5–14	1–2	100–200	4–7
Tensile strength, MPa	To 25	To 25	To 25	To 25
Filtration coefficient, cm/s	$<6 \times 10^{-10}$	1×10^{-8} – 1×10^{-10}	6×10^{-10} – 2×10^{-9}	1.0×10^{-11} – 1.5×10^{-11}
Laying on slopes	1:1–1:3 and more	1:3	1:1–1:2.5	At least 1:3
Chemical stability, pH	4–12.5	0.5–14	4–6.5	4–11
Service life, years	More than 50	More than 50	Less than 30	More than 50

of bentonite mats are the need for additional loading of the material, as well as low resistance to freeze–thaw cycles.

3 Problem Statement

The purpose of this study is to develop design and process solutions for the irrigation canals destroyed concrete linings creation and restoration with the modern composite materials usage.

4 Theoretical Part

The serious problem irrigation and principal canals throughout the world is seepage losses, which make up a significant part of the total water volume. For example, in Iraq, most canal linings for reclamation purposes are in concrete lining and are subject to seepage through the facing slabs joints [12]. The authors research purpose A. Al-adili, O. A. Al-ameer, A. Al-sharbati [13] was to reduce or prevent seepage from open canals through the new alternative materials for filling joints usage.

Geosynthetic clay liners, developed in 2005, are a relatively new material technology in the geosynthetic world and have been recognized as highly effective for rapid construction, including land reclamation facilities. The material physical properties were verified by the authors [15] by conducting laboratory tests. To evaluate the process performance, the material was applied to a section of the canal with an area about 4000 m².

The estimated service life of such a coating exceeds 50 years, the material is easy to install and operate, and cost savings compared to the construction of concrete cladding is about 24% [16].

The cracks formation in concrete coatings occurs by a change in external and internal loads formed with the concrete pavements operating technologies non-compliance, the wrong ratio in the mortar preparation and wrong laying methods and also the coating aging under the external factors influence. To eliminate cracks in concrete linings, the method shall be used with the various polymeric additives. This method consists in lowering the concrete surfaces capillary moisture saturation with a device for clogging the concrete pore space by materials with much less than concrete permeability.

The sediments carried by the water flow fill the damage, cracks, joints and expansion concrete linings joints, thereby reducing water losses due to filtration. Irrigation canals clogging is a “simple” and at the same time quite effective impervious measure reducing seepage losses for 3–6 times [1].

In [10], cracks and holes in various facing coatings were examined, and filtration was assessed. The results showed that cracks in the of two precast concrete slabs joints and holes in the geomembrane cause an increase in seepage losses. New combined concrete and geomembrane lining usage reduces seepage by 86% compared to an earth channel, while after three years of operation seepage can be reduced by 68 The authors established a statistical relationship between the decrease in seepage and the lining repairing time, which made it possible to estimate the water loss for seepage from the lined channels. According to the calculations carried out by the authors, without taking into account the service life of the lining, seepage losses shall be underestimated by 58%, and the water usage efficiency in the canal shall be overestimated.

Unlike the anti-filtration materials discussed above, the concrete-filled coating has a number of advantages:

- The speed of work
- Convenience and ease of installation
- Environmental friendliness of the material
- Service life
- Increased strength
- Puncture resistance
- Waterproof
- Protection against germination of plants
- Possibility of laying in all weather conditions
- Resistance to aggressive environments.

In addition, the concrete web can be used on complex objects, steep slopes, without an additional attachment device (unlike other rolled materials that require additional attachment to the base). No additional construction materials and skilled labor are required for laying the material. A minimum amount of preparatory work is required before installation.

5 Study Results

To repair damage to concrete canals linings (local large fractures and expansion joints) and other feeding hydraulic structures made with concrete and reinforced concrete linings, a method has been developed for repairing damage to channel linings using concrete-filled materials (Fig. 3) [20].

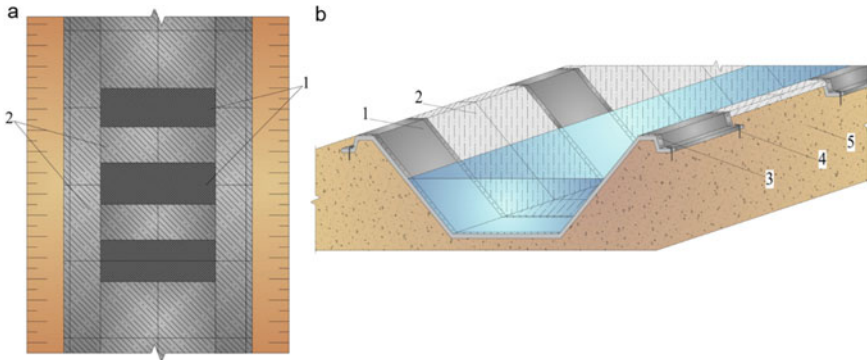


Fig. 3 Scheme of repair of major damages of concrete channel linings: **a** plan; **b** section 1—concrete cladding; 2—concrete-filled material; 3—bracing (self-tapping screw, dowel-nails); 4—steel stakes; 5—ground of the base

To repair major damages on concrete channel linings, presented in the form of partial or complete destruction of slabs, a pre-fabricated concrete-filled coating is used, arranged in the form of a patch over the defective area and attached to the surface of the anti-filtration concrete or reinforced concrete lining (Fig. 4).

The method includes the defective area preparation, which consists in clearing, the remains destroyed concrete and dust removing. Next, a binder material shall be applied, forming an adhesive layer, the defective area shall be filled with building material (filling with fine gravel or sand), and it shall be leveled. For large damage repairing on the canals concrete lining, a prefabricated concrete-filled coating shall be used, like a patch over the defective area and it shall be attached to the impervious concrete or reinforced concrete lining surface using self-tapping screws, anchors or other fasteners. To seal the prefabricated concrete pavement connection with a concrete lining, an polymer sealant adhesive layer shall be arranged. Patch sagging shall be prevented by laying a flat geogrid on the concrete lining surface. This solution shall be distinguished by easy installation, low labor costs and also the need to use large-sized specialized equipment absence. In addition, the pre-fabricated concrete-filled material coating has durability and water resistance.

The fiber reinforced concrete application for repairing concrete pavements damage is an effective alternative to the currently used traditional cement mortar. Depending on the type of introduced fiber, it is possible to obtain fiber reinforced concrete with the characteristics required for a particular object. Fiber reinforced concrete is distinguished by its strength properties, water resistance, temperature extremes resistance, durability

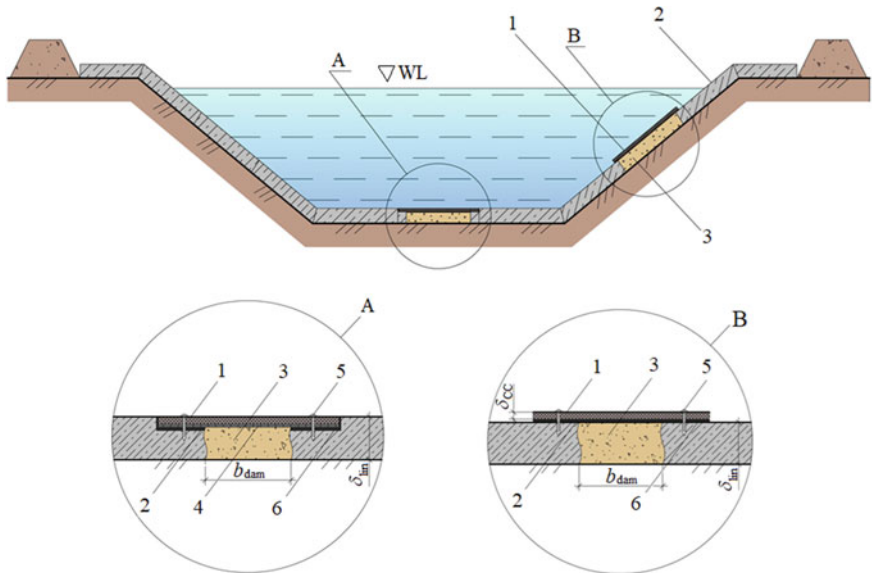


Fig. 4 The method large damage to the concrete lining repairing along the bottom (node A) and on the slope (node B): δ_{lin} —lining thickness; b_{dam} —damage width; b_{CC} —concrete canvas thickness; 1—concrete canvas; 2—concrete lining; 3—backfill; 4—self-tapping screw; 5—a polymer sealant layer; 6—base

and other physical and mechanical characteristics. In addition, fiber-concrete is environment friendly and low cost (depending on the type of fiber), that's why it can be used at irrigation and drainage facilities.

For the expansion joints and connections of concrete and reinforced concrete coatings repairing, a structural and technical solution has been developed for the concrete linings restoration using fiber-reinforced concrete and other composite materials (Fig. 5).

This design and technical solution aimed at restoring the canal concrete lining includes: the voids filling on destroyed expansion joint with fiber-reinforced concrete and applying a waterproofing material to the frozen surface. During concrete lining expansion joint repairing, it is necessary to prepare the repaired area, which consists in cleaning it from debris, removing loose concrete in the damage zone, chasing along the deformable area and cleaning it from dust.

Option (a) includes: laying the sealer into the cavity of the deformation seam, ramming and filling with a fiber-concrete mixture. After the fiber concrete solidifies, an elastic waterproofing tape applied to a layer of epoxy glue is laid on its surface. Option (b) includes: filling the destroyed under-slab space with a geopolymer composition that stabilizes the natural base and prevents further soil subsidence. After hardening, the expansion joint shall be filled with a fiber-reinforced concrete mixture, over which polyurethane sealant shall be applied. Option (c) includes: filling the expansion joint with a fiber-reinforced concrete mixture, on which, after hardening, an elastic cement-based waterproofing shall be applied.

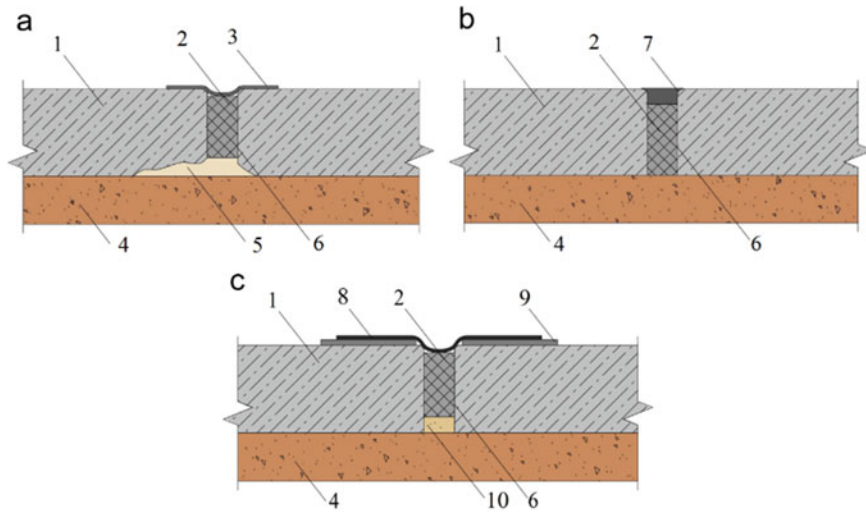


Fig. 5 Design and process solutions for the expansion joints of canals repairing with composites (options **a**, **b**, **c**): 1—concrete lining; 2—expansion joint; 3—polyurethane sealant; 4—ground of the base; 5—geopolymer composition; 6—fiber-reinforced concrete; 7—elastic cement-based waterproofing; 8—elastic waterproofing tape; 9—a layer of epoxy glue; 10—sealer (sand, gravel, crushed stone, geocomposite materials)

The use of fiber concrete for sealing cracks, expansion joints and joints of concrete linings will extend the service life of concrete linings by reinforcing cement-sand mortar with fiber. In addition, the most important performance characteristics of concrete coatings are significantly improved: strength, resistance to bending and stretching, water resistance, crack resistance, resistance to external influences.

Such process solutions shall be distinguished by increased efficiency and reliability, which consists in eliminating seepage losses, while increasing the repaired area durability due to the increased physical and mechanical characteristics fiber-reinforced concrete and other composite materials used in coatings.

6 Practical Relevance

Let us consider a methodology for calculating clogging, which allows calculating the seepage-control concrete lining water permeability, namely, the specific seepage flow through damage, the average seepage coefficient, the water permeability coefficient with clogged damage, the seepage rate and the pressure gradient at the permeable boundaries.

Initial data for calculation: water depth h_0 , m; damage width b_{dam} , m; damage length l_{dam} , m; lining thickness δ_{lin} , m; clogged layer seepage coefficient in damage to the lining k_{cl} , m/day; soil permeability coefficient k_s , m; lining damage average length L_{dam} , m; canal length L_c , m; canal width B_c , m; critical head gradient I_{cr} .

The piezometric head acting on the concrete lining shall be determined by the formula:

$$H = h_0 + \delta_{lin}, \text{ m.} \quad (1)$$

Substituting the piezometric flow rate value into the formula for the specific flow rate through damage to the lining, obtain:

$$q_f = 2 \cdot k_{cl} \cdot H \cdot k'_2, \text{ m}^2/\text{day}, \tag{2}$$

where k'_2 is the ratio of elliptic integrals.

Let us determine the seepage flow through the clogged damage to the lining from the expression:

$$q'_f = \frac{\pi \cdot k_{cl}(h_0 + \delta_{lin})}{\ln\left(\frac{\exp\left(\frac{\pi \cdot \delta_{lin}}{b_{dam}}\right)}{\sin\left(\frac{\pi \cdot m}{2 \cdot b_{dam}}\right)}\right)}, \text{ m}^2/\text{day}. \tag{3}$$

Comparison of the calculation results with the most famous formulas of scientists V. P. Nedriga and Yu. M. Kosichenko showed in Table 2.

Table 2 The results comparison calculation the clogged damage seepage flow rate to the lining

Seepage flow through damage (m ² /day)			
Formula (3)	V. P. Nedriga Formula	Yu. M. Kosichenko Formula (1980)—the exact	Yu. M. Kosichenko Formula (1980)—approximate
$\frac{0.112 \text{ (m}^2/\text{day)}}{- [\%]}$	$\frac{0.145 \text{ (m}^2/\text{day)}}{-29.46 \text{ (\%)}}$	$\frac{0.208 \text{ (m}^2/\text{day)}}{-85.71 \text{ (\%)}}$	$\frac{0.210 \text{ (m}^2/\text{day)}}{-87.5 \text{ (\%)}}$

Note The numerator shows specific flows, m²/day; in the denominator—the deviation of the values from the exact formula of the article authors, %

Next, we compare the calculation the water permeability coefficient with clogged damage and the pressure gradient at its base.

Let us calculate the amount of damage to the seepage-control lining:

$$n = \frac{L_c}{l_{dam}}, \text{ pcs.} \tag{4}$$

The lining area shall be determined by the formula:

$$F_{lin} = B_c \cdot L_c, \text{ m}^2. \tag{5}$$

Let's find the average seepage coefficient with clogged damage:

$$k'_{lin} = \frac{2k_{cl} \cdot \delta_{lin} \cdot L_{dam} \cdot n}{F_{lin}}, \text{ cm/s.} \tag{6}$$

7 Conclusions

As a study result, new design and technical solutions for repairing damage to irrigation canal linings have been developed, which usage will ensure the impervious coating impermeability, increase reliability and prevent the under-slab voids formation. The solutions advantages lie in the repairing possibility major damage to concrete and reinforced concrete channel linings, restoring expansion joints, and also a longer further structures operation. The calculation method through clogged damages in concrete canal linings makes it possible to determine the seepage flow through the coatings seepage-control elements in the cracks presence or other damage there.

References

1. Kosichenko YM, Baev OA (2014) Impervious coating of geosynthetics. RosNIIPM, Novocherkassk
2. Kosichenko YM, Baev OA (2016) Design of impervious coatings with enhanced reliability made from innovative materials. *Procedia Eng* 150:1503–1509. <https://doi.org/10.1016/j.proeng.2016.07.096>
3. Kosichenko YM, Baev OA (2014) Highly reliable designs of impervious coatings for channels and reservoirs, the criteria for their efficiency and reliability. *Hyd Eng* 8:18–25
4. Kosichenko YM, Garbuz AY (2018) Hydraulic model of water permeability of concrete lining during long-term operation of the channel. *Prirodoobustrojstvo* 4:30–40. <https://doi.org/10.26897/1997-6011/2018-4-30-40>
5. Abdrazakov FK, Rukavishnikov AA (2019) Elimination of unproductive losses of water resources from the irrigation network through the use of modern facing materials. *Agric Sci J* 10:91–94. <https://doi.org/10.28983/asj.y2019i10pp91-94>
6. Abdrazakov FK, Rukavishnikov AA, Povarov AV, Trushin YE (2019) Intensification of melioration through decreasing maintenance load on irrigation canals. *E3S Web Conf* 140:09009. <https://doi.org/10.1051/e3sconf/201914009009>
7. Bandurin MA, Bandurina IP, Vanzha VV, Pasnichenko PG, Tkachenko VT (2021) Modelling of the optimal height of the variable edge of a volumetric anti-filtration geotextile coating for restoring failed water supply structures. *IOP Conf Ser Mater Sci Eng* 1064:012001. <https://doi.org/10.1088/1757-899X/1064/1/012001>
8. Ding K, Gao L (2020) Development in canal lining technology in China. *Irrig Drain* 69:36–40. <https://doi.org/10.1002/ird.2438>
9. Plusquellec H (2019) Overestimation of benefits of canal irrigation projects: decline of performance over time caused by deterioration of concrete canal lining. *Irrig Drain* 68:383–388. <https://doi.org/10.1002/ird.2341>
10. Han X, Wang X, Zhu Y, Huang J (2021) A fully coupled three-dimensional numerical model for estimating canal seepage with cracks and holes in canal lining damage. *J Hydrol* 597:126094. <https://doi.org/10.1016/j.jhydrol.2021.126094>
11. Han X, Wang X, Zhu Y, Wu J, Huang J (2022) Effects of canal damage characteristics on canal seepage based on a three-dimensional numerical model. *J Hydrol* 605:127295. <https://doi.org/10.1016/j.jhydrol.2021.127295>
12. Abd-Elhamid HF, Abdelaal GM, Abd-Elaty I, Said AM (2019) Efficiency of using different lining materials to protect groundwater from leakage of polluted streams. *J Water Supply Res Technol-AQUA* 68:448–459. <https://doi.org/10.2166/aqua.2019.032>

13. Al-adili A, Al-ameer OA, Al-sharbaty A (2016) Experimental investigation of joint filling materials performance on preventing seepage in lined open concrete canal (laboratory and field model). *KSCE J Civ Eng* 20:1936–1947
14. Elkamhawy E, Zelenakova M, Abd-Elaty I (2021) Numerical canal seepage loss evaluation for different lining and crack techniques in arid and semi-arid regions: a case study of the river Nile, Egypt. *Water (Switzerland)* 13:3135. <https://doi.org/10.3390/w13213135>
15. Crawford W, Kujawsk M (2019) Geosynthetic cementitious composite mats: essential characteristics and properties. In: Abstracts of the 17th European conference on soil mechanics and geotechnical engineering, Harpa Conference Centre, Iceland, Reykjavik, 1–7 Sept 2019
16. Blond E, Boyle S, Ferrara M, Rimoldi P, Stark T (2019) Applications of geosynthetics to irrigation. *Drainage Agric* 68:67–83. <https://doi.org/10.1002/ird.2300>
17. Li Q, Wu B, Zhou H (2022) Damage simulation analysis of canal concrete lining plates based on temperature-stress-water load coupling. *Sustainability* 14(15):9202. <https://doi.org/10.3390/su14159202>
18. El-Molla DA, El-Molla MA (2021) Reducing the conveyance losses in trapezoidal canals using compacted earth lining. *Ain Shams Eng J* 12(3):2453–2463. <https://doi.org/10.1016/j.asej.2021.01.018>
19. Prabakaran PA, Sathyamoorthy GL, Adhimayan M (2019) An experimental and comparative study on canal lining exploitation geo synthetic material, cement mortar and material lining. *Int J Recent Technol Eng* 7(4S):81–83
20. Baev OA, Talalaeva VF (2022) Method of repair of concrete channel linings. *RUS Patent* 2,779,173, 5 Sept 2022



Development of Single-Node Finite Elements for the Calculation of Systems with Unilateral Constraints by FEM in the Form of the Classical Mixed Method

M. I. Bochkov^(✉) and V. A. Ignatyev

Volgograd State Technical University, 1, St. Akademicheskaya, Volgograd 400074, Russia
maxim.bochckow@yandex.ru

Abstract. This article investigates the features and advantages of using single-node finite elements of Finite Element Method in the form of the Classical Mixed Method. The research was conducted on one-dimensional problems with various types of unilateral constraints (rigid, elastically flexible, with a gap between the structure and the support). A special algorithm for switching the condition of the support was developed by modifying the response matrix of the single-node finite elements. This algorithm allows switching of connections without changing the calculation scheme of the structure. Verification was carried out by comparing the calculated results with the results of the calculation of the LIRA SAPR software package, which calculation schemes are built using single-node finite elements that implement the displacement method. The article demonstrates the advantages of solving problems that include single-node finite elements that simulate various types of constructive nonlinearity, including ease of algorithmization in the decision-making area on switching the state of unilateral constraints, due to the inclusion in the response matrix of both the force that arises in the connection and displacement along its direction, and the ability to solve the problem of elastic connection, which is included in the work after the section gap reaches a certain value.

Keywords: Constructive nonlinearity · Structural mechanics · Finite element

1 Introduction

In modern engineering practice, real properties of soil are usually taken into account with a substantial number of rough assumptions. The use of modern soil mechanics models, such as the hardening soil model [1–4], is complicated not only by the increase in the number of variables but also by the absence of regulations governing the use of the normative base. Similar problems are encountered in the class of constructive nonlinear problems, such as problems with supports accounting for friction [5], or dynamic problems that take into account the operation of vibration dampers [6, 7]. Thus, modern structural mechanics faces the task not only of developing new methods for calculating

structures that take into account the real properties of the considered systems, but also of optimizing the algorithms that implement them in order to make these methods more applicable in practical design of real buildings and structures.

The use of single-node finite elements is widely used in the calculation of systems that take into account the peculiarities of soil foundation work using the finite element method in the displacement form. The LIRA SAPR software package [8] uses two main types of single-node finite elements that are used to simulate linear elastic connections, as well as a number of nonlinear single-node finite elements that simulate constructive nonlinear behavior of elastic connections, due to their disconnection when the ultimate force or displacement is reached. In our works [9, 10], the effectiveness of using the Finite Element Method in the form of the Classical Mixed Method to solve constructive nonlinear problems and problems involving elastic flexible connections has already been demonstrated. Therefore, the development of single-node finite elements is a logical development of the proposed approaches, which will allow for their systematization and the development of the proposed advantages of calculating structures on an elastic flexible, linear and nonlinear working foundation.

2 Materials and Methods

When using the Finite Element Method in the form of the Classical Mixed Method (FEM in CMM form), both displacements and forces are included in the response matrix. This allows us to determine both the displacement and force that arise in a single-node finite element at the calculation stage of the resolving equations. This ability eliminates intermediate steps in determining this force based on the deformed scheme, providing an advantage in calculation accuracy. In addition, such an approach is convenient for solving constructive nonlinear problems, in which changes in connection characteristics depend on the forces that arise in them. It is worth noting that problems of changing the elastic properties of connections with increasing load are common in real engineering practice. Such changes can include changes in the properties of the soil foundation due to a decrease in porosity under load.

A mixed-type single-node finite element, taking into account the elastic flexible properties for all linear displacements and rotations for a three-dimensional problem in the finite element method in the classical mixed method form, is shown in Fig. 1. Such a finite element has twelve degrees of freedom, six translations along the directions of the global axes and six forces arising in the elastic flexible connections. Since the element represents a node, its use does not require the introduction of a local coordinate system, i.e., the forces are oriented in the global coordinate system. The relationship between displacements and forces for the finite element will be determined by six stiffness characteristics, depending on the equivalent elastic properties that our element should model at the location point. Thus, as mentioned earlier, after solving the resolving equations, we will obtain the reaction values in supports, i.e., we will have comprehensive information necessary for decision-making on the operation of supports in a nonlinear statement.

To simplify the presentation of the material reflecting the fundamental principles of using the developed finite elements, we will describe single-node finite elements of a planar problem in the text of the article. Such elements will have 6 degrees of freedom—3 displacements along the directions of the global axes and 3 forces arising in the links.

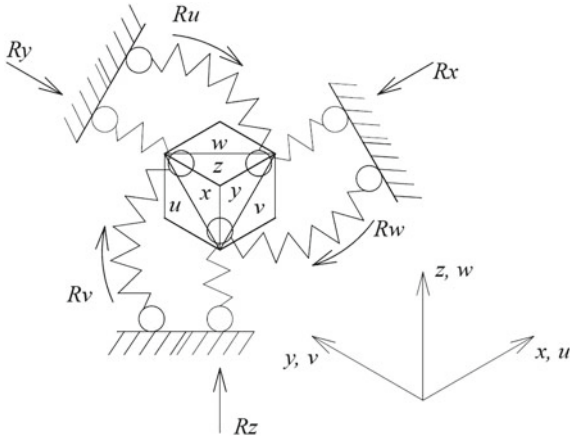


Fig. 1 Single-node mixed finite element

The response matrix of such a finite element can be written in the form of expression (1).

$$\begin{bmatrix} r_{1,1} & r_{1,2} & r_{1,3} & \tilde{r}_{1,4} & \tilde{r}_{1,5} & \tilde{r}_{1,6} \\ r_{2,1} & r_{2,2} & r_{2,3} & \tilde{r}_{2,4} & \tilde{r}_{2,5} & \tilde{r}_{2,6} \\ r_{3,1} & r_{3,2} & r_{3,3} & \tilde{r}_{3,4} & \tilde{r}_{3,5} & \tilde{r}_{3,6} \\ \tilde{\delta}_{4,1} & \tilde{\delta}_{4,2} & \tilde{\delta}_{4,3} & \delta_{4,4} & \delta_{4,5} & \delta_{4,6} \\ \tilde{\delta}_{5,1} & \tilde{\delta}_{5,2} & \tilde{\delta}_{5,3} & \delta_{5,4} & \delta_{5,5} & \delta_{5,6} \\ \tilde{\delta}_{6,1} & \tilde{\delta}_{6,2} & \tilde{\delta}_{6,3} & \delta_{6,4} & \delta_{6,5} & \delta_{6,6} \end{bmatrix} = \begin{bmatrix} 0 & 0 & 0 & -1 & 0 & 0 \\ 0 & 0 & 0 & 0 & -1 & 0 \\ 0 & 0 & 0 & 0 & 0 & -1 \\ 1 & 0 & 0 & 1/C_x & 0 & 0 \\ 0 & 1 & 0 & 0 & 1/C_y & 0 \\ 0 & 0 & 1 & 0 & 0 & 1/C_\varphi \end{bmatrix} \tag{1}$$

where C_x, C_y, C_φ —is the equivalent stiffness of the element, which corresponds to horizontal, vertical and angular stiffness, respectively.

The stiffness of the element is calculated separately depending on the physical properties we want to transmit depending on the support. An example of such stiffness is the reduced nodal stiffness coefficient for the Winkler model of foundation operation.

The integration of the developed single-node finite elements into the computational scheme built using bar finite elements, regardless of the type of finite elements [11–13], is carried out by combining the unknowns that determine the displacements at the nodes of the bar finite element with the displacements of the single-node finite element installed at this node.

The presence of support stiffness in the solving equations allows modeling both rigid connections—by introducing a stiffness coefficient C_x, C_y, C_φ greater than the stiffness of the main elements of the problem (where $\frac{1}{C_{on}} \rightarrow 0$), and the absence of support connection - by introducing a stiffness coefficient C_x, C_y, C_φ less than the stiffness of the main elements of the problem (where $\frac{1}{C_{off}} \rightarrow \infty$). Thus, the use of a single-node finite element allows modeling one-way work of elastic-pliable or rigid supports without changing the calculation scheme, which simplifies the algorithmization of the iterative process of calculating a constructively non-linear problem.

3 Results and Discussion

Let's demonstrate the above on an elementary example of a beam supported by different types of supports and loaded with a concentrated load.

Example 1 Calculation of a beam on two-sided elastic-pliable supports (Fig. 2).

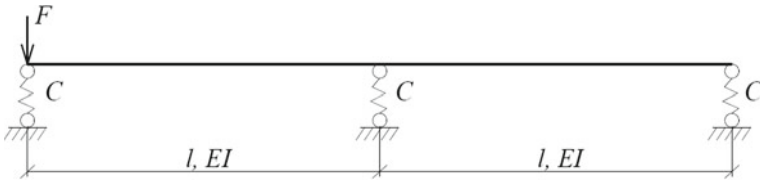


Fig. 2 Example 1. Calculation scheme of a beam on two-sided resilient supports

The primary system uses the first type beam finite element [14]. The primary finite element method system in the form of a classic mixed method for such a beam is shown in Fig. 3.

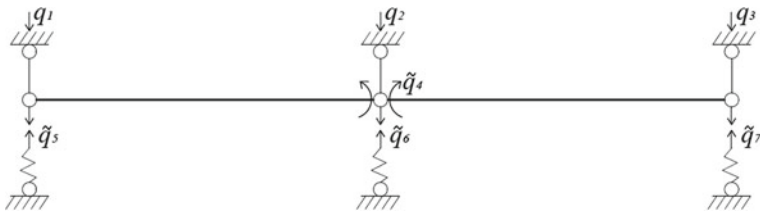


Fig. 3 The main FEM system in the form of a mixed method for a beam on two-sided resilient supports

The solving equations in matrix form have the following view (2).

$$\begin{bmatrix}
 0 & 0 & 0 & -1/l & -1 & 0 & 0 \\
 0 & 0 & 0 & 2/l & 0 & -1 & 0 \\
 0 & 0 & 0 & -1/l & 0 & 0 & -1 \\
 1/l & -2/l & 1/l & 2l/3EI & 0 & 0 & 0 \\
 1 & 0 & 0 & 0 & 1/C & 0 & 0 \\
 0 & 1 & 0 & 0 & 0 & 1/C & 0 \\
 0 & 0 & 1 & 0 & 0 & 0 & 1/C
 \end{bmatrix} \cdot \begin{bmatrix}
 q_1 \\
 q_2 \\
 q_3 \\
 q_4 \\
 q_5 \\
 q_6 \\
 q_7
 \end{bmatrix} = \begin{bmatrix}
 1000 \\
 0 \\
 0 \\
 0 \\
 0 \\
 0 \\
 0
 \end{bmatrix} \quad (2)$$

Table 1 shows a comparison of the accuracy of the calculation with the calculation made using the LIRA SAPR 2013 R5 software package. In the computational scheme of the software package, FE 51 (single-node) and FE 2 (two-node) were used.

The deformed shape of the beam obtained is shown in Fig. 4.

Table 1 The calculation results for example 1

	FEM in CMM form	LIRA SAPR 2013 R5	Discrepancy, %
q_1 , mm (movement in 1 support)	18.4848	18.4832	~ 0
q_2 , mm (movement in 2 support)	3.0304	3.0303	~ 0
q_3 , mm (movement in 3 support)	-1.5152	-1.5152	0
M_2 , kN*m (bending moment over the second support)	-454.55	-454.6	~0

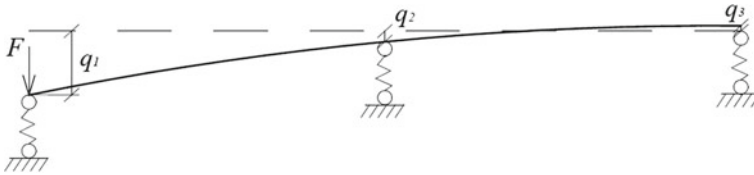


Fig. 4 Example 1. Deformation scheme of the beam

Example 2 Calculation of a beam on one-sided elastic-pliable supports.

Let’s perform the calculation of the beam from Example 1, assuming that the elastic-pliable supports are one-sided. To find the working scheme, we will use the Rabinovich algorithm adapted by us for calculating systems using the Finite Element Method in the form of the Classical Mixed Method in [9]. As mentioned above, using a single-node finite element, we can model the one-way work of supports, when they are disconnected, by changing the stiffness. In this case, the solving equations in the second step, when support 3 is disconnected, will have the following form (3):

$$\begin{bmatrix}
 0 & 0 & 0 & -1/l & -1 & 0 & 0 \\
 0 & 0 & 0 & 2/l & 0 & -1 & 0 \\
 0 & 0 & 0 & -1/l & 0 & 0 & -1 \\
 1/l & -2/l & 1/l & 2l/3EI & 0 & 0 & 0 \\
 1 & 0 & 0 & 0 & 1/C & 0 & 0 \\
 0 & 1 & 0 & 0 & 0 & 1/C & 0 \\
 0 & 0 & 1 & 0 & 0 & 0 & 1/C_{off}
 \end{bmatrix} \cdot \begin{bmatrix} q_1 \\ q_2 \\ q_3 \\ q_4 \\ q_5 \\ q_6 \\ q_7 \end{bmatrix} = \begin{bmatrix} 1000 \\ 0 \\ 0 \\ 0 \\ 0 \\ 0 \\ 0 \end{bmatrix} \tag{3}$$

where $C_{off} \rightarrow 0$.

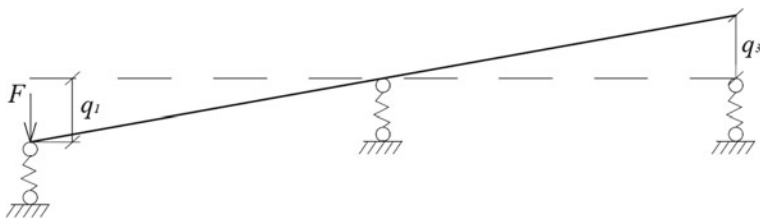
The deformed scheme after the second step of the calculation is shown in the figure, and the comparison of the calculation results with the LIRA SAPR 2013 R5 calculation is presented in Table 2.

The obtained deformed shape of the beam is shown in Fig. 5.

Thus, the use of a single-node finite element of the mixed method, which includes the stiffness of the elastic-pliable support, allows solving a problem with unilateral

Table 2 The calculation results for Example 2

	FEM in CMM form	LIRA SAPR 2013 R5	Discrepancy, %
q_1 , mm (movement in 1 support)	20	20	0
q_2 , mm (movement in 2 support)	0	0	0
q_3 , mm (movement in 3 support)	-20	-20	0
M_2 , kN*m (bending moment over the second support)	~ 0	0	0

**Fig. 5** Example 2. Deformation scheme of the beam

constraints without changing the calculation scheme using the mechanism of changing the stiffness of the connections. The error in the value of some of the parameters is explained by the fact that the connections are not absolutely rigid, but such an error can be neglected.

The application of the mixed form of the finite element has also shown its effectiveness in solving problems with hardening or softening one-sided connections using an algorithm based on the idea of the method of compensating loads proposed by Alyonin and Ignatyev [15, 16]. The essence of the method of compensating loads is to model the change in support stiffness by introducing compensating loads with their subsequent iterative refinement to a certain coefficient for exiting the algorithm. When modeling such a problem using the finite element method in the form of a classic mixed method, these compensating loads will be applied to the single-node finite elements themselves and will enter the external load vector, affecting only the values of one of its rows. In addition, the values of compensating loads are calculated depending on the force arising in the support, which enters the solving equation of the mixed method when using the single-node finite element developed by us. Therefore, the application of this method based on the mixed FEM, unlike displacement-based FEM, will not require additional calculations, which simplifies the calculation algorithm.

In the case of using a single-node finite element, the method of compensating loads can be adapted by introducing not compensating loads, but directly compensating displacements into the calculation scheme. This effect allows achieving the fact that the

external load vector in the mixed form of the finite element method explicitly includes displacements in the directions of the disconnected supports. This approach allows algorithmizing the calculation of supports with gaps by introducing compensating displacements in the supports where the deflection has exceeded the size of the gap.

Example 3 Let us consider the beam from Example 2, which has a one-sided resilient support in support 3, but is fixed against upward movement by a rigid support with a clearance of 10 mm. The design scheme is shown in Fig. 6.

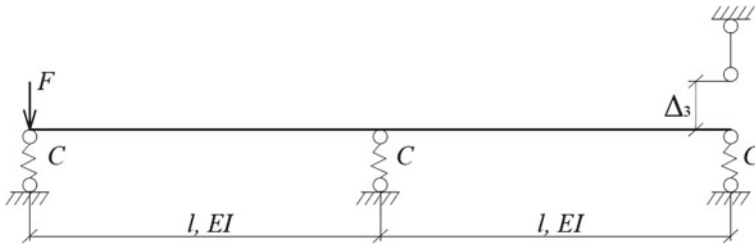


Fig. 6 Example 3. Calculation scheme

The calculation of such a beam on steps 1 and 2 will correspond to the calculation of the beam from Example 2, as described above. However, further, on the third step, due to the fact that the displacement in the beam has exceeded the clearance value, the main system will take the form (4).

$$\begin{bmatrix}
 0 & 0 & 0 & -1/l & -1 & 0 & 0 \\
 0 & 0 & 0 & 2/l & 0 & -1 & 0 \\
 0 & 0 & 0 & -1/l & 0 & 0 & -1 \\
 1/l & -2/l & 1/l & 2l/3EI & 0 & 0 & 0 \\
 1 & 0 & 0 & 0 & 1/C & 0 & 0 \\
 0 & 1 & 0 & 0 & 0 & 1/C & 0 \\
 0 & 0 & 1 & 0 & 0 & 0 & 1/C_{on}
 \end{bmatrix} \cdot \begin{bmatrix} q_1 \\ q_2 \\ q_3 \\ q_4 \\ q_5 \\ q_6 \\ q_7 \end{bmatrix} = \begin{bmatrix} 1000 \\ 0 \\ 0 \\ 0 \\ 0 \\ 0 \\ \Delta \end{bmatrix} \tag{4}$$

where $C_{on} \rightarrow \infty$; $\Delta = -10$.

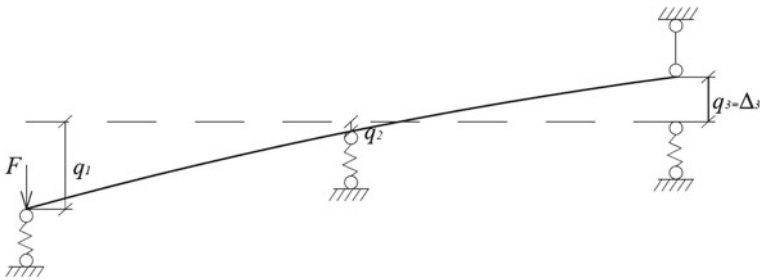
The deformed scheme after the second calculation step is shown in the figure, and the comparison of the calculation results with the calculation of LIRA SAPR 2013 R5 is summarized in Table 3.

The obtained deformed scheme of the beam is shown in Fig. 7.

The introduction of compensating movements in the directions of the rejected supports also allows taking into account in the calculation schemes the inclusion of one-sided resilient connections with clearances. However, solving such problems in the LIRA SAPR 2013 software without involving a complex iterative process with a large number of iterations is impossible. The finite element method in the form of a classical mixed method allows reducing such a calculation to a simple step-by-step process with decision-making at the beginning of each step.

Table 3 The calculation results for Example 3

	FEM in CMM form	LIRA SAPR 2013 R5	Discrepancy, %
q_1 , mm (movement in 1 support)	19,1788	19,1803	0
q_2 , mm (movement in 2 support)	1,6393	1,6393	0
q_3 , mm (movement in 3 support)	-10	-10	0
M_2 , kN*m (bending moment over the second support)	-245,902	-245,912	0

**Fig. 7** Example 3. Deformation scheme of the beam

Example 4 Let us consider the beam from Example 3, which has a one-sided resilient support in support 3, but is fixed against upward movement by a resilient support with a clearance of 10 mm.

The system of resolving equations for such a beam on the third step of the calculation will have the form (5).

$$\begin{bmatrix} 0 & 0 & 0 & -1/l & -1 & 0 & 0 \\ 0 & 0 & 0 & 2/l & 0 & -1 & 0 \\ 0 & 0 & 0 & -1/l & 0 & 0 & -1 \\ 1/l & -2/l & 1/l & 2l/3EI & 0 & 0 & 0 \\ 1 & 0 & 0 & 0 & 1/C & 0 & 0 \\ 0 & 1 & 0 & 0 & 0 & 1/C & 0 \\ 0 & 0 & 1 & 0 & 0 & 0 & 1/C \end{bmatrix} \cdot \begin{bmatrix} q_1 \\ q_2 \\ q_3 \\ q_4 \\ q_5 \\ q_6 \\ q_7 \end{bmatrix} = \begin{bmatrix} 1000 \\ 0 \\ 0 \\ 0 \\ 0 \\ 0 \\ \Delta_3 \end{bmatrix} \quad (5)$$

As a result of the calculation, the displacement in the third support is obtained: $q_3 = -10,7576$ mm. Let us compare this value with the results of the calculation in LIRA SAPR from Example 3, by adding to them the value of the transverse force Q in the beam multiplied by the stiffness coefficient of the support. Such a calculation will not give an accurate displacement value since it does not take into account the joint work of the support and the beam, but it will give an idea of the order of magnitude of

displacements. $q'_3 = -10 - 40,9853 * 0,02 = -10,8197(\text{mm})$. We assume that the value obtained by us is more accurate since it takes into account the joint work of the beam and the resilient supports.

The developed single-node finite element of the finite element method in the form of a classical mixed method allows efficiently solving problems involving any types of one-sided supports. Such possibility is provided by including both displacements and forces in the resolving equation, which allows making a decision on the inclusion/exclusion of unilateral constraints without additional calculations and by turning them on/off by making changes to the response matrix of the finite element. The efficiency of the developed finite element is demonstrated through the comparison of the calculation results with the LIRA SAPR 2013 software, as well as by expanding its area of application to a problem with a one-sided resilient support with a clearance, which the software cannot solve in a linear formulation.

References

1. Alexanderov AS, Dolgikh GV (2016) Modification of the criterion of Kulon-Mora for raschet constructive roads on the resistance of the sdvyh. Part 1. Enter the third parameter of the motherhood. *Mezhdunarodnyi nauchno issledovatel'skii zhurnal* 6–2(48)
2. Bhatto AH et al (2019) Mohr-Coulomb and hardening soil model comparison of the settlement of an embankment dam. *Eng Technol Appl Sci Res* 9(5):4654–4658
3. Kudasheva MI, Kaloshina CV (2017) Comparison of the Mohr-Coulomb model and the hardening ground model in the Plaxis software complex. *Stroitel'stvo i arhitektura. Opyt i sovremennyye tekhnologii*. <http://sbornikstf.pstu.ru/council/?n=9>. Accessed 3 Apr 2023
4. Xiang X, Zi-Hang D (2017) Numerical implementation of a modified Mohr-Coulomb model and its application in slope stability analysis. *J Modern Transp* 25(1):40–51
5. Lukashevich AA, Lukashevich NK (2019) Modelling and numerical solution of problems of structural mechanics with unilateral constraints and friction. *IOP Conf Ser: Mater Sci Eng* 687:033024
6. Potapov AN, Tazeev NT (2023) Time analysis of a constructively nonlinear system with one-way connections. *Int J Comput Civ Struct Eng* 19(1):135–146. <https://doi.org/10.22337/2587-9618-2023-19-1-135-146>
7. Wang L, Jiang TL, Dai HL, Ni Q (2018) Three-dimensional vortex-induced vibrations of supported pipes conveying fluid based on wake oscillator models. *J Sound Vib* 422:590–612
8. Strelec-Strelecky EB, Zhurvlev AV, Vodopyanov Ryu (2019) LIRA-SAPR. Book 1. Basics. LIPALAND publ
9. Ignatyev AV, Ignatyev VA, Bochkov MI (2017) Application of the finite element method in the form of a classical mixed method to the calculation of systems with one-way constraints. *Stroitel'naya mekhanika i raschet sooruzheniy* 2:52–61
10. Ignatyev AV, Bochkov MI, Kurochkina IV (2019) Comparative analysis of the efficiency of some algorithms for calculating systems with one-way connections. *Izvestiya vysshikh uchebnykh zavedeniy. Stroitel'stvo* 11(731):87–98
11. Ignatyev AV, Gabova VV (2007) Algorithm for static design of bar systems using the finite element method in mixed form. *Vestnik Volgogradskogo gosudarstvennogo arkhitekturno-stroitel'nogo universiteta. Ser.: Yestestvennyye nauki* 6(23):72–77
12. Voronkova GV, Rekunov SS (2007) Features of the calculation of plates by the finite element method in mixed form. *Vestnik Volgogradskogo gosudarstvennogo arkhitekturno-stroitel'nogo universiteta. Ser.:Stroitel'stvo I Arhitektura* 7(26):74–77

13. Ignatyev AV, Ignatyev VA, Onishchenko YeV (2017) Analysis of flexible bars and frames with large displacements of nodes by finite element method in the form of classical mixed method. In: IOP conference series: materials science and engineering, vol 262: International Conference on Construction, Architecture and Technosphere Safety (ICCATS 2017), 21–22 September 2017, Chelyabinsk, Russian Federation
14. Ignatyev VA, Ignatyev AV (2022) Finite element method in the form of a classical mixed method of structural mechanics (theory, mathematical models and algorithms). ASV, Moscow
15. Alyonin VP (1988) Alyonin VP Calculation of systems with one-sided Winkler constraints. *Izv. Vuzov. Stroitel'stvo i arkhitektura* 3:33–36
16. Alyonin VP (2002) Iterative methods for calculating systems with external and internal one-way connections. Dissertation, Volgograd



Technique for Solving Finite Element Systems of High-Order Linear Algebraic Equations Describing the Stress–Strain State of One-Dimensional and Two-Dimensional Structures

A. V. Ignatyev^(✉) and I. S. Zavyalov

Volgograd State Technical University, 1, St. Akademicheskaya, Volgograd 400074, Russia
alignat70@yandex.ru

Abstract. The article discusses the problems that arise when applying the finite element method to design models of complex structures and structures represented by design schemes with a large number of finite elements. The development of an algorithm for reducing finite element systems of high-order equations describing the stress–strain state of one-dimensional and two-dimensional structures based on linear interpolation, which allows to significantly reduce the order of these systems, while maintaining sufficient accuracy of calculations, is described. The article presents a mathematical model for a two-dimensional plate and describes a method for solving a system of equations based on linear interpolation at the nodes of a fine grid. To test the effectiveness of the algorithm, numerical experiments were carried out comparing the results obtained using the proposed method with the analytical and results obtained on the basis of the FEM in the form of a classical mixed method. The results of numerical experiments have shown that the proposed algorithm has a sufficiently high accuracy and efficiency in solving problems of solid mechanics. The proposed approach can be applied to reduce systems of high-order algebraic equations describing the stress–strain state of one-dimensional and two-dimensional structures, and to speed up calculations in large and complex problems of solid mechanics, which is an urgent problem in engineering practice.

Keywords: FEM in the form of a classical mixed method · Flexible thin plate · High-order SLAE · Reduction method · Algorithm for constructing a reduced system of equations

1 Introduction

The finite element method (FEM) is one of the most common and effective methods of numerical analysis, which is widely used in engineering calculations and scientific research. When solving structural mechanics problems, FEM is most often used in the

form of the displacement method. A study of existing publications on the theory of FEM and the practice of its application in software systems revealed that the traditional form of FEM in displacements, which is the basis of many software systems, has its advantages, but there are also a number of unresolved problems that can affect the accuracy of the calculation results and require additional verification. Unresolved problems of the traditional form of FEM in displacements contributed to the development of other forms of FEM, such as FEM in stresses, FEM in the form of the method of forces, FEM in a mixed form and hybrid variants [1–6]. In particular, the authors develop the finite element method, presented in the form of the classical mixed method of structural mechanics. Its theoretical justification, the development of the corresponding physical and mathematical models of finite elements and algorithms for calculating various types of structural elements and structures in linear and nonlinear formulations are given in [7, 8].

Taking into account the tendencies towards complication and greater accuracy of computational finite element models of buildings and structures, calculations for statics, dynamics and stability using software systems that implement the finite element method lead to an increase in the dimension of problems (the order of coefficient matrices for unknowns reaches 2 million equations and more). In addition, most of the problems of structural mechanics are ill-conditioned, due to the use of different types of finite elements, a large spread of stiffness, and irregular grids.

It is also worth noting the fact that when searching for an acceptable design solution, it is necessary to repeatedly make changes to the calculation model and repeat the calculation at each stage of the change in the calculation scheme.

It should be noted that usually the solution of SLAE takes most of the time for calculating the problem on a computer. In addition, the quality and accuracy of the solution of the problem as a whole directly depends on this stage. The operation of the entire complex largely depends on the choice of the SLAE solution method, the algorithm and the quality of its implementation, so it is worth paying special attention to these issues.

In this case, traditional methods for solving SLAEs turn out to be inefficient and, therefore, it is necessary to develop high-performance methods that take into account the sparseness of matrices, are resistant to bad conditioning and can work effectively on a limited amount of memory under conditions of high-dimensional problems.

Based on these requirements, there is a need to develop and implement in the computational software systems highly efficient methods for solving systems of high-order finite element equations.

To date, two options for solving or circumventing this problem have been outlined and are being used.

The first is to develop methods and algorithms related to the direct solution of large SLAEs (various options for ordering and transforming the matrix of coefficients for unknowns, the use of iterative procedures, etc.) [9–14]

The second way is the development of physical models of complex structures with a phased transition from a simple model to a more complex one, using the calculation result of the previous rough model when building a more complex subsequent one. Here

it should be noted the method of superelements (substructures) [15–18], interpolation methods (grid methods) [19], as well as spline methods [20–23].

We propose a technique for solving high-order finite element SLAEs describing the stress–strain state of one-dimensional and two-dimensional structures, which is based on an algorithm for reducing this SLAE based on linear interpolation of functions describing the stress–strain state of the structure under consideration.

2 Materials and Methods

The algorithm for constructing a reduced system of finite element equations that describe the stress–strain state of a one-dimensional or two-dimensional structure in each of the coarse grid cells is based on the approximation of the main unknowns of the mixed method at the fine grid nodes through the values of the same unknowns at the coarse grid nodes. This algorithm can be greatly simplified if we accept a linear interpolation of the main unknowns between the nodes of the coarse grid.

The choice of linear interpolation is due to the fact that in some cases it is very difficult to choose a non-linear approximating function and justify its choice.

The algorithm for constructing a reduced system of equations consists of five stages.

1. Two finite element grids are applied to the structure under consideration: a grid with large cells with the designation of nodes I, J (main nodes) and a grid with small cells with the designation of nodes i, j . (secondary nodes). The area under consideration, formed by a coarse finite element grid applied to a two-dimensional structure, is shown in Fig. 1. The number of fine grid nodes is a multiple of the coarse grid nodes, and it is the same for all regions of the coarse grid.

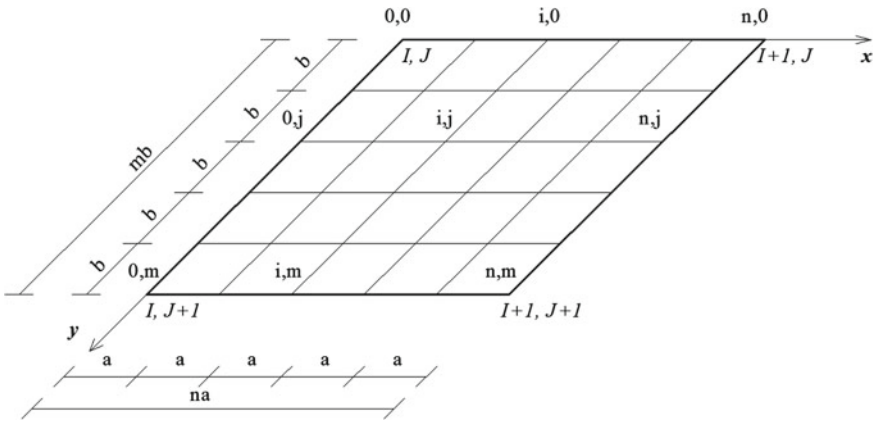


Fig. 1 The area under consideration formed by partitioning into a large finite element grid

2. A relationship is established between the displacements and forces of nodes i, j and I, J . In the area under consideration, a linear interpolation of the values of the main

unknowns of the mixed method at the nodes of the fine grid through the values of the same unknowns at the nodes of the coarse grid is performed. A formal representation of such an interpolation for a one-dimensional construction is shown in Fig. 2, for the two-dimensional construction in Fig. 3. To establish a connection between the displacements and forces of nodes i, j and I, J , the coefficients of linear interpolation polynomials are found, which allow expressing the values of the main unknowns of the mixed method at the nodes of the fine grid through the same values of the unknowns at the nodes of the coarse grid for all areas of the coarse grid.

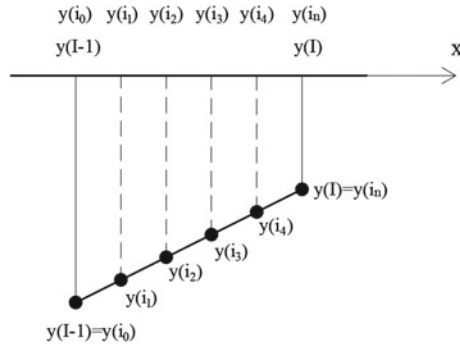


Fig. 2 Linear interpolation between displacements and forces of nodes i, j and I, J for one-dimensional construction

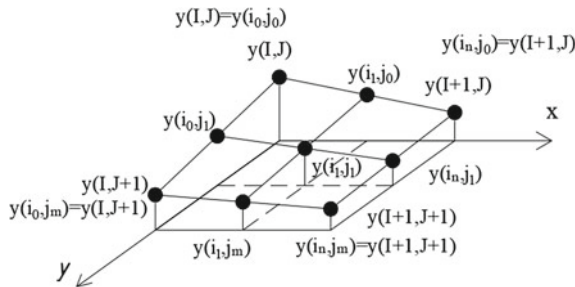


Fig. 3 Linear interpolation between displacements and forces of nodes i, j and I, J for a two-dimensional construction

3. The values of the main unknowns of the mixed method at the nodes of the fine grid, expressed through the values of the same nodal unknowns of the coarse grid, are substituted into the system of finite element equations of the finite element method in the form of the classical mixed method (FEM in the form of CMM) for each of the considered design areas. The global system of resolving equations is written as (1).

$$\begin{bmatrix} r & \tilde{r} \\ \tilde{\delta} & \delta \end{bmatrix} \begin{Bmatrix} q^* \\ \tilde{q}^* \end{Bmatrix} + \begin{Bmatrix} R_F \\ \Delta_F \end{Bmatrix} = \{0\}, \tag{1}$$

where

$[r]$	a matrix that translates the displacement vector into a vector of forces. The physical meaning of its element $r_{i,j}$ is the force arising in the direction of the i -th degree of freedom from a single movement of the j -th degree of freedom;
$[\tilde{r}]$	a matrix that translates a vector of forces into a vector of forces. The physical meaning of its element $\tilde{r}_{i,j}$ is a force arising in the direction of the i -th degree of freedom from a single force in the j -th degree of freedom;
$[\tilde{\delta}] = -[\tilde{r}]^T$	a matrix that translates a displacement vector into a displacement vector. The physical meaning of its element $\tilde{\delta}_{i,j}$ is a displacement arising in the direction of the i -th degree of freedom from a single displacement of the j -th degree of freedom;
$[\delta]$	a matrix that translates a vector of forces into a vector of displacements. The physical meaning of its element $\delta_{i,j}$ is the displacement that occurs in the direction of the i -th degree of freedom from a single force in the j -th degree of freedom;
$\{R_F\}$	the vector of reactions in the introduced connections from nodal loads, to which the local load is given, distributed over the elements of the main system;
$\{\Delta_F\}$	vector of displacements in the direction of force unknowns from the load in the main system;
q^*	kinematic unknowns expressed through the values of the same nodal coarse grid unknowns,
\tilde{q}^*	force unknowns expressed in terms of the values of the same coarse grid nodal unknowns.

The resulting system of equations for coarse grid unknowns (reduced system of equations) is solved by any of the most efficient methods.

4. In reverse order, we find the stress–strain state in the finite elements of the area under consideration.
5. The next stage of the calculation is to reduce the size of the grid cell with nodes I, J .

3 Results and Discussion

To demonstrate the applicability of the proposed algorithm for constructing a reduced system of finite element equations, a calculation was made of a square thin bending plate hinged along the contour (Fig. 4) to the action of a constant uniformly distributed load.

Initial data:

$$a = b = 1(m); \quad h = 0.01(m); \quad \mu_x = \mu_y = 0.3;$$

$$E = 1.092 \cdot 10^7(\text{ton}/m^2); \quad q = 1(\text{ton}/m^2).$$

When calculating the stress–strain state of a thin bendable plate based on FEM in the form of a classical mixed method, the system is represented by an ensemble of rectangular FE with three unknowns in each node (Fig. 5).

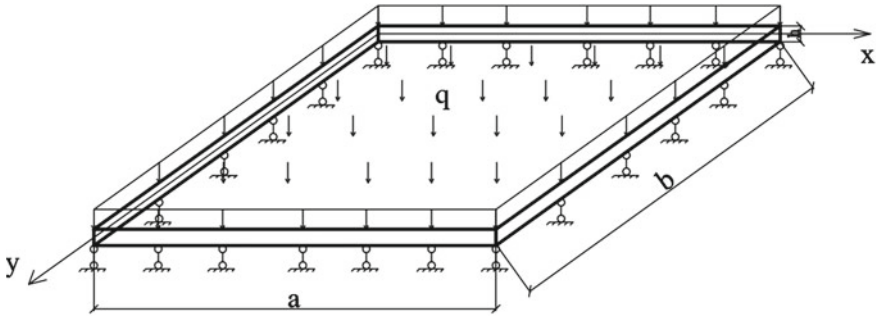


Fig. 4 A plate pivotally supported along the contour

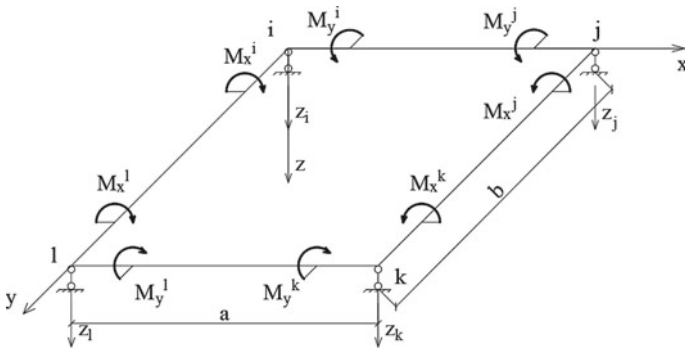


Fig. 5 Rectangular finite element used in the calculations of a rectangular bendable plate according to FEM in the form of CMM

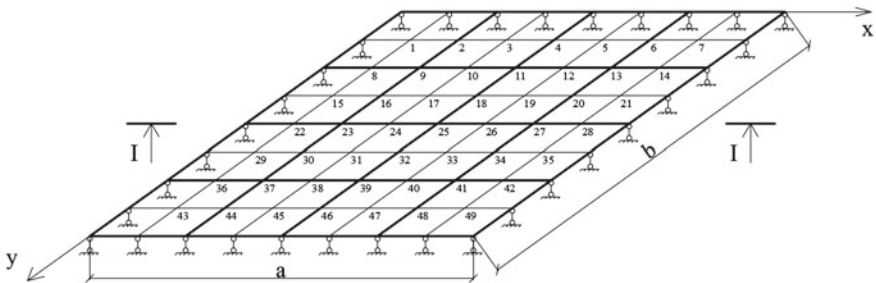


Fig. 6 Pivotedly supported plate, represented by a large and small finite element grid

Two finite element grids are applied to the plate: a grid with large 4×4 cells and a grid with small 8×8 cells (Fig. 6).

The function for approximating the main unknown displacements is written as a linear polynomial (2).

$$w(i, j) = c_1 + c_2 \cdot i + c_3 \cdot j + c_4 \cdot i \cdot j \tag{2}$$

Then, for an area of size axb bounded by coarse grid nodes $(I-1, J-1)$, $(I, J-1)$, $(I-1, J)$, (I, J) , with a step between nodes equal to m and n , the displacements in fine grid nodes can be represented by in the form of (3).

$$w(i, j) = \frac{w(I-1, J-1)}{a \cdot b} (a - m \cdot i) \cdot (b - n \cdot j) + \frac{w(I, J-1)}{a \cdot b} (m \cdot i) \cdot (b - n \cdot j) + \frac{w(I-1, J)}{a \cdot b} (a - m \cdot i) \cdot (n \cdot j) + \frac{w(I, J)}{a \cdot b} (m \cdot i) \cdot (n \cdot j) \quad (3)$$

Similarly, a connection is established between the forces in nodes i, j and I, J .

Table 1 compares the results of calculating the displacement w of the nodes of this plate according to the proposed algorithm with the analytical solution and the solution obtained on the basis of FEM in the form of CMM without reduction for finite element grids 4×4 and 8×8 .

Table 2 compares the results of calculating bending moments M_x at the nodes of this plate according to the proposed algorithm with an analytical solution and a solution obtained on the basis of the FEM in the form of CMM without regard to reduction with finite element grids 4×4 and 8×8 .

Table 3 compares the results of calculating bending moments M_y at the nodes of this plate according to the proposed algorithm with an analytical solution and a solution obtained on the basis of the FEM in the form of CMM without regard to reduction with finite element grids 4×4 and 8×8 .

4 Conclusions

The results obtained allow us to draw the following conclusions:

- The advantage of the proposed algorithm for reducing high-order SLAEs based on linear interpolation of the main unknowns at the nodes of a fine grid is the absence of operations for inverting the matrix of coefficients for unknown SLAEs for sparse grid nodes, which can also be of a rather high order and is a highly expensive operation in terms of computer time.
- Comparison of the results of calculations obtained using the algorithm for reducing the finite element system of equations obtained on the basis of the FEM in the form of CMM with the analytical solution showed a high degree of accuracy of the calculated displacements and forces, not inferior to the results obtained using the FEM in the form of CMM without the reduction procedure finite element system of equations.
- The above algorithm for constructing reduced SLAEs that describe the stress-strain state of one-dimensional and two-dimensional structures can be formalized and generalized to finite element areas of a structure with a design scheme of finite elements of any shape.
- The algorithm can be extended to handle 3D structures, although this would require further development and testing.
- The proposed algorithm has significant practical implications in the field of structural mechanics. The reduction of the size of the system of equations can be particularly useful in the analysis of complex structures with many degrees of freedom and high-order equations, which is an urgent problem in modern engineering practice.

Table 1 Comparison of the results of calculating the displacement $w(m)$ of the nodes of a square hinged plate, represented by a large 4×4 grid and a fine 8×8 grid, performed according to the proposed algorithm with an analytical solution and the solution obtained on the basis of FEM in the form of CMM without reduction

	Node number									
	8	9	10	11	22	23	24	25		
Analytical Solution (AS)	0.001182	0.002132	0.002733	0.002938	0.001623	0.002938	0.003776	0.004062		
FEM in the form of CMIM (FE grid 4×4) with reduction	0.001077	0.002154	0.0025475	0.002941	0.0014705	0.002941	0.003481	0.004021		
Percent difference from AS	9.75%	-1.02%	7.28%	-0.10%	10.37%	-0.10%	8.47%	1.02%		
FEM in the form of CMIM (FE grid 4×4) without reduction	-	0.00212	-	0.00295	-	0.00295	-	0.00411		
Percent difference from AS	-	0.57%	-	-0.41%	-	-0.41%	-	-1.17%		
FEM in the form of CMIM (FE grid 8×8) without reduction	0.00118	0.00213	0.00274	0.00294	0.00162	0.00294	0.00379	0.00408		
Percent difference from AS	0.17%	0.09%	-0.26%	-0.07%	0.19%	-0.07%	-0.37%	-0.44%		

Table 2 Comparison of the results of calculating the bending moments $M_x(on \cdot m)$ at the nodes of a square hinged plate, represented by a coarse 4×4 grid and a fine 8×8 grid, performed according to the proposed algorithm with an analytical solution and a solution obtained on the basis of the FEM in the form of CMM without reduction

	Node number									
	8	9	10	11	22	23	24	25		
Analytical solution (AS)	0.019	0.029	0.034	0.036	0.025	0.039	0.046	0.048		
FEM in the form of CMIM (FE grid 4×4) with reduction	0.01416	0.02832	0.0318965	0.035473	0.0188045	0.037609	0.042593	0.047577		
Percent difference from AS	34.18%	2.40%	6.59%	1.49%	32.95%	3.70%	8.00%	0.89%		
FEM in the form of CMM (FE grid 4×4) without reduction	-	0.03046	-	0.03626	-	0.04022	-	0.04922		
Percent difference from AS	-	-4.79%	-	-0.72%	-	-3.03%	-	-2.48%		
FEM in the form of CMM (FE grid 8×8) without reduction	0.0196	0.02966	0.03438	0.03578	0.0251	0.03922	0.04614	0.04819		
Percent difference from AS	-3.06%	-2.23%	-1.11%	0.61%	-0.40%	-0.56%	-0.30%	-0.39%		

Table 3 Comparison of the results of calculating the bending moments $M_y(ton \cdot m)$ at the nodes of a square hinged plate, represented by a coarse 4×4 grid and a fine 8×8 grid, performed according to the proposed algorithm with an analytical solution and a solution obtained on the basis of the FEM in the form of CMM without reduction

	Node number									
	8	9	10	11	22	23	24	25		
Analytical solution (AS)	0.017	0.029	0.037	0.039	0.021	0.036	0.045	0.048		
FEM in the form of CMIM (FE grid 4×4) with reduction	0.01416	0.02832	0.0329645	0.037609	0.0177365	0.035473	0.041525	0.047577		
Percent difference from AS	20.06%	2.40%	12.24%	3.70%	18.40%	1.49%	8.37%	0.89%		
FEM in the form of CMIM (FE grid 4×4) without reduction	-	0.03046	-	0.04022	-	0.03626	-	0.04922		
Percent difference from AS	-	-4.79%	-	-3.03%	-	-0.72%	-	-2.48%		
FEM in the form of CMIM (FE grid 8×8) without reduction	0.01735	0.02966	0.03686	0.03922	0.02058	0.03578	0.04507	0.04819		
Percent difference from AS	-2.02%	-2.23%	0.38%	-0.56%	2.04%	0.61%	-0.16%	-0.39%		

Also, the application of the proposed algorithm can also be extended to the field of structural dynamics, where frequency equations need to be solved to find the natural frequencies and mode shapes of a structure. By reducing the size of the system of equations, the proposed algorithm can enable more efficient and accurate simulations in structural dynamics problems.

In conclusion, the proposed algorithm for reducing finite element systems of equations based on linear interpolation has significant practical implications for the field of structural mechanics, including the analysis of complex structures, solving frequency equations, and optimization. Its potential to reduce computational resources and enable more efficient simulations can have immense benefits for various engineering applications and is an urgent need in modern engineering practice.

References

1. Muller B, Starke G (2016) Stress-Based Finite Element Methods in Linear and Nonlinear Solid Mechanics. *Advanced Finite Element Technologies*, p 69–104
2. Auricchio F, Beirão da Veiga L, Lovadina C, Reali A, Taylor R, Wriggers P (2013) Approximation of incompressible large deformation elastic problems: some unresolved issues. *Comput. Mech.* 52:1153–1167
3. Boffi D, Brezzi F, Fortin M (2013) *Mixed finite element methods and applications*. Springer, Heidelberg
4. Storn J (2019) Topics in least-squares and discontinuous petrov-galerkin finite element analysis. <https://doi.org/10.18452/20141>
5. Schneider P, Kienzler R, Boehm M (2014) Modeling of consistent second-order plate theories for anisotropic materials. *ZAMM J Appl Math Mech: Zeitschrift für angewandte Mathematik und Mechanik* 94(1–2)
6. Meyer-Coors M, Kienzler R, Schneider P (2021) Modularity of the displacement coefficients and complete plate theories in the framework of the consistent-approximation approach. *Continuum Mech Thermodyn* 33:1805–1827
7. Ignatyev VA, Ignatyev AV (2022) Finite element method in the form of a classical mixed method of structural mechanics (theory, mathematical models and algorithms). ASV, Moscow
8. Ignatyev V, Ignatyev A, Zavyalov I (2023) The efficiency of application of triangular bending finite elements for plate calculation using the classical mixed-type approach to the finite-element method. In: Guda A (eds) *Networked control systems for connected and automated vehicles*. NN 2022. Lecture notes in networks and systems, vol 509. Springer, Cham. https://doi.org/10.1007/978-3-031-11058-0_98
9. Benzi M, Tũma M (2003) A robust incomplete factorization preconditioner for positive definite matrices. *Numer Linear Algebra with Appl* 10:385–400. <https://doi.org/10.1002/nla.320>
10. Scott J, Tũma M (2023) Algorithms for sparse linear systems. Birkhäuser, pp 89–111. <https://doi.org/10.1007/978-3-031-25820-6>
11. Scott J, Tũma M (2023) Sparse LU factorizations. https://doi.org/10.1007/978-3-031-25820-6_6
12. Chen Q, Jiao X (2021) HIFIR: hybrid in-complete factorization with iterative refinement for preconditioning ill-conditioned and singular systems. <https://doi.org/10.48550/arXiv.2106.09877>
13. Marín J, Mas J (2023) Balanced incomplete factorization preconditioner with pivoting. *Rev Real Acad Cienc Exactas Fis Nat Ser A-Mat* 117(5). <https://doi.org/10.1007/s13398-022-01334-1>

14. John P, Jennifer P (2020) Preconditioners for Krylov subspace methods: an overview. *GAMM-Mitteilungen*. <https://doi.org/10.1002/gamm.202000015>
15. Tsybenko A, Konyukhov A, Tsybenko H (2015) Numerical method for determining stiffness characteristics of an arbitrary form superelement. *Appl Comput Syst* 18(1). <https://doi.org/10.1515/acss-2015-0019>
16. Papadrakakis M, Bitoulas N, Hatjikonstantinou K (1991) An efficient superelement-by-superelement method for large finite element computations. *Comput Syst Eng* 2:535–540. [https://doi.org/10.1016/0956-0521\(91\)90055-A](https://doi.org/10.1016/0956-0521(91)90055-A)
17. Galanin MP, Savenkov E (2003) Substantiation of the finite superelement method. *Comput Math Math Phys* 43:680–695
18. Mokryakov V (2018) Numerical simulation of functionally graded plane elastic medium by finite superelement method. *AIP Conf Proc*. <https://doi.org/10.1063/1.5019038>
19. Wang H, Wang F (2023) A sparse reconstruction algorithm based on constrained inhomogeneous grid optimization. *Circuits Syst Signal Process*. <https://doi.org/10.1007/s00034-023-02333-2>
20. Kumari R (2017) Topical advancements in various spline techniques for boundary value problems. *Int J Res Appl Sci Eng Technol* 5:105–125
21. Burova I (2022) Local interpolation splines and solution of integro-differential equations of mechanic's problems. *Wseas Trans Appl Theor Mech* 17:103–112. <https://doi.org/10.37394/232011.2022.17.14>
22. Burova I, Alcybeev G (2022) Solution of integral equations using local splines of the second order. *Wseas Trans Appl Theor Mech* 17:254–258. <https://doi.org/10.37394/232011.2022.17.31>
23. Han J-G, Ren W-X, Huang Y (2006) A spline wavelet finite-element method in structural mechanics. *Int J Numer Meth Eng* 66:166–190. <https://doi.org/10.1002/nme.1551>



Experimental Studies of Reinforced Concrete Beams, Taking into Account the Reaction of Thrust on Compliant Supports Under Short-Term Dynamic Loading

O. Kumpyak, Z. Galyautdinov, D. Galyautdinov^(✉), and N. Zboykova

Tomsk State University of Architecture and Civil Engineering, 2, Solyanaya Sq, Tomsk 634003, Russia

DaudG@yandex.ru

Abstract. When designing reinforced concrete beam structures with limited horizontal displacement on supports under short-term dynamic loading, it is necessary to take into account the occurrence of a thrust reaction. The presence of a thrust leads to a significant increase in strength and crack resistance of structures, and when yielding supports are used, to the increase in their energy intensity. The purpose of the experimental study is to study the feasibility of using yielding supports in dynamically loaded spacer structures. The paper presents the results of experimental studies of reinforced concrete beam structures with a thrust on yielding supports under short-term dynamic loading. The influence of yielding supports on the strength, deformability and crack resistance of reinforced concrete structures with thrust was considered. The results of experimental studies indicate a positive effect of the use of yielding supports in dynamically loaded structures with a thrust.

Keywords: Reinforced concrete beam · Yielding supports · Thrust · Short-term dynamic load · Support reaction · Displacement

1 Introduction

Because of the continuous development of chemical, oil, gas and other industries, the probability of occurrence and impact on the structures of buildings and constructions of random short-term dynamic loads of high intensity is increased. Structures designed for special dynamic impacts are often built from prefabricated and precast-monolithic reinforced concrete according to the frame and frame-braced design schemes. Due to a number of reasons, the horizontal and vertical yielding of prefabricated element joints takes place. In this case, in bending structures, due to the limitation of the horizontal displacement in the support fastenings, a thrust reaction occurs.

The results of experimental and theoretical studies [1–7] show that the thrust phenomenon leads to increasing the bearing capacity of the bent reinforced concrete structures and is well studied under static loading. With a single short-term dynamic loading,

the effect of thrust on the work of the structure is ambiguous. On the one hand, the action of thrust increases the structure bearing capacity, on the other hand, its deformability decreases. The decrease in deformability negatively affects the plastic properties of the reinforced concrete structure and often leads to the decrease in its dynamic strength.

Experimental and theoretical studies of reinforced concrete structures under intense dynamic impact at their vertical yielding on supports are reflected in the works of domestic [7–16] scientists. It was established that one of the effective ways to increase the resistance of structures to these influences is the use of yielding supports. In this case, the degree of reduction of the dynamic response is determined by the elastic–plastic properties of the yielding support and the ratio of rigidity of the support and the structure.

2 Subject, Tasks and Methods

For the purpose of experimental assessment of the stress–strain state of reinforced concrete beam structures on yielding supports with thrust under short-term dynamic loading a research program has been developed and implemented (Table 1). Fourteen experimental structures were designed and manufactured. The difference between the structures is in the nature of loading (static or short-term dynamic), the presence or absence of thrust and the nature of deformation of yielding supports (elastic–plastic, elastic–plastic with hardening).

In Table 1, the following designations are adopted: “B”—reinforced concrete beam; “S”—static load; “D”—dynamic load; “T”—the presence of thrust; “Y”—the presence of yielding supports deforming in the elastic–plastic stage “e” or elastic–plastic with hardening “h”; “1...14”—the serial number of the construction. For example, the construction “BDTYH-6” stands for beam “B” subjected to dynamic loading “D”, taking into account the limitation of horizontal displacement “T” on yielding supports “Y” deformed in the stage of hardening “h” at number 6.

Samples were of rectangular section, 150×220 mm in size and 1900 mm long. Concrete was heavy of class B35. Reinforcement of experimental structures was carried out with a spatial frame. The reinforcement of the lower zone of beams was carried out from the hot-rolled bar reinforcement of class A500s $2\text{Ø}10$, the upper zone from reinforcement of class A240 $2\text{Ø}6$. The transverse reinforcement was made of bound clamps of cold-formed reinforced steel $\text{Ø}5$ Vr500 installed with a step of 50 mm in the support zone and 130 mm in the middle of the span. To reinforce the end sections of the beams the meshes with a cell of 50×50 mm were used from the cold-formed reinforcement $\text{Ø}5$ mm class Vr500, 7 meshes on each side, and the corners 100×10 mm were installed (see Fig. 1).

A set of measuring instruments was placed on the samples (see Fig. 2): to determine the displacement of the beam and the collapse of pliable supports, Waycon inductive position sensors of the RL150 and RL50 series, respectively. To measure accelerations—accelerometers (DHE 100,023). To determine the reaction of the system—a force-measuring tensoresistor sensor DST 4126 and to determine the magnitude of the support reactions—dynamometric supports (RF Patent for utility model No. 161908). The instruments were connected to Mic-036R and Mic-400D computers. To determine the thrust value, strain gauges with a base of 50 mm were glued onto the strands. Visualization of the pattern of crack development in the process of short-term dynamic loading

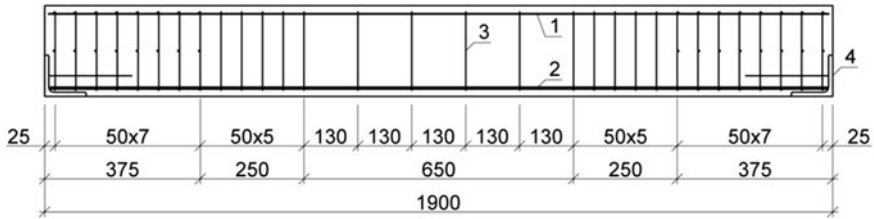


Fig. 1 Scheme of reinforcement of reinforced concrete structures: reinforcement $\text{\O}6$ mm class A240 (1); reinforcement $\text{\O}10$ mm class A500s (2); reinforcement $\text{\O}5$ mm class Vr500 (3); equal-shelf corner 100×10 mm (4)

was performed using a high-speed camera with a shooting frequency of 2500 frames per second.

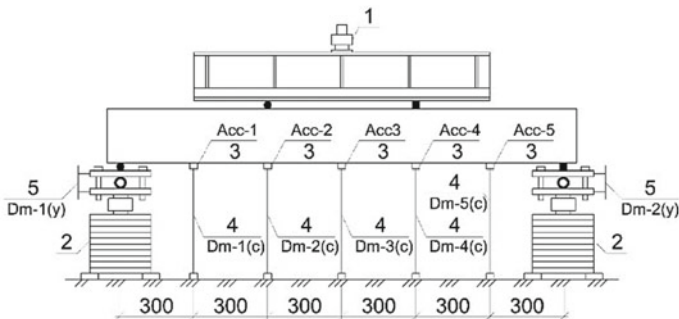


Fig. 2 Measuring instruments layout: force-measuring unit DST-4126 (1); dynamometric support (RF patent No. 176603) (2); accelerometer (DHE 100,023) (3); Waycon displacement sensors RL150 series (4); Waycon displacement sensors RL50 series (5)

Studies of experimental structures for static load were carried out on a test bench (see Fig. 3). The structures were considered as beams freely lying on supports. The thrust was created using a restrictive contour consisting of end traverses connected to each other by two strands with a diameter of 60 mm. The traverses rested against the ends of the beams with the possibility of rotation through two plates and a solid section pipe between them. Milled grooves were provided in the plates. Before testing, an initial compression was created at the level of the location of the tensioned reinforcement using a jack installed at the end of the traverse. Then the restrictive contour was fixed using nuts screwed on

the strands. The precompression value was taken according to the results of static tests and amounted to 5 . . . 10% of H_{\max} . Under static loading, the concentrated load on the experimental structures was applied in stages through the distribution traverse with a load value of 4 kN at each stage. The load was set using a hydraulic jack DG-25.

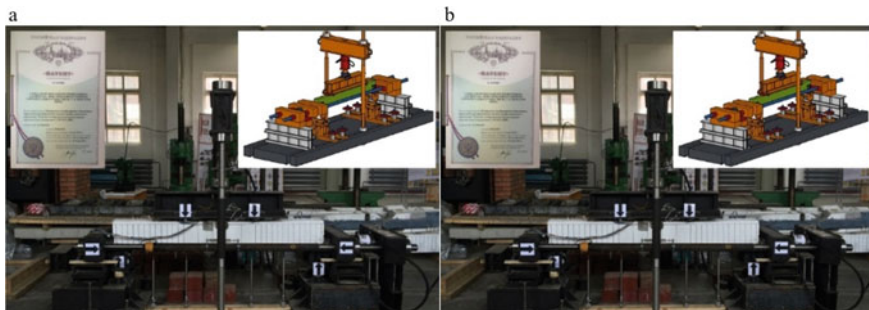


Fig. 3 Stands for testing beams with spacers on rigid supports under static loading (a) and under short-term dynamic loading on yielding supports (b). Utility model patents of the Russian Federation No. 148401 and No. 147262

A short-term dynamic load on the structure was applied through the distribution beam (see Fig. 3). A load weighing 450 kg was dropped along the fixed guides from a height determined by calculation equal to 750 mm and 1150 mm. Height 750 was assigned for the BD-3 hinged structure without thrust and yielding supports brought to complete destruction. In order to assess the effect of thrust on strength and deformability at a load drop height of 750 mm the BDT-4 design was also tested. For the operation of the structure in the elastic–plastic stage subjected to the limitation of its horizontal displacement on the supports, the height of the fall of the load was 1150 mm (BDT-5). Further tests were carried out by varying the stiffness of the yielding supports in order to compare the results with the experimental data obtained for the BD-3 and BDT-5 specimens at a fall height of 750 mm and 1150 mm respectively.

3 Research Results and Discussion

Statics. According to the program of experimental studies, (see Table 1) two samples were tested under static load: without thrust (BS-1) and with thrust (BSR-2). Diagrams of deformations of reinforcement, concrete and strands as well as the displacement of the structure depending on the load were obtained (see Figs. 4 and 5). As a result of static tests for a hinged beam BS-1 without thrust the destructive load was $F_u = 60$ kN and for the beam BST-2 with thrust $F_u = 176$ kN the increase in bearing capacity was 2,93 times, while the maximum deflections decreased by 235% (see Fig. 5). From the development of deflections, one can see that the limitation of horizontal displacement affects the deflection of the structure from the initial stages of loading. Appearance of the first cracks in the beam without thrust was noted under the load $F_{crc} = 24$ kN, but with thrust $F_{crc} = 36$ kN (see Fig. 5). It indicates the deformation reduction of the

structures with thrust. Considering the deformation of strands, one can see that the thrust in the structure occurs from the first stages of loading. A significant increase in thrust is observed after opening the first cracks. In this case, the growth of expansion forces during loading is non-linear. According to the patterns of sample destruction and crack development, it can be seen that the presence of thrust leads to the increase in crack resistance in the beams while destruction occurs along the concrete of the compressed zone, and the stresses in the tensile reinforcement reached the physical yield strength (see Figs. 4 and 5).

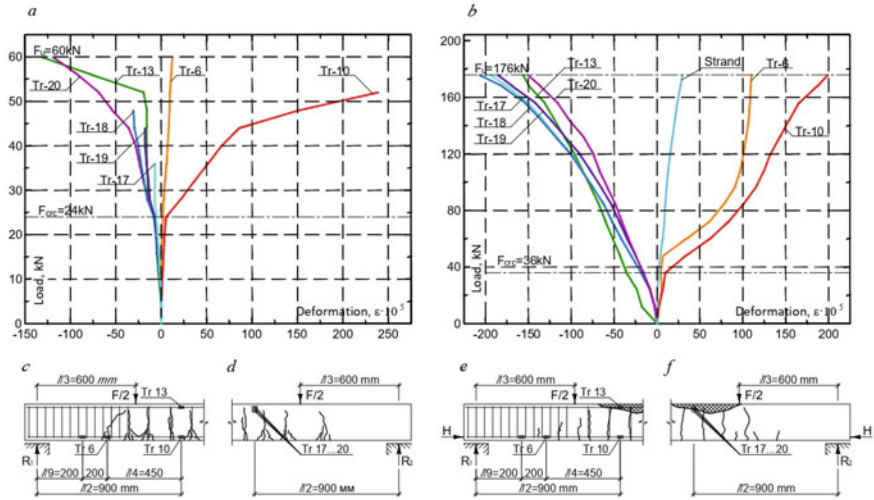


Fig. 4 Diagrams of the development of deformations of reinforcement and concrete: **a** BS-1 beams under static loading, arrangement of tensoristors on reinforcement and concrete, **c, d** pattern of cracking; **b** beams BST-2 with thrust under static loading, **e, f** arrangement of tensoristors on reinforcement and concrete, pattern of cracking

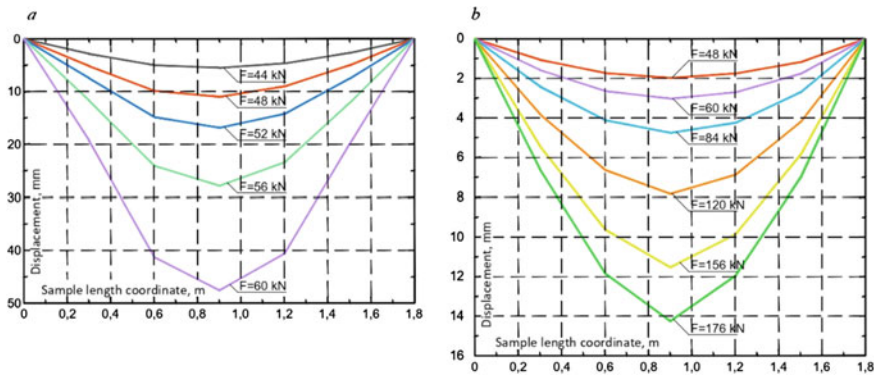


Fig. 5 Displacements of beam BS-1 (a) and BSR-2 (b) under static loading

There is a delay in time of support reactions and the inclusion of reinforcement and concrete in the work by a value of 0.003 s. Structures BD-3 and BDT-5 were brought to the plastic stage. The forces of inertia begin to develop at the initial stage of the system reaction increase. At the maximum value of the system reaction, the greatest value of the inertia force is observed. There is a decrease in deflections, the number and width of crack opening in the BDT-4 beam in relation to the BD-3 sample due to the presence of thrust at the same level of loading. For the sample BDT-5 with the height of the load drop equal to 1150 mm, the dynamic reaction increased by 2 times in relation to the sample BD-3 with equal displacements. The presence of thrust leads to earlier peak values of the measured parameters.

According to the test results of the sample BDT-5 in the limit state, a brittle fracture of concrete of the compressed zone was established simultaneously with the achievement of the physical yield strength in the tensile reinforcement. The response of the structure to dynamic impact is stronger. The reaction of the beam to the external impact BDT-5 is two times greater than that of the BDT-4 beams. For the BDT-4 structure at the horizontal displacement limit, a significant decrease in cracking is observed (see Fig. 7).

Dynamics. Yielding supports. Load drop height 750 mm. Two beams with a thrust BDTYH-6, BDTYH-7 on elastic–plastic yielding supports with hardening were tested (see Figs. 8 and 9). According to the tests of the construction BDTYH-6, one can see the decrease in the support reaction relative to BDT4 by 40% and the increase in the moment of reaching its maximum value from to $t = 0, 0175s$. According to the movements of the yielding supports (see Fig. 8d) the time for the transition of the support to the plastic stage $t_{SY_el} = 0, 005s$ and to the hardening stage $t_{SY_pl} = 0, 016s$ was established. In addition, when the support passes into the hardening stage a sharp increase in the support reaction arises due to the decrease in the deformability of the crushed inserts and the increase in inertial forces. There is a decrease in the maximum movement of the structure (see Fig. 6b). For the BDTYH-7 sample, a decrease in the support reaction relative to BDR-4 by 50% and an increase in the time point for reaching its maximum value from $t = 0, 009s$ to $t = 0, 021s$. That is, the construction works more plastically, and the yielding supports increase the system power consumption. According to the movements of the yielding supports, the time for the transition of a support to the plastic stage $t_{SY_el} = 0, 005s$ as well as hardening was determined. At the time, $t = 0, 02s$ one sees a sharp increase in the support reaction due to the decrease in deformability of the crushed inserts and the increase in inertial forces, when the structure stops due to the complete collapse of the yielding supports. There is a decrease in the maximum displacement of the structure (see Fig. 6b) by 68% relative to the BDT-4 sample and by 81% relative to the BD-3 sample. Thus, comparing the process of dynamic deformation of specimens BDTYH-6 and BDTYH-7 with BDT-4, one observes the effect in terms of the parameters of dynamic deformation of the structures: the decrease in support reaction, the time of reaching the maximum values of the support reactions increases by 2 times. The zone of crack formation is limited, and the width of crack opening is insignificant.

On elastoplastic yielding supports, three beams with a thrust were tested—BDTYe-8, BDTYe-9, BDRTYe10 (see Figs. 8 and 9). The decrease in the support reaction for the BDTYe-8 sample relative to BDT-4 by 40% and the increase in time of reaching the

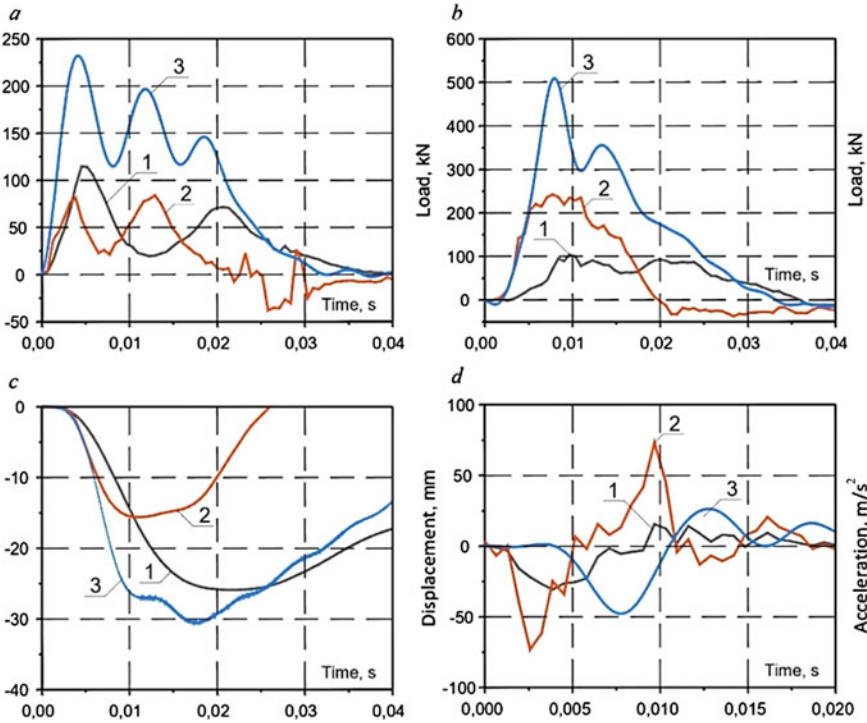


Fig. 6 Diagrams of changes in time of system reactions (a), support reactions (b), displacements (c) and accelerations (d) according to the results of tests of reinforced concrete beams BD-3(1), BDT-4(2), BDT-5(3) on rigid supports under dynamic loading



Fig. 7 Pattern of crack development at the moment of reaching maximum displacements of reinforced concrete beams BD-3 (a), BDT-4 (b), BDT-5 (c) on rigid supports under short-term dynamic loading

maximum value from $t = 0,009s$ to $t = 0,017s$ was established. The transition time of the support to the plastic stage was $t_{SY_el} = 0,007s$. There is a decrease in the maximum displacement of the structure by 38% relative to the BD-3 sample. Concerning the BDR-4 sample, the displacements of the structure did not change, but the time to reach the maximum value was reduced. At the same time, the supports stopped at the border of the transition to the hardening stage. The BDTYe-9 construction has the decrease in the support reaction relative to BDT-4 by 54% and the increase in time of reaching its maximum value from $t = 0,009s$ to $t = 0,015s$. According to the movements of the yielding supports, the time for transition of the support to the plastic stage was equal to $t_{SY_el} = 0,006s$. There is a decrease in the maximum displacement of the structure

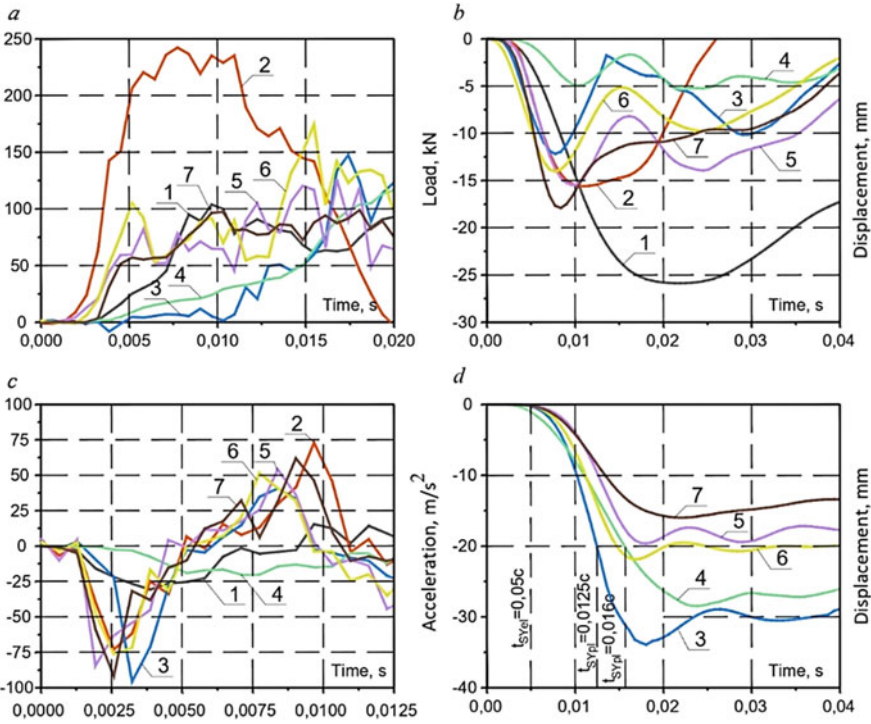


Fig. 8 Diagrams of changes in time of support reactions (a), displacements of samples (b), accelerations (c) and deformation of yielding supports (d) according to test results of reinforced concrete beams BD-3 (1), BDT-4 (2), BDTY-6 (3), BDTYH-7(4), BDTYe-8(5), BDTe-9(6), BDTYe-10(7) under dynamic

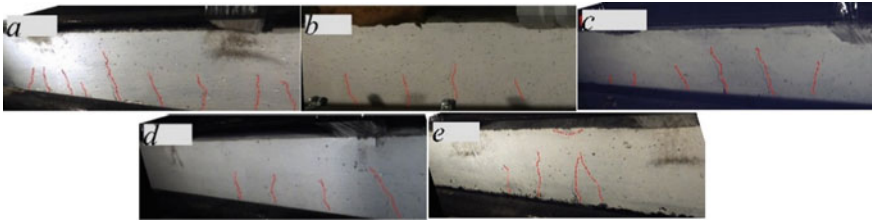


Fig. 9 The pattern of crack development at the moment of reaching maximum displacements of reinforced concrete beams BDTY-6 (a), BDTY-7 (b), BDTYe-8 (c), BDTYe-9 (g), BDTYe-10 (d) under short-term dynamic loading

by 40% relative to the BD-3 sample. As for the sample BDT-4, the displacements of the structure did not change, but the time to reach the maximum value was reduced. Based on the results of testing the BDRPu-10 construction, the decrease in the support reaction relative to the BDR-4 by 60% and the increase in the moment of reaching the maximum value from $c t = 0, 009s$ to $t = 0, 018s$ were recorded. The transition time

of the support to the plastic stage was $t_{SY_el} = 0,0065s$. There is a decrease in the maximum movement of the structure (see Fig. 8b) by 30% relative to the sample BD-3 and relative to the sample BDT-4 it was increased by 13%.

Dynamics. Yielding supports. Load drop height 1150 mm. Below are the data on testing the structures with a thrust on yielding supports at a load drop height of 1150 mm. Based on the test results of the BDTYH-11 construction (see Figs. 10 and 11), the decrease in the support reaction relative to BDT-5 by 2, 5 times and the increase in time of reaching the maximum value from $t = 0,008s$ to $t = 0,0175s$. The transition time of the support to the plastic stage $t_{SY_el} = 0,007s$, and hardening $t_{SY_pl} = 0,0135s$ (see Fig. 10d). When the support enters the hardening stage, a sharp increase in the support reaction is observed (see Fig. 10a), due to the decrease in deformability of the crushed inserts and the increase in inertial forces, when the structure stops due to the complete collapse of the yielding supports. There is a decrease in the maximum.

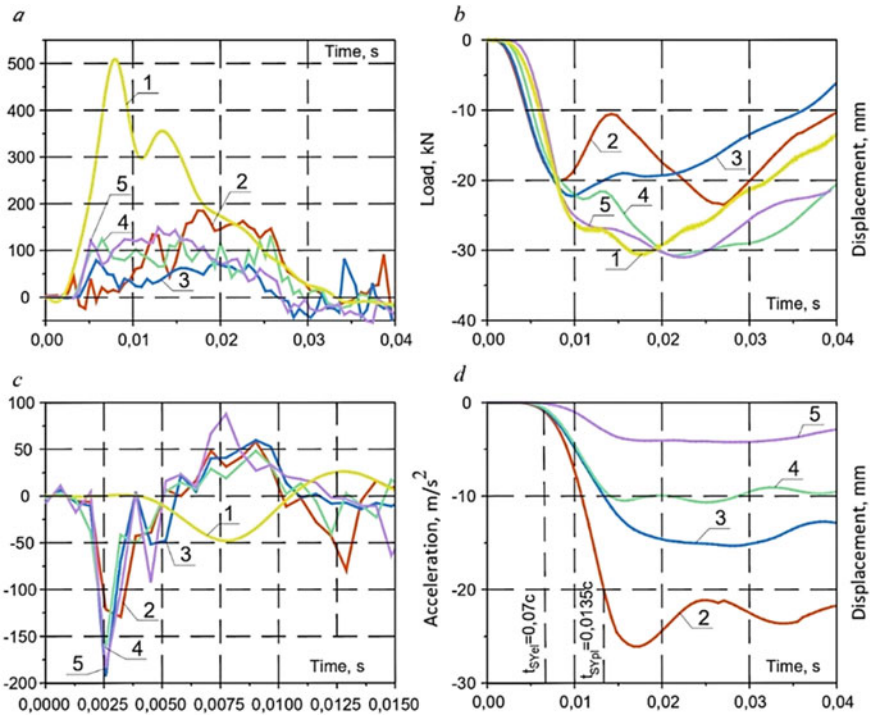


Fig. 10 Diagrams of changes in time of support reactions (a), displacements (b), accelerations (c), samples and deformation of yielding supports (d) according to the results of tests of reinforced concrete beams BDT-5 (1), BDTY-11 (2), BDTYe- 12(3), BDTYe-13(4), BDTYe-14(5) under short-term dynamic loading

Tests of the BDTYe-12 construction showed the decrease in the support reaction relative to the BDT-5 by 80% and the decrease in the moment of reaching the maximum value from $t = 0,004s$ to $t = 0,023s$. The transition time of the support to the plastic



Fig. 11 The pattern of crack development at the moment of reaching the maximum displacements of reinforced concrete beams BDTY-11 (a), BDTYe-12 (b), BDTYe-13 (c), BDTYe-14 (g) under short-term dynamic loading

stage was $t_{SY_el} = 0,007$. There is a decrease in the maximum displacement of the structure by 27% relative to the BDRTY sample. Flexible supports are actively involved in the deformation process, deformations decrease, and the thrust increases, that is, the limitation of the horizontal displacement of the support sections prevents the growth of deflections, the resistance time and the plastic stage of the structure deformation increase. The sample BDTYe-13 made it possible to establish the decrease in the support reaction of the beam relative to BDT-5 by 75% and the increase in the moment of reaching the maximum value from $t = 0,008s$ to $t = 0,020s$. Support transition time to the plastic stage $t_{SY_el} = 0,0087s$.

The displacements of the structure correspond to the displacements of the sample BDT-5. For the BDTYe-14 construction, the decrease in the support reaction relative to the BDT-5 by 72% and the increase in time of reaching the maximum value from $t = 0,008s$ to $t = 0,013s$. Support transition time to the plastic stage was $t_{SY_el} = 0,0097s$. The displacements of the structure correspond to the displacements of the sample BDT-5.

From the video footage of structures BDTYe-12, BDTYe-13, BDTYe-14 (see Fig. 11) during operation of yielding supports in the elastic–plastic stage, one sees that with the increase in rigidity of the supports, more severe destruction occurs. During the operation of yielding supports at the stage of hardening for the sample BDRP-11, one sees that with a decrease in the rigidity of the supports, there is less formation and development of cracks relative to the structures BDTYe-12, BDTYe-13, BDTYe-14.

4 Conclusions

Thus, as a result of static tests, it was found that the presence of thrust in the reinforced concrete beams leads to the increase in their bearing capacity by 2.93 times and the decrease in deflections by 235%.

Under short-term dynamic loading, the presence of thrust leads to a sharp increase in support reactions (see Fig. 6a and 8a) by a factor of 2, 4 and to an earlier achievement of their maximum value. With the use of yielding supports deforming in the elastic–plastic region, the support reactions decrease by up to 5 times, while the higher the rigidity of the supports, the greater the support reaction. The maximum decrease in support reactions is observed during operation of yielding supports in the hardening stage, and the development of support reactions is smoothed out and the peak value is observed much later at $t = 0,02s$. The time of reaching the maximum values of reactions of the structure on yielding supports, in comparison with the structure on rigid supports, increases three times. The maximum decrease in the structure displacements up to 5 times is observed during the operation of yielding supports in the initial stage of hardening,

in the case of further deformation, a sharp increase in accelerations occurs (see Fig. 8c and 10c) and the inertia forces significantly increase.

Acknowledgements. This work was carried out within the government contract FEMN-2022-0004 of the Ministry of Science and Higher Education of the Russian Federation.

References

1. Abdul'-Rakhman AS (1995) Increasing the bearing capacity of reinforced concrete structures under explosive effects. Dissertation. State Construction University
2. Vinogradova TN (1977) Influence of thrust on the operation of reinforced concrete beam structures under short-term dynamic impacts. Dissertation. Moscow Engineering and Construction University
3. Gvozdev AA (1976) New about the strength of reinforced concrete. Moscow
4. Kumpyak OG, Galyautdinov ZR (2015) Experimental research of reinforced concrete edge supported slabs with spacers. *Vestnik Tomsk State Univ Architect Build* 3:113–120
5. Popov NN, Rastorguyev BS (1964) Calculation of reinforced concrete structures for the action of short-term dynamic loads. Moscow
6. Tikhonov IN (2013) Principles of strength calculation and design of reinforcement for floor beams of buildings made of monolithic reinforced concrete to prevent progressive destruction. *Housing Construct* 40–45
7. Kumpyak OG, Galyautdinov ZR, Kokorin DN (2016) Strength and deformability of reinforced concrete structures on yielding supports under short-term dynamic load. Tomsk
8. Kumpyak OG, Meshcheulov NV, Lyulevich YS (2016) Dynamic strength and deformability of oblique planes in compressed and bended yielding supports. *Vestnik Tomsk State Univ Architect Build* 6:150–159
9. Kumpyak OG, Meshcheulov NV (2017) Numerical simulation of yielding supports in the form of annular tubes under static and dynamic loads. *Vestnik Tomsk State Univ Architect Build* 5:121–134
10. Kumpyak OG, Galyautdinov ZR, Galyautdinov DR (2018) Experimental study of beams on yielding supports with thrust. *MATEC Web Conf* 143. <https://doi.org/10.1051/1.4973016>
11. Chiaia B, Kumpyak O, Placidi L, Maksimov V (2015) Experimental analysis and modeling of two-way reinforced concrete slabs over different kinds of yielding supports under short-term dynamic loading. *Eng Struct* 96:88–99
12. Kumpyak OG, Meshcheulov NV (2017) Numerical simulation of yielding supports the shape of annular tubes under static and short-term dynamic loadings. *Int J Comput Civ Struct Eng* 13(4):103–113
13. Elfetori FA (2013) Experimental testing of composite tubes with different corrugation profile subjected to lateral compression load. *World Acad Sci Eng Technol Int J Mech Indus Sci Eng* 7(2):183–186
14. Fan Z, Shen J, Lu G (2011) Investigation of lateral crushing of sandwich tubes. *Twelfth East Asia-Pacific Conf Struct Eng Construct Proc Eng* 14:442–449
15. Lion KH, Amir RAG, Prasetyo E, Khairi Y (2009) Impact energy absorption of concentric circular tubes. *Wseas Trans Appl Theor Mech* 4(3):95–104
16. Lipa S, Kotelko M (2013). Lateral impact of tubular structure—theoretical and experimental analysis. Part 1—Investigation of single tube. *J Theor Appl Mach* 51(4):873–882



Freeform Surfaces in Architectural and Structural Design

V. A. Korotkiy^(✉), E. A. Usmanova, and L. I. Khmarova

South Ural State University, 76, Lenin Avenue, Chelyabinsk 454080, Russia
Korotkiiva@susu.ru

Abstract. Freeform surfaces, unlike traditional linear surfaces and surfaces of revolution, are used in modern architecture in the design of structures of various shaping. If the surface to be designed does not have large gradients relative to some base plane xy , both bicubic polynomials from scalar quantities x , y and surface patches in Bezier form can be used for its modeling. The most natural shape of the surface comes about when the skeleton of the constructed surface is formed by physical splines (elastic elements passing through the given points). The paper deals with experimental evaluation of deflection effect on the accuracy of approximation of physical splines by composite cubic curves. An algorithm for the bicubic surface formation on a fixed skeleton has been developed to reduce the size of the characteristic matrix of the constructed surface by almost two times. A comparative analysis of advantages and disadvantages of mathematical models of surfaces formed by bicubic and Bezier patches is performed. The authors provide examples of composite surfaces modeling on a fixed skeleton. The relevance of the work is due to the widespread use of curvilinear shapes in architectural design, the emergence of new building materials and the introduction of digital technology in design.

Keywords: Nature-like curve · Physical spline · Fixed skeleton · Bicubic surface · Bezier curve

1 Introduction

Freeform surfaces, different from traditional linear and surface of revolution, are used in modern architecture in the design of structures with great spatial freedom of shaping. In particular, the search for new non-linear forms gave rise to the *tent architecture* [1] and *fold architecture*. [2], using slabs with complex non-rectilinear outlines. If the surface to be constructed does not involve large gradients with respect to some base xy plane, both bicubic polynomials from scalar x , y values and surface Bezier segments can be used for its modeling. [3–5].

Scientific novelty. The authors provide experimental estimation of the deflection effect on the accuracy of approximation of real physical splines by composite cubic curves (mathematical splines). An algorithm for the formation of a bicubic surface on a fixed

framework has been developed to reduce the size of the characteristic matrix of the constructed surface by almost two times. The comparative analysis of advantages and disadvantages of mathematical models of surfaces formed by bicubic and Bezier patches has been performed.

The relevance of the work arises from the widespread use of non-rectilinear shapes in architecture, the emergence of new building materials and the introduction of digital technology in design.

2 Problem Statement

Problem 1

The most natural shape of the surface results from the case when the framework of the constructed surface is formed by physical splines (curves passing through the given points with minimal curvature). A physical spline is a “nature-like” curve [6–9]. The scientific sources [10, 11] indicate that for the case of weak deflections, the physical spline is adequately approximated by a compound piecewise cubic function with a steady change in curvature (the so-called “mathematical spline”). We should evaluate experimentally the deflection effect on the adequate accuracy.

Problem 2

The bicubic surface is formed by bicubic patches of bounded by cells of a rectangular grid on the xy plane of the cartesian reference system [12, 13]. The surface on the grid consists of mn patches of (1), each of them is defined by its own set of 16 a_{ij} coefficients.

$$\Phi(x, y) = \sum_{i=0}^3 \sum_{j=0}^3 a_{ij} x^3 y^3 \quad (1)$$

Calculation of the coefficients is limited to the solution of the system of 16 mn linear algebraic equations. We should develop an algorithm to form a bicubic surface to reduce the number of equations.

Problem 3

A cubic Bezier surface [14, 15] is formed by segments of

$$r(u, v) = \sum_{i=0}^3 \left[\sum_{j=0}^3 r_{ij} g_j(v) \right] g_i(u);$$

$$g_k(t) = \frac{3!}{k!(3-k)!} t^k (1-t)^{3-k}, \quad t \in [0, 1], \quad k = 0, 1, 2, 3. \quad (2)$$

We should compare the advantages and disadvantages of surfaces designed by bicubic patches (1) and by Bézier surface segments (2). We propose to solve this problem by mathematical manipulations to shape free-form surfaces by means of three-dimensional computer graphics. doc.

3 Physical Spline Simulation

A physical spline is a curve with minimum internal strain energy and minimum average curvature (an example of a physical spline: a thin metal ruler running through the given points). A mathematical spline is a composite piecewise cubic curve running through the same points and continuous up to the second derivatives [16–18].

3.1 A Cantilever Beam

The photograph (Fig. 1a) shows a cantilever beam with a strong deflection running through the point (30, −10). There are also traces of the cantilever beams with weak and average deflection.

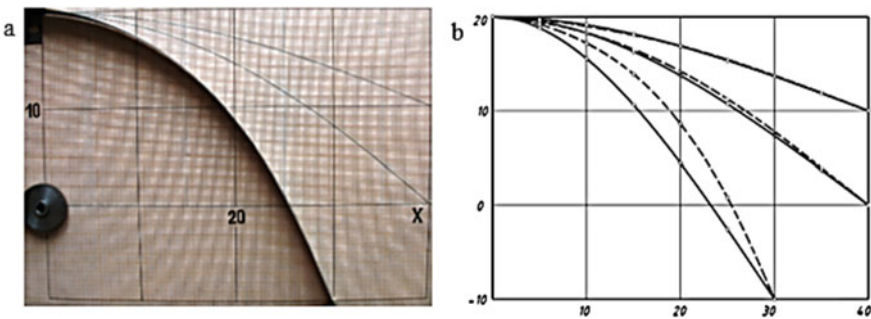


Fig. 1 Cantilever beams: **a** is a photo; **b** is calculation (continuous lines) and the experiment (dashed lines)

We propose to evaluate the deflection of the beam by the value of the maximum relative deflection $\delta y/l$, where l is the length of the beam, δy is the greatest value of the deflection along the length of the beam. For example, for a beam with an average deflection, we obtain $\delta y/l \sim 0.5 = 50\%$. For a beam with a weak deflection, we obtain.

Figure 1b compares physical splines (dashed lines) and mathematical splines (continuous lines) $y = b_0 + b_1x + b_2x^2 + b_3x^3$. A larger approximation error (more than 15%) is obtained for the beam with a strong deflection. An error of 1% ... 2% was obtained for cantilever beams with a weak and average deflections. Thus, the approximation error does not exceed 2% for relative deflections up to 50%.

3.2 An Elastic Segment Passing Through Three Points

We consider a physical spline, a thin metal ruler passing through points P_0, P_1, P_2 (Fig. 2a). Figure 2b compares a mathematical spline (a continuous line) and a physical spline (a dashed line). The maximum relative deflection is equal to $\delta y/l \approx 0.3 = 30\%$. The maximum approximation error does not exceed 4%.

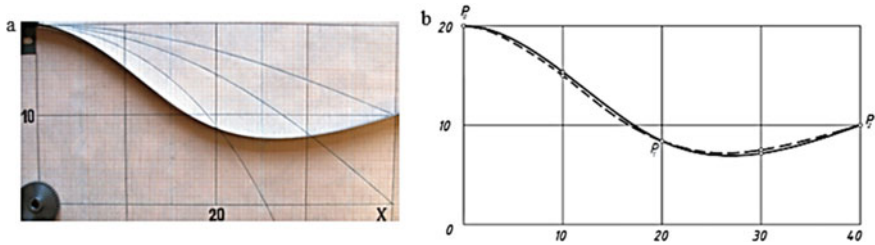


Fig. 2 Two-segment cantilever beam: **a** is a photo; **b** is calculation (continuous lines) and the experiment (dashed lines)

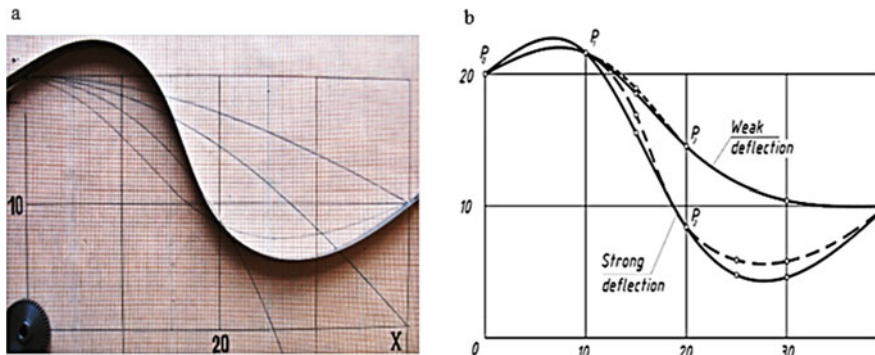


Fig. 3 Three-segment cantilever beam: **a**—photo; **b**—calculation (continuous lines) and an experiment (dashed lines)

3.3 An Elastic Segment Passing Through Four Points Three Points

Figure 3a is a picture of an elastic segment with strong deflections. Figure 3b shows the axial lines of the elastic segment with strong and weak deflections (dashed lines).

Mathematical splines (continuous lines) are formed by a set of cubic parabolas connected to each other with C2 smoothness (continuous curvature change). For example, a mathematical spline approximating the elastic segment of P0-P1-P2-P3 with small deflections is the following:

$$\begin{aligned}
 y_{P_0-P_1}(x) &= 20 + 0,408043x - 0,00248043x^3, \quad x \in [0, 10], \\
 y_{P_1-P_2}(x) &= 21,6 - 0,336087(x - 10) - 0,074413(x - 10)^2 \\
 &\quad + 0,00370217(x - 10)^3, \quad x \in [10, 20], \\
 y_{P_2-P_3} &= 14,5 - 0,713695(x - 20) + 0,0366522(x - 20)^2 \\
 &\quad - 0,000610869(x - 20)^3, \quad x \in [20, 40].
 \end{aligned} \tag{3}$$

The relative deflections of the elastic segments are equal to $\delta y/l \approx 0.4 = 40\%$ and $\delta y/l \approx 0.25 = 25\%$. For an elastic segment with a strong deflection, the maximum error of approximation is about 20%. For the segment with a weak deflection, the approximation error does not exceed 2%.

Thus, the analysis of experimental data (see Figs. 1, 2 and 3) shows that with a relative deflection of the elastic segment $\delta y/l = 25\dots30\%$ less the approximation error does not exceed $1\dots4\%$

4 A Composite Bicubic Surface

We should construct a surface “pulled up” on a fixed frame (Fig. 4a). The equations of “left” and “right” $F_{left} = ABCD$ and $F_{right} = BMNC$ patches will be calculated by the formula (1). The equations of ABCD and BMNC bicubic patches contain 32 scalar coefficients to be determined [19–21].

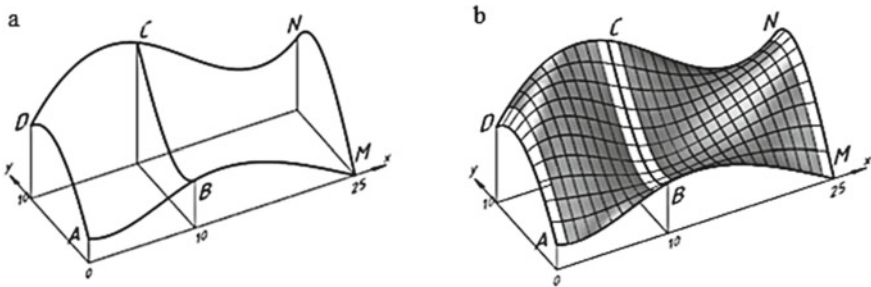


Fig. 4 A bicubic surface on a fixed skeleton

Let us assume that the equations of AD, BC, MN, ABM, DCN frame lines are defined as mathematical splines. For example, the equation of the longitudinal skeleton line ABM is the following:

$$\begin{aligned}
 AB &= z_{AB}(x) = 2,5 - 0,4x + 0,1285x^2 - 0,00635x^3, \quad x \in [0, 10], \\
 BM &= z_{BM}(x) = 5 + 0,265(x - 10) - 0,062(x - 10)^2 \\
 &\quad + 0,001474074(x - 10)^3, \quad x \in [10, 25].
 \end{aligned}
 \tag{4}$$

The frame line equations contain 14 fixed coefficients included in Eqs. (1). The other 18 coefficients are derived from the C2-smooth coupling conditions of the left and right bicubic patches.

Theorem. If the bicubic patches $F_{left}(x, y)$ and $F_{right}(x, y)$ have a common transversal joint BC, and the first and second partial derivatives coincide at the points B, C

$$\frac{\partial F_{left}}{\partial x} \Big|_B = \frac{\partial F_{right}}{\partial x} \Big|_B, \quad \frac{\partial F_{left}}{\partial x} \Big|_C = \frac{\partial F_{right}}{\partial x} \Big|_C,
 \tag{5}$$

$$\frac{\partial^2 F_{left}}{\partial x^2} \Big|_B = \frac{\partial^2 F_{right}}{\partial x^2} \Big|_B, \quad \frac{\partial^2 F_{left}}{\partial x^2} \Big|_C = \frac{\partial^2 F_{right}}{\partial x^2} \Big|_C,
 \tag{6}$$

and also the first and the second mixed derivatives coincide

$$\frac{\partial^2 F_{left}}{\partial x \partial y} \Big|_B = \frac{\partial^2 F_{right}}{\partial x \partial y} \Big|_B, \quad \frac{\partial^2 F_{left}}{\partial x \partial y} \Big|_C = \frac{\partial^2 F_{right}}{\partial x \partial y} \Big|_C,
 \tag{7}$$

$$\left. \frac{\partial^4 F_{left}}{\partial x^2 \partial y^2} \right|_B = \left. \frac{\partial^4 F_{right}}{\partial x^2 \partial y^2} \right|_B, \quad \left. \frac{\partial^4 F_{left}}{\partial x^2 \partial y^2} \right|_C = \left. \frac{\partial^4 F_{right}}{\partial x^2 \partial y^2} \right|_C \quad (8)$$

then the following equations $\frac{\partial F_{left}}{\partial x} = \frac{\partial F_{right}}{\partial x}$, $\frac{\partial^2 F_{left}}{\partial x^2} = \frac{\partial^2 F_{right}}{\partial x^2}$ are fulfilled at any point of the joint.

This means that the curvature of the composite bicubic surface changes continuously (C2 smoothness is ensured).

We supplement smoothness conditions (5...8) with “plane angles” conditions (the first mixed derivatives at angular points A, M, N, D are equal to zero), solve the resulting system of linear algebraic equations, and find coefficients a_{ij} included in (1). Figure 4b shows the longitudinal and transverse formations of the constructed surface.

Thus, the algorithm for forming a bicubic surface on a fixed skeleton is reduced to solving $9n$ linear algebraic equations in relation to $9n$ unknown coefficients, where n is the number of surface patches. Fixing the framework almost halves the size of the characteristic matrix of the simulated surface [22].

Example 1 Figure 5 shows the architectural design of a three-segment ($n = 3$) slab pulled up on a fixed frame. We had to solve a reduced system of $9n = 27$ linear equations (instead of $16n = 48$ equations) to calculate all the coefficients of Eqs. (1).

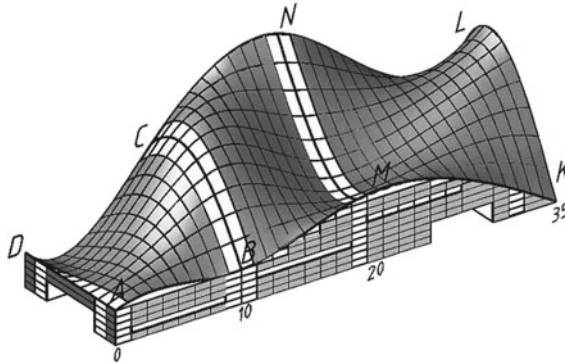


Fig. 5 Architectural design (three-segment free-form slab)

Example 2 Figure 6 shows a C2-smooth surface on a fixed frame formed by four bicubic patches. Instead of a system of $16n = 64$ linear equations, we needed to solve a system of $9n = 36$ linear equations.

A disadvantage of the designs made using the patches of bicubic surfaces is related to the severe restrictions on the shape of the frame load-bearing elements: all frame elements must be flat curves located in the vertical planes oriented along the x and y axes [23, 24]. We can eliminate this disadvantage using Bézier surfaces. We should convert the equations of the skeleton lines into cubic Bézier curves [25].

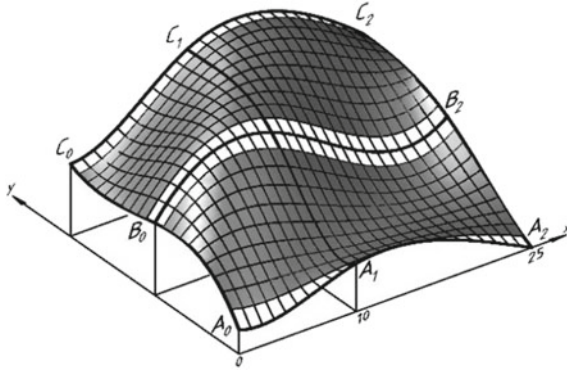


Fig. 6 Four-segment C2-smooth bicubic surface

5 Converting a Cubic Parabola to a Bézier Curve

The equation of a cubic parabola is

$$y = b_0 + b_1(x - x_0) + b_2(x - x_0)^2 + b_3(x - x_0)^3, \quad x \in [x_0, x_1]. \tag{9}$$

We represent (9) in the Ferguson form [10]:

$$r(t) = a_0 + a_1t + a_2t^2 + a_3t^3, \quad t \in [0, 1] \tag{10}$$

Putting $h_x = x_1 - x_0$ in Eq. (9), we replace the variable $x = h_x t + x_0$. If the parameter t changes within the range $[0, 1]$, the value of x changes within the range $[x_0, x_1]$. We obtain Eq. (9) in parametric form:

$$\begin{aligned} x(t) &= x_0 + h_x t, \\ y(t) &= b_0 + b_1 h_x t + b_2 h_x^2 t^2 + b_3 h_x^3 t^3, \quad t \in [0, 1]. \end{aligned} \tag{11}$$

Putting $t = 0$, we obtain the coordinates of vector a_0 :

$$a_{0x} = x_0, \quad a_{0y} = y_0. \tag{12}$$

Putting $t = 1$, we obtain:

$$\begin{aligned} a_{0x} + a_{1x} + a_{2x} + a_{3x} &= x_1, \\ a_{0y} + a_{1y} + a_{2y} + a_{3y} &= y_1. \end{aligned} \tag{13}$$

The system of Eqs. (10, 11) contains 4 equations and eight unknown variables a_{ix} , a_{iy} ($i = 0, \dots, 4$). One must add four more conditions.

Differentiating (11), we obtain:

$$\begin{aligned} \dot{x}|_{t=0} &= h_x, \quad \dot{y}|_{t=0} = b_1 h_x, \\ \dot{x}|_{t=1} &= h_x, \quad \dot{y}|_{t=1} = b_1 h_x + 2b_2 h_x^2 + 3b_3 h_x^3. \end{aligned} \tag{14}$$

Differentiating (10), we obtain:

$$\begin{aligned} \dot{x}|_{t=0} = \dot{x}|_{t=1} = a_{1x}, \quad \dot{y}|_{t=0} = \dot{y}|_{t=1} = a_{1y}, \\ \dot{x}|_{t=1} = \dot{x}|_{t=1} = a_{1x} + 2a_{2x} + 3a_{3x}, \quad \dot{y}|_{t=1} = \dot{y}|_{t=1} = a_{1y} + 2a_{2y} + 3a_{3y}. \end{aligned} \quad (15)$$

Equating (14) and (15), we obtain:

$$\begin{aligned} a_{1x} = h_x, \quad a_{1y} = b_1 h_x, \\ a_{1x} + 2a_{2x} + 3a_{3x} = h_x, \quad a_{1y} + 2a_{2y} + 3a_{3y} = b_1 h_x + 2b_2 h_x^2 + 3b_3 h_x^3. \end{aligned} \quad (16)$$

The system of Eqs. (12), (13), (16) contains 8 equations and 8 unknown coefficients a_{ix} , a_{iy} ($i = 0, \dots, 4$) included in (10). Solving this system of equations, we obtain:

$$\begin{aligned} a_{0x} = x_0, \quad a_{0y} = b_0 = y_0, \quad a_{1x} = h_x, \\ a_{1y} = h_x b_1, \quad a_{2x} = 0, \quad a_{2y} = h_x^2 b_2, \quad a_{3x} = 0, \quad a_{3y} = h_x^3 b_3. \end{aligned} \quad (17)$$

Expressions (17) provide an single-valued conversion of the scalar algebraic Eq. (9) of the cubic parabola to the vector parametric Ferguson Eq. (10).

The Ferguson equation, in its turn, is recorded in the Bezier form [15]:

$$r_i(t) = (1-t)^3 R_0 + 3t(1-t)^2 Q + 3t^2(1-t)P + t^3 R_1, \quad t \in [0, 1], \quad (18)$$

where $R_0(x_0, y_0)$, $R_1(x_1, y_1)$ are end-points, Q and P are control points of the Bezier curve. The coordinates of the control points are defined by the expressions:

$$Q = \frac{1}{3}(a_1 + 3a_0), \quad P = \frac{1}{3}(a_2 + 2a_1 + 3a_0) \quad (19)$$

Decomposing (19) into x , y , and considering (17), we obtain:

$$\begin{aligned} Q_x = \frac{1}{3}(a_{1x} + 3a_{0x}) = \frac{1}{3}(h_x + 3x_0), \quad Q_y = \frac{1}{3}(a_{1y} + 3a_{0y}) = \frac{1}{3}(h_x b_1 + 3y_0), \\ P_x = \frac{1}{3}(a_{2x} + 2a_{1x} + 3a_{0x}) = \frac{1}{3}(2h_x + 3x_0), \quad P_y = \frac{1}{3}(a_{2y} + 2a_{1y} + 3a_{0y}) \\ = \frac{1}{3}(h_x^2 b_2 + 2h_x b_1 + 3y_0). \end{aligned} \quad (20)$$

Converting the algebraic cubic parabola (9) to a Bézier curve (18) is completely solved.

6 Bezier Surface

One must “pull up” the surface on a skeleton formed by cubic curves AB , BC , CD , DA (Fig. 7a). The surface is not rectangular (trapezoidal), so the bicubic surface cannot be used to solve the problem.

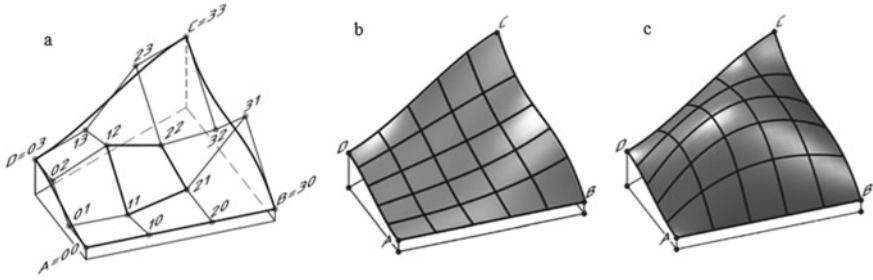


Fig.7 Bézier surface pulled on a quadrangular skeleton: **a** is a characteristic polyhedron; **b** is a concave surface; **c** is a convex surface

Example 3 The Bézier surface patch (2) is formed using a characteristic polyhedron containing 16 vertexes. The skeleton of the surface formed by cubic Bézier curves is fixed, hence, 12 vertexes 00, 10, 20, 30, 31, 32, 33, 23, 13, 03, 02, 01 are fixed. The shape of the surface can be controlled by changing the positions of four “inner” vertexes 11, 21, 22, 12 (see Fig. 7a). For example, when the inner vertexes are lowered, we obtain a “concave” patch of the Bézier surface, and when they are raised, we obtain a “convex” patch (Fig. 7c).

Example 4 In contrast to a bicubic surface, a Bezier surface can be pulled over a triangular skeleton. A quadrangular patch becomes triangular if one of the boundary curves of the quadrangular patch degenerates into a point [10]. For example, Fig. 8a shows a characteristic polyhedron with side CD degenerated to a point $03 = 13 = 23 = 33$. Changing the positions of internal control points 11, 21, 22, 12 we obtain triangular patches of different shapes pulled on the triangular skeleton ABC (Fig. 8b, c).

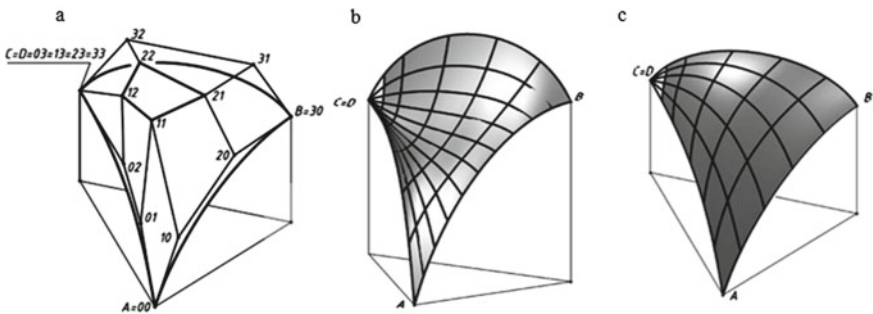


Fig. 8 Bézier surface pulled on a triangle skeleton: **a** is a characteristic polyhedron; **b** is a concave surface; **c** is a convex surface

Example 5 (composite Bézier surface). Let the surface be pulled over the skeleton formed by the composite cubic curves ABE and DCE (Fig. 9a). Curves AB and BE , DC and CE are connected with smoothness G1 (smoothness G1 means that there is a common tangent at the junction point [26, 27]). The surface to be constructed must

pass through the transverse guides AD and BC . One should note that the skeleton of the surface is formed by randomly positioned cubic curves in space.

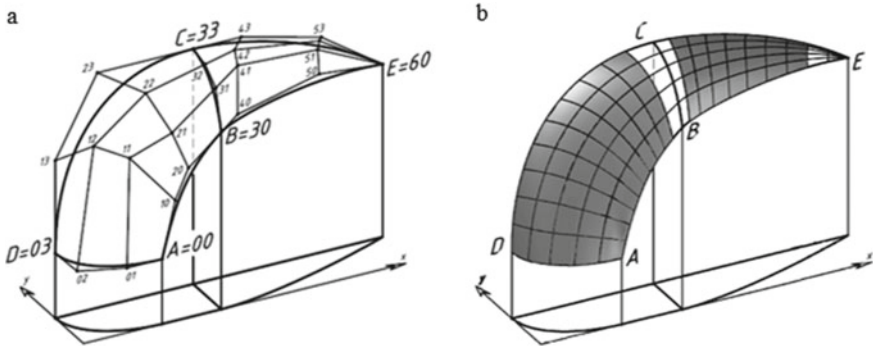


Fig. 9 Composite G1-smooth Bézier surface: **a** is a fixed skeleton; **b** is a grid of generators

We will form the surface from two patches of the Bézier surface (2). The quadrangular patch $ABCD$ and the triangular patch BCE are connected along the joint BC with smoothness G1. The condition of G1-smooth joint of the patches is: $|20-30|=\lambda|30-40|$, $|21-31|=\lambda|31-41|$, $|22-32|=\lambda|32-42|$, $|23-33|=\lambda|33-43|$, where λ is any positive number. In the example λ equals 0.5.

The longitudinal formations of the composite surface begin at the points on the guiding line AD and end at the point E (Fig. 9b). Any longitudinal formative consists of two cubic Bézier curves connected with smoothness G1 at some point on the guiding line BC .

7 Conclusion

The approximation of the physical spline by a mathematical one (a set of C2-smoothly connected cubic parabolas) is possible at relative deflections up to $\delta y/l = 25\% \dots 30\%$. In this case the approximation error does not exceed $1\% \dots 4\%$.

We have proposed an algorithm for the formation of a bicubic surface on a fixed skeleton in order to almost halve the size of the system of linear algebraic equations relative to the equation coefficients (1).

We have considered the advantages and disadvantages of surfaces constructed on the basis of bicubic patches (1) and Bézier surface patches (2). The use of Bézier surface patches allows us to form a G1-smooth surface pulled on an arbitrary spatial skeleton, but not to ensure the smoothness of G2 (continuous change of curvature).

In contrast to the Bézier surface, the composite bicubic surface (1) is characterized by increased smoothness (up to G2 level), but the shape of the skeleton is strictly restricted (the skeleton lines should be placed in mutually perpendicular vertical planes). In the implementation of architectural projects, this restriction is not significant, so the bicubic surfaces can be recommended for use in architectural and structural design.

Acknowledgements. The work was supported by Act 211 Government of the Russian Federation, contract № 02. A03.21.0011.

References

1. Udler E, Tostov E (2001) Awning design. *CADmaster* 1(6):43–47
2. Kirichkov I (2018) Refraction of the Category of Fold through the Prism of Architecture. *Architect Design* 3:1–11
3. Hoschek J, Lasser D (1996) *Fundamentals of computer aided geometric design*; A K Peters, CRC Press, England, pp 213–247
4. Germain-Lacour P, Georges PL, Pistre F et al (1989) *Mathematics and CAD: 2 volumes*, vol 2. Mir, Moscow, p 264
5. Farin G (2002) *Curves and surfaces for computer aided geometric design. A Practical Guide*. Arizona State University, Academic Press, pp 285–308
6. C. de Boor. *A Practical Guide to Splines* (1985) Radio and communication, Moscow
7. Ahlberg J, Nilson E, Walsh J (1972) *Theory of splines and their applications*. Mir, Moscow
8. Korotkiy VA (2020) Cubic curves in engineering geometry. *Geometry Graph* 3(8):3–24
9. Korotkiy VA (2022) Irregular curves in engineering geometry and computer graphics. *J Sci Visualization* 14(1):1–17. <https://doi.org/10.26583/sv.14.1.01>
10. Fox A, Pratt M (1982) *Computational geometry. Application in design and production*. Mir, Moscow, 304 p
11. Bartels RH, Beatty JC, Barsky BA (1987) *An introduction to splines for use in computer graphics and geometric modeling*; Morgan Kaufmann Publishers, Los Altos, Inc., CA, USA, pp 6–12, 149–152
12. Jarke JV (1986) Bicubic patches for approximating non-rectangular control-point meshes. *Comput Aided Geometric Des* 3(1):456–459
13. Levner G, Tassinari P, Marini D (1988) Simple general methods for ray tracing bicubic surfaces. *Theoretical Foundations of Computer Graphics and CAD*. Springer-Verlag, New York, pp 805–820
14. Gallier J (2018) *Curves and surfaces in geometric modeling: theory and algorithms*. University of Pennsylvania, Philadelphia, PA, USA, pp 61–114
15. Bezier P (1989) *Geometric methods*. Mathematics and CAD, vol 2. Mir, Moscow, pp 96–257
16. Panchuk KL, Myasoedova TM, Lyubchinov EV (2021) Spline curves formation given extreme derivatives. *J Math* 9(1):47. <https://doi.org/10.3390/math9010047>
17. Panchuk KL, Yurkov VY, Kaygorodtseva NV (2020) *Mathematical foundations of geometric modeling of curved lines: textbook*. Publishing House of OmSTU, Omsk, p 198
18. Knott GD (1999) *Interpolating cubic splines*. Birkhauser, Boston, MA, USA, pp 133–138
19. Shikin EV, Plis AI (2020) *Curves and surfaces on a computer screen. A Guide to Splines for users*. Dialogue-MEPHI, Moscow
20. Golovanov NN (2020) *Geometric modeling*. DMK-Press, Moscow
21. Marsh D (2005) *Applied geometry for computer graphics and CAD*. Springer-Verlag, London, p 350
22. Korotkiy VA, Usmanova EA (2023) Bicubic ribbon surface. *Omsk Sci Bull* 2(186):10–16
23. Agoston MK (2005) *Computer graphics and geometric modeling. Implementation and algorithms*. Springer, London, pp 373–471
24. Schneider PJ, Eberly DH (2003) *Geometric tools for computer graphics*; Morgan Kaufmann Publishers, Inc.: San Francisco, CA, USA, pp 109–170, 356–358

25. Korotkiy VA (2022) Constructive algorithms for forming compound cubic bezier curves in space and on plane. *Omsk Sci Bull* 2(182):10–16
26. Gotovtsev AA (2012) Autodesk alias: what to start with? *CADmaster* 5(66):42–44
27. Kornishin MS, Paimushin VN, Snigirev VF (1989) *Computational geometry in shell mechanics problems*. Nauka, Moscow



Transformation of Vectors the Formation of Unique Architectural Objects When the Frame of the Situation Changes

N. A. Saprykina^(✉)

The Moscow Architectural Institute (State Academy), 11/4 Rozhdestvenka Street,
Moscow 107031, Russia
nas@markhi.ru

Abstract. The study examines the precedents of unique architectural objects that have appeared in scientific and design developments in connection with the transformation of the vectors of their formation when the frame of the situation changes. The purpose of this article is to critically comprehend the trend of the emergence of new or transformation of existing unique architectural objects due to their emergent properties. Alternative concepts of the formation of architectural objects are revealed in connection with the evolution of the views of the organization of ritual events: organizing a memorial complex as a place of spiritual comfort for family members of deceased people; using the potential of information technology to organize cemeteries and create virtual spaces; the creation of a vertical or underground necropolis. Modern approaches to the organization of penitentiary facilities in connection with the change in the frame of prevention of relapse of crimes are determined: a healing approach to psychological and cognitive rehabilitation of prisoners in the spatial cluster of the prison; the economic concept of a vertical prison with the possibility of habitat and working prisoners. Compensatory techniques for adjusting the instability of the urban environment in its dense building with the help of objects of “parasitic” architecture by restoring unused urban spaces are considered. The presented selection of design proposals for unique architectural objects allows you to outline the directions for searching and conducting further promising research in this area.

Keywords: Emergent properties · Changing the frame of the situation · Transformation of formation vectors · Memorial complexes · Ritual events · Penitentiary facilities

1 Introduction

In accordance with the needs of the dynamic development of society based on the use of modern scientific paradigms and concepts in many aspects of life, the appearance occurs new or transformations of existing unique architectural objects occur due to the modification of the vectors of their formation. Solving problems in today’s architectural

activity requires reducing the gap between humanitarian and natural science knowledge, expanding the study of areas amenable to formalization and the study of emergent properties of architectural objects. This is happening against the background of a change in the foundations of the worldview, changes in the philosophical outlook of society and as a result of the formation of new knowledge through its transformation from separate independent sciences into an interdisciplinary science.

The problem is that various sciences study the dynamics of properties and relations of their research objects in specific subject areas, without investigating and without taking into account the fundamental nature of general properties and relations, despite the fact that knowledge of this nature is valuable for any particular science [1]. The use of the principle of emergence makes it possible to determine certain special properties of the object of study find out their source and understand their genesis. This is due to the fact that the properties of the system, which are not inherent in its elements individually, arise due to the unification of these elements into a single, integral system [2].

The current practice of insufficient use of the concept of emergence is explained by its complexity. The task is to consider the practice of using this system concept in architectural and urban planning science, to clarify the interpretation of the system principles of thinking as much as possible, to identify its overdue contradictions and to propose a scheme for applying the principle of emergence in the study of unique architectural objects [3].

1.1 Relevance of the Issue

A new approach to the use of the principle of emergence allows us to reveal potential opportunities in the development of methods of modeling, organization and development of the life activities environment, as well as the design of unique architectural objects in a changing reality.

In this case, it will be relevant to consider obtaining completely different properties of the system in the process of changing the frame of the situation, which is considered in sociology as its structure of human interaction. The theory of frames in the direct interaction of people with each other or with objects allows us to understand what is the structure of everyday communications, and according to what laws they develop. The frame logic of analysis is often transferred to new areas of research and used in the theory of architecture [4].

Considering architecture as a living organism, responsive to the needs of society, allows you to reveal the potential of shaping in architecture and moves from the conceptual aspect to the actual approach. In this case, the architectural system can be represented as the interaction of several hierarchical levels, where the upper mega-level is represented by an architectural form, understood in the broadest sense as the material embodiment of an architectural phenomenon, a real physical product of architectural activity [5]. The ability to work with such systems becomes a discovery, especially with the use of effects similar to the so-called feedback, as well as purposeful logical transitions to another trajectory.

1.2 Problem Statement

The purpose of this article is to critically comprehend the trend of the emergence of new or transformation of existing unique architectural objects due to changes in the vectors of their formation based on the analysis of theoretical and design experimental developments. The main scientific task of this article is to determine the features of the formation of unique objects and to identify the most rational ways to design them in connection with the change in the frame of the situation. This will require solving the following specific research tasks:

- To identify alternative concepts of architectural formation of objects in connection with the evolution of the views of the organization of ritual events.
- To identify modern approaches to the organization of penitentiary facilities in connection with the change in the frame of prevention of recidivism.
- To consider compensatory techniques for correcting the instability of the urban environment

This approach to the study necessitates the identification of methods and reception for the formation of unique architectural objects for various environmental conditions, which are practically not used in modern architecture and construction practice. In this case, it will be relevant to consider obtaining completely different properties of such objects in the process of changing the vectors of their formation, manifested in the following concepts.

2 Theoretical Part

2.1 Alternative Concepts of the Formation of Architectural Objects in Connection with the Evolution of the Views of the Organization of Ritual Events

This delicate concept is connected with a new attitude to the formation of a cemetery as a place where the deceased acquires peace after life and where he is remembered by the survivors. In Buddhist culture, there is a concept called “reincarnation”, in which it is believed that the death of life is actually a new beginning. This is not only a renewal of the life and eternity of the spirit, but also a new starting point of tradition, since every mortal eventually dies. The cemetery is often considered a place where the deceased acquires peace after his life, which is coming to an end. However, the end of life does not mean practically “meaningless sleep” underground. Therefore, a cemetery is not only a place where the living remember the deceased, but also the last refuge where he can reincarnate and continue to return to nature in another form of life.

Based on this, the project “*The Reincarnation: Buddhist Skyscraper*” (authors QiLong Wu, WuHong Fang, HuiFang Duan, Chenhui Bao) 2018 (China) puts forward the idea of using the remains of the dead as nutrients used for seed germination. This symbolizes the process of reincarnation of life in the germinating and growing seed. At the same time, some parts of the plant, through processing, can also become a reminder for living people who will feel that the deceased is still around them. The authors of the idea believe that the architectural space of the cemetery, made in the form of a vertical volume, is significantly different from a cold tombstone. It allows you to continue the

memory of the values of the dead that existed and can become a bridge between the living and the dead to make a spiritual dialogue between these two substances [6].

Another concept of solving the problem of burial of deceased people is associated with population growth and accelerating global aging. At the same time, cities with an increasing population and high-density buildings face problems of reducing the amount of resources for organizing cemeteries. This problem is especially acute in Japan with the highest level of aging in the world. The price of a cemetery in Tokyo is so high that most poor people cannot afford to place their relics and loved ones in the cemetery.

As a result, it is proposed to solve the problem of traditional cemeteries using the skyscraper “*Vertical Cemetery*” (authors GuoChao Deng, QingMing Xiao, Yuan Feng, Liwei Shen, Qin Xiong) 2018 (China), which could adjust its height. The authors of the concept are based on humane care for family members of deceased people—“we are not only building a place to store the remains and ashes of the dead, but also creating a place of spiritual comfort for living relatives. In this regard, they never disappear and will not be forgotten”. The memorial complex consists of a series of spatial structures floating above the city in the form of a tornado shape, where the urns are made in the form of lanterns. This can not only save land, but all residents of the city can see the light from the tombstones of their family members.

As the number of people who have died increases, the top of the building rises, raising the height of the cemetery to accommodate more burials. A laser emitting device is provided at the bottom of the cemetery. When living people worship their relatives, the laser will always glow to illuminate the city. When relative or friends completely forget the dead, the laser will go out and the urn will fall into the device under the cemetery. The authors hope that the proposed building will be able to solve the modern problems of a traditional cemetery [7].

Another frame arises when using the potential of information technology, which makes it possible to solve various problems and create virtual spaces to perpetuate the cultural and mental heritage of deceased people as an information cluster. The emergence of virtual space as a new form of communication, a new worldview and a means for a person to express himself, anew forms a person’s idea of the world as a whole. For architecture, it is essential that virtual involves moving away from the usual categories and values to their new forms. As a result, architecture becomes more abstract, and the architect, in turn, gets more freedom to experiment [8].

Nowadays people tend to forget about the importance of the achievements of our ancestors. The ever-changing world needs a new means to perpetuate the cultural impact of people on society as a testament to civilization. Cemeteries are usually located very close to settlements and occupy a lot of valuable land in the city center, which can be returned to citizens as a new public space. However, it is very important to take care of your history and personal experiences and share them with other people [9].

The authors of the concept “*In Two Minds: Magnetic Cemetery*” (authors Marine Joli, Judith Haggiag) 2017 (France, Canada) suggest that in the near future there will be a standardization of the practice of beliefs, where attachment to the body will become non-existent. This raises the question of the cemetery’s future. Currently, due to the increase in population, the vertical development of facilities is presented as a solution to the problem of lack of urban spaces. There is a separation of space from the main uses of the cemetery

as a vertical building, which represents an image of the evolution of morals in relation to death, body and spirit. The building itself lifts off the ground. It looks like an allegory of the gradual removal of a person from the body. Inside the cemetery there is a magnetic wave generator and a reserve for the retransmission of energy. Being lightweight, this system propels platforms and makes them move horizontally and vertically. This method provides more freedom in the design of the building.

This project offers a new way of perceiving space. By creating code, platforms can levitate from one point in space to another. At the same time, the user has the opportunity to choose the type of space in which he wants to be, in accordance with his needs. Such a cemetery modulates the space around a person who is static while remaining on one of the platforms. Here there is a revision of the functions of the cemetery and its capabilities, by magnetizing the space. The cemetery itself offers infinity of routes and spaces capable of meeting the needs of visitors. To do this, the basic screen with artificial intelligence recognizes users thanks to his fingerprints in order to offer him possible routes according to his moods, desires and habits [10].

Environmental problems, as a rule, do not occupy a prominent place due to the severe loss of loved ones and relatives, perhaps because of the sensitivity of this situation. This point of view is changing as these issues become more important [11]. The main problem is the negative impact on the environment of traditional methods of handling the bodies of the dead used by various religions. The concept of a vertical necropolis is presented as a way to meet future needs with the skillful exploitation of limited urban land. In this concept, it is proposed to solve the problem of traditional cemeteries using a skyscraper.

The use of the vertical memorial necropolis in Delhi “*Vertical Necropolis*” (architect Ankit Kumar) 2012 (India) makes it more convenient to conduct a memorial ritual and frees up a significant amount of land (for example, for the organization of memorial parks or wildlife reserves). The vertical necropolis will free up a significant part of the land for use and provide a place for the remains of the deceased in it. It will also create a space where different groups of people, grieving together, can feel comfortable [12].

The Seal of cities and the exponential growth of their population leave very few areas for facilities that do not contribute to its urban life and economy. In particular, there is very little land dedicated to cemeteries in Paris, and every ten years burials are “recycled” and as a result thousands of remains remain without a proper location palace. The idea of a vertical cemetery is to remember the deceased as part of society by creating a symbolic tower with a specific place in the city. The skyscraper will become a new landmark for the city, where families could gather.

In the center of the tower-cemeteries “*Vertical Cemetery*” for Paris (architects Fillette Romaric, Chandrasegar Velmourougan) 2011 (France) there is a skylight opening a hole into the sky that reflects light into the pond below. A spiral wrap around the skylight organizes a passage along the graves and leads to the top of the tower with a beautiful view of Paris. Each burial has a memorial plaque and a flexible rod attached to the exterior facade, which during the movement of the wind reminds of the deceased person [13].

Due to the extreme limitation of the building area in Mexico City, its growth is possible only in the direction of the outskirts of the city with the subsequent loss of agricultural land and environmental consequences. Overpopulation Accounting, limited

land, as well as the psychological and sensual experience of grief at the burial of the deceased is carried out in the project of an underground vertical cemetery for Mexico City “*Towers for the dead*” (architects Israel Lopez Balan, Elsa Mendoza Andres, Moises Adrian Hernandez Garcia) 2011 (Mexico). The object is made in the form of a large-scale screw with a curved retaining wall and ramps with good lighting, which provides comfortable light and ventilation for visiting. The authors of the project believe that such a cemetery allows family members of the deceased to get closer after traveling to the underworld, where they have just buried their loved one [14].

The considered some concepts of modification of vectors of formation of unique architectural objects when changing the frame of the situation associated with the evolution of the views of the organization of ritual events allow us to identify new approaches to their design. Thus, the typology of architecture is being updated with new types of architectural objects that are cultural and informational denominators of the future.

2.2 Modern Approaches to the Organization of Penitentiary Facilities in Connection with the with the Change in the Frame of Prevention of Relapse of Crimes

One of the most important activities of the modern penitentiary system for the restoration of social justice, along with the punitive function, is the prevention of relapse of crimes. Many proposals for the organization and location of penitentiary facilities in the urban environment have appeared in the conceptual and design developments. The penitentiary penal enforcement system, within the framework of State institutions, is engaged in the execution of criminal penalties imposed on citizens in accordance with the law. It also ensures the execution of punishments both related and unrelated to deprivation of liberty, as well as the detention of persons under investigation from the moment of detention to trial (until the change in the measure of procedural restraint in the form of detention). It is also necessary to identify the huge impact on the decisions of the promising developments of the twentieth century, presented in the design practice of the precedents of utopian design using information technologies, which are further embodied in the work of modern architects [15].

So, in the project “*Healing Matrix*” (authors Jie Liu, Wen Sun, Hewen Suo) in 2016 (Canada), they are trying to change the usual organization of the personality correction center in a penitentiary institution and solve a socio-psychological problem by architectural means. The idea is that the spatial cluster of healing replaces the nature of the traditional detention of prisoners at various stages of the rehabilitation process. Prisoners have the opportunity to interact with each other and with the control center in a specially organized rehabilitation space throughout their stay, which allows them to fundamentally cure personality disorder and achieve full recovery [16].

In order to achieve crime prevention, as well as psychological and cognitive rehabilitation, in addition to the correction center, six independent and related types of spaces are being created. Each space is a cluster of several cubes and has its own functions and approach to self-healing and self-correction: for prayer (religious support), for meditation (inner peace power), for accompaniment (interpersonal interactions and support), for anger or depression management (cognitive behavioral therapy) and social learning space (communication and polishing of humane skills) [17].

Each prisoner has his own personal independent space in a cube ($3 \times 3 \times 3$ m), which ensures the protection of prisoners' lives and their privacy. Information is instantly transmitted through the building's command center, and network of the matrix automatically transfers the prisoner to the spaces to optimize the healing effect. In order to ensure the free multi-purpose movement of each unit, the building itself has an internal space matrix that allows its three-dimensional movement. The mobility of space creates not only a healing effect for the recovery of prisoners based on a multi-layered treatment system, but also implements interactions between prisoners.

The concept of a vertical prison "*Vertical Prison*" (authors Chow Khoo Toong, Ong Tien Yee, Beh Ssi Cze) 2010 (Malaysia) is based on the fact that, according to the results of some studies, the imprisonment of a criminal is only a temporary residence, since he not have the opportunity to rehabilitate himself in the community he desires. The project is considering the possibility of creating a vertical prison where prisoners will have to live and work in communities in agricultural fields and factories for recycling. These products will be exploited by offenders in the community, and will continue to be used in the city below. Lou offenders will live "for free" until they finish the phrase in their re-education. The vertical prison has its own transportation system, which combines various blocks for officers, prisoners, firefighters and other workers [18].

One of the highest crime rates in the United States has the city of Detroit, which was an economic center in the past, and now its economy is collapsing due to residents leaving it. Since prisoners are seen as an economic burden for taxpayers, it is logical to rethink the methods of imprisonment and the idea of organizing here production arises. The goal is to allow prisoners to serve their prison sentences while remaining a labor force in the economic sector. As many areas of Detroit remain abandoned, there is a need to create an architecture that is flexible to meet unsustainable economic needs. [19].

In this regard, the idea of the project "*City Rehab*" (authors: Yassin Nour Al-tubor, Fawzi Bata, Boran Al-Amro, Yazeed Balqar) 2018 (Jordan) is to rehabilitate the city of Detroit by creating a penitentiary facility there in order to economically rebuild the city. The vertical tower with the function of incarceration consists of modular units that can be added or removed, and then recycled. In the event that the population of prisoners decreases and moves to other parts of the city, the tower can be used for another purpose. The structure of the tower mainly includes the following blocks: living quarters for prisoners, production units for prisoners and maintenance and officer housing units. The production units contain training and working sectors, such as plantations, seminar rooms and training courses.

The structure of the tower consists of a main core, which acts as a vertical transit and consists of 4 elevators-stairs. Around the core are stacked blocks of housing, services and manufacturing. The blocks are connected to the core through bridges, and at each height through four floors a slab is organized, which serves as a communal courtyard for the inhabitants. The gaps between the blocks are filled with glass so that natural sunlight penetrates into the space. Despite the fact that prisoners remain isolated from public life, production units are part of the local market and meet its needs by adapting work units and allowing prisoners to specialize in economic activities. The overall goal is to reduce

the prison population and move the units to different parts of the city, where their use will be retrained [19].

Another example is project of the prison “*Prison in the Sky for Urban Areas*” (authors Greg Knobloch and Andreas Tjeldflaat) 2012 (Malaysia). This concept challenges all preconceived notions of “prison” and offers simple but original ideas that reinterpret a high-rise facility as a city prison. The complex consists of three towers in the form of an arch, where three main stages of prevention of relapse of crimes are carried out in each arch: Conclusion, Transformation and Integration. At the initial stage, the conclusion process of conclusion place in isolation, and further the physical unification takes place and at the end, at the integration stage, the system is programmed. As prisoners master education, they are exposed to an increasing degree of social interaction in order to make the transition back to society as humane as possible. To speed up this process, the state program and residential units are introduced at the integration stage [20].

2.3 Compensatory Techniques for Correcting the Instability of the Urban Environment: “parasitic” Architecture

In connection with solving the problems of densely built-up cities, a modern trend has emerged in architecture—“parasitic” architecture as a new way to increase living space and organize affordable social housing in megacities. Most often, examples of such projects are based on the principle of reclaiming unused urban spaces. Such buildings are fixed or built either inside existing buildings or outside in such a way as to depend on the communal infrastructure of the main building. The trend of parasitic architecture is gradually developing with the consolidation of modern cities.

By purpose and size, the precedents of “parasitic” architecture arise in extraordinary situations and have various forms. The analysis of design and experimental developments revealed the following types of “parasitic architecture”: art objects, seasonal buildings, symbiont objects, integrated extensions, buildings between the main buildings, suspended buildings—“parasites”, saprophyte objects, transplant extensions, parasitic objects on the facade, parasitic megastructures. The most interesting are the unique precedents using compensatory techniques for correcting the instability of the urban environment.

For the organization of additional premises on the roof of almost any existing building in urban conditions, *objects of symbiont* are being developed. The project of a small structure “*Bird’s Nest*” (ONZ Architects, Turkey) 2013 (architects Onat Oktem, Zia Imren and Zeynep Okte) is designed as a music room for schools that lack space and proper insulation. The sloping roof of the facility, according to the authors, is designed to collect rainwater and place photovoltaic panels for maximum absorption of solar energy. The extension can be used to provide housing for homeless citizens, a studio for artists or a small additional room for guests [21].

The project of prefabricated house “*Prefab Parasite*” prefabricated house (studio Lara Calder Architects) 2009 (Australia) is an *integrated extension* designed for the development of unused spaces in urban landscapes. The shape of the object, developed using software by parametric 3D modeling is a flexible structure in which all components, such as the load-bearing system, facade cladding, ceilings and stairs, are integrated into a

single parametric model. Design system integration improves the efficiency and accuracy of the construction process [22].

A well-known example of *buildings between the main buildings* is one of the projects of the architectural bureau “Za Bor Architects” in Moscow “*Parasite Office*” (authors Arseniy Borisenko and Petr Zaitsev). The building was planned to be built of polycarbonate and glass, at the height of the second floor, between two residential buildings. The purpose of the construction was to use the free spaces between the houses to create offices that do not restrict access to the yards. The new building compensates for the lack of space in the densely built-up capital. Such construction does not require expensive land plots [23].

In the design of a *parasitic suspended building* for a nightclub (Urbanplunger), Hong Kong (China), in accordance with the current situation, which is characterized by an extremely compact layout of the area, the main criterion is the compactness of the building. Suspended structural structure allows the entire building to “float” in space. Below, under the building, it is planned to create a small green area for walking, from which special elevators for visitors and their cars lead directly to the nightclub. It is also planned to set up a small garden on the roof of the hotel [24].

Buildings that are being introduced into buildings that have already ceased to function, for example, in former factories, warehouses, industrial facilities, are *saprophyte objects*. At the same time, the goal is to revive the degrading territory, to introduce new functions. So, in order to expand the music school of Amy Friarson in Louviers, a concert hall was built on top of the former monastery of the XVII century (architects of the Opus 5 firm) in the former monastery of Notre-Dame-de-Consolation (France (Paris)). The object was conceived in a very narrow area, which caused the filling of all free spaces, raising it above the existing walls [25].

The project “Flux Haus” in Hong Kong (authors Kammil Karransoy, Jitendra Farkade and Vinay Khare) is designed as a parasitic housing megastructure that will be suspended from a spatial structure with single pods above the five towers of the Green Harbor Tower complex (China). The structure is a grid of robot-built rails on which all the cubic AI-equipped habitation pods, which include robot swarm technology, are located. This allows you to quickly adapt to create the desired layout of the room or furniture, allowing you to instantly transform cubic capsules from the living room or dining room to the bedroom [26].

3 Practical the Significance

With the advent of a new paradigm, due to the emergence of many scientific and technical discoveries, the field of architectural thought is expanding, accompanied by a huge amount of information and the expansion of all kinds of communications. Architecture not only meets the new paradigm, but also opens up new knowledge and stimulates science to new inventions, as evidenced by the methods of forming unique architectural objects discussed above [27]. The precedents of unique architectural objects that have appeared in scientific and design developments in connection with the transformation of the vectors of their formation when the frame of the situation changes provide a continuous transition from traditional approaches to new ones based on innovative technologies.

The presented developments of concepts of a natural-scientific nature make it possible to bring architecture closer to the sciences of a technical plan related to it in construction activities. Such processes should be reflected in the content of the subject of architectural activity, which by its structural organization forms the emergent principles of creating unique objects as a system. Technological and economic requirements for the creation of such architectural objects cause a leap in the search for new principles of their creation that meet innovative concepts.

This review shows that studies of unique architectural objects in connection with changes in the vectors of their formation can become a “road map” for the implementation of measures related to the use of emergent principles. The implementation of the theoretical provisions and practical recommendations set out in the article will allow us to outline the directions of further research in this area and will contribute to the development of scientific and technological progress, which is of great socio-economic importance.

4 Conclusion

As a result of the research, the precedents of unique architectural objects that has appeared in scientific and design developments in connection with the change in the vectors of their formation when the frame of the situation changes are considered. This made it possible to determine the features of the formation of unique objects in the following areas considered and to obtain the results discussed in this review:

1. Alternative concepts of the formation of architectural objects have revealed in connection with the evolution of the views of the organization of ritual events:
 - Using the remains of the dead as nutrients for the ascent of plant seeds allows you to continue the memory of the pre-existing values of the deceased, and can also become a bridge between the living and the dead to make a spiritual dialogue between these two substances.
 - The concept of organizing a memorial complex not only as a place to store the remains and ashes of the dead, but also as a place of spiritual comfort for family members of deceased people. In this regard, humane care for living relatives creates a situation where deceased people will never be forgotten.
 - Using the potential of information technologies makes it possible to solve various problems of organizing cemeteries and create virtual spaces to perpetuate the cultural and mental heritage of deceased people as an information cluster.
 - The concept of a vertical necropolis is presented as a way to meet future needs in the exploitation of limited urban land. In this regard, it is proposed to solve the problem of traditional cemeteries by using a skyscraper or an underground vertical cemetery.
2. Modern approaches to the organization of penitentiary facilities have defined in connection with the change in the frame of prevention of relapse of crimes:
 - The healing approach to psychological and cognitive rehabilitation of prisoners consists in the fact that the spatial cluster of the prison replaces the nature of the traditional detention of prisoners at various stages of the process of personality correction. The mobility of the prison space creates not only a healing effect for the recovery of prisoners, but also implements interactions between prisoners.

- The concept of a vertical prison considers the possibility of providing prisoners with housing and work in communities in agricultural fields and factories for processing industrial raw materials. The resulting productions will be exploited by offenders in the community, and further used in the city below.
 - An economic concept that allows prisoners to serve a prison sentence in isolation from public life, while remaining a labor force. This allows prisoners to adapt to production classes, allowing them to specialize in economic activities.
3. Compensatory techniques for correcting the instability of the urban environment have considered:
- The problems of densely built-up cities in architecture can be solved with the help of objects of “parasitic” architecture as a new way to increase the housing stock while restoring unused urban spaces.
 - Unique precedents that use compensatory techniques for adjusting the instability of the urban environment are: symbiotic objects, integrated extensions, suspended the objects between the main buildings, saprophyte objects, and parasitic mega structures.

Acknowledgements. The research was carried out within the framework of the Program of Fundamental Scientific Research of the Russian Academy of Architecture and Building Sciences and the Ministry of Construction and Housing and Communal Services of the Russian Federation for 2023.

References

1. Lutsenko EV (2008) Existence, non-existence and change as emergent properties of systems. <http://quantmagic.narod.ru/volumes/VOL512008/p1215>
2. Korosov AV (2012) The principle of emergence in ecology. *Sci Electron J “Principles of Ecology”* 3:48–66. <http://ecopri.ru/journal/atricle.php?id=1481>
3. Saprykina NA (2014) The use of the principles of emergence in the formation of spatial habitat as a system. In: *Science, education and experimental design. Proceedings of the International scientific and practical conference. April 7–11. MARHI, Moscow*, pp 344–347
4. Vakhstein V (2013) Sociology of an architectural object. Between formal and practical rationality. In: *New Literary Review. “Architecture and Utopia”* 121:3. <http://www.nlobooks.ru/node/3561>
5. Kholodova LP (2010) Concepts of modern theory of architecture. “Architecton: news of universities”, 31. http://archvuz.ru/2010_3/1
6. Wu Q, Fang W, Duan H, Bao C (2018) The reincarnation: Buddhist skyscraper (China). <http://www.evolo.us/the-reincarnation-buddhist-skyscraper/#more-36105>
7. Deng G, Xiao Q, Feng Y, Shen L, Xiong Q (2018) Vertical cemetery (China). <http://www.evolo.us/vertical-cemetery/#more-36100>
8. Saprykina NA, Saprykin IA (2012) “Paperless” architecture in the context of virtual reality. *Arch Modern Inf Technol* 12:1–7. http://www.marhi.ru/AMIT/2012/special_12/saprykina/abstract.php
9. Dutsev M (2020) The city as an art integration space. In: *Proceedings of the 2nd international conference on architecture: heritage, traditions and innovations (AHTI 2020). Series: advances in social science, education and humanities research*. <https://doi.org/10.2991/asschr.k.200923.061>

10. Joli M, Haggiag J (2017) In two minds: magnetic cemetery (France, Canada). <http://www.evolo.us/in-two-minds-magnetic-cemetery/#more-35727>
11. Cirella GT, Russo A, Benassi F, Czermański E, Goncharuk AG, Oniszczyk-Jastrzabek A (2021) Energy re-shift for an urbanizing world. *Energies* 14:5516. <https://doi.org/10.3390/en14175516>
12. Kummur A (2012) Vertical necropolis in Delhi (India). <https://www.evolo.us/vertical-necropolis-in-delhi/>
13. Romaric F, Velmourougane C (2011) Vertical cemetery for Paris (France). <https://www.evolo.us/vertical-cemetery-for-paris/>
14. Balan IL, Andrés EM, García MA (2011) Underground tower for the dead (Mexico). <https://www.evolo.us/tower-for-the-dead/>
15. Tribelskaya E (2020) Revitalization of the penitentiary complexes in the historic centre of Florence. In: Proceedings of the 2nd international conference on architecture: heritage, traditions and innovations (AHTI 2020). <https://doi.org/10.2991/assehr.k.200923.033>
16. Kalyanov GN, Kuprianov BV, Fiodorov IG (2017) The role of decomposition in organizational system modeling. In: CEUR workshop proceedings. 2nd international scientific conference "convergent cognitive information technologies, (135056), 2064:380–387
17. Liu J, Sun W, Suo H (2016) Healing matrix (Canada). <http://www.evolo.us/competition/healingmatrix/#>
18. Toong CK, Yee OT, Cze BS (2010) Vertical prison (Malaysia). <https://www.evolo.us/vertical-prison/>
19. Al-tubor YN, Bata F, Al-Amro B, Balqar Y (2018) City rehab—Detroit (Jordan). <http://www.evolo.us/city-rehab-detroit/#more-36054>
20. Knobloch G, Tjeldflaat A (2012) Prison in the sky for urban areas (Malaysia). <http://www.evolo.us/prison-in-the-sky-for-urban-areas/>
21. Leylin T (2013) Bird's Nest: Solar-Powered Studio Perches on School Roofs (Turkey). <https://www.greenprophet.com/2013/07/birds-nest-solar-powered-studio-perches-on-school-roofs/>
22. Cimento K (2009) Parasite Prefab/Lara Calder architects (Australia). <https://www.archdaily.com/35859/parasite-prefab-lara-calder-architects>
23. Zaitsev P (2011) Parasite office in Moscow/ Za Bor architects (Russia). <https://www.evolo.us/parasite-office-in-moscow/>
24. Rosenfield K (2012) Elevated night club hotel in Hong Kong/Urbanplunger (China). <https://www.archdaily.com/210547/elevated-night-club-hotel-in-hong-kong-urbanplunger>
25. Frearson A (2012) Music school Louviers extension/Opus 5 Architectes (France). In: *Dezeen*, July 2012. <https://www.dezeen.com/2012/07/16/music-school-louviers-extension-by-opus-5/>
26. Crook L (2019) IAAC graduates propose parasitic pods as alternative to cage homes in Hong Kong (China). In: *Dezeen*, August 2019. <https://www.dezeen.com/2019/08/19/iaac-flux-haus-conceptual-architecture-china-housing/>
27. Baitenov E (2020) Modern challenges and the outline of the future of architecture. In: Proceedings of the 2nd international conference on architecture: heritage, traditions and innovations (AHTI 2020). <https://doi.org/10.2991/assehr.k.200923.002>



The Process of Progressive Limiting State and Determination of the Residual Strain Energy of a Structure Based on the Force Method

L. Yu Stupishin¹, K. E. Nikitin^{1,2}(✉), and M. L. Moshkevich³

¹ Moscow State University of Civil Engineering, 26, Yaroslavskoe Shosse St., Moscow 129337, Russia

niksbox@ya.ru

² RUDN University, 6, Miklukho-Maklaya St., Moscow 117198, Russia

³ Southwest State University, 94, 50 Let Oktyabrya St., Kursk 105040, Russia

Abstract. A methodology for investigating the progressive limiting state of the structure is proposed. To solve this problem, the criterion of critical strain energy levels in the form of the force method is used. The criterion for violation of the limiting state of the structure is a change in the state of self-stress of the structure. The problem is posed as an eigenvalue problem and the values of the maximum values of the design parameters are found for the flexibility matrix. The resulting forces correspond to a critical level of energy. They can be used to find the maximum possible value of the strain energy of the structure. By subtracting from it the amount of work of external forces, it is possible to determine the residual load-bearing capacity of the structure. An example of calculating a simple statically indeterminate truss structure is demonstrated. It clearly shows the change in the energy of deformation of the structure, its self-stress, and the possibility of modeling the progressive limiting state of the structure.

Keywords: Truss · Strain energy · Limiting state · Critical strain energy levels · Matrix methods

1 Introduction

Currently, the most popular formulation of problems of structural mechanics in the form of Lagrange. It allows you to get a construction design corresponding to a given load [1–9]. Geometric features of the cross-sections of structural elements are taken according to the most loaded cross-section in the elements. When design structures, its elements are typified, and their dimensions are unified. As a result, the structures obtained with this approach include elements with geometric parameters that are not economic sounded. They have a significant reserve of bearing capacity.

The choice of the type of the limiting state of the structural elements by the designer in accordance with the requirements of the codes also leads to a significant reserve of the

load-bearing capacity of the structure. Calculations in the elastic stage of deformation lead to a rational form of the cross-section of the cambered beam in the form of an I-beam, where the material is concentrated in the extreme fibers. At the same time, the calculation in the elastic–plastic stage of deformation recommends concentrating the material at the neutral axis of the element, which gives a rational rhombus shape. The theory of optimal design of structures [10–13], designed to reduce the load-bearing capacity of load-bearing structures, does not allow to significantly reduce its value [14] (by no more than 20%).

When assessing the technical status of an exploited structure or its element, it is important to know such a parameter as its residual load-bearing capacity [15–24]. But determining the complete (maximum) load-bearing capacity of structures is usually difficult. For example, if we are based on the Lagrange approach, and consider all possible options for loading load-bearing structures, this leads to the need to solve an infinite sequence of problems. Their solution is impossible even with the capabilities of modern FEM packages. This does not allow to find the residual bearing capacity of the structures after the application of the design load.

To overcome these difficulties, a criterion of Critical strain internal energy levels was proposed [25]. It allows us to estimate the residual value of the load-bearing capacity of the structure by the value of the deformation energy [26].

In addition, finding the minimum of the critical strain energy makes it possible to find the most loaded structural element (the ‘weak link’), in which the limiting state will first occur. This approach allows us to set and solve the problem of the progressive limiting state of the load-bearing structures of the building. We investigate the process of progressive limiting state and determine the residual strain energy of the structure using the example of a simple rod system.

2 Methods and Materials

To obtain the criterion of critical energy levels, it is necessary to separate the energy of the fields of external influences and the energy of the field of internal deformations. These energies have different sources of origin and laws of existence [25]. The condition of the critical state of the strain energy of the structure includes the following three requirements.

The first requirement is a minimum variation of the strain energy of the structure:

$$\delta^2 U(\chi) = 0 \quad (1)$$

The second is the condition of orthonormality of the design parameters of the structure:

$$\sum_j U_j(\chi) = 1 \quad (2)$$

The third requirement is the implementation of conditions at the boundary of the area of acceptable design parameters:

$$\Gamma(\chi) = 0 \quad (3)$$

Here $U(\chi)$ is the potential strain energy of the structure; χ is the extremals of the internal design parameters, which represent generalized displacements and forces.

Switching from one level of critical energy to another is followed by a change in the state of self-stress of the structure. The potential strain energy of the structure at a given level of loading balances the work of external influences. The remaining part of the potential strain energy is in a self-stressed state.

$$U(\chi) = U_{cr}(\chi) + U_{ex}(\chi) \quad (4)$$

Since the work of external forces is balanced by a part of the potential strain energy, which is provided for by the construction design, the limiting state of the structure is not violated. The remaining part of the self-stressed energy can be spent on increasing the load. The load-bearing capacity of the structure will be exhausted as soon as this part of the deformation energy runs out.

Experience shows that before the self-stressed strain energy is completely exhausted, various things can happen:

- change in the type of deformation of the material, such as the transition from elastic to plastic stage of deformation, etc.;
- loss of form of the initial type of deformation (buckling);
- change of the design model due to the breakout of the load of structural elements;
- exceeding the acceptable values of the displacement of the points of the structure entailing a violation of regular (safe) operating conditions;
- other reasons that are related to the violations of the conditions of the limiting state of the structure.

Therefore, in the future we will investigate the critical strain energy of the structure. To do this, we will create a small perturbation of the internal field of forces or deformations. The conditions of the critical state of the structure in the form of the force method obtained from the variational principle (1–3) have the form [26–28]:

$$[L]\{\delta\Phi\} = [\lambda^L]\{\delta\Phi\} \quad (5)$$

Here $[L]$ is the flexibility matrix of the structure; $\{\delta\Phi\}$ is the vector of amplitude values of the distribution of generalized reactive self-stress forces in the structure. It is represented by a set of orthonormal functions; $[\lambda^L]$ —the matrix of eigenvalues, which has the meaning of unitary angular displacements of the structure.

The vector of maximum nodal displacements of the structure is calculated as:

$$\{Z_{\max}\} = [\lambda_{\max}^L]\{\delta\Phi_{\max}\} \quad (6)$$

The algorithm for determining the greatest internal forces and the potential strain energy based on them is written through the well-known matrix procedures of structural mechanics.

We construct the matrices of the internal stiffness of the structure $[C]$ and the static matrix of the problem $[A]$. We will consider all degrees of freedom of the system in

the selected design constraints, where we will monitor generalized displacements and forces.

$$[K] = [A]^T [C][A] \quad (7)$$

The flexibility matrix $[L]$ is found as the inverse of the stiffness matrix $[K]$:

$$[L] = [K]^{-1} \quad (8)$$

We solve the eigenvalue problem (5) and find the vector of maximum displacements (6).

The vector of strains of the rods caused by extreme nodal displacements is defined as:

$$\{\varepsilon\} = -[A]^T \{Z_{\max}\} \quad (9)$$

We calculate the distribution of forces in the structural elements caused by the extreme vector of nodal displacements as:

$$\{N\} = [C]\{\varepsilon_{\max}\} \quad (10)$$

The potential strain energy is determined by the formula:

$$U = \{N\}^T [L]\{N\}/2 \quad (11)$$

3 Results and Discussion

Let us illustrate the proposed methodology using the example of a statically indeterminate truss. This computing scheme, with its sufficient simplicity, allows us to show the main features of changing the computational scheme and self-stress. The limiting states for extended and compressed rods are described uniformly by strength constraints. We will assume that the dimensions of the rods are selected in such a way that there is no loss of stability, and restrictions on the movement of nodes are not violated.

The last two assumptions about the kinds of limit states, if necessary, are easy to consider, as are any others. This is because they are placed on the right side of the inequalities describing the limiting state of the structure:

$$\begin{aligned} U(\Phi, \xi) &\leq U_{ult}, \\ \{\Phi_{\max}\} &\leq \{\Phi_{ult}\}, \\ \{\xi_{\max}\} &\leq \{\xi_{ult}\}. \end{aligned} \quad (12)$$

Here $\{\Phi\}$ is the vector of generalized forces, and $\{\xi\}$ is the vector of generalized displacements. The indexes correspond to the maximum and ultimate values.

Let us consider the methodology for determining the extreme values of the strain energy, generalized forces, and displacements, including their values at the boundary of the range of acceptable parameters. These values are located on the left side of the

inequality and are determined only by the geometrical and mechanical features of the structure, including the support conditions.

In the case of the occurrence of a limiting state in one or more rods, they stop resisting external influences. For example, due to the yielding state. Or any other mentioned in the right part of the conditions (12). We will refer further to the “elimination of the rod” meaning that the rod has stopped taking the load properly. Further, in the figures illustrating the progress of solving the problem, such rods will not be shown.

Consider the truss shown in Fig. 1, in which the lengths of the rods and stiffness are the same. Figure 1 also shows the numbering of elements and nodes of the truss. The truss nodes are numbered in blue, the rods are numbered in red.

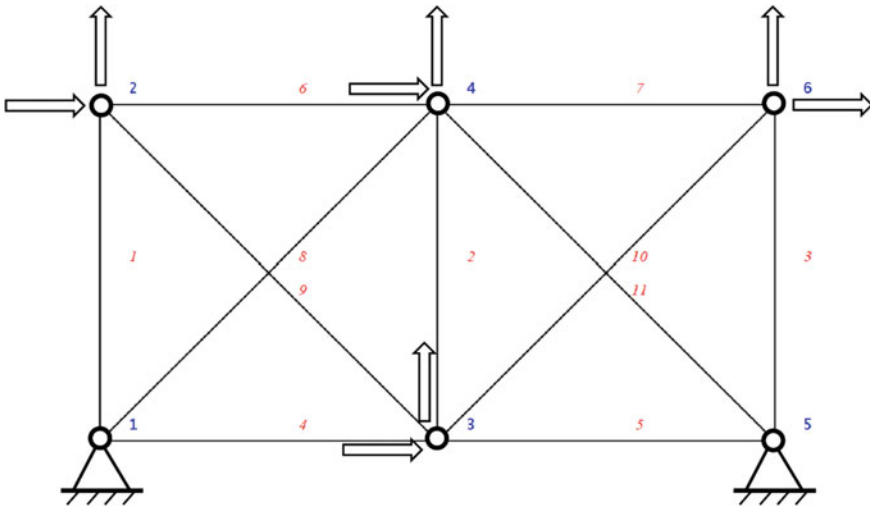


Fig. 1 Design scheme of a statically indeterminate truss: degrees of freedom of nodes and numbering of nodes and truss elements

We solve the problem of determining the first state of self-stress of the structure. We obtain the forces in the rods from the unit vectors applied in the direction of the degrees of freedom shown in Fig. 1 near the nodes.

Figure 2 shows the forces in the truss rods from unitary nodal variations of reactive forces. We will assume that the external influences in the calculated truss are applied in the same directions as the variations of reactive influences arising in the direction of the originally selected degrees of freedom.

Figure 3 shows the forces calculated from the maximum nodal displacements. Calculations were performed in a software package for the analysis of structures by the method of critical energy levels ‘CLE’ [29].

Comparing the values of the forces in the rods obtained for two loading cases, we notice that the forces arising from the maximum values of the displacement of the nodes significantly outweigh the forces from the action of unitary nodal forces. Note that these forces illustrate a possible external load here. Thus, the principal magnitudes of the forces in the rods are greater than from possible external influences.

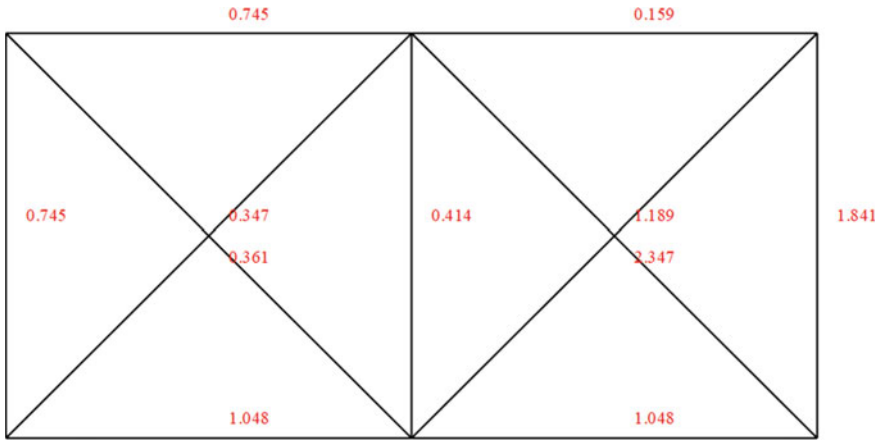


Fig. 2 The self-stress force in the rods from unitary variations of reactive forces in the nodes of the truss

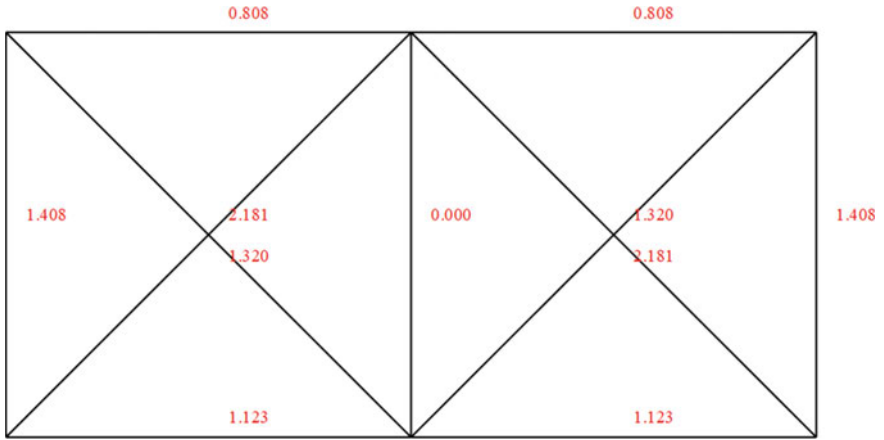


Fig. 3 The self-stress principal values of the forces from the maximum nodal displacements

The maximum possible potential strain energy of the truss calculated from the principal (maximum) forces in the rods of the truss is $U_{cr}^{max,I} = 13.09 \cdot EA/l$. It can be taken in relative form as: $\bar{U}_{cr}^{max,I} = 1$. The work of external unitary influences in relation to the maximum possible strain energy for the truss is $W_{ex}/U_{cr}^{max,I} = 0.65$. The residual relative value of the strain energy of the truss: $U_{res}^I/U_{cr}^{max,I} = (U_{cr}^{max,I} - W_{ex})/U_{cr}^{max,I} = 0.35$. That is, the residual resource of the load-bearing capacity of the truss is 65% of its maximum value, even if external loads are applied in all nodes of the truss in all directions of degrees of freedom.

At the first stage of self-stress, we obtain the top values of forces in rods 8 and 11, which are the ‘weak link’. If we are concerned about which of the rods will break down at the next stage of loading the truss, we must remove the 8 and 11 rods from the design

scheme. And then perform the calculation for the new design scheme shown in Fig. 4. Repeating the calculations until the structure becomes geometrically changeable, we obtain a method of progressive limiting state of the structure.

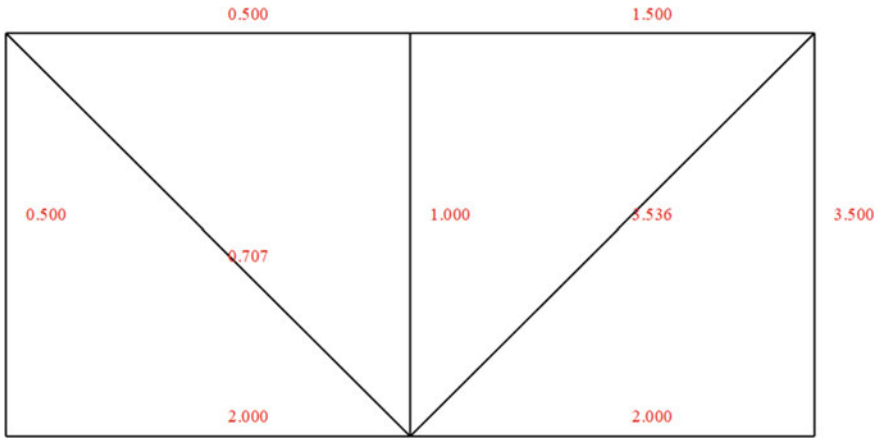


Fig. 4 The self-stress forces in the rods from unitary variations of reactive forces in the nodes of the truss at the second stage of self-stress

Figures 4 and 5 show the internal forces for cases of a unitary force action in the nodes of the truss and the maximum possible values of forces in the same rods from nodal reactive actions. The forces from the principal (maximum) nodal influences also have greater magnitudes than from unitary forceful influences in the nodes.

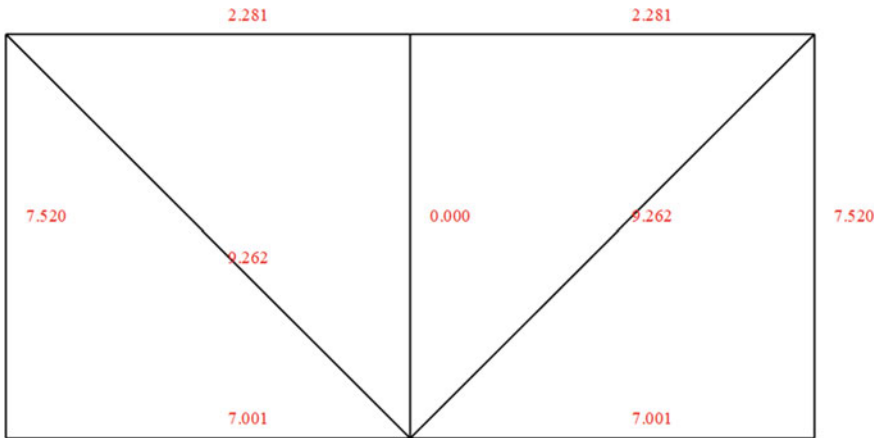


Fig. 5 The self-stress principal magnitudes of the forces from the maximum nodal displacements at the second stage of self-stress

The relative potential strain energy at the second stage of self-stress is $\overline{U}_{cr}^{\max,II} = 1$. The ratio of the work of the nodal forces at the second stage of self-stress to the maximum potential strain energy is $W_{ex}/U_{cr}^{\max,II} = 0.1$. The relative residual potential strain energy is $U_{res}^{II}/U_{cr}^{\max,II} = (U_{cr}^{\max,II} - W_{ex})/U_{cr}^{\max,II} = 0.9$.

At the second stage, rods 9 and 10 are eliminated from work on the load. After that, the calculation scheme of the truss becomes an unstable system.

4 Conclusion

The methodology of the progressive limit state, based on the variational principle of critical strain energy levels of structure, allows us to overcome a number of problems that cannot be solved based on the principle of the minimum of the total energy of the structure:

- obtaining a single criterion describing the limiting state of the structure. This is a change in self-stressed structures when passing through a critical level of strain energy of the structure;
- the ability to calculate the maximum possible potential strain energy of the structure and the residual potential strain energy of the structure after the application of external influences;
- formulation and solution of the problem of finding the “weak link” of the structure in the form of the method of forces;
- formulation and solution of problems of the progressive limiting state of the structure in the form of the method of forces. Sequential application of the methodology of finding the weak link of the structure;
- calculation of the residual load-bearing capacity of the structure. In the example of a statically indeterminate farm, it is rather large.

The growth of residual energy in the design schemes of trusses with removed rods is explained by the fact that the remaining rods of the farm must have the ability to bear the load applied initially. And for this, they must have large values of stiffness.

References

1. Ba K, Gakwaya A (2018) Thermomechanical total Lagrangian SPH formulation for solid mechanics in large deformation problems. *Comput Methods Appl Mech Eng* 342:458–473. <https://doi.org/10.1016/j.cma.2018.07.038>
2. Coombs WM, Augarde CE, Brennan AJ et al (2020) On Lagrangian mechanics and the implicit material point method for large deformation elasto-plasticity. *Comput Methods Appl Mech Eng* 358:112622. <https://doi.org/10.1016/j.cma.2019.112622>
3. Lin Y, Zhang X, Xu W et al (2019) Importance assessment of structural members based on elastic-plastic strain energy. *Adv Mater Sci Eng* 2019:1–17. <https://doi.org/10.1155/2019/8019675>
4. Nairn JA, Hammerquist CC, Smith GD (2020) New material point method contact algorithms for improved accuracy, large-deformation problems, and proper null-space filtering. *Comput Methods Appl Mech Eng* 362:112859. <https://doi.org/10.1016/j.cma.2020.112859>

5. Portillo D, Oesterle B, Thierer R et al (2020) Structural models based on 3D constitutive laws: variational structure and numerical solution. *Comput Methods Appl Mech Eng* 362:112872. <https://doi.org/10.1016/j.cma.2020.112872>
6. Renaud A, Heuzé T, Stainier L (2020) The discontinuous Galerkin material point method for variational hyperelastic–plastic solids. *Comput Methods Appl Mech Eng* 365:112987. <https://doi.org/10.1016/j.cma.2020.112987>
7. Samaniego E, Anitescu C, Goswami S et al (2020) An energy approach to the solution of partial differential equations in computational mechanics via machine learning: Concepts, implementation and applications. *Comput Methods Appl Mech Eng* 362:112790. <https://doi.org/10.1016/j.cma.2019.112790>
8. Wang X, Xu Q, Atluri SN (2020) Combination of the variational iteration method and numerical algorithms for nonlinear problems. *Appl Math Model* 79:243–259. <https://doi.org/10.1016/j.apm.2019.10.034>
9. Xiang CS, Li LY, Zhou Y et al (2020) An efficient damage identification method for simply supported beams based on strain energy information entropy. *Adv Mater Sci Eng* 2020:1–11. <https://doi.org/10.1155/2020/9283949>
10. Tamrazyan AG, Alekseytsev AV (2019) Optimal'noe proektirovanie nesushhih konstrukcij zdaniy s uchetom odnositel'nogo riska avariij (Optimal structures design: accounting of costs and relative accidents risk). *Proceed Moscow State Univ Civil Eng* 14(7):819–830. <https://doi.org/10.22227/1997-0935.2019.7.819-830>
11. Lalin VV, Lalina II, Golovchenko Y et al (2022) Metod minimizacii usilij v sterzhnevyyh sistemah s pomoshh'ju uzlovyyh nagruzok (Method for minimizing stress resultant in rod systems using nodal loads). *The Eurasian Scient J* 14(2):35
12. Repetckii OV, Nguyen VV (2020) Issledovaniya vliyaniya rasstrojki parametrov na dolgovechnost' rabochih koles turbomashin s uchetom analiza chuvstvitel'nosti (Research of influence mistuning parameter on the durability bladed disks turbomachines based on sensitivity analysis). *Bulletin NGIEI* 10(113):5–16. <https://doi.org/10.24411/2227-9407-2020-10090>
13. Alekseytsev A, Al Ali (2022) Mohamad optimization of bearing structures subject to mechanical safety: an evolutionary approach and software. *Inter J Comp Civil Struct Eng* 18(2):131–142
14. Perelmuter AV, Slivker VI (2007) Raschetnye modeli sooruzhenij i vozmozhnost' ih analiza (Calculation models of structures and the possibility of their analysis). DMK Press, Moscow
15. Golik VI, Dmitrak YV, Gabaraev OZ et al (2019) Ispol'zovanie ostatochnoj prochnosti porod v nesushhih konstrukcijah pri podzemnoj dobyche rud (Use of residual rock strength in bearing structures in underground ore mining). *RUDN J Eng Res* 20(2):193–203. <https://doi.org/10.22363/2312-8143-2019-20-2-193-203>
16. Lugantsev LD (2020) Tischenko SL (2020) Komp'yuternyj monitoring ostatochnogo resursa jelementov konstrukcij pri korrozionnom vozdejstvii (Computer monitoring of the residual life of structural elements under corrosion). *Math Methods Eng Tech—MMTT* 3:52–55
17. Lyudmirsky YG, Assaulenko SS, Kramskoi AV (2022) Metodiki i oborudovanie dlja jeksperimental'noj ocenki rabotosposobnosti obolochkovykh i korpusnykh konstrukcij (Methods and equipment for experimental evaluation of the performance of shell and hull structures). *Adv Eng Res* 22(3):252–260. <https://doi.org/10.23947/2687-1653-2022-22-3-252-260>
18. Mandritsa DP (2020) Vyjavlenie rezervov jekspluatacionnoj prigodnosti materialov i konstrukcij pri osobykh nagruzkah (Identification of reserves of operational suitability of materials and structures under special loads). *Proceed Tula State Univ Tech Sci* 12:355–361
19. Minasyan AA (2022) Kriterii prochnosti korrozionno povrezhdennogo betona pri ploskom napryazhennom sostojanii i ostatochnyj resurs nesushhej sposobnosti plit perekrytija (Criteria for the strength of corrosively damaged concrete in a flat stressed state and the residual life of the bearing capacity of the floor slabs). *Modern Const Architect* 5(29):11–16

20. Shalyi EE, Leonovich SN, Kim LV et al (2018) Remont i prognozirovanie dolgovechnosti otremonirovannyh zhelezobetonnyh gidrotehnicheskikh sooruzhenij (Repair and forecasting of durability of repaired reinforced concrete hydraulic structures). In: SMARTBUILD'2018: Object-spatial design of unique buildings and structures. First scientific and practical forum, Ivanovo, November, pp 97–102
21. Shmelev GD, Ishkov AN, Drapalyuk DA (2022) Metod prognoza ostatochnogo sroka sluzhby po veroyatnomu snizheniju nesushhej sposobnosti jekspluatiruemykh stroitel'nykh konstrukcij (A method for predicting remaining service life according to the probable decrease in the bearing capacity of the operated building structures). Housing Utilities Infrastruct 2(21):9–18. <https://doi.org/10.36622/VSTU.2022.21.2.001>
22. Shmelev GD, Ishkov AN, Shmelev AG (2022) Raschet ostatochnogo sroka sluzhby zhelezobetonnykh konstrukcij shahty reaktora jenergobloka AJES (Calculation of the residual life of reinforced concrete structures in the reactor shaft of the NPP power unit). Housing Utilities Infrastruct 4(23):9–20. <https://doi.org/10.36622/VSTU.2022.23.4.001>
23. Smolyago GA, Frolov NV (2019) Sovremennye podhody k raschetu ostatochnogo resursa izgibaemykh zhelezobetonnykh jelementov s korrozionnymi povrezhdenijami (Modern approaches to residual life calculation of flexural steel concrete elements with corrosion damage). Bull Tomsk State Univ Architect Civil Eng 21(6):88–100. <https://doi.org/10.31675/1607-1859-2019-21-6-88-100>
24. Utkin VC, Soloviev CA (2019) Opredelenie ostatochnoj nesushhej sposobnosti i nadezhnosti nesushhih jelementov zhelezobetonnykh konstrukcij na stadii jekspluatsii (Determination of residual load-bearing capacity and reliability of load-bearing elements of reinforced concrete structures at the operational stage). Vologda State University Publication, Vologda
25. Stupishin LYu (2022) Kriticheskie urovni vnutrenney potentsialnoy energii deformatsii tverdykh deformiruemykh tel (Critical levels of internal potential energy of deformation of solid deformable bodies). NRU MGSU Publication, Moscow
26. Stupishin LY (2018) Predelnoe sostoyanie ctroitelnykh konstruksiy i kriticheskie urovni energii (Structural limit state and critical energy levels). Indust Civil Eng 10:102–106
27. Stupishin LY, Mondrus VL (2022) Critical energy properties study for unsymmetrical deformable structures. Buildings 12(779):1–12. <https://doi.org/10.3390/buildings12060779>
28. Stupishin LY, Moshkevich ML (2022) Limit states design theory based on critical energy levels criterion in force method form. Magazine Civil Eng 111(3):11. <https://doi.org/10.34910/MCE.111.1>
29. Stupishin LY, Nikitin KE (2021) Komp'yuternaja sistema analiza sooruzhenij na osnove metoda kriticheskikh urovnej jenerгии (Computer system for the analysis of structures based on the critical energy levels method). In: BIMAC'2021: BIM modeling in construction and architecture. St. Petersburg, April. pp 223–230. <https://doi.org/10.23968/BIMAC.2021.000>



Historic Building Information Modeling in the Context of Architectural Education

G. Zakharova^(✉)

Ural State University of Architecture and Art, 23, K. Liebknechta St., Yekaterinburg 620075,
Russia
zakharova@usaaa.ru

Abstract. One of the most demanded areas of digitalization in the architecture and construction industry is BIM—building information modeling as an effective tool for managing an object throughout its entire life cycle. In recent decades, worldwide interest in the application of this technology to architectural heritage has been steadily increasing, as evidenced by the large number of publications on HBIM—historical building information modeling. Researchers note great opportunities in the application of information models for the preservation and study of heritage. At the same time, there are barriers to wider dissemination of the technology. Firstly, this is a definite complexity of creating the model through laser scanning and photofixation with next processing and elaboration unique parametric elements in computer programs. Secondly, the group of specialists involved in heritage projects as a rule is poorly versed in information technology, and specialists are not always ready to work with models. But at a minimum architects working with historic buildings should become guides in applying and explaining modern approaches and methods of working with heritage. Therefore, the topic of teaching HBIM in architectural universities needs to be given more attention both in practical work and in scientific research. This article contributes to this relevant and necessary topic. Examples of the implementation of BIM models for historical buildings in Yekaterinburg, including constructivist objects, made by students of the Applied Informatics in Architecture department of the Ural State University of Architecture and Art are given, the use of BIM for computer-aided design of solid 3D model is shown, for which an appropriate technology was developed. With a small number of BIM curricula that are slowly being implemented at the university level, a practice-oriented methodology for learning new technologies is offered.

Keywords: BIM · Building information modeling · HBIM · Historic BIM · Architectural education · BIM teaching · Historic buildings · Applied informatics in architecture

1 Introduction

Over the past decades, digital methods in the architectural and construction industry have been increasingly used. Among them, one of the most popular areas is building information modeling—BIM. The complex work of all project participants with different

roles at different stages has shown its productivity, in a number of countries BIM is being introduced as a mandatory technology at the government level. Thanks to a systematic approach, information modeling allows you to maintain the integrity of the representation of the created object both in time due to its relevance at all stages of the life cycle, and in space: all related information, characteristics, documents and data are systematized and stored in a single environment. The protocol adopted in the UK [1] as one of the countries with the most developed BIM defines BIM as a collaborative way of working based on digital technologies that open up more efficient methods for designing, delivering and maintaining physical built assets. BIM embeds key product and asset data into a computer 3D model that can be used to effectively manage information throughout the asset's lifecycle.

BIM is successfully implemented for newly created objects, as it is built in stages, taking into account all the requirements for project documentation. As for buildings built in the "pre-information" era, the use of BIM also brings a significant effect for their fixation, study, restoration, reconstruction, condition monitoring, and much more [2].

The events of April 2019, when Notre Dame Cathedral was significantly damaged by fire, showed the relevance and urgent need for a detailed digital representation of World Heritage sites. For restoration work, Autodesk was able to create a BIM model of the Notre Dame Cathedral in the form in which it existed before the fire based on data obtained before the fire using Reality Capture technologies [3]. Thus, conditions were created for the joint work of all project participants in the cloud and access to up-to-date data and plans. The data for the BIM model was obtained thanks to Professor of Vassar College Andrew Tallon, who thanks to his passion for Gothic architecture scanned the Cathedral with an accuracy of 5 mm [4]. This tragic event calls for every major cultural heritage site to be digitized so that it can be restored in the event of destruction or degradation.

The relevance of HBIM is also explained due to the fact that over time the number of heritage buildings that need a restoration, repair, reconstruction is increasing, these works make up a high percentage in the construction industry. In addition, the workflow in historical architecture projects is poorly formalized, information is scattered, and outdated tools are used. The stakeholders involved in the project—archaeologist, archivist, architect, civil engineer, restorer, etc., often work separately, create disparate data, sometimes duplicating work [5]. As one of the solutions of the problem, article [5] proposes the web platform for implementing the HBIM protocol, called BIMlegacy, which covers all stages of working with an heritage object: registering a building, determining intervention options, developing an intervention project, planning physical intervention, physical intervention, transmission, maintenance and dissemination of culture and historical information. The protocol is intended for the work of all interested parties in a common information field.

For unique buildings of architectural heritage, the task of building an information model is quite complicated [6], and this also prevents the widespread practical implementation of HBIM technology in the restoration and reconstruction of historical buildings.

Another deterrent to the spread of technology is that the group of professionals involved in heritage projects as a rule does not always know modern technologies and

express doubts about the validity of using BIM. The economic benefit is also not obvious: laser scanning and design are more expensive than traditional methods, and it is not always possible to save money at the production stage [7].

In such a situation it is important that architects working with historic buildings be guides in applying and explaining modern approaches and methods of working with heritage. For this, it is necessary to introduce systematically relevant topics into the educational process of architects. The public education system is slowly responding to the challenges of the time, BIM technologies at universities at the level of educational standards and new educational programs are just beginning to be implemented at some universities. Therefore, it seems important to find ways to quickly introduce innovative technologies into the educational process in order to receive specialists who meet modern requirements.

Next, we will briefly present the essence of HBIM technology, and then we will present our experience in BIM modeling of historical buildings: we will show a practice-oriented methodology for teaching new technologies and some HBIM projects completed by students of the Applied Informatics in Architecture program at the Ural State University of Architecture and Art.

2 HBIM Technology

HBIM technology over the past decade has become increasingly widespread in the world. In the Google Scholar search engine, more than 1200 articles on this topic are identified in 2022 and 2023 alone, and 4400 in all time. There are a lot of individual case studies, as well as summaries on methods, tools and software. Thus, in a systematic review of the literature [8], based on about 200 primary studies, a modern HBIM workflow was elaborated, and possible difficulties that may be encountered are given. It has been suggested that HBIM will replace the traditional survey and restoration process in the near future. The review [9] noted the integration of HBIM with such innovative technologies as virtual and augmented reality (VR / AR), artificial intelligence (AI) methods and identified the potential of HBIM in these areas. In [10] it is described how an ontology of a digital model of a heritage object is formed as a digital twin, which includes not only a graphical 3D representation of the object, but also all information related to it in the form of a knowledge graph.

From the point of view of the geography of HBIM distribution, the study [11] noted many European countries, it is shown that this topic is most actively developed in Italy and the UK. In Russia, academic research on heritage information modeling is beginning to become more widespread. For example, a wide range of such studies is presented in the review [12], which covers more than 50 references. Here, in particular, links are given to the works of the Department of Historical Informatics of Moscow State University named for M.V. Lomonosov, Novosibirsk State University of Architecture and Civil Engineering (Sibstrin), Ural State University of Architecture and Art. We also note here the work of the Department of Architecture and Urbanism of the Perm National Research Polytechnic University on the development of methods and tools for digital documentation of historical objects [13].

Further in this section, the essence of HBIM will be briefly introduced, some typical examples will be given. Promising areas of application of this technology collected from many sources will also be listed.

2.1 The Essence of HBIM, Some Examples

The term HBIM was introduced in 2007 in an article [14] as BIM, whose parametric rules can be derived from “architectural pattern books of the eighteenth century”. Papers [14, 15] describe the HBIM process, which starts with remote data collection using a ground-based laser scanner in combination with digital cameras, then uses a series of computer programs to combine images and scanned data. Parametric objects for historical buildings are unique and usually have complex, irregular shapes, which requires additional processing in computer programs to build unique parametric elements. The model is also saturated with the results of measurements and field studies, as well as historical documentation.

The non-profit organization Historic England published the book in 2017 [16], which reveals the essence of information modeling and provides examples of its application for a large number of heritage sites, highlights their features and the diversity of BIM modeling goals: preventive maintenance, conservation, adaptive reuse, heritage management, research and excursion and educational activities, etc. Here are some examples from the source [16], for every one the visualization is presented and the goals and results of modeling are described: the Waverley railway station in Edinburgh, the Woodseat Hall mansion, the East Club in the Stratford House mansion near Oxford Street in London, etc. The technology of embedding unique building decor elements into the BIM model is also shown using examples. The scanned element on the facade of the building was built as a Mesh model, processed in the CloudCompare, MeshLab and 3ds Max programs and then imported into the Revit family as an object that is geometrically correct in size and location, which looks correct when rendered and reflected in the documentation.

2.2 Applications for HBIM

The variety of architectural heritage objects and their condition determines the variety of goals that HBIM can support, thereby determining the possibilities and benefits of this technology. Next we note some of them found in papers [2, 5, 10, 16–19].

The information model of an architectural heritage object allows:

- to monitor the state of the object and subsequent preventive maintenance;
- develop an optimal plan for the conservation of the object or adaptation for reuse;
- carry out reconstruction with simultaneous maintenance of construction documentation indicating information about each element of the building: material, color, structure, strength, dimensions, features;
- perform cataloging and computer certification of the object, being the source of a detailed element-by-element representation of the object;
- link historical documents to the object (links to Internet sources, adding text and graphic documents to the model), combining the geometric and physical characteristics of the object and digitized documentary and historical evidence;

- to form a library of architectural elements of the past that can be used in modern construction;
- to be a virtual interactive exhibit of a modern museum, contributing to excursion and educational activities;
- to be a model for teaching students;
- to be a model for testing scientific hypotheses and to conduct a comprehensive analysis, taking into account the historical context;
- to save and structure information about the climatic factors of the construction area, the historical context, the cultural landscape;
- to ensure measures aimed at protecting and preserving the cultural heritage site and to preserve the local culture and identity.

3 HBIM in the Educational Process of Universities

BIM technologies are necessary for a modern architect, the relevance of teaching BIM technologies at universities is determined by the growing demand for specialists with relevant competencies in a new dynamically developing digital environment.

Recently, the topic of teaching HBIM in architectural universities is becoming more widespread [19–21]. There are degree courses with specific addresses in “Conservation of Architectural and Environmental Heritage” [22]. Students acquire skills in the field of knowledge, protection, conservation, reuse and enhancement of architectural and environmental heritage. They studied modern instruments and tools for collecting and managing data, from on-field survey to sharing projects and ideas and project management in general.

3.1 Interdisciplinary Education for Work with Heritage

The set of specialists involved in the work for preserving historical buildings is quite wide and is represented by specialists in related fields. Their competencies differ depending on the tasks solved at different stages. Along with specialization in certain areas, it is necessary to form an interdisciplinary holistic vision of all interrelated issues when teaching future architects. The example of such integrative approach is presented in [23], where heritage education is seen as a synthesis of six dimensions: the urban heritage as preserved history; as a geographical context; heritage as an architectural project in the new surrounding development; heritage in its cultural dimension, conveying the traditions and social life of past communities; adaptive reuse designs with sustainability and green architecture in mind; urban heritage as a meaningful sense of place.

In the interdisciplinary educational program “Applied Informatics in Architecture” (the only one in Russia, existed at the Ural State University of Architecture and Arts from 2001 to 2018), the skills of applying information technologies in the design of objects of cultural and historical heritage were formed. The study of BIM, and at the same time the humanities, such as the history of architecture, called the interest of students in the virtual reproduction of heritage objects. Most HBIM projects were developed as final graduate work. In our case, HBIM was a hindsight tool.

3.2 Examples of HBIM Models in the Educational Program “Applied Informatics in Architecture”

Figure 1 shows the information model of the first city theater built in Yekaterinburg in 1845–1847 according to the project of the architect of the Ural Mining Administration K.G. Tursky. This is the first specialized theater building in the Urals, which for a long time was the main theater in Yekaterinburg. The building was repeatedly rebuilt during the time and has survived to this day in a distorted form. The HBIM model reflects the original appearance of the building, which is of aesthetic and cultural-historical value.



Fig. 1 3D reconstruction of the first city theater in Yekaterinburg built in 1845–1847 and the building plan of 1845

3D reconstruction was carried out in the BIM software: Renga and Autodesk Revit in order to compare these programs and identify the advantages and disadvantages of each. The building plan of 1845 and a photograph of the 1880s were the initial data. The plan of the current building was used as reference material. The original drawings have been scaled to fit the remaining elements in the existing building. The scanned plans were used as a substrate for drawing the base plan in AutoCAD and importing it into BIM programs.

The following two examples are 3D reconstructions of historical and architectural heritage of constructivism of federal significance in Yekaterinburg: The House for Officers, built in the period 1932–1941 (Fig. 2) and the Dzerzhinsky House of Culture, built in 1931, where the local history museum is now located. The work was carried out in the Russian BIM software Renga.

To carry out work on modeling and prototyping of the Dzerzhinsky House of Culture (Fig. 3), the archive of the Museum of Architecture and Design of the Ural State Architectural and Art University provided drawings, photographs, a technical passport and documents of the 30 s. The complexity of the work was that the original drawings did not contain dimensions, only the total size of the building was known from the technical passport—72 × 35 m. To obtain the remaining dimensions, the Corel Draw program was used. The drawings of each floor were loaded and outlined and the dimensions were set.

For the interests of the museum, the solid 3D model of the building was further carried out, which ensured the exact transfer of the object from the drawings to the real space. The solid 3D model was glued by hand from drawings obtained in BIM-model and cut out on a plotter. This technology of computer-aided design of solid 3D models of historic buildings based on BIM can be useful for the formation of museum collections.

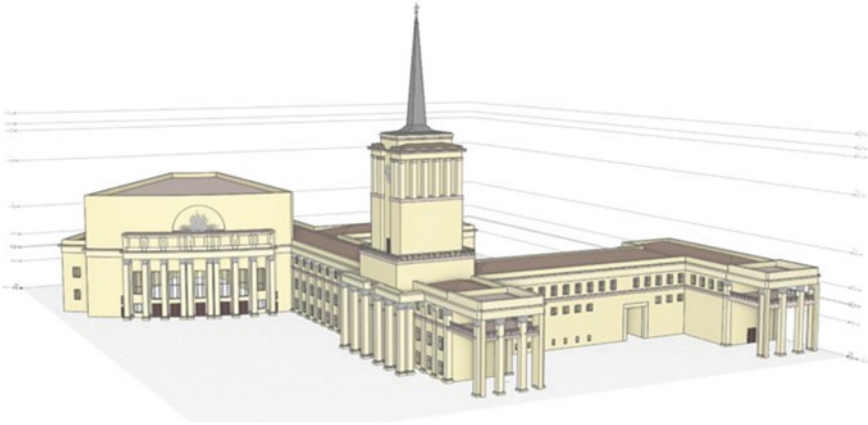


Fig. 2 3D reconstruction of the heritage of constructivism: The House for Officers (1932–1941)

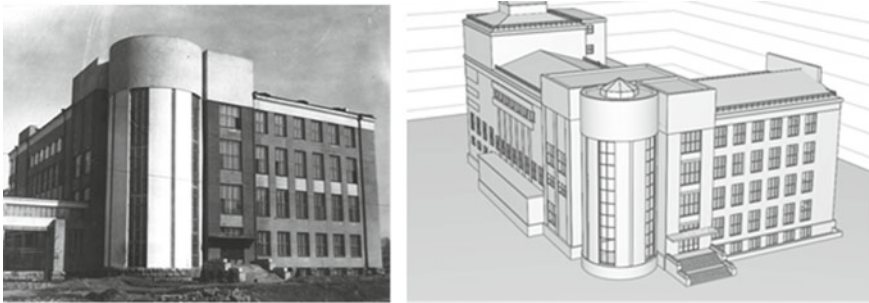


Fig. 3 Dzerzhinsky House of Culture: photo of the 30 s and BIM-model in Renga software

When working with informatics-architects students, a number of projects on heritage information modeling were implemented. Thanks to the study of modern IT technologies, along with the direct use of BIM programs (Revit, Civil3D, InfraWorks, etc.), interactive 3D projects were implemented in game engines (Unreal Engine, Unity) for the implementation of virtual reality, such as shown in Fig. 4.

The educational program should quickly respond to the emergence of new tools, it is necessary to add new topics to the course programs. For teaching, it is useful to involve representatives of IT companies. Also, companies willingly accept students for practice, thereby educating their future employees.

One of the key points in the implementation of a modern educational program is the interaction of educational departments with the mostly developed in BIM IT companies.

We can say that we have formed a practice-oriented methodology for teaching BIM as a basis for working with heritage objects. The methodology allows developing both technical and managerial and communicative competencies. Here are some of the components of this technique:

- introduction of new sections in the computer-aided design disciplines;

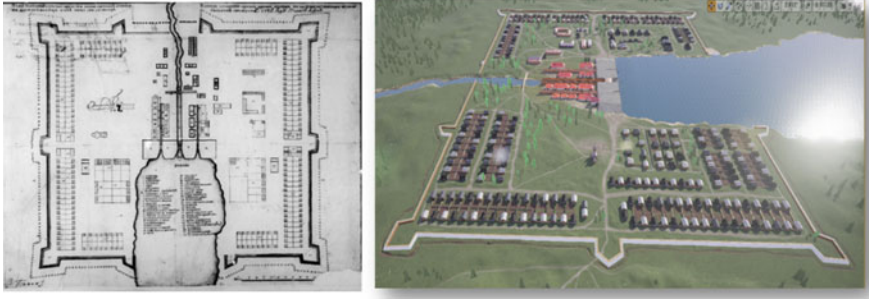


Fig. 4 The plan of Yekaterinburg fortress (1726) and screenshot of its interactive 3D reconstruction

- master classes with the participation of companies that have implemented BIM and BIM software suppliers;
- excursions in the companies, as well as on construction sites;
- conferences and round tables with the participation of students;
- participation of students in competitions of various levels;
- virtual tours projects of any complexity and remoteness;
- interactive sessions to discuss topics including the world's best examples of architecture and preservation of cultural and historical heritage.

4 Conclusion

Information modeling of historic buildings is an urgent need of our time. In order to be able to restore the masterpieces of world architecture in case of their destruction, the heritage must be digitized. The number of historical objects requiring reconstruction or restoration is steadily increasing over the time. Specialists from various fields working in heritage projects often do not know new modern technologies. Therefore, one of the most important tasks of architectural education is the formation of interdisciplinary approaches based on new information technologies.

Building information modeling is fundamentally changing the architecture, engineering, and construction industries and therefore influence the requirements for the educational process. Changes are needed in the curricula and programs of academic disciplines; the development of new educational programs is also necessary.

Understanding the principles of information modeling and mastering the technologies of building models will allow future architects to work competently and carefully with heritage objects.

References

1. AEC (UK) BIM Technology Protocol (2015) Practical Implementation of BIM for the UK Architectural, Engineering and Construction (AEC) Industry, Version 2.1.1. The AEC Initiative: Jakarta, Indonesia

2. Talapov VV (2021) BIM-tehnologiya i arhitekturnye pamyatniki derevyannogo zodchestva (BIM-technology for the restoration of architectural monuments of wooden architecture). <https://integral-russia.ru/2021/12/07/bim-tehnologiya-i-arhitekturnye-pamyatniki-derevyannogo-zodchestva/>. Accessed 15 Jun 2023
3. Hartigan R (2019) Historian uses lasers to unlock mysteries of Gothic cathedrals. *J National Geographic*. <https://www.nationalgeographic.com/adventure/article/150622-andrew-tallon-notre-dame-cathedral-laser-scan-art-history-medieval-gothic>. Accessed 15 Jun 2023
4. Nadeau BL (2019) Professor who scanned all of Notre Dame died months before fire. <https://www.thedailybeast.com/notre-dame-fire-vassar-professor-andrew-tallon-who-scanned-the-cathedral-died-months-before-the-disaster>. Accessed 15 Jun 2023
5. Jordan-Palomar I, Tzortzopoulos P, García-Valldecabres J et al (2018) Protocol to manage heritage-building interventions using heritage building information modelling (HBIM). *J Sustainability* 10(4):908. <https://doi.org/10.3390/su10040908>
6. Murphy M, McGovern E, Pavia S (2009) Historic building information modelling (HBIM). *J Structural Survey* 27(4):311–327. <https://doi.org/10.1108/02630800910985108>
7. Nesterova A (2022) Kak BIM i lazernoe skanirovanie spasayut pri rekonstrukcii i restavraczii istoricheskikh zdaniy (How BIM and laser scanning save the reconstruction and restoration of historic buildings). <https://digital-build.ru/kak-bim-i-lazernoe-skanirovanie-spasayut-pri-rekonstrukcii-i-restavraczii-istoricheskikh-zdaniy/>. Accessed 17 Jun 2023
8. Bastem SS, Cekmis A (2022) Development of historic building information modelling: a systematic literature review. *J Build Res Info* 50(5):527–558. <https://doi.org/10.1080/09613218.2021.1983754>
9. Hussein KA, Ismael EH (2020) State-of-the-art of historic building information modelling—HBIM trends in the built heritage: review paper. *J Eng Sci* 13(3):77–90
10. Niccolucci F, Felicetti A, Hermon S (2022) Populating the data space for cultural heritage with heritage digital twins. *J Data* 7(8):105. <https://doi.org/10.3390/data7080105>
11. Ewart I, Zuecco V (2018) Heritage building information modelling (HBIM): a review of published case studies. In: 35th CIB W78 International Conference: IT in Design, Construction, and Management, 1–3 October, Chicago, Illinois, USA, pp 35–41. <http://centaur.reading.ac.uk/79742/>. Accessed 15 Jun 2023
12. Ermolaeva EI, Mainicheva AY (2020) Opyt primeneniya tehnologii BIM v izuchenii, vossozdanii i muzeifikacii zdaniy i sooruzhenij v Rossii (Experience in the application of BIM technology in the study, reconstruction and museumification of buildings and structures in Russia). *Balandinskie chteniya XV*:460–470. <https://doi.org/10.24411/9999-001A-2020-10051>
13. Maksimova S, Shamarina A, Semina A (2022) Digital survey and information modelling application experience for the historical and cultural heritage objects. In: Rocha A, Isaeva E (eds) *Science and global challenges of the 21st century—science and technology*, Perm, Russia, vol 342, October. *Lecture Notes in Networks and Systems*, Springer Nature Switzerland AG, pp 927–935
14. Murphy M, McGovern E, Pavia S (2007) Parametric vector modelling of laser and image surveys of 17th century classical architecture in Dublin. In: Arnold D, Chalmers A, Niccolucci F (eds.) *VAST 2007 Future technologies to empower heritage professionals*, The 8th International Symposium on Virtual Reality, Archaeology and Intelligent Cultural Heritage, Short and Project Papers, 26–29 November. Brighton, UK, pp 79–84
15. Murphy M, McGovern E, Pavia S (2013) Historic Building Information Modelling – Adding intelligence to laser and image based surveys of European classical architecture. *ISPRS J Photogram. Remote Sens.* <https://doi.org/10.1016/j.isprsjprs>. 2012.11.006
16. *BIM for Heritage: developing a historic building information model* (2017) Swindon, UK, Historic England
17. Logothetis, S, Delinasiou A, Stylianidis E (2015) Building information modelling for cultural heritage: a review. *ISPRS Ann Photogramm Remote Sens. Spatial Inf Sci* II-5/W3:177–183

18. Chiabrando F, Sammartano G, Spano A (2016) Historical buildings models and their handling via 3d survey: from points clouds to user-oriented HBIM. *ISPRS International Archives Photogramm, Remote Sens Spatial Inf Sci XLI-B5*:633–640. <https://doi.org/10.5194/isprs-archives-XLI-B5-633-2016>
19. Khodeir LM, Aly D, Tarek S (2016) Integrating HBIM (heritage building information modeling) tools in the application of sustainable retrofitting of heritage buildings in Egypt. *J Procedia Enviro Sci* 34:258–270. <https://doi.org/10.1016/j.proenv.2016.04.024>
20. Jadresin MR, McPherson P, McConchie G et al (2022) Architectural history and sustainable architectural heritage education: digitalization of heritage in New Zealand. *J Sustainability* 14:16432. <https://doi.org/10.3390/su142416432>
21. Redweik P, Cláudio AP, Carmo MB et al (2017) Digital preservation of cultural and scientific heritage: involving university students to raise awareness of its importance. *J Virtual Archaeol. Rev.* 8:22–34
22. Lombardini N, Achille C, Tommasi C et al (2021) Enhancing and managing data and digital competencies for architecture teaching and training in the field of protection of Heritage (the on-line catalogue of research publications produced by scholars and researchers at the Politecnico di Milano). <https://re.public.polimi.it/handle/11311/1195841>. Accessed 15 Jun 2023
23. Helmy M (2019) The role of architectural education in promoting urban heritage: opportunities and challenges. *IEREK Press The Acad Res Community Publ* 2(3):196

Urban Engineering and Planning



The Rationale and Principles of “Smart Urban Planning”

V. Yu Spiridonov¹, V. A. Kolyasnikov², and S. G. Shabiev²(✉)

¹ Russian Academy of Architecture and Construction Sciences, 24, Bolshaya Dmitrovka St., Moscow 107031, Russia

² South Ural State University, 76, Lenina Ave, Chelyabinsk 454080, Russia
shabievsg@susu.ac.ru

Abstract. This paper considers issues of information and technological support for strategic urban planning. These include goal-setting, forecasting, design, and the effective development of spatial urbanization based on the synergy of modern urban planning theory and the emerging scientific foundations of artificial urban intelligence. The paper proposes a variation of the theoretical model of “smart urban planning”, including the structure of the rationale and principles, as well as the basic information technologies and methods corresponding to these principles. Within this variant, a mechanism is proposed for the introduction of a “cyberphysical urban planning system”, an urban information platform, a “digital twin”, and a “town planning system for self-monitoring”. This mechanism takes into account the need for introducing artificial intelligence to urban planning in order to provide solutions to the problems of smart Big Data collection, the smart introduction of scientific and technological knowledge, smart analysis and systematization of Big Data, smart forecasting, modeling, and design, the smart integration of successful global practices, smart control for implementation, smart transformation and modernization, and self-organization in decision-making. The paper also establishes dialectical contradictions and threats connected with the issues of goal setting, planning, design, and implementation of the development of the spatial object of urbanization. They are presented in the form of a structure of principles of dialectical unity of goal formation, goal structuring, development and self-development, global and regional specialization and cooperation, unity of construction and measurability, and unity of management.

Keywords: Smart urban planning · Theoretical model · Regularities · Principles

1 Introduction

In modern urban development, the mechanisms of strategic urban planning (SUP) are based on the methodological provisions of modern systems theory and urban planning theory. At the same time, the new domain of “smart” technologies is starting to offer an interdisciplinary approach applicable to different field of socio-economic and urban and regional planning (including social and environmental) [1]. By analogy, the concept of “systems” has become a basis for the scientific research.

The relatively new concept of smart specialization focuses on the SUP of any spatial urban object. This is due to the effective concentration of scientific, material, and investment resources in its unique features, considered as competitive advantages in terms of adaptation to the global economy [2, 3]. It is currently being used in more than 130 regions and states of Europe [4] for the development of strategies for economic, innovative, and urban development. Smart specialization is recommended by the European Commission for use in all territories of the European Union. The existence of an approved Smart Specialization Strategy (Regional Research and Innovation Strategy for Smart Specialization—RIS3) is a requirement for funding regional development programs from the European Union Development Fund [5].

Accordingly, a smart city and a smart region is considered as part of a higher-level settlement system which effectively develops a system of knowledge and competencies based on its unique territorial-organizational, socio-economic, innovative-infrastructure, territorial-planning, architectural-planning and innovative features [6–9].

This development is directly related to the organization of economic, socio-cultural, ecological and other partnerships in the relationships between spatial urban objects, in the structure of higher-ranking urban planning systems (subsystems, clusters) and within the system itself [10, 11].

Globalization has given the SUP of urban planning systems a special role in urbanization, taking into account socio-economic, landscape, ecological, natural, and climatic integration and communication, and to resolving relevant problems, crises, and threats. The aim is to ensure the relations among socio-economic macro-regions, “world cities”, and transnational and transcontinental structures, as well as the interaction between the natural-ecological, anthropogenic environment and humanity [12, 13]. There has also been a rapid increase in the unpredictability of the SUP of urban systems, and this is directly reflected in the emergence of a significant number of new methods, mechanisms, and approaches to SUP of an urban object as a complex system.

There is also a rapid progression in the unpredictability of urban planning systems and this is directly reflected in the emergence of a significant number of new methods, mechanisms, and approaches to urban planning as a complex system. Such methods, mechanisms, and approaches include planning for sustainable and inclusive development, strategic, predictive probabilistic, implementing, institutional, participatory, initiative planning, as well as other types of urban planning [2, 14–18].

This situation requires a unique individual system of SUP for the progressive development of a spatial urban object, based on advanced information and communication, other digital and intellectual technologies, the effective use of accumulated scientific, technological knowledge and achievements in spatial transformation and modernization [19–24]. Therefore, it is difficult to overestimate the role of the integration of AI, Big Data, and digital twins in SUP for innovative and spatial development.

An effective mechanism of SUP for the development of a large urban planning system, necessitates the introduction of intelligent infrastructure to automate the monitoring and systematization of Big Data, communications, intelligent analysis, modeling and design, and the automated control of implementation and self-organization in decision-making (data-driven decision-making systems).

Taking the above into account, the scientific foundations of “smart urban planning” should be established to form a synergy of the methodology of modern SUP with the emerging foundations of urban AI [25–28].

The main purpose of this study is to develop a theoretical model for smart urban planning, consisting of principles and the basic information technologies and methods corresponding to these principles. According to the data above, such a structure needs to take into account the dialectical contradictions and threats related to the SUP of spatial urban objects.

2 Foundation: The Theoretical Model of “Smart Urban Planning”

Based on the synergy of modern SUP and urban AI, the present work proposes a structure of the laws and principles of smart urban planning for the development of complex urban planning systems. Four groups of rationale can be established: smart goal setting; smart forecasting; smart design; and smart implementation. Each of these four groups contains the principles of digitalization—integration, implementation, and automation.

The principles of digitalization are connected with the integration of Big Data, digital twins, and AI into the innovative and spatial development of the urban planning system at all levels of the forecasting, planning, design, and management of the urban planning system. They are based on the necessity and possibility of introducing advanced information and communication, other digital and intelligent technologies, as well as on the effective use of the Internet of Things, accumulated scientific and technological knowledge, and achievements in spatial transformation and modernization. These principles also take into account the availability of appropriate technological infrastructure, human capital, and internet literacy, access to infrastructure, including institutional regulation, and inclusion in the technology market.

The rationales of smart goal setting for the development of urbanization ensure the dialectical unity in goal formation and goal structuring. They can be seen in the principles of the balance of (1) stages and uniformity; (2) realism and idealization; (3) complexity and autonomy; (4) controllability and self-determination; (5) conformity and individuality; and (6) the goals.

The implementation of these rationales and principles is by introducing a “cyber-physical urban planning system” into the goal-setting process as a complex distribution system of the interconnections of the computational and physical elements (resources) of an urbanized object. It constantly receives data from the environment (via the Internet of Things) and uses them to further optimize the processes of urban planning and management of the development of a city or region.

The balance of stages and uniformity is associated with the establishment of planning goals based on the stages of development of spatial systems: transitional, homeostatic, and coevolutionary. The goals of the co-evolutionary stage are aimed at harmonizing the interaction of society and nature in the movement towards the noosphere (according to V.I. Vernadsky).

This principle takes into account the planning and the changing cycles of urban development, including the cycles of the quantitative territorial growth (extensive phase) and the qualitative development (intensive phase) of the architectural and spatial environment.

The balance of realism and idealization is linked to the dependence of goals on the stage of cognition of the object, as well as on the time perspective of planning. The long-term goal is an ideal achieved by consistent realistic decisions related to the order of the implementation of strategies, methodologies, programs, and projects. The main goal of the spatial development of the urban planning system should be the harmonization of architectural and planning by means of the joint development of people, nature, and architecture. This also needs to take into account the consistency and compromise of global, regional, and local solutions and to highlight the tasks of ensuring a healthy and safe environment, social security, reproduction of people and nature, the rational use of the environment and resource conservation in the interests of present and future generations.

The balance of complexity and autonomy considers the balance of external influences and internal factors in order to effectively develop an urban object. Such development is based on the features and objectives of the system at a higher level. The goals of architectural and planning development must comply with the requirements of applicable laws and regulatory documentation, international, federal, regional and local norms and regulations, and national security requirements. They must be coordinated with previously developed proposals, plans and programs for the strategic socio-economic, urban planning, historical, cultural, environmental, and ecological development of the territory.

The balance of controllability and self-determination is associated with the effect of the objectives of the urban planning systems above the hierarchical level, when compared with the objectives of the underlying ones. It is also closely linked to the awareness and acceptance of the motivational features of the overlying urban planning system such as will, self-determination, and freedom of choice of the planning for the object under consideration.

The balance of conformity and individuality requires the use of tree-like, matrix, or network forms of representation of the objectives which correspond to the stages of cognition.

The balance of goals is based on the structure of the goals for the effective development of the urban planning system. It takes into account the balance of global, state, regional, and local interests, economic and environmental goals, functional and aesthetic goals, and the goals of continuity and innovative development in urban planning, as well as the prioritization of these goals.

The rationales of smart forecasting include the principles of dialectical unity for the development and self-development, both global and regional. These are the principles of the balance of (1) management and self-organization; (2) economy and ecology; (3) innovation and traditions; (4) sustainability, in order to identify and take into account the interests of the regional population and future generations; (5) inclusiveness and exclusivity; and (6) communicative integrality and alienation.

The implementation of the rationales and principles of smart forecasting is associated with the introduction of an “urban information platform”, considered as an AI platform for managing databases of big spatial data with the functions of automated information and analytical support for the exercise of powers of property and urban planning, including social and environmental activities. The characteristics of such a

platform are smart forecasting, the smart analysis of Big Data, and the smart processing and systematization of this data.

The balance of management and self-organization is associated with the acceptance of compromise in the management and self-organization of the planning object as a complex urban planning system characterized by stochasticity and non-deterministic behavior, and is based on the variability, alternativeness, and probabilistic nature of planning decisions.

This principle takes into account the need to understand the compromises between the directive management of urban development and the natural self-development of the spatial system, and the role of management processes in matters of strategic urban planning.

The balancing of economic and environmental decisions is aimed at ensuring environmental and technological safety, resource conservation, and ensuring the reproduction of the ecological environment. It is connected with the balance of solutions between the natural environment (including geological, morphological, and general climatic features), the anthropogenic environment, and humanity (with its various forms of community and communication), while ensuring the interaction and interdependence of the natural and anthropogenic environment and humanity, as well as with the greening of the architectural and spatial system by means of engineering. It focuses on the internal socio-ecological conditionality which determines the ecological priority in the formation of economic, functional, urban, historical, cultural, and aesthetic frameworks and structures of the planning object.

The balance of innovation and traditions is associated with the traditions of urban culture. It defines the study and modeling of the spatial urban object as an object of urban art and urban culture; the development of ideas about the beauty and aesthetic expressiveness of the architectural and spatial environment; measures to protect historical and cultural monuments; and the identification and use the unique features of the spatial system as a special resource.

The balance of sustainability is associated with the establishment of a balance of interests of the present population of the territory and the comfort and safety of future generations. It also takes into account the possible damage and conditions for its repair for these future generations. This principle takes into account three types of possible damage to sustainable development: economic, social, and environmental. The balance of sustainability determines the trade-offs between the interests of the regional level with the 17 global goals adopted at the 2015 United Nations Summit on Sustainable Development.

The priorities of spatial planning for the sustainable development of the urban planning system include ensuring a sustainable balance between the infrastructural, ecological, socio-economic, functional-economic, historical-cultural, and aesthetic well-being of the territory. Other objectives include a sustainable balance between urban planning and engineering solutions; a balance of economic and environmental processes; the coordinated development of territories at various levels; and the rational use of natural resources in the interests of present and future generations.

The balance of inclusiveness and exclusivity is aimed at ensuring the creation of equal social, legal, and other conditions with different socio-economic opportunities for different groups of the population. For example, the introduction and promotion of different classes and categories of housing for consumers with different purchasing capabilities. This is connected with an awareness of the resources which allow an improvement in the quality of life and ensuring equal opportunities for all groups of the population. This principle is directly related to the international rules of inclusive growth: Economic development, Standard of Living, and Inequality [29].

This balance of inclusivity and exclusivity is also characterized by the priority of interests of the local residents in relation to the external population, where these residents are bearers of unique cultural skills, knowledge, and competencies. They are both competitive and predominant factors.

The balance of communicative integrality and alienation takes into account the variety of contradictory interdependencies of the planning object in global urban and infrastructural communication. This principle is aimed at integrating the spatial object of planning into the global system of interaction of socio-economic macro-regions, world cities, and transcontinental links, as well as resolving possible conflicts and threats associated with these processes. This principle is characterized by interests of national security.

The rationales of smart design are revealed in the principles of dialectical unity of specialization and cooperation, unity in construction and measurability. These are the principles of the balance of (1) uniqueness and universality; (2) partnership and competition; (3) structuring and amorphousness; (4) hierarchy and equivalence; (5) diversity and homogeneity; (6) dynamism and staticism; (7) integrity and fragmentation; (8) being open and being enclosed; (9) accessibility and autonomy; (10) attraction and rejection; (11) rationing and personalization; and (12) optimization and harmonization.

This group of principles is connected with the establishment of a balance of priorities between the unique features of an urban development, in terms of its competitive advantages and partner relationships, and with the establishment of quantitative indicators of the quality of the urban environment. In this study, the design state for the estimated period is considered as standard, and in the forecast as optimal and harmonious.

The rationales of smart design are directly related to the introduction of digital twins. This is an interactive digital model of an urban development object embedded in its planning and management system. It is based on a comprehensive analytical urban information computer platform whose main objectives are smart modeling, smart design, and the smart integration of successful practices.

The balance of uniqueness and universality is based on the effective concentration of scientific, material, and investment resources in the unique features of the spatial planning object. These factors are considered competitive advantages in terms of the object's adaptation to the global economy. The uniqueness of urban planning resources is determined by the identification and development of the unique features of historical, cultural, natural, functional, economic, communication, innovative, and aesthetic character, as the spatial potential of the development of the territories under consideration, as well as the formation of appropriate urban planning frameworks based on these features. This principle is connected with the awareness of the use of the priorities described

above and the application of the best international practices as universal mechanisms of SUP in resolving the issues of a specific territory.

The balance of partnership relations and competition is based on the understanding of the need, or lack of such, to establish interstate, macro-regional, and local administrative-legal, socio-economic, natural-climatic, natural-geographical, historical, cultural, and other relationships and the corresponding areas of joint interest.

There are several levels of significance for territories of joint interest and partnerships: interstate; state; inter-macro-regional; macro-regional; and local. According to these levels, the types of possible competition are determined by one or another party using this resource as an initiative advantage.

The balance of structuring and amorphousness is aimed at zoning the territory of the urban planning system; the identification of subsystems, stable zones, elements, and connections; the identification of the most significant objects of capital construction; and the formation of the structures and frameworks of spatial development. In order to implement this principle, methods are used to identify and model stable and changeable elements and connections; significant capital construction projects; the construction of ecological, economic, functional (urbanized), historical, cultural and aesthetic frameworks; ecological and urban planning; economic and urban planning; functional planning; and the historical, cultural and aesthetic zoning of the territory as necessary conditions for the effective development of the architectural and spatial system.

The balance of hierarchy and equivalence is aimed at controlling the effects of overlying urban planning systems at higher level in comparison with the underlying ones, as well as influencing the underlying systems on the overlying ones. It is connected with the hierarchy of structures and frameworks of the urban planning system, its zones, elements, connections, and the distribution of major and minor capital construction projects. This principle defines the establishment of a hierarchy of: urban planning systems and their subsystems; ecological, economic, functional (urbanized), historical, cultural, and aesthetic structures of architectural and spatial systems; their zones, elements, connections, and capital construction objects; and modeling taking into account their dependence and subordination.

The balance of diversity and uniformity establishes the presence of functional-planning, ecological, and other heterogeneities of the territories in the architectural-planning system. This principle is connected with the identification and development of various hierarchical and morphological subsystems of the design object. This includes: its ecological, economic, functional, historical, cultural, and aesthetic structures and frameworks; their zones, elements, and connections; the diversity of capital construction objects; and the use of typology and the development of diversity as a necessary condition for the effective development of the object under consideration.

The balance of the dynamism and static nature of the main structures (administrative-legal, socio-economic, environmental, natural-geographical, socio-cultural and historical-cultural) and elements of the urban planning system. This principle is aimed at the growth, adaptability, and transformation of the architectural and planning system, as a reaction to external disturbing influences and internal processes.

The balance of integrity and fragmentation concerns the functional urbanized and natural-ecological zones and structures of the urban planning system. This principle

establishes the internal connectivity of subsystems, structures and frameworks of the urban planning system; its zones, elements, and the most significant objects of capital construction, as well as the interaction of the system with adjacent systems. The methods of implementing this principle are the spatial consistency of the structures and frameworks of the system under consideration with the structures and frameworks of the systems overlying the hierarchy; ensuring the functional and compositional connectivity of the elements of the architectural and planning system itself; and the identification and modeling of zones and areas of influence of the elements in the system.

The balance of being open and being enclosed is associated with ensuring the flexibility of the urban planning system by the open or enclosed nature of ecological, economic, functional, historical, cultural, and aesthetic structures and frameworks of a spatial urbanized object and its modeling, taking into account architectural and planning continuity and modernization.

The balance of accessibility and autonomy or barrier determines the regulatory, socio-cultural and other forms of differentiation and relative independence of various social forms expressed in spatial activities.

The balance of attraction and rejection or delaying of socio-economic and urbanization activities is associated with the preservation of the integrity of the urban planning system in conditions of internal competition.

The balance of rationing and personalization of the urban planning system determines the measurability and efficiency of the projected state of the architectural and planning environment based on its compliance with the requirements of regulatory documentation. The methods are the balance of design solutions based on the requirements of norms and standards. These take into account the threshold indicators of the development of the urban planning system. Such documentation should include international norms and standards and an index assessment of sustainable and inclusive development; international, state, and regional norms and standards and indexes of urban planning design (including smart cities and smart regions); and standards of urban planning design at all levels.

The optimization of an urban-planning object establishes the measurability and efficiency of the projected state of its architectural and planning environment based on the identification and consideration of local characteristics and development strategies of specific territories.

The principle of harmonization establishes the measurability and efficiency of the projected state of the architectural and planning environment of a spatial urbanized object, based on compositional orderliness, and in strategic terms the compositional unity of the natural and architectural-spatial environments. Compositional orderliness is characterized by artistic and figurative content, the morphological integrity and expressiveness of the architectural and planning system. The compositional unity of the natural and architectural-spatial environment is aimed at ensuring the co-evolutionary harmonious development of people, nature, and architecture.

The composition of the architectural and planning system is largely determined by the development of urban culture, urban tradition, and urban art. Urban culture is understood as the general artistic and aesthetic level of urban planning. Urban tradition is the continuity of urban objects, while urban art is architectural creativity, consisting

of the ability of architects and urban planners to create planning and spatial stylistic compositions of urban objects with the involvement of elements of the natural landscape. The harmonization of the architectural and planning system include the identification and modeling of conceptual, morphological, sign, and information structures of such a system, as well as the synthesis of natural and urbanized landscapes.

The rationales of the smart implementation of the development of the urban planning system are established by the principles of dialectical unity in management: (1) the balance of the implementation and regional interests; (2) the balance of strategic and tactical management; (3) the balance of institutionality and private interests; (4) the balance of regulation and self-determination; (5) the balance of participation and state interests; and (6) the balance of controllability and self-management.

The implementation of these rationales and principles is characterized by the introduction into the urban information platform of an “urban implementation monitoring system”. This system will ensure the processes of smart control, smart transformation and modernization, and smart self-organization in decision-making.

The balance of implementation and regional interests will establish the requirements for the implementation of international obligations at the domestic, including at the regional and local levels, while maintaining internal regional needs and priorities.

The balance of strategic and tactical management establishes the need for the inter-related development of urban planning documents and strategic plans for the spatial development of the architectural planning system and the corresponding programs and implementation projects. This principle is also associated with the possibility of changes in urban planning documents and strategic spatial development plans when required by the state.

The balance of institutionality and private interests is conditioned by the need to take into account the existing spatial institutions as processes of social consolidation for individual territories with the subjects and objects of certain functions. This principle takes into account the development of spatial institutions with their social norms, rules, and restrictions.

The balance of regulation and self-determination is associated with the formation of rules for the use of territories based on documents regarding urban planning, the historical-cultural context, the environmental, and ecological zoning. Zoning documents are considered to be flexible documents of urban planning regulation, allowing appropriate deviations from the established regulations.

The balance of participation and state interests is connected with the interests of residents, businesses, and scientific and public institutions, as well as with ensuring the formation of a comfortable, safe, and well-maintained living environment within the development of the urban planning system. This principle also takes into account the priority of state issues and objectives.

The balance of controllability and self-management establishes the need to monitor the implementation of design solutions, analyze and evaluate the effectiveness of their results, as well as to adjust the proposals of project documentation, including the revision of the development objectives of the architectural and planning system.

3 Conclusion

This study proposes a variation of the theoretical model of smart urban planning, as represented by the system of goal-setting–forecasting–design–implementation. It is based on the synergy of the methodology of modern SUP and the emerging scientific foundations of urban AI. This version of the theoretical model consists of the principles and the basic information technologies and methods which correspond to these principles. The study also defines the mechanism for implementing the cyberphysical urban planning system, the urban information platform, the digital twin, and the urban planning system of self-monitoring.

The rationales of smart goal-setting are established in the balance of (1) stages and uniformity; (2) realism and idealization; (3) complexity and autonomy; (4) controllability and self-determination; (5) conformity and individuality; and (6) the domination of goals. The regularities of smart forecasting are determined by the principles of the balance of (1) management and self-organization; (2) economy and ecology; (3) innovation and traditions; (4) sustainability in order to identify and take into account the interests of the regional population and future generations; (5) inclusiveness and exclusivity; and (6) communicative integrality and alienation. The rationales of smart design are established in the balance of (1) uniqueness and universality; (2) partnership and competition; (3) structuring and amorphousness; (4) hierarchy and equivalence; (5) diversity and homogeneity; (6) dynamism and staticism; (7) integrity and fragmentation; (8) being open and being enclosed; (9) accessibility and autonomy; (10) attraction and rejection; (11) rationing and personalization; and (12) optimization and harmonization. The rationales of smart implementation lie in the balance of (1) implementation and regional interests; (2) strategic and tactical management; (3) institutionality and private interests; (4) regulation and self-determination; (5) participation and state interests; and (6) controllability and self-management.

References

1. Lyshchikova J, Stryabkova E, Glotova AS (2019) The ‘smart region’ concept: the implementation of digital technology. *J Adv Res Law Economics* 10. [https://doi.org/10.14505/jarle.v10.4\(42\).34](https://doi.org/10.14505/jarle.v10.4(42).34)
2. Markkula M, Kune H (2015) Making smart regions smarter: smart specialization and the role of universities in regional innovation ecosystems. *J Tech Innov Manage Rev* 5:7–15
3. Manolov G, Orlova D (2020) A Smart specialization strategy for sustainable development of regions. In: E3S Web of Conferences 208. <https://doi.org/10.1051/e3sconf/202020808009>
4. Stryabkova EA, Lyshchikova YV (2018) From smart city to smart region: concept evolution or new development paradigm. *J Econ: Yesterday, Today* Tomo 8:248–255
5. Polido A, Pires SM, Rodrigues C, Teles F (2019) Sustainable development discourse in smart specialization strategies. *J Clean Product* 240. <https://doi.org/10.1016/j.jclepro.2019.118224>
6. Sinkienė J, Grumadaitė K (2014) Sumanaus regiono konceptualusis modelis. *J Viešoji politika ir administravimas public policy and administration* 13:414–426. <https://doi.org/10.5755/j01.ppa.13.3.8305>
7. Mazza PI, Mavri M (2019) From smart cities to smart regions as a solution to improve the sustainability of urban communities. *J Studia Ekonomiczne* 389:60–80

8. Bauer M, Helbig D, Mokhov V, Eltsova M (2019) Smart region concept as a solution for sustainable development for region with a rural and urban character. *J Phys* 1415. <https://doi.org/10.1088/1742-6596/1415/1/012018>
9. Matern A, Binder J, Noack A (2020) Smart regions: insights from hybridization and peripheralization research. *J Europ Plann Stud* 28:2060–2077. <https://doi.org/10.1080/09654313.2019.1703910>
10. Sutriadi R (2018) Defining smart city, smart region, smart village and Technopolis as an innovative concept in Indonesia’s urban and regional development themes to reach sustainability. *J Earth Environ Sci* 202. <https://doi.org/10.1088/1755-1315/202/1/012047>
11. Billones RKC, Guillermo MA, Lucas KC, Era MD, Dadios EP, Fillone AM (2021) Smart region mobility framework. *J Sustain* 13. <https://doi.org/10.3390/su13116366>
12. Spiridonov V, Shabiev S, Aliukov S (2022) Scientific aspects of the study of transcontinental relations and global settlement. *J Land* 11. <https://doi.org/10.3390/land11030342>
13. Robinson J (2002) Global and world cities: a view from off the map. *J Urban Reg Res* 26:531–554. <https://doi.org/10.1111/1468-2427.00397>
14. Cialfi D (2021) Smart Regions in the Italian context. From a theoretical to an empirical framework. <https://doi.org/10.20944/preprints202110.0271.v1>
15. Anthopoulos LG, Vakali A (2012) Urban planning and smart cities: interrelations and reciprocities. *J FIA* 7281:178–189
16. Karvonen A, Cook M, Haarstad H (2020) Urban planning and the smart city: projects, practices and politics. *J Urban Planning* 5:65–68. <https://doi.org/10.17645/up.v5i1.2936>
17. Fialová J, Bamwesigye D, Łukaszkiewicz J, Fortuna-Antoszkiewicz B (2021) Smart cities landscape and urban planning for sustainability in Brno City. *J Land* 10. <https://doi.org/10.3390/land10080870>
18. Allam Z, Newman P (2018) Redefining the smart city: culture, metabolism and governance. *J Smart Cities* 1:4–25. <https://doi.org/10.3390/smartcities1010002>
19. Yamamura S, Fana L, Suzuki Y (2017) Assessment of urban energy performance through integration of BIM and GIS for smart city planning. *J Proced Eng* 180:1462–1472. <https://doi.org/10.1016/j.proeng.2017.04.309>
20. Jucevičius R, Patašienė I, Patašius M (2014) Digital dimension of smart city: critical analysis. *J Procedia—Soc Behav Sci* 156:146–150. <https://doi.org/10.1016/j.sbspro.2014.11.137>
21. Jupp J (2017) 4D BIM for environmental planning and management. *J Proced Eng* 180:190–201. <https://doi.org/10.1016/j.proeng.2017.04.178>
22. Re CF, Tagliabue LC, Maltesea S, Zuccaro M (2016) A multi-criteria framework for decision process in retrofit optioneering through interactive data flow. *J Proced Eng* 180:859–869. <https://doi.org/10.1016/j.proeng.2017.04.247>
23. Bibri SE, Krogstie J (2020) The emerging data-driven Smart City and its innovative applied solutions for sustainability: the cases of London and Barcelona. *J Bibri and Krogstie Energy Info* 3. <https://doi.org/10.1186/s42162-020-00108-6>
24. Marsal-Llacuna M-L (2013) Smarter urban planning through a citizen-based approach. The smart urban planning method. Dissertation, Universitat de Girona
25. Spiridonov VY (2012) The evolution of the concepts of architectural and planning development of resettlement systems. Dissertation, Ural State University of Architecture and Art named after N.S. Alferov
26. Kolyasnikov VA, Spiridonov VY (2016) Modern theory and practice of urban planning: settlement spatial development. Architecton, Yekaterinburg
27. Spiridonov VY, Shabiev SG (2020) Smart urban planning: modern technologies for ensuring sustainable territorial development. *J Mat Sci Eng* 962. <https://doi.org/10.1088/1757-899X/962/3/032034>

28. Spiridonov VY, Shabiev SG (2020) The urban planning information platform: progressive methods of planning and managing the sustainable development of territories. *J Mat Sci Eng* 962. <https://doi.org/10.1088/1757-899X/962/3/032035>
29. Eurasian Economic Commission, United Nations Conference on Trade and Development (2019) Inclusive growth of the Eurasian economic union member states: assessment and opportunities



Concept Project for the Comprehensive Renovation of the Urban Area of the Microdistrict

Dr., Ph.D. Arthur Manko¹(✉), Valeria Vinogradova², Maria Voropaeva², Alina Ganshina², and Olga Matyukhova²

¹ Department of Soil Mechanics and Geotechnics, National Research Moscow State University of Civil Engineering, 26, Yaroslavskoe Sch., Moscow 129337, Russia

MankoAV@mgsu.ru

² Institute of Hydraulic and Power Engineering, National Research Moscow State University of Civil Engineering, 26, Yaroslavskoe Sch., Moscow 129337, Russia

Abstract. For multiple decades, people attempted, sometimes quite successfully, to set up unique city districts. These districts were mostly one-of-a-kind options for forming the urban environment. The general construction was centered around the high-rise districts matching the average urban environment comfort requirements. However, today these districts do not match the exiting residential standards and must be redeveloped and renewed to match the modern residential comfort concepts. Developing a blueprint of complex high-rise areas renovation require benchmarking against the international practices of the latest decades, actively investigating the renovation possibilities open for the city building concepts of the past. The article researches the national and foreign blueprint projects of high-rise districts. It also presents a methodology for the suggested blueprint projects of an urban micro-district renovation.

Keywords: Renovation · Concept · Project · Microdistrict · Residential district · Multistory development · Urban planning

1 Introduction

The National Research University Moscow University of Civil Engineering fosters student extracurricular research teams supervised by the university departments. The members of the research team supervised by the Department of Soil Mechanics and Geotechnical Engineering were suggested solving a case aiming at urban district renovation involving the underground space based on any existing district. The research aims at developing a blueprint project of urban district renovation making use of underground space based on the best national and international practices.

2 Research Problem

The Russian urban planners took the idea of high-rise districts of apartment blocks from foreign practices, which were considered advanced at the time. However, this type of urban arrangement had never been analyzed against its prospects, the evolution of the quality of life and the needs of its residents over the following several decades [1].

Achieving the aim of the research requires solving the following tasks:

- Reviewing the USSR urban areas design basics.
This is to use various research into the USSR urban planning history to analyze the basic urban planning principles and further identify the renovation focus areas, which will not prejudice the residents of such districts.
- Reviewing the foreign urban areas planning experience and practices.
- The residential high-rise areas began growing out of use in the 1970-s, followed by the emergence of the urban areas' reconstruction concepts. Accounting for the mistakes made over the course of such renovation abroad shall minimize the financial losses of the national developers.
- Reviewing the current advance national and international urban environment renovation practices.
Designing a blueprint renovation project for major cities requires studying the best current national and international practices used to set up comfortable residential environment.
- Proposing a blueprint project for the renovation of an existing urban district based on the analyzed practices.

No project aiming at creating a comfortable residential environment can ignore the development of the underground space [2]. It is due to that a complex urban district renovation solution is being reviewed and proposed herein.

3 The USSR Urban Areas Design Basics in Respect to Their Renovation

Renovating urban areas and districts is the reorganization and redeveloping the functions of such. As life spins, the society requires new, changed functional aspects, novel leisure activities and residential environment. Starting from the 1950-s over the history of the USSR all the basic area and micro-district zoning principles had been drawn. According to [3], in 1952 the residential districts, i.e. micro-districts were divided into quarters hosting the intra-block ring-ways. The houses were arranged in the groups of four adjacent buildings forming a quadrangle. This arrangement was called a close. The quarters consisted of 3 closes. Each close featured a public utility site and a playground. The quarter featured an additional area used for the recreation of adults, a flowerbed and a sportsground. The remaining areas were greened with trees.

The industrial and public quarters and districts were zoned similarly. However, it was a change compared to the zoning used from the beginning of 1920-s, when a quarter could host adjacent residential, public, sports or industrial buildings. The industrial quarters were to be laid out to match the production cycles, meaning that the warehouses had to be

located immediately by the site consuming the stored goods. For instance, the plywood and chipboard production sites were located by a furniture plant, etc. [4].

By 1966 the idea of the residential blocs zoning had changed, as new concepts of residential areas and commuter districts appeared [5]. Novye Cheremushki was one of such new districts, divided into quarters and designed according to the new concept [6]. Take quarter 9 as an example. The concept identified the zones for residential buildings. The number of apartments and the consequent number of possible residents were used to calculate how many kids the kindergartens built mandatorily in each quarter should have been able to accommodate. The quarter has 16 houses hosting 982 apartments in total. The school capacity, usually one per quarter, was also calculated. If no site for the school was available, a major study complex for several adjacent quarters was built [7]. The quarter project also featured sports grounds, playgrounds and resting sites, a splash pool, public utility sites, arbors, parking lots, and even a cinema. Over the 1960–1970s a great number of such quarters and areas were build across the cities of our country.

Today the renovation features multiple residential buildings, micro-districts, districts, and quarters redevelopment projects. A blueprint project for the renovation of quarter 9 in Novye Cheremushki has been developed [8]. This project has been developed around the decision to maintain the historical and cultural value of the sites. At the same time, some of the sites' functions will have to be changed which, in its turn, would require changes of the construction project and space and layout design. The authors consider that this project will work to preserve the historical look of the quarter and create additional workplaces. This project also allows reclaiming the underground space.

4 Basic Principles of Urban Areas Design Abroad

Renovating urban areas and districts is the reorganization and redeveloping the functions of such. As life To facilitate the integrated development of poorly designed microdistricts or those with no concept as well as for the renovation of morally and physically outdated areas, one can appeal to international experience [9]. Judging by the international expertise, four environments for the formation of a foreign city can be distinguished:

- Downtown is a financial, cultural and administrative center of any foreign city. Geographically, it is not always a central part in terms of geometry. Most often, Downtown is located below the geometric city center as if at the bottom, and this is why it's got such a name. Depending on the size of the city, the Downtown may consist of two or three buildings.
- Suburbs are located in the immediate vicinity of Downtown, as a rule, westwards and eastwards of the city center. In large cities, the Suburbs are also located from southward. As a rule, suburbs are one- and two-storey private houses, less frequently for two families, households. This part of the city is functionally similar to the Russian residential areas of the 1950s.
- Industrial area is a place where all the warehouses and production facilities of the city are located; oftentimes, shopping centers are also located there. Sometimes the industrial area is divided into two parts, the northern one, where production is concentrated, and the southern one (below Downtown or just outside the Suburbs), where the cultural and leisure facilities, sports facilities, nightclubs, etc. are situated.

- Social area is an area where high-rise buildings dominate. This area is located in the north of any city and is intended for people with low income, the poor, etc.

Each of the Suburban and Social districts has its own infrastructure (schools, hospitals, children institutions). In its turn, the suburbs can also be divided into microdistricts according to the price of real estate. At the same time, separate settlements are formed inside, to admit them, a special permission is necessary. If the first three district groups are not quite (maybe, except for a part of Industrial districts) suitable for the study of renovation of some functional residential areas, the Social group concept is very suitable for Soviet and Russian urban development.

During the renovation and changing the functionality of urban areas, we are primarily interested in the foreign experience of the so-called tactical urbanism of the areas with high-rise buildings [10]. In the USA, for example, back in 1970 the authorities realized that building up a separate enclave consisting of people with social problems results in the degradation of society and crime growth [11].

As an example, this is the district of New York—the Bronx, one of its quarters is shown in Fig. 1. This photo was taken from the New York Times newspaper [12]. This quarter is visually similar to the dormitory district in any large city in the post-Soviet space. However, the problem of this area is the absence of any leisure facilities and a variety of sports grounds. Therefore, the districts of US cities where there are only high-rise residential buildings, are being renovated with a partial change of the functions adding industrial buildings with small-scale handicraft production, retail premises and offices, i.e. creating new jobs [13].



Fig. 1 A typical Bronx neighborhood

However, the legislative part was still lagging behind since at that time the authorities often practiced compulsory purchase of real estate from private individuals. Under the guise of the economic development program in the district, the purchase of territories for development was conducted to attract investors. Ghettos were the first to be included in the program. Legislatively, such activities could be restricted only in 2012 because

only in 42 of the 50 states, court cases were conducted back in 1954 in Washington and in 1984 in Hawaii, when 73% of the island real estate belonged to 22 owners [14].

The problem of renovation and redevelopment of residential areas is urgent not only in the USA, but also in other countries where there is a high-rise typical building. Another example may be seen in France [15] where there are so-called “priority areas”; these are districts whose development and subsequent financing is of the paramount importance relative to other areas. At the same time, priority areas can be located both within the city and in the suburbs. These are districts with low-rise buildings where housing is quite expensive and it is hard to be bought for people with low income, and social housing is not provided in priority areas. This division occurred after the Marshall’s Plan declaration of 1945 when people began to divide their places of residence according to their income level. In the 1960s, following the declaration of independence from France for many of its colonies, a flow of emigrants from these colonies rushed into the country. This was the time the Marshall’s plan emerged again; high-rise houses were started to build for migrants in the poor districts. Due to the fact that the number of sites for new construction was limited, especially in cities such as Tours, Le Havre, Brest, Cergy, Saint-Quentin, Senart and others, the authorities began to seize yard spaces between the houses with the status of social housing for construction. The low-rise social houses were demolished for the construction of higher houses (9–16 floors) with social housing for low-income population strata and emigrants. A few years ago, the French government announced a “National Urban Renewal Program”, which finished in 2020. 50 billion euros have been allocated for the transformation of 600 such districts in the cities across France. This program was aimed at making social areas more secure due to crime reduction by creating new jobs in the districts, the renovation of districts with the creation of socio-cultural places of leisure and recreation, attracting people to the area for temporary migration to reduce social tension. As a result, the program actually was finished after the repainting and partial repair of houses with the allocated money. Journalists interviewed the residents of social districts with high-rise buildings where this renovation program was conducted, and 72% of the respondents reported about not only the crime rate being unchanged, but also significantly worsened social conflicts. Sometimes, under the guise of renovation, even those socio-cultural areas existing in the district were destroyed. With minor exceptions, playgrounds were made (Fig. 2).

Meanwhile, the program contained the items suggesting the demolition of a part of high-rise buildings to free up the territory for socio-cultural and commercial development. But this was not actually done. The final report of the Accounting Chamber of France revealed that the main reason was that some municipalities spent only 0.1% of the estimated renovation budget. According to the explanations of some city leaders, this is because they “... do not see the point of changing anything if we can keep the old and renovate it ...”. A technical problem of the renovation in the social districts of high-rise buildings in French cities consists in the absence of a comprehensive renovation solution. The project stipulated for the demolition and construction of even higher social houses, while the vacant place was designated for building some object indicated in the program as “at the discretion of municipalities”, i.e. no concepts for the development of districts were proposed to relieve social tension in ethnic enclaves.



Fig. 2 An example of the renovation of a high-rise building in France under the national urban renewal program

5 Examples of a New Approach to the Design and Renovation of Urban Areas

For large cities, in particular for Moscow, various design projects have been developed for renovation, conversion and reconstruction of former residential areas into modern ones due to the formation of cultural and leisure facilities [16]. Apparently, the study above indicates that it is necessary to renovate existing areas and form new areas in a universal way: it is necessary to live comfortably, work, relax and have fun in the district while children should have not only schools and preschool institutions, but also leisure facilities.

As an example of the development and renovation of existing districts, as well as the creation of substantially new districts, consider the example of the city of Irkutsk [17], which has been actively being built recently. There are both old, already established neighborhoods in the city, which are gradually being renovated and reconstructed (for example, Quarter 130), and new districts are being built. As an example, take the Raduzhny district, which began to be built back in the Soviet times but the construction continued already in the conditions when the living and construction requirements are governed not by the state but by private investors' needs. The new districts are completely different. There is example of poorly designed districts, such as the Yerшовsky district, where there are no conditions for pedestrian movement, there is no transport within the district, public transport is poorly developed as the district can only be reached by a minibus No. 68 k. There are no schools, kindergartens, polyclinics, sports, public and socio-cultural facilities in the district, there is an urgent need of convenience stores. There is a new Union microdistrict that has a better urban planning. It is located on the left bank of the Angara in the Sverdlovsk district, which has its own kindergarten, socio-cultural, sports facilities and healthcare facilities. Unfortunately, the neighborhood does not have its own school, and transport communications have not been fully developed; however, the introduction of the Soyuz-Priority residential complex shall improve transport accessibility. One of the newest and most interesting districts of Irkutsk, described

by the researchers as “the area between a dormitory and a private suburb”, is the Berezovy microdistrict. This microdistrict is part of the Markov work settlement. Berezovy is built up mainly with three- and five-storey houses with a developed infrastructure. The only drawback of the neighborhood is a significant distance from transport communications and Irkutsk.

It is also necessary to pay special attention to the development of underground space, and for this purpose, it is necessary to have a clearly stated program [18]. Generally, such programs allocate 3–5 directions in underground urbanization. The main ones in terms of the renovation of existing areas are transport facilities, engineering infrastructure and public facilities. During the renovation of the district, existing utilities and other engineering infrastructure facilities are subject to renovation alongside with the construction of underground structures for public (social, commercial) purposes. First of all, it is necessary to make parking lots from underground structures for transport purposes. It is also necessary to upgrade the transport accessibility of the micro-district. The underground system of the off-street transport copes with this problem perfectly. The station should be located directly in the area of the microdistrict.

6 Blueprint Project of the Renovation in the Existing Areas with High-Rise Buildings

Summing up the available domestic and foreign experiences, we can conclude that the design of the urban development plan of a district or microdistrict should be carried out within the future “life cycle” of the territory, which contributes to the most correct definition of the stage and direction of its development [19]. The most striking example of the implementation of the district life cycle concept is the USA where the districts are built for certain categories of people. For retired people, the availability of schools and kindergartens is not important, while for other categories of people such as young families, on the contrary, the availability of a school within walking distance as well as various sports and other leisure sections can be crucial [20]. After they stop having need in educational, cultural, etc. institutions people move to another area mostly adapted for the retired.

In our country, where the concept of a megapolis—a city with high-rise buildings—has long been established, it is necessary to provide all the necessary infrastructure for all age groups in the district, if possible. But it is not always possible to implement due to various conditions. For example, in a microdistrict located in the central part of a large city, it is almost impossible to organize a park for walking and recreation. Therefore, in the district where it is possible to organize recreation areas, sports grounds, cultural facilities, etc., it is necessary to stipulate that citizens from other areas will come to such a district as there is no such infrastructure in the place of their residence.

However, it is possible only due to the transport accessibility of this multifunctional area. Transport accessibility should be both for personal motor transport and for public transport. It is quite logical that people living in the suburbs will go to the district by private vehicles to have recreation and entertainment at weekends. In turn, people living in the city itself, and especially in the city center, will go to a multifunctional district for recreation and cultural pastime on any day by public transport. At the same time,

there should be no transfers between the transport types, and thus, the most suitable is an off-street transport system (metro, premetro).

Theoretically, all of the aforementioned can be very attractive, but how one can actually attract people to come to the district for leisure? First of all, according to the authors of this article, there is a greater need for jobs in the district than in housing. The people living in this area will already visit the places of recreation and cultural leisure. For making people come to the district (especially if it is located on the border of a city and a suburb), it is necessary for them to know this area well. If a person works in some place, over time he or she will definitely learn the infrastructure of this area. Clearly, it is better to bring your family, loved ones, friends to a place where a person can definitely have some rest and cultural leisure. Thus, the inflow of people from the outside to the area will be ensured.

Further, consider the blueprint project for the renovation of the existing area in the city. Once again, it is worth reminding that this plan is intended for a district that best fits the concept of a “multifunctional area” mentioned above. To do this, follow these steps:

- Analysis of the existing area in order to identify the existing transport accessibility (by road and off-street transport), ways of developing transport accessibility, existing development, urban zoning, the ways of renovation of housing, public and industrial stock.
- Analysis of the history of the district development to create its future image. One shall determine what objects cannot be located here. For example, Yakimanka used to be an industrial area with manufacturing facilities and factories, but today it is impossible. Based on the purpose of the building, it is possible to save and redesign some of them.
- Identification of the target audience for which it is necessary to renovate this area. It is necessary to divide the district residents into target groups “by age” and “by income”. At first, it is necessary to determine for which target group “by income” the renovation of the district will be conducted; next, one needs to define the infrastructure facilities designated only for the target group “by age” within a larger target group “by income”.
- Identify the target groups of visitors to the district on the same principle as described in paragraph 3.
- Defining the district priority object which would bear the greatest load of visitors’ attraction. If possible, this facility should meet the needs of all target groups.
- Identification of related objects required for various target groups.
- Identification of jobs to attract people to the district (number, type of activity, etc.).
- Comparison of numerical indicators to identify priority objects of future construction (passability per day and certain hours, statistics on workplaces and visitors to the facility).
- Possible options of architectural, landscape and structural solutions, their justification of both the main object and additional ones.
- Financial justification for the construction of the main facility as it will be the main place to attract an additional flow of people. Financial justification of auxiliary facilities is also necessary as they will also attract their own target group. Sometimes auxiliary facilities can make up a significant percentage of the profit.

- Drafting the life cycle of the main and auxiliary facilities to adjust the calculation of future profits and determining the payback period, taking into account a future renovation or demolition of facilities and possible area redevelopment.

7 Conclusions

Based on the results of this scientific study, the following conclusions can be drawn:

- Urban planning projects for the arrangement of microdistricts of cities with high-rise buildings in the USSR are considered.
- Various concepts for microdistrict design are currently considered in our country by various examples.
- The examples of designing areas with high-rise buildings abroad are considered.
- Various approaches to the renovation of areas with high-rise buildings in the USA and France are considered
- All approaches (domestic and foreign) to the renovation of existing areas with high-rise buildings are analyzed.
- The authors propose a model for the methodology of a blueprint project for the comprehensive renovation of a microdistrict (district) with existing buildings.

References

1. Chekmeneva DA (2018) Identity formation of cultural and leisure centres in Moscow bedroom communities. In: Abstracts of International Scientific-Practical Conference, faculty, young scientists and students, Moscow, 02–06 April, pp 607–608
2. Rodionovsky AN (2022) Formation of a system of local urban centres based on existing metro stations. *Innov Invest* 11:240–243
3. Improvement and renovation. Approaches and challenges (2018). Publishers A-Print. Moscow
4. Ashimin AV, Shestopalova NV (2021). Problems of Russian town planning of XX-XXI centuries in the context of cultural and civilizational decay of post-industrial society. <https://doi.org/10.46916/18052021-3-978-5-00174-233-3>
5. Ovsyannikova VE (2019) Parallels in the mass construction of the 1920s–1950s (Sokol settlement and the 9th quarter of Novye Chermushki). In: Materials of the international scientific-practical conference, St. Petersburg, March 21–22, pp 330–333
6. Gorlov VN (2014) Novye Chermushki. Transition to mass implementation of microdistrict development in the USSR in the 50–60s of the twentieth century. *Bull Moscow State Regional Univ Series: History Polit Sci* 2:61–68
7. Bobkova IA (2016) School unification. Will the economy win over metropolitan education? *Concepts* 1(35):65–77
8. Mitryaev EA, Popov AV (2022) Prospects for reconstruction of the 9th quarter of new Chermushki with a change of function. *Ecol Urban Territ* 1:80–85. <https://doi.org/10.24412/1816-1863-2022-1-80-85>
9. Potashova MD, Tsitman TO (2019) Integrated development of urban areas. microdistrict renovation. *Eng Const Bull Caspian Sea Reg* 2:40–50
10. Zazulya VS, Lobanov YN, Rusanov GE, Volkov VI (2019) Tactical urbanism as a method for rapid ‘renovation’ of dormitory areas of the cityю. *Bull Civil Eng* 5:5–9. <https://doi.org/10.23968/1999-5571-2019-16-5-5-9>

11. Alov IN (2018) African-American ghettos: characterization and typology. *Urban Res Pract.* <https://doi.org/10.17323/usp31201863-77>
12. Kimmelman MA (2021) Rebirth in the Bronx: is this how to save public housing? *The New York Times*, Aug.5
13. Fedchenko IG (2020) Community centre” as a new type of public architecture in the residential environment. *Modern World Archit* 1:248–262. <https://doi.org/10.25995/NIITIAG.2020.81.27.011>
14. Denisova EL (2022) Foreign experience in the implementation of renovation programmes: a comparative analysis. *Herald of Saint Petersburg Law Acad* 4:35–38
15. Bouhassoun K (2023) Remplaçons les ghettos par des villes: *Factuel.info.* <https://www.factuel.info/remplacons-les-ghettos-par-des-villes>. Accessed 29 Apr 2023.
16. Chekmeneva DA (2018) Shaping the identity of cultural and leisure centres in Moscow bedroom communities. *Abstracts of the International Scientific-Practical Conference, Faculty, Young Scientists and Students* 2:607–608
17. Abdulova IT (2019) New microdistricts of Irkutsk: between suburbs and “bedroom communities”. In: peripheral urban areas in the post-Soviet space: Collection of abstracts of the international scientific conference. In 2 parts, Ulan-Ude, 14–16 Nov. <https://doi.org/10.31554/978-5-7925-0571-1-2019-1-92-97>
18. Korolevsky KY, Egorychev OO, Zertsalov MG, Konyukhov DS (2007) Main principles of forming the programme of complex development of Moscow underground space. *Metro Tunnels* 6:34–35
19. Ramírez-Villegas R, Eriksson O, Olofsson T (2019) Life cycle assessment of building renovation measures—trade-off between building materials and energy. *Energies* 12(3):344. <https://doi.org/10.3390/en12030344>
20. Kashef M (2017) Residential developments in small-town America: assessment and regulations. *City, Territ Archit.* <https://doi.org/10.1186/s40410-017-0070-4>



Contextual Approach in the Process of Integrating Modern Buildings into the Architectural and Spatial Environment of Historical Centers in Large Cities

I. N. Maltseva^(✉) and N. N. Kaganovich

Ural Federal University Named After the First President of Russia B. N. Yeltsin, 19, Mira,
Yekaterinburg 620002, Russia
i.n.maltceva@urfu.ru

Abstract. The article is devoted to the problem, which in the process of further development of modern, especially large, cities, becomes more and more relevant—these are the issues of interaction of the historical context with modern architecture and innovations in the field of urban planning. Due to the fact that the city, being a complex and constantly developing socio-economic system, has a very important characteristic—its historical past, it is necessary to consider approaches and methods for integrating objects of modern architecture into the existing material and spatial environment of the city. This determined the purpose of this work—the study of methods for including newly built objects in the historical environment based on a contextual approach. The problems of synthesizing the old and the new, their optimal combination in terms of preserving the historical integrity of the development, taking into account legislation, regulatory requirements and modern technologies in this area, in the restoration or reconstruction of cultural heritage sites, including the inclusion of new buildings and the organization of public spaces. In the process of analyzing examples from architectural practice, the main methods of environmental adaptation and the role of new buildings in a specific historical context are identified. As a result of the study, a project proposal for the renovation of a quarter in the historical center of a large city is considered as approbation.

Keywords: Urban environment · Historical buildings · Cultural heritage · Integration methods · Building rehabilitation · Public spaces

1 Introduction

The modern city, being a complex multifactorial system, has another very important characteristic—its historical past. The time during which it existed and developed, its architectural and construction framework and urban infrastructure were formed. As a result, it is the time factor that the city in the process of development accumulates historical and architectural values and forms its socio-cultural component. The time factor

reflects not only the historical past, but also determines the urban development potential, and therefore the strategies and prospects for the development of cities in the future [1]. On the other hand, the problem of the relationship between “old and new” is determined by the current level of development of society: new trends in architecture and technology, aesthetic and socio-cultural views. Of particular importance in urban development programs are historical and cultural objects, including architectural monuments that bear the imprint of past eras in style or are associated with memorable historical events. Such objects that exist on the outskirts of cities, as a rule, are not numerous, fit into modern buildings or natural landscape environment. A completely different situation develops in historical centers, especially in large and rapidly growing cities: it is the historical, as a rule, ensemble building, being unique, that creates a holistic impression, makes the city unique and recognizable. At the same time, the development of historical cities leads to changes in their spatial structure, artistic image and the emergence of new public spaces [2]. Exceptionally careful integration of modern architecture objects into the historical environment, competent use of the functional potential of urban spaces and objects of cultural and historical heritage are important conditions for the formation of a coherent spatio-temporal and sustainable urban environment. The best preservation of architectural monuments is achieved with their active life, service to the city and people [3].

2 Basic Principles and Methods of Integrating New Construction Objects into the Historical Urban Environment

Revitalization or modernization of a historical building in some cases turns out to be the only way to restore and preserve it, thereby extending its life cycle [4]. Most often, it requires revitalization and renovation, as a rule, the depressive territory in which it is located. On the other hand, in some cases (taking into account the historical status of the object) it becomes necessary to supplement the historically established ensemble or fragment of the preserved building with a new building. In these cases, the problem of integrating the new object into the historical context arises, associated with a number of contradictions and a certain conflict between the “old and the new.” In the process of reconstruction of the urban environment, it is important not only to preserve the objects of historical and cultural heritage, but to harmoniously fit modern buildings into the existing environment [5]. Any new object that arises within an already established environment is an element of the reconstruction of the fabric of this environment. It must fit into the environment and coexist in the old architectural environment without causing emotional rejection in people [6].

The first method of concealed reconstruction is used when it is necessary to update the historical site of urban development or its adaptation with elements of modernization. It is also optimal for the reconstruction of closed or “intermediate”, so-called non-structural urban spaces (closed courtyards, quarters, wastelands, dead ends), which are not associated with areas of public activity and generally do not affect the perception of the existing elements of urban space.

There are two fundamentally different applications of covert reconstruction:

- The reconstructed object is included in the structural frame of the central part of the city.
- The reconstructed object is located in the zone of influence of this frame, but is not included in its composition, forms “tissue”, predominantly residential formations, isolated from the actively visited zone of the urban core.

The purpose of reconstruction in the first case is to create a rich and diverse urban environment, permeable in all directions and designed for mass flows of citizens. At the same time, for a number of reasons, it may not be possible to use the old residential development in its former function. The traditional method of reconstructing old residential buildings is typical for the second case [7].

The second method of stylistic imitation and application is based on the imitation of the compositional techniques of historical architecture and is mainly used to restore the facade appearance of buildings without disturbing the familiar appearance of urban development. In practice, there are many examples of successful “integration” into ordinary historical buildings that do not violate the architectural and artistic appearance of the street. This is how the development object was formed on Krasnoarmeiskaya Street in Yekaterinburg: the building on the left is historical, the building on the right is made in stylistic imitation, in general, the complex organically blends into modern residential development (Fig. 1a).



Fig. 1 a Krasnoarmeiskaya Street in Yekaterinburg; b the Big City shopping center in Tomsk

An example of an unsuccessful stylistic imitation is the Big City shopping center built in 2005 in Tomsk, whose name became a household name for the entire Tomsk architecture of the early 2000s, and the blue color was firmly entrenched in buildings in the “kaprom” style (Fig. 1b).

The application method is a kind of stylistic imitation with the introduction of elements of new architecture on the historical facade, while the general character and scale of the facades, the rhythm of its segmentation and details are not distorted by modern means of architectural design, an example is a fragment of the embankment building in Haarlem, a suburb of Amsterdam (Fig. 2a), the historical development of the embankment in Amsterdam (Fig. 2b).

The third method of “old and new” contrast, popular in modern, especially in foreign architectural practice, and creating a bright and strong impression when perceived, opposes the new object to the familiar and familiar architectural environment by use:



Fig. 2 **a** A fragment of the embankment in Haarlem; **b** a fragment of the embankment in Amsterdam; **c** the Museum “Kunsthau Graz”; **d** the Cultural Industries Quarter

- Innovative materials and structures.
- “Contrasting”, often “provocative”, shaping technique or color solution.
- Physical and visual separation of volumes of an architectural object.
- Deliberate violation of the principle of “coscale” when using elements of a “contrasting” scale.

This principle is used when rebuilding a building associated with modernization or reconstruction (changing the shape or volume) [8]. Examples include the building of the Kunsthaus Museum in Graz (Austria), architect Cooke Fournier (Fig. 2c). and the building of the Elbe Philharmonic in Hamburg (architectural bureau Herzog & de Meuron), where the architects used the building of a former goods warehouse as the basis for a futuristic volume of glass and steel, as well as the building in Sheffield at 192 Shoreham Street, a Victorian brick industrial a building located on the edge of the protected zone of the Cultural Industries Quarter, which is considered to be of local significance (Fig. 2d).

The office building “Cocoon” is compositionally and logically inscribed in the existing building of the Novosibirsk city [9], which can be attributed to a successful example of a “contrasting” integration method (Fig. 3a), as well as the “Building with three towers” in the Rotermanniv quarter of the Tallinn city (Studio KOKO architects). The project of the Estonian architectural studio in 2009 was nominated for the European Union Prize for Contemporary Architecture—Mies van der Rohe Prize.

The fourth method of surgical intervention is often reduced to the contrasting interaction of the “old and new”, as a result of which not only the scale, but also the architectural

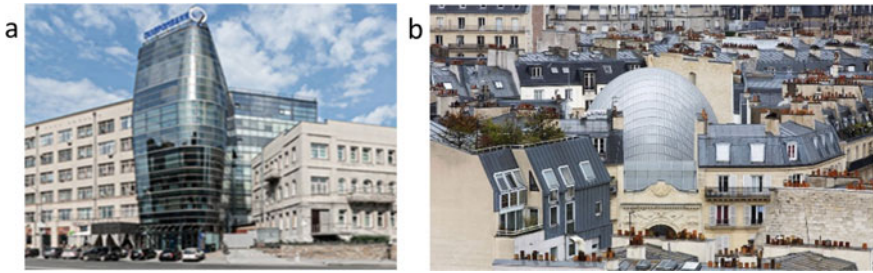


Fig. 3 **a** The office building “Cocoon”; **b** the building of the fund of the Pathé film studio in Paris

landscape and the environmental context change. For example, the building of the fund of the Pathé film studio by the architect Renzo Piano in Paris (Fig. 3b).

3 Environmental Adaptation Methods

Considering the main methods of interaction between “old and new architecture”, we can conclude that it is the contextual principle of adaptation in the conditions of the current urban environment that allows us to preserve the originality and uniqueness of historical buildings and ensembles, the “memory of place” in urban landscapes, and at the same time competently structure the further development of the city environment [10]. At the same time, in some cases it is necessary to assemble or supplement the existing composition of a street or square with a volume defined in terms of dimensions and morphology. All these tasks are solved, first of all, at the urban planning level to fit the building into the structure of the urban fabric. Then, at the compositional level and further at the stylistic, coloristic, semiotic or typological levels, the volume-spatial composition of the building, the overall dimensions of the building, depending on the need and environment, are determined [11].

The interaction of historical and modern architecture considers a number of typical and traditional approaches:

- “*Symbiosis of the old and the new*” involves the use of compositional expressiveness techniques through individual, characteristic of a historical object, architectural elements by means of new materials and technologies, combining the “old” and “new” with a common color scheme or the principle of shaping in order to create a single architectural ensemble in a certain historical environment [12]. Examples of a new “reading” of historical buildings are the object in Barking and Dagenham in the East London area (Fig. 4a), the development of the historical center of Lithuanian Kaunas, the complex of buildings in Gdansk, where the historical building perfectly “gets along” with a modern building, restored anew after complete destruction during World War II (Fig. 4b). A good example of the combination of old and new is Tate Modern 49. The historic Bankside Power Station building was converted in 2000 into a modern art gallery to preserve the building’s historic character (architects George Scott, Herzog and de Meuron). In 2016, the ensemble organically complemented the

new modern building of the same authors, which became a link between the river bank and the picturesque Southwark area.

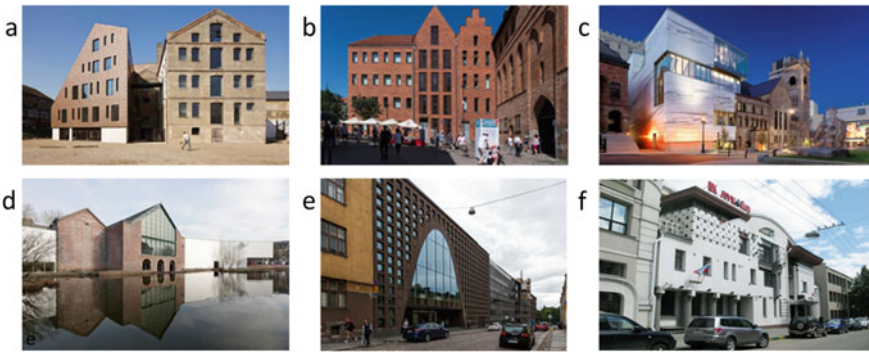


Fig. 4 **a** the object in Barking and Dagenham in the East London area; **b** the complex of buildings in Gdansk; **c** the Memorial Museum in Mons city (Belgian); **d** the Romanesque church-museum in Montreal; **e** the building of the University Library in Helsinki; **f** the office building of the bank “Lukoil” in Nizhny Novgorod

- “*Subordination*”, in which it is the historical building that dominates, and the modern building serves as a “background” and “dissolves” in space due to laconic forms, active glazing of facades or the introduction of “blind” sections of walls, neutral color scheme; this technique was used in the building “Memorial Museum” in the Belgian Mons city (architectural studio of Pierre Hebelinck). In this architectural solution, the white plastered walls of the new extension with flat-roofed play the role of a “neutral background” to achieve greater expressiveness of the preserved historical part (Fig. 4c). The Romanesque church-museum in Montreal, which survived almost complete destruction, was restored and became part of a wonderful modern building (Provencher Roy studio), which housed the museum and theater (Fig. 4d).

“Inscribing” into a historical ensemble or building, in which architectural integrity is achieved by repeating and supplementing such means of harmonization as “rhythm and mass”, subordinating building parts, scaling, maintaining the level of horizontal divisions with highlighting the basement, central and cornice parts, identifying the axis of symmetry, in general, characteristic techniques in historical buildings, in particular, built in the style of classicism. The building of the University Library in Helsinki (Anttinen Oiva Architects) was inscribed between two old buildings, while the number of storeys was preserved, the exterior finish was made of similar materials, which is why the modern building does not seem to be something foreign (Fig. 4e).

In the process of integrating a new building into the historical environment, the principles of integrity and order, the classification type and the role of the historical building in the structure of a specific historical environment are important, which is achieved by certain methods of environmental adaptation, such as:

- *Typological*, in which the new building becomes part of the existing typological range in the historical building, the overall harmony is achieved by mutually coordinating scales and proportions, using the principle of modularity.
- *Stylistic*, based on the stylization and subordination of the new building to the overall composition in the historical environment.
- *Compositional*, in which the project of a new building uses such means of harmonization in the architectural composition as rhythmic, metric, scale, horizontal and vertical divisions, symmetry and asymmetry and other characteristics of a historical building.
- *Artistic and aesthetic* uses modern modernization of architectural details on the facade, present in one or another original form in a historical building (belts, bas-reliefs, ornaments, etc.).
- *Figurative-symbolic* (semiotic) to identify and preserve the associative image, important for the historical “memory of the place”.
- *Coloristic*, using the color, texture of modern exterior materials to identify the historical environment or “fit” into it.

An example of successful environmental adaptation is the office building of the Lukoil bank in Nizhny Novgorod on Gruzinskaya street, 26 (Fig. 4f). As a result of the modern stylistic interpretation of the compositional techniques of the neighboring historical building (the main articulations and the multifaceted relief of the facade, the introduction of bright associative details), the unity of the image was achieved, and the new building tactfully blended into the historical environment.

The need for a harmonious synthesis of modern and historical architecture is one of the most important problems that arise in the design of buildings. It is due to the rapidly changing lifestyle and mentality of the population, aesthetic views and the development of modern technologies, including innovations in the field of construction. All these are factors for the formation of new trends in architecture. In modern conditions, the relevance of reconstruction as a “normal” architectural practice has revived. Architects are increasingly reconstructing historical buildings, giving them qualitatively new functional characteristics [13].

4 Approbation (Conceptual Project Proposal) Based on the Results of the Analysis of Environmental Adaptation Methods in the Historical Center of a Large City

The purpose and concept of the project approbation are determined taking into account the study and study of archival documents on the protection of cultural heritage objects, the need to organize an urban socio-cultural platform, given that the world experience in the development of large cities shows that the nature of the city, its significance and success is determined by the historical center, namely the quality his public spaces [14]. The quarter in the historical center of Yekaterinburg, bounded by Proletarskaya (former Officerskaya), Pervomaiskaya (former Clubnaya), Gorky (former 2nd Beregovaya) and Clara Zetkin streets, was considered as a design object; this is a degrading territory with preserved cultural heritage sites, including the estate of F.A. Zlokazov.

The urban planning and architectural and historical context represents a good transport and pedestrian accessibility of the quarter, the proximity of public parking lots, social and cultural facilities and public spaces of urban significance, the presence of preserved cultural heritage sites, temporary structures and objects subject to demolition on the site. The estate of F.A. Zlokazov is a monument of regional significance and is dated to the 1880-1890s, the territory of the object belongs to the lands of historical and cultural purpose (Fig. 5a). The general condition of the object is recognized as unsatisfactory. The objects of the complex have lost their original purpose and at present, for the most part, these are small commercial premises for various purposes, the Zlokazov residential building (Fig. 5b, 2) is empty.

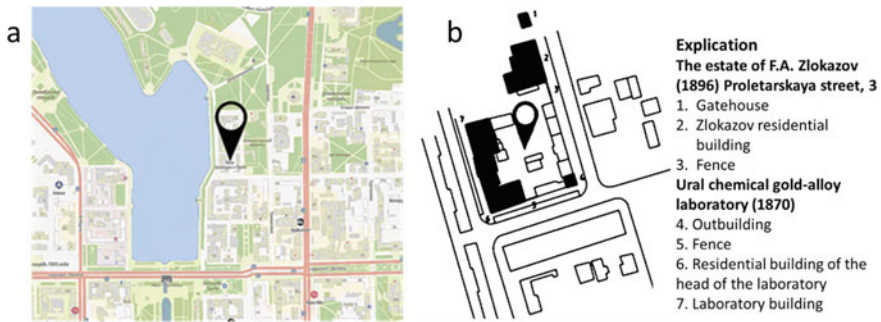


Fig. 5 a Situational plan; b scheme of the location of objects in accordance with the general plan of the technical passport (objects of cultural heritage in the scheme are highlighted in black)

The socio-cultural context is represented by the complex of the tourist-excursion program “Literary Quarter” existing in the immediate vicinity. The designed object can potentially become a continuation of this scenario in terms of meaning and organization. In addition, a cultural cluster and social activity zones (the embankment of the city pond, places of recreation and festivals) have formed in this area of the city. It can be successfully supplemented with new public spaces, which really become the most important part of the formation of the climate of urban life [15].

The urban planning concept involves the historical and social rehabilitation of the site, the transformation of the existing urban complex by restoring its historical appearance, planning and spatial structure, compositional integrity and functional activity. Along with the restoration of the cultural heritage site, it is planned to include new buildings and open public spaces within the historical boundaries of the site, which will allow the complex to become part of the urban cultural and information cluster and the Literary Quarter excursion route, an attractive urban facility that most fully realizes its cultural, educational and tourist potential, thus being part of a cost-effective project [16].

The architectural and planning concept (Fig. 6) involves the creation of an urban socio-cultural center of a multifunctional structure with the preservation of cultural heritage objects in its composition, taking into account a set of measures for restoration, functional reorganization, the inclusion of new construction objects within the boundaries of the site in accordance with archival data on the general development of the historical quarter [17, 18].

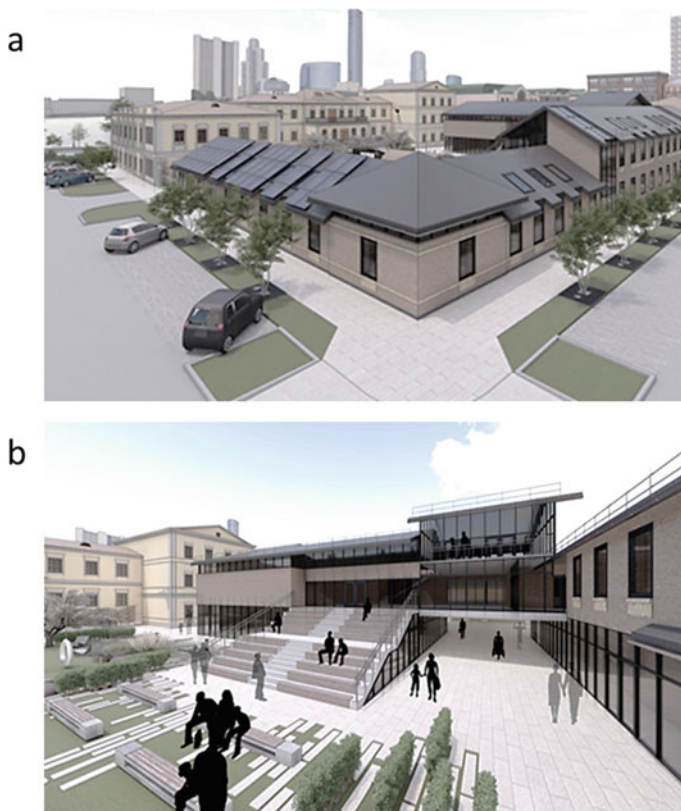


Fig. 6 Sociocultural center: **a** general view; **b** fragments of the complex

This determined the main functional tasks:

- Organization of an open public space on the territory of the courtyard and an underground exhibition center to accommodate the permanent historical exposition “Ural gold-smelting laboratory”.
- Reconstruction by placing a city mini hotel in the historic building “Residential building of the head of the laboratory”.
- Placement of the Yekaterinburg Museum Center of Folk Art “Gamayun” and the complex of premises of the city socio-cultural center in newly erected buildings, including the reconstruction of historical buildings—an outbuilding and residential building.
- Imagine the center as a system of open structures and indoor premises, an integral and functionally zoned space with convenient communications, while maintaining the principle of separation of flows and the possibility of autonomous use of individual blocks.
- In accordance with the general context, use the methods of “stylistic imitation” and “restrained contrast of old and new” through a combination of such environmental adaptation techniques as stylistic, compositional, figurative, aesthetic, coloristic.

Preserve the uniqueness of the ensemble building and the “memory of the place” by “symbiosis of the old and the new”.

5 Conclusion

The need for social, architectural and environmental rehabilitation of historical sites, which is due to the presence in degrading territories, requires, first of all, a contextual approach, taking into account the factors of development of the urban environment and its historical center. The expediency of including new buildings in the historical environment, the choice of methods of environmental adaptation depends on the analysis of these factors: urban planning, architectural and historical, sociocultural and many others. The main tasks are to achieve compositional integrity, stylistic unity and artistic expressiveness of the environment and the maximum humanization of space [19, 20]. An important role in the rehabilitation of historical centers is given to the creation of public spaces. If public spaces are created in a historical environment, then the main task is to preserve the historical and cultural heritage and create a variety of viewpoints for the perception of unique historical objects. “Currently, the tasks of updating the urban environment are being solved in accordance with the existing legislative framework, the state of the environment and the capabilities of society. It should be borne in mind that any reconstructions measures suggest a long implementation period, require strong investment support and the participation of city authorities in the development of environmental renewal programs.

References

1. Komarova KA (2023) Aktualnye problemy ekspluatatsii i prispособleniya pamyatnikov arkhitektury (Actual problems of operation and adaptation of architectural monuments). *J Young Scientist* 13(460):36–40
2. Hatherley O (2012) Na ploshchadi. V poiskakh obshchestvennykh prostranstv postsovetskogo goroda (Across the plaza: the public voids of the post-Soviet City). Strelka Press, Moscow, p 52–60
3. Sakharova OA (2011) Opyt formirovaniya sovremennogo kompleksa zdaniy iz ob"yektov, otnesennykh k pamyatnikam istorii i arkhitektury (Experience of formation of a modern complex of buildings from the objects carried to monuments stories and architecture). *J Bulletin of MGSU* 1–2:184–186
4. Gelfond AL (2011) Arkhitekturnaya tipologiya v aspekte zhiznennogo tsikla zdaniya (Architectural typology in the aspect of the life cycle of a building). *J Acad Architect Construct* <https://doi.org/10.22337/2077>
5. Nyakina PA (2023) Sochetaniye sovremennosti i kul'turnogo naslediya v arkhitekturnykh prostranstvakh Katara (The combination of modernity and cultural heritage in the architectural spaces of Qatar). *J Young Scientist* 6(453):47–51
6. Khasieva SA (2001) Arkhitektura gorodskoy sredy (Architecture of the urban environment). Stroyizdat, Moscow, pp 78–82
7. Volkova TF (2015) Metody rekonstruktsii gorodskoy sredy (Methods of reconstruction of urban environment). *J Modern Scientific Research Innovation* 4–5:113–117
8. Sinitsyn V (2013) Evropeyskiy opyt vitalizatsii ob"yektov kul'turnogo naslediya (European experience of vitalization of cultural heritage objects). *J World Art: Bull Internat Institute Antiques* 4(04):40–47

9. Glushakova ES (2012) Sintez sovremennoy i istoricheskoy arkhitektury v arkhitekturno-prostranstvennoy srede gorod (Synthesis of modern and historical architecture in the architectural and spatial environment of the city). *J Intellectual potential of the 21st century: Stages Knowl* 10–11:10–17
10. Gelfond AL (2015) Obshchestvennoye zdaniye i obshchestvennoye prostranstvo. Dualizm otnosheniy (Public building and public space. Dualism of relations). *J Acad Architect Construct* <https://doi.org/10.22337/2077-9038>
11. Zaitsev AA (2019) Osobennosti ispol'zovaniya priyemov adaptatsii kontekstual'noy arkhitektury v gorodakh Rossii (Features of using contextual architecture adaptation techniques in Russian cities). <http://www.opentextnn.ru/space/?id=4780>. Accessed 14 Nov 2022
12. Sokolov YuV (2016) Sovremennoye ispol'zovaniye pamyatnikov arkhitektury (The Modern use of Architectural Heritage Monuments). In: *Humanities scientific research Vol. 7*. <https://human.snauka.ru/2016/07/15840>. Accessed 04 Feb 2023
13. Solntsev IV, Petrov AA (2013) Primeneniye kontseptsii naiboleye effektivnogo ispol'zovaniya v otsenke pamyatnikov arkhitektury (Application of the best use concept in the valuation of listed buildings). *J Econ Strat* 15-4(112):70–77
14. Kozlova LV (2016) Obshchestvennyye prostranstva kak osnova formirovaniya istoricheskogo tsentra krupnogo goroda (na primere Irkutsk) (Public spaces as the basis for the formation of the historical center of a large city (on the example of Irkutsk)). In: *Abstracts of the Balandinsky readings, Ural Federal University, Yekaterinburg*, p 1
15. Skuratov S (2013) Obshchestvennyye prostranstva vazhneye arkhitektury (Public spaces are more important than architecture). <https://archi.ru/russia/47440/sergei-skuratov-obshchestvennyye-prostranstva-vazhnee-arhitektury> Accessed 18 Feb 2023
16. Nazarova AM (2018) Ob'yekt kul'turnogo naslediya kak instrument razvitiya territorii (Object of cultural heritage as a tool for the development of the territory). *J Sciences of Europe* 29–3(29):9–13
17. Kalnitskaya E (2008) Novye puti muzeyifikatsii pamyatnika arkhitektury: Mikhaylovskiy zamok (New ways of museofication of an architectural landmark: Mikhailovskiy palace). *J Scient J Herzen Univ* 75:123–131
18. Gryaznukhina KA (2014) Sokhraneniye promyshlennykh ob'yektov kak istoriko-arkhitekturnykh pamyatnikov (Preservation of industrial facilities as historical and architectural monuments). *J Achiev of High School Sci* 13:7–10
19. Votinov MA (2013) Sovremennyye priemy formirovaniya obshchestvennykh prostranstv v istoricheskoy srede goroda (Modern methods of forming public spaces in the historical environment of the city). *J Bulletin of BSTU named after V.G. Shukhov* 5:11–14
20. Votinov MA (2015) Renovatsiya i gumanizatsiya obshchestvennykh prostranstv v gorodskoy srede (Renovation and humanization of public spaces in the urban environment). *KhNUH them A.N.Beketova, Kharkiv*, pp 102–114



Dynamics of Development of Public Green Spaces in the City of Simferopol

O. O. Korenkova^(✉)

Moscow State University of Civil Engineering (National Research University), 26, Yaroslavskoe Shosse, Moscow 129337, Russia
o.o.korenkova@mail.ru

Abstract. The city is a whole system and is an integral part of the modern representation of the image of the state. In the urban greening system, the main environment-forming role belongs to plantations of common use. It has been established that the quantitative and qualitative parameters of green spaces in the city of Simferopol have changed over the centuries, depending on the action of a group of factors. Currently, green spaces account for only 6.6% of the entire city area. The level of provision of the population with green spaces for general use is lower than the normative one and in different years varied from 1.5 ha to 20 ha. At the same time, only in the late Soviet period did this indicator correspond to the norms and amounted to 20 m²/person. The size of the area of green spaces in the landscaping system of the city of Simferopol was largely influenced by the following conditions: an increase in the area of the city, the addition of forest fund territories to the green spaces, an increase in the area and the allocation of these territories for development. Consequently, depending on the action of one or another factor, there was an increase or decrease in the percentage of green areas for common use. The totality of the factors acting on the process of greening the city can be attributed to the socio-economic and legal group.

Keywords: Green spaces · Retrospective analysis · Urban environment · Urban landscaping · Simferopol

1 Introduction

The city is a whole system and is an integral part of the modern image of the state. At the same time, cities historically perform a number of functions that satisfy the vital needs of a person in it [1]. The current stage of social development is characterized by the rapid growth of settlements and an increase in the population, due to which a special environment is formed, which is called urban.

Man, as the main element of the city, during his life has a significant impact on its ecological system as a whole. Thus, with his own hands, a person can both turn the city into a center for the development of civilization, and become the cause of the destruction of the surrounding nature [2, 3].

The formation of the urban environment takes place within a special natural landscape and includes both abiotic components of nature—relief, climate, water resources, and biotic—flora and fauna. In addition to these components, as a result of the urbanization of cities, elements of the technosphere are added, which include production results, the urban architectural complex, and transport [4–6].

The components of the urban environment are interconnected, and as a result of their interaction, contradictions between its individual parts are intensified. The greatest impact is exerted by the transforming human activity, which resulted in the emergence of a new ecological environment with a high concentration of anthropogenic factors [7]. Today, an acute environmental problem is the problem of “green spaces”—deforestation and reduction of green areas due to construction can lead to serious consequences. That is why it is so important to preserve as much urban green space as possible, which is a projection of the natural ecosystem.

Green spaces are one of the factors for optimizing the environment. They make it possible to improve the microclimatic and ecological conditions of certain sections of the city, and as a result, create places for comfortable and safe recreation and stay of people. Green areas are one of the mandatory elements of cities. They not only improve sanitary and hygienic conditions, but also largely determine the appearance of the city and its aesthetic merits [8, 9].

The territory of the city is changing, and as a result of the creation of new and reconstruction of old districts, the single green zone is also changing, which is interconnected by various “arteries” in the form of boulevards, parks, gardens, squares and landscaped pedestrian streets, forming a system of landscaped common areas. Undoubtedly, the main place in the landscaping system of the urban area belongs to green areas of common use, which have a beneficial effect on the state of the environment and are not only a place for mass recreation of the population, but also a place for pedestrian transit routes [10].

In recent years, the active activity of the population in the form of recreational running, gymnastics and other events—the so-called sanation amateur performance of the population, as well as walking their pets—has become massive [11]. Thus, many parks and squares take on the load along with the stadiums, covering alleys, playgrounds and glades. But not all public places are ready for such loads. The functioning of green areas of common use is affected by the proximity of public service centers. This implies an increased level of transit pedestrian flows and an increase in the number of visitors. Thus, in order to prevent negative consequences on natural resources, it becomes necessary to improve the system for planning planning, landscaping and landscaping of construction sites.

The neighborhood of public green spaces with places of residential formations increases the level of comfort for the population [12]. In many ways, even this is the main factor in the acquisition of housing. In recent years, the main problem of the urban environment for green spaces has become “spot” buildings that arise in the middle of parks and squares, disrupting the balance of the green area and reducing not only the quantitative indicators of greening, but also the qualitative conditions of existence in these conditions. To prevent such actively developing negative ones, it is necessary to legally fix compensatory landscaping under similar conditions for developers.

In order to create comfortable living conditions in urban areas, it is fundamentally important to fix the balances of the biotechnosphere in the form of normative ones, which, by law, will ensure a gradual transition to achieving a balance [13].

In the Republic of Crimea, the process of urbanization is actively taking place, actualizing the problem of creating a comfortable urban environment. Of particular importance in obtaining a high-quality environment in a large city is given to favorable conditions for the population's recreation, which contribute to effective labor activity [14].

In the urban greening system, the main environment-forming role belongs to plantations of common use. Today in Simferopol there are quite a few parks, gardens, squares and boulevards, which are a legacy of the Soviet period and require significant renovation. The structure of the city is very diverse, as evidenced by the maps of previous years, showing the dynamics of the growth of the city along the periphery and the development of developed territories. At the same time, the pressure on the state of the environment increases. In the conditions of pollution of emissions from vehicles and industrial enterprises, the improvement and landscaping of populated areas are of particular importance.

In recent years, the main problem of the urban environment for green spaces has become "spot" buildings that arise in the middle of parks and squares, disrupting the balance of the green area and reducing not only the quantitative indicators of greening, but also the qualitative conditions of existence in these conditions.

The purpose of the study is to identify the basic principles of the formation of public green spaces in the city of Simferopol.

To achieve this goal, the following tasks were set: to identify patterns of development of green spaces for general use; perform a systematic analysis of the influence of socio-economic factors on the quantitative and qualitative parameters of green areas for common use.

2 Materials and Methods

The scientific research was carried out in several stages. At the first stage, cameral work with archival materials was carried out. We searched for cartographic material of the city of Simferopol. In the course of the research, the most detailed maps and general plans of the city were selected.

At the second stage, work was carried out with the obtained illustrative material, and its comparison was carried out. The available data was divided into six time periods: the first stage—the Russian Empire; the second stage is the Soviet period; the third stage is the Late Soviet period; the fourth stage is the Post-Soviet period; the fifth stage is the Ukrainian period; the sixth stage is the Russian Federation. The maps revealed areas of green spaces of common use. The next step of the work was the calculation of the area of the studied green spaces using the AutoCAD computer-aided design systems. Subsequently, the obtained data were statistically processed [15, 16].

3 Results and Discussion

In the urban greening system, the main environment-forming role belongs to plantations of common use. They are the most important indicators of the city greening degree [17, 18].

The modern landscaping system developed gradually and changed along with the boundaries of the city (Fig. 1), the population and its provision with green spaces. As Simferopol expanded along the periphery and new territories were annexed, the area of green spaces changed.

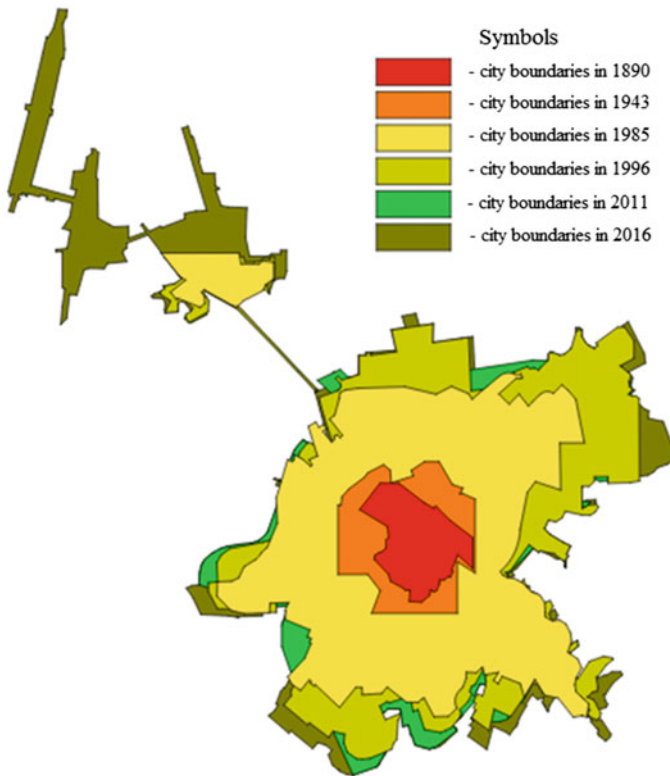


Fig. 1 Scheme of changing the boundaries of the city of Simferopol

One can observe a complete picture of the dynamics of changes in the landscaping system, depending on the influence of a group of factors. The analysis is based on socio-economic factors, depending on which the quantitative parameters of green spaces changed in different periods.

As you know, the landscaping of Simferopol began in the 1950s after the end of the war and gained momentum every year. The landscaping system gradually took shape, if initially the process was more chaotic than practical, then later it was thoughtful and

planned, thanks to the emergence of a unified regulatory framework and the level of specialists involved in the matter.

The area of public green spaces, including parks, gardens, squares, boulevards, urban forests and forest parks, is: for 1890–7.2 ha for 1943–10.05 ha, for 1985–696 ha, for 1996–453.7 ha, for 2011–550.2 ha, for 2016–543.1 ha. If we consider these green areas in the city system, it turns out that the percentage of green spaces in the total area of the city is: for 1890–1.65%, for 1943–1.03%, for 1985–13.9%, for 1996–8.22%, for 2011–10.37%, for 2016–6.62%. Figure 2 shows a histogram of the ratio of the area of green spaces for general use to the area of the city of Simferopol.

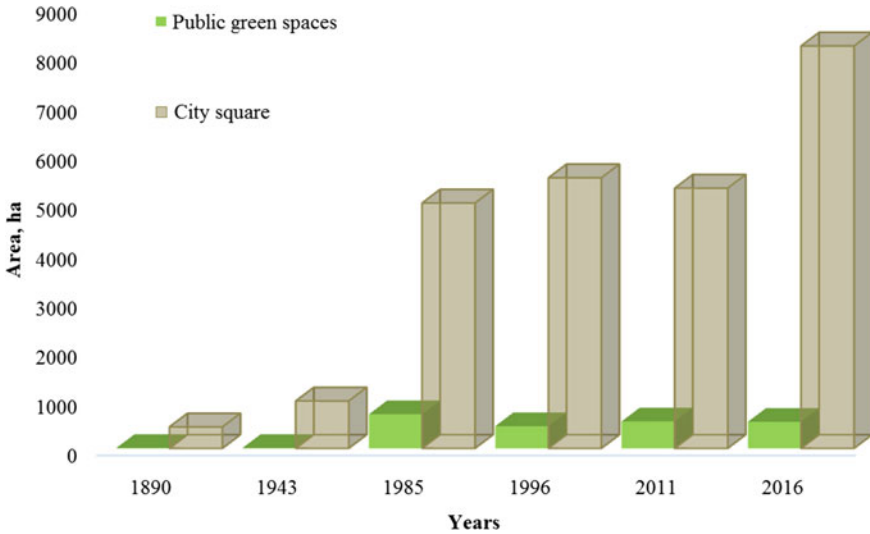


Fig. 2 The ratio of the area of green spaces for general use to the area of Simferopol

At the same time, if we do not take into account the areas of urban forests and recreation, but take into account only parks, gardens, squares and boulevards, then the area of greenery in public places will have lower indicators (Table 1).

Table 1 Indicators of the area of green spaces in common use, excluding urban forests

Parameter	Years					
	1890	1943	1985	1996	2011	2016
The area of green spaces for general use, ha	7.2	10.05	212.5	161.5	175.4	143.5
Share of the total area of the city, %	1.65	1.03	4.25	2.93	3.31	1.75

One can observe a direct dependence of the growth in the number of green areas, their area and share in the city system, depending on the increase in the area of the settlement and the number of inhabitants in it, which we see on the graph at the beginning (Fig. 3), but not always the growth of the city and the population is accompanied by an increase in the number of green spaces, even including urban forests.

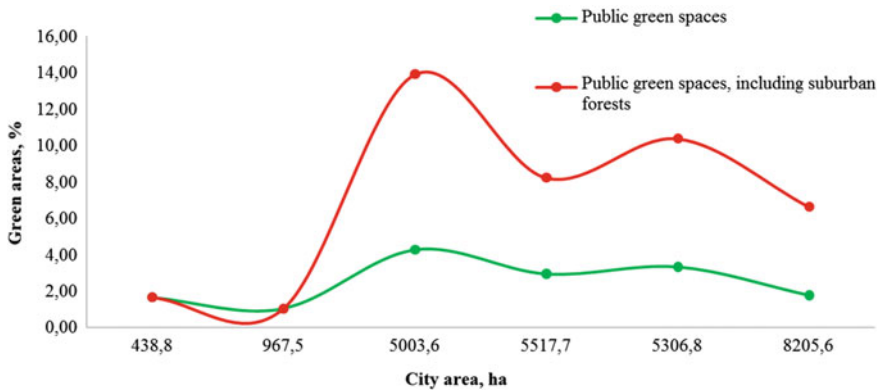


Fig. 3 Dependence of the percentage of green areas on the area of the city

A sharp rise in indicators in 1985 is characterized by the inclusion of urban forests in the plantations, as well as the display of these forests on the general plan, although afforestation in the Crimea began to be actively engaged in since the 1950s in accordance with the program for the creation of artificial forests. A significant decline in 1996 is explained by the change in the area of urban forests in the central region due to the development of the Ak-Mechet and Pnevmatika microdistricts. In subsequent years, there is again an increase in indicators due to an increase in the area of the city along the periphery and the annexation of territories, including lands of the forest fund.

In the process of city development, there is a reduction in green areas—parks, gardens, squares, street gardening and other green areas, but what is important, these objects come to a neglected state. There is a so-called process of destruction of a unified system of gardening. The problem lies not only in the reduction of green areas, but also in many respects the preservation of such areas depends on the quality selection of planting material, selection of plants depending on climatic conditions and qualified care for them [19–23].

Green areas of common use are the most important indicators of the degree of greening of the city. The provision of each resident with green spaces speaks of the state of urban green building and largely determines the future plan for the development of the urban system in the future. Therefore, data on the level of provision of the population with green areas are fixed at the technical and regulatory level and are mandatory.

To determine the indicator of landscaping, the calculation of the area of green spaces per 1 person in the whole city for all years was carried out (Table 2). The calculations are based on legal acts—SNiP II-K.2-62, SNiP II-60-75 and SNiP 2.07.01-89* [24–27].

Table 2 Comparison of indicators of provision of the population with green spaces for general use in different periods

Parameter	Years					
	1890	1890	1890	1890	1890	1890
Population, pers	38,000	67,000	338,000	343,565	336,330	336,460
Population density, person/km ²	8675.79	6928.64	67,600	62,352.99	63,458.49	41,031.70
City area, km ²	4.38	9.67	50.03	55.17	53.06	82.05
Area of common areas, ha	7.2	10.05	698.0	453.7	550.2	575.3
The level of provision with green areas, m ² /person	1.9	1.5	20	13.2	16.3	17.1
Normative level of provision with green areas, m ² /person	–	–	18	18	18	18

In accordance with the current standards of urban planning at the federal level for cities with a population of 250 to 500 thousand people. the area of green areas for common use should be at least 16 m²/person. and 18 m²/person. for the Southern regions (at the local level of a constituent entity of the Russian Federation) [28]. An analysis of the quantitative characteristics of the normalized parameters showed that the landscaping of public facilities of all years does not adequately comply with the standards given in SNiP 2.07.01-89* [24].

In 1890, the rationing of green areas was not carried out, there was no any regulatory and technical basis for regulating this area, therefore, it is not possible to assess the ratio of the level of provision of the population to the current standards. We can only state that the number of green spaces per person was 1.9 m². landscaped areas of common use (gardens) accounted for only 1.65% of the total area of the city.

The same situation is typical for 1943 as well. rationing in the period of the Soviet Union begins only in 1958 with the document SN 41–58 “Rules and norms for the planning and development of cities” [29], which regulates exclusively the balance of territories for public facilities. Therefore, we can only talk about the number of green spaces per person in 1943, which is 1.5 m².

The highest indicators of provision with green spaces are typical for 1985 and amount to 20 m²/person. when presented by the standard 18 m²/person. The used normative act SNiP II-60-75 allows an increase in the number of green spaces by no more than [26] than by 20% for the southern regions. Such high rates are explained by the fact that during the period of perestroika much attention was paid to programs for the restoration of landscaping. Accordingly, each resident was sufficiently provided with green spaces for a comfortable life in the city.

Already by 1996, these figures decreased and began to amount to 13.2 m²/person. Such a decline compared to 1985 is associated with the collapse of the Soviet Union and, accordingly, a reduction in city greening programs, as well as the development of green areas for other needs. Work on the creation of new and reconstruction of existing

landscaping facilities is constantly being reduced, and the quality of their maintenance is declining.

It should be noted that despite the non-compliance with the norms, the number of green spaces in common use since 1996 tends to increase over the years. This indicates that the city is gradually recovering and in the near future, subject to the necessary measures, it will be able to fully provide residents with comfortable living conditions. Already in 2011, these figures are 16.3 m²/person, and in 2016–17.1 m²/person, which indicates an increase in the area of green spaces (Fig. 4).

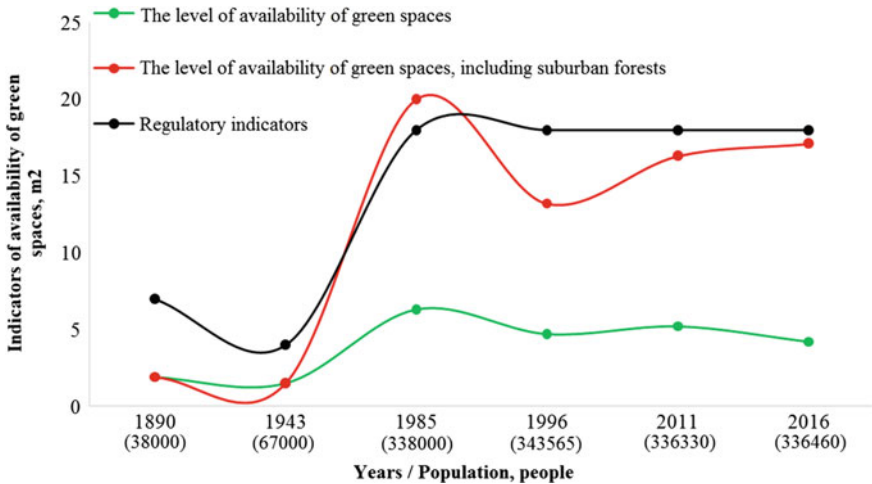


Fig. 4 The level of provision of the population with green spaces for general use

According to the master plan for 2016, a prospective increase in the number of plantings for common use is planned to reach 29.8 m²/person.—this is 57.4% higher than the current indicator. This is possible only if all measures to restore landscaping are observed. This indicator is taken into account together with the area of urban forests, but with unregulated use of their territories, the sanitary condition, aesthetic appeal, and ecological value of landscapes may deteriorate [30]. Therefore, it is necessary to fix the requirements for the exploitation of forests in a regulatory manner in order to prevent irreversible consequences in the future.

4 Conclusion

The quantitative and qualitative parameters of green spaces have changed over the centuries depending on the action of a group of factors. The share of green spaces in the landscaping system of Simferopol was largely affected by the following conditions: an increase in the area of the city, the addition of forest fund territories to green spaces, an increase in the area and the allocation of these territories for development. Consequently, depending on the action of one or another factor, there was an increase or decrease in the percentage of green areas for common use. The totality of acting factors can be attributed to the socio-economic and legal group.

It has been established that in 1985 the indicators of the provision of green spaces for residents of the city of Simferopol were the highest and amounted to 20 m²/person. when presented by the standard 18 m²/person. By 1996, these figures decreased and began to amount to 13.2 m²/person. Over the next 20 years, this indicator slightly increased (in 2011–16.3 m²/person, and in 2016–17.1 m²/person). However, it is below the normative indicators (18 m²/person).

References

1. Sanaev IV (2006) The role of green spaces in creating an optimal urban environment. *Forest Bulletin* 6:71–76
2. Dyupin MV (2021) The role of green spaces in cities. *Sci Works Stud Izhevsk State Agric Acad* 2(13):141–143
3. Pastukhov MA, Smirnova DO (2020) Urban green spaces. Experience of the world's largest cities. *Sci Works KubGTU* 8:791–795
4. Zemtsova AM, Racheev NO (2021) The functional role of green spaces in urban ecosystems on the example of the city of Kirov. Knowledge of the young: science, practice and innovation: collection of scientific proceedings of the XX international scientific and practical conference students and young scientists, Kirov, March 12, 2021, pp 11–15
5. Isaeva LG, Khimich YR (2020) Assessment of the state of green spaces in the city of Monchegorsk (Murmansk region). *Proc Kola Sci Center Russ Acad Sci* 11(2–8(8)):168–179. <https://doi.org/10.37614/2307-5252.2020.2.8.018>
6. Savchenkova VA, Pionkova KA, Malyshev DA (2020) Assessment of the state of green spaces in the city of Korolev. *Academy* 11(62):20–23
7. Runova EM, Gnatkovich PS (2013) Ecology and rational environmental management. *Syst. Methods. Technol. Species Compos* 2:156–159
8. Nizamutdinov TI, Kolesnikova EV, Alekseev DK (2021) Influence of green spaces on the dynamics of air pollution in cities. *Bulletin of the perm national research polytechnic university. Appl Ecol. Urbanistics* 1(41):58–73. <https://doi.org/10.15593/2409-5125/2021.01.05>
9. Bystrova AS (2016) Dust-collecting capacity of green spaces within the residential area of the city of Abakan. *Ecology of Southern Siberia and adjacent territories, Abakan, November 23–25, 2016*, pp 140–141
10. Belyaeva YuV (2019) Evaluation of the effectiveness of green spaces in the city of Tolyatti. *Synergetics Nat. Tech Socio-economic Syst* 16:283–289
11. Bukharina IL, Zhuravleva AN, Bolyshova OG (2012) *Urban plantations: ecological aspect: monograph. Izhevsk*
12. Mikhhalcheva SG, Rylyakin EG (2018) Modern problems of organizing urban green areas for common use. *Sursky Bull* 2(2):49–52
13. Borisov MV, Bakaeva NV, Chernyaeva IV (2020) Normative and technical regulation in the field of landscaping the urban environment. *Vestnik MGSU* 15(2):212–222
14. Skopenko DV, Korenkova OO (2018) Green spaces of the city of Simferopol. *Materials of the IV scientific conference of the faculty, graduate students, students and young scientists. Simferopol*, pp 876–878
15. Shadrina IA, Lavrova OP (2021) Analysis of methods for monitoring and managing green spaces in Russian cities using digital technologies. *Landscape architecture and the formation of a comfortable urban environment: proceedings of the XVII regional scientific and practical conference, Nizhny Novgorod, March 25, 2021*, pp 94–101

16. Ionova MN, Degteva ZhF (2020) The use of remote sensing for monitoring green spaces in the city of Yakutsk. In: Ionova MN (ed) Bulletin of the north-eastern federal university; Ammosov MK. Ser: Earth Sci 4(20):57–64. <https://doi.org/10.25587/SVFU.2020.20.4.003>
17. Atkina LA, Bulatova LV (2017) Rationing and placement of landscaped public areas in Yekaterinburg. Perm Agrarian Bull 4(20):146–152
18. Boyko TA, Zbrueva II (2021) The state of green spaces in the landscaped areas of common use of the central planning area of the city of Perm. Ecol Urbanized Territ 4:63–67. <https://doi.org/10.24412/1816-1863-2021-4-63-67>
19. Morozova GY (2010) Problems of landscaping in the Far Eastern cities. Proc Samara Sci Center Russ Acad Sci 12(3):772–775
20. Vershinina IV, Kuposova NN (2022) Ecological assessment of green spaces in the square 70th anniversary of the victory in the city of Bor, Nizhny Novgorod region. Nat Techn Sci 6(169):63–66
21. Zubareva ON, Prysov DA, Bulanova OS (2021) Analysis of the state of green spaces in the Central Park of the city of Krasnoyarsk. Siberian For J 6:46–58. <https://doi.org/10.15372/SJF S20210605>
22. Al-Mossavi BA, Al-Shebillawi ID (2021) The system of urban green spaces as a factor in the sustainable development of cities in Iraq (on the example of the city of Samawa). Actual problems and prospects for the development of the construction complex: proceedings of the international scientific and practical conference: at 2 o'clock, Volgograd, December 07–08, 2021, pp 35–38
23. Julia VB (2019) Ecological and biological monitoring of urban green spaces in the conditions of technogenesis. West-Russia-East 13:189–191
24. Building codes and regulations of RF 2.07.01-89* (1994) Urban planning. Planning and building urban and rural settlements: normative material
25. Building codes and regulations of RF II-K.2-62 (1967) Planning and development of populated areas. Design standards: normative material
26. Building codes and regulations of RF II-60-75** (1985) Planning and development of cities, towns and rural settlements. Design standards: normative material
27. Ilbulova GR, Buskunova GG, Khasanova RF (2020) Assessing the availability of green spaces in microdistricts of the city of Sibay (Republic of Bashkortostan). Ecology and nature management: applied aspects: X International scientific and practical conference, Ufa, March 15–20, 2020, pp 104–108
28. Rules for the creation, maintenance and protection of green spaces located on the territory of the municipality of the city district of Simferopol of the Republic of Crimea: regulatory material; input. 04.02.2015, Simferopol
29. Rules and norms for planning and building cities: SN 41–58: normative and technical material (1959)
30. Bakaeva NV, Sporysheva EA, Shcherbakova AA, Konstantinova VS (2016) Ecological problems of development of modern cities. Des Constr 7–12



Long-Term Risks of Urban Landscape Transformation

A. Gushchin^(✉) and M. Divakova

Ural State University of Architecture and Art Named for N.S. Alferov, 23, K. Liebknecht Str.,
Ekaterinburg 620075, Russia
alexanderNG@yandex.ru

Abstract. This article analyses different approaches to defining the concept of landscape. The author's approach to the definition of the concept of landscape, allows to substantiate the original interpretation of urban planning activity as an activity to replace some components of the landscape by others: natural components by man-made ones. Further, the authors note that the replacement of some components in such a complex system as landscape is always associated with risks. Risks of this type are referred to by the authors as Landscape risks. The authors describe the main characteristics of landscape risks and give specific examples for the largest city, which is Ekaterinburg in Russia. Then the authors analyse various ways of identification and management of landscape risks and come to a conclusion that the best way to identify not only risks but also chains of cause and effect describing changes in landscape, is the system DPSEEA: driver, pressure, state, expansion, effect, action. The authors have constructed chains of indicators for the examples of landscape violations given in the article. Further the possibilities of including landscape risks in spatial urban development planning procedures are analyzed. It concludes that such opportunities are not sufficient.

Keywords: Risk · Landscape · Landscape risk · Risk management · Spatial planning

1 Introduction

The concept of landscape was introduced into science by the famous Russian scientist A. Humboldt, who borrowed this word from his native German, where it had been used since ancient times and meant “die Landschaft”—“a kind of land”, “a kind of terrain”, “... a large surface area visible to the general eye, which differs from neighbouring areas by characteristic individual features” [1]. Over time, the concept of landscape has been part and parcel of a scientific discipline such as geography. Today, landscape science is at the core of physical geography. Under the influence of geography, a normative definition of landscape was adopted and enshrined in the state standard GOST 17.8.1.01-86 [2]: landscape is “a territorial system consisting of interacting natural or natural-anthropogenic components and complexes of lower taxonomic rank”. This definition makes it possible to divide landscapes into two types: natural landscapes and

anthropogenic landscapes. A natural landscape is a landscape consisting of interacting natural components or complexes of lower taxonomic rank. Anthropogenic landscape is a landscape consisting of interacting anthropogenic components. The state standard GOST 56891.4-2016 defines the concept of cultural landscape as follows: “Territorial complex formed as a result of evolutionary interaction between nature and man, his socio-cultural and economic activities and consisting of characteristic combinations of natural and anthropogenic components that are in a stable relationship and interdependence” [3]. The authors emphasize two fundamental characteristics in this definition: (1) cultural landscapes are the result of evolutionary interactions between nature and humans, and (2) natural and anthropogenic components are in a stable relationship and interdependence. This is the starting point for further considerations.

2 The Concept of Landscape Risk

The concept of landscape risk is relatively little used in the Russian scientific school. There is no systematic theory of landscape risks. Individual aspects of landscape risks are considered. An example is the work of Pershina et al. [4], devoted to the risk analysis of the landscape design process (landscape design). Accordingly, landscape risks are also design risks. The concept of landscape risk is more common in foreign scientific schools. Scientific research has already entered the methodological stage. The result of methodological research was a Guide to the assessment of environmental risks [5]. The Guide and the works, based on it, use concept of the ecological risk, but do not give its exact definition.

Here are some definitions of environmental (ecological) risks. In the study X. Li and co-authors environmental risk is interpreted as “Landscape environmental risk is a negative consequence of the interaction between landscape characteristics and external threats when the landscape is exposed to one or more sources of risk” [6]. The authors of the paper see the cause for environmental risks in growing urbanization: “With rapid urbanization, the expansion of artificial (developed) lands occurs at the expense of ecological lands and can increase landscape fragmentation and vulnerability” [ibid.]. In the study by W. Xu et al. the reasons for the risks are that “The complex impact of factors from many sources changes the structure of the landscape and reduces the quality of landscape ecology in the area of large-scale open-pit coal mines, which leads to an ecologically unstable environment” [7]. An example of a practical approach to assessing the consequences of risks without their precise definition is given in the work of R. S. Leven, I. Pudevina “The purpose of environmental risk assessment is to assess the likelihood that an anthropogenic disturbance will have a negative impact on ecosystems, which will lead the ecosystem to a new dynamic equilibrium with a simpler structure and less potential energy. The probability of risk depends on the threshold capacity of the system (resistance) and on the ability of the system to return to a state of equilibrium (elasticity)” [8]. An approach based on external factors allows the use of advanced mathematical tools. In general, the presented research area is characterized by the following features: In general, the research direction presented is characterized by the following features:

- close linkage to ecology—risks are often referred to as landscape ecological risks;

- the cause of risks is the action of various kinds of factors external to the landscape system; examples of factors may be very diverse: mining, urbanization and others;
- orientation on practical approach—many authors do not define the concept of risk, but go straight to the methods of its assessment.

The author's interpretation of landscape risk differs in his understanding of the nature of risks. Earlier it was said that urban planning is considered as an activity that results in some components of the landscape being replaced by others. Natural components are replaced by anthropogenic ones. The author's view set out in more detail below.

3 Urban Planning Activities—Landscape Modification Activities

The concept of urban planning activity is defined in the Urban Planning Code of the Russian Federation: “Urban planning activity is an activity on the development of territories, including cities and other settlements...” [9]. What is the result of this activity? Urban planning and architecture create an urban environment that develops not according to natural laws, but according to the laws of aesthetic, economic, social and other laws. It is the way in which the environment is formed that distinguishes one scientific discipline from another. More precisely, the way it is formed determines the competences needed to study the newly created environment. According to the authors, there is nothing to prevent us from extending the original understanding of landscape as a visual representation before our eyes to the urban environment. The urban environment also contains natural and anthropogenic components, but it is mainly shaped by human activities and evolves not only according to natural laws, but also according to economic, social and societal laws. As we can see, the difference lies in the way the landscape is formed. Figure 1 a and b demonstrate urban landscapes of different genesis. Another difference is that the natural landscape was not created to meet human needs, on the contrary, man is forced to adapt to it. The urban landscape, on the other hand, has been created from the outset to meet human needs. The urban landscape is therefore a manageable system, if not in practice then at least in theory.



Fig. 1 a Anthropogenic landscape shaped by industrial activities. Magnitnaya Mountain. *Source* [11]; b. Urban landscape shaped by urban development activities

Managing a system as complex as the landscape is a process that does not always lead to the desired results. As evidence, we present the assessment presented in the Spatial

Development Strategy of the Russian Federation. The strategy notes “the low level of comfort of the urban environment in most cities, including large urban agglomerations, large urban settlements and urban-type agglomerations”, “the unsatisfactory state of the environment in most cities with more than 500 thousand inhabitants and industrial cities, the lack of green spaces, fragmentation and violation of their integrity in these cities” [10].

The laws of behavior of complex systems are described in many works on systems theory [12], but we will be interested in the laws formulated by Jay Forrester in computer modelling of cities [13]. According to Forrester, every management decision aimed at solving a problem generates two types of systemic reactions: short-term and long-term. The short-term response is a response to actions taken to solve a specific problem. After the problem is solved, there is a long-term response. The long-term reaction is negative in nature and is associated with the unintended consequences of solving the problem. The existence of long-term reactions is a consequence of incomplete and limited knowledge about the behavior of complex systems. It follows from what has been said that solving any urban development problem will also have long-term negative reactions. The most obvious example is the creation of a transport network in cities and the long-term rehabilitation in the form of traffic congestion. Let’s return to the understanding of urban development as a landscape-altering activity. Everything that has been said about long-term responses applies to urban planning as a landscape-altering activity. Because of our limited knowledge, any urban development activity will create long-term risks. It is precisely these risks—the risks generated by the activity of changing the landscape—that we will call landscape risks. Thus, landscape risks are characterized by the following features:

- long-term nature aimed at degradation of the urban landscape,
- multi-scale structure characteristic of the landscape as a whole [14].

4 Examples of Landscape Risks

Let us consider the risks of urban landscape transformation using the example of the creation of green infrastructure in the city of Ekaterinburg. The territory of the modern city of Ekaterinburg has a developed river network of 11 rivers and many wetlands. In the 1960s, the possibilities for spatial development were exhausted and the drainage and development of wetlands began. Figure 2a shows the modern development of Ekaterinburg and the contours of the developed peatlands. The development of the peatlands has disturbed the water balance of the area, and this imbalance has created a long-term trend that has led to the degradation of the green infrastructure.

The current state of the city’s green infrastructure can be assessed using remote sensing data (multispectral satellite imagery). The urban greening system (green infrastructure) is studied using images in different channels of the optical spectrum and different combinations of channels. In particular, the vegetation index is constructed to highlight the part of the spectrum absorbed by plant chlorophyll during photosynthesis. Absorption in this part of the spectrum makes it possible to assess the state of vegetation. The index indicates the presence and condition of vegetation (relative biomass). The importance of studying the vegetation index is due to the fact that the methodology

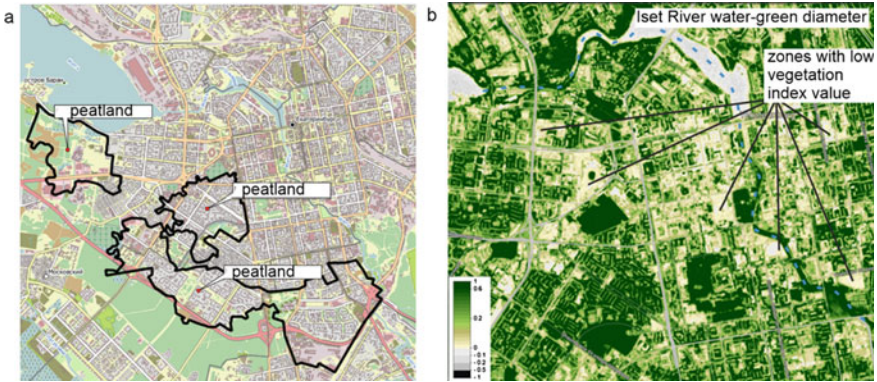


Fig. 2 a Fragment of the 1947 Sverdlovsk plan, superimposed on the modern development. Source [16]; b. NDVI vegetation index values for central Yekaterinburg. Imagery date 30.08.2022. Sentinel-2 satellite. Source [16]

for assessing the quality of the urban environment [15] uses remote sensing data for this part of the optical spectrum. In general, the urban environment quality index includes six “spaces”—blocks, each of which is evaluated according to six criteria, each of which is evaluated by a set of indicators. One of the “spaces” is the “green spaces” block. The indicator system of this block includes indicator N14—“The share of green areas of common use”, which is “calculated by interpreting satellite images and determining the share of the urban area covered by vegetation in the total area of the city”. The next important indicator is indicator N15 “Green area coverage”, which is ‘calculated based on the interpretation of satellite images and the calculation of the vegetation index as the proportion of the area with high biomass plantations in the total green area of the city. The guidelines for assessing the quality of cities do not provide a specific methodology for calculating the index. In general, the vegetation index makes it possible to assess the relative biomass of vegetation and its potential for the development of a city’s green infrastructure.

The spatial distribution of the vegetation index is shown in Fig. 2b. Data from the European Space Agency. The color scale of the vegetation index is based on color intensity—the most saturated color corresponds to dense vegetation (trees), less saturated color corresponds to shrubs, weakly saturated color corresponds to grass, colorless and dark values correspond to disturbances. Figure 2b shows the presence of gaps—large empty areas of the territory. In such areas there is little total plant biomass: trees, shrubs and grasses. The figure also shows the riparian area of the Iset River—the green water frame of the city. In the river area, there is also a lack of the biomass necessary for the formation of a water-green frame. All of the above: gaps, free vegetation, a deteriorating water-green frame, indicate the deterioration of the drainage system in the area. The drainage system in the area used to include wetlands and streams. Thus, the landscape risks associated with the development of peatlands have materialized.

The landscape risks of the formed green infrastructure configuration are as follows. Modern green infrastructure is a circular structure formed by a system of forest parks. The spatial configuration of the green infrastructure is shown in Fig. 3a, which is part of

the master plan. The main disadvantage of this concept is that it is not scalable and, over time, will no longer meet the needs of urban development. The complexity of scaling the spatial structure of the ring is explained by simple geometric considerations: the area of the circle enclosed by the ring is proportional to the square of the ring radius, so the cost of extending the ring is proportional to the square of the ring radius. The spatial structure that ensures growth must include linear (quasi-linear) spatial elements. In this case, the cost of providing growth is proportional to length. Returning to green infrastructure, we conclude that the existing spatial configuration of green infrastructure hinders urban development and requires high-rise buildings. The importance of linear elements in the spatial configuration of green infrastructure was emphasized by V.V. Vladimirov, the author of the term “green frame” of the territory [16]. Thus, the spatial configuration of green infrastructure creates one of the possible scenarios (development risks)—landscape risks in the terminology of this article.

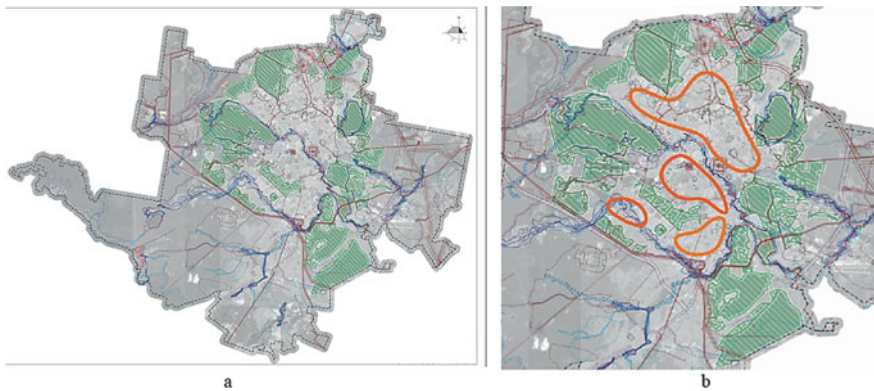


Fig. 3 **a** Areas with special conditions of use. *Source* [17]; **b** The contours of the thermal island predicted by the authors for Yekaterinburg

Another risk posed by the circular spatial configuration of green infrastructure is climate risk. Climate risk arises from the lack of linear elements in the spatial configuration of green infrastructure. The importance of green wedges is that they contribute to the free movement of air—the “ventilation” of the city center, thereby normalizing the microclimate and eliminating the heat island effect characteristic of large cities. Linear elements are often referred to as ‘green wedges’. In their work, the authors predicted the contours of the heat island [17]. The predicted contours are shown in Fig. 3b.

The general approach to risk management is set out in the national standard of the Russian Federation GOST R ISO 31000–2019 [18]. The standard describes risk management in the form of step-by-step procedures, starting with the identification (detection) of risks. In order to carry out the procedure of identifying risks, it is necessary to classify them beforehand. To classify risks, we use the work of Akimov et al. [19]. According to this classification, landscape risks are classified. In terms of risk: natural and technospheric, since the urban landscape contains both natural and man-made components. For the reason: to the possible implementation (scenario) of negative development trends. As far as is possible, landscape risks are classified as non-insurable risks. As a result,

landscape risk losses are expressed in terms of long-term consequences and are not always amenable to precise calculation. By its very nature, the assessment of landscape risk damage is often a cost–benefit assessment. This leads to the conclusion that there is a need for systematic monitoring of landscape risks. According to the authors cited, landscape risk assessment can be carried out using phenomenological or expert methods. Phenomenological methods of landscape risk assessment require long-term monitoring: in the example of peatland development above, it took several decades. This leaves expert methods—methods of qualitative risk assessment. There are several well-tested techniques for qualitative risk assessment:

- Probability-impact matrix—the method involves creating a matrix in which the probability of a risk occurring is assessed on one axis and the impact on the project is assessed on the other. Each potential risk is then assigned an appropriate value in the matrix, allowing the most significant risks to be identified.
- SWOT analysis. This method uses a SWOT (Strengths, Weaknesses, Opportunities and Threats) matrix to identify risks. It helps to identify the internal and external factors that can affect a situation and to determine what the risks are.
- Expert approach. This method uses the knowledge and experience of experts to assess risks.
- Historical data analysis. This method relies on the analysis of past data and experience to identify potential risks. By analyzing data from past projects or events, general trends and factors that may affect the current project can be identified.
- Decision tree method. This method presents risks in the form of a tree, with each branch representing the potential consequences and probability of occurrence. Probability and impact analysis is then used to identify the most significant risks.

Unfortunately, most of the known risk identification methods are difficult to use for their own reasons. The Probability Impact Matrix method is of little use because of the aforementioned complexity of damage assessment and the long-term impact of the risk. The SWOT analysis method aims to assess the current situation rather than trends. The expert approach requires a certain level of expertise and credibility of the experts. Historical data analysis can not only be used, but is also an important component of landscape risk identification. The decision tree method allows identification and prediction of trends, but can lead to combinatorial explosion—exponential growth of options, so should be used in conjunction with expert judgement to eliminate known unrealistic options.

According to the authors, one of the most promising methods for assessing landscape risks is an indicative approach, i.e. an approach based on indicators. Many different indicators have been developed on the basis of the indicative approach. For example, the urban environment quality index mentioned above. Indicator—on the basis of which the state of the urban environment is monitored, consisting of six blocks. Landscape risks require a separate indicator structure. We will use the DPSEEA scheme: Driver—Source, Pressure—Pressure, State—State, Expansion—Rapid (Extensive) Growth, Effect—Result, Action—Action [20]. The idea of this technique is as follows: drivers (D) refer to factors that cause different processes. Driving forces create pressure factors—pressure (P). In response to the resulting pressure, the state (S) of the object (environment, landscape) changes. Changes in the state of an object lead to

“explosive” factors—factors that act more strongly than others. As a result of the “explosive” factors, a spectrum of consequences (effects) appears—effects (E). At the end of the chain is an action that can be directed at any stage of the chain (A). The DPSEEA method is considered to work well for risks related to environmental pollution [21].

For the examples of landscape risk discussed above, the DPSEEA chain might look like this the source (driver) is the reduction of wetlands within the city. The driver is the total moisture content of the soil, calculated using the water balance equation [22]. As a result of the action of the stress factor, the state of the system *S* changes, as an indicator of which soil moisture can be selected. Soil moisture varies spatially inhomogeneously, so we choose the spatial heterogeneity of soil moisture as the explosion factors. And the last indicator (effects) is the total mass of vegetation, calculated on the basis of the vegetation index mentioned above. This is the chain of cause and effect relationships. Taking into account the development of this system of indicators, we can assess the real existence of the constructed system of cause-effect relationships and take timely measures to prevent negative consequences. The proposed indicator chain can also serve as a basis for analyzing climate impacts. The first two links in the chain remain unchanged: this is a decrease in the area of the wetland (source), the load factor is the total moisture reserve in the soil. Differences begin at this level: the amount of evaporated moisture can be chosen as a factor in the state of the system. Furthermore, a decrease in the amount of evaporated moisture leads to an increase in surface temperature and the formation of a heat island, as shown in Fig. 3b.

The next important issue is the question of risk management procedures. The Russian Federation provides for the creation of a territorial safety passport for each subject [23]. However, the Safety Data Sheet reflects natural emergencies that require immediate response, and landscape risks are only trends. Potential landscape risks can be reflected in master plans or development strategies of the municipality. The composition of the schemes of the master plan is determined by Article 23 of the Town Planning Code “Content of the master plan of the settlement and the master plan of the urban district”. The content of the master plan provides for “a list and description of the main risk factors for natural and man-made emergencies”. The problem is that landscape risks form negative trends, but do not always lead directly to emergencies. A good example of this is the situation with the state of the vegetation in the riparian area of the Iset River, which is important for creating a green water frame for the city. The state of the vegetation is shown in Fig. 2b. Of course, the condition can be described as poor, but this is not an emergency. The trends created by landscape risks worsen the general state of the urban environment and can be taken into account in the integral assessment of the quality of the urban environment using known methods—according to the Urban Environment Quality Index. The Urban Environmental Quality Index focuses on the needs of administrative management and encourages the elimination of the consequences of previous decisions rather than the elimination of the causes. For example, the index includes the indicator “green space area”, to improve the quality there is an obvious solution—to increase the green space area. The reasons for the lack of green spaces are not important for improving the urban environment quality index. For these reasons, the urban environment quality index is not suitable for managing landscape risks. The most appropriate way to manage landscape risks is to develop a municipal development strategy, the need for which

is regulated by the Federal Law “On Strategic Planning” [24]. Article 39—“Strategic planning documents developed at the municipal level” can be attributed to the urban landscape level. According to the content of the document, there are no methodological recommendations. Paragraph 2 of the article states that “according to the decision of the local governments, a strategy for the socio-economic development of the municipality can be developed, approved (adopted) and implemented”. In general, it can be concluded that the issue of landscape risk management is not sufficiently reflected at the level of regulatory documents.

5 Conclusion

The article analyses different approaches to landscape definition and concludes that the normative method of landscape definition is the most appropriate. The approach adopted allows us to consider urban planning as an activity that changes the components of the landscape, leading to a change in the landscape as a whole. Furthermore, based on system-wide methods, it is concluded that landscape changing activities are associated with the formation of long-term trends, called landscape risks. Landscape risks are ultimately due to a fundamental problem: the incompleteness of our knowledge about the properties of a complex system. The article gives examples of landscape risks. The article then suggests ways to assess causal relationships in order to analyze the long-term effects of landscape change. The possibilities of including landscape risks in regulatory documents are analyzed. It is concluded that such opportunities are insufficient.

References

1. Kolbovsky EY (2006) Landscape science. Academy
2. GOST 17.8.1.01-86 (1987) Landscapes. Terms and definitions nature conservation: national standard of the Russian Federation
3. GOST 56891.4-2016 (1986) Preservation of cultural heritage objects. Terms and definitions: national standard of the Russian Federation
4. Pershina AP, Khrul TS, Ivanova EO (2017) Risk analysis in landscape design. *Lesnoy Vestnik. For Bull* 21(2):20–25
5. US Environmental Protection Agency Risk Assessment Forum (1998) Guidelines for ecological risk assessment. US Environmental Protection Agency, Washington DC
6. Li X et al (2021) Landscape ecological risk assessment under multiple indicators. *Land* 10(7):739
7. Xu W et al (2021) Construction of landscape ecological network based on landscape ecological risk assessment in a large-scale opencast coal mine area. *J Clean Prod* 286:125523
8. Leuven RS, Poudevigne I (2002) Riverine landscape dynamics and ecological risk assessment. *Freshw Biol* 47(4):845–865
9. Federal Law (2004) Urban planning code of the Russian Federation N 190-FZ (ed. from 13.06.2023)
10. The spatial development strategy of the Russian Federation for the period up to 2025 (2019) Approved by decree of the government of the Russian Federation of 13 February 2019 N 207-г
11. Magnitogorsk. Construction (2023). https://www.skyscrapercity.com/threads/МАГНИТ_ОГОРСК-СТРОИТЕЛЬСТВО.989821/page-50

12. Tsvetkov VY (2018) Theory of systems. MAKSPress, Moscow, p 877
13. Forrester J (1974) Dynamics of urban development. Translation from English Orlov MG; Foreword: Kozlov YK, Progress, Moscow, p 286
14. Khoroshev A (2022) Polyscale organisation of the geographical landscape. Association of Scientific Publications KMK, p 412
15. Index of the quality of the urban environment (2023) <https://индекс-городов.рф/#/>
16. Vladimirov VV (1986) Ecological bases of the methodology of settlement and district planning. Dissertation. Moscow
17. Gushchin AN, Divakova MN (2022) Green infrastructure of Yekaterinburg. Modern state and ways of development. Architekton: Izv vuzov 4:80. [https://doi.org/10.47055/1990-4126-2022-4\(80\)-23](https://doi.org/10.47055/1990-4126-2022-4(80)-23)
18. GOST R ISO 31000-2019 (2019) Risk management. Principles and guidelines, Standard-inform, Moscow
19. Akimov VA (2004) Risks in nature, technosphere, society and economy. Moscow Business Express, EMERCOM of Russia, p 352
20. Environmental Health Indicators: Framework and Methodologies (1999) World health organization sustainable development and healthy environments. Geneva. http://whqlibdoc.who.int/hq/1999/WHO_SDE_OEH_99.10.pdf
21. Gushchin AN (2015) The theory of sustainable urban development. Directmedia, Moscow-Berlin, p 233
22. Methods for calculating the water balance (1976) International manual on research and practice. Hydrometeoizdat, Leningrad, p 120
23. Model Security Passport for territories of constituent entities of the Russian Federation and municipalities (2004) Annex to order no 484 of the ministry of emergency situations of the Russian Federation of 25 October 2004
24. Federal Law (2014) On strategic planning in the Russian Federation (of 28.06.2014 N 172-FZ)



Hydropower System of the Ural Factory City as a Unique Object of Industrial Heritage

T. Bystrova¹(✉), E. Alekseeva², and V. Litovskiy²

¹ Ural Federal University Named After the First President of Russia B. N. Yeltsin, 51, Ave.
Lenina, Ekaterinburg 620075, Russia
taby27@yandex.ru

² Ural Branch of the Russian Academy of Sciences, 16, S. Kovalevskoy St.,
Ekaterinburg 620108, Russia

Abstract. The authors focus on the economic, sociocultural significance, and impact on the urban planning of dams and ponds created in the Ural factory cities in the 18–nineteenth centuries. The article provides the data on dams’ construction and their technical and design features. A number of hydroenergetic systems created in the 18–nineteenth centuries at the territory of modern Greater Ekaterinburg are presented: the dams and ponds in Ekaterinburg proper and its districts (former Nizhne-Issetski and Verkh-Issetski ironworks); the dams and ponds in Polevskoy, Revda, and Mariinsk. Their distinctive features are shown in comparison with dams of the seventeenth century in other regions of Russia, and updated quantitative data on these objects are given. The authors use a multicomponent model for the analysis (a dam from the architectural, urban, economic, sociocultural points of view), which contributes to better comprehension of the changing role of dams and ponds in the structure of industrial settlements and outline reasonable ways for their revalorization.

Keywords: Factory city · Dam · Pond · Ironworks · System-structural analysis · Historical landscape · Industrial heritage · Architectural and urban heritage

1 Introduction

Relevance of the topic and problem statement. Modern man does not always realize that large hydrotechnical structures of the 18–nineteenth centuries in the industrial Urals—dams and ponds—radically changed the original landscape (while, in fact, “growing” out of it) and became an integral part of not only factories, but also the cities of the region as a whole. The systemic nature of the creation of objects and the flexibility of implementing the initial matrix of small industrial settlements allowed the Urals to become by the end of the eighteenth century the leading metallurgical center of Russia and the world. It is in this vein, taking into account the diverse economic use, on the one hand, and understanding the initial connection of housing with water as the main energy resource of its time on the other hand, we propose to comprehend it, speaking of the historical and architectural heritage, including the reconstruction of its objects, first of all, dams.

In purely architectural terms, we rely on an extensive (but still not complete) pool of historical data. The engineering and technical features of the Ural dams are reflected in the fundamental works by Gennin [1], Danilevsky [2], Kozlov [3], Artobolevsky and Blagonravov [4], Chugaev [5] and Shterenlicht [6]. Their architecture has been thoroughly studied by Barabanov [7, 8], and recently, in combination with historical and archival materials, by Korepanov [9, 10]. From their works it follows that in the Urals in the eighteenth–nineteenth centuries, classical examples of hydrotechnical structures were created that impacted spatial organization of settlements. Many of these works were completed quite a long time ago, and their materials need to be included in a new context, primarily due to a change in the paradigm of working with heritage. Today, it is moving from purely conservation to issues of rehabilitation, revalorization, inclusion in educational, economic, touristic and other activities.

Hence, the task of the work is to present large hydraulic structures—factory dams—in the unity of the architectural, technical and urban planning component, taking into account the processes of transformation of cities in the eighteenth–twenty-first centuries.

Work methodology. The most productive for this work is the synthesis of two concepts—the “second modernity” of U. Beck and the topological approach. The concept of “second modernity” that appeared at the end of the twentieth century proves the possibility of rethinking industrial objects in new sociocultural and economic conditions. The authors usually explore this stage itself, which is distinguished by globalization processes, while we emphasize the “reflexivity” of the “second modernity”, which U. Beck writes about. This is a time of reassessment of everything that was created in the industrial period. Within the framework of our work, this means that the dam is no longer considered in isolation from the space and era in which it was created; we can see its city-forming and cultural significance, which is important for an architectural object (Fig. 1).

Topology, which is becoming more and more widespread (A. P. Obedkov, L. V. Polubichenko, F. S. Korandey, etc.), is a method of identifying a constant, stable and relatively unchanged, “what characterizes a particular object, despite the presence of certain variables parameters, and ensures its relative identity to itself at different stages of development in time and space” [11], as well as in the specific meaning of the relationship of the object (or its various elements) to space, place and structure. To study the history of individual territories of an industrial settlement born by a pond, this approach is productive in that it makes it possible to analyze the space systematically. In other words, a pond and a dam associated with it, becoming part of a natural, carefully chosen landscape, are the constants of the place and, at the same time, the natural limits of all its subsequent physical and functional changes.

2 Results

Consideration of the dams of Ekaterinburg and its immediate surroundings, created in the eighteenth century, shows their specific regional differences, primarily due to the peculiarity of the economic use of the water wheel energy in a particular area. It is shown that the structure of the Ural dam is determined by its location on the terrain

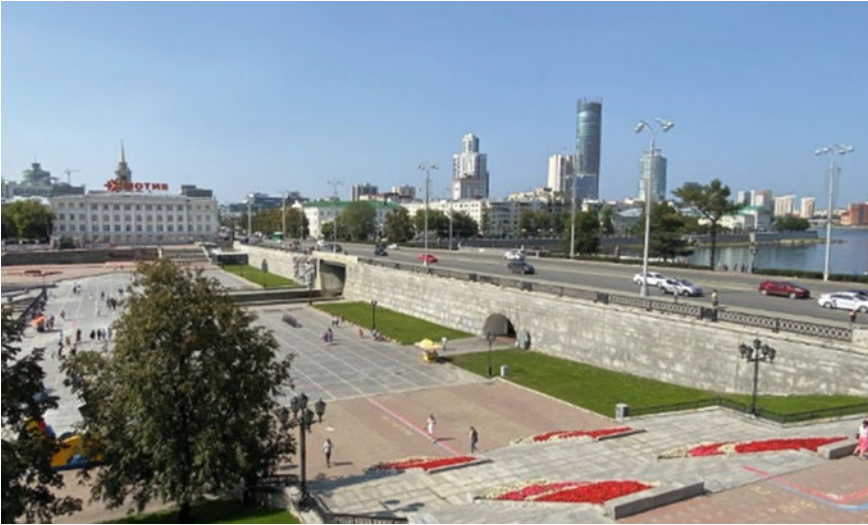


Fig. 1 View of the historical square and the dam. Ekaterinburg. *Photo* by E. Alekseeva. 2021

and the tasks of regularly supplying the plant (with the features of its blast furnace and sawmill) with energy.

A comprehensive analysis of the construction processes of a dam, a factory, an industrial settlement in the Urals of the eighteenth century, based on a topological approach, reveals their additional connectivity—with a decisive influence of the structure, size, location of the dam on the rest of the elements and levels of Ekaterinburg as a system, starting with the location of “factories” (workshops) of the plant in the center of the settlement and along the river at the point of its exit from the dam, and ending with larger urban planning solutions. This determines the uniqueness of the Ural dams as objects of historical-architectural and historical-cultural heritage (Fig. 2).



Fig. 2 **a** Production buildings at Plotinka before the start of work on the creation of the historical square. Sverdlovsk. Early 1970s GASO (State archives of the Sverdlovsk region). F-1. Op. 6. D. 6376; **b** Dam before reconstruction. Sverdlovsk. Early 1970s GASO. F-1. Op. 6. D. 6388

The study of the Ural dams in the unity of architectural and urban planning aspects shows their connection with all other city processes of the eighteenth–twenty-first centuries, in particular, the change in their significance within the settlement from purely economic to sociocultural. Changing externally and functionally, the dams have remained key locations of industrial Ekaterinburg and satellite towns for three centuries already.

The refined parameters of a number of dams of the eighteenth century located in Ekaterinburg and its environs are given. In particular, the dimensions and specifics of the creation of dams at the Isetsky, Verkh-Isetsky, Nizhne-Isetsky plants in Ekaterinburg, dams in Polevskoy, Revda and Mariinsk are indicated.

3 Discussion

3.1 The Dam Gives Birth to a Settlement

The stability and efficiency of the mining industry functioning in the eighteenth century, the rhythm of its activities were determined not only by mining reserves and factory capacities, but also by the reliability, stability of the operation and the potential of its hydropower system. The system of water and energy resources of the factory cities in the eighteenth century Urals predetermined the planning structure of factory settlements, influencing the formation of a specific identity of the place, which makes it possible to consider it as a complex architectural and town-planning object of industrial heritage.

Analyzing the water and energy heritage of Ekaterinburg, a quite typical industrial settlement of that period, which was part of a rationally equipped and rather dense settlement system, we should primarily consider that the plant would not exist without a dam. The entire subsequent town-planning structure depended on its location on the river, the features of the relief. As a point of connection between the given natural environment and technical and technological processes in the age of the water wheel, the dam set the volume of factory production, the orientation of the settlement and the direction of the streets, always regularly organized according to the town planning guidelines of the Enlightenment.

The first water-operating enterprises appeared in Russia in 1620–30s—Nitsynsky ironworks (1631) and Pyskorsky ironworks (1633) [2]. According to the reconstruction of the Porotovskiy ironworks of the seventeenth century, carried out by N. B. Baklanov, the settlement next to such plants was not designed as a regular one and occupied one bank of the river next to the dam. Both the dam itself and the settlement differ from those that arose in the Urals in the eighteenth century. The dams of the European part of Russia, for example, the Verkhnetsninskaya dam in Vyshny Volochek (1703), which were created almost simultaneously with the Urals, were wooden two-span (beishlots) with wooden lockshields. The dam served purely hydrotechnical purposes—maintaining the water level in the canal between Tvertsa and Tsna, so it is not tied to residential areas.

On the territory of the industrial Urals, a characteristic canon for the construction of mining settlements has developed around their key elements—a dam, in the downstream of which there was a plant with mechanisms driven by water, and a pond where water was concentrated. The presence of the required amount of water in the pond and the rhythm of its supply to water wheels or turbines completely predetermined the seasonal and monthly efficiency of factories of any profile. On the contrary, insufficient water

supply led to long shutdowns and significant downturns in the activities of enterprises. For example, the insufficient supply of water resources to the metallurgical Nizhne- and Verkhne-Uktusky plants caused their uneven work and by 1750 led to the closure [12].

3.2 Technical and Technological Features of the Ural Dams

For all its “invisibility” for a modern person, the dam is a cluster of construction and landscape engineering technologies, and over time, a certain part of the urban planning ensemble is formed on it, which will be discussed separately. The architectural value of dams must be taken into account in restoration work, since they are an essential element in the development of technological progress and constitute a capital heritage of great originality, which must be preserved.

The hydrotechnical complexes of the Ural factories assumed the construction of water reservoirs with a desirable uniform distribution of water energy throughout the year with the necessary safety measures during critical periods of spring floods [13]. The hydraulic structures of ironworks in Germany, France and Sweden that existed at the time of V. de Gennin’s arrival in the Urals in 1722 used, as a rule, the bottom shot wheels which were here inappropriate due to the harsh Ural winters and often freezing of shallow rivers.

The size and dimensions of the Ural dams—for example with a crest width of up to 30–40 m [14]—were aimed to completely exclude the possibility of the dam’s break. In order to avoid seepage of water through the body of the dam and its destruction due to floods, the earthen dam was made solid right at the time of the construction, and then it was constantly strengthened, by dumping production waste on the crest and slopes. Builders led by dam master Leonty Zlobin relied on this approach during the construction of a short, but wide and high dam on the Iset river—in contrast to the long and low European dams of the seventeenth century—with a large and fairly deep pond, and in the dam itself with a large main slot for discharging the main water drain and two parallel side conduits for supplying water to chests with water wheels to drive factory mechanisms.

The place of the future dam was marked with stakes, a ditch was dug along its entire length, reaching solid layers of soil. The edge of the moat on the side facing the pond was reinforced with two or three rows of piles. Between them lay a lattice of logs. The gaps between the bars were filled with clay. The holes for the slots were enclosed with quadrangular wooden log cabins, which were also filled with clay (“pigs”). Since the 1740s the lower part of the dam was often reinforced with a vertical frame. The back wall of the moat was strengthened with bundles of brushwood with turf [7]. At the same time, the bottom of the future pond was being cleared from the forest. The earthen embankment towards the pond was made as sloping as possible, from a third to half the width of the entire dam. Later, slag, a waste from metallurgical production, could be used as a reinforcing addition.

The main working element of the entire dam structure were water conduits, i.e. a piping system that carried water from a pond to the wheels of factory machinery. The conduit system included chest wells—hollow wooden log cabins connected by pipes to the chest, a kind of intermediate reservoirs to increase water pressure.

The diameter of wooden factory wheels at the Ural water driven ironworks averaged 3.6 m. Later, the iron wheels of the nineteenth century had a diameter of up to 2 m. In order to avoid freezing of the wheels in winter due to the weak pressure of water and the difference in its level in the chest, the latter at the Ekaterinburg plant fundamentally differed from the chests of the seventeenth century not only by the absence of an inclination, but also by the greater depth of the chest with a constant cross section throughout its length and in the branches to the factories. Moreover, since the late 1730s chests that were previously open from above began to be closed from above and rounded, so that in the middle of the eighteenth century, almost round “pipes” were already leading from the chests to the wheels, and the closed sections of the chests were additionally upholstered with iron to be able to heat them with fires during frosts. As a result, in the XIX century chests almost everywhere in the Urals acquired a round or oval cross-section, were made of metal, and were much larger than the former wooden ones. Optimum water pressure in them was achieved by placing a chest window and regulating the level of the pond through the spillway, and additionally in the chest itself, where it was regulated by a system of mechanical pistons installed in the slot directly behind the window entering the chest and further at the joints along its entire length. The chest bottom was arranged parallel to the water horizon in the river, and the chest itself was located as low as possible, which gave more energy to the water, and together with the chest wells, hollow wooden log cabins made it possible to regulate the water pressure and change the water flow to the desired direction. The higher the trough of the chest was attached above the wheels, the greater the energy of the falling water from them could be transferred to the wheels, rotate them faster and provide more mechanisms with proper energy [15].

The logic of the water wheel also dictated the layout of the plant and its “factories” (workshops). So, the blast furnace factory was built in the immediate vicinity of the dam and was technically connected with it. Ore and coal were brought along the top of the blast furnace. Near the dam, but at a safe distance from the blast furnace, a sawmill was built. Workshops that did not need the power of a water engine were located further from the dam.

The thoughtfulness and experimentally verified pragmatics of the construction of dams and the operation of their mechanisms is evidenced by the fact that the methods of their construction indicated by V. de Gennin in the “Description of the Ural and Siberian Plants”, which he called the “fundamental doctrine”, existed for earthen mill dams and small ponds until the beginning of the twentieth century [15].

3.3 Architectural Elements of the Ural Dams

The materials on them are scarce. But those that exist show that the dam was conceived as an integral structure, not only in the physical, but also in the aesthetic sense.

The Verkh-Isetsy plant, including the dam, constituted a single architectural ensemble in the style of classicism. The connection between the topography of the place and architecture is evidenced by the solution of the factory office, which had multi-storey facades due to the level difference between the dam and the factory site. The main facade was one- and two-storey, and those facing the entrance from Ekaterinburg—two- and three-storey (Fig. 3).



Fig. 3 a The dam of the Verkh-Isetsy Pond in its current state. Architect K. Gordeev. *Photo* by V. Litovski. 2021; Model of the old office of the Verkh-Isetsy plant. Architect M. P. Malakhov. 1820s–1830s. Ekaterinburg, 28, Kirova st Fund “Drugoi Mir”. *Photo* by E. Alekseeva. 2021

Nizhne-Isetskaya dam [16], originally built on the Iset in the 1780s with production buildings of the local branch of the Ekaterinburg Mint, had a width of about 5 m at the base and about 2.5 m on the crest, with a length of 16 m and a height of more than 6 m [17]. It had one spillway and two chest slots (Fig. 4). A guardhouse was built into the body of the dam between the spillway and the left chest slot. The construction of such a structure was carried out for one season [10].

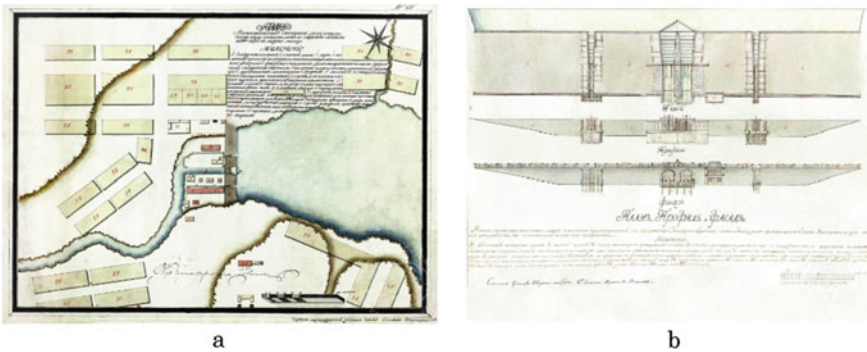


Fig. 4 a Plan of the Nizhne-Isetsy plant. 1807 *Source* https://xn--80aebf3an9auge0i.xn--p1ai/german_2 b Nizhne-Isetskaya dam in the 1800s *Source* https://xn--80aebf3an9auge0i.xn--p1ai/german_2

The Nizhne-Isetskaya dam shows that any architectural elements of dams are made in the style of the time, with all the seriousness of the then approach to architectural design. These are neat and devoid of decoration objects, built into the body of the dam and not violating the overall rational harmony. For example, the dam of the Nizhne-Isetsy plant in Ekaterinburg, built in the 1800s, includes a two-storey guard building, the shape of which refers to the military architecture of the Petrine era. It is a simple, neat rectangular volume with a symmetrical façade and a high hipped roof (Fig. 5b). Its

proportions were continued in 1804 by the Nizhne-Isetsy steel factory, located nearby, forming a recognizable industrial ensemble.



Fig. 5 a Nizhne-Isetskaya dam. Ekaterinburg. Modern look. Photo. *Source* The first bulb of Nizhneisetsk. Museum of Energy of the Urals. URL: <http://musen.ru/chronicle/1921/>; b “Profile plan and facade of the Nizhne-Isetsy state-owned plant to the dam, rebuilt according to the design of the Ekaterinburg Mint by the foreman Egor Usoltsev”. GASO. F. 25. Op. 2. D. 7927. *Source* 14, p. 11. Fragment

Later, the dams in Ekaterinburg and other Ural settlements are landscaped, improved, turning into a kind of a promenade.

3.4 Genesis and Development of Hydraulic Structures of Ironworks in Ekaterinburg

On March 12, 1723, the Ekaterinburg fortress with a rampart, a moat and a bastion was laid, and after that, in April, under the leadership of the dam master L. S. Zlobin, the construction of a factory dam began.

Dam and pond of the Ekaterinburg plant. The hydropower base of the plant consisted of a pond and a dam 211.1 m long, 42.7 m wide, 6.4 m high, with a spillway and two working slots, later the dam was filled up and lined with rubble stone. The technologies for erecting a dam in Ekaterinburg have been studied in detail by historians and architects: “The dam was constructed from larch, which became stonelike in the water, log grating was clogged with clay. English cloth was laid between the rows of larches in a log grating. The clay in the log grating had to be tamped” [18]. In the middle of the dam there was a spillway, to the right and left of which there were chest slots through which water was supplied to the water wheels that set the factory mechanisms in motion. At the same time, the conduits had locks, which, opening, let water through. The channels were covered with stone vaults. After backfilling and leveling the surface in the southern part of the dam, a road was made connecting the banks of the Iset river. In the northern part lay wooden shields on which pedestrians walked. Here, the connections between the purely technical, construction characteristics of the dam with urban planning and, further, sociocultural ones are clearly visible. Not only production, but also the city is

organized thanks to the presence of a dam, and until now the main streets of most of the Ural city-factories cross the pond along this line [19]. The dam and pond powered the production system of the ironworks.

Ekaterinburg became a model for most other places here. Factories of the Ural ironworks were built along the river, perpendicular to the dam, they towered over the residential buildings surrounding them, becoming a kind of spatial dominants [20].

One of the most interesting points that should be remembered in today's protection actions is the improvement of dams in the nineteenth–twentieth centuries: as their economic function was lost, their sociocultural function came to the fore, because they were in the center of any industrial settlement in the Urals. So, in 1886, due to the Siberian-Ural Scientific and Industrial Exhibition of 1887, important for the city, in Ekaterinburg, on the upstream of the city dam in its northern part, a square with an area of half a hectare was laid out. From the time of the factory fortress the dam was the starting planning structure, the main road, but earlier it was not equipped with vegetation. Dmitry Ivanovich Lobanov (1852–1916), an employee of the railway and a member of the Ural Society of Natural Science Amateurs (UOLE), played the main role in the implementation of the idea. The square had a free layout with islands of lawns, groups of trees and shrubs, and flower beds. The forms of the dam slots were played up in the final version of the organized space, dividing it into four sections. Bronze busts of Emperor Peter I and Empress Catherine II were also installed there. The square was separated from the roadway by a metal fence along which a hedge was planted. In the warm season, the place was buried in greenery.

By the middle of the twentieth century, the layout of the square began to change towards a regular one. The total area has grown slightly due to the fact that the spillways of the dam were hidden. The lawns were enlarged, and small semi-circular areas were laid out next to the entrances to the square. In close proximity to the pond there was a through path. The trees have almost disappeared, replaced by shrubs. In 1958, a bust of P. P. Bazhov (sculptor M. G. Manizer, architects B. E. Rogozhin, A. P. Velikanov) with stone benches around was installed in the center of the square on the dam. In 1987, a bronze bust of D. N. Mamin-Sibiriyak (sculptor A. Antonov) was installed nearby. During the reconstruction of 1962–73 the dam was expanded, lined with granite, and a through passage was made from the side spillway. In the 2000s the territory of the square has lost a significant part of the vegetation, becoming a transit pedestrian zone.

Verkh-Isetskaya dam and pond. Since the dry summer of 1724 showed that the water reserves in the pond of the Ekaterinburg plant were not enough for full-fledged work, it was decided to build an additional dam upstream of the Iset. The dam of the Verkh-Isetsy plant, more than 300 m long, was built in 1725–1726, as a result of which the Verkh-Isetsy pond was formed, five times larger than the pond of the Ekaterinburg plant. The general management of the project was carried out by V. de Gennin, and the construction was directly supervised by Konstantin Gordeev, Larion Pozharov, Danila Borsky, Ivan Melentiev and Leonty Zlobin. The dam was built by the peasants of the settlements assigned to Ekaterinburg—Aramil'skaya, Kamyshevskaya, Kamenskaya, Okunevskaya, as well as regiments from Tobolsk.

The dam is elongated in the meridional direction, forming one of the main compositional and planning axes of the development of the plant and the vicinities, as well as

the western border of the territory of the historical ensemble. Now it is a dam, dissected by new locks for the discharge of spring waters. Structurally, it was made in the form of wooden cages, clogged with selected clay and stone. The dimensions of the dam are: length 320 m, minimum width is 50 m, and height is 5–7 m. Undoubtedly, at present the dam is of historical and architectural value as a genuine element of the plant's hydraulic engineering system, preserving its historical city-forming significance. In terms of identified and recognized cultural and industrial heritage, today this is the only enterprise founded in the eighteenth century that has survived. There are old production buildings, a factory dam, an office, which requires not only the preservation of their special historical and cultural status, but also tactful updating and refunctionalization.

3.5 Dams and Ponds in Polevskoy

Decree on the construction of the dam of the Upper Pond of the Polevskoy plant on the river Polevaya was signed by Peter I in January 1722. It was erected in 1724, now becoming a monument of engineering art of that time and the “heart” of Polevskoy (Fig. 6). Water not only powered the Polevskoy plant, but also fed below the Shtangovy pond, and partly, together with the river Severushka, the Seversky pond. Below the Upper pond, at the confluence of the Polevaya river with Severushka, another dam was built in 1738, at which the Seversky pond with an area of 2.4 km² and an ironworks were formed.



Fig. 6 The dam of the Seversky plant. Polevskoy. *Photo by V. Litovski. 2022*

Now the eastern bank of the dam is reinforced by a bulk dam for 1.5 km, and the pond itself stretches for 8 km, reaching a width of 500 m. In the southern part of the pond, along the flooded floodplain of the Polevaya river was formed by a large arm, regulated above by the Shtangovy pond. The height of the water level in the Shtangovy Pond is 350 m, and in the Seversky pond—339 m.

Nevertheless, in the hydrocascade, the dominant is not the Upper pond with a water level of 365 m above sea level, but the Glubochensky pond, with a water surface in the reservoir of 412 m. Elongated from west to east, it is formed by an embankment dam 800 m long, more than 30 m wide at the base and up to 25 m high, has two small bays formed by the main river Glubokaya and the small river Kamenushka. In general, the length of the Glubochensky pond is 2.1 km, the width in the middle part is from 450 to 800 m, the average depth varies in the range of 5–7 m, and the maximum (near the dam on the site of the old channel of the Glubokaya river) reaches 23 m with a total area reservoir in 1.28 km². From this it follows that the volume of water concentrated in it varies from 6.4 to 9 million m³, and the mass—from 6.4 to 9 million tons.

Polevskoy with its Gumeshevsky deposit and the function of supplying copper raw materials to the Isetsky plant is the place where a unique engineering and technical system of regulating ponds was created from the Glubochensky pond to the Seversky pond (1876–1887). The author of the project of the Glubochensky pond and canal was Fedor Alekseevich Khvoshchinsky [21], who from 1837 to 1853 served as the chief manager of the Sysert plants. The uniqueness of the canal is that it has not only a bed laid on the surface more than 4 km long to the Svetlaya river, but also an artificial underground tunnel 1,780 m long. Its construction was led by the plant owner D. P. Solomirsky and the merchant A. S. Vyatkin.

3.6 Dams and Ponds in Revda

On the Revda river, the dam—also under the leadership of Leonty Zlobin—began to be erected in May 1732 by order of Akinfiy Demidov. Its length was about 160 m, height—8.5 m, and the width of the base—57.5 m. At the base of each of the dikes, a “tooth” was cut—larch wells measuring 2 × 2 and 3 × 3 m. They were clogged with rammed clay. These “teeth” protected the dikes from erosion. The bed of the Revda river was blocked with stones and clay between the mountains ... The stream was diverted closer to the right bank. A pond with an area of 800 hectares was formed ... at the plant, water turned 33 wheels, each with a diameter of about 4 m, a width of about 2 m. In the spring of 1733, the Revda river showed its temper, and the newly built dam was demolished” [22]. Below, three more dams were formed, which created a water reserve for two auxiliary plants—Sharaminsky and Baranovsky (Fig. 7).

In 1964, the old Revda dam was reconstructed, the wooden spillway system was replaced with a reinforced concrete one (Fig. 8a). “Before backfilling the old spillways, two beams with a section of 600 × 600 mm were removed from their base, stacked one on top of the other. Between them a green cloth pad was found. Larch and cloth, which had lain in the water for 230 years, were like new. The spillway from the new dam started in 1965. The size of the dam: length—70 m, height—8 m” [21].

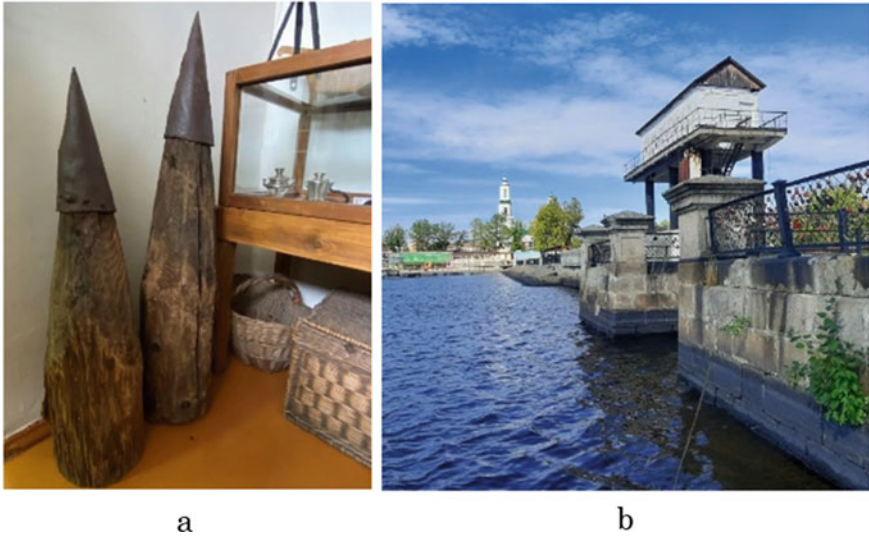


Fig. 7 **a** Fragments of spiles driven into the base of the dam's log grating. From the exposition of the museum "Ural antiquity" in Revda. *Photo* by E. Alekseeva. 2022; **b** Water intake complex at the dam of the Sysert pond. Sysert. *Photo* by V. Litovski. 2022



Fig. 8 **a** The Revda dam. Modern look. *Photo* by E. Alekseeva. 2022; **b** Wooden dam of the Mariinsky ironworks. The village of Mariinsk. *Photo* by E. Alekseeva. 2022

3.7 The Dam of the Mariinsky Ironworks

In 1840, on the Revda river, 25 km from the main Revdinsky plant, an auxiliary Mariinsky ironworks was founded. It specialized in the production of strip, section, sheet and roofing iron and was closed during the Civil War. In the village of Mariinsk, an old wooden dam is still preserved (albeit partially destroyed) (Fig. 8b). The factory dam with a release slot for 6 locks had a length of about 320 m, and full height of water was 7.3 m. However,

there was still not always enough water in the factory pond, so the factory often worked only 7–8 months a year. At the heart of the dam is a ribbed structure made of larch, filled with earth and clay. The slope is lined with rubble stone. On the left side of the dam, one more spillway is visible—a working one. It is partially covered with wooden structures sticking out there. It was through him that water entered the plant and set its mechanisms in motion. The buildings of the Mariinsky ironworks stood below the dam. They were wooden, by now nothing remains of them. But near the dam there is a lot of slag. From 1945 until the 1950s, a hydroelectric power station operated on the dam of the Mariinsky pond, supplying the village with electricity [23].

Thus, the experience of building dams in Ekaterinburg and nearby industrial settlements was deeply successive: following the dams of the Uktusky, and then the Isetsy plant, it diffused during the creation of a dam at the Verkh-Isetsy, Polevskoy and other plants.

3.8 Historical and Architectural Significance of Dams in the Context of the History of the Ural Region

The industrial and cultural heritage of any Ural settlement that arose as a mining settlement or a factory city [20] can now be judged, first of all, by the preservation of its three main components: a pond, a dam and the structure of the settlement, which determines the historical development of the factory city. If the settlement also served as an outpost, then the degree of preservation of the heritage is also determined by the degree of preservation of the fortress or its elements. In this regard, the key cultural heritage of Ekaterinburg as a factory city (ironworks at the Plotinka) and as an outpost (fortress) have been lost. At the same time, if the fortress was lost in the process of expanding the city, then the plant, due to the “cultivation of the center”—the organization of the Historical Square—is irreplaceable, despite the best intentions, such as the development of the city in line with the concept of “garden city”, the creation of recreational and cultural public spaces, etc.

The range of values of water in the process of development and the nature of the settlement system of the Urals is very wide, from purely economic to state-symbolic. Quite in the spirit of its time, able to “read” any iconological systems and loving allegories [24], the confluence of waters is interpreted as an increase in the power and strength of not only nature, but also power. By the nineteenth century, this value-semantic continuum was losing its integrity, making it possible to transform the original forms and often lose their integrity. So, in 1808, the retaining wall of the dam of the Verkh-Isetsy plant was lined with cut stone from the downstream side, which led to the loss of a wooden construction over the lifting mechanisms. With the construction of a new sluice and a building of locking mechanisms, the old water conduits were dismantled and the chest and spillways were filled in. Later, the plant’s dam was reconstructed many times [25]. Ultimately, road and rail access roads are arranged on the surface of the dam. At present, the locks of its spillways have not been preserved, and the new one is made of reinforced concrete. The preserved retaining walls of the dam and canals lined with stone are of historical value.

Comprehending the architectural, urban planning and socio-cultural value of the ponds and dams of Ekaterinburg and its vicinities has a long history. Its completeness

and adequacy largely depend on museum representations. A large-scale and successful example of the representation of industrial, including hydraulic, heritage is the Sever-skaya blast furnace Museum Complex, which is based on a monument of urban planning and industrial architecture of the nineteenth century, an object of cultural heritage of federal significance in the city of Polevskoy. Together with the plant and the dam, it is one of the few industrial complexes of the middle of the nineteenth century that have been saved in such a high degree of preservation, not only in Russia, but also in Europe, giving a complete picture of the production metallurgical process, and the hydropower infrastructure of factory city of that time [26].

4 Conclusion

It is necessary to draw the attention of scientists and citizens to ponds and dams, if only because many people do not perceive them as an industrial heritage. Based on the idea of heritage revalorization [27], we can say that the very fact of designating a place plays a big role in attracting attention in this way.

The city-forming role of water and energy facilities and their unique function in shaping the settlement system of the mining Urals are obvious. This is largely due to the connection of the energy of the water wheel, later the hydro turbine, with production, on the one hand, and the layout of the city-factory, on the other. In turn, the totality of such connections sets the boundaries of the settlement and significantly affects the mentality of its inhabitants.

Speaking of industrial processes and objects of the eighteenth century, we cannot lose sight of their value-semantic aspects for contemporaries. In addition to the originality of building technologies and structures noted above, there was a specific symbiosis of pragmatic and symbolic principles that well characterize the era.

The transformation of the dams in the region under consideration in history has been repeatedly associated with capital work to increase, strengthen or change the structure. Decorative landscaping was also timed to coincide with image or anniversary events. The dams have come down to us in a significantly altered form, but at their base the original structural elements have been preserved—log cages filled with clay and lined with rubble on the outside, currently “chained” in concrete and granite shells.

The remains of the ancient dam of the Isetsy pond with fragments at the locations of spillways are part of the cultural heritage site of federal significance “Buildings and structures of the Ekaterininsky plant “Monetka” (Sverdlovsk region, Ekaterinburg, the central part of the city), and included in the unified state register of cultural heritage objects (monuments of history and culture) of the peoples of the Russian Federation.

It is difficult to overestimate the hydrotechnical, urban planning, infrastructure and cultural significance of the dam for Ekaterinburg and the surrounding cities. Its location set the direction of the main streets, the vectors of further development of settlements. The central highway always ran along the axis of the dam. Among the many dams that blocked the Iset and other rivers of Ekaterinburg in different places (Sukhaya, Olkhovka, Melkovka, Osnovinka) to ensure the operation of saw and flour mills, gold washing factories, the dam of the Ekaterinburg plant, of course, is of particular importance, especially since most of the old dams over time were dismantled, their ponds were

lowered, and the rivers themselves were covered up. In varying degrees of preservation in the urban environment, the remains of the log-earth dam of the Uktus plant, the Nizhne-Isetskaya and Verkhne-Isetskaya dams are represented.

Thus, the fundamental technological construction of metallurgical plants of the eighteenth century has been the main “backbone” of the settlements under study for three centuries, linking the banks of the rivers and symbolically connecting generations. The technological functions of dams in the nineteenth century came to naught. In the last quarter of the XIX century their role has increased as a part of urban improvement, a communicative, household, leisure component of urban everyday life, a road and transport artery. Throughout history, the town-planning and town-forming (holding the pond) functions of the dam continue to be preserved. At the same time, its utilitarian purpose is transformed into a symbolic, cultural, aesthetic, commemorative significance. As the functions of the dam changed—from production and hydropower to infrastructure and transport—in practice, the industrial heritage object was revalued.

Acknowledgements. The research was carried out with the financial support of topic 2.2.2.2. Russian Academy of Architecture and Building Sciences 2021–2023 “Scientific foundations of urban development of the rural settlement system”.

The article was prepared in the frameworks of the approved for 2023 research plan “Region in the context of Russian history: landscapes and actors” of the Institute of History and Archaeology of the Ural Branch of the Russian Academy of Sciences.

The materials of the article were prepared as part of the approved for 2023 research plan of the Institute of Economics of the Ural Branch of the Russian Academy of Sciences.

References

1. Gennin W de (2009) *Opisaniye Ural'skikh i Sibirskikh zavodov* (Description of the Ural and Siberian plants). Alfaret, St. Petersburg (reprint edition)
2. Danilevsky VV (1949) *Russkaya tekhnika* (Russian technology). Leningrad newspaper-magazine and book publishing house, Leningrad
3. Kozlov AG (1981) *Tvortsy nauki i tekhniki na Urale XVII—nachalo XX veka*. Biograficheskii spravochnik (Creators of science and technology in the Urals in the 17th—early 20th centuries. Biographical guide). Sredneuralskoe book publishing house, Sverdlovsk
4. Artobolevsky II, Blagonravov AA (1975) *Ocherki istorii tekhniki v Rossii (1861–1917)*. (Essays on the history of technology in Russia (1861–1917)). Nauka, Moscow
5. Chugaev RV (1967) *Zemlyanye gidrotekhnicheskiye sooruzheniya* (Earthen hydraulic structures). Energiya department of Leningrad, Leningrad
6. Shterenlikht DV (2005) *Ocherki istorii gidravliki, vodnykh i stroitel'nykh iskusstv* (Essays on the history of hydraulics, water and construction arts), vol 6. Geos, Moscow
7. Barabanov A (2002) Les monuments de l'art hydraulique de l'Oural du XVIIIe au debut du XXe siècle. In *L'eau industrielle, l'eau industrieuse*. Ed. Dorel-Ferre G. Cahier de l'APIC n°2. CRDP de Champagne-Ardenne, 2002
8. Barabanov A (2009) Les ouvrages hydrotechniques de l'Oural ancien. *Historiens & Géographes* 405:20–32
9. Korepanov NS (2003) *V provintsial'nom Ekaterinburge (1781–1831 gg.)* (In provincial Ekaterinburg (1781–1831)). BKI, Ekaterinburg

10. Korepanov NS (2013) Nizhne-Isetskii zavod, 1789–1915 gg. (Nizhne-Isetsy plant, 1789–1915). Grachev and Partners, Ekaterinburg
11. Polubichenko LV (2017) Topologicheskaya paradigma gumanitarnogo znaniya: mif ili real'nost'? (Topological paradigm of humanitarian knowledge: myth or reality?). Bulletin of Moscow University. Ser. 19. Linguistics and intercultural communication 4:102–117
12. Baidin VI, Grachev VYu, Kononov YuV, Mosin AG (2011) Uktus, Uktusskiy zavod i yego okrestnosti v XVII–XVIII vv. (Uktus, Uktus plant and its environs in the 17th–18th centuries). LLC Grachev and Partners, Ekaterinburg
13. Barabanov A (2009) Les ouvrages hydrotechniques de l'Oural ancien. *Historiens Géographes* 405:20–32
14. Stroitel'stvo plotin na Urale (Construction of dams in the Urals). Available via Kray Ural. <https://krayural.ru/raznoe/250-uralskih-plotin>. Accessed 14 March 2021
15. Baklanov NB (1935) Tekhnika metallurgicheskogo proizvodstva XVIII veka na Urale (Technique of metallurgical production of the XVIII century in the Urals). Sotsekgiz, Moscow, Leningrad
16. Pervaya lampochka Nizhneisetska: Nizhneisetskaya plotina posluzhila trom zavodam i odnoy gidroelektrostantsii (The first light bulb of Nizhnesetsk: The Nizhnesetsk dam served as three factories and one hydroelectric power station). <http://musen.ru/chronicle/1921/>. Accessed 12 Mai 2021
17. Ekskursiya po Nizhneisetsku. Chast' 1. Istoriya Nizhneisetskoj plotiny (Excursion around Nizhnesetsk. Part 1. History of the Lower Iset Dam). <http://ekb7.ru/micro-nigneisetsk>. Accessed 10 June 2023
18. Desyatov VG (2013) Stareysheye sooruzheniye na reke Iseti (The oldest structure on the Iset River). *Academic Bulletin UralNIiproekt RAASN* 1:96–98
19. Barabanov AA (1977) Razvitiye arkhitektury gidrotekhnicheskikh sooruzheniy na Urale (Development of the architecture of hydraulic structures in the Urals). Dissertation, Moscow Architectural Institute
20. Lotareva RM (1993) Goroda-zavody Rossii XVIII—pervaya polovina XIX veka (Cities-factories of Russia in the 18th—first half of the 19th century). Publishing house of the Ural University, Ural Institute of Architecture and Art, Ekaterinburg
21. Surenkov V (2010) Iz istorii Glubochenskogo pruda (From the history of the Glubochensky Pond). *Rabochaya Pravda. Polevskoy*. June 23 (No. 25):1
22. Plotina Revdinskogo zavoda. Kto, kak i kogda yeye stroil (The dam of the Revdinsky plant. Who, how and when built it). Available via revda-info.ru (revda-info.ru). Accessed 16 March 2023
23. Raspopov P. Starinnaya derevyannaya plotina v sele Mariinsk (Ancient wooden dam in the village of Mariinsk). Available via [Uraloved](http://uraloved.ru) (uraloved.ru). <https://uraloved.ru/mariinsk>. Accessed 14 Mar 2023
24. Likhachev DS (1998) Poeziya sadov. k semantike sadovo-parkovykh stiley. Sad kak tekst (Poetry of gardens. to the semantics of landscape gardening styles. Garden as a text). 3rd ed., rev. and add. Novosti, Moscow
25. Plotina Verkh-Isetskogo pruda (The dam of the Verkh-Isetsy pond). Available via [Photoputevoditel](http://photoputevoditel.ru). <http://ekb7.ru/viz-photoputevoditel>. Accessed 5 Mai 2023
26. Alekseeva EV (2017) Revalorizatsiya industrial'nogo naslediya v Rossii i stranakh Zapadnoy Evropy: podkhody, ob'yekty, landshafty, aktyory (Revalorization of the industrial heritage in Russia and Western Europe: approaches, objects, landscapes, actors). *Econ Hist* 1:9–23
27. Severskaya domna. https://stz.tmk-group.ru/severskaya_domna. Accessed 10 Mar 2023



Forming the Coherence of the Cultural and Social Framework in the Arctic Settlements Using GIS-Technologies

A. Korobeynikova^(✉), N. Danilina, and I. Teplova

Moscow State University of Civil Engineering, 26, Yaroslavskoye Shosse, Moscow 129337, Russia

anna-chega@mail.ru

Abstract. The Arctic is unique natural landscapes, resources, rich culture of the small peoples of the North, and as a consequence, the high tourist potential of the region. The development of the cultural and social framework (CSF) of Arctic cities will help to develop a network of public spaces and provide connections between them, which can have a positive impact on both the comfort of the environment for local residents and tourists. However, the formation of a comfortable urban environment in Arctic cities is a difficult task that is complicated by the harsh climate of the Arctic territories, low temperatures, precipitation, high wind speed, as well as the peculiarities of daylight and polar nights. These factors can significantly reduce the comfort of being outdoors and as a consequence reduce the variety of outdoor recreation for both residents of Arctic cities and tourists. It is also worth mentioning a decrease in the safety of staying in the open spaces of Arctic cities, since low temperatures and high wind speeds can lead to a significant reduction in frostbite time. Ensuring connectivity of CSF objects is the key to the development and improvement of all the components of the cultural and social framework. The article analyzes the factors influencing the cohesion of cultural and social frameworks of Arctic cities, uses modern GIS-technologies to model the cultural and social framework, developed an algorithm to assess the pedestrian accessibility of CSF, using GIS-technology, as an approbation of theoretical research an experiment on the example of Norilsk.

Keywords: Arctic · Public spaces · Arctic tourism potential · Cultural and social framework · GIS · Territorial cohesion · Connectivity of linear objects · Comfortable environment in the Arctic · Sustainable development

1 Introduction

The Arctic zone occupies more than 28% of the territory of the Russian Federation [1]. It is home to 2.6 million people, which is more than half of the world's Arctic population. Despite the difficult climate, polar nights, and the problem of permafrost soils, interest in this area has always remained at a high level [2, 3]. Increased interest in

the development of the Arctic zone of Russia is associated not only with the opening of the Northern Sea Route, but also with great economic, social, raw material and tourist potential of the territory [4–6]. The development of the Arctic city is impossible without taking into account its public spaces, their condition and their connectivity. It is the inseparability of cultural, historical and natural objects of the city that makes it possible to create a sustainable, development-capable cultural and social framework (CSF) [7–9]. The development of the cultural and social framework in the Arctic cities is an urgent task for modern urban development [10]. First of all, the relevance of the problem is associated with the development of spatial development documents of the Arctic zone. The research presented in this article was conducted on the basis of the “Strategy for the Development of the Arctic Zone of the Russian Federation and National Security until 2035”, as well as other key documents defining the goals, development and expected results related to the development of the Arctic zone of Russia [11–13]. In connection with the publication of the Strategy, there are more developments on this topic and mechanisms for the management of these territories is being created at an accelerated pace.

Despite the importance of the development of the territories of the ASRF settlements, it is important to understand that the urban development of the Arctic has a number of features [14–16]. Such features include:

- low temperatures,
- high wind speeds,
- high precipitation,
- polar night.

In conditions of low temperatures, high wind speeds and complex topography, moving between objects of attraction becomes a very difficult and unsafe task for human health [17, 18]. Based on the above difficulties it is obvious that creating a cultural and social framework in the Arctic cities, as well as ensuring its connectivity and accessibility is not only a question of comfort, but also of safety [19]. A great number of scientists such as Ratner E. M., Serebrovsky F. L. and others have dealt with the issue of climatic comfort and creation of comfortable urban conditions, taking into account climatic factors [20, 21]. Among foreign researchers in area of influence of a climate on the person it is possible to allocate Blocken B., Oszczewski, R. J., etc. [22, 23] Ensuring the connectivity of objects of attraction in Arctic cities is not only a criterion for the comfort of living in an urban environment, but also security.

2 Cultural and Social Framework (CSF) of the Arctic Cities

2.1 CSF Structure

Cultural and social framework (CSF) of the city is a set of objects of social and social significance both for the population of the city and business development, including the attraction of external flow of tourists.

This study identifies three groups of objects:

- Natural objects from squares and boulevards (the most compact green spaces in cities) to Specially protected natural territories;

- Historical objects—buildings, complexes of buildings, historical centers of cities, having the signs of historical value;
- Cultural objects—theaters, cinemas, clubs, museums, entertainment centers, sports facilities and many other objects of entertainment and cognitive nature, which are the focus of public attraction outside of work activities.

The objects of the cultural and social framework in the Arctic cities also have a number of features (Fig. 1).

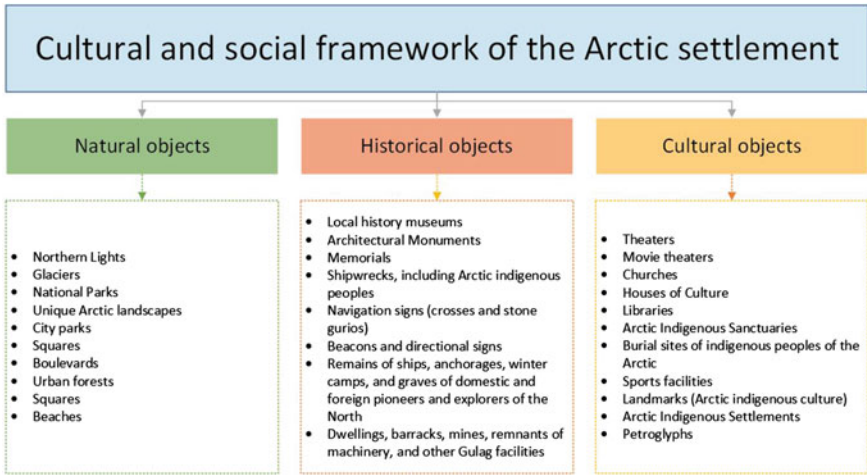


Fig. 1 The composition of the cultural and social framework, taking into account the specifics of cities in Arctic cities

The natural objects of the Arctic territories include traditional parks, squares, boulevards, squares, as well as urban forests and arctic deserts. Also the natural objects in the Arctic zone can include beaches, which, despite the climate not quite suitable for beach recreation, have a unique natural landscape and become an active focus of attraction for visitors.

Historical sites of Arctic cities are represented mainly by local history museums, which reflect the unique life and culture of indigenous peoples of the North. Also historical objects of the cultural and social framework of the cities of the Arctic Region are represented by memorial monuments—monuments to polar explorers and discoverers of the Arctic, memorial complexes of the Great Patriotic War, memorial complexes to the victims of the Gulag. Many Arctic cities have a large number of monuments of architecture and urban planning from the time of its development and construction of cities, including UNESCO World Heritage Sites.

As objects of culture, it is proposed to consider first of all objects of cultural and community services—theaters, cinemas, stadiums, etc. However, the Arctic zone of the Russian Federation is also represented by unique objects typical only for the Arctic—petroglyphs, camps of indigenous peoples, etc. [24].

The most important task is to connect all these objects to each other in a single cultural and social framework and ensure the accessibility of all objects within the framework of CSF. The cultural and social framework should have the following essential parameters (Fig. 2):

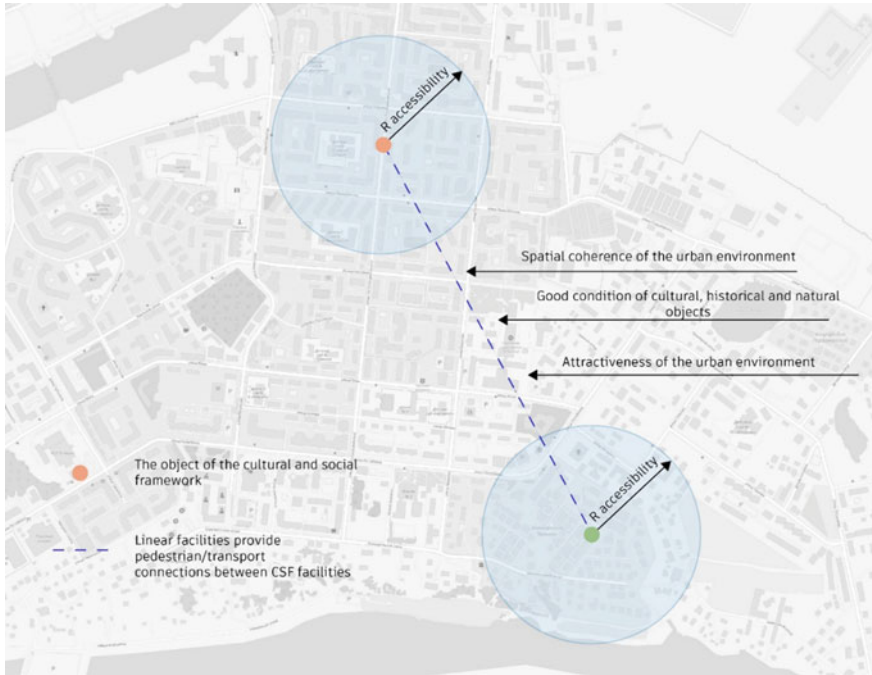


Fig. 2 Diagram of the CSF in Arctic cities

- spatial coherence of the urban environment,
- good condition of cultural, historical and natural objects,
- attractiveness of the urban environment.

The purpose of the Arctic settlement CSF is to concentrate the objects of cultural and social significance in the cities within a coherent system of territories.

2.2 Connectivity of CSF Objects

Connectivity is a mandatory requirement for the formation of CSF in the Arctic settlements, as it is primarily a question of environmental safety. In this study we will pay attention to the requirement for connectivity of the cultural and social framework of the Arctic cities. The provision of CSF connectivity in the Arctic is considerably complicated by low temperatures, strong winds, polar ngoches, and difficult terrain. The transport infrastructure and the availability of accessible navigation in the city also play a significant role. All of the above factors have a direct impact on the connectivity of

CSF. The connectivity of the cultural and social framework can be considered through pedestrian and vehicular accessibility. In this study, we consider pedestrian temporal isochrones. Based on a review of existing site connectivity studies, the following factors affecting the connectivity of CSF were identified (Figs. 3):

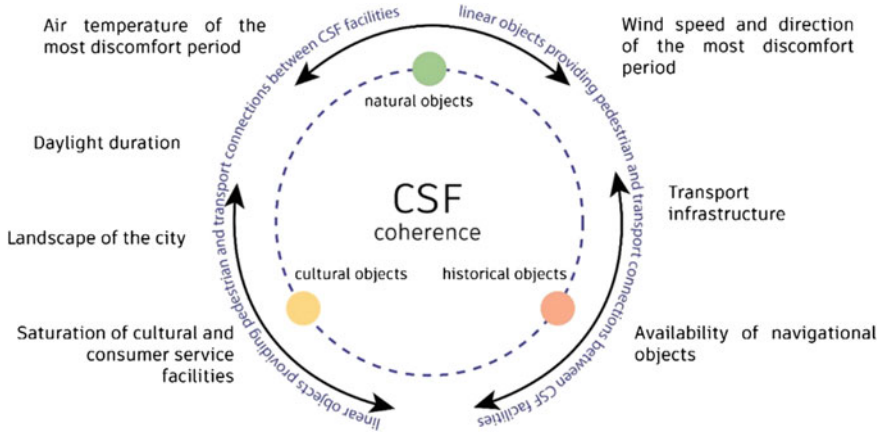


Fig. 3 Factors affecting the connectivity of the CSF in the Arctic cities

- air temperature of the most discomfort period,
- wind speed and direction of the most discomfort period
- daylight duration,
- landscape of the city,
- transport infrastructure,
- saturation of cultural and consumer service facilities,
- availability of navigational objects.

In this study we will consider in detail two factors—air temperature of the most discomfort period and wind speed and direction of the most discomfort period and their influence on the connectivity of CSF objects. It should be noted that the existing methods of assessing the accessibility of CSF facilities for cities with a more comfortable climate are not acceptable for cities in the ASRF—the movement of pedestrians at low temperatures and high wind speeds may not be safe.

2.3 Assessment of CSF Connectivity Parameters—Temperature and Wind Speed

In order to determine the maximum permissible time for moving between CSF objects it is suggested to refer to the WindChill Index table data [25]. The WindChill Index is a way to measure the severity of the weather, that is, the subjective feeling of a person when simultaneously exposed to frost and wind [26]. Polar explorers Paul Sayplu and Charles Passlu during the Antarctic expedition in the winter of 1941 conducted a series of experiments that consisted in observing the rate of freezing of water depending on

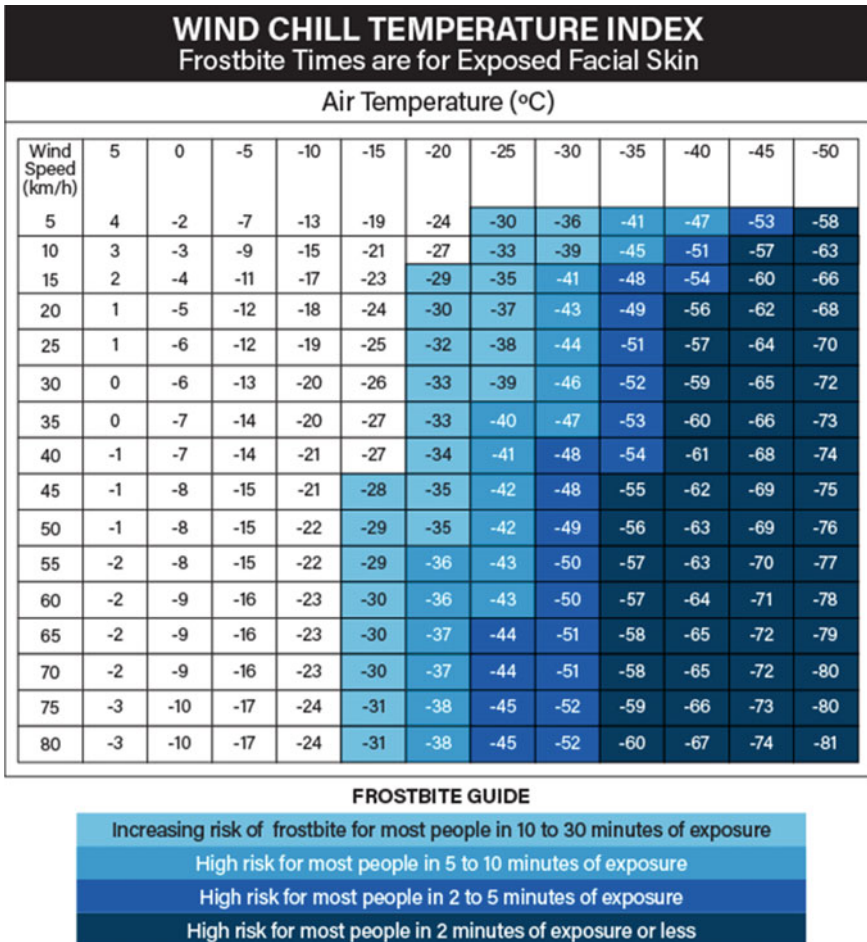


Fig. 4 Table of WindChill index values

air temperature and wind speed. The results formed the basis for the development of the table of values of the wind-cold index.

The wind-cold index weather hardness is calculated as follows: the air temperature in degrees Celsius is added to the wind speed multiplied by the hardness coefficient. For ease of use, different combinations of air temperature and wind speed are gathered into a table of weather hardness by wind-cold index (Fig. 4).

Thanks to the table we can determine the maximum time during which pedestrians can move between CSF objects safely, without risk of frostbite or feeling of discomfort. To determine the maximum distance between objects we propose to use the method of constructing temporal isochrons. As the initial formula we will take the formula of distance calculation on the basis of speed and time. Time is determined on the basis of

the WindChill Index frostbite table.

$$S_{csf} = V \times t_{wci} \tag{1}$$

S_{csf} —distance between CSF objects; V —pedestrian speed; t_{wci} —the allowable time when moving on the street between objects, taking into account the WindChill Index.

Since in this study we consider pedestrian temporal isochrones, we choose 5 m/s as the speed of a pedestrian (V). As a tool to find S_{csf} we will use geoinformation analysis, specifically network analysis in the form of temporal isochrones. As a recommendation for urban planners, we have developed an algorithm for assessing the pedestrian connectivity of CSF facilities for cities in the Arctic (Fig. 5).

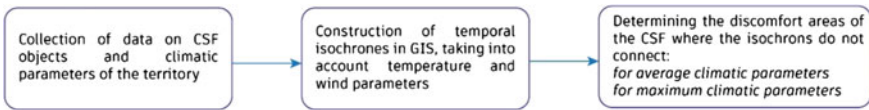


Fig. 5 Algorithm for assessing the connectivity of the framework in Arctic cities

The first stage of the algorithm consists in collecting information about the objects of the cultural and social framework of the city, as well as climatic parameters of the territory in question. At the second stage it is necessary to construct temporal isochrones, the availability zones of which are determined through climatic parameters and WindChill Index. The third stage identifies the discomfort areas of the cultural and social framework, where the isochrons do not connect for the average and maximum parameters of temperature and wind speed. To confirm the applicability of the algorithm it is necessary to conduct an approximation on the real territory of the Arctic city. For the study it is proposed to use modern GIS-technologies, which help to optimize and automate the work with spatial data [27–29].

3 Project Experiment on the Example of Norilsk

As an appraisal we will consider a fragment of the cultural and social map of the city of Norilsk. Norilsk is a large city, a city of regional subordination of Krasnoyarsk region with the population of 174 453 people (as of 2021) (Fig. 6). Norilsk is considered the world’s most northern city with a population of more than 150 thousand people. Norilsk is the largest center of non-ferrous metallurgy in the Russian Federation.

Norilsk is one of the most interesting cities in the Arctic zone in terms of tourism—special northern nature, culture of the small peoples of the North and Siberia, unique life of local residents of the city. Norilsk is home to many natural and cultural attractions. However, Norilsk is also characterized by the harshest climate, even for the Arctic [30]. The average temperature in the most uncomfortable period in January is $-18.8\text{ }^{\circ}\text{C}$, and the minimum can reach $-57\text{ }^{\circ}\text{C}$. The average wind speed is 6.7 km/h and the maximum wind speed is up to 144 km/h (Fig. 5). Considering the safety requirements for traveling at such low temperatures and high wind speeds, it is proposed to analyze two travel scenarios—at average temperature and wind speed parameters and at maximum ones.

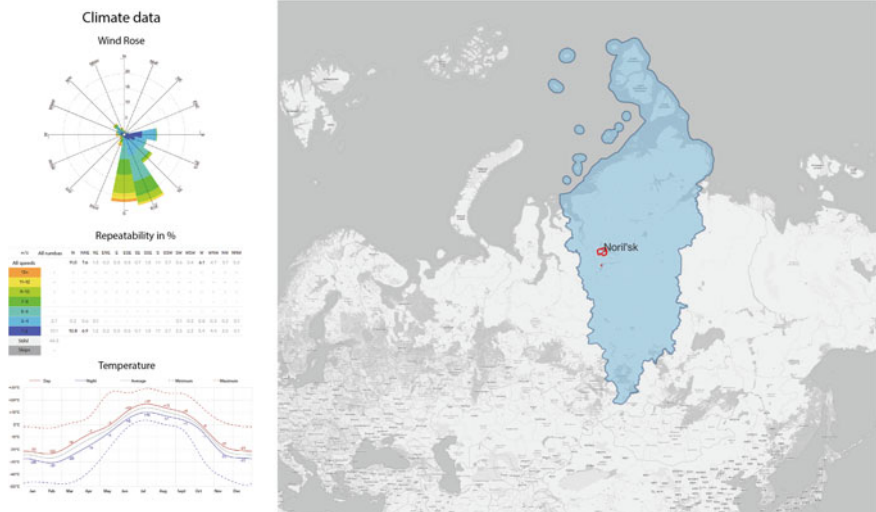


Fig. 6 Norilsk city layout and climatic parameters

According to WindChill Index this means that for average and maximum values of temperature and wind speed we take time availability isochrones of 2, 5 and 10 min.

In accordance with the developed algorithm, the *first step* is to collect data on the existing objects of the cultural and social framework (cultural, historical and natural) and enter them into the GIS in the form of vector geometry with attributes (Fig. 7).

In Norilsk, historical and cultural objects of CSF predominate within the city boundaries, while natural objects are mostly located outside the city, within the boundaries of the urban district. Natural sites located outside the city should be considered separately, taking into account both transport and pedestrian accessibility. This study proposes to consider objects within the city of Norilsk and in its immediate vicinity.

At the *second stage*, it is necessary to construct temporal isochrones of pedestrian accessibility, taking into account climatic factors. To build temporal isochrones we use the software package QGIS and a module for network analysis ORS Tools. The range of temporal accessibility choose 5 and 10 min for the average values and 2 min for the maximum.

On the *third stage* it is necessary to connect all objects of CSF in a single frame and to determine areas of the frame where isochrones are not connected, and hence the connectivity between objects is broken. To connect the objects by the existing transport-pedestrian lines we use also the program complex QGIS and network analysis module QNEAT3 (Shortest Path). First, we conduct an analysis for the average parameters of temperature and wind speed -18.8°C and 6.7 km/h (Fig. 8). The availability ranges for the average parameters are 5 and 10 min.

The diagrams show that with average parameters of temperature and wind speeds there are only a few uncomfortable areas where connectivity is broken. The first small section is located on Vokzalnaya Street. The second section, much longer, runs along Oktyabrskaya Street to the memorial to the victims of the Gulag or Norilsk Golgotha.

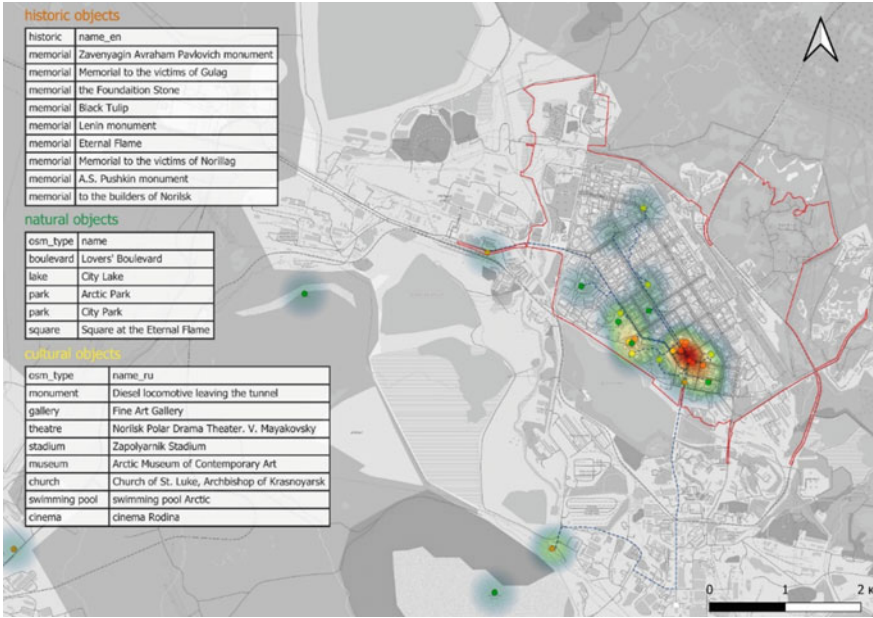


Fig. 7 Elements of the cultural and social framework by type and their density

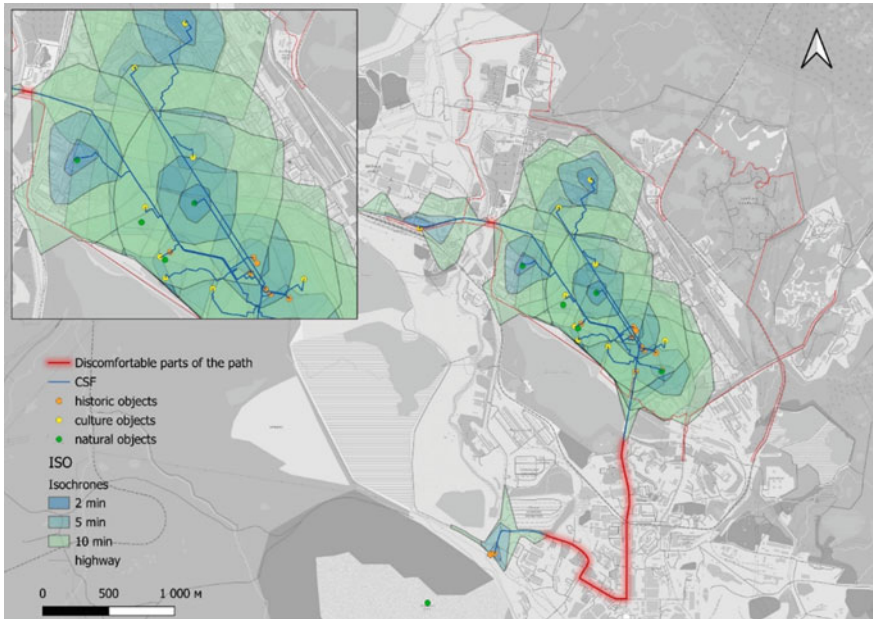


Fig. 8 Isochrones of the availability of CSF for average climatic parameters

Despite the fact that the memorial is outside of the city it is worth to include it in the cultural and social framework of Norilsk, as the theme of Gulag and Norillag is one of the main in the history and in forming the identity of the city. It is necessary to note, that the way to the memorial runs through the area of Old Town where many historical buildings of historical value of Norilsk are preserved. Creation of intermediate CSF facilities and modernization of public transport routes will allow to achieve connectivity in this area.

Then we need to conduct a similar analysis for the maximum parameters of temperature and wind speed -57°C and 144 km/h (Fig. 9). The accessibility ranges for the maximal parameters are 2 min.

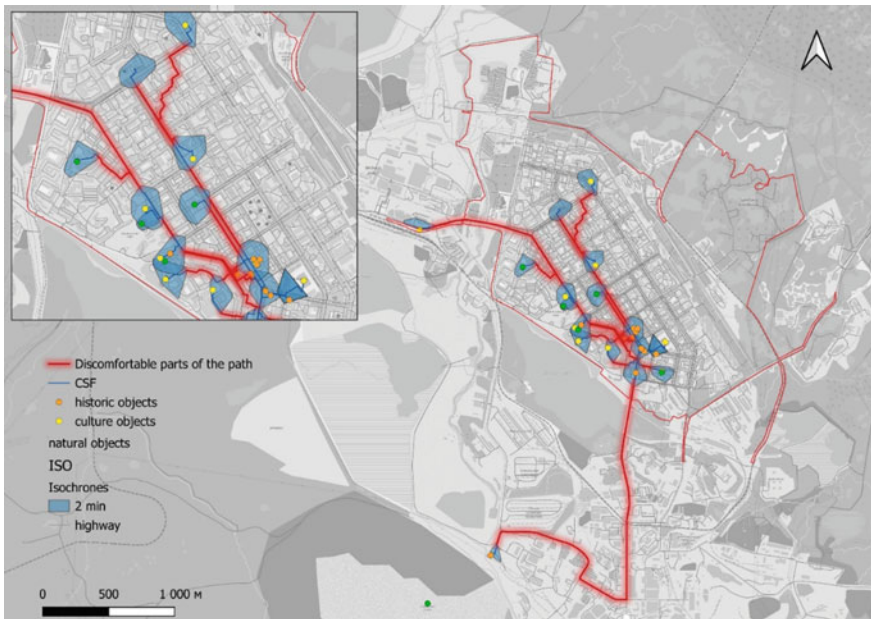


Fig. 9 Isochrones of the availability of CSF for maximum climatic parameters

The resulting scheme shows that the uncomfortable areas are much more than those where connectivity is maintained. In contrast to the first scheme these are not only remote objects, but also the objects located within the limits of kilometer or even hundreds meters. It is obvious that these sites require measures to increase the connectivity of CSF objects.

4 Conclusions

As a conclusion, it can be argued that there are problems with connectivity in the Arctic cities. Even taking into account the average air temperatures and wind speeds in the cultural and social framework of the city there are uncomfortable areas of the pedestrian path. When the maximum possible temperatures and wind speeds are taken into account,

there are considerably more of these areas. As recommendations to increase the connectivity of the cultural and social framework we can offer: the organization of warm stops, improving the system of public transport, as well as the creation of intermediate points of interest.

The developed methodology of CSF connectivity assessment through the parameters of temperature and wind speed makes it possible to determine the uncomfortable areas of the cultural and social framework (CSF) of the Arctic city and to work out proposals on the improvement of connectivity. Ensuring of spatial coherence of cultural and social framework is extremely important in the complex climatic conditions of the Arctic zone of the Russian Federation. The project experiment on the example of the city of Norilsk confirmed the applicability of the methodology for assessing the connectivity of the cultural and social framework through the parameters of temperature and wind speed. As a conclusion it is also necessary to say that for a full assessment of the coherence of the cultural and social framework of the Arctic cities it is necessary to take into account other factors—daylight duration, landscape of the city, transport infrastructure, saturation of cultural and consumer service facilities, availability of navigational objects. To optimize the process of CSF connectivity assessment it is necessary to create a script in Python programming language in the GIS environment. The creation of a coherent cultural and social framework of the Arctic city will help to develop a network of public spaces and ensure the connection between them, which in turn will increase the comfort and safety of the living environment for the residents, as well as help to develop tourist routes in the city.

References

1. Alekseev GV et al (2016) Arctic space of Russia in the XXI century: factors of development, management organization. Nauka Publishing House, Saint Petersburg, p 1016
2. Semenova A, Konstantinov P, Varentsov M (2019) Modeling the dynamics of comfort thermal conditions in Arctic cities under regional climate change. IOP Conf Ser: Earth Environ Sci 386(1). <https://doi.org/10.1088/1755-1315/386/1/012017>
3. Drozdova IV, Alievskaya NV, Belova NE (2022) Problems and prospects for the development of the Arctic zone of the Russian Federation. In: Proceedings of ARCTD 2021: Arctic territorial development. Cham: Springer International Publishing, pp 137–143
4. Prokopova S (2022) The concept of a warm city in the arctic: basic ideas of comfort in the urban environment (the case of Western Siberia, Russia). Technical Aesthetics and Design Research 3(4):22–28. <https://doi.org/10.34031/2687-0878-2021-3-4-22-28>
5. Serteser N, Karadag I (2018) Design for improving pedestrian wind comfort: a case study on a courtyard around a tall building. Archit Sci Rev 61(6):492–499
6. Korobeynikova AE (2019) Trend of development and formation of residential environment of settlements on the sloping terrain in the conditions of the Arctic zone of the Russian Federation. Bull Eurasian Sci 11(4):26
7. Medeiros E, Rauhut D (2020) Territorial cohesion cities: a policy recipe for achieving territorial cohesion? Reg Stud 54(1):120–128
8. Korobeynikova A, Danilina N, Makisha N (2021) Sustainable development of the slope lands of the Russian arctic: investigation of the relationship between slope aspects, wind regime and residential wind comfort. Land 10(4):354. <https://doi.org/10.3390/land10040354>
9. Kuklina V, Sizov O, Fedorov R (2021) Green spaces as an indicator of urban sustainability in the Arctic cities: case of Nadym. Polar Sci 29:100672

10. Rauhut D, da Costa NM (2021) Territorial cohesion in Denmark, Finland, Norway and Sweden 2007 and 2017. *Geogr Tidsskr—Dan J Geogr* 121(1):1–14
11. Strategy for development of the Arctic zone of the Russian Federation and ensuring national security for the period up to 2020. <https://docs.cntd.ru/document/499002465>
12. Presidential Decree of 26.10.2020 № 645 On the strategies of development of the Arctic zone of the Russian Federation and ensuring national security for the period up to 2035. <http://www.kremlin.ru/acts/bank/45972>
13. Decree of the President of the Russian Federation from 05.03.2020 № 164 On the basis of state policy of the Russian Federation in the Arctic for the period up to 2035. https://minec.gov-murman.ru/activities/CERArctic/npa_arctic/
14. Belyaev IS (2021) Problems of Arctic construction: trends and prospects. *Bull Civil Eng* 2:248–255
15. Barsukova NI (2022) Creation of public spaces for the Arctic cities of Russia. Civilization aspects of the development of the Arctic regions of Russia: proceedings of the III scientific-practical conference, pp 8–17
16. Barsukova NI, Fomina EV (2022) Parks in extreme conditions of the Arctic. *Principles Organ* 18:8–17
17. Carder M et al (2005) The lagged effect of cold temperature and wind chill on cardiorespiratory mortality in Scotland. *Occup Environ Med* 62(10):702–710
18. Shui T et al (2018) Assessment of pedestrian-level wind conditions in severe cold regions of China. *Build Environ* 135:53–67
19. Loginov V, Ignatyeva M, Balashenko V (2018) Consistent approach to assess the comfort of living in the northern and arctic areas. *Econ Reg* 14(4):1399–1410. <https://doi.org/10.17059/2018-4-26>
20. Serebrovsky FL (1985) Aeration of settlements. Stroyizdat, Moscow, p 172
21. Ratner EM (1967) Method of physiological assessment of local climate by its impact on human thermal state. *Vop Kulturologii* 5:446–451
22. Blocken B, Stathopoulos T, Van Beeck JPAJ (2016) Pedestrian-level wind conditions around buildings: review of wind-tunnel and CFD techniques and their accuracy for wind comfort assessment. *Build Environ* 100:50–81
23. Oszcewski RJ (1995) The basis of wind chill. *Arctic* 372–382
24. Milosz H, Galina Z, Mariya M (2022) Geoheritage of the Kandalaksha region (Kola Peninsula, white sea, Arctic Russia), evaluation, and geotourism opportunities. *Geoheritage* 14(4). <https://doi.org/10.1007/s12371-022-00726-4>
25. Kokotis P, Katsavos S (2015) Effects of wind chill factor, temperature and other meteorological parameters on the incidence of Bell's palsy: results based on a retrospective, 7-year long, Greek population study. *Neuroepidemiology* 45(1):44–49
26. Ahmad T, Rashid T, Khawaja H, Moatamedi M (2016) Study of wind chill factor using infrared imaging. *Int J Multiphys* 10(3):325–342
27. Stevens D, Dragicevic S, Rothley K (2007) ICity: a GIS–CA modelling tool for urban planning and decision making. *Environ Model Softw* 22(6):761–773
28. Van Maarseveen M, Martinez J, Flacke J (2019) GIS in sustainable urban planning and management: a global perspective. Taylor & Francis, p 364
29. Bogdanova AY (2020) Application of GIS technologies in urban planning. International scientific and technical conference of young scientists, pp 174–178
30. 131.13330.2012 C. (2012) Building climatology. Revised edition of SNiP 23-01-99. Ministry of Regional Development of Russia, p 108



Ecopositive Environment at a Preschool Educational Institution

N. V. Lamekhova^(✉)

Ural State University of Architecture and Art, 23, Karl Liebkneht Street, Ekaterinburg 620075, Russia

Lamekhova@mail.ru

Abstract. The article discusses the basic principles of an eco-positive environment at a preschool educational institution. Such principles provide a basis for an environmentally comfortable space and teaches preschool children a right attitude to the environment. Special attention is paid to ecological comfort zones in preschool educational institutions. The article also identifies the prerequisites and considers several techniques and tools used to form an environmentally friendly (eco-positive) environment at a preschool institution. The possibilities to organize a roofing space as part of an environmentally oriented architectural environment are revealed. The main directions for the development of an on-roof exclusive space at a preschool institution have been identified as follows: an exploitable roof with playgrounds and phyto-modules; a “building–hill”, which involves using horizontal surfaces of the flat exploitable roof along with the slopes (embedded, raised) of the roof, involving the horizontal, angled and even vertical planes and facilitating the development of the exploitable roofing space in conjunction with the site; an exploitable roof featuring mini-gardens and greenhouses, “green” slopes used to establish eco-trails; a resource-saving roof. The research outcomes are both practical and theoretical, with the latter capable of being the basis for further research.

Keywords: Ecology · Ecological comfort · Ecopositive environment · Green architecture

1 Introduction

Setting-up an environmentally comfortable architectural space has long been a matter of interest both nationally and internationally. The basics of environmental culture and environmental education should be taught starting from the preschool age [1–4], as otherwise educating the younger generation is impossible without broadcasting these principles. Individuals’ perception of environment is not limited to vision, it involves other senses, such as hearing, smell and touch, which constantly work together. These functions affect a person on a deeper level than we might think.

It is worth noting that preschool age is highly suitable for the environmental upbringing and understanding natural relationships. According to S. N. Nikolaeva, N. N. Konratieva, A. M. Fedotova, N. A. Ryzhova, O. Yu. Tyutyunik, I. A. Haidurova, etc. “5–7-

year-old kids are capable of acquiring ecological knowledge about plants, animals, man, cause-and-effect relationships and interactions of nature, human-nature relationships and the versatility of nature” [5].

The architect’s role in the design of the architectural environment for preschool education is underestimated. The fact that the architect, a creator with various plots at hand, is capable of directly or indirectly influencing the human perception of the world, human emotions, of working with subconscious feelings is highly important. The most amazing thing is that the impressions that we relieve, physical actions and especially the memories caused by them are rooted in our consciousness and permanently impact the development of our personality.

On a global scale, boosting the level of environmental culture lays the foundation for the growth of national welfare and saving public expenses on the elimination of natural and environmental disasters, often caused by humans themselves. In this regard, the role of an eco-positive approach based on the principles of caring for the environment and the child as an integral part of nature, is increasing [6].

The studies into preschool ecological education in the 1980s [7]. Despite the currently available developed and tested methods and various pre-school ecological education programs proposed, in practice there is a discrepancy between the facilities and resources and the content of the educational process.

This study considers the main means to form a favorable eco-positive architectural environment being an integral architectural component of a preschool educational institution. The term “eco-sustainability” is understood here as a result of “green” construction, aimed at erecting buildings with minimal environmental impact and rational energy use [8].

The study is particularly relevant due to the ecological comfort problems faced in pre-school, which arise due to the modern requirements to the educational process.

The article aims to identify the sustainable architecture techniques building up the basis the eco-positive pre-school environment.

The research methodology is based on a transdisciplinary approach that considers the study of children’s psycho-physiological characteristics through the prism of the educational process building up the knowledge about ecology within a certain architectural environment. Scientific research in the form of project proposals referenced in the article are justified by the preschool architectural environment ecological comfort ideology. They serve as a basis to identify sustainable architectural space forming techniques that preserve cognitive foundations, form the preschoolers’ desire for harmonious unity with nature, and comply with optimal freedom of movement, comfort, and minimal environmental interference requirements.

2 Environmental Practices Used to Form a Sustainable Worldview in Preschool Children

The following authors researched the issues of education by nature and ecological culture: Abramova N. L., Archegova I. B., Vinogradova T. A., Ivanov S. A., Kondratieva N. N., Kulikova E. Yu., Markova T. A., Mindzayeva M. R., Parfentieva T. A., Shkolnikov D. I., Shilenok T. A., etc. Improving the energy efficiency of preschool buildings was

considered in many foreign overviews and studies by Bjarke Ingels, Cardelus C., Day C., Dudek M., Exley P., Henning Larsen, etc. Vatin N. I., Nemova D. V., Yezersky V. A. and others researched cutting the preschool construction costs.

Many scientists were engaged in the development of environmental practices for children. During the Soviet period, preschool environmental activities were mainly based on nature conservation viewed as the most important social activity. Environmental knowledge was included in multiple training programs and manuals. However, this was not enough to solve the publicly set tasks of environmental education. In the 1970s, an integrated approach to environmental studies was formed. It studied the environment as an integral inter-connected system and involved children in useful extracurricular and social environmental activities. From that moment on, education has viewed nature protection as a system of scientific knowledge and practical measures for the rational use of natural resources, environment protection, and preventing the destruction of natural objects and complexes.

It is important that humanism towards nature was already developing in that historical period: the children's attention was focused on the difficulties animals and plants experience and the possible assistance from humans (equipment of feeders, weeding, etc.). The pupils acquired the environmental ethics that is paramount for a growing personality, i.e., knowledge how to protect nature and what one should not do to nature.

The preschool ecological practices developing over the latest decade provide nature conservation guidelines along with ecological and naturalistic (studying nature by observing living organisms, creating educational ecological trails, conducting outdoor excursions); ecological and local history (studying the influence of human activity on the state of natural and cultural heritage objects; identifying conditions to preserve the historical landscapes); ecological and educational (collection, processing, analysis, dissemination of ecological and educational information, studying and modeling of environmental problems, creation of information products (posters, wall newspapers, crafts, etc.) on environmental protection); and agroecological (planting and caring for plants) guidelines.

It is important that such activity of a problem-oriented, creative nature allows children to think about their lifestyle, place and purpose in the world, discuss and become aware of global problems, form an active environmental position and feel its value, form their own attitude to it [7].

The ecological education outcome is the emergence of ecological culture which coordinates natural and social security in one's life and ensures the natural environment preservation [5]. Environmental practices allow children to conduct comprehensive ecosystems studies with special equipment, along with experiments and observations that bring them to perceive the nature and interact with it.

Having analyzed the content, form, methods and techniques of environmental protection measures as part of the present study, the authors have identified the following main directions: "activation" of the building's protective function—making up a "barrier" protecting from the negative external influences (gas pollution, noise, overheating); creation of a favorable and safe environment for games and leisure, sports and experimentation, taking into account the children's age and preferences; identification of ways and resources to create an environmentally friendly environment for the children's daily

life at a preschool educational institution. Formation of conditions conducive to the development of ecological culture and a conscious attitude to nature.

The programs on ecological education of preschool children view the following as the components of human ecological culture: resource conservation, low-waste/non-waste and the degree of energy resources use, creating conditions for the development and existence of future generations [9–11]. Therefore, this issue will be considered from the point of view of resource conservation by architectural means and creation of conditions for the development and existence of future generations, as setting up comfortable environmental conditions is one of the strongest factors affecting human health and well-being.

The everyday design process usually focuses on the general compositional and pictorial aspects of an object with little attention being paid to how the object functions and interacts with human life. It is about how people who use objects, that is, preschool children, actually perceive, live in and understand them. The influence of building environments on cognitive and social development is usually given little or no time at all. The task of the study is to determine the design solutions of environmental comfort zones that convey the correct ecological worldview.

Based on the experience of implementing environmental practices, it is possible to identify areas requiring ecological comfort zones. The developed eco-comfortable preschool environment concept states that these zones can be located on site, as well as embedded in the internal structure. The main purpose of such zones is the children's feeling of closeness to and harmony with nature in an open or closed space. Nature has a very profound positive impact on our physical and spiritual health, and also enhances the sense of community with the world around us.

Swedish scientists compared children treated in different conditions: the playground for some was located in a quiet place, surrounded by tall buildings, with low plants and paved paths; others, on the contrary, followed the outdoors-at-any-weather principle and played on a playground in an overgrown garden. The study showed that children in constant contact with nature who spent the whole day outdoors regardless of the weather had better coordination and better ability to concentrate [12, 13]. It was also found that the proximity of trees could help reduce the symptoms of attention deficit disorder in children [14].

Christopher Day, Andrea Faber Taylor, Francis Kuo and William K. Sullivan found that places with green spaces stimulate the creative imagination in playing children, increase their ability to interact positively with adults and reduce the manifestations of disorders associated with low ability to concentrate [15–18]. All this indicates that environmental practices create unique opportunities for various children's outdoor activities.

One of the most common areas of preschool environmental education over the past decades has been environmental practices involving the study of man-nature relationships. Any environmental practice is based on a comprehensive study of the ecosystem by preschool children. It is included in the educational process and involves three channels of the surrounding world perception: cognitive (mastering knowledge about the world and humans and the related mental activity), perceptual (involvement of emotions

and feelings in the educational process) and practical (inclusion of personality in social activity).

The analysis of the forms, methods and technologies of environmental practices used over the last decade has revealed the following types of children's activities: support of objects of animate and inanimate nature (breeding fish, feeding animals in winter); environmental monitoring and research, including various methods: observation, experiment, modeling, etc.; design and creative activities aimed at solving local environmental problems: collection and disposal of solid household waste, landscaping and landscape design, etc.; ecological and educational activities—broadcasting (promoting) ecological and environmental knowledge in various forms, creative works (newspapers, drawings, posters); ecological and health-improving activities aimed at developing healthy and environmentally safe lifestyle skills and abilities; mass outdoor events: games, trainings, discussions, holidays, contests, excursions, hiking, etc.; ecological and artistic activities: writing fairy tales and stories about animate and inanimate objects, photographing, drawing [7].

Despite the trends towards the development of creative, problem-oriented, interactive activities, the aforementioned areas still mostly involved the kids' intellect in the perception and understanding of the world around them. The development of the emotional, spiritual and moral components requires new sensory forms, methods and technologies of interaction between nature and architecture along with the corresponding educational content.

Thus, for the last decade of the twenty-first century, the practice of sensory nature cognition and sensory pedagogics, based on the person's ability to perceive the outside world using one's senses: sight, hearing, smell, touch, taste, start developing in the national eco-education.

In the framework of sensory pedagogics, the children activities on eco-trails (paths), which can be organized both in the natural and urbanized environment, on the territory of educational organizations, have a great psychological impact. When organizing the cognitive activity of children on the eco-trail, it is possible to get information not only from the guide or the inscriptions on the tablets, but also by influencing the emotions (color contrast, colors, smells of different types of plants) that greatly affect the perception of the student senses.

In terms of organizing contemporary environmental practices, the pedagogical experience of Yu. V. Sheshina is noteworthy [16] as she annually organizes a country camp "Solnechnaya Chasha" for children of different ages in the vicinity of Yekaterinburg. It naturally combines the following: research activities (observations of natural objects, changes in nature, the study of the species composition of plants and animals, etc.); creative activities (floristry, landscape design, Ikebana, journalism, acting, needlework); ethno-cultural component (traditions of different countries in the world, including the traditions of the human-nature relations); recovery by natural means (morning jogging, swimming, sauna, natural nutrition, herbal tea, etc.); local history component (acquaintance with natural monuments, cultural sights of the region); demonstration of video materials on environmental and moral orientation topics; simple relaxation and meditation practices in the natural environment; sensory communication with the natural world and its contemplation; acquisition of the ethical-philosophical and ecological knowledge

in the form of a problematic dialogue and heuristic conversations; socially significant environmental activities (cleaning natural areas from debris, planting, etc.). Thus, the eco-activity of children in this camp is versatile, complex, involving mind, emotions and feelings, rational and irrational elements, science and art, theory and practice in the process of understanding nature and the surrounding world. Within this pedagogical approach to the organization of children's environmental practices it is possible to form a comprehensive child's noospheric worldview.

The efficiency of an integrated approach to the children activities during environmental practices was pointed to by foreign researchers as early as in the 80-s of the twentieth century. Thus, G. W. Knamiller distinguished the priority personality traits the environmental education should develop and considered to be the most important for a person with a noospheric worldview: a sense of unity with the environment, admiration for it and respect for its underlying processes; a sense of community with other people and living beings; a sense of responsibility for the choice made; developed imagination and creativity; a sense of continuity between past, present and future; ability to find the necessary information; critical attitude to the information received; the ability to predict and evaluate; the ability to formulate and test hypotheses.

To define the content, forms and methods of children environmental practices, the pedagogical approach of J. Elstgeest is of interest as it proposes to build the pedagogical process of the child's cognition of the environment based on the following definition of the latter: "The environment is simply the world that surrounds us. It starts from the skin of our body and extends in all directions, in ever-expanding circles until it encompasses even the Universe" [1]. In compliance with this, the education, based on the unique experience and child feelings, should gradually expand the horizons of knowledge and understanding of the surrounding world starting from the immediate natural environment to understanding the structure and beauty of the Universe, feeling the "filial feeling of the space" (K. N. Wentzel). Thus, the true sacralization of life by a person is possible on the education path since the very earliest years of a special attitude to nature, water, air, earth, sky, plants, animals as the "moral personalities" [1]. We consider the task of captivating children with this idea, giving them appropriate content and active methods and technologies, including sensory ones, for cognizing nature, to be one of the primary tasks of modern education.

3 Architectural Techniques of Ecopositive Architectural Environment

Some of the techniques creating an eco-positive architectural environment are quite simple and effective and do not require additional capital investments.

The playground is one of the main zones that forms a sustainable and comfortable environment of a preschool educational institution. Preserving the original components, as well as the possibility of transformation in order to create conditions for children to feel the closeness between the nature and humans are very important. "The positive side of children noticing, observing, experiencing, creating a variety of worlds embedded in everyday life is the richness and depth of their spiritual communication with the landscape, the ability to receive maximum personally important information in this contact

and achieve a sense of unity with the world...The development of the human ability to discover multiple worlds can be left to chance—which happens most often in our modern culture. And you can teach a person to realize, manage and give verified traditions of many generations of people, cultural forms. Such, for example, is the teaching of meditative contemplation that takes place in Japanese gardens” [19].

Landscape modeling is one of the techniques that ensures an environmentally oriented architectural environment, and it should, undoubtedly, account for the psychophysiological characteristics of preschool children. We further establish the preschool age categories and the corresponding preferences:

- playgrounds for toddlers (up to 3 years old) are quiet, sunny, isolated sites surrounded with greenery which have a sandbox and small swing springs. It is important to keep in mind that this is the kids’ first meeting with the outside world and strangers, the first independent platform, so it is of great importance for the toddlers;
- playgrounds for children aged 3–5—mainly for experimental games of children with sand and water;
- playgrounds for children aged 5 to 6 (7) are characterized by a variety of activities and additional educational functions. They can feature outdoor horizontal platforms for creative, theatrical and educational activities added to the artificially created elements of the natural environment (slides, hills, small dams), which is determined by age (craving for active physical development) when studying natural elements, phenomena in the educational and cognitive process in the air in the form of small amphitheaters.

The elements for experimental activities can be different: artificially constructed; made from natural elements (remnants of wood, old trees, etc.) which are compelling due to their low cost and high information and artistic potential. Here, it is possible to identify a group of means to create an artificial barrier—the screening of the territory, contributing to the protective function formation for the structural elements of the territory that prevents the external adverse influences through the use of:

- fences (creation of a protected yard due to a deaf or semi-deaf fence, phyto-walls);
- the volume of the building (the formation of semi-enclosed recreation courtyards due to the main volume of the building and the use of the exploitable roofing space for playgrounds) [20];
- creation of a protected courtyard for the formation of the building volume, or by using an active landscape component [21];
- shadow canopies (shadow canopies can form the perimeter of the site, creating a visually impenetrable surface) and due to the changes in the terrain of the site.
- enabling the protective functions of the site. Due to the correct formation of the volume of the building and the modeling of the site, wind protection can be carried out; relief differences on the site can act as protective architectural measures to eliminate and reduce the negative impact on the health of pupils, creating wind protection, forming a shadow curtain, being a comfortable area for children’s games.

The building and the site are characterized by the harmonious inclusion of the architectural object in the urban and landscape environment and is manifested in the principle of sustainable development of architecture in the form of the integration principle [8].

Another direction for the development of the structural elements of the building volume within the framework of the comfortable environment generation can be the interconnection of the object with the environment and the development of safe and affordable “green roofs” on the building and slopes, earthed parts. In this regard, the building is like a game element of a walking area, expanding the range of opportunities for the environmentally comfortable space.

The roof has great potential. The roof is of crucial importance in the organization of a three-dimensional solution for the preschool object in the development of a microdistrict of the city when perceived from the upper floors. Based on the variety of techniques and approaches to the accessible roofing space organization, the following areas can be identified as having firmly established themselves in international practice (Fig. 1):



Fig. 1 Trends in the development of the exclusive space of the roofing part in a preschool institution

(a) *the exploitable roof with playgrounds and phyto-modules*, which involves the use of a flat operated roof with canopies for playing (installation of playgrounds and themed playgrounds on the roof), where part of the roofing surface can compensate for the territory under the building [22], including the green areas. The problem of forming walking areas on the roof of a building is usually aggravated by the complexity of wind-protection. Possible solutions include options with side protection, which can be designed in the form of a slope to the inner surface of the roof or in the

form of a wall [23]. Layout solutions can be varied, it is important to create a wind-protector around the perimeter, which would allow using the open-air space for physical activity, expanding the range of means presented on the ground surface.

A flat operated roof with platforms and phyto-modules makes it possible: to compensate for the built-up area; to provide fire passage around the building; to use canopies to protect from sun and precipitation, various types of coatings, plants; to increase the aesthetic potential of the roof plane; to form highly artistic landscape compositions in the roof plane; to protect the roof from overheating.

Disadvantages: seasonal use, or restriction due to the lack of the ability to remove snow in the winter season.

- (b) *“Building–hill”*—which synthesizes horizontal parts of a flat roof in use and slopes (embedded, raised parts of the roof), using space not only in the horizontal plane, but at an angle and even vertically, which in turn allows developing the exploitable roofing space in conjunction with the site. Such roof has the following advantages: compensation for the built-up area; provision of fire passage around the building (subject to the use of a raised volume, the width of which is not more than 18 m, adjacent to the ground plane, where the entrance of the fire truck is possible from 2 sides); the possibility of using canopies to protect from sun and precipitation; increasing the aesthetic expediency of the roof plane; the possibility of forming highly artistic landscape compositions in the roof plane with the use of different types of coatings, plants; the possibility of using natural slopes and obstacles for pupils; protection from overheating; the possibility of snow removal in winter.

The presence of a “green” roof and slopes near the building, as well as the presence of grounded parts, contributes to the development of the pupils’ coordination [8], conducting collective games (competitions), which is confirmed by the scientific results by S. V. Ilvitskaya and I. V. Mikhailova. The roof can be arranged with a green coating along the entire length of the building, which guarantees energy efficiency, sound insulation, and comfortable internal environment parameters.

- (c) *the operated roof with mini-gardens and greenhouses, the presence of “green” slopes for the organization of eco-trails*—allows involving pupils in light labor (agricultural) activities, as well as for the opportunity to grow alimentary products. Additional features include the collection of rainwater and its reuse for irrigation; cultivation of a wide range of different types of plants; increasing the aesthetic expediency of the roof plane; protection from overheating.
- (d) *resource-saving roofing*—the use of energy-efficient technologies, which involves placing solar panels on the roof, collecting rainwater. Excellent practical experience exists in Germany, Holland, Belgium and other European countries. As it is impractical to spend tap water on toilet flushing in a toilet tank, the Europeans have come up with many schemes for using absolutely free, but no less useful natural water. Thanks to the use of rainwater, the cost of depreciation of pumping and cleaning equipment is reduced, personal budget savings occur. Reuse of energy resources (collecting rainwater, solar energy), improving the aesthetic qualities of the roof plane (by searching for optimal roof slopes); protection of the roof from overheating—all these translate into the careful attitude to nature, its resources, which educates the younger generation.

As a result, the identified directions for the organization of a particular roofing solution allow the architects and designers to choose an architectural solution, they can also serve as a basis for further scientific.

The analysis of the above roofing space set up techniques identifies the potential of the roofing space with an environmentally oriented architectural environment: the use of grass covering on the roof for active games, sports activities; creation of artificial slopes, vertical landscaping on the roof together with other gaming equipment; careful preservation of existing trees and shrubs, their inclusion in the overall composition of the complex, the general idea of active games.

Thus, the identified characteristics and capabilities of the roof spaces will help the architect and the designer to cope with the tasks in a substantive and meaningful way, which will contribute to the creation of the environmentally comfortable roof zones.

Searching for an eco-positive environment forms *open amphitheater platforms at ground level, or in the volume of the building*, which form small stairs-amphitheatres. The increase in natural zones, playground elements made of natural materials (wood, stone, sand, etc.), the expanded use of nature objects—the presence of different points of perception, the creation of conditions for educational, creative and sports activities increase the comfort of children’s stay in the preschool, contribute to ensuring a safe, health-saving and environmentally oriented environment.

Ecological trails (paths) that can be organized both in the natural environment, on the territory of an educational institution, and in an urban zone. When involved in cognitive activity on an ecological path, children can get information both from a mentor, and by means of impressions about the surrounding world.

The territory of a kindergarten is not a simple arrangement of isolated structural elements, it should be a system of objects distinguished by age preferences and groups, connected by an “ecological path”, which will correspond to a logically organized space that serves as a source of full-fledged development for each child. Thus a preschooler can develop the necessary personal traits with the help of an educator.

The internal structure of a preschool educational institution can include: a sensory garden, a phyto-module, ensuring a close connection between a veranda and a walking area.

Sensory garden. New ecological practices related to the contemplation of nature have begun to spread recently (E. N. Dzyatkovskaya, A. N. Zahlebny, G. P. Sikorskaya, etc.). Scientists have also found out that green spaces in a child’s everyday environment, even viewed through the window, reduce the symptoms of attention deficit.

G. P. Sikorskaya states that only the direct contact with nature opens an amazing world for a child. He will have to master it in life and harmoniously fit into it. But at the same time, urban conditions cannot always provide an opportunity to establish the necessary contact with wildlife, compensate for the lack and fulfill the strive for feelings, curiosity, sensitivity and empathy by expanding the educational space of the “sensory garden”, where the pedagogical process can acquire new semantic turns aimed at such natural phenomena as harmony, rhythm, symmetry and other stable signs of beauty [24].

Such garden can be arranged in the public area of an educational institution as an *atrium* with overhead light or upper side lighting. A sensory garden at a preschool

educational institution can partially solve problems with outdoor activities in cold or windy weather.

Phyto-module. Phyto-modules are small rooms with a wide range of plants with good light transmission capacity designed for educational and play activities of preschool children. The phyto-module can have a permanent translucent enclosing structure, which allows it to be used in winter, and also can have a removable or transformable system, which is open in summer and closed with translucent material in winter [25]. The transforming frame or partition will allow using the space adjacent to the phyto-module in summer and winter for the purpose of conducting experimental activities, expanding the boundaries of the room. It is assumed that the phyto-module will contain a natural component (indoor plants of different sizes, climbing plants for vertical gardening, a water resource) and various educational activities (sensory, design, museum, sports, music, etc.).

Ensuring the close connection of a veranda with the walking area. The walking areas in the close vicinity to the entrance of the preschool institutions based on the “uniting with nature” principle are based on the approximation of the basic parameters of the residential cell of an individual residential building. Bringing the walking area close to the exit from the group site contributes to strengthening the educational function, the emergence of a sense of ownership and belonging of this object to a certain group of pupils.

The study of ecologically comfortable zones for preschool education revealed that these zones, included in the structure of a preschool educational institution, are a place for inspiration, creative self-realization, intellectual and physical development, leisure, recreation and communication, a place for the implementation of ideas for younger generation education.

4 Conclusion

The competent use of modern approaches to equipping the identified environmental comfort zones will make the preschool educational process more accessible. This will significantly help increase the children’s motivation to learn and warm up their love for the world around them, nature. To do this, it is necessary to involve the kids’ emotions and feelings, while forming a wide environmentally comfortable environment. The scientific novelty of this study lies in the identification of a number of architectural techniques and means for organizing an eco-positive architectural environment at a preschool institution, which promotes the fullest stimulation of the pupils’ the abilities, the activation of their mental activities, and will ultimately serve to stimulate the research activities (observation of natural objects, changes in nature, the study of plant species, etc.); the ability to conduct recreational activities, jogging on the “green” slopes, skiing downhill in winter); local history component (acquaintance with the herbs of the region, acquaintance with rare plant species); the ability to conduct simple relaxation and meditation practices in the natural environment; sensory communication with the outside world; mastering ethical, philosophical and environmental knowledge in the form of problematic dialogue, conversations.

References

1. Arhegova I (2003) Ecological worldview is the basis of development. *Bull Russ Acad Sci* 73:114–116
2. Iovlev V (2006) Architectural space and ecology. Architecton, Ekaterinburg
3. Kulikova E (2000) Architecture and ecology of modern megalopolises. *GIAB* 8:26–28
4. Cardelus C (2018) Green architecture today. Booq Publishing
5. Goncharova E (2008) Theory and methodology of ecological education of preschool children. Nizhnevartovsk, Nizhnevartovsk Humanitarian Institute. A course of lectures for students of higher pedagogical educational institutions
6. Novitskaya E (2018) Architectural aspects of ecopositive design of home kindergartens, pp 46–49
7. Ivanov S, Abramova N (2016) Genesis of children’s ecological practices: from the study of ecosystems to sensory interaction with nature. *Sci Dialogue* 9(57):283–296
8. Ilvitskaya S, Mikhailova I (2020) Sustainable architecture as a vector of development in the design of preschool educational organizations. *Bull TSASU* 22(6)
9. Markova T, Vinogradova T, Kondratieva N, Shilenok T (2006) WE: environmental education program for children. Press, Moscow
10. Myasishchev V, Bodaleva A (1995) Psychology of relationships. Institute of Practical Psychology, Modek, Voronezh, Moscow
11. Sokolov Y (2021) Problems and risks of renewable energy sources. *Probl Risk Anal* 18(4):28–47. <https://doi.org/10.32686/1812-5220-2021-18-4-28-47>
12. Zazulya V (2020) Ecological comfort and public spaces. *Urbanistics* 3. <https://doi.org/10.7256/2310-8673.2020.3.31732>
13. Lowe R (2007) *The last child in the forest*. Good Book, Moscow
14. Lowe R (2021) *Our wild call*. Bombora, Moscow
15. Day C (2007) Environment and children. Passive lessons from the everyday environment (Midbjer A. Chennai)
16. Dudek M (2005) *Children’s spaces*. Architectural Press, London
17. Broto C (2006) *Great kinds’ spaces*. C. Broto i Comerma, Barcelona
18. Broto C (2006) *Preschol and kindergarten architecture*. C. Broto i Comerma, Barcelona
19. Osorina M (2007) *The secret world of children in the space of the adult world*. Speech, St. Petersburg
20. Zhelnakova L (2017) Principles of ecologization of the architectural environment for children with physical health disorders. Dissertation, Nizhny Novgorod State University of Architecture and Civil Engineering
21. Lamekhova N (2021) Regional specific features of architectural space ecologization for preschool education in the Urals. *E3S Web Conf* 311:02010. <https://doi.org/10.1051/e3sconf/202131102010>
22. Merenkov A, Akchurina N, Matveeva T, Yankovskaya Y (2019) The basic principles of “green” architecture in the foreign experience of implementation. *IOP Conf Ser: Mater Sci Eng* 687. <https://doi.org/10.1088/1757-899X/687/5/055058>
23. Lamekhova N (2019) Formation of healthy environment for early childhood education. *Architecton* 2:62–65
24. Sikorskaya S (2007) Sensory garden for children, including for children with disabilities. Rarity, Yekaterinburg
25. Dorozhkina E (2017) Constructive problems of green architecture. *Urban Stud* 4. <https://doi.org/10.7256/2310-8673.2017.4.24150>



Use of Water Resources and the Irrigation Network of the Chui Valley

M. T. Abylgazieva^(✉) and T. A. Ableshev

Kyrgyz State University Named After I. Arabaev, 51, St. Razzakova, Bishkek, Kyrgyzstan
muni.83@mail.ru

Abstract. The Kyrgyz Republic has the richest water and energy resources. The main asset of Kyrgyzstan is water resources. The main indicators of the water supply of the territory is the amount of river flow per one km² of area. All water supply and water balance assessment data were obtained from the Department of water resources and melioration of the Ministry of Agriculture and Melioration of the Kyrgyz Republic. According to the Ministry of Agriculture and Melioration of the Kyrgyz Republic, 321,119 ha of irrigated agricultural land are concentrated in the Chui region. There is drainage on 102,068 ha, where 576.6 km of the inter-farm collector and drainage network are dispersed, of which 114.6 km (or 20%) is in poor condition, as well as 3450.9 km of on-farm CDS, of which 1292.2 km (or 36%) is also in poor condition, including 642.2 km of open and 650 km of closed networks. An extensive network of irrigation facilities has been created in the Chui Valley. Initially, the Boroldoi and Krasnorechensk main canals were created then 18 km from Bishkek, the At-Bashy Canal was built.

Keywords: Water resources · Water supply · River runoff · Economic sectors · Water consumption · Water consumption · Irrigation · Water regime · Atmospheric precipitation · Natural pollution

1 Introduction

Kyrgyzstan is the only country in Central Asia that is fully provided with maximum reserves, not only of drinking water, but also of irrigation water. In total, there are more than 1000 large and medium water sources, of which 850 are used for irrigated agriculture. Their total average annual runoff is more than 60 billion m³, of which about 70% falls during the growing season.

2 Materials and Methods of Research

The main indicators of the water supply of the territory is the amount of river flow per one km² of area. According to Moldoshev K.O. for the Chui valley, the natural water supply is 266 thousand m³. On average, 1 km² of the territory of the Chui Valley accounts for 266 thousand m³ of water per year. Across the republic, this figure is 258 thousand m³

of water per year per 1 km². The largest amount of water falls in the Issyk-Ata region, where 419 thousand m³ of water falls on 1 km² of area. The least prosperous region is the Moscow region, where the water resources of the river runoff is 143 thousand m³ of water per year per 1 km² [1].

Water supply in the Chui valley is 2.7 thousand m³/year. This figure is more than three times less than the figure for the republic. If we distribute the water resources of the river valley for each inhabitant, then the water supply in the Chui valley is 2.1 thousand m³ per inhabitant (as of January 1, 2020), which is approximately 3 times less than in the entire republic. In particular, the Chui Valley is characterized by a high amplitude of specific water supply. In the Kemin district, there are 21.6 thousand m³/year of water per inhabitant. For the Alamedin district and the city of Bishkek, the same figure is 0.5 thousand m³/year. This is due to the fact that there is a high population density. Lakes make up only 0.2% of the entire territory. The vast majority of lakes are located in the highlands. On the territory of the Chui Valley there are a large number of reservoirs of long-term and seasonal regulation, pools of ten-day and daily regulation, as well as ponds.

A complex irrigation system has been created in the Chui Valley. In this valley, where a dry and hot climate prevails, without irrigation, agriculture is not possible. A dense and rather extensive system of irrigation facilities has been created in the studied valley. In the 1930s, Boroldoi and the Krasnorechensk canals were built. Then the At-Bashy Canal, 60 km long, was built. In 1940, the Big Chui Canal was dug, 175 km long [2].

On the territory of Kyrgyzstan, including the Chui valley, the first stage of a large-scale land and water reform was carried out during 1926–1928. During these years, water management construction was launched on a large scale, private ownership of land and water was eliminated, the poor peasants were endowed with land and water. These activities contributed to the rapid restoration of the area of irrigated land. Already at the beginning of 1929, it reached 465 thousand hectares. The development of the textile, hemp-jute and sugar industries, as well as public animal husbandry, required a significant expansion of the areas of regularly irrigated lands, the reconstruction of existing irrigation systems, taking into account the placement of industrial crops and the peculiarities of the soil and climatic conditions of individual zones.

In 1927, the construction of the Krasnorechensk Canal was completed in the Chui Valley, with an irrigation area of 17,000 ha. The population took an active part in the construction of irrigation facilities.

Since 1929, the construction of new engineering irrigation systems began, such as the Krasnorechensk and Samsonovsk main canals, as well as the reconstruction of the irrigation systems of the Issyk-Ata, Kara-Balta, Shamsi and other river basins. These measures made it possible by 1930 to bring the area sparing of irrigated lands only in the Chu River basin up to 265 thousand hectares.

In 1940, the grandiose (for that time) project of the Orto-Tokoi reservoir and large Chui canals was completed, providing irrigation of lands on an area of 80 thousand hectares and increasing water supply by 43 thousand hectares. As a result of a large volume of water management works in 1940, the area of irrigated land in the republic reached 723 thousand hectares [3].

According to the Great Soviet Encyclopedia, the workers of the republic, inspired by the positive experience of high-speed construction, decided to build the Big Chui Canal (BCC) using the methods of folk construction [4]. It was envisaged that collective farms would take a share in the construction of the BCC in the amount of up to 50% of the cost of all work. On May 10, the division of the canal route into sections was completed (a total of 12 construction sites, on 10 of which worked Kyrgyz people, and 2 Kazakh people). Since that day, work has been in full swing along the 140-km route of the canal, which has turned into a true holiday of labor. On average, each worker fulfilled the norms by almost 160%. For 40 working days (from May 10 to June 23, 1941), the annual plan for the construction of the Great Chui Canal was completed by 39%. It was a national building, the building of the century. The current generation should follow the example of those courageous people, because they, one might say, dug the canal with their bare hands.

In the period 1941–1945. At-Bashy engineering system was built in the Chui valley, which gave the opportunity to irrigate more than 20 thousand hectares of new land.

During this period, the largest Orto-Tokoi reservoir in the republic with the Western and Eastern branches of the Big Chui Canal was put into permanent operation. Much attention is paid to the technical improvement of irrigation systems. So, if in 1955 there were 9 thousand hydrotechnical structures in the irrigated systems of the republic, then in 1964–1965. there were already 17 thousand of them. The length of canals with artificial anti-filtration clothing increased by more than 3 times.

Today, the Irrigation Facility of the Chui region is a large, complex water management complex of the republic with interstate water distribution. The main sources of irrigation are:

- the Chu river, regulated by the Orto-Tokoi reservoir;
- tributaries of the river. Chu, rr. Chon-Kemin, Shamsi, Issyk-Ata, Ala-Archa, Alamedin, Sokuluk, Ak-Suu, Kara-Balta, Chon-Kainda, Zharly-Kainda, Aspara.

According to the Ministry of Agriculture and Melioration of the Kyrgyz Republic [3], 321,119 hectares of irrigated agricultural land are concentrated in the Chui region. There is drainage on 102,068 ha, where 576.6 km of the inter-farm collector and drainage network are dispersed, of which 114.6 km (or 20%) is in poor condition, as well as 3450.9 km of on-farm CDS, of which 1292.2 km (or 36%) is also in poor condition, including 642.2 km of open and 650 km of closed networks.

BCC is a large irrigation canal, one of the large complexes of irrigation and irrigation canals in Kyrgyzstan, consisting of three branches: the Western BCC, the Eastern BCC and the Southern BCC. The Big Chui Canal crosses the capital of Kyrgyzstan Bishkek from east to west in its northern part. The route of the canal runs along the Chui valley from the foothill part of the Chu river, northeast of the village of Chym-Korgon, from east to west parallel to the Western Big Chui Canal. The mountain section of the Eastern BCC as the southern distribution channel reaches the Ala-Archa River. The head structure of the Eastern BCC is designed for water flow up to 350 m³/s. Built in 1958. The total length is 100 km, the irrigated area is 41.5 thousand hectares. The main practical focus is to provide water to cities, villages and adjacent territories. The water intake unit is telemechanized. BCC has several branches: [5].

- **Eastern Big Chui Canal (EBCC):** A major irrigation canal in Kyrgyzstan. Construction completed in 1958. The route of the canal runs along the Chui valley from the foothill part of the Chu river, northeast of the village of Chym-Korgon, from east to west parallel to the Western Big Chui Canal. The mountain section of the EBCC as the southern distribution channel reaches the Ala-Archa River. The head structure of the EBCC is designed for water flow up to 350 m³/s. The total length is 100 km, the irrigated area is 41.5 thousand hectares. It is designed to increase the water supply of the city and the territories adjacent to the city. The water intake unit is telemechanized.
- **Western Big Chui Canal (WBCC):** The largest irrigation canal in the country. It originates from the Chu River, about 40 km downstream of the water intake facility of the Eastern Big Chui Canal (about 8 km east of the Ivanovka village). Its route crosses the entire Chui valley from east to west, enters the territory of Kazakhstan. The total length of the canal is 145 km, the irrigation area is 82,000 ha. The normal water flow in the canal head is 43.0 m³/s, the forced flow is 55 m³/s. Construction started in 1940. A 70 km section of the canal, which allows irrigating 10 thousand hectares of land, was built during the Great Patriotic War (1943) using the folk construction method.
- **South Big Chui Canal (SBCC):** Construction started in 1976. It originates from the Issyk-Ata River (near the village of Yuryevka), passes along the southern outskirts of Bishkek, crossing the embankment of the Alamedin River, through the Orto-Sai forest area, the Southern forest area and, as expected, will reach the Merke region (Kazakhstan). The total length is 158 km, within the city—4.5 km. Designed for irrigation of 3000 ha of land. The water flow in the head of the canal is 90 m³/s, within the city—45 m³/s. The width within the city is 10.5 m, in the section between the 5th and 6th microdistricts from the embankment of the Alamedin River to Yunusaliev Avenue it expands to 20 m, the depth reaches 2 m.

In addition to surface waters within the Chui depression, the so-called “karasuch” tributaries flow into the Chu River, originating from sources that form at the end of alluvial cones and along the Chu River itself, starting east of the city of Tokmok. The largest of them is the Red River, which collects water from many springs and has a length of 50 km. The average annual water consumption is 2.5–3.5 m³ sec. On the right bank of the Chu River is the Chernaya River, which also has a main source of pound waters.

Below the exit line of pound waters, the Chui valley is indented by a network of dens that collect and carry “karasuch” waters. The course of such “karasuch” rivers is calm, the banks are swampy, ponds are created along the logs. Part of the water is disassembled for irrigation, a smaller part reaches the Chu River.

A significant part of groundwater is used in the national economy and, above all, in agriculture for irrigation.

The underground waters of the piedmont plume and most of the piedmont plain are of good drinking quality [6]. Below the karasuk zone, they are somewhat mineralized. In some places of the lower part of the depression, they sometimes cause soil salinization. But this does not reduce the great importance of the groundwater of the Chui depression for the water supply of settlements, primarily the city of Bishkek. The water supply of Bishkek is currently carried out at the expense of the ground waters of the Baityk depression, which are located at a considerable depth (up to 80–90 m). The underground

water reserves of the Ala-Archa and Alamudun alluvial fans can fully meet the needs of the city of Bishkek [7].

Through numerous discharges, longitudinal and transverse, in the Kyrgyz Range, deep waters come to the surface in the form of mineral-thermal springs that are used for medicinal purposes. Most of these sources are confined to the northern slopes of the ridge. The Kara-Balta terms in the upper reaches have a temperature of 20–28°. Alamudun springs emerge from granite cracks on the left bank of the Alamudun River south of the city of Bishkek; their temperature is 29.5–33°. Numerous springs of the Ysyk-Ata gorge with temperatures of 36–55 °C also come out of granites. They have a hydrotherapy resort. In the valley of the Kyzyl-Suu River there is a spring of the same name with a temperature of 20–23 °C, etc.

To regulate winter water flow, such large reservoirs as Orto-Tokoi, Nizhne-Ala-Archinskoe, Ala-Archinskoe, Sokulukskoe, Spartak and a number of smaller reservoirs and BDRs, 246 in total, were built.

The Orto-Tokoy reservoir is located on the Chu River, 2 km west of the village of Orto-Tokoi, on the border of the Naryn and Issyk-Kul regions. The plan for the construction of the reservoir was approved by a resolution of the Central Committee of the All-Union Communist Party of Bolsheviks and the Council of People's Commissars of the USSR of March 19, 1940. Construction began in 1941, completed in 1960. Height above sea level—1700 m. Water surface area—26 km², volume—470 million m³. Length—18 km, maximum width—5 km, maximum depth—47 m. Dam height—52 m, length—365 m, width—6 m. Spillway tunnel length—567 m, diameter—4.5 m. an average of 12.8 m³/s. Regulates the flow of the Chu River. The water of the reservoir is used for irrigation of 120 thousand hectares of agricultural land: 86 thousand hectares in Kyrgyzstan, 34 thousand hectares in Kazakhstan [8].

The Chu River in the Chuy district receives its left tributaries Shamschy and Kegeti. The Shamschy River originates from the glaciers of the northern slope of the Kyrgyz Range, at an absolute elevation of over 4000 m and is formed by the confluence of the Tuyuk River. In its upper stream, it flows through a narrow gorge and enters the Chui valley. The valley of the Shamschy River is divided by the Tuyuk and Kol-Tor spurs into three parts—the Tuyuk, At-Zhailoo and Kol-Tor basins. The total length of the Shamschy River is 58 km. The watershed area of the river is 457 km². The average annual water flow rate is 5.68 m³/sec. The maximum flow rate is 20.4 m³/sec, and the minimum flow rate is 1.13 m³/sec. The largest tributary is the Tuyuk River. Its length is 24 km, watershed area — 132 km². The Shamschy River forms a huge cone of outflow as it leaves the mountains and becomes low. At the watershed area, the river has a gradient of 0.035 and runs in a floodplain 26 m wide, in boulder and pebble deposits with an average diameter of 157 mm and a maximum diameter of 484 mm.

The Shamschy River carries about 61,000 m³ annually at the junction, of which 22,000 m³ of sediment and 39,000 m³ of suspended sediment. In winter, ice formation and pike processes take place on the river. The water intake unit is an improved mountain type of water intake unit with a curvilinear convex threshold. It was built on the Shamschy River in 1977. Water intake is carried out from the Shamschy River into the right bank Novyi canal up to 16 m³/s for irrigation of 9.9 thousand hectares.

As can be seen from Table 3, snow, glacial and groundwater take part in the feeding of the valley's rivers.

Chui district has a well-developed river network. The main water artery is the Chu River, which belongs to glacial- and snow-fed rivers characterized by two water level rises (Schultz 1964). The first spring rise is caused by snowmelt in the lower part of the watershed, and the second summer rise is a longer and more powerful water rise caused by the melting of eternal spurs and glaciers in the highlands [9–11].

The Chu River in the Chuy district receives its left tributaries Shamschy and Kegeti. The Shamschy River originates from the glaciers of the northern slope of the Kyrgyz Range, at an absolute elevation of over 4000 m and is formed by the confluence of the Tuyuk River. In its upper stream, it flows through a narrow gorge and enters the Chui valley. The valley of the Shamschy River is divided by the Tuyuk and Kol-Tor spurs into three parts—the Tuyuk, At-Zhailoo and Kol-Tor basins. The total length of the Shamschy River is 58 km. The watershed area of the river is 457 km². The average annual water flow rate is 5.68 m³/sec. The maximum flow rate is 20.4 m³/sec, and the minimum flow rate is 1.13 m³/sec. The largest tributary is the Tuyuk River. Its length is 24 km, watershed area – 132 km². The Shamschy River forms a huge cone of outflow as it leaves the mountains and becomes low. At the watershed area, the river has a gradient of 0.035 and runs in a floodplain 26 m wide, in boulder and pebble deposits with an average diameter of 157 mm and a maximum diameter of 484 mm.

The Shamschy River carries about 61,000 m³ annually at the junction, of which 22,000 m³ of sediment and 39,000 m³ of suspended sediment. In winter, ice formation and pike processes take place on the river.

The water intake unit is an improved mountain type of water intake unit with a curvilinear convex threshold.

Built on the Shamschy River in 1977, water intake is carried out from the Shamschy River into the right bank Novyi canal up to 16 m³/s for irrigation of 9.9 thousand hectares.

The Kegeti River originates from the glaciers of the Kyrgyz Range and enters the Chuy Valley. The upper stream of the river is narrow, the channel is rocky and porous. The length of the river to the site, and catchment area is 2900 m and area is 256 km². The river is fed by glacial and snow with groundwater recharge. The flood maximum is in July–August. During the period of mudflow floods more than 65 thousand m³ of loose clastic material can be carried down the river in some years. The average perennial discharge during the low-water period is 1.58–3.58 m³/s. The Kol-Tor River, a major tributary of the Kegeti River, originates from beneath the Anastasia Glacier. The length of the river is 17 km. The Kegeti River has a gradient of 0.026 at the watershed site and runs in a floodplain 80 m wide in pebble and boulder deposits. In winter, ice formation and pike processes take place on the river. The duration of all ice phenomena on the river averages 39 days. The water of the Kegeti River is used for irrigation.

The Burana River originates from the glaciers of the Kyrgyz Range, at an absolute height of over 4000 m above sea level. The total length of the river from the water intake site is 19.4 km, the area of the water intake basin is 61 km². The type of river feeding is glacial and snow with groundwater recharge. The flood maximum occurs in July–August and reaches more than 20 m³/s. Flood growth is characterized by rapid increase due to the intensity of snow and ice melting in the mountains and precipitation in the form of

rain. The average perennial discharge during the low-water period is 0.1–0.9 m³/s. At the water intake site, the river has a gradient of 0.039 and runs in a 30 m wide floodplain and boulder and pebble deposits with an average diameter of 176 mm and a maximum diameter of 530 mm. In winter, the river is subject to ice and pike formation. The water intake unit is located in the village of Kalinovka. Hydrological characteristics of the rivers are given in Tables 1, 2 and 3. Besides these rivers, the Eastern Big Chuy Canal is laid on the territory of the district. It was built in 1957 and laid in an earthen channel with a bottom slope varying within 0.00014–0.00035. The canal discharge capacity varies from 55 m³/s at the head to 8 m³/s at the end of the canal [3].

Table 1 Balance assessment of the water resources of the Chui valley in comparison with the nationwide data

No	Region	Area, thousand. km ²	Precipitation, km ³	Effluent, km ³			Evaporation, km ³	Gross moisture, km ³
				Full	Surface	Underground		
1	Chui valley	15.3	8.6	4	2.4	1.7	4.5	6.2
2	Across Kyrgyzstan	198.5	104	51.2	30.9	20.3	52.8	73.1

Table 2 Reservoirs in the Chu River basin used for irrigation

Reservoir	Year of putting into operation	Mirror area at NPG, km ²	Design volume of water, million m ³	Dam height, m	Irrigated area
Orto-Tokoi	1956	25.0	470.0	52	100
Nijnyaya-Ala-Archa	1966	5.21	39.0	22	20
Sokuluk	1968	1.77	13.0	28	4

Table 3 Feeding source of the rivers of the Chuy valley

River–point	Area km ²	Proportion of feeding sources row				In % of total	
		Snow		Glacial		Underground	
		mm	%	mm	%	mm	%
Shamshy	317	171	25	209	33	253	43
Kegeti-forest cordon	256	75	27	87	31	118	42

Source Bakirov N.B., Chuy valley, Bishkek, 1994

The length of the canal reaches 97.3 km, with a huge area of 41.5 thousand hectares suspended from it. On its way the canal route overlaps a number of mountain rivers: Burana, Kegeti, Shamshy. In its large part the canal runs in an earthen bed, except for

the Kegeti site, where it is represented by three strings of parallel fast-flowing streams paved with cobblestone for 6 km. Lakes.

A large lake of rubble origin Koltor Kegetinsky lies at an altitude of 2733.6 m. Its length is 0.7 km, width—0.5 km, and area—0.2 km². The dam of the lake is a huge moraine and rockfall formation. Lake water is filtered through the dam body, coming out at its foot in the form of a powerful spring. A deep gully has been formed at the outflow of spring water, which clearly has a tendency to further cut into the dam body. In addition, there is evidence that, especially in wet years, the lake has surface runoff (as was the case in 1979). Both of these circumstances make a catastrophic breach of Kol-Tor Lake possible. In the continental arid climate of the Chuy region, rivers are used for irrigated agriculture and cheap electricity. The summer extended floods provide water for numerous irrigation systems.

Water in the Chui Valley is accumulated in various forms: in the form of eternal snows and glaciers of high mountains, groundwater, springs, rivers, lakes, swamps, as well as artificially in reservoirs, ponds and canals. All of them are of great importance in life and economic activity of the population.

All rivers in the region belong to the basin of the Chu River, which belongs to the number of large rivers in Central Asia. It is the second in terms of valley and high water content in the Kyrgyz Republic. The area of the basin is about 50 thousand km, and the length of the river is 50 km. The sources of the Chu River are located on the southern slopes of the western part of Teskei Ala-Too, in the west its waters are lost in the desert at the western edge of Betpak-Dala [2].

The Chu River is formed by the confluence of Kochkork and Dzhoon-Aryk. From the Kochkor Basin, the Chu River flows northeastward to Issyk-Kul Lake, crossing the Orto-Tokoi Basin along the way. The Chu receives its second right tributary Kichi Kemin, 80 km long, at the exit from the Boom Gorge. The Chu River also receives the so-called “karasuchny” tributaries, which originate from springs that form at the end of the cones of removal and along the Chu itself, starting from Tokmok. The turbidity of the Chu River increases downstream. The average annual turbidity at Kochkorka village is 101 g/m in Kazakhstan (Furmanovo village)—659 g/m. The highest turbidity occurs in May–June. The average annual flow of the Chu River is 20–40 m³/C. Various river networks cut through mountain ranges and form the Chu River basin. Consequently, not all products of rock destruction remain on the territory of Chuy Region, often they are transported beyond its boundaries. First of all, the most mobile compounds of elements are alkalinized and carried away: Ca, Mg, Mn, NaCl, Na₂CO₃, KCl, and others.

High mountain ranges are powerful condensers of moisture. Here, from year to year, snowfields are accumulated, and glaciers are formed. As a result of high solar radiation, glaciers and snowfields are subjected to melting, and summer rains make this area a source of surface water.

3 Conclusions

Chui valley is the main granary of the republic. Its area is 3.5 million hectares. The vast majority of this territory—2.2 million hectares, suitable for the development of irrigated agriculture, is located in Kazakhstan and 610 thousand hectares—in Kyrgyzstan. About

30% of the total area of regularly irrigated lands of the republic is located in the Chui valley. In 1973, it amounted to 268 thousand hectares against 109.3 thousand hectares.

An extensive network of irrigation facilities has been created in the Chui Valley. Initially, the Boroldoi and Krasnorechensk main canals were created then 18 km from Bishkek, the At-Bashy Canal was built.

Today, the Irrigation Facility of the Chui region is a large, complex water management complex of the republic with interstate water distribution. The main sources of irrigation are:

- the Chu river, regulated by the Orto-Tokoi reservoir;
- tributaries of the river. Chu, rr. Chon-Kemin, Shamsi, Issyk-Ata, Ala-Archa, Alamedin, Sokuluk, Ak-Suu, Kara-Balta, Chon-Kainda, Zharly-Kainda, Aspara.

References

1. Moldoshev KO, Shakhin S (2017) Water availability of the Chui valley in Kyrgyzstan. *Hydrometeorol Ecol, Almaty* 3(86):100–104
2. Bolshakov MN (1974) Water resources of the rivers of the Soviet Tien Shan and methods for their calculation. *Ilim, Frunze*, p 306
3. Materials of the department of water resources and land reclamation of the ministry of agriculture (2010) Bishkek
4. Great Soviet Encyclopedia (1970) Soviet encyclopedia. Moscow, p 547
5. Bolshakov MN (1974) Water resources of the rivers of the Soviet Tien Shan and methods for their calculation. *Ilim, Frunze*, p 26
6. Hydrogeology of the USSR. v.XI. Kirghiz SSR (1971) Nedra, Moscow, p 487
7. Mamatkanov DM, Bazhanova LV, Romanovsky VV (2006) Water resources of Kyrgyzstan at the present stage. *Ilim, Bishkek*, p 60
8. Usubaliev RA, Moldoshev KO, Bredikhin NV (2017) The development of glaciation in the conditions of modern climate change. *Proc Univ Kyrgyzstan* 8:43–45
9. Moldoshev KO (2009) Scientific and methodological foundations of economic and geographical studies of water resources. *Kishovarz, Dushanbe* 2:41–42
10. Materials of the JV. Chui ecological laboratory (2005)
11. Dikikh AN (2001) Problems and forecast of the development of glaciation and water content of the rivers of Central Asia. *Compilation: water and sustainable development of Central Asia, Bishkek*, pp 75–86

**Engineering Structure Safety,
Environmental Engineering
and Environmental Protection**



Reagent Treatment of Domestic Wastewater in Arctic Settlements from Ammonium Ions

A. M. Fugaeva^(✉) and E. I. Vialkova

Industrial University of Tyumen, 38, Volodarskogo Street, Tyumen 625000, Russia
nastyafugaeva@mail.ru

Abstract. The problem of treatment and disposal of domestic wastewater is very relevant for remote small settlements in the Arctic. Biological purification, as a traditional method, is problematic in conditions of low temperatures and high flow irregularity of wastewater. The organic substances characterized by BOD, COD and nitrogen compounds, which can be harmful when poorly treated wastewater is discharged into water bodies, are particularly difficult to extract from the water. In the conditions of the deteriorating environmental situation around the world, effective methods of wastewater treatment are being sought. This study examines the method of physical and chemical treatment of domestic wastewater from the small Arctic settlements. The experiment is carried out according to the standard laboratory research methods. For the study, real wastewater from the septic tanks was taken. These water samples were similar in composition to wastewater from the remote northern settlements. Particular attention is paid to the purification of water from ammonium ions at a temperature of 5 °C. It turned out that it was possible. It is possible to reduce the concentration of ammonium ion by 96% by using the chemical precipitation method in combination with preliminary coagulation, oxidation and filtration. In addition, the effectiveness of physical and chemical treatment does not depend much on the temperature of incoming wastewater.

Keywords: Arctic settlements · Domestic wastewater · Ammonium ions · Reagent treatment

1 Introduction and Review

The Arctic zone of Russia is quite large and covers 9 regions, while the area of the Arctic territories is 4.8 million km² ($\approx 28\%$ of the country's territory). About three million people live here, which is more than half of the world population of the Arctic. Currently, in the process of rapid climate change and intensive anthropogenic activity in the northern regions, permafrost melting, soil degradation, deterioration of water quality in the rivers, lakes and the coastal zone are observed. Therefore, the following tasks are primarily considered to mitigate the negative effects of natural and human factors: adaptation of the population and sustainability of regional development; preservation and restoration of the environment; rational use of the natural resources; maintaining

the health of the Arctic ecosystems. The development of the infrastructure of the small northern settlements is included in the Strategic Development Program of the Russian Arctic. At the same time, much attention is paid to the protection of the natural tundra clusters and the preservation of the northern water bodies, especially those that belong to the highest fishing category and are included in the zone of the main economic activity of the local population. The problem urgency of the wastewater proper management is growing with the increasing degree of improvement of the Arctic settlements around the world.

The content of ammonium ions in the natural waters varies in the range from 0.01 to 0.2 mg/L. The presence of ammonium ions in the uncontaminated natural water bodies is mainly due to the processes of biochemical degradation of the protein substances, deamination of amino acids, decomposition of urea under the action of the enzymes. The main sources of ammonium ions entering the water bodies are livestock farms, household wastewater, surface runoff from farmland in the case of the ammonium fertilizers, as well as wastewater from the food, coke, forestry and chemical industries. The effluents of the industrial enterprises contain up to 1 mg/L of ammonium; in the municipal effluents is 2–7 mg/L; up to 10 g of ammonium nitrogen per inhabitant enters the sewage systems daily with household wastewater [1, 2]. In wastewater from the private residential storage tanks, the concentration of ammonium nitrogen can reach 70–200 mg/L, that is associated with a low water consumption rate [3, 4]. The maximum permissible concentration of ammonium ions in the water of reservoirs of household drinking and cultural water use is set at 2–0.5 mg/L, depending on the category of the system (GN 2 0.1.5.1315–03 RU). The toxicity of ammonium increases with an increase in the pH of the medium. The increased concentration of ammonium ions can be used as an indicator reflecting the deterioration of the sanitary condition of a water body. In this case, the process of contamination of surface and groundwater, primarily by household and agricultural effluents, has had a place [5].

One of the most promising chemical methods of wastewater treatment from ammonium ions is the precipitation of ammonium in the form of insoluble ammonium magnesium phosphate hexahydrate (AMP), or struvite ($\text{NH}_4\text{MgPO}_4 \cdot 6\text{H}_2\text{O}$). This method provides a high degree of purification and allows the secondary use of ammonia, since struvite is a valuable product and can be used as a fertilizer [6–8]. To study the wastewater treatment process, the authors analyzed the precipitation of AMP with the sodium hydrophosphate, sodium hydroxide and magnesium chloride. It turned out that the maximum degree of wastewater treatment from ammonium ions is achieved at $\text{pH} = 8.5\text{--}10$ and a slight increase of the amount of sludge (by 5%). And also, the optimal mode of AMR precipitation is a direct instantaneous supply of reagents, while first Na_2HPO_4 and NaOH solutions are added to the wastewater, and then MgCl_2 solution is added there. In addition, it was found [9] that AMR is mainly formed during precipitation at a ratio of the ion concentrations in wastewater $[\text{Ca}^{2+}]: [\text{Mg}^{2+}] = 0.25:1$ and lower.

According to research [7, 9], in the small northern settlements, the temperatures of wastewater entering the Wastewater Treatment Plant (WWTP) during the longest cold period do not exceed 12–13 °C. On average, for small wastewater treatment stations, it is only 6–7 °C. The water temperature in the small septic tanks reaches only 2–4 °C in winter. This is due to the uneven formation of a small amount of effluent and their long

accumulation in the receiving tanks of the pumping stations and averages. In addition, wastewater is characterized by high values of the suspended solids, BOD, COD and ammonium ions. All these factors affect the low efficiency of biological WWTP, which does not exceed 70% [7].

Taking into account the specific northern conditions and the requirements of regulatory documents (SP 32.13330.2018 RU), in such areas it is possible to replace the biological purification stage with chemical or physical–chemical treatment stages at the WWTP. According to [10], it is preferable to arrange physical–chemical treatment plants (PCTP) for small settlements characterized by a large uneven of the wastewater inlet, low temperature and pollutant concentration. In this case, the structures will work more stably, regardless of the wastewater flow schedule, temperature differences and changes in external conditions.

Over the past few decades, Russia has accumulated quite a lot of experience in the introduction of the PCTPs [11–13], the main stages of which are reagent treatment (coagulation, oxidation) and filtration. The main problem that is not solved by the proposed schemes is the removal of ammonium ions and the reduction of COD to the established norms. There are also methods of solving these problems in foreign practice. In Greenland and Denmark, the preliminary coagulation with polyaluminum chloride allowed to reduce suspended solids by 73%, phosphates by 28% [14, 15]. In the State of Alaska (USA), it is proposed to introduce a technological scheme that includes physical–chemical oxidation in the presence of hydrogen peroxide, which reduces COD to 0.7 mg/L [16].

An example of using a chemical method is the nitrogen oxidation with the reagents containing active chlorine. Active chlorine oxidizes ammonium compounds, ammonia and organic substances containing amino groups to mono- and dichloramines, as well as to nitrogen trichloride in wastewater. The article [17] describes a method for the oxidation of ammonium ions with sodium hypochlorite to determine the optimal conditions for its conduct in the absence and presence of organic compounds. In the conducted series of experiments, the maximum degree of ammonium ion removal was 98% in the organic compounds' absence; at a reagent dose of 200 to 220 mg/L, the decrease in ammonium occurred from 2.5 to 0.5 mg/L.

In Spain, optimization of the coagulation and flocculation processes at the urban WWTPs led to the use of 25 mg/L of ferric chloride (FeCl_3) in combination with 25 mg/L of a flocculant consisting of silicon (SiO_2 3%), aluminum (Al_2SO_4 64.5%) and iron salts (Fe_2O_3 32.5%) in 1 min of rapid mixing process at 200 rpm and slow mixing for 30 min at 30 rpm, followed by a final 30-min settling process. Numerical and statistical results of process optimization achieved 91.5%, 59.1% and 95.2% efficiency of removal of turbidity, COD and suspended solids, respectively. These performance indicators theoretically support an improved coagulation/flocculation process as a pretreatment for a higher recovery rate of NH_4^+ [18].

The authors of the article [19] propose a treatment scheme that includes primary deposition, which leads to the production of an upper super-settling liquid and a lower solid precipitate. The contaminated liquid phase is treated by electrochemical purification, which effectively allows to obtain non-drinking water suitable for use in agriculture and reuse in the toilets. The lower solid residue undergoes biohumus formation, or microwave

irradiation, or biogasification, or phytoremediation. In addition, these methods provide satisfactory removal of BOD (>85%), COD (81–91%) and pathogenic microorganisms, as well as decomposition of the heavy metals and micro-pollutants. These methods are not specific to any region and can be used all over the world in certain places in the absence of centralized WWTPs.

Recently, the intensive oxidation (AOP) technologies have been gaining popularity abroad, which effectively remove the pollutants from wastewater, as well as disinfect, which makes it possible to discharge wastewater in accordance with current legislation [20]. The AOPs method consists of ultraviolet irradiation using hydrogen peroxide as an oxidizer.

This article discusses the method of wastewater reagent treatment based on coagulation, sedimentation, chemical oxidation, filtration and chemical precipitation of ammonium ions. At the same time, in order to get as close as possible to the real conditions of water purification in the northern settlements, the studies were carried out in two temperature regimes—for warm and cold water.

2 Description of Studies

An experiment on the physical–chemical treatment of household wastewater in the laboratory of the Department of Engineering Systems and Structures (Tyumen Industrial University, Russia) was conducted.

The purpose of the study was to develop a technological scheme of a physical–chemical treatment plant (PCTP) for Arctic settlements. This scheme was supposed to provide the reagent treatment of domestic wastewater from ammonium ions and other organic substances.

The object of the study is household wastewater taken from septic tanks of the areas with low–rise buildings, whose composition similar to the wastewater of the small northern settlements. The subject of the study is the physical and chemical methods of household wastewater treatment.

The following order of technological processes of domestic wastewater treatment was subject to research: preliminary aeration (compressed air treatment for 20 min); coagulation (addition of aluminum-based coagulant “Aqua-Aurat–30” or AA); flocculation (addition of polyacrylamide or PAA); sedimentation of suspended solids; chemical oxidation of organic substances (by potassium permanganate or KMnO_4); filtration through quartz sand layer (granule size from 0.5 to 1.7 mm); chemical precipitation of ammonium ions (addition of sodium hydrophosphate solution Na_2HPO_4 , magnesium chloride solution MgCl_2 at pH = 9–10); filtration through a layer of granular activated carbon (granule size from 1 to 3 mm). During the work, the wastewater temperature was modeled in the normal ($T = 18\text{--}22\text{ }^\circ\text{C}$) and extreme ($T = 3\text{--}7\text{ }^\circ\text{C}$) conditions. Table 1 shows a detailed plan of the experiment.

The peculiarity of the experiment: the study was conducted for three weeks; the samples of Initial wastewater from the septic were taken every week, so there were some differences in the indicators of the initial wastewater. The effectiveness of a particular purification stage was evaluated by the following control indicators: pH, suspended solids, COD, turbidity, chromaticity, various cations and anions. All indicators in the

samples were measured according to the standard methods; at least three measurements were carried out, followed by the determination of error, which generally do not exceed 10%. The indicators were measured using instruments: pH meter "pH 150MI"; spectrophotometer "PE 5400VI"; liquid analyzer "Fluorate-0.2 M"; capillary electrophoresis system "Drops 105M".

During the deposition of suspended solids and reaction products, a visible precipitate was formed, the volumes of which were also measured. The results of the first stage, when

Table 1 Experiment design

Process name	Code	Wastewater treatment technology
<i>1. Coagulation of wastewater</i>		
Coagulation + Flocculation + Precipitation at $T = 18-22\text{ }^{\circ}\text{C}$	A	The wastewater samples should have a temperature of $T = 20\text{ }^{\circ}\text{C} \pm 2$. A coagulant AA (with a dose of 70 mg/L) and a flocculant PAA (with a dose of 1 mg/L) are added, which are mixed quickly for 1 min at a rate of 2–3 rpm. Then the mixing rate is reduced to 0.5 rpm and the sample is slowly mixed for another 20 min. Next, the mixture is sedimented for 60 min
Coagulation + Flocculation + Precipitation at $T = 3-7\text{ }^{\circ}\text{C}$	B	The wastewater samples should be cooled to temperature of $T = 4\text{ }^{\circ}\text{C} \pm 1$. The coagulant AA (with a dose of 70 mg/L) and flocculant PAA (with a dose of 1 mg/L) are added, which are mixed with water quickly for 1 min and mixed slowly for 20 min; then the mixture is sedimented for 60 min
Pre-aeration + Coagulation + Flocculation + Precipitation at $T = 18-22\text{ }^{\circ}\text{C}$	C	The wastewater samples should have a temperature of $T = 20\text{ }^{\circ}\text{C} \pm 2$. The water is aerated for 20 min with compressed air. The coagulant AA (with a dose of 70 mg/L) and flocculant PAA (with a dose of 1 mg/L) are added, which are mixed with water quickly for 1 min and mixed slowly for 20 min; than the mixture is sedimented for 60 min
Pre-aeration + Coagulation + Flocculation + Precipitation at $T = 3-7\text{ }^{\circ}\text{C}$	D	The wastewater samples should be cooled to temperature of $T = 4\text{ }^{\circ}\text{C} \pm 1$, then it is aerated for 20 min with compressed air. The coagulant AA (with a dose of 70 mg/L) and flocculant PAA (with a dose of 1 mg/L) are added, which are mixed quickly for 1 min and mixed slowly for 20 min; than the mixture is sedimented for 60 min

(continued)

Table 1 (continued)

Process name	Code	Wastewater treatment technology
Oxidation + Pre-aeration + Coagulation + Flocculation + Precipitation at T = 18–22 °C	E	The wastewater samples should have a temperature of $T = 20\text{ °C} \pm 2$. An oxidizer solution KMnO_4 with a dose of 10 mg/L is added to the wastewater samples. The mixture of water and oxidizer is aerated for 20 min with compressed air. The coagulant AA (with a dose of 70 mg/L) and flocculant PAA (with a dose of 1 mg/L) are added, which are mixed with water quickly for 1 min and mixed slowly for 20 min; than the mixture is sedimented for 60 min
Oxidation + Pre-aeration + Coagulation + Flocculation + Precipitation at T = 3–7 °C	F	The wastewater samples should be cooled to temperature of $T = 4\text{ °C} \pm 1$. The oxidizer solution KMnO_4 with a dose of 10 mg/L is added to the wastewater samples. The mixture of water and oxidizer is aerated for 20 min with compressed air. The coagulant AA (with a dose of 70 mg/L) and flocculant PAA (with a dose of 1 mg/L) are added, which are mixed with water quickly for 1 min and mixed slowly for 20 min; than the mixture is sedimented for 60 min

Based on the results of the control indicators measurement, the best version of the wastewater treatment technology is selected

It should be compared the water cleaning efficiency under normal and extreme temperature conditions

2. Chemical oxidation of wastewater

Chemical oxidation + Mechanical filtration through sand at T = 18–22 °C	G	Pre-purified water in the coagulation process should have a temperature of $T = 20\text{ °C} \pm 2$. The oxidizer solution KMnO_4 with a dose of 10 mg/L is added to the wastewater samples. The sample is mixed quickly for one minute and slowly for 20 min. The mixture is filtered through a pre-washed layer of sand (speed $\approx 1\text{--}2$ drops in second, $h = 10\text{ cm}$)
---	---	--

(continued)

only wastewater coagulation under various conditions was carried out, are presented in Table 2.

Table 1 (continued)

Process name	Code	Wastewater treatment technology
Chemical oxidation + Mechanical filtration through sand at $T = 3-7\text{ }^{\circ}\text{C}$	H	Pre-purified water in the coagulation process should have a temperature of $T = 5\text{ }^{\circ}\text{C} \pm 1$. The oxidizer solution KMnO_4 with a dose of 10 mg/L is added to the wastewater samples. The sample is mixed quickly and slowly, then the mixture is filtered through a pre-washed layer of sand
Chemical oxidation + Air bubbling + Mechanical filtration through sand at $T = 18-22\text{ }^{\circ}\text{C}$	I	Pre-purified water in the coagulation process should have a temperature of $T = 20\text{ }^{\circ}\text{C} \pm 2$. The oxidizer solution KMnO_4 with a dose of 10 mg/L is added to the wastewater samples. The mixture of water and oxidizer is bubbled with compressed air for 20 min, then it is filtered through a pre-washed layer of sand
Chemical oxidation + Air bubbling + Mechanical filtration through sand at $T = 3-7\text{ }^{\circ}\text{C}$	J	Pre-purified water in the coagulation process should have a temperature of $T = 5\text{ }^{\circ}\text{C} \pm 1$. The oxidizer solution KMnO_4 with a dose of 10 mg/L is added to the wastewater samples. The mixture of water and oxidizer is bubbled with compressed air for 20 min, then it is filtered through a pre-washed layer of sand

Based on the results of the control indicators measurement, the best version of the wastewater treatment technology is selected

It should be compared the water cleaning efficiency under normal and extreme temperature conditions

3. Chemical ammonium precipitation

Chemical ammonium precipitation + Sorption filtration through coal at $T = 18-22\text{ }^{\circ}\text{C}$	K	Pre-purified water (after coagulation and oxidation) should have a temperature of $T = 20\text{ }^{\circ}\text{C} \pm 2$. Sodium hydrogen phosphate Na_2HPO_4 and magnesium chloride MgCl_2 are injected. The resulting sample is stirred for 1 min, then alkalinized with a 10% solution NaOH to $\text{pH} = 9$. Then it is mixed for 5 min and sedimented for 60 min. Next, the sample filtered through a layer (10 cm) of pre-washed activated carbon (speed $\approx 0.5-1$ drop in second)
---	---	--

(continued)

Table 1 (continued)

Process name	Code	Wastewater treatment technology
Chemical ammonium precipitation + Sorption filtration through coal at T = 3–7 °C	L	Pre-purified water (after coagulation and oxidation) should have a temperature of T = 6 °C ± 1. Sodium hydrogen phosphate Na ₂ HPO ₄ and magnesium chloride MgCl ₂ are injected. The resulting sample is stirred for 1 min, then alkalized with a 10% solution NaOH to pH = 9. Then it is mixed for 5 min and sedimented for 60 min. Next, the sample filtered through a layer (10 cm) of pre-washed activated carbon (speed ≈ 0.5–1 drop in second)
Chemical ammonium precipitation + Sorption filtration through coal + second coagulation at T = 18–22 °C	M	Pre-purified water (after coagulation and oxidation) should have a temperature of T = 20 °C ± 2. Sodium hydrogen phosphate Na ₂ HPO ₄ and magnesium chloride MgCl ₂ are injected. The resulting sample is stirred for 1 min, then alkalized with a 10% solution NaOH to pH = 9. Then it is mixed for 1 min and added coagulant AA with dose 30 mg/L. The mixture is mixed quickly for 1 min and mixed slowly for 20 min; then it is sedimented for 60 min. Next, the sample filtered through a layer (10 cm) of pre-washed activated carbon (speed ≈ 0.5–1 drop in second)
Chemical ammonium precipitation + Sorption filtration through coal + second coagulation at T = 3–7 °C	N	Pre-purified water (after coagulation and oxidation) should have a temperature of T = 6 °C ± 1. Sodium hydrogen phosphate Na ₂ HPO ₄ and magnesium chloride MgCl ₂ are injected. The resulting sample is stirred for 1 min, then alkalized with a 10% solution NaOH to pH = 9. Then it is mixed for 1 min and added coagulant AA with dose 30 mg/L. The mixture is mixed quickly for 1 min and mixed slowly for 20 min; then it is sedimented for 60 min. Next, the sample filtered through a activated carbon

Based on the results of the control indicators measurement, the best version of the wastewater treatment technology is selected

It should be compared the water cleaning efficiency under normal and extreme temperature conditions

Table 2 Results of the first experiment stage (Coagulation of wastewater)

Water quality index	Initial wastewater	Process code					
		A	B	C	D	E	F
pH	7.14	6.79	6.87	7.30	7.26	7.42	7.29
Suspended solids, mg/L	440	315	270	255	230	269	261
COD, mg/L	490	350	300	284	256	300	290
Ammonium, mg/L	82.45	28.95	48.44	88.22	61.34	84.74	86.19
Nitrites, mg/L	0.28	0.1<	0.1<	0.18	0.25	0.30	0.33
Nitrates, mg/L	1.42	1.37	5.96	2.51	1.22	3.06	2.89
Phosphates, mg/L	19.42	1.7	1.11	4.48	0.98	4.4	2.2
Chlorides, mg/L	100.5	171.3	170.8	171.9	178.7	166.2	171.3
Sulphates, mg/L	19.35	13.2	13.26	14.28	18.37	15.85	16.87
Sludge volume, L	–	0.025	0.029	0.031	0.032	0.029	0.030

The best result in reducing the concentration of ammonium ions was achieved with the following sequence of processes: pre-aeration—coagulation and flocculation—settling. It turned out that the decrease in temperature negatively affected the efficiency of purification, this is especially evident in relation to the ammonium ion: with a decrease in temperature, the residual concentration increased by almost two times.

The second stage of the experiment investigated the chemical oxidation of water purified during coagulation. Oxidation was carried out with a solution of potassium permanganate (KMnO_4) 10 mg/L; the effluents were quickly mixed for 1 min and kept with bubbling air for 20 min or without air-bubbling, then filtered through a layer of washed quartz sand. The results of the second stage are presented in Table 3.

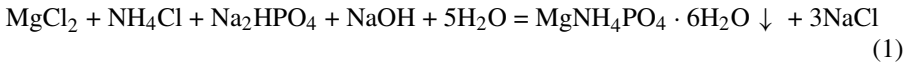
Table 3 Results of the second experiment stage (Chemical oxidation of wastewater)

Water quality index	Water quality		Process code					
	After A	After B	C	D	G	H	I	J
pH	7.05	7.15	6.88	6.86	7.27	7.32	7.98	7.71
Suspended solids, mg/L	160	300	104	172	59	109	51	82
COD, mg/L	390	452	250	259	141	164	126	123
Ammonium, mg/L	29.4	28.6	35.6	36.4	19	21	18.2	17.2
Turbidity mg/L	89.78	78.42	4.47	7.71	2.44	2.2	1.57	2.32
Chromaticity, degrees	360.78	350.76	54.5	62.98	45.65	41.71	31.61	35.27

The variant with chemical oxidation during bubbling of water with compressed air (processes I and J) gave a more effective reduction of the such indicators as suspended

solids, COD, chromaticity, turbidity and concentration of ammonium ions. This was due to an increase in the activity of the reagent oxidants with additional oxygen saturation of the water and confirmed previously published data [21, 22]. To further experiment, the wastewater samples after preliminary coagulation and chemical oxidation during air-bubbling were used.

The third stage considered the chemical precipitation of ammonium ions by adding phosphate ions and magnesium ions to the water, followed by precipitation of magnesium-ammonium-phosphate in an alkaline medium by the following mechanism (1) [6]:



Considering that for the production of magnesium-ammonium phosphate $\text{MgNH}_4\text{PO}_4 \times 6\text{H}_2\text{O}$ reagents were supplied in a molar ratio $\text{Mg}:\text{NH}_4:\text{PO}_4 = 1:1:1$, the number of reagents (per 1 L of wastewater) (2–3) was calculated:

$$\frac{m_{\text{ammonium chloride}}}{M_{\text{ammonium chloride}}} = \frac{X}{M_{\text{magnesium chloride}}} \Rightarrow \frac{0.191}{53} = \frac{X}{95} \Rightarrow X = 0.342\text{g} \quad (2)$$

$$\frac{m_{\text{ammonium chloride}}}{M_{\text{ammonium chloride}}} = \frac{X}{M_{\text{sodium hydrophosphate}}} \Rightarrow \frac{0.191}{53} = \frac{X}{142} \Rightarrow X = 0.512\text{g} \quad (3)$$

To intensify precipitation, the alkalization with a 10% NaOH alkali solution was performed. After stirring for 1 min and settling for 60 min, the effluents were filtered through a layer of granular activated carbon. Figure 1 shows how the intensity of precipitation of the magnesium ammonium phosphate varied depending on the temperature and the addition of coagulant: The first two laboratory glasses (look from left to right) were filled with warm water; the next glasses were filled with cold water; the coagulant was added into only two glasses: 2 and 4. In the water samples where the coagulant was added, the sediment volumes were approximately 20% larger. Figure 1 shows that the precipitate had a creamy color characteristic of struvite. The results of the third stage are presented in Table 4.

Secondary coagulation increased the effect of ammonium precipitation, but at the same time enlarged the content of COD and chromaticity. At the next stage of the work, it is planned to more carefully select the coagulants for secondary water treatment and to control the additional indicators associated with secondary water pollution as a result of the reagents' use. A comparison of the effects of water purification depending on temperature conditions was made: for cold ($T = 3\text{--}7^\circ\text{C}$) and warm ($T = 18\text{--}22^\circ\text{C}$) water. The results show that at the slightly different concentrations in the initial water samples, the all concentrations at the outlet were approximately equal. Changes in water temperature under normal and extreme conditions had little effect on the final result. The concentration of suspended solids in water decreased by 98%. After mechanical filtration (stages I and J), the proposed scheme was equally effective regardless of the discrepancy in the quality of the initial water samples. In a practical implementation, this can only affect the service life of the filter loading and the number of the load wash cycles.



Fig. 1 Chemical ammonium precipitation

The COD concentrations were reduced by more than 10 times, while the overall removal efficiency of chemically oxidized organic substances was 91%. After coagulation and precipitation (stages A and B), the water samples became approximately the same in quality, regardless of discrepancies in the indicators at the inlet. This suggests that the proposed coagulation and flocculation scheme is very effective for a significant deviation of the COD concentration (700 ± 250 mg/L) from the average value, which is usually observed when domestic wastewater enters. A certain increase in COD (by 10–20 mg/L) after secondary coagulation (purification stages M and N) was obviously associated with the entry of organic molecules of PAA flocculant into the water. Experimental data showed that additional coagulation after chemical precipitation of ammonium ions introduces secondary contamination into the water. Based on this, it was decided to abandon the M and N stages in the future.

Figure 2 shows the graphs of changes in the content of ammonium ions after each stage of purification. The total effect achieved for ammonium ions was 96%. The growth of ammonium at the purification stages A, B, I and J was associated with an effect on the measurement of this indicator of other types of pollutants contained in real wastewater samples. It was obvious that the main removal of ammonium ions occurs at the stage of chemical precipitation (R and L).

The general scheme of water purification processes used in laboratory modeling, which will serve as the basis for the development of the PCTP-technological scheme in the future, is shown in Fig. 3. The sequence of processes is as follows: Pre-aeration → Coagulation, Flocculation → Precipitation → Oxidation → Mechanical filtration (through sand) → Ammonium precipitation → Sorption filtration (through activated carbon).

In the practical implementation of this scheme, it is necessary to add the disinfection and pH stabilization at the end. The facilities for collecting, processing and utilization of sludge are also needed. At the same time, the sediments at different stages of purification have different composition and properties: the sludge after coagulation is a waste and is

Table 4 Results of the third experiment stage (Chemical ammonium precipitation)

Water quality index	Warm water T = 18–22 °C (Normal conditions)					Cold water T = 3–6 °C (Extreme conditions)				
	Initial water	Process code				Initial water	Process code			
		A	I	R	M		B	J	L	N
Suspended solids, mg/L	190	70	16	5	2	160	30	17	4	3
COD, mg/L	850	445	395	57.4	77.5	956	435	391	75.5	86.3
Turbidity mg/L	94.02	25.87	2.73	1.74	0	92.22	8.47	3.19	0.93	0
Chromaticity, degrees	370.66	170.37	50.86	11.24	0.75	372.79	83.99	56.01	7.87	2.32
pH	6.78	6.92	7.95	9.05	9.13	7.01	6.83	7.77	9	9.25
Ammonium, mg/L	58	64.2	60.1	5.48	2.36	63.27	66.15	70.32	2.7	2.2
Potassium, mg/L	15.04	14.96	16	9.68	6.86	14.81	15.17	18.64	5.59	8.02
Manganese, mg/L	0.35	–	–	0.03	0.03	0.4	–	–	0.03	0.02
Magnesium, mg/L	16.41	16.1	–	492.5	679.6	16.49	16.52	–	773.3	640.7
Sodium, mg/L	55.15	54.81	–	359.3	717.6	56.37	56.73	–	595.6	840.7
Chlorides, mg/L	87.86	–	–	2173	3735	88.49	–	–	3766	3918
Sulphates, mg/L	19.69	–	–	160.1	117.36	29.6	–	–	139	94.72
Phosphates, mg/L	20.05	–	–	0.88	0.25	17.87	–	–	0.25	0.25
Nitrites, mg/L	0.2	–	–	0.2	0.2	0.2	–	–	0.2	0.2
Nitrates, mg/L	1.1	–	–	0.48	0.82	1	–	–	0.96	0.87

subject to additional special treatment; the sludge after chemical precipitation of ammonium is a ready-made fertilizer for agricultural needs. The total volume of dewatered sludge will be no more than 0.5% of the capacity of the PCTP.

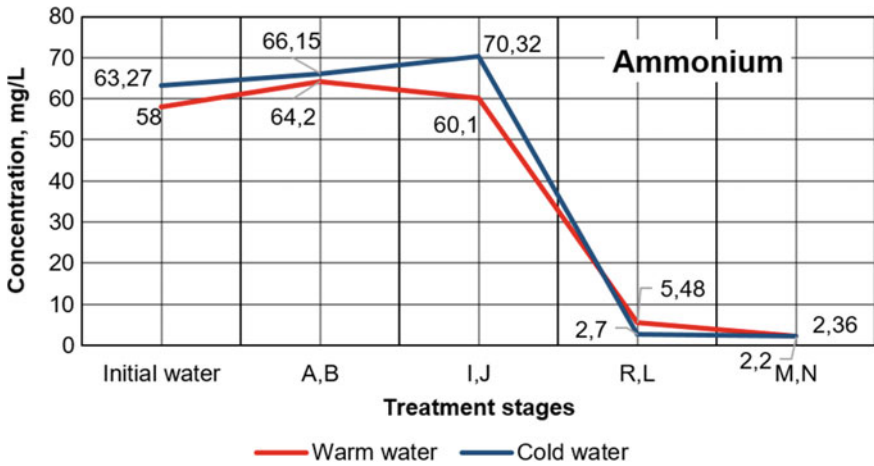


Fig. 2 Change in the ion-ammonium concentration at the treatment stages: for warm water (T = 18–22 °C) and cold water (T = 3–6 °C)

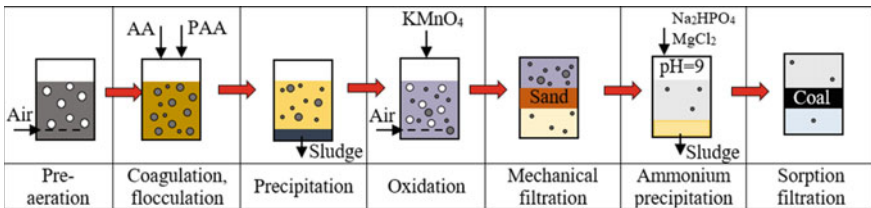


Fig. 3 Diagram of laboratory modeling of the wastewater treatment stages

3 Conclusion

A water purification scheme was developed and tested in the laboratory, including the following processes: Pre-aeration → Coagulation, Flocculation → Precipitation → Oxidation → Mechanical filtration (through sand) → Ammonium precipitation → Sorption filtration (through activated carbon). The adopted scheme excludes the stage of biological treatment and is completely based on physical and chemical methods. This scheme is quite acceptable for the implementation of the project of the PCTP (physical and chemical treatment plant).

As a result of the experiment, it was possible to achieve the water quality indicators permitted by the Russian Standards, established for small and ultra-small treatment facilities when discharged into a water body of category “B”. At the same time, purification effects were achieved: for suspended solids, 98%, COD 91%, ammonium ion 96%, turbidity 100%, chromaticity 99%. In connection with the use of many reagents, it is necessary to control the quality of purified water for the content of aluminum, sulfates, phosphates, magnesium, manganese and other specific substances.

It turned out that this technology depends less on the temperature of the water and is suitable for domestic wastewater with a temperature of 3 to 22 °C. This fact allows

the use of physicochemical treatment of non-centralized sewerage systems in remote northern settlements in the Arctic.

References

1. Arctic regions of Russia (2021) <https://arctic-council-russia.ru/useful/?ysclid=lg4r3edy6s26890718>. Accessed 10 March 2023
2. Handbook of Hydrochemistry (1988) In: Nikanorov AM (ed) Hydrometeoizdat. Leningrad
3. Vialkova E, Maksimova S, Zemlyanova M, Maksimov L, Vorotnikova A (2020) Integrated design approach to small sewage systems in the arctic climate. *Environ Process* 7:673–690
4. Harmful chemicals (1989) Inorganic compounds of groups V–VIII: Reference ed. In: Filov VA (ed) Chemistry. Leningrad
5. Wang H, Qian M, Zhang D, Wu Q, Zhao Z (2023) Ammonia-nitrogen removal by hydroxyapatite prepared from waste fish scale. *Water* 15:1274. <https://doi.org/10.3390/w15071274>
6. Lobanov SA, Poilov VZ (2006) Treatment of wastewater to remove ammonium ions by precipitation. *Russ J Appl Chem* 79:1473–1477
7. Vialkova E, Glushchenko E (2021) Wastewater treatment in remote arctic settlements. *Water* 13:919. <https://doi.org/10.3390/w13070919>
8. Mitani Y, Sakai Y, Mishina F, Ishiduka S (2001) Second international conference on recovery of phosphate from sewage and animal wastes. Center for European studies of polyphosphates, Amsterdam
9. Glushchenko E, Vialkova E, Sidorenko O, Fugaeva A (2020) Physical–chemical wastewater treatment in Arctic conditions. *E3S Web Conf* 157:02014
10. Hendriksen K, Hoffmann B (2018) Greenlandic water and sanitation systems—identifying system constellation and challenges. *Environ Sci Poll Res* 25:32964–32974. <https://doi.org/10.1007/s11356-017-9556-6>
11. Mochalov IP (2016) Wastewater treatment and disinfection for small settlements (in far north conditions). Russia, Moscow
12. Trunova NA (1984) Wastewater treatment and its reuse in cotton industry. Dissertation, Moscow, Russia
13. Ershov AV (2015) Physico–chemical wastewater treatment in block-modular structures. Penza, Russia
14. Koivunen J, Heinonen-Tanski H (2005) Peracetic acid (PAA) disinfection of primary, secondary, and tertiary treated municipal wastewaters. *Water Res* 39:4445–4453. <https://doi.org/10.1016/j.watres.2005.08.016>
15. Chhetri RK, Klupsch E, Andersen HR, Jensen PE (2018) Treatment of Arctic wastewater by chemical coagulation, UV and peracetic acid disinfection. *Environ Sci Pollut Res* 25:32851–32859. <https://doi.org/10.1007/s11356-017-8585-5>
16. Wu T, Englehardt JD, Guo T et al (2018) Applicability of energy-positive net-zero water management in Alaska: technology status and case study. *Environ Sci Pollut Res* 25:33025–33037. <https://doi.org/10.1007/s11356-017-0743-2>
17. Nebukina IA, Smirnova NN, Rvachev IS (2015) The effect of organic compounds on removal efficiency of ammonium ions from wastewater by oxidation method. *Probl Contemp Sci Pract Vernadsky Univ* 2:28–33
18. Barros A, Vecino X, Reig M, Cortina JL (2022) Coagulation and flocculation optimization process applied to the sidestream of an urban wastewater treatment plant. *Water* 14:4024. <https://doi.org/10.3390/w14244024>

19. Anusuyadevi PR, Kumar DJP, Jyothi ADHVO, Patwardhan NSVJ, Mol A (2023) Towards viable eco-friendly local treatment of blackwater in sparsely populated regions. *Water* 15:542. <https://doi.org/10.3390/w15030542>
20. Lado Ribeiro AR, Rodríguez-Chueca JJ, Giannakis S (2021) Urban and industrial wastewater disinfection and decontamination by advanced oxidation processes (AOPs): current issues and future trends. *Water* 13:560. <https://doi.org/10.3390/w13040560>
21. Kofman VY (2013) New oxidizing technologies (part 1). *Water Supply San Equip* 10:68–78
22. Kofman VY (2013) New oxidizing technologies (part 2). *Water Supply San Equip* 11:70–77



Use of Non-magnetic Fraction of Metallurgical Slags in Carbon Dioxide Sequestration Technology

E. V. Kolodezhnaya¹(✉), M. S. Garkavi², I. V. Shadrunkova³, O. E. Gorlova^{1,3},
and K. A. Vorobyev¹

¹ Research Institute of Comprehensive Exploitation of Mineral Resources of the Russian Academy of Sciences, 4, Kryukovskiy tupik, Moscow 111020, Russia
kev@uralomega.ru

² Company “Ural-Omega”, 89/7, Lenina Ave, Magnitogorsk 455037, Russia

³ Nosov Magnitogorsk State Technical University, 38, Lenina Ave, Magnitogorsk 455000, Russia

Abstract. Russia’s environmental industrial policy is aimed at increasing the resource efficiency of production, minimizing the negative impact on the environment, strengthening competitiveness and ensuring technological sovereignty. One of the directions of carbon dioxide sequestration is mineral carbonation. The idea of the article is to use for mineral carbonation, as an alternative to natural materials, a non-magnetic fraction obtained as a result of recycling of high-tonnage metallurgical waste-slugs. Carbon sequestration technologies by mineral carbonation of technogenic raw materials are at the research stage, therefore it is necessary to assess the suitability of the use of metallurgical slags. To solve the tasks set, the material composition of steelmaking and blast furnace slags has been studied in detail. The content of minerals capable of participating in carbonation in the non-magnetic fraction of slags was determined, and the carbonation potential was evaluated based on calculated and practical data. The requirements for man-made waste for their use as raw materials for carbonation are formulated. The factors that have a restraining effect on the introduction of mineral carbonation technologies are highlighted. An assessment of the carbon cycle at the ferrous metallurgy enterprise is given.

Keywords: Technogenic waste · Metallurgical slag · Ash and slag waste · Mineral carbonation · Sequestration · Phase composition · Carbonation potential

1 Introduction

In 2021, the Government of the Russian Federation set the executive authorities the task of decarbonizing Russian industry and developing an action plan for the transition to carbon regulation and sequestration of carbon dioxide emissions [1, 2]. Carbon dioxide emissions generated as a result of the functioning of enterprises of various industries

significantly increase the anthropogenic impact on the environment and make changes in the climate system of our planet. Global anthropogenic emissions are estimated at 57×10^9 tons of CO_2 equivalent in year [3]. The main sources of emissions are coal-fired power plants, large industrial enterprises and agriculture. According to the International Energy Agency, the largest share of carbon dioxide emissions falls on ferrous metallurgy enterprises (30% or 17×10^9 tons CO_2 equivalent) and the cement industry (26% or 14×10^9 tons CO_2 equivalent) [4], therefore, in the foreseeable future, work to reduce the carbon footprint of anthropogenic origin must be carried out in this direction. The use of CO_2 capturing and storing technologies (CCS Carbon Capture & Storage) is one of the processes of technological transformation taking place in the XXI century. and, in particular, refers to the national criteria for sustainable (including green) development projects in the Russian Federation [5].

The development of the main provisions of carbon sequestration technologies in a situation of functioning of ferrous metallurgy enterprises is topical scientific and technical task.

The development of algorithms for carbon dioxide sequestration of industrial enterprises has been reported in the literature since the early 1990 [6]. At the moment, the main directions have been proposed and investigated, of varying degrees of complexity: geological storage in developed underground spaces—geosequestration; reuse in technological processes; mineral carbonation.

The subject of our research is the mineral carbonation of carbon dioxide as the most accessible technology for domestic enterprises. In the process of mineral carbonation, carbon dioxide interacts with natural minerals to form stable solid carbonates. Chemical reactions of mineral carbonation contribute to the exothermic removal of energy during the formation of carbonates.

Conditionally, two main approaches can be distinguished for mineral carbonation technologies (Fig. 1).

Carbonation under natural conditions at the storage site of raw materials	Carbonation in industrial installations
<input type="checkbox"/>	<input type="checkbox"/>
<input type="checkbox"/> Eliminating the effects of excessive mining activity, by integrating carbonation	<input type="checkbox"/> High rate of carbonization reaction and the possibility of almost complete carbonization of the starting materials
<input type="checkbox"/> No costs for crushing, grinding and transporting raw materials	<input type="checkbox"/> The ability to manage the process
<input type="checkbox"/> Use of carbonation reaction energy	<input type="checkbox"/> Possibility of separation of undesirable substances and production of relatively pure carbonates
<input type="checkbox"/> High cost of drilling and injection of carbon dioxide	<input type="checkbox"/> Huge scale of preparation and transportation of raw materials
<input type="checkbox"/> Linking the location to suitable mountain complexes	<input type="checkbox"/> High energy costs for raw material preparation, process and product deposit
<input type="checkbox"/> Very low reaction rate	

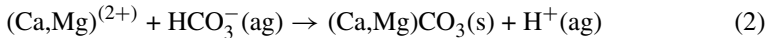
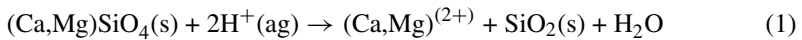
Fig. 1 Features of different carbonation approaches

The first approach involves the introduction of CO₂ in the form of gas or liquid directly into the array of mineral raw materials at the place of its storage—carbonation takes place in natural conditions. With the second approach, the process is carried out in industrial installations under optimal temperature and pressure conditions [7]. At the same time, the rate of carbonization reactions increases significantly.

2 The Purpose of Research

The most active components for CO₂ sequestration are calcium and magnesium oxides. In nature, such minerals occur in the form of silicates, aluminosilicates and hydroxides: serpentinite (Mg₃Si₂O₅(OH)₄), olivine ((Mg, Fe)₂SiO₄), wollastonite (CaSiO₃). The process of mineral carbonation will require 3,2–7,4 tons of natural silicates for sequestration of 1M³ CO₂ [8].

An alternative to the use of natural minerals is the use of mining waste. In the waste of metallurgical production, Ca²⁺ and Mg²⁺ ions are part of oxides, hydroxides and mainly silicates. The process of carbonation of silicates from slags can be divided into two stages. At the first stage, minerals are hydrated with the formation of reactive phases (1), and at the second stage, carbon dioxide is directly bound (2).



The mass fraction of calcium and magnesium ions in soluble compounds capable of hydration in technogenic raw materials is crucial. The completeness and speed of the carbonization reactions, as well as the economic feasibility of the entire technological process will depend on the hardware and the optimality of the conditions (temperature, pressure, time).

During carbonization in an aqueous medium, the speed and completeness of solubility of calcium and magnesium compounds usually increase with a decrease in the pH of the medium, an increase in temperature and pressure, and an increase in the specific surface area of the particles. Thus, it was noted that dicalcium silicate (β-Ca₂SiO₄) dissolves well already at pH = 10, and tricalcium aluminate (Ca₃Al₂O₆) and mayenite (Ca_{11.3}Al₁₄O_{32.3}) at pH = 10 and pH = 7 [9]. The concentration of carbon dioxide will only affect the speed of carbonation, but does not affect its completeness [10].

The activity of technogenic mineral phases is lower than that of natural minerals, and varies greatly depending on the quantitative composition, crystal structure of minerals and the presence of elements such as Fe, Pb, Cr, Al and metallic impurities. For example, metallurgical slags from steel smelting contain 22–24% Fe in the form of various technogenic phases and metal particles. The use of metallurgical slags as raw materials for carbon sequestration is possible only after the extraction of metal impurities.

Taking into account the above, production waste for use as a raw material for mineral carbonation must have the following properties:

- high mass fraction of calcium and magnesium in phases capable of hydration,
- low degree of harmful impact on the environment,

- fine grain size and high specific surface area,
- have a sufficient amount of stored waste close to the sources of emissions.

The analysis of the phase composition of waste from the extraction and processing of mineral raw materials formed at the enterprises of the mining and metallurgical industry showed that the phases required for mineral carbonation are present in slags and slurries of ferrous metallurgy, ashes of heat and power plants, as well as in slags from the combustion of solid household waste (Table 1).

Table 1 The resource suitability of waste for carbonation

Technogenic waste	Mass fraction of CaO, %	Mass fraction of MgO, %	Mass fraction of phases containing Ca and Mg capable of hydration, %	Accumulation volume, million tons (Russia)
Converter slag	40–54	1,9–12,6	35–40	500
Blast furnace slags	30–50	1–18	17–20	
Waste from incineration	14–30	1,9–3,5	20–35	Not installed
Ashes of the CHP	2–45	1–6	0–15	1400

In the construction industry, blast furnace slags are widely used and disposed of in concrete technology, for example, in the production of binders, but steelmaking slags are not widespread in this industry [11]. One of the constraining factors on the way to the use of steelmaking slags in the production of building products and structures is the presence of free CaO and MgO in them, which cause an uneven change in volume during hardening and low strength of the slag binder without an activator [12]. Carbonation of slags will remove this restriction. Assessment of the carbonation potential of steelmaking and blast furnace slag, as the most multi-tonnage stored technogenic waste, will allow us to move to the next stage of the development of technologies for sequestration of emissions of metallurgical enterprises. The carbonation potential is the required amount of mining waste (in units of mass) to bind 1m³ of carbon dioxide [13].

As an object of research, a sample of the current converter slag of the Magnitogorsk Iron and Steel Works with a fraction of 0–50 mm (after sorting) was selected.

3 Object of Research

The experience of processing metallurgical slags has shown that the processing of this raw material faces technological difficulties even at the stage of crushing and grinding [14, 15]. The processes of disintegration, the schemes of crushing and grinding of slags

should be adapted to maximize the extraction of metal kings in the process of disintegration, taking into account the morphometric features and physic-mechanical properties of technogenic raw materials [16]. Using a modern mineralogical and analytical complex, it was found that metal particles in a slag sample have a size from 0,5 to 5 mm (Fig. 2).

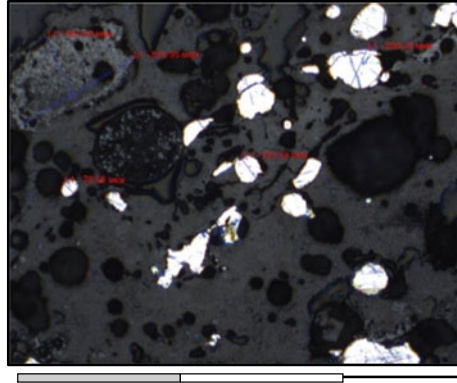


Fig. 2 Micrographs of crushed slag: light grains—metal; dark grains—silicates

Consequently, the efficiency of metal extraction, with subsequent slag enrichment, will directly depend on the amount of the size class 0–5 mm formed during crushing. To implement such disintegration by technical means without over-grinding, it is necessary to adapt the parameters of the crusher operation.

Analysis of the methods of disintegration of complex-structured technogenic raw materials has shown that a high degree of selectivity of disintegration at rational energy costs is provided by centrifugal impact crushers [17]. These devices have a vertical axis of rotation, which contributes to the removal of material from the workspace after the act of crushing, and, as a result, reducing the number of equipment breakdowns. The granulometric composition of the crushed material can be adjusted in a certain range by changing the speed of rotation of the accelerator and the size of the supplied material [18].

To extract metal inclusions, a sample of converter slag was crushed in a centrifugal impact crusher at an accelerator rotation speed of 70 m/s in a cycle with a roar [19]. Crushed slag with a size of 0–5 mm was fed to magnetic separation in a weak magnetic field to obtain magnetic and non-magnetic products (Fig. 3).

All slag processing products are in demand. Magnetic fractions are a circulating product and are used as a charge material in the production of cast iron and steel. Non-magnetic fractions are sold as construction rubble and sand, and, in addition, can serve as raw materials for mineral carbonation at a metallurgical enterprise as part of industrial recycling.

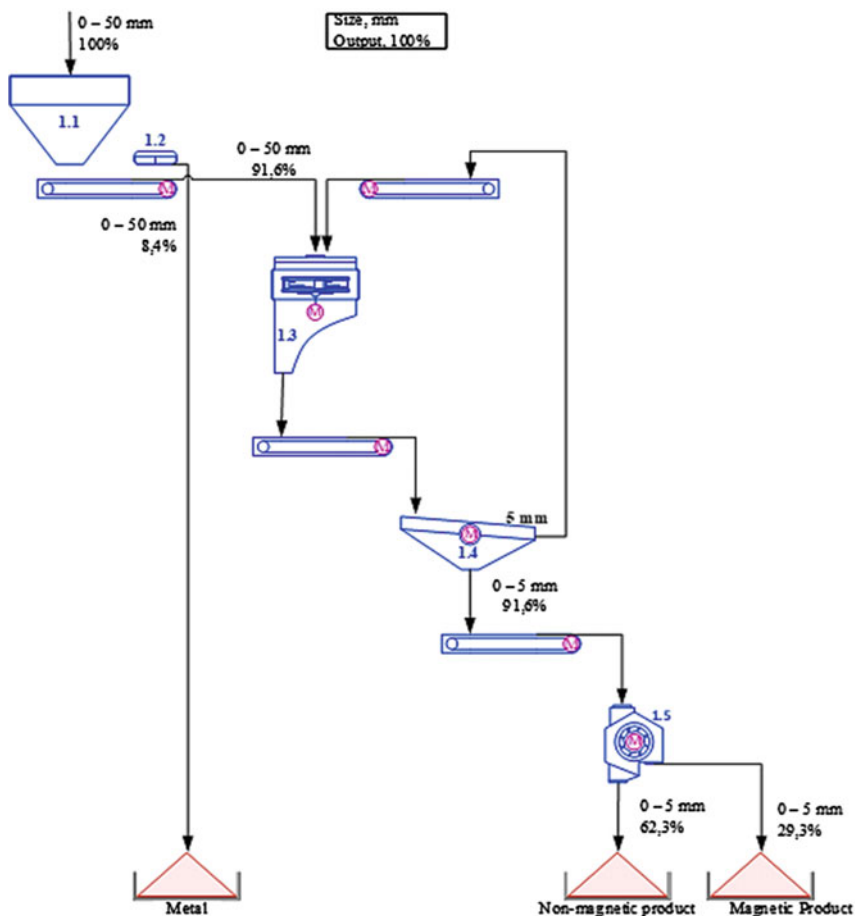


Fig. 3 Technological scheme of slag processing: 1.1—Hopper with feeder, 1.2—Iron separator, 1.3—Centrifugal impact crusher DC, 1.4—Screen, 1.5—Magnetic separator

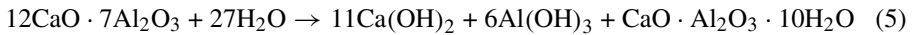
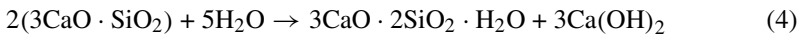
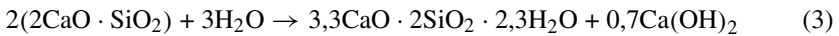
4 Calculation of Carbonation Potential

The chemical composition of the non-magnetic slag processing product is determined by X-ray fluorescence, which allows us to quantify the mass fractions of a wide range of elements in technogenic raw materials of complex material composition (Table 2).

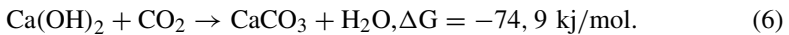
Table 2 Chemical composition of the slag sample

Mass fraction of oxide, %										
FeO	SiO ₂	CaO	Al ₂ O ₃	SO ₃	MgO	Cr ₂ O ₃	TiO ₂	MnO	P ₂ O ₅	V ₂ O ₅
22.4	12.4	39.4	4.2	0.3	14.6	0.3	0.5	2.6	0.5	0.3

A sample of a non-magnetic product of converter slag processing contains a sufficient amount of Ca and Mg oxides and can be considered as a raw material for mineral carbonation after the phase composition is established. The phase composition of the non-magnetic fraction was determined using a diffractometer “D2 PHASER” and license databases “Topas 4.2”. The main slag minerals are: Larnit (C2S)—23,7%, Brownmillite (4CaO·Al₂O₃·Fe₂O₃)—14,2%, Hardened periclase (MgO)—15%, Tricalcium silicate (C3S)—12,5%, Solid solution of oxides (RO-phase)—12,7, Calcium Ferrite (2CaO·Fe₂O₃)—8,7%, Mayenite (12CaO·7Al₂O₃)—3,4%, Magnesiovustite (Mg, Fe)O—3%, Lime—3,5%. Larnite, tricalcium silicate and mayenite are capable of hydration with the formation of calcium hydroxide according to the reaction Eqs. (3, 4, 5):



Calcium hydroxide, formed by reactions (4, 5, 6), participates in the sequestration of carbon dioxide. The isobaric-isothermal potential ΔG of the carbonization reaction (6) indicates the possibility of its occurrence:



According to the results of the slag phase analysis and the reaction equations, the carbonation potential of the non-magnetic product of converter slag processing (Table 3) was calculated.

Table 3 Calculation of the carbonization potential of converter slag

Active slag phases	Mass fraction of active phases in the slag, %	Hydration products capable of binding CO ₂	Mass fraction of hydration products formed, %	Mass Ca(OH) ₂ required for binding 1 m ³ of CO ₂ , kg	Carbonization potential of converter slag, kg
Larnit (C2S)	23.7	Ca(OH) ₂	15.0	3.3	28
Tricalcium silicate (C3S)	12.5		50.0		
Mayenite (12CaO · 7Al ₂ O ₃)	3.4		60.0		

According to the calculation results, 28 kg of non-magnetic slag fraction is needed to bind 1 m³ of carbon dioxide. Thus, the use of non-magnetic products of converter slag processing as raw materials for mineral carbonation will allow to bind greenhouse gases of industrial enterprises.

5 Results and Discussion

The process of carbon dioxide absorption is studied by scientists from many countries of the world as a promising process applied to a large number of substances and materials of various origin and purpose [20–23]. Carbonation of industrial waste, as well as cement and lime-based materials, is a real way to improve the properties of materials in terms of physical and mechanical characteristics and increase their resistance to environmental influences.

Binders based on man-made waste can be activated by carbonation [24–26]. During carbonization of the non-magnetic slag fraction, dense carbonate products may be formed, which will increase the rate of strength gain, water-sealed slag binder, which will allow more extensive utilization of slags in construction products.

The non-magnetic product of converter slag processing has a fineness of less than 5 mm, contains free lime and has weak hydraulic properties. After carbonization, this material can be used as a substitute for fine aggregate in concrete and mortar (Table 4).

Table 4 Granulometric composition and modulus of slag size

Residues on sieves	Residues on sieves with a cell, mm, %						The size module
	2,5	1,25	0,63	0,315	0,16	Bottom	
Private residues on sieves	2,6	15,5	17,2	20,1	15,6	29,0	1,8
Complete residues on sieves	2,6	18,1	35,3	55,4	71,0	100,0	

Carbonation of a non-magnetic product of converter slag processing was carried out at atmospheric pressure. Samples of the material were placed in a container, which was filled with carbon dioxide to a concentration of 50% and maintained a relative humidity of 70%, and then stored for 5, 10, 28 and 56 days. At the end of the experiment, a differential thermal analysis (DTA) was performed and the dependence of the mass fraction of carbonates in the sample on the storage time was determined (Fig. 4).

As a result of the experiment, the presence of carbonates in all samples of the non-magnetic slag product was established, which is indicated by an increase in mass loss at a temperature from 710 to 735 °C. After 5 days of carbonization, the mass fraction of calcium carbonate in the slag was 4.16%. The nature of the graph in Fig. 4 indicates the slow process of carbonation of the material. It was not possible to set the end time of the process for the selected time interval. So, after 56 days of slag storage in a container, the mass fraction of carbonates was 13.62%.

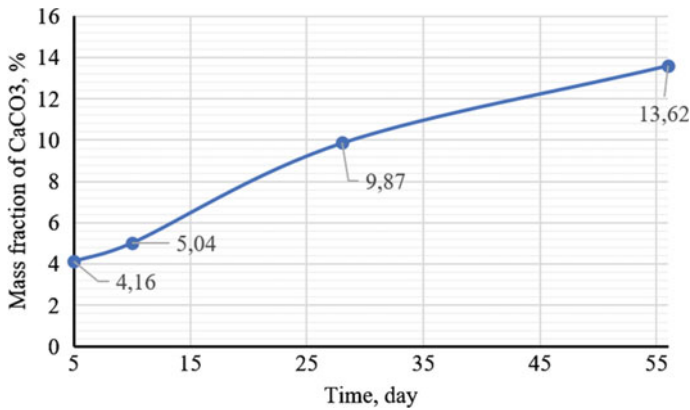


Fig. 4 Dependence of the mass fraction of carbonates on the exposure time

The analysis of the theoretical and practical data obtained indicates the effectiveness of using the non-magnetic fraction of converter slag processing as a raw material for sequestration of greenhouse gases. The results of practical tests confirmed the course of the mineral carbonization process at normal pressure. However, it is also necessary to study the process of accelerated carbonation of technogenic raw materials and the physico-chemical characteristics of the raw material that affect the final products and the rate of carbonation, which will reduce the processing time of the material.

6 Conclusion

To assess the possibility of organizing a closed carbon dioxide cycle in the conditions of blast furnace production of metallurgical enterprises, the calculation of the annual volume of greenhouse gas emissions was carried out on the example of the Magnitogorsk Iron and Steel Works (MMK). The average productivity of the blast furnace at MMK is 1,75 million tons per year. With an average total emission of 2 tons of CO₂ per ton of metal products, the annual emission of the blast furnace will be 3,5 million tons or 1,77 million m³ of gas [27].

According to the results of the carbonation potential assessment, 49,6 million tons of non-magnetic converter slag processing product will be required for sequestration of annual greenhouse gas emissions.

Further work should be aimed at developing the technological design of the process of capturing emissions and mineral carbonation of metallurgical slags, clarifying the parameters and characteristics of the reactions in real conditions. The analysis carried out and the results presented indicate the possibility of sequestration of emissions from metallurgical enterprises and the organization of a closed cycle of carbon dioxide circulation based on mineral carbonation technologies of steelmaking and blast furnace slags.

Acknowledgements. The work was carried out with the financial support of the Russian Science Foundation for Basic Scientific Research and exploratory scientific research No. 22-27-00526 dated 12/29/2021.

References

1. On limiting carbon dioxide emissions: Federal Law of 02.07. 2021, no. 296-FL. <http://www.kremlin.ru/acts/bank/47013>. Accessed 20 December 2022
2. On approval of the strategy of socio-economic development of the Russian Federation with a low level of greenhouse gas emissions until 2050: decree of the Government of the Russian Federation No. 3052-r dated October 20, 2021. <http://publication.pravo.gov.ru/Document/View/0001202111010022>. Accessed 20 December 2022.
3. Special report “global warming by 1.5°C”: summary for policy makers. Intergovernmental Panel on Climate Change. 2018. <https://www.ipcc.ch/sr15/chapter/spm/>. Accessed 15 October 2021
4. Annual report of the international energy agency. “On the prospects of world energy up to 2050” (World Energy Outlook 2022). <https://in.minenergo.gov.ru/knowledge-base/analitics/perspektivy-mirovoy-energetiki-do-2050-goda>. Download file: World Energy Outlook 2022.pdf. Accessed 20 December 2022
5. Shadrinova IV, Zelinskaya EV, Orekhova NN, Gorlova OE, Chekushina TV (2023) ESG-transformation in processing of man-made mineral raw materials. Russian Mining Indus 1:71–78. <https://doi.org/10.30686/1609-9192-2023-1-71-78>
6. Moazzem S, Rasul MG, Khan MMK (2012) A review on technologies for reducing CO₂ emission from coal fired power plants. J Thermal Power Plants, 227–254. <https://doi.org/10.5772/31876>
7. Olajire AA (2013) CO capture by aqueous ammonia 2 process in the clean development mechanism for Nigerian oil industry. Front Chem Sci Eng 7:366–380. <https://doi.org/10.1007/s11705-013-1340-7>
8. Garkavi MS, Shadrinova IV, Kolodezhnaya EV (2020) Technological aspects of waste incinerator slag processing. IOP Conf Series: Materials Sci Eng 962:042058. <https://doi.org/10.1088/1757-899X/962/4/042058>
9. Kelemen PB, Matter J (2008) In situ carbonation of peridotite for CO₂ storage. Proc Natl Acad Sci USA 105:17295–17300. <https://doi.org/10.1073/pnas.0805794105>
10. Olajire AA (2013) A review of mineral carbonation technology in sequestration of CO₂. J Petrol Sci Eng 109:364–392
11. Shishken VI (2005) Technologies of building materials from local raw materials and man-made waste. Magnitogorsk State Technical University, Russia Magnitogorsk
12. Huijgen, WJJ (2005) Mineral CO₂ sequestration by steel slag carbonation. Environmental science and technology, American Chemical Society, USA
13. Shadrinova IV, Gorlova OE, Kolodezhnaya EV, Kutlubayev IM (2015) The mechanism of disintegration of metallurgical slags in centrifugal impact crushing apparatuses. J Phys Tech Prob Mineral Develop 2:149–155
14. Kolodezhnaya EV, Shadrinova IV, Gorlova OE (2019) Technologies for obtaining high-quality concentrates from dump metallurgical slags. J Obogashchenie Rud 4:54–60. <https://doi.org/10.1088/1755-1315/1061/1/012040/>
15. Chanturia VA, Shadrinova IV, Gorlova OE, Kolodezhnaya EV (2020) Development of technological innovations of deep and complex processing of technogenic raw materials in the conditions of new economic challenges. Izvestiya Tula State University. Earth Sci 1:159–171

16. Gorbatova EA, Ozhogina EG (2017) The feasibility of integration of mineralogical and analytical methods of study of metallurgical slag. *Bulletin Magnitogorsk state technical University G. I. Nosova* 4:31–39. <https://doi.org/10.18503/1995-2732-2017-15-4-31-39>
17. Shadrinova IV, Artomonov VA, Vorobiev VV, Kozin AJ, Kolodezhnaya EV (2008) Selection decomposition of metallurgical slag by Vapart-impact devices. In: *The XXIV International Mineral Processing Congress Beijing*, p 3943–3946
18. Paladeeva NI (1996) Impact crushers. *Mining J* 10–11:139–145
19. Kolodezhnaya EV, Gorlova OE, Orekhova NN, Kolkova MS, Glagoleva IV (2022) Determination of criterion for selectivity of disintegration of technogenic raw materials for environmentally oriented processing. *IOP Conf Ser: Earth Environ Sci* 1061:012040. <https://doi.org/10.1088/1755-1315/1061/1/012040>
20. Artamonova AV, Voronin KM (2011) Slag-alkaline binders based on blast-furnace granular slag of centrifugal impact grinding. *Cement Its Appl* 4:108–113
21. Lyuborsky N, Vorobyev D (2011) The current state of research on artificial carbonation of limestone systems. *Journal Motrol* 13C:165–176
22. Andreevich RA (2018) Utilization of steelmaking slags by accelerated carbonation. *Bull South Ural State Univ Series: Construct Architect* 18(3):68–72
23. Lyubomirsky NV, Fedorkin SI (2016) The effect of carbon dioxide pressure on the kinetics of forced carbonation of semi-dry pressed calcareous stone and the formation of its strength. *Const Techn Saf* 3(55):28–38
24. Gerdemann's SJ, Oconnor W (2007) Ex situ aqueous mineral carbonation. *Environ Sci Technol* 41(7):2587–2593. <https://doi.org/10.1021/es0619253>
25. Renforth P, Washbourne C-L (2011) Silicate production and availability for mineral carbonation. *Environ Sci Technol* 45(6):2035–2041. <https://doi.org/10.1021/es103241w>
26. Kovalenko NE, Kalinichenko AU (2011) Disposal of ash and slag waste from solid waste incineration as components of building materials. *Bull North Caucasus State Univ* 3:65–69
27. The Federal State Statistics Service (Rosstat) has published a report Key indicators of environmental protection. *Statis Bull* https://rosstat.gov.ru/storage/mediabank/oxr_bul_2021.pdf/. Accessed 20 December 2022



Study of the Composition of the Activating Mixture for the Production of Foamed Geopolymer Materials

A. V. Ryabova, A. I. Izvarin^(✉), A. A. Timofeeva, L. A. Yatsenko, and P. O. Orlovsky

Platov South-Russian State Polytechnic University (NPI), 132, Prosveshcheniya St.,
Novocherkassk 346428, Russia
andre.izvarin@yandex.ru

Abstract. The accumulated of ash and slag waste necessitates their processing. The processing of ash and slag wastes through their use for the synthesis of geopolymers is a very promising area of research. Geopolymer materials are obtained by alkaline activation reaction. The role of the activator on the technological properties of foamed geopolymer materials has been studied. It has been established that solutions of alkali hydroxides and/or solutions of alkali silicates are used as an activating solution. The synthesis of samples with different content of liquid glass and sodium hydroxide was carried out. It is shown that the content of both liquid glass and sodium hydroxide affects the properties. Technological properties and microstructure of synthesized samples are determined. Conclusions are drawn about the optimal amount of liquid glass and sodium hydroxide in the composition of the activating solution for obtaining foamed geopolymer materials with a minimum density. Pore size distribution studied.

Keywords: Geopolymer materials · Ash and slag waste · Alkaline activation · Porous structure · Recycling · Pore formation

1 Introduction

Currently, energy saving in construction has become a major problem. [1, 2]. Thermal insulation materials are the main tool for improving energy efficiency in the construction of buildings [3–5]. The use of energy-efficient thermal insulation materials reduces heat loss, which results in lower energy costs. [6, 7]. Even though there is currently a strong growth in renewable energy sources, electricity generation from solid fossil fuels is still relevant. Worldwide, about 70% of electricity is generated using natural resources, while coal accounts for about 38% [8, 9].

Also in the modern world there is a problem associated with environmental pollution (soil, groundwater, air) by ash and slag waste (ASW), which are produced during the operation of thermal power plants [10–12]. During the combustion of coal, a mechanical mixture of ash and slag is formed in a ratio of 4:1 [13]. Annually in Russia, the coal power industry produces more than 75 million tons of ASW, of which only about 11%

is processed. [14]. The search for ways to dispose of such wastes is a very topical area of research [15, 16]. ASW is an aluminosilicate material and can be used in road construction, in the production of cement and building materials. [17–20].

Processing of ASW is very promising due to the possibility of their use in the synthesis of geopolymers [21, 22]. Geopolymer materials (alkaline-activated materials) are new environmentally friendly binder materials obtained by alkaline activation reaction [23]. They have the following advantages: fire resistance, chemical, corrosion resistance, durability. The mechanism of alkaline activation is as follows: substances containing a large amount of Al and Si in their composition interact with an activator solution, most often these are solutions of alkali hydroxides (KOH, NaOH) and/or solutions of alkaline silicates ($K_2O \cdot nSiO_2$ or $Na_2O \cdot nSiO_2$). In this case, silicate and aluminate tetrahedral units dissolve at high pH values and begin to polymerize [24].

The modulus of the activator is the most important factor and is defined as the mass ratio of SiO_2 to Na_2O or (K_2O) in the alkaline activator. The dosage or total mass of Na_2O in the alkaline activator solution generally includes the sum of the masses of Na_2O present in the sodium silicate solution and/or sodium hydroxide.

At the same time, it is promising to obtain foamed geopolymer materials with low density and thermal conductivity. There are several foaming methods. The most popular are direct foaming, replica method, sacrificial filler, sintering, mechanical foaming and additive manufacturing [25].

Among them, direct foaming is the simplest and most widely used method of foamed geopolymer materials [26]. Direct foaming typically involves a reaction that uses various blowing agents and an alkaline environment to induce pores during geopolymerization. The pores formed by this foaming method are usually closed. Therefore, a material with such pores will have high thermal insulation properties. Compared to other methods, direct foaming has a significant effect on the viscosity of the reaction mixture and, accordingly, on geopolymerization, thereby affecting both the internal and external porosity of the foamed geopolymers. This is because most porosity reactions either consume or release water.

The main advantage of geopolymers is their high fire resistance compared to other existing heat-insulating materials [27]. Therefore, the purpose of this work is to study the influence of the composition of the activating mixture on the properties of the obtained foamed geopolymer materials.

2 Materials and Methods

ASW from the Novochoerkassk State District Power Plant was chosen as the main raw material for the production of geopolymer materials. The chemical composition of ASW is presented in Table 1. The main substances are SiO_2 and Al_2O_3 , the total content of which is 70%. A mixture of liquid sodium glass and sodium hydroxide solution was used as an activator, and aluminum powder was used as a pore-forming additive.

The raw mixture for obtaining geopolymer materials is prepared as follows: drying of ASW until a moisture content of no more than 5% is reached, and their subsequent grinding to a particle size of 250 microns. After that, a solution of sodium hydroxide is prepared in a separate container; for this, NaOH powder is mixed with water in a given

Table 1 Chemical composition of ash and slag wastes

Chemical composition, wt. %											
SiO ₂	Al ₂ O ₃	Fe ₂ O ₃	K ₂ O	MgO	SO ₃	TiO ₂	CaO	Na ₂ O	P ₂ O ₅	MnO	LOI
51,23	18,78	10,27	3,04	2,08	0,31	0,78	3,10	0,92	0,13	0,13	9,23

ratio. Then liquid glass is added to the resulting sodium hydroxide solution, stirred for 5 min and an activating solution is obtained. After that ASW is activated by adding an activating solution to them. Next, aluminum powder is added to the resulting mixture and stirred for 5 min. At the final stage, the resulting compositions are poured into molds and cured at a temperature of 80 °C for 12 h. After that, a visual inspection of the samples is carried out, during which conclusions are drawn about the size of the pores and the homogeneity of the structure. The component composition of the raw mixture is shown in Tables 2 and 3.

Table 2 Component composition of the raw mixture to study the effect of liquid glass on the properties of geopolymer materials, wt. %

Sample	Sample composition, wt. %				
	ASM	Waterglass	NaOH (powder), over 100	Water, over 100	Aluminum powder
1.1	80.0	18.0	2.0	4.0	2.0
1.2	77.5	20.5	2.0	4.0	2.0
1.3	75.0	23.0	2.0	4.0	2.0
1.4	72.5	25.5	2.0	4.0	2.0
1.5	70.0	28.0	2.0	4.0	2.0

Table 3 Component composition of the raw mixture to study the effect of sodium hydroxide on the properties of geopolymer materials, wt. %

Sample	Sample composition, wt. %				
	ASM	Waterglass	NaOH (powder), over 100	Water, over 100	Aluminum powder
2.1	75.0	23.0	-	-	2.0
2.2	75.0	23.0	1.0	2.0	2.0
2.3	75.0	23.0	2.0	4.0	2.0
2.4	75.0	23.0	3.0	6.0	2.0
2.5	75.0	23.0	4.0	8.0	2.0

Sample density ρ , kg/m^3 , was determined by the Eq. (1):

$$\rho = \frac{m}{V} \cdot 1000, \text{ kg/m}^3 \quad (1)$$

where m —sample weight, g ; V —sample volume, cm^3 .

The compressive strength of the samples was determined on a hydraulic press brand TP-1-350 TestPress, Russia.

The porosity of the material was calculated by Eq. (2):

$$P = \frac{1 - d_b}{d_t} \cdot 100, \% \quad (2)$$

where d_b —sample bulk density, kg/m^3 ; d_t —sample true density, kg/m^3 .

The thermal conductivity of the synthesized samples was determined using a thermal conductivity meter ITP-MG4'100/Zond', SKB StroyPribor, Russia.

3 Results and Discussions

Synthesis of geopolymers consists in alkaline activation of aluminosilicate components of ASW. In this case, the dissolution of aluminum and silicon in an alkaline medium, the transport of dissolved particles, and polycondensation occur, during which a three-dimensional silicoaluminate structure is formed (Fig. 1) [28, 29].

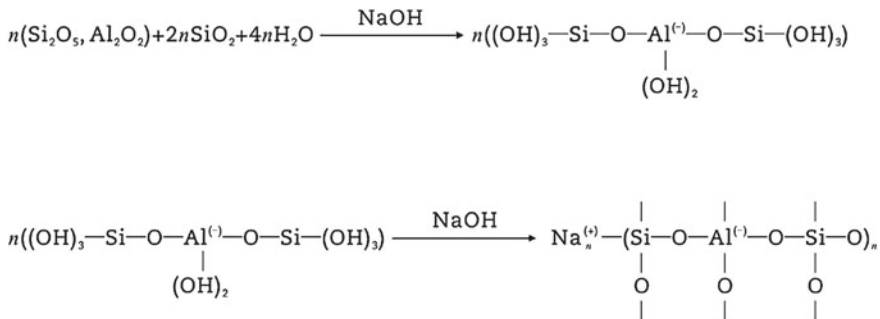


Fig. 1 Schematic diagram of the formation of geopolymer compounds

To study the influence of the amount of liquid glass on the properties of geopolymers, the optimal amount in the composition of ASM and liquid glass was investigated. The structure of the synthesized samples is shown in Fig. 2.

As can be seen from Fig. 2, sample 1.3 has the most porous and uniform structure, with a pore size of up to 2 mm. Samples 1.1 and 1.5 do not have pores, since they contain insufficient and excessive amounts of liquid glass, respectively. Samples 1.2 and 1.4 have a weakly expressed porous structure. Technological properties of these samples are shown in Table 4.

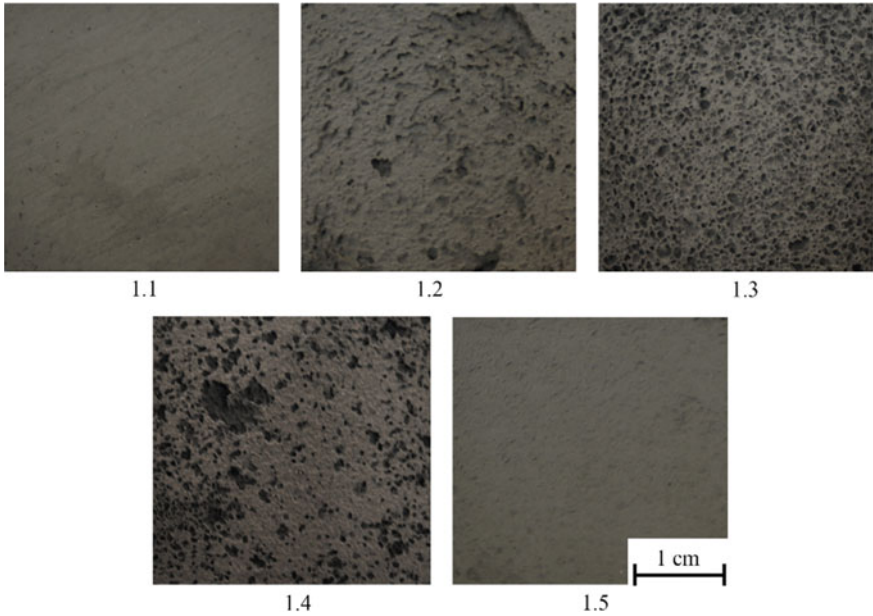


Fig. 2 The structure of geopolymer materials in the study of the influence of liquid glass

Table 4 Technological properties of the obtained geopolymer materials in the study of the influence of liquid glass

Sample	Density, kg/m ³	Compressive strength, MPa	Porosity, %	Thermal conductivity, W/(m · K)
1.1	1136	2,37	51,29	0,26
1.2	709	1,67	69,60	0,16
1.3	467	0,83	79,97	0,10
1.4	663	1,46	71,57	0,15
1.5	954	2,48	59,09	0,21

Sample 1.3 has the best thermal insulation properties (Table 4). Consequently, a composition containing 75.0% ASW and 23.0% liquid glass was chosen for further studies.

The structure of the obtained geopolymer materials with different content of sodium hydroxide is presented in Fig. 3.

As can be seen from Fig. 3, in the absence of sodium hydroxide in the composition (sample 2.1), the formation of a porous structure practically does not occur. As the alkali content increases, the pore size increases. The pore formation of foamed geopolymers using aluminum powder as a pore former consists in the interaction of the alkaline component with aluminum powder, with the formation of hydrogen, which foams the

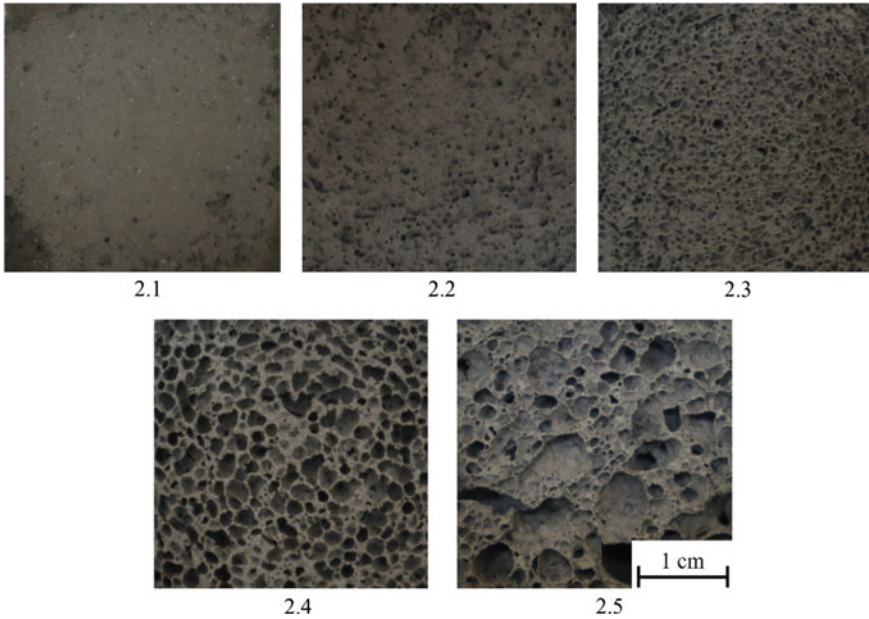
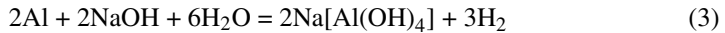


Fig. 3 The structure of geopolymer materials in the study of the effect of sodium hydroxide

geopolymer suspension according to the reaction (3) [30]:



Therefore, the more alkali in the reaction mixture, the more actively the foaming of the geopolymer material occurs.

On Fig. 4 shows the distribution of pore size ranges for samples 2.3, 2.4 and 2.5. For samples 2.1 and 2.2, it was decided not to distribute the pore size ranges, since the samples have a monolithic slightly porous structure.

In sample 2.3, the predominant amount is macropores in the size range of 0.2–1.0 mm, in sample 2.4 in the range of 0.6–1.2 mm, in sample 2.5, the predominant amount is in the range of 0.4–1.2 and a large number of pores with a size of more than 2 mm.

Technological properties in the study of the role of sodium hydroxide are shown in Table 5.

The best technological properties were found in sample 2.4 (Table 5), since it has the lowest density.

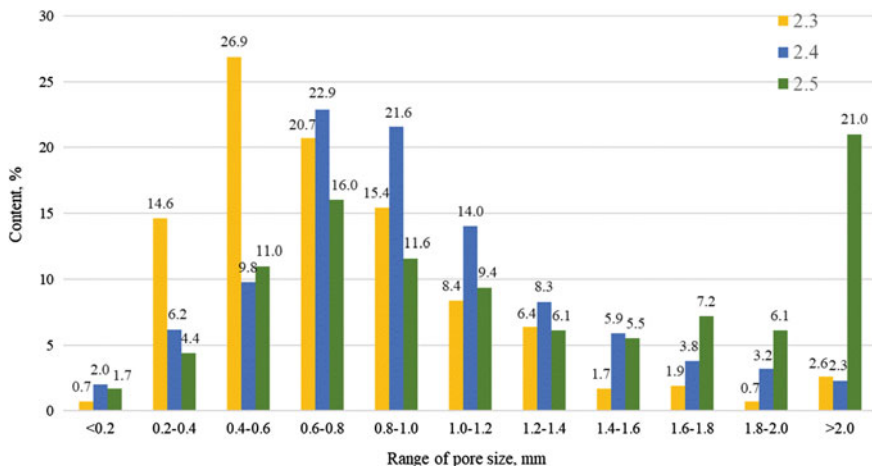


Fig. 4 Histogram of the distribution of the range of pore sizes for samples 2.3, 2.4, 2.5

Table 5 Technological properties of the obtained geopolymer materials in the study of the role of sodium hydroxide

Sample	Density, kg/m ³	Compressive strength, MPa	Porosity, %	Thermal conductivity, W/(m·K)
2.1	1192	3.52	48.89	0.27
2.2	732	1.78	69.42	0.16
2.3	467	0.83	79.97	0.10
2.4	357	0.54	84.69	0.08
2.5	385	0.39	83.49	0.09

4 Conclusion

Thus, the possibility of obtaining foamed geopolymer materials based on ash and slag waste from the Novochoerkassk State District Power Plant was shown. The chemical composition of ASW was studied. It was revealed that the main substances are SiO₂ and Al₂O₃, the total content of which is 70%.

Upon receipt of geopolymers, an alkaline activation reaction of aluminosilicate components of ASW occurs. In this case, the dissolution of aluminum and silicon in an alkaline medium, the transport of dissolved particles and polycondensation occur, during which a three-dimensional silicoaluminate structure is formed.

The mechanism of foaming geopolymer material with aluminum powder is the interaction of aluminum with alkali to form hydrogen, which has a foaming effect.

It has been established that in the absence of sodium hydroxide in the composition, the formation of a porous structure practically does not occur. As the alkali content increases, the pore size increases and the density decreases. Therefore, the more alkali in

the composition of the reaction mixture, the more actively the foaming of the geopolymer material occurs.

It has been established that when the activating mixture contains 23.0% liquid glass and 3.0% sodium hydroxide, a foamed geopolymer material with the best technological properties is formed (sample 2.4). The density of this sample is 357 kg/m³, the compressive strength is 0.54 MPa, the porosity is 84.69%, and the thermal conductivity is 0.08 W/(m·K).

Acknowledgements. The work was performed as part of the project under an agreement on the provision of grants from the federal budget in the form of subsidies in accordance with Paragraph 4 of Section 78.1 of the Budget Code of the Russian Federation, Agreement # 075-15-2022-1111, from June 29, 2022, topic “Carbon-neutral technologies for recycling large-tonnage fuel energy waste with the production of functional geopolymer materials”.

References

1. Jelle BP (2011) Traditional, state-of-the-art and future thermal building insulation materials and solutions—properties, requirements and possibilities. *Energy Build* 43:2549–2563. <https://doi.org/10.1016/j.enbuild.2011.05.015>
2. da Cunha SRL, de Aguiar JLB (2020) Phase change materials and energy efficiency of buildings: a review of knowledge. *J Energy Storage* 27:101083. <https://doi.org/10.1016/j.est.2019.101083>
3. Papadopoulos AM (2005) State of the art in thermal insulation materials and aims for future developments. *Energy Build* 37:77–86. <https://doi.org/10.1016/j.enbuild.2004.05.006>
4. Korjenic A, Petránek V, Zach J, Hroudová J (2011) Development and performance evaluation of natural thermal-insulation materials composed of renewable resources. *Energy Build* 43:2518–2523. <https://doi.org/10.1016/j.enbuild.2011.06.012>
5. Alam M, Singh H, Limbachiya MC (2011) Vacuum Insulation Panels (VIPs) for building construction industry—a review of the contemporary developments and future directions. *Appl Energy* 88:3592–3602. <https://doi.org/10.1016/j.apenergy.2011.04.040>
6. Aditya L, Mahlia TMI, Rismanchi B et al (2017) A review on insulation materials for energy conservation in buildings. *Renew Sustain energy Rev* 73:1352–1365. <https://doi.org/10.1016/j.rser.2017.02.034>
7. Al-Homoud MS (2005) Performance characteristics and practical applications of common building thermal insulation materials. *Build Environ* 40:353–366. <https://doi.org/10.1016/j.buildenv.2004.05.013>
8. Abu-Jdayil B, Mourad A-H, Hittini W et al (2019) Traditional, state-of-the-art and renewable thermal building insulation materials: an overview. *Constr Build Mater* 214:709–735. <https://doi.org/10.1016/j.conbuildmat.2019.04.102>
9. Bódis K, Kougias I, Taylor N, Jäger-Waldau A (2019) Solar photovoltaic electricity generation: a lifeline for the European coal regions in transition. *Sustainability* 11:3703. <https://doi.org/10.3390/su11133703>
10. Menshov PV, Khlupin YV, Nalesnik OI, Makarovskikh AV (2014) Ash and Slag waste as a secondary raw material. *Procedia Chem* 10:184–191. <https://doi.org/10.1016/j.proche.2014.10.032>
11. Tiwari MK, Bajpai S, Dewangan UK, Tamrakar RK (2015) Suitability of leaching test methods for fly ash and slag. a review. *J Radiat Res Appl Sci* 8:523–537. <https://doi.org/10.1016/j.jrras.2015.06.003>

12. Yatsenko EA, Goltsman BM, Novikov YV et al (2022) Review on modern ways of insulation of reservoirs for liquid hydrogen storage. *Int J Hydrogen Energy* 47:41046–41054. <https://doi.org/10.1016/j.ijhydene.2022.09.211>
13. Aleksandrova TN, Korchevenkov SA (2017) Ecological and technological aspects of ash and slag wastes utilization. *J Ecol Eng* 18:15–24. <https://doi.org/10.12911/22998993/74363>
14. Murko V, Khyamyalyainen V, Baranova M (2018) Use of ash-and-slag wastes after burning of fine-dispersed coal-washing wastes. *E3S Web of Conf* 41:1042. <https://doi.org/10.1051/e3sconf/20184101042>
15. Romanyuk VS, Klimova LV, Kurdashov VM et al (2023) Prospects for the use of painted ceramic facing materials using man-made waste. In: *Proceedings of the 6th International Conference on Construction, Architecture and Technosphere Safety: ICCATS*, pp 35–44. https://doi.org/10.1007/978-3-031-21120-1_4
16. Cherkasova TG, Cherkasova EV, Tikhomirova AV et al (2022) Study of matrix and rare elements in ash and slag waste of a thermal power plant concerning the possibility of their extraction. *Metallurgist* 65:1324–1330. <https://doi.org/10.1007/s11015-022-01278-2>
17. Lyapin AA, Parinov IA, Buravchuk NI et al (2021) The use of burnt rocks of mine dumps and ash-slag waste in road construction. *Improv Road Pavement Charact Appl Ind Waste Finite Elem Model*, p 77–112
18. Lyapin AA, Parinov IA, Buravchuk NI et al *Improving road pavement characteristics*, 10:973–978
19. Bahn-Walkowiak B, Bleischwitz R, Distelkamp M, Meyer M (2012) Taxing construction minerals: a contribution to a resource-efficient. *Europe Miner Econ* 25:29–43. <https://doi.org/10.1007/s13563-012-0018-9>
20. Malchik AG, Litovkin SV, Rodionov et al (2016) Analyzing the technology of using ash and slag waste from thermal power plants in the production of building ceramics. *IOP Conf Ser: Mat Sci Eng* 127:12024. <https://doi.org/10.1088/1757-899X/127/1/012024>
21. Yatsenko EA, Ryabova AV, Vil'bitskaya NA et al (2022) Eco-geopolymers based on CHP plant ash-slag waste: promising materials for road construction in the arctic zone. *Glas Ceram* 78:490–493. <https://doi.org/10.1007/s10717-022-00438-9>
22. Yatsenko EA, Smolii VA, Klimova LV et al (2022) Solid fuel combustion wastes at CHPP in the arctic zone of the Russian Federation: utility in eco-geopolymer technology. *Glas Ceram* 78:374–377. <https://doi.org/10.1007/s10717-022-00414-3>
23. Cong P, Cheng Y (2021) Advances in geopolymer materials: a comprehensive review. *J Traffic Transp Eng* 8:283–314. <https://doi.org/10.1016/j.jtte.2021.03.004>
24. Zhang Z, Zhu Y, Yang T et al (2017) Conversion of local industrial wastes into greener cement through geopolymer technology: a case study of high-magnesium nickel slag. *J Clean Prod* 141:463–471. <https://doi.org/10.1016/j.jclepro.2016.09.147>
25. Novais RM, Buruberri LH, Ascensão G et al (2016) Porous biomass fly ash-based geopolymers with tailored thermal conductivity. *J Clean Prod* 119:99–107. <https://doi.org/10.1016/j.jclepro.2016.01.083>
26. Bai C, Colombo P et al (2018) Processing, properties and applications of highly porous geopolymers: a review. *Ceram Int* 44:16103–16118. <https://doi.org/10.1016/j.ceramint.2018.05.219>
27. Łach M, Mierzwiński D, Korniejenko K, Mięka J (2018) Geopolymer foam as a passive fire protection. *MATEC Web of Conf* 247:31. <https://doi.org/10.1051/matecconf/201824700031>
28. Abdullah MMA, Hussin K, Bnhussain M et al (2011) Chemical reactions in the geopolymerisation process using fly ash-based geopolymer. A review. *Aust J Basic Appl Sci* 5:1199–1203
29. Villa C, Pecina ET, Torres R, Gómez L (2010) Geopolymer synthesis using alkaline activation of natural zeolite. *Constr Build Mater* 24:2084–2090. <https://doi.org/10.1016/j.conbuildmat.2010.04.052>

30. Yatsenko EA, Goltsman BM, Trofimov SV et al (2023) Influence of various coal energy wastes and foaming agents on foamed geopolymer materials' synthesis. *Materials* 16:264. <https://doi.org/10.3390/ma16010264>



Changes in Runoff During the Growing Season in the Upper Reaches of the Naryn River in the Context of Global Climate Change

R. T. Akmatov¹✉, O. A. Karymshakov¹, Zh. O. Karamoldoev²,
and T. M. Choduraev¹

¹ Ecology and Tourism of the Kyrgyz State University Named After I. Arabaev, 51, I. Razzakov St., Bishkek 720026, Kyrgyzstan
nalsur24@list.ru

² Institute of Geology Named After M. Adyshev of the National Academy of Sciences of the Kyrgyz Republic, 30, Erkindik St., Bishkek 720481, Kyrgyzstan

Abstract. In this article, attention focused on the analysis of the tightness of relationships between the runoff during the growing season and the main climatic factors of the formation of river flow in the annual and growing season. Long-term fluctuations in runoff during the growing season determined by cold precipitation in the catchment areas and the temperature regime of the summer months. 2000 to 2019 the amount of precipitation in the upper reaches of the Naryn River between October to April increased significantly. The sum of positive air temperatures has increased most significantly over the past twenty years in the alpine zone and over the past forty years—in the lower reaches of the catchment. The number of days with positive temperatures is also increasing. For example, in the high mountain zone over the past 20 years it has increased from 109 to 122 days, and in the middle mountain zone of the river—from 220 to 236 days over the past 40 years. As a result, the air temperature above 0 °C shifted from mid-May–June to April–May at the Tien-Shan meteorological station, from mid-March to the first half of March at the Naryn meteorological station. Therefore, the runoff of the upper reaches of the Naryn River during the growing season, according to the data from the Naryn gauging station, Naryn city, has been increasing the average growing water discharge since 1992.

Keywords: Summer runoff · Vegetation period · Water consumption · Climatic factors · Hydrological regime · Water supply · Gauging station

1 Introduction

The Naryn River is the largest water artery in Kyrgyzstan. In the outlet section (hydropost Uchkurgan), the area of the basin is 58400 km², the annual discharge is estimated at 432 m³/s [1–4]. Its runoff used for hydropower and water management purposes. In the future, it planned to build 24 hydroelectric power stations in the Naryn river basin. At

the same time, their construction in the upper reaches of the Naryn River was planned for the coming years. This determines the relevance of studying the water regime of the Naryn River.

The hydrological regime of the upper reaches of the Naryn River was described according to the data of a hydrological station located in the city of Naryn; climatic characteristics were determined according to long-term data of the Tien Shan meteorological station (3614 m above sea level) and Naryn (2040 m above sea level).

2 Relevance, Scientific Significance of the Issue

The problem of water supply for the population and various sectors of the economy has become relevant for many regions of the world. The uneven distribution of river flow within regions is becoming a serious problem, especially in arid regions of the world. These regions include the Central Asian region.

Kyrgyzstan has changed water relations with neighboring Republics. According to previous agreements, the use of water from the Toktogul reservoir, compared to energy, was focused on irrigation purposes. Energy is currently at the forefront.

This is due to the fact that Kyrgyzstan uses only 2% of the total volume of water from the Nizhne-Naryn HPP for irrigation. In addition, Toktogul HPP cannot provide electricity in autumn and winter. Due to the fact that an average of 11 billion m³ of water per year from the Toktogul reservoir used to irrigate the territories of Uzbekistan, Tajikistan and Kazakhstan. Under such conditions, Kyrgyzstan faces difficulties in managing the water regime of the Toktogul HPP due to a decrease in electricity supply in the winter.

At the same time, population growth observed in Kyrgyzstan, new houses and enterprises are being built. The expansion of irrigated lands is becoming an urgent task, the solution of which is necessary to provide the growing population with agricultural products.

3 Formulation of the Problem

The paper sets the task to investigate the hydrological regime of the upper reaches of the Naryn River (Narynhydropost, Naryn city) since 1930. Therefore, it is necessary to modernize and develop the systems of water supply, energy and water resources management. In this regard, one of the most important scientific and practical issues is the hydrological analysis of the flow of the Naryn River and the forecast of fluctuations in water content in the Toktogul reservoir to optimize the cost-effective operation of the Toktogul HPP.

4 Theoretical Part

The distribution of runoff within a year determined by the time when water enters the river system from genetic sources—snow, glaciers and rains. In the conditions of Kyrgyzstan, regulated by the peculiarities of orography and relief—the distribution of watershed areas in altitudinal zones and exposures—relative to moisture-bearing air masses, synoptic conditions of the cold and warm periods of the year.

Many scientists have developed theoretical foundations and methods for studying the hydrological characteristics of the rivers of Kyrgyzstan, including the Naryn river basin. These include V.L. Schultz “Rivers of Central Asia”, 1965, D.M. Mamatkanov “Modeling and prediction of fluctuations in river flow”, 1973, M.N. Bolshakov “Water resources of the rivers of the Soviet Tien Shan and methods for their calculation”, 1974, S.K. Alamanov “Study of the formation and long-term forecast of river flow in the north-west of Kyrgyzstan”, 1977, A.G. Grinevich, E.K. Pospaeva “Characteristics of vegetation runoff in the basin of the river. Naryn and questions of its forecasting”, 1975, I.V. Ratsek “Oscillations and evolution of glacial runoff in the basin of the river. Naryn”, 1991.

5 Practical Significance, Suggestions and Results of Implementations

To assess the situation in the upper reaches of the Naryn River, hydrological and meteorological data from the archive of the Hydrometeorological Service of the Kyrgyz Republic used for the period 1930–2020. Were applied Statistical, geographical and hydrological methods.

According to the data of the gauging station in the city of Naryn for 1930–2020, it can be seen that the average water discharge for the growing season has increased since 1992 (Fig. 1). So, if the average vegetation flow in 1931–1991 was 144.7 m³/s, later for the period from 1992 to 2020 it increased to 173.9 m³/s, or by 120%.

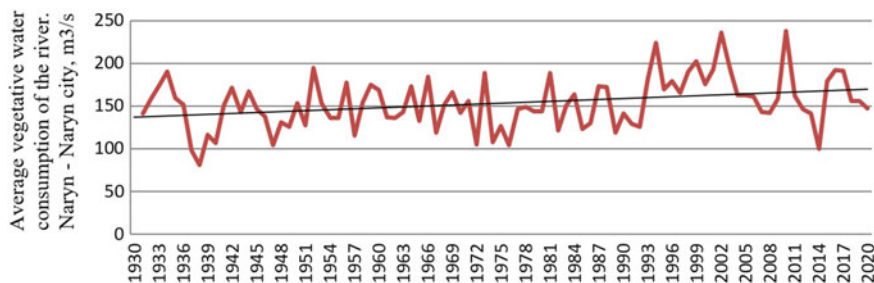


Fig. 1 Changes in water discharge on the river Naryn (hydropost Naryn from 1930 to 2020)

The study of the Naryn River’s feeding sources during the growing season showed that in upper reaches the increasing of water inflow in April–June occurs mainly due to snow melting, and in July–September—due to ice and high-mountain snow melting [5–7]. Calculations based on data for 1992–2020 showed that the ratio of the water content of the Naryn River by months of the growing season distributed as follows: 26% of the flow fell on July, 23% on June and August, 13% on May, 10% on September and 5% in April, as seen in Fig. 2.

The results of analyze Fig. 3, show that the supply of the river with glacial water decreased compared to its supply with snow water (Fig. 3). Since 1992, the part of the July runoff in the vegetation season of the total runoff has decreased by 10%, (Fig. 4).

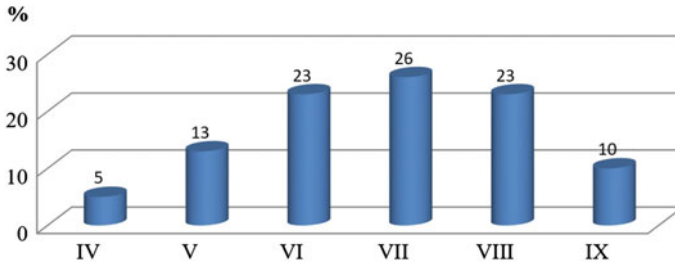


Fig. 2 Percentage of monthly runoff to vegetation runoff (Naryn gauging station)

According to V.A. Kuzmichenok and A.N. Dikikh [7–9], the relative decrease of glacial water part in the river associated with a decreasing of the glacier's area and the attraction of the lower boundary of the firn upwards. In August, the share of runoff did not change, while in September, on the contrary, it increased (about 1%). As shown on Fig. 4 the share of river feeding by melt waters (April–June), on the contrary, increases. Following this trend, the maximum water inflow gradually shifts from July to May–June.

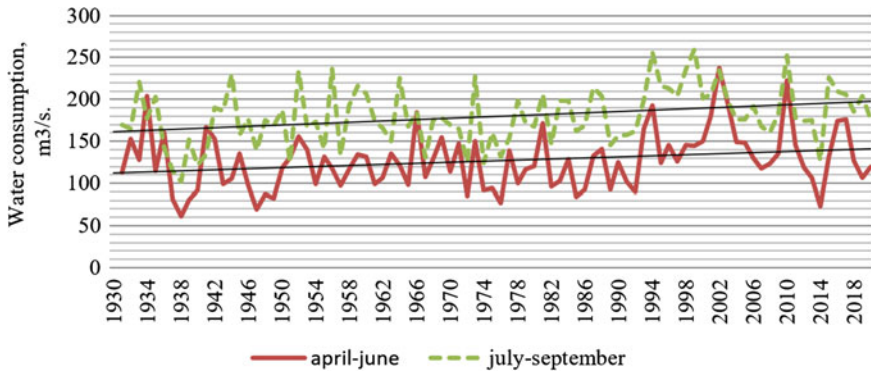


Fig. 3 The ratio of the river's supply of melted snow water (April–June) and melted glacial water (July–September)

The temperature regime of the summer months and precipitation falling on the river catchment during the cold season play a key role in the formation of long-term runoff fluctuations during the vegetation season. In other words, climatic factors determine the formation of runoff [10–13]. For example, over the past 20 years, compared with 1930–1999 [14, 15], the amount of precipitation in the cold seasons of the year has increased, (Fig. 5). So, in October–April in 1930–2019p Precipitation in the upper reaches of the Naryn River increased from 646.8 mm to 1168 mm at the Tien Shan meteorological station and from 977.5 to 1401.8 mm at the Naryn meteorological station. As a result, the flow of the Naryn River also increased [16], as shown in Fig. 1. A.N. Dikikh [7] noted a decrease in the water level in the upper reaches of the Naryn River due to a precipitation decrease during the cold periods of the year in 1930–1998.

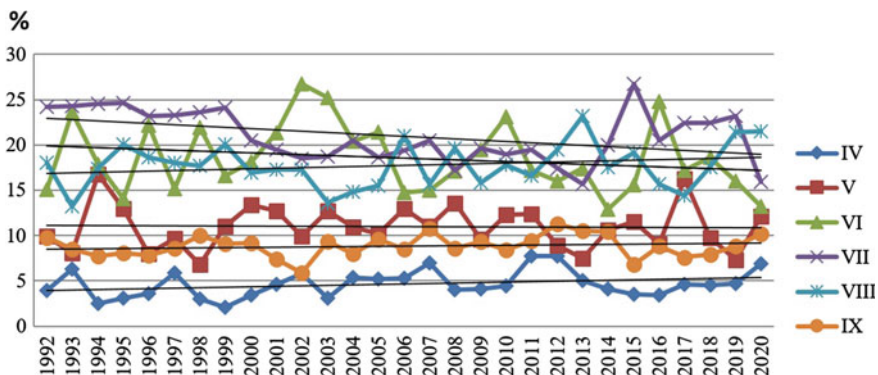


Fig. 4 Changes in the share of monthly runoff in the total runoff of the vegetation season

Analyzing the data of the Naryn and Tien Shan weather stations, we notice climatic conditions changes in the upper reaches of the Naryn River over the past 20–40 years [6].

The sum of positive air temperatures at the Tien Shan weather station increased from 95.4 to 168.7 °C, at the Naryn weather station from 827.4 to 947 °C (Fig. 6).

The number of days with positive temperatures also increased. For example, in the high mountain zone over the past 20 years it increased from 109 to 122 days, and in the middle mountain zone of the river—from 220 to 236 days over the past 40 years. As a result, the air temperature above 0 °C shifted from mid-May–June to April–May at the Tien-Shan weather station, from mid-March to the first half of March at the Naryn weather station [17, 18].

The analysis of the average annual water consumption at the Naryn hydropost and the correlations of the average monthly air temperatures at the Naryn and Tien Shan weather stations showed that the correlation between summer air temperatures and runoff at the Tien Shan weather station is very close (Fig. 7). According to O. Yu Kalashnikova. Studies [19, 20], the summer runoff of the upper reaches of the Naryn River during the vegetation season was 72% of the annual volume. In the summer months, the tendency of the air temperature raised. At the Tien Shan weather station, the air temperature in the summer months of 1930–2019 increased by 1.2 °C (Fig. 8). In the summer months, there is a tendency to increase the air temperature.

In addition to climatic parameters, the vegetation period of runoff is influenced by low water flow (October–March) Fig. 9. For example, Fig. 10 shows that the low water flow runoff has been increasing since 1992. The low water flow runoff was 29.9 m³/s in 1931–1991 and increased by 37.7 m³/s or 120% in the period from 1992 to 2017.

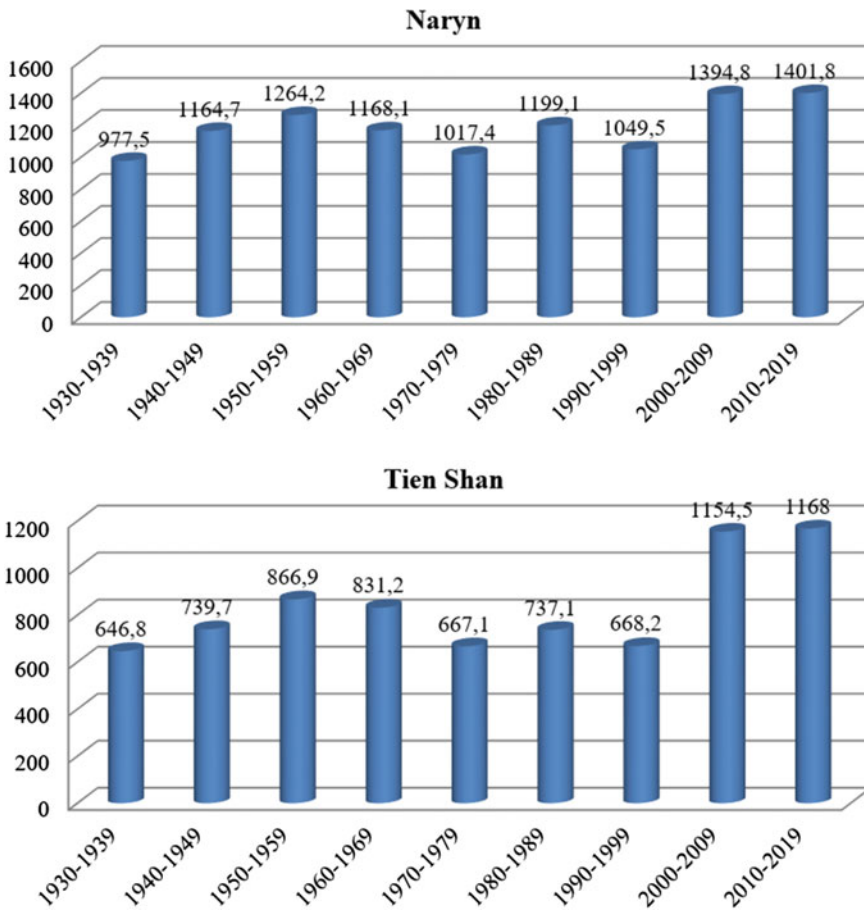


Fig. 5 Changes for precipitation (in mm) from October to April at Naryn and Tien Shan weather stations

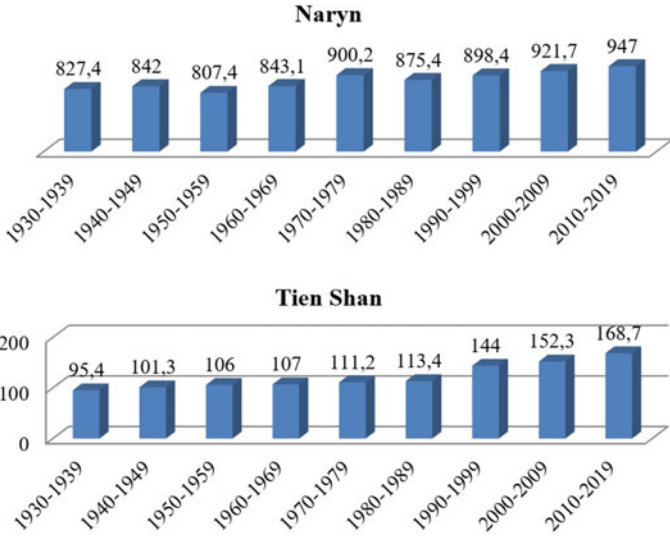


Fig. 6 Sum of average annual positive air temperatures at Naryn and Tien Shan weather stations

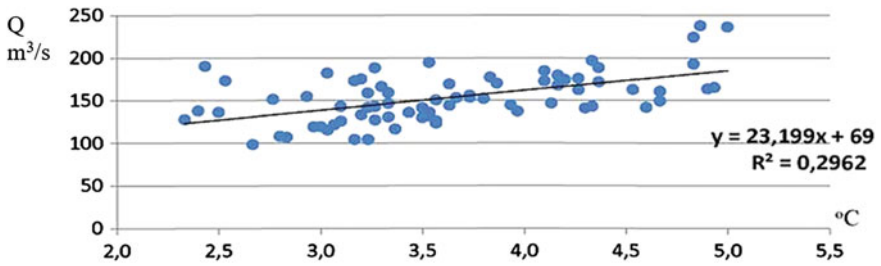


Fig. 7 Dependence of the average vegetation water consumption at the Naryn hydropost on the average air temperature in June–August at the Tien Shan weather station

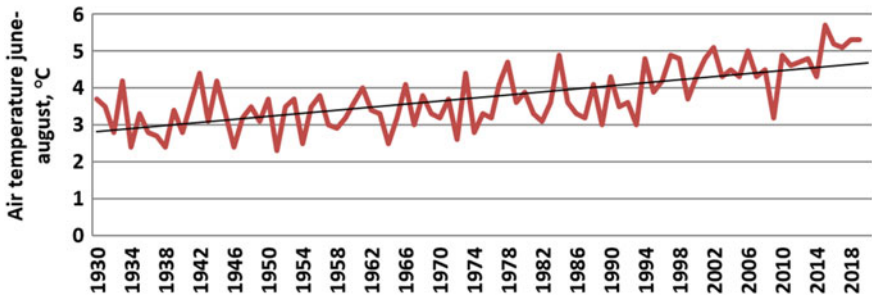


Fig. 8 Changes in the average air temperature in June–August according to the data of the Tien Shan weather station

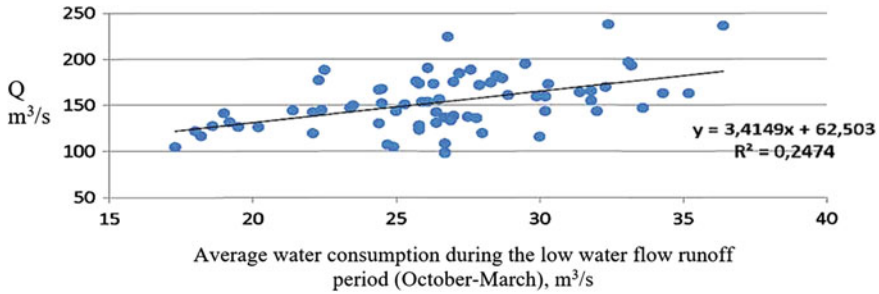


Fig. 9 Dependence of the average vegetation water consumption at the Naryn hydropost on the average water consumption during the low water flow runoff period

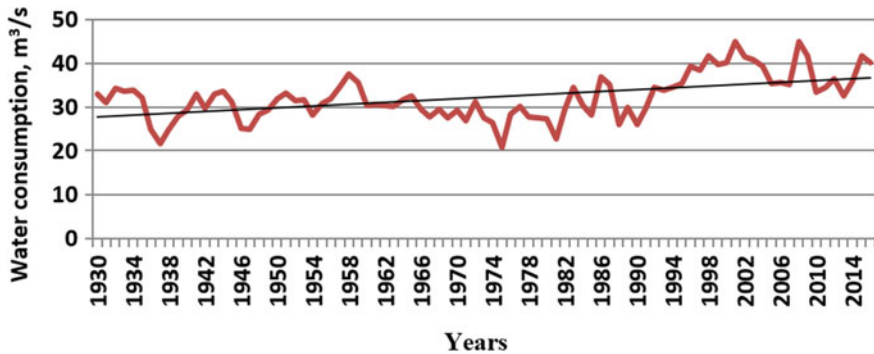


Fig. 10 Change in water consumption of the Naryn hydropost during the low water flow runoff period (m³/s)

6 Conclusion

Since 1992, according to the data of the Narynhydro postwater discharges increased in the upper reaches of the Naryn River. The average vegetation period runoff was 144.7 m³/s in 1931–1991, and over the period from 1992 to 2017 it increased by 173.9 m³/s or 120%. In 1992–2017, the share of runoff in July (powered by melting glaciers) decreased by 10% at the Narynhydro post. In 1930–2019, in the upper reaches of the Naryn River, the amount of precipitation in October–April increased from 646.8 to 1168 mm at the Tien Shan weather station and from 977.5 to 1401.8 mm at the Naryn weather station. The sum of positive air temperatures at the Tien Shan weather station increased from 95.4 to 168.7 °C, and at the Narynweather station from 827.4 to 947 °C.

References

1. Mamatkanov DM, Bazhanova LV, Romanovsky VV (2006) Water resources of Kyrgyzstan at the present stage. Ilim, Bishkek, 60 p
2. Report on the sustainable development of mountain areas, their potential and response to various types of impact (the Naryn river basin) (2005) Project manager, PhD., S.K. Alamanov, Institute of Geology MM Adyshev NAS KR, Bishkek, 109 p

3. Ilyina IA (ed) (1969) Resources of surface waters of the USSR. Vol. 14. Is. 1. Central Asia, River basin Syr Darya, Gidrometeoizdat, Leningrad, 49 p
4. Shults VL (1965) Rivers of Central Asia. GIMIZ, Leningrad, p 91
5. Bolshakov MN (1974) Water resources of the rivers of the Soviet Tien Shan and methods for their calculation. Ilim, Frunze, 26 p
6. Report hydrological forecast for the flow of the Naryn River (2017) Project leader, Doctor of Geographical Sciences, Professor TM Choduraev. Department of Science of the Ministry of Education and Science of the Kyrgyz Republic, Bishkek, 41 p
7. Dikikh AN (1999) Glacial runoff of the Naryn River and the scenario of its possible change with climate warming. *Izv. National AN Kyrgyz Rep. Problems of geology and geography in Kyrgyzstan*, Bishkek, pp 74–79
8. Dikikh AN (2001) Problems and forecast of the development of glaciation and water content of the rivers of Central Asia. *Compilation: Water and sustainable development of Central Asia*, Bishkek, pp 88–92
9. Kuzmichenok VA (2010) Glaciation and runoff in the Naryn river basin. Inventory, temporary changes, forecast. Study of formation factors and assessment of the influence of reservoirs of the Lower Naryn cascade of HPPs on the quality of water resources in the Naryn river basin by isotope methods (according to the results of the ISTC project KR-1430, 2007–2010), Bishkek, pp 19–39
10. Akmatov RT, Alamanov SK, Choduraev TM (2017) The long-term runoff regime of the river. Naryn. Priority directions of development of education and science: collection of materials of the III International Scientific and Practical Conference, Cheboksary
11. Akmatov RT, Alamanov SK, Choduraev TM (2017) Glacial runoff of the Naryn River. Scientific research: theory, methodology and practice. In: *Collection of materials of the III International Scientific and Practical Conference*, vol 1, pp 20–21
12. Akmatov RT, Alamanov SK, Choduraev TM (2019) The role of precipitation and air temperature in the formation of summer runoff. In: VII International Scientific Practical Conference “Modern problems of reservoirs and their catchments”, Perm State University, IOP Conf. Series: Earth and Environmental Science, vol 321, p 012017. <https://doi.org/10.1088/1755-1315/321/1/012017>
13. Akmatov RT, Alamanov SK, Choduraev TM, Pochechun VA (2019) Glacier runoff and regime of rivers with glacial power (a case of study: Naryn river, Kyrgyzstan). In: VII International Scientific Practical Conference “Modern problems of reservoirs and their catchments”, Perm. State University, IOP Conf. Series. Earth and Environmental Science, vol 321, p 012016. <https://doi.org/10.1088/1755-1315/321/1/012016>
14. Akmatov RT (2018) The perennial flow of the Naryn River, its distribution during the year. *Izv. University of Kyrgyzstan* 11:84
15. Akmatov RT (2018) Changes in the regime of atmospheric precipitation in the upper part of the Naryn river basin. *Izv. University of Kyrgyzstan* 11:87
16. Alamanov SK, Lelevkin VM, Podrezov AO et al (2006) Climate change and water problems in Central Asia. Textbook for Universities, OAO IPO Lev Tolstoy, Moscow, Bishkek, p 107
17. Akmatov RT (2022) Geocological influences of large reservoirs in Kyrgyzstan. Dissertation, Bishkek, 122 p
18. Akmatov RT (2021) Changes in the thermal regime in the upper part of the Naryn river basin. *Science, New Tech Innov to Kyrgyzstan* 4:18–19
19. Kalashnikova OY (2003) On the issue of hydrological forecasts of spring-summer runoff of mountain rivers, collection of scientific papers. *Mete Hydrol Kyrgyzstan. KRSU* 3:14–22
20. Kalashnikova OY (2022) Study of the influence of climatic factors on the formation of runoff in the rivers of the Naryn basin and their long-term forecast. Dissertation, Bishkek, 57 p



Subject-Economic Groups for the Information-Measuring System for Determining the Ecological Well-Being of a Person

D. V. Martynov¹(✉), O. E. Bezborodova², O. N. Bodin¹, M. Yu Rudyk¹,
and A. A. Trofimov²

¹ Penza State Technological University, 1a / 11, Baidukova str. / Gagarin str., Penza 440039,
Russia

dimka.martinov.95@gmail.com

² Penza State University, 40, Krasnaya str., Penza 440026, Russia

Abstract. The article examines the problem of choosing corrective measures to ensure the ecological well-being of a person in the territorial technosphere. The purpose of the study is to develop a methodology for the reasonable choice of corrective measures. To achieve the goal, it is proposed to use the relative risk as a measure of the ecological well-being of a person. Based on Pigou's model of environmental externalities, an algorithm for creating a list of corrective measures for two situations is proposed: when the actual risk values exceed the norm and the decision maker needs to know how much investment is needed to improve the environmental well-being of a person; when the decision maker has some financial resources at his disposal and it is necessary to find out how the ecological well-being of a person will change if they are invested in appropriate activities. The results obtained allow us to conclude that the use of risk as a measure of a person's environmental well-being, as well as subject-economic groups, makes it possible to form a list of corrective measures, taking into account the mutual influence of the components of the territorial technosphere and the combined action of risk factors.

Keywords: Environmental human well-being · Territorial technosphere · Risk · Subject-economic group · Corrective measures

1 Introduction

Currently, there is a problem of ensuring the environmental human well-being in the territorial technosphere. The source of this problem is a historically formed approach based on the assessment of the quality of individual elements of the territorial technosphere. Such an approach does not take into account the mutual influence of elements of the territorial technosphere (neutralism, predation, parasitism, competition, symbiosis) and the joint action of risk factors (synergism, antagonism, summation), does not allow solving

the problem comprehensively, increasing the effectiveness of corrective measures [1–3]. Taking into account these features will increase the reliability of the assessment of human environmental well-being in the territorial technosphere; increase the environmental efficiency of the technosphere object; reduce the risk of negative impact of technosphere objects on the functional state of the human body and the environment; save resources for determining individual parameters of elements of the territorial technosphere [4–7].

To solve this problem, it is necessary to develop an information and measurement system for determining the environmental human well-being which allows measuring parameter control of the components in the territorial technosphere, operational analysis of measurement control data (assessment, modeling, forecasting), comparative analysis and zoning of the territorial technosphere for the environmental human well-being, forming a list of corrective measures (therapeutic and preventive (LPM), environmental (POM), technological (TM)) with an indication of their effectiveness and implementation costs [8–10]. At the same time, measurement control is understood as control carried out with the use of measuring instruments [11].

To form a reasonable list of corrective measures, a special methodology is required to establish the relationship between the environmental human well-being in the territorial technosphere and the need to implement corrective measures.

The purpose of the study is to develop a methodology for the reasonable selection of corrective measures.

To achieve the purpose, the authors set and solved the following objectives:

- to substantiate and propose a measure for determining the environmental human well-being in the territorial technosphere;
- to establish the relationship between the environmental human well-being in the territorial technosphere and the cost of corrective measures;
- to propose an algorithm for the formation of a reasonable list of corrective measures.

The objects of research are subject-economic groups (SEG) (medico-economic (MEG), environmental-economic (EEG), industrial-economic (IEG)) to provide the environmental well-being of a human in the territorial technosphere.

The study was conducted using an integrated system approach and methods of analysis and synthesis, grouping and generalization.

2 Materials and Methods

As a measure of human environmental well-being, the authors propose to use relative risk (hereinafter referred to as a “risk”) [12], showing the existence of a link between the risk factor and a change in the state of the studied component of the territorial technosphere (human, environment, object of the technosphere). In statistics, relative risk is the ratio of the frequency of consequences among the studied objects that were influenced by the risk factor (P_{exposed}) to the frequency of consequences among the studied components of the territorial technosphere that were not influenced by this factor ($P_{\text{non-exposed}}$) [13]

$$R = P_{\text{exposed}} / P_{\text{non-exposed}} \cdot \quad (1)$$

Table 1 Ratio of the consequences of exposure to the risk factor

Presence of a risk factor/Presence of consequences	Yes	No	Total
There is a risk factor (1)	a	b	$a + c$
No risk factor (0)	c	d	$b + d$
Total	$a + c$	$b + d$	$a + b + c + d$

Table 1 shows the relationship between the risk factor, the aftermath of its impact and the number of analyzed territorial technosphere components.

This table shows the a, b, c, d as the number of objects under study that have certain ratios of the values of the impact of the risk factor and the consequences.

The value of risk (R) is determined by the formula

$$R = \frac{a/(a + b)}{c/(c + d)} \quad (2)$$

The resulting risk value is compared with the value 1 in order to define the nature of the relationship between the risk factor and the consequences of its impact on the object.

If $R = 1$, thus, the studied risk factor has little effect on the state of the territorial technosphere component.

At values $R > 1$, the risk factor significantly affects the state of the territorial technosphere component increasing the frequency of aftermath occurrence.

At values $R < 1$, the risk factor does not affect the state of the element of the territorial technosphere.

Obtain the values of the boundaries of the confidence interval with a confidence probability of 95%.

The formula for calculating the upper limit of the confidence interval

$$R^{up.line} = e^{\ln(RR)+1,96\sqrt{\frac{b}{a \cdot (a+b)} + \frac{d}{c \cdot (c+d)}}} \quad (3)$$

The formula for calculating the lower limit of the confidence interval

$$R^{bot.line} = e^{\ln(RR)-1,96\sqrt{\frac{b}{a \cdot (a+b)} + \frac{d}{c \cdot (c+d)}}} \quad (4)$$

If both boundary values ($R^{up.line}, R^{bot.line}$) are on the same side with 1, i.e. the confidence interval does not include 1, we draw a conclusion on the statistical significance of the revealed relationship between the factor and the outcome with the probability of error $P < 0, 05$.

If the lower limit of the 95% confidence interval is less than 1, and the upper one is greater, it is concluded that there is no statistical significance of the risk factor impact on the frequency of consequences, regardless of the value R ($P < 0, 05$).

To form a reasonable list of corrective measures, the authors introduced the concept of a “subject-economic group” of parameters as a set of data (medical-economic, environmental-economic and industrial-economic) characterizing the state of the territorial technosphere components, expressed in terms of risk values, and allowing one to

reasonably form a list of therapeutic and preventive, environmental and technical measures, the implementation of which facilitate the reduction of risk to human health to safe values and increase human environmental well-being [14].

Each subject-economic group consists of data collected according to certain templates (questionnaires, schemes, etc.). Each subject-economic group includes several states of the territorial technosphere characterized by certain risk values (R_{\min} , R_{low} , $R_{moderate}$, R_{high}) and organized according to the principle of similarity of risk factors affecting humans, the environment, technosphere objects, measurement control procedures, modeling and forecasting of human environmental well-being, corrective measures.

The subject-economic group of parameters combines the initial data, measurement control data of each territorial technosphere component, reference data and calculation results obtained by the information and measurement system for determining human environmental well-being. These data are accumulated and combined into databases that have the following structure.

The subject-economic group of parameters is divided into three parts: general, subject (medical, environmental and technological) and economic.

The general part contains data that allows converting the request of the decision-maker into an action plan for fulfilling such a request. These are, first of all, data that characterize the territorial technosphere for which the environmental human well-being is determined (geographical coordinates of the territory or the administrative name of the district). As well as data specific to this group, for example, one or more risk factors for which it is necessary to assess the environmental human well-being or an age, professional or social group of the population for which it is necessary to assess environmental well-being.

The subject part includes three subgroups of parameters: reference data, measurement control data and calculation data.

The subgroup of reference data includes reference books containing reference data and constants characterizing the properties and possible states of a human, the environment and objects of the technosphere.

The subgroup of measurement control data includes the results of measurement control obtained during the monitoring of the functional state of the human body, environmental and sanitary-hygienic monitoring, monitoring of technological processes.

The calculated subgroup of parameters contains the results obtained using reference data and measurement control data, that is, the results of intermediate and final calculations.

The economic part includes data on the content and cost of corrective measures aimed at improving or maintaining the necessary environmental well-being of a human. These data can be obtained from reference books of the best available technologies and correspond to risk ranges by qualitative and quantitative characteristics.

For each part, standards are generated, consisting of measures in various combinations, taking into account not only the need for improving human environmental well-being, but also the ability of a technosphere object or a state structure to additionally invest in the implementation of corrective measures.

The composition of the general part of each medical and economic group, in addition to the geographically determined parameters of the territorial technosphere necessary for defining the index of environmental comorbidity (geoclimatic, environmental and social features of the region of human residence), includes the name of the nosological form and the code assigned to it according to the ICD-10 classification, the average duration of treatment for this group or organ system.

The subgroup of reference data of the medical part contains data on the maximum permissible values of risk factors for human health, expressed in absolute units, for example, the maximum permissible concentrations of heavy metal salts in organic liquids, threshold toxodoses of chemicals. As well as templates for filling in personally determined parameters to determine the index of environmental comorbidity (age, time of residence in the natural and climatic zone, the presence of disability and occupational pathologies).

This subgroup also contains criteria for restoring health and the average duration of treatment.

The subgroup of measurement control data of the medical unit contains data on the names and number of laboratory and instrumental diagnostic measures (measurement control). The data is provided with links to the relevant standards.

The calculated subgroup of the parameters of the medical part contains the results of calculating the functional state of the human body, the index of environmental comorbidity and health risk for each risk factor separately (r_i^{HUM}), health risk for all risk factors (R_j^{HUM}) and risk in the territorial technosphere (R_j^{TT}).

The economic part contains data on the necessary therapeutic and preventive measures (medication, physiotherapy, surgical treatment, medical and nursing procedures, nutrition, sanitary and hygienic treatment) as well as the quantitative data on the cost of treatment, medicines, consumables, tools, food, etc.

The general part of each environmental and economic group, in addition to data that allows converting a decision-maker's request into an action plan for fulfilling the request, includes data on environments (atmosphere, lithosphere, hydrosphere) and risk factors of greatest interest to operational analytics.

The subgroup of reference data of the environmental part contains reference books of maximum permissible values of risk factors (chemical, physical, biological) in various environments (atmosphere, lithosphere, hydrosphere) and for various conditions (in the air of the working area, average daily, maximum one-time, settlements, residential premises, etc.; in the water of fishing ponds, cultural-household use, drinking, etc.).

The subgroup of measurement control data includes the results of measuring background and actual concentrations of chemicals, microbiological objects in various media and the actual levels of physical impacts.

The subgroup of calculated parameters includes the results of calculating environmental indices, as well as environmental risk for each risk factor separately (r_i^{ENV}), environmental risk for all risk factors (R_j^{ENV}) and risk in the territorial technosphere (R_j^{TT}).

The economic part contains data on the cost of environmental protection measures (liquidation of landfills, reclamation of land plots, planting of certain types of green

spaces, making up some protected areas (reserves, nature reserves), organizing sanitary protection zones), the amount of payment for negative environmental impact.

Each production and economic group includes a set of parameters that characterize the intensity of formation of risk factors during technological processes. Production and economic groups consist of data characterizing the operation of technological, environmental protection equipment, local treatment facilities and waste management systems collected according to certain templates (questionnaires, schemes, etc.).

The general part of the production and economic group includes industry affiliation and operating modes of enterprises in the region (number of working days per year, shift).

The subgroup of reference data of the technical part contains a list of technosphere objects located in this region, for each of these objects the names of technological equipment units (main, environmental protection, cleaning), the name and volumes of raw materials and materials used, technical and technical characteristics, adopted environmental impact standards (standards of permissible emissions, discharges, waste generation, physical impacts).

The subgroup of measurement control data includes the results of measurement control in manual and automatic modes of temperature ($^{\circ}\text{C}$), humidity (%), air velocity (m/s), mass release of chemicals (kg/h); volumetric water flow (m/h), temperature of discharged wastewater ($^{\circ}\text{C}$); hydrogen index of discharged wastewater (pH), chemical oxygen consumption (mg/dm), as well as the indicators of physical and biological risk factors.

The subgroup of calculated parameters includes the results of calculating gross emissions, discharges, waste generation volumes, as well as technogenic risk for each risk factor separately (r_i^{OT}), technogenic risk for all risk factors (R_j^{OT}) and risk in the territorial technosphere (R_j^{TT}).

The economic part contains quantitative data on the cost of technological measures, including the use of the best available technologies.

Figure 1 shows the relationship of human health risk (R_j^{HUM}), technogenic (R_j^{OT}) and environmental (R_j^{ENV}) with the costs for providing human environmental well-being.

The relationship between the values of risk factors and the costs of implementing corrective measures in each of the subject-economic groups is obtained on the basis of the conventional model of environmental externalities by A. Pigou [15].

The essence of the adaptation of Pigou's approach to the definition of environmental well-being of a human consists in the fact that the object of the technosphere, which is a risk source, carries out therapeutic, preventive, environmental and technical measures (costs) aimed at reducing (excluding) this risk, the amount of which should be sufficient to reduce (eliminate) this risk.

The "Pigou's approach" to determining the cost of measures that correct the values of risk factors is to include the costs of implementing corrective measures in the total costs of (G_S)

$$G_S = G_P + P, \quad (5)$$

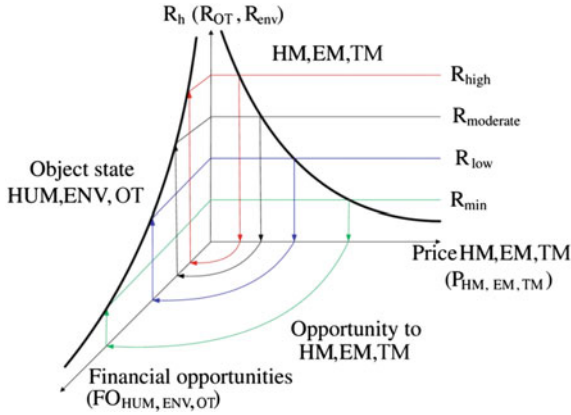


Fig. 1 The relationship between risks and costs of ensuring human environmental well-being

where G_P —production costs of the TO, P —the costs of implementing the entire set of corrective measures as part of the subject-economic groups, determined by the formula

$$P = \sum_{i=1}^n P_i^{HM} + \sum_{i=1}^m P_i^{EM} + \sum_{i=1}^k P_i^{TM}, \tag{6}$$

where P_i^{HM} , P_i^{EM} , P_i^{TM} is the cost of implementing corrective measures aimed at minimizing and/or eliminating the i -th risk factor as part of medical-economic, environmental-economic, industrial-economic groups.

The costs of implementing each corrective action depend on the required risk reduction

$$P_i^{HM(EM, TM)} = f\left(R_i^{HUM(ENV, OT)}\right). \tag{7}$$

3 Results and Discussion

A simplified diagram of the information and measurement system for determining the environmental well-being of a human in the territorial technosphere is shown in Fig. 2a. It includes tools for determining the values of risk factors (3), data entry tools (4), an environmental monitoring device (5) containing software tools for identifying risk factors (5.1), software tools for determining human environmental well-being (5.2), software tools for forming a list of corrective measures (5.3), computing devices (5.4) and the database (5.5) [16].

The means for determining the values of risk factors (3) are laboratory devices and equipment where, in accordance with sanitary and hygienic requirements following GOST, the content of technogenic impurities is determined in samples taken simultaneously during the year from atmospheric air, soil and wastewater. The results of instrumental control of risk factors and all data obtained by the computing device (5.5) are stored

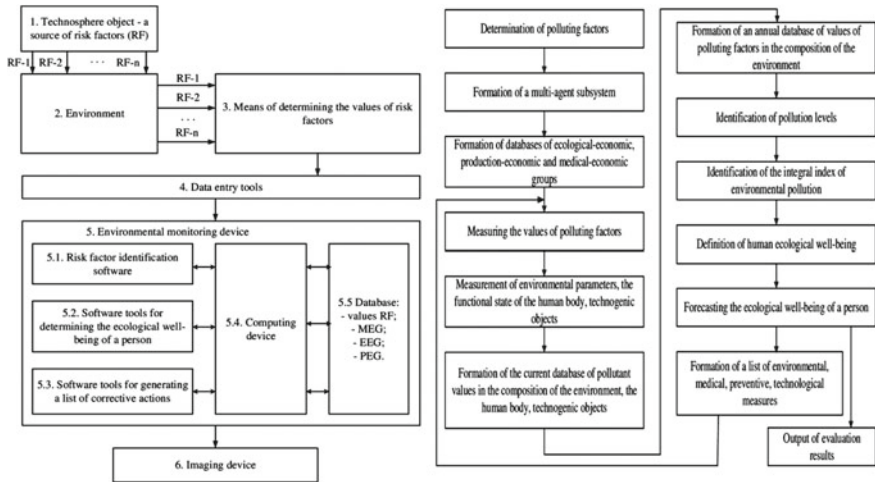


Fig. 2 a Simplified scheme of the system for determining the environmental well-being of a human in the territorial technosphere; **b** scheme of the algorithm of the proposed method for determining the environmental well-being of a human

in a database of risk factor values. The database (5.5) also contains subject-economic groups of parameters.

With the accumulation of a sufficient number of measurement results for a specified period, using software tools for identifying risk factors (5.1), the environmental well-being of a human in the territorial technosphere is determined (5.2). Depending on the values obtained, using which software tools for forming a list of corrective measures (5.3) implementing Pigou's method, make a list of corrective measures, the implementation of which leads to an increase in human environmental well-being. This list is displayed in the prescribed form on the visualization devices (6) for presentation to the decision-maker.

The scheme of the algorithm for implementing the proposed method to assess the environmental well-being of a human in the territorial technosphere in order to form a list of corrective measures is shown in Fig. 2b.

When forming a list of corrective measures, two approaches are possible [17–19].

Firstly, when the actual risk values exceed the norm and the decision-maker needs to know how much investment will be required to improve the environmental well-being of a human in the considered territorial technosphere (see Fig. 3a).

Secondly, when the decision-maker has some financial resources at its disposal and it is necessary to find out how the environmental well-being of a human will change if they are invested in appropriate measures (see Fig. 3b).

At the same time, it is possible to form a list of corrective measures with a gradual reduction of risk in the territorial technosphere, if the object of the technosphere does not currently have the necessary amount of funds to implement the entire set of measures proposed by the system.

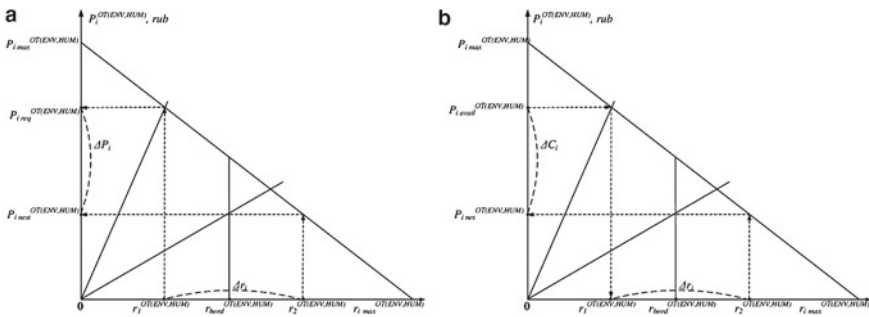


Fig. 3 Improved Pigou graphs for the reasonable formation of a list of environmental, therapeutic, preventive and technological measures for two situations: **a** when the risk is known, and it is necessary to determine the amount of funds to reduce it, **b** when it is necessary to determine which risk reduction will be achieved due to the investment of available funds

4 Conclusions

Currently, one of the problems is to provide the environmental human well-being in the territorial technosphere. In the course of the conducted research, some tools have been developed for the reasonable choice of corrective measures to ensure human environmental well-being. A measure for determining the environmental well-being of a human in the territorial technosphere is substantiated and proposed. The relationship between the environmental well-being of a human in the territorial technosphere and the cost of corrective measures is shown. The scheme of the information and measurement system for determining the environmental well-being of a human and the algorithm for forming a reasonable list of corrective measures have been developed. The concept of a “subject-economic group” of parameters is proposed as a set of data (medical-economic, environmental-economic and industrial-economic) characterizing the state of the territorial technosphere components expressed in terms of risk values, and allowing reasonably forming a list of therapeutic, preventive, environmental and technical measures, the implementation of which facilitates the reduction in the risk for human health to safe values and increases human environmental well-being.

References

1. Kiselev MV et al (2018) Automatic meteorological measuring systems for microclimate monitoring. In IOP Conference Series: Earth Environmental Science 190:012031. <https://doi.org/10.1088/1755-1315/190/1/012031>
2. Bazarov A et al (2018) Mobile measurement system for the coupled monitoring of atmospheric and soil parameters. Russ Meteorol Hydrol 43:271–275. <https://doi.org/10.3103/S106837391804009X>
3. Korolkov VA et al (2015) Pilot project of measuring and computing system for mesoscale monitoring of atmospheric boundary layer. In: 21st International Symposium on Atmospheric and Ocean Optics: Atmospheric Physics, Proceedings of SPIE 9680, 96805. <https://doi.org/10.1117/12.2205475>

4. R 2.1.10.1920-04. Guidelines for assessing the risk to public health from exposure to chemicals that pollute the environment
5. Kovalevskaya OY, Blinovskaya YY, Agoshkov AI, Vasyanovich YA, Petukhov VI, Doryshev YS (2013) The risk of emergencies during the operation of offshore oil platforms. Problems of development of georesources of the Far East. Issue 4: Mining information and analytical bulletin (scientific and technical journal). Individual articles (special issue), no. 12, 144 p
6. Mamelina TY, Pushkareva AV, Veipan VE (2021) The software complex for biochemical indicators monitoring taking into account ecological background of the region. J Phys: Conf Series 1889(3)
7. Zhigula LD, Petukhov VI, Zhigula EA (2013) Criteria for identifying natural hazard factors and problems of risk management in the field of recreation. Modern problems of science and education, no. 3. <http://science-education.ru/ru/article/view?id=9182>. Accessed 04.08.2023
8. Bezborodova OE (2022) Intelligent information-measuring and control system for control of the state of the territorial technosphere. Izmereniya. Monitoring. Upravlenie. Kontrol' = Measurements. Monit Manag Cont 2:21–28. <https://doi.org/10.21685/2307-5538-2022-2-3>
9. Bezborodova OE (2022) Hierarchical structure of a multi-agent system. Izmereniya. Monitoring. Upravlenie. Kontrol' = Measurements. Monit Manag Cont 2:29–38. <https://doi.org/10.21685/2307-5538-2022-2-4>
10. Mikhailov PG, Ualiyev Z (2020) Issues of ensuring the stability of thin-film heterostructures of multifunctional sensors of information-measuring systems. In: International Multi-Conference on Industrial Engineering and Modern Technologies, FarEastCon 2020
11. GOST R 50.05.08-2018, Conformity assessment system in the field of atomic energy use. Conformity assessment in the form of control, unified methods. Visual and measuring control
12. Petrov VI, Ryazanova AY (2021) Basic statistical knowledge necessary for the interpretation of modern data from clinical studies. Med Bull 1(81):3–11
13. Bezborodova O, Bodin O, Martynov D (2023) Forecasting the state of the environment based on the assessment of technogenic risk. AIP Conf Proc 2700(1):050002. <https://doi.org/10.1063/5.0127012>
14. Golovanov AV, Kovalev IV, Chistyakova OB, Tyukov DI, Kuznetsova NV, Grishko BV, Rogalev VI, Berezina NI, Dolinina VV (2006) Method and system for optimizing therapeutic and diagnostic medical care. Patent No. 2325100 RF, 3MPK, A61B5/00
15. Stokov AS, Ternovskiy DS, Potashnikov VY, Potapova AA (2020) Assessment of environmental externalities as consequences of foreign trade expansion. J New Econ Assoc 4(48):113–137. <https://doi.org/10.31737/2221-2264-2020-48-4-5>
16. Bezborodova OE (2022) Information-measuring system for assessing the ecological well-being of a person. Models, Syst, Netw Econ, Techn, Nat Soc 4(44). <https://cyberleninka.ru/article/n/informatsionno-izmeritelnaya-sistema-dlya-otsenki-ekologicheskogo-blagopoluchiya-cheloveka>. Accessed 05.20.2023
17. Afanasiev SV, Lukmanov AD, Karimov GR (2021) Environmental protection measures in the rural settlement of the Meselinsky Village Council of the Aurgazinsky District of the Republic of Bashkortostan. Priority areas of regional development: Collection of articles based on materials of the II All-Russian (national)) scientific and practical conference with international participation, Kurgan State Agricultural Academy. T.S. Maltseva, Kurgan, pp 331–334
18. Kravets ED (2015) Efficiency of therapeutic and preventive measures to improve the health status of workers in the petrochemical industry. Occupational Med Human Ecol 4. <https://cyberleninka.ru/article/n/effektivnost-lechebno-profilakticheskikh-mer-po-ozdorovleniyu-sosvoyaniya-zdorovya-u-rabotnikov-neftehimicheskoy-promyshlennosti>. Accessed 05.20.2023

19. Manzhilevskaya SE, Petrenko LK, Alshenko DN (2019) Organizational, technological and urban planning measures aimed at improving the level of environmental safety of the territory of Rostov-on-Don. Bull Eurasian Sci 4. <https://cyberleninka.ru/article/n/organizatsionno-technologicheskiei-gradostroitelnye-meropriyatiya-napravlennye-na-povyshenie-urovnya-ekologicheskoy-bezopasnosti>. Accessed 05.20.2023



Removing Biogenic Elements from Urban Sewage: Technology Review

M. Dyagelev^(✉)

Kalashnikov Izhevsk State Technical University, 7, Studencheskaja, Izhevsk 426069, Russia
m.yu.dyagelev@istu.ru

Abstract. Protecting the environment and water bodies from pollution and depletion is one of the key problems of today's world. Aggravating pollution of water sources due to insufficient capacities and efficiency of the existing sewage treatment facilities, as well as the discharge of poorly-treated or untreated sewage, causes the violations of the sanitary, chemical, and hydrobiological regimen of water bodies. The increased content of nitrogen and phosphorus compounds in sewage propagates eutrophication leading to the destruction of water flora and fauna. The removal of biogenic elements from sewage in current conditions is one of the key problems in wastewater treatment. This article analyzes the existing techniques of nitrogen and phosphorus compound removal from wastewater as the most efficient and affordable method of sewage treatment. The authors analyzed research and review publications from international citation bases. Further, they compared the advantages and disadvantages of biogenic element removal techniques based on the analysis performed. The authors compared the following techniques: A/O (anaerobic/oxic), AA/O (anaerobic/anoxic/oxic), the UCT (University of Cape Town) process, the Modified UCT process, the Bardenpho process, and the JHB (Johannesburg) process.

Keywords: Sewage · Biogenic elements · Sewage treatment · Nitrogen removal · Nitrification · Denitrification · Phosphorus removal

1 Introduction

Sewage treatment is one of the key components of environmental protection [1]. New trends and approaches have been arising in this area that form the notion of the 21st Century Equipment and Technology that aim to solve problems not considered before. According to the existing views, the main cause of the deterioration of potable water quality is the eutrophication of surface sources [2–5].

The increased content of nitrogen and phosphorus compounds in sewage propagates the weediness of water (eutrophication), which causes the destruction of water flora and fauna. The removal of biogenic elements from sewage in current conditions is one of the key problems in wastewater treatment. Therefore, it is necessary to improve the efficiency of nitrogen and phosphorus compound removal from wastewater. Of all the

possible methods (biological, chemical, and physical/chemical) used to remove these compounds from wastewater, the biological method of treating large volumes of urban sewage is the most efficient and affordable [6–9].

The biological method of the deep removal of biogenic substances (nitrogen and phosphorus) from the wastewater combining aerobic, anoxic, and anaerobic treatment stages allows achieving a total content of phosphorus of 1.0–1.5 mg/dm³ and a total content of nitrogen of 8–10 mg/dm³ (including proteins, ammonia, nitrite, and nitrate) in the treated water using actual biological treatment facilities [10, 11].

The purpose of this research work is to review the key biogenic element removal techniques and determine their advantages and disadvantages during both the construction and operation.

2 Theoretical Basis

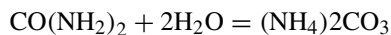
Global practice includes several conventional combinations [6–11] of anaerobic and aerobic treatment stages for the deep removal of biogenic elements from the sewage of various compositions.

Biogenic elements are substances that can always be found in organisms where they perform specific biological functions. Key biogenic elements include oxygen, carbon, hydrogen, nitrogen, phosphorus, sulfur, calcium, potassium, sodium, and chlorine. All of these elements take a significant part in the biological processes occurring in the environment, including the water bodies [11].

Wastewater treatment practices focus on two main biogenic elements: nitrogen (N) and phosphorus (P).

Wastewater nitrogen can be found in several compounds: ammonia nitrogen (NH₄⁻), nitrite nitrogen (NO₂⁻), nitrate nitrogen (NO₃⁻), and organic nitrogen (as part of organic compounds).

The presence of nitrogen compounds in wastewater is a result of the decomposition of proteins found in household sewage. Through metabolism, proteins in living beings produce urea CO(NH₂)₂ that undergoes hydrolysis induced by putrefactive bacteria in wastewater, which results in the production of ammonium salt nitrogen [12]:



Most of the nitrogen in wastewater is in this state of ammonium carbonate. Further on, ammonium carbonate can decompose and produce ammonia. Ammonia production occurs according to the following equation:



The production of various amounts of ammonia, nitrites, and nitrates can indicate protein oxidation stages and treatment facility operation specifics, and it can be used to assess the sanitary condition of water bodies.

Phosphorus compounds can be found in household sewage in different states: dissolved, colloidal, and suspended. Insoluble phosphorus is mostly found in suspended particles, as well as poorly-soluble phosphates and proteins. Insoluble phosphorus is

bound with other compounds and does not react to biological treatment. Most of the phosphorus compounds in the sewage that needs to be treated are made up of colloidal or dissolved phosphates, orthophosphates, and dissolved polyphosphate forms. Organic phosphorus in household sewage mainly includes human metabolites, organic polyphosphates (nucleic acids), as well as human and hydrobiont wastes. The dissolved mineral phosphorus is represented by orthophosphoric acid and its anions (H_2PO_4^- , PO_4^{2-} , PO_4^{3-}) [11].

Currently, there are several methods and techniques for the biological removal of nitrogen and phosphorus. There are numerous variations of biological treatment options aiming for the removal of specifically nitrogen or phosphorus, as well as the simultaneous removal of both elements [13–21].

3 Materials and Methods

The review of the techniques used in different countries for the biogenic element removal from sewage scopes the publications dating from 1965 to 2023. We worked with Russian and foreign databases, such as Elibrary, Science Direct, PubMed, and Global Pesticide Bans, as well as the Yandex and Google search engines using keywords like biogenic elements, biogenic element removal from wastewater, nitrogen removal, nitrification, denitrification, phosphorus removal. The obtained information was compared with the existing laws of the Russian Federation, European Union, USA, and China, and systematized according to the sections of the article.

4 Results

All of the flow charts for wastewater biogenic element removal can be divided into two groups. The first group includes the options with oxidation ditches, and the second one includes the options that can be implemented in regular corridor aerotank. The second group is interesting in terms of re-technification (the replacement of some of the existing water treatment technology that is morally and/or physically obsolete with new technology to improve the efficiency of treatment without significant capital costs). Based on the number of mixing and aeration zones [22, 23], there can be two-, three-, four-, and five-stage options.

The main flow chart organization options are as follows: A/O (anaerobic-oxic) (Fig. 1), AA/O (anaerobic-anoxic-oxic) (Fig. 2), the UCT process (University of Cape Town) (Fig. 3), the Modified UCT process (Fig. 4), the Bardenpho process (Fig. 5), the JHB process (Johannesburg) (Fig. 6) with different modifications, etc. The flow charts of these biogenic element removal techniques are reviewed below [24–43].

Following the flow chart shown in Fig. 1, the return sludge is mixed with the incoming sewage and supplied to the anaerobic reactor. Further, wastewater undergoes aerobic treatment and enters the secondary sedimentation tanks. This is the simplest and cheapest nitrogen and phosphorus compound removal option. However, it can only be used for industrial sewage with high active sludge loads in terms of carbon-bearing organics, and moderate nitrification with high concentrations of phosphorus compounds. Low-load

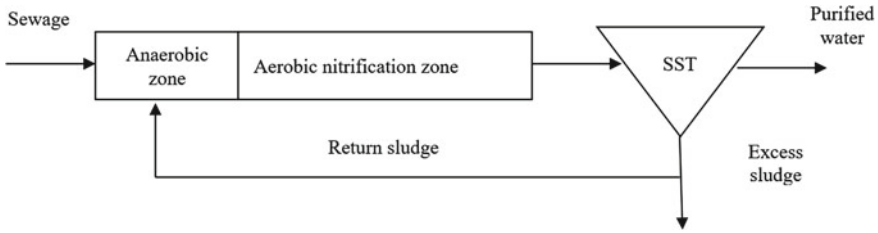


Fig. 1 The A/O (anaerobic-oxic) flow chart

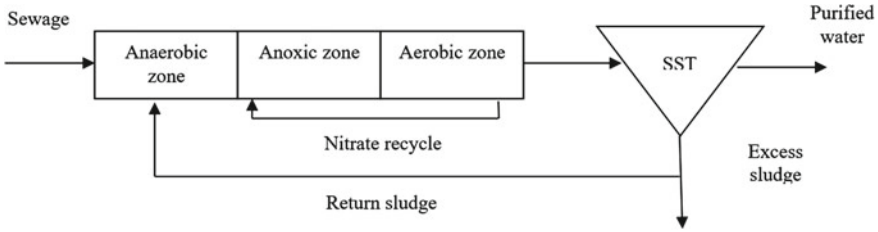


Fig. 2 The AA/O slow chart

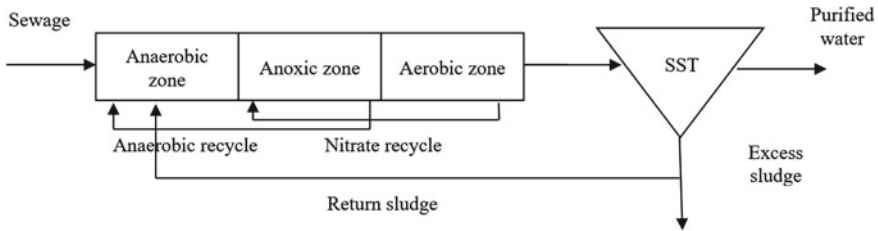


Fig. 3 The UCT process flow chart

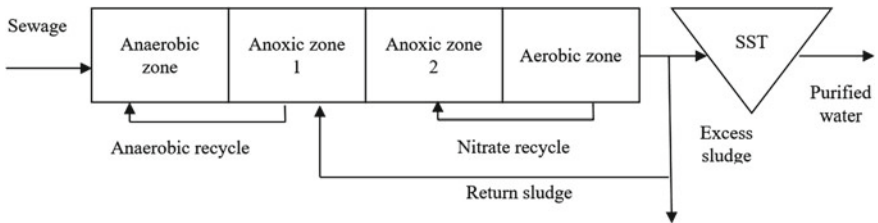


Fig. 4 The modified UCT process flow chart

facilities feature an additional anoxic stage for more efficient removal of nitrate and nitrite nitrogen.

The AA/O (Anaerobic/Anoxic/Oxic) process is designed to remove nitrogen and phosphorus. This process includes a sequence of anaerobic, anoxic, and aerobic zones.

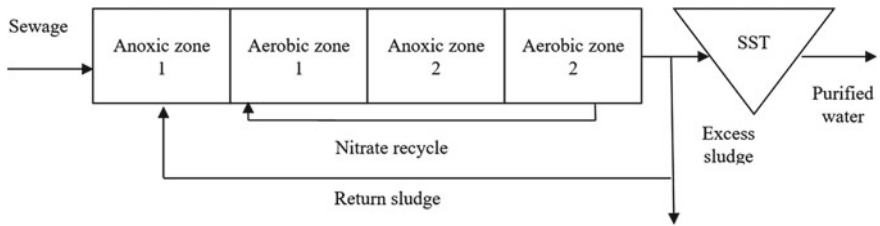


Fig. 5 The Bardenpho process flow chart

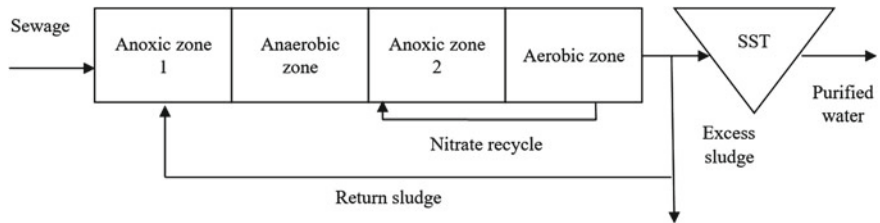


Fig. 6 The JHB process flow chart

In the AA/O process, the anaerobic, anoxic, and aerobic zones are split into several perfect mixing compartments.

The UCT process was proposed at the University of Cape Town in 1984. It is a modification of the previous processes with three recirculating flows (the previous processes had two). This option allows for the minimization of nitrates entering the anaerobic zone of the facility thus improving the efficiency of the biological removal of phosphorus. Unlike the options reviewed above, this process supplies the return sludge recycle and nitrate recycle to the anoxic zone.

This process includes a sequence of anaerobic, two anoxic, and aerobic zones. The first anoxic zone in this process is designed to remove nitrate nitrogen from the return sludge, and the second anoxic zone removes the nitrates formed during the nitrification in the aerobic zone to assure the required quality of treated water in terms of N-NO_3 .

The key factors affecting the efficiency of the biological removal of phosphorus include the time of sewage stay in the anaerobic zone, the time of stay in anoxic and aerobic zones, the amount of easily oxidable organic compounds, the age of active sludge, and the concentration of nitrates in the anaerobic zone.

This treatment option is well-known and widespread in Europe. It allows for the efficient removal of nitrogen and phosphorus compounds at low-load facilities. Its name can be broken down as follows: Bar—its developer, Barnard, den—denitrification, pho—phosphorus removal).

In this process, wastewater treatment starts with the anoxic stage which includes denitrification. Sewage is supplied to the said zone to be used as the source of carbon for denitrification, along with the post-nitrificator sludge mix that contains nitrites and nitrates. This is followed by the aerobic stage where the content of organic pollutants in the sewage is reduced, and nitrification takes place. The nitrate-bearing sludge mix

from this zone is supplied simultaneously to the next and the previous anoxic denitrification zone. The process is finished in the aerobic zone where nitrification and partial dephosphorization take place.

The Johannesburg (JHB) process is a sequence of an anoxic zone (denitrification), an anaerobic zone (phosphorus concentration reduction), another anoxic zone (nitrate and nitrite nitrogen removal), and an aerobic zone (ammonia oxidation).

Deep removal of nitrogen and phosphorus from sewage often focuses on a few methods, while overlooking the advantages of the others. To assess the advantages and disadvantages of the methods discussed, we compared them in Table 1.

Table 1 The comparison of conventional deep biogenic element removal options from wastewater

Technique	Advantages	Disadvantages
The A/O (anaerobic/oxide) process	This option is simple This option is cost-efficient It can be used for industrial sewage with high active sludge loads	Designed for high-output facilities Maintain the BOD:R proportion of at least 10:1
The AA/O (anaerobic/anoxic/oxic) process	Can be used for urban sewage with low active sludge loads Can remove both nitrogen and phosphorus; Simple operation Low energy costs due to the oxidation of the majority of organic compounds during denitrification and the presence of only 2 recycles	Limited efficiency of the biological removal of phosphorus The anaerobic zone is supplied with active sludge that did not undergo denitrification, which reduces the efficiency of the biological removal of phosphorus The efficiency of denitrification is limited by the flow of the nitrate recycle
The UCT process	Simultaneous removal of organics, nitrogen, and phosphorus compounds The anaerobic zone is supplied with the denitrified mix allowing for the stable and efficient biological removal of phosphorus High nitrogen removal efficiency, including nitrite nitrogen Extensive process control over phosphorus and nitrogen removal	Nitrate nitrogen undermines the efficiency of phosphorus removal in the anaerobic zone Complex control algorithm for internal recycles This is a relatively complex option in terms of both construction and operation This option requires more energy than the AA/O because of the additional sludge mix recycle

(continued)

Table 1 (continued)

Technique	Advantages	Disadvantages
<p>The modified UCT process</p>	<p>The negative impact of nitrate nitrogen on the efficiency of phosphorus removal in the anaerobic zone is eliminated A dedicated return sludge denitrificator helps reduce the concentration of nitrates in it almost to zero before it is supplied to the anaerobic zone. This results in high efficiency and stability of the biological removal of nitrogen, including for low-concentration sewage High nitrogen removal efficiency, including nitrite nitrogen Extensive process control over phosphorus and nitrogen removal</p>	<p>A large number of controlled parameters is required for successful nitrogen and phosphorus removal This is a relatively complex option in terms of both construction and operation This option requires more energy than the AA/O because of the additional sludge mix recycle</p>
<p>The Bardenpho process</p>	<p>Can be used at low-output facilities Can remove both nitrogen and phosphorus Facilitates the total amount of nitrogen in the treated water of 2.5–5.0 mg/l</p>	<p>The anaerobic zone is supplied with active sludge that did not undergo denitrification, which reduces the efficiency of the biological removal of phosphorus The required volumes at the facility are larger than for the AA/O process</p>
<p>The JHB process</p>	<p>Easy to control Efficient usage of the denitrification reactor The anaerobic zone is supplied with the partially denitrified active sludge, which helps improve the efficiency of the biological removal of phosphorus compared to the AA/O and Bardenpho processes High nitrogen removal efficiency</p>	<p>Less efficient than the Modified UCT process Incomplete denitrification Medium efficiency in terms of the biological removal of phosphorus Requires additional volumes for the denitrification of the return sludge</p>

5 Conclusions

The aggravating pollution of water sources due to the insufficient capacities and efficiency of the existing sewage treatment facilities results in the violations of the sanitary, chemical, and hydrobiological regimens of water bodies. This is especially relevant for the content of nitrogen and phosphorus compounds in wastewater that propagates the weediness of waters with subsequent destruction of the water flora and fauna. The removal of biogenic elements from sewage in current conditions is one of the key problems in wastewater treatment.

The combined, or chemo-biological method of phosphorus removal requires the implementation of engineering and technological solutions typical of the biological method, along with a backup agent dispensing system for periods of low organic compound loads. This solution can help avoid high operating costs typical of the chemical method and assure stable high-quality phosphorus removal during periods of low organic compound loads.

The biological method helps achieve high treatment quality in terms of phosphorus removal, but this process is highly susceptible to the current quality of the sewage to be treated and requires highly qualified process engineers and maintenance personnel at sewage treatment facilities.

References

1. Dyagelev MY (2023) Improving the efficiency of biological treatment of industrial wastewater as part of urban wastewater. *Theoret Appl Ecol* 2:96–103. <https://doi.org/10.25750/1995-4301-2023-2-096-103>
2. Adolph ML, Dreßler M, Troelstra V et al (2023) Eutrophication and contamination dynamics of Schweriner See, NE-Germany, during the past 670 years—a multi-proxy approach on lacustrine surface sediments and sediment cores. *Sci Total Environ* 877:162745. <https://doi.org/10.1016/j.envc.2023.100733>
3. Dyagelev M (2022) An Example of practical training on the discipline “wastewater treatment” for students in the field of construction engineering. *AIP Conf Proc* 2647:030030. <https://doi.org/10.1063/5.0104524>
4. Dash S, Kalamdhad AS (2022) Systematic bibliographic research on eutrophication-based ecological modelling of aquatic ecosystems through the lens of science mapping. *Ecol Model* 472:110080. <https://doi.org/10.1016/j.ecolmodel.2022.110080>
5. Li Y, Shang J, Zhang C et al (2021) The role of freshwater eutrophication in greenhouse gas emissions: a review. *Sci Total Environ* 768:144582. <https://doi.org/10.1016/j.scitotenv.2020.144582>
6. Zhou Q, Sun H, Jia L et al (2022) Simultaneous biological removal of nitrogen and phosphorus from secondary effluent of wastewater treatment plants by advanced treatment: a review. *Chemosphere* 296:134054. <https://doi.org/10.1016/j.chemosphere.2022.134054>
7. Peng YY, He S, Wu F (2021) Biochemical processes mediated by iron-based materials in water treatment: enhancing nitrogen and phosphorus removal in low C/N ratio wastewater. *Sci Total Environ* 775:145137. <https://doi.org/10.1016/j.scitotenv.2021.145137>
8. Habyarimana JL, Juan M, Nyiransengiyumva C et al (2022) Critical review on operation mechanisms to recover phosphorus from wastewater via microbial procedures amalgamated with phosphate-rich in side-stream to enhance biological phosphorus removal. *Biocatal Agric Biotechnol* 45:102484. <https://doi.org/10.1016/j.bcab.2022.102484>

9. Kang D, Zhao X, Wang N et al (2023) Redirecting carbon to recover VFA to facilitate biological short-cut nitrogen removal in wastewater treatment: a critical review. *Water Res* 238:120015. <https://doi.org/10.1016/j.watres.2023.120015>
10. Hu K, Li W, Wang Y et al (2023) Novel biological nitrogen removal process for the treatment of wastewater with low carbon to nitrogen ratio: a review. *J Water Proc Eng* 53:103673. <https://doi.org/10.1016/j.jwpe.2023.103673>
11. Wu T, Yang SS, Zhong L et al (2023) Simultaneous nitrification, denitrification and phosphorus removal: what have we done so far and how do we need to do in the future? *Sci Total Environ* 856:158977. <https://doi.org/10.1016/j.scitotenv.2022.158977>
12. Kharkina OV (2015) Effektivnaia ekspluatatsiia i raschet sooruzhenii biologicheskoi ochistki stochnykh vod (Efficient operation and calculation of biological wastewater treatment facilities). Panorama. Volgograd
13. Al-Hazmi HE, Maktabifard M, Grubba D et al (2023) An advanced synergy of partial denitrification-anammox for optimizing nitrogen removal from wastewater: a review. *Biores Technol* 381:129168. <https://doi.org/10.1016/j.biortech.2023.129168>
14. Li J, Feng M, Zheng S et al (2023) The membrane aerated biofilm reactor for nitrogen removal of wastewater treatment: principles, performances, and nitrous oxide emissions. *Chem Eng J* 460:14169. <https://doi.org/10.1016/j.cej.2023.141693>
15. Mishra S, Singh V, Cheng L et al (2022) Nitrogen removal from wastewater: A comprehensive review of biological nitrogen removal processes, critical operation parameters and bioreactor design. *J Environ Chem Eng* 10:107387. <https://doi.org/10.1016/j.jece.2022.107387>
16. Su D, Chen Y (2022) Advanced bioelectrochemical system for nitrogen removal in wastewater. *Chemos* 292:133206. <https://doi.org/10.1016/j.chemosphere.2021.133206>
17. Zhang SZ, Chen S, Jiang H (2022) A back propagation neural network model for accurately predicting the removal efficiency of ammonia nitrogen in wastewater treatment plants using different biological processes. *Water Res* 222:118908. <https://doi.org/10.1016/j.watres.2022.118908>
18. Deng L, Dhar BR (2023) Phosphorus recovery from wastewater via calcium phosphate precipitation: a critical review of methods, progress, and insights. *Chemosphere* 330:138685. <https://doi.org/10.1016/j.chemosphere.2023.138685>
19. Capua FD, de Sario S, Ferraro A et al (2022) Phosphorus removal and recovery from urban wastewater: current practices and new direction. *Sci Total Environ* 823:153750. <https://doi.org/10.1016/j.scitotenv.2022.153750>
20. Rios-Miguel AB, van Bergen TJHM, Zillien C et al (2023) Predicting and improving the microbial removal of organic micropollutants during wastewater treatment: a review. *Chemosphere* 333:138908. <https://doi.org/10.1016/j.chemosphere.2023.138908>
21. Guo G, Ekama GA, Wang Y et al (2019) Advances in sulfur conversion-associated enhanced biological phosphorus removal in sulfate-rich wastewater treatment: a review. *Biores Technol* 285:121303. <https://doi.org/10.1016/j.biortech.2019.03.142>
22. My D (2022) The review of methods of post-treatment of urban wastewater with a high content of industrial effluents. *IOP Conf Series: Earth Environ Sci* 981:042007. <https://doi.org/10.1088/1755-1315/981/4/042007>
23. Dyagelev MY, Pavlov II, Nepogodin AM et al (2021) The review of aeration systems for biological wastewater treatment. *IOP Conf Series: Earth Environ Sci* 839:42035. <https://doi.org/10.1088/1755-1315/839/4/042035>
24. Lei S, Zhang J, Hu B, Zhao J et al (2023) Improving nutrients removal of Anaerobic-Anoxic-Oxic process via inhibiting partial anaerobic mixture with nitrite in side-stream tanks: role of nitric oxide. *Biores Technol* 382:129207. <https://doi.org/10.1016/j.biortech.2023.129207>
25. Xu L, Zhao J, Wang J et al (2023) Elucidating performance failure in the use of an Anaerobic-Oxic-Anoxic (AOA) plug-flow system for biological nutrient removal. *Sci Total Environ* 880:163320. <https://doi.org/10.1016/j.scitotenv.2023.163320>

26. Rajab AR, Salim MR, Sohaili J et al (2022) Feasibility of nutrients removal and its pathways using integrated anaerobic-aerobic sequencing batch reactor. *Bioresou Techn Rep* 17:100912. <https://doi.org/10.1016/j.biteb.2021.100912>
27. Huang L, Lu Z, Xie T et al (2022) Nitrogen and phosphorus removal by coupling anaerobic ammonia oxidation reaction with algal-bacterial symbiotic system. *J Environ Chem Eng* 10:108905. <https://doi.org/10.1016/j.jece.2022.108905>
28. Li N, Zeng W, Wang B et al (2019) Nitritation, nitrous oxide emission pathways and in situ microbial community in a modified University of Cape Town process. *Biores Technol* 271:289–297. <https://doi.org/10.1016/j.biortech.2018.09.107>
29. Zeng W, Bai X, Zhang L et al (2014) Population dynamics of nitrifying bacteria for nitritation achieved in Johannesburg (JHB) process treating municipal wastewater. *Biores Technol* 162:30–37. <https://doi.org/10.1016/j.biortech.2014.03.102>
30. Wang X, Ma Y, Peng Y et al (2007) Short-cut nitrification of domestic wastewater in a pilot-scale A/O nitrogen removal plant. *Bioprocess Biosyst Eng* 30:91–97. <https://doi.org/10.1007/s00449-006-0104-x>
31. Zeng W, Wang X, Li B et al (2013) Nitritation and denitrifying phosphorus removal via nitrite pathway from domestic wastewater in a continuous MUCT process. *Biores Technol* 143:187–195. <https://doi.org/10.1016/j.biortech.2013.06.002>
32. Ge S, Peng Y, Qiu S et al (2014) Complete nitrogen removal from municipal wastewater via partial nitrification by appropriately alternating anoxic/aerobic conditions in a continuous plug-flow step feed process. *Water Res* 55:95–105. <https://doi.org/10.1016/j.watres.2014.01.058>
33. Mannina G, Capodici M, Cosenza A et al (2016) Carbon and nutrient biological removal in a University of Cape Town membrane bioreactor: analysis of a pilot plant operated under two different C/N ratios. *Chem Eng J* 296:289–299. <https://doi.org/10.1016/j.cej.2016.03.114>
34. Hu X, Xie L, Shim H et al (2014) Biological nutrient removal in a full scale anoxic/anaerobic/aerobic/pre-anoxic-MBR plant for low C/N ratio municipal wastewater treatment. *Chin J Chem Eng* 22:447–454. [https://doi.org/10.1016/S1004-9541\(14\)60064-1](https://doi.org/10.1016/S1004-9541(14)60064-1)
35. Zhao W, Huang Y, Wang M et al (2018) Post-endogenous denitrification and phosphorus removal in an alternating anaerobic/oxic/anoxic (AOA) system treating low carbon/nitrogen (C/N) domestic wastewater. *Chem Eng J* 339:450–458. <https://doi.org/10.1016/j.cej.2018.01.096>
36. Zeng W, Li L, Yang Y et al (2010) Nitritation and denitrification of domestic wastewater using a continuous anaerobic–anoxic–aerobic (A2O) process at ambient temperatures. *Biores Technol* 101:8074–8082. <https://doi.org/10.1016/j.biortech.2010.05.098>
37. Østgaard K, Christensson M, Lie E et al (1997) Anoxic biological phosphorus removal in a full-scale UCT process. *Water Res* 31:2719–2726. [https://doi.org/10.1016/S0043-1354\(97\)00125-5](https://doi.org/10.1016/S0043-1354(97)00125-5)
38. Huang X, Dong W, Wang H et al (2017) Biological nutrient removal and molecular biological characteristics in an anaerobic-multistage anaerobic/oxic (A-MAO) process to treat municipal wastewater. *Biores Technol* 241:969–978. <https://doi.org/10.1016/j.biortech.2017.05.161>
39. Ashrafi E, Zeinabad AM, Borghai SM et al (2019) Optimising nutrient removal of a hybrid five-stage Bardenpho and moving bed biofilm reactor process using response surface methodology. *J Environ Chem Eng* 7:102861. <https://doi.org/10.1016/j.jece.2018.102861>
40. Xue J, Schmitz BW, Caton K et al (2019) Assessing the spatial and temporal variability of bacterial communities in two Bardenpho wastewater treatment systems via Illumina MiSeq sequencing. *Sci Total Environ* 657:1543–1552. <https://doi.org/10.1016/j.scitotenv.2018.12.141>

41. Zeng W, Li L, Yang YY et al (2011) Denitrifying phosphorus removal and impact of nitrite accumulation on phosphorus removal in a continuous anaerobic–anoxic–aerobic (A2O) process treating domestic wastewater. *Enzyme Microb Technol* 48:134–142. <https://doi.org/10.1016/j.enzmictec.2010.10.010>
42. Abyar H, Nowrouzi M, Rostami AA (2022) Comprehensive study of biological phosphorus removal systems from economic and environmental perspectives based on the optimization approach. *Environ Technol Innov* 28:102811. <https://doi.org/10.1016/j.eti.2022.102811>
43. Ramin E, Flores-Alsina X, Gaszynski C et al (2022) Plant-wide assessment of alternative activated sludge configurations for biological nutrient removal under uncertain influent characteristics. *Sci Total Environ* 822:153678. <https://doi.org/10.1016/j.scitotenv.2022.153678>



Environmental and Economic Balance in the Refurbishment of the Sewage Treatment Plant

N. G. Vurdova^(✉)

JSC “GMS Neftemash”, 44 Voennaya St., Tumen 625003, Russia
nadya_vurdova@mail.ru

Abstract. Enterprises of the petrochemical industry are objects having a significant impact on the environment, they are obliged to develop and implement programs for improving environmental sustainability, which should reflect the compliance of technological processes, equipment, technical methods, techniques used at the enterprise with the best available technologies (BAT). Therefore, the growing demand for the practices of solving the problems of environmental protection efficiency in the activities of specific economic entities stimulates the search and development of both new methods and private indicators of effectiveness of environmental investment projects of various levels. The study shows the results of application of proactive measures related to the implementation of the investment environmentally oriented project on reconstruction of water supply and sanitation systems of the enterprise. Technical measures aimed at increasing the efficiency of water recycling systems, reducing the volume of effluent discharged by the plant and reducing raw water intake from the surface water source have been elaborated.

Keywords: Sustainable development of the enterprise · Investment project · Feasibility study · Life cycle of the investment project · Environmental and economic risks · Closed water systems · Wastewater treatment plants

1 Introduction

In current environment, global environmental trends have gained widespread international support, affecting both national and company economies, and are an integral part of sustainability standards for business operations. The company is managed as a business, which includes loss management, improvement of equipment effectiveness and value management in order to have a positive economic impact on the entire ecosystem in which it operates. Recently, the Russian Federation has adopted uniform criteria for evaluating projects that are aimed at sustainable, including “green development”, which allows the formation of economic incentives for the transition to advanced environmental standards.

In this study, the sequence of implementation of the investment project on reconstruction of wastewater treatment plant (WWTP) of oil refinery is investigated. Despite

the substantial capital costs, it was possible to qualitatively justify to the customer the necessity and possibility to implement the project with acceptable efficiency, based on the principle of ecological and economic equilibrium.

1.1 Relevance of the Study

Any investment project starts with an investment appraisal. When implementing a large project, it is customary to start with a feasibility study or preFEED [1–3].

The initial (pre-investment) stage is of fundamental importance to the potential investor (customer, lender). In this case, a lot of money is often spent to clarify all the circumstances affecting the outcome—"to be or not to be". Stage preFEED—the process of conceptual development of the projects, applied in processing industries, such as exploration and extraction of oil, the oil refining and petrochemical industry, etc. Pre-engineering is inherent in industries that require very large capital expenditure with long project life cycles. Thereby the project should pass certain milestones of clearly defined milestones during the project life cycle before being funded to start the next design stage (Fig. 1). In international practice, independent peer review is often undertaken before a final investment decision is made. Experts verify calculations, make proposals for commercial and technical optimization, and identify hidden risks. A positive decision is made if the conditions are met:

- all indicators are calculated with accuracy 3 class based on AACE methodology [4];
- the calculations are made according to the principle of "minimum technical solution";
- all risks (political, technical, organizational, market, environmental) and methods of their localization are elaborated;
- an independent review of all preliminary solutions was carried out.

Some domestic companies-investors set stricter requirements to the volume of documentation prepared at this stage, comparable with the "Project documentation" stage adopted in the Russian Federation (Regulation No.87). The principal difference is in the accuracy of the project budget estimate, for FEED it is 80–90%, which allows proceeding immediately with the ordering of the main equipment. There are also differences in approaches to risk assessment, description of environmental protection, prevention of emergencies and industrial safety declaration.

Thus, the importance of pre-investment calculations is great, without their quality, the terms of the project will be disrupted, and the customer may incur unexpected costs [5].

1.2 Results and Discussion

Let us take a closer look at the tasks of risk identification and assessment. Risk is commonly understood as the possibility of an adverse event that may lead to certain losses for people, economic objects or the environment [6–8]. Modern approaches and methods of risk management are widely researched and legislated by numerous documents: standards and methodologies, for example [9–13]. The best-known are:

1. ISO 31000 et al. Risk management. Principles and guidelines.

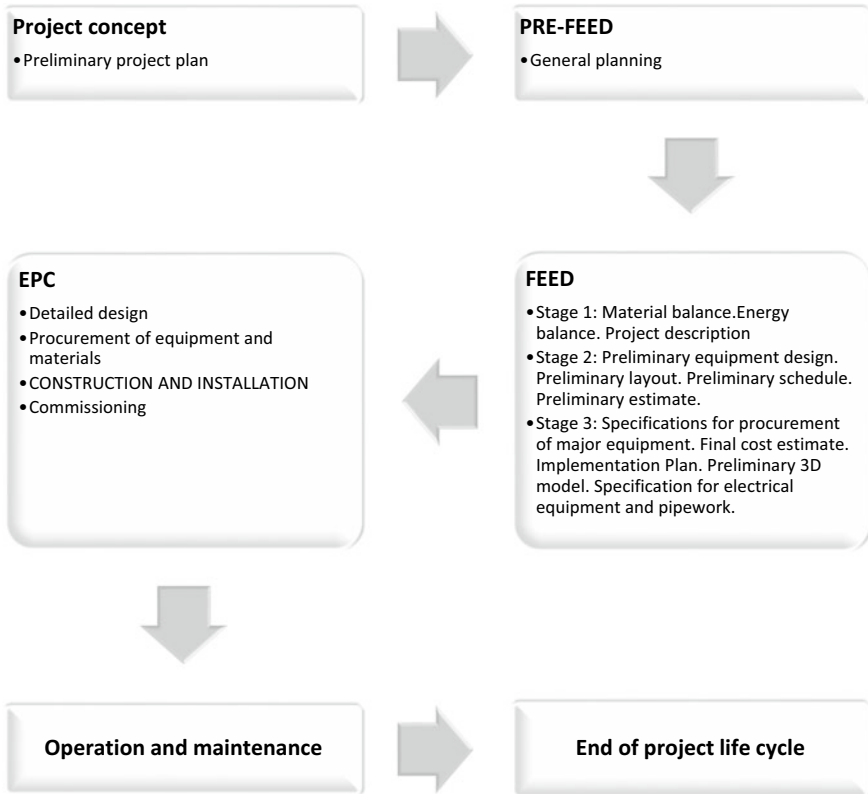


Fig. 1 Life cycle of a construction investment project

2. ISO 14000 et al. Environmental management standards.
3. HAZID—separate procedures for the identification and assessment of risks; used for the preliminary identification and description of risks at the initial stage of design of industrial objects.
4. ENVID—identification of environmental risks.
5. PHSER—procedures for assessing occupational safety, health and environmental protection.
6. HAZOP—Hazard identification and operability procedures for an industrial facility; detailed structuring of hazards for individual process assemblies.
7. ESIA—environmental and social impact assessment.
8. ESAP—environmental and social action plan.

In domestic practice, the ESIA section is a mandatory part of the design documentation for any construction projects, but the HAZID and HAZOP procedures are applied only at hazardous production facilities. Assessment of environmental risks consisting in determination of hazard types, identification of risks (threats), obtaining quantitative assessments of the probability of adverse events and their consequences, as a rule, is not carried out.

Environmental and Economic Risks for an Industrial Plant (EERIP) are manifested in the possibility of economic losses because of environmental degradation from the activities of the enterprise [14–16]. Prof. L. Mochalova offers the methodology of EERIP management based on methodologies of environmental management system (EMS) in accordance with ISO 14000 standards and risk management methodologies, which contains the algorithm of choice of effective method from passive low-cost to active, with significant losses or costs. Economic justification is based on the cost estimate of benefits from the implementation of risk prevention measures of these damages (natural, manufactured and social), assessment of the cost of these activities and assessing the effectiveness of management decisions that increase the "environmental value" of the enterprise. The proposed methodology provides for the presence of not only an effectively functioning EMS at an IP, but also gives guidelines for its further improvement.

However, practice shows that not many IPs are able to apply the approaches in question. Only large companies with international capital, or seeking to enter global markets, really have a highly organized EMS [17–19]. These businesses have been producing ESG reports for many years and have high ratings, including international ratings, e.g. [20]. Medium and small businesses prefer to follow formal signs, declaring the presence of an EMS according to ISO 14000 standards. In fact, activities such as: environmental planning and management; emergency preparedness and response; reviewing and revising processes and responses; and documenting information appropriately and to the extent necessary, are conducted formally or not at all. This situation may be explained by the following, in our opinion:

1. There is a lack of environmental awareness between both decision-making managers and other employees of an IP, which manifests itself, first, in a low awareness of the environmental policy implemented at an IP.
2. There is a persistent opinion that "environmental" problems are secondary to "economic" ones. This is especially true for mining, oil and gas BCPs. This is facilitated by the remoteness and closeness of such facilities.
3. There is no unified mechanism for assessing EERIP.
4. When justifying investments in the development of BCPs or environmental projects, the risks of not starting a project are not taken into account, e.g., [21].
5. EMS is most often used by enterprises to improve their image and competitive advantage in the market, sometimes to meet the requirements of legislation and to improve relations with regulatory authorities and the public.

Of course, following global trends in sustainable development in general, and environmental sustainability in particular, is a worthy goal. However, in the face of constant resource constraints: financial and human, IPs always choose to maximize profits through increased output, improved operational, financial or investment performance. Environmental performance is present in the reports, except in the form of losses for environmental violations.

1.3 Findings of the Study

This situation can be solved, in our opinion, by applying simpler procedures for decision-making at all levels of management of IRs. Let us show it on the example of a real

non-financial investment project of reconstruction of the WWT of an oil refinery. The objective was to prepare materials for preFEED stage "Reconstruction Project WWT for refinery of 15.5 ml tons". We know, first, the construction project for an industrial facility must include an ESIA section where environmental risks of the project's implementation are reviewed. However, most measures can be described already at this stage, guided by [22]. Secondly, if an enterprise has a highly organized EMS, the best existing (environmental protection) technology is adopted, which is based on the latest achievements in the development of production processes, installations or modes of their operation that have proven practical suitability for limiting the negative impact on the environment (emissions, discharges, waste, etc.). Special account shall be taken of [23]:

- comparable processes, installations or regimes of their operation that have been successfully tested recently;
- technical progress and changes in scientific knowledge and understanding of the problem;
- economic efficiency of the technology;
- timing of implementation in both new and existing plants;
- nature and extent of the negative impact on the environment;
- level of waste-free technology.

Thirdly, life cycle costs (LCC), equipment and material costs (OPEX), and total cost of ownership (CAPEX) are calculated.

The following tasks were carried out in the course of the work:

- (a) analysis of operation of water recycling units (WRU) and wastewater disposal systems;
- (b) development of optimal solutions and schemes of WRU;
- (c) elaboration of technical measures aimed at increasing efficiency of water recycling system, reduction of wastewater discharged by the plant and reduction of raw water intake due to organization of feeding with treated wastewater of modern units of WRU.

Modern WRU cannot operate without water stabilization treatment. Comprehensive reagent treatment of recycled water is the most economical way to protect water-cooled heat exchange equipment, cooling tower elements and water pipelines from metal corrosion, scaling and biofouling.

To implement a comprehensive reagent program at the enterprise, a methodology has been developed that includes three stages: preparatory, analytical and testing [24]. At the first stage, the aggressive properties of water in the current circulating water supply system were assessed and requirements for its quality were established. At the second stage, a qualitative selection of chemical reagents was carried out and their quantity necessary for the stabilization of water treatment was determined. At the third stage, industrial approbation and experimental verification of the effectiveness of the developed recommendations for the treatment of recycled water were carried out simultaneously. The effectiveness of corrosion inhibitors selected in accordance with the proposed water treatment methodology was determined by the corrosion rate on coupons maintained in the clean cycle of the water supply system for 30–45 days [25].

We have investigated the water-chemical regime of some WRUs and analyses the operation of the refinery's sewage treatment facilities. The current inhibition regime of water recycling systems was investigated based on monitoring data from January 2019 to July 2022. The following problems were identified.

1. In general, the circulating systems operate in a stable mode. To eliminate the described shortcomings at WRU-6 consider the possibility of automatic supply of reagents to WRU-6 and WRU-9 by analogy with WRU-11, since according to the received data the indicators of circulating systems at WRU-11 are significantly better, i.e. install "True Sense" automation units with 24-h access to analytical data.
2. As measures to improve the performance of WRU, it has been proposed to replace the phosphate inhibition technology with a fully organic technology using complex inhibitors based on phosphonates, phosphonocarboxylates and polymers. This technology allows operation in the pH range of 7.0–9.5 and the Langelier Index of 3.0–3.5, while effectively inhibiting both corrosion and salt deposits. The advantage of this technology is its environmental friendliness. The orthophosphate content of the effluent is reduced. Orthophosphates cause eutrophication of water bodies.
3. In addition, as a second non-oxidizing biocide, use biocides with high bio dispersing capacity to flush out and kill slime-forming and sulphate-forming bacteria (for example, based on dibronitrile propionamide); using two biocides with different main substance in the composition prevents the microbiological contamination of water circulation system to get used to the reagents.
4. Measures need to be developed to improve the efficiency of the existing WWTP. Exactly, conduct pilot tests and develop a feasibility study for upgrading the WWTs aimed at improving the efficiency of the water recycling system, reducing the volume of discharged wastewater from the plant and reducing the volume of raw water intake through the organization of feeding treated wastewater with modern WRUs.

The treated water from the refinery was tested for corrosion rate (Table 1) and microbiological parameters such as sulphate reducing bacteria (SRB), mucus forming bacteria (MFB), heterotrophic aerobic bacteria (HAB) (Table 2). In all samples, except river water, significant amounts of slime-forming, sulphate-reducing and heterotrophic aerobic bacteria were detected. It was concluded that the wastewater is not recommended for use as make-up water. Re-use in cooling systems can lead to significant contamination of modern recycling systems for the following reasons:

Table 1 Corrosion rates and total microbial number (TMN) in river and treated wastewater

Indicator	River recharge	Treated wastewater
Corrosion rate, mm/year	1239	1138
TMN, KOE/cm ³	<10 ²	>10 ⁴

1. High COD and BOD values indicate high levels of organic matter, which is a nutrient for various microbiological contamination in the water. Even when using 10%

Table 2 Examination of microbiological indicators of treated wastewater

Indicator	Units, KOE/cm ³
SRB	$4.4\text{--}6.7 \times 10^4$
MFB	5.4×10^6
HAB	1.0×10^6

wastewater as make-up and 90% river water for cooling systems with an evaporation factor of "2", the COD value will be doubled, resulting in a doubling of biocide consumption.

2. Phenols cause corrosion and should not be in the feed at all.
3. Sulphides are extremely corrosive to carbon steel and copper. They will cause microbiological growth in the recycling system (SRB in particular).
4. Petroleum products—will cause an increase in microbiology and corrosion.
5. Ammonia—will significantly increase the need for halogen-containing reagents and will accelerate the corrosive effect on copper and brass.

Can be done now:

- A. Install sand filtration or via floc followed by chlorination before this water is sent to the cooling systems.
- B. Return treated effluent as make-up in an amount not exceeding 10% of the total volume, with the expectation that:
 - an increase in microbiology growth will result in a 2-threefold increase in the consumption of biocide BD1501E;
 - sulphides, phenols, COD and BOD, oil and hydrocarbons will increase Hypo/OX1201 reagent consumption by at least 2 times;
 - copper inhibitor input will be required.

Thus, for reuse in recycling water supply, as well as to stop the discharge of excessive amounts of treated wastewater to the urban WWTP, it is proposed to carry out reconstruction of treatment facilities to bring wastewater performance to the requirements for the first stage of the WRU. Then successive stages of construction of new biological wastewater treatment facilities with a post-treatment unit will be implemented, which will fully return all treated wastewater into circulation and reduce water intake from the river for technical needs.

A technical and economic comparison of various technological solutions according to the most commonly used methods was carried out [26]. After determining the key technical and technological indicators of the project according to the ACE methodology (5th assessment class), the project targets were adjusted to achieve the technical results (according to BAT), which were broken down into three stages with consecutive implementation (Table 3).

Recently, customers have started to pay attention to methodologies for estimating the total cost of ownership of purchased products. In the case of water supply and

Table 3 A list of the main activities to modernize the sewage treatment plants and the achieved result

Stages	Stage objectives	Result
1	Carry out reconstruction of the existing sewage treatment plants: concrete restoration; re-laying of networks; partial replacement of equipment	Improving the degree of treatment indicators, such as petroleum products, suspended solids, sulfides, etc. The developed measures will allow to return a part of the treated effluents to separate blocks of recycled water supply and reduce penalties from the city the urban sewerage operator (Vodokanal) for excesses, where pre-treated plant effluent is discharged
2	Build new facilities—biological treatment units	The measures will make it possible to return treated wastewater to separate blocks of recycled water supply, to stop the discharge of wastewater to the city treatment facilities, to return some of the wastewater as technical water for user enterprises. The surplus can be directed to discharge into the river
3	Build new facilities—post-treatment units	The measures will make it possible to return all treated wastewater to water recycling units, stop discharging wastewater to the city's treatment facilities, stop taking river water from the river for technical needs, and return all water as technical water for user enterprises and cogeneration plants

wastewater disposal facilities, GOST R 58785-2019 can be followed. Water quality. Life cycle costing for the efficient operation of water supply and wastewater disposal systems and facilities. For management planning and analysis of production capacity of the enterprise, other methods are more often used, for example [27]. It is based on the definition of technical and economic indicators of the enterprise that are the basis for the development of a production and financial plan of the enterprise, as well as the establishment of standards for future periods in the planning framework at the enterprise.

Costs for modernization of sewage treatment facilities with a phased implementation of the latest technology that allows the organization of closed circulation cycles at the enterprise were determined. The results are summarized in Table 4.

Payments for discharges (items 13, 14) are attributed as benefits from the carried out measures. The data in Tab.4 show that these benefits cannot be achieved at the first stage of reconstruction, but the payback period of the investment is the fastest—2 y. Further investment in subsequent phases will generate an economic effect of up to 0.5 billion rubles.

Table 4 Technical and economic calculations of wastewater treatment plant reconstruction options

No.	Name of costs	Unit	Costs of modernization			Note
			Stage I	Stage II	Stage III	
1	Capacity of sewage treatment plants	m ³ /day	45,000,00	45,000,00	45,000,00	
2	Capital expenditures	thousand rubles	500,000,00	2,650,000,00	3,365,000,00	
3	Dismantling of equipment from item 2 (1%)	thousand rubles	3000,00	15,000,00	21,500,00	
4	Unrecorded costs, 20% of item 2	thousand rubles	66,000,00	330,000,00	473,000,00	
5	Total: Investment costs	thousand rubles	569,000,00	2,995,000,00	3,859,500,00	Including unaccounted expenses 20%
6	Operating costs, per year (assuming a standard service life of structures of 25 years):	thousand rubles	62,244,00	311,220,00	446,082,00	
7	Change in operating costs after modernization:					“+” overspending, “-” savings
8	electricity for technological purposes	thousand rubles	-268,00	12,612,00	11,332,00	
9	maintenance, operation and repair of new equipment	thousand rubles	-62,244,00	311,220,00	446,082,00	

(continued)

In the study under consideration, the obtained results proved to be sufficient to justify investments in the project of reconstruction of the existing refinery's WWTPs. In some cases, the calculations can be supplemented by using the method [28]. After performing the GOST LCC calculation, the compensating costs associated with the

Table 4 (continued)

No.	Name of costs	Unit	Costs of modernization			Note
			Stage I	Stage II	Stage III	
10	maintenance, operation and repair of old equipment	thousand rubles	90,000,00	-90,000,00	-90,000,00	
11	Total change in annual operating costs, per year	thousand rubles	-27,488,00	233,832,00	367,414,00	
12	Payments for discharges to the city's wastewater treatment plant:	thousand rubles				
13	penalties for exceeding VAT	thousand rubles	5000,00	-5000,00	-5000,00	
14	toll	thousand rubles	800,000,00	800,000,00	-800,000,00	
15	The main technical and economic indicators:	thousand rubles				
16	Net income growth	thousand rubles	-587,109,12	430,287,68	874,620,16	24%—taxes
17	The economic effect of the project by reconstruction stages	thousand rubles	-646,959,12	131,037,68	445,695,16	The deposit rate, 15%, is taken into account
18	Payback period	year	2	6	4	

possibility of environmental and economic risks are added to the OPEX data. These will be 'payments to organizations that experience deterioration in economic performance during the rehabilitation of the sewerage facility, costs directly related to failures and additional costs related to environmental protection measures'. Examples of calculations of such risks are given in the following material.

2 Conclusion

The study contains an analysis of the approaches of international and domestic design practices, as well as the sequence of implementation of the investment project for the reconstruction of WWTP of petrochemical plant. Despite significant capital expenditures, it was possible to substantiate qualitatively the necessity and possibility of the project implementation with acceptable efficiency based on the principle of ecological and economic balance.

The author present the results of calculations for the feasibility study of reconstruction according to different international methodologies. A preliminary qualification survey of companies, specializing in the supply of technologies and equipment for wastewater treatment of refineries and petrochemical plant, resulted in an estimate of the cost of investment meeting the requirements of Class 5 in accordance with the AASE methodology. For more accurate results, the author carried out an assessment in accordance with the methodology in accordance with local standard—GOST R 58785-2019, according to which the full LCC of the construction project were determined.

Having assessed the investment costs at the preliminary stage, the client decided to carry out further works in stages. In accordance with the customer's assignment, technical and economic calculations of three options for the reconstruction of WWTP of petrochemical plant, that the author were carried out, which made it possible to develop an investment justification program with a phased construction.

In the first stage, are reconstructed the existing WWTP. The result of implementation should be of the projected solutions: improvement of the degree of purification for certain indicators, such as oil products, suspended substances, sulphides, etc. The developed measures will allow returning a part of the treated effluents to separate WRU and reduce penalties from the domestic utilities for exceeding the normative allowable discharge of pollutants.

In the second stage, are being built new biological treatment units. Measures will allow returning the treated effluents to separate water-recycling units, to stop the discharge of effluents to the municipal sewage treatment plant and to return a part of the effluents as technical water for the enterprises-subscribers. Can be directed the surplus to discharge into the river.

In the third stage, are being built new additional treatment units. Actions will allow returning all treated sewage to WRU, to stop discharge of sewage to municipal sewage treatment plants, to stop river water intake for technical needs, to return all water as technical water for enterprises-customers and cogeneration plants.

For the enterprise in question, adherence to sustainability standards is a priority. To increase its sustainability, as well as to ensure industrial and environmental safety, the enterprise has introduced a risk management system. Therefore, accounting, analysis of various risks and development of risk mitigation measures are carried out on a systematic basis. Author were considered the variants of quantitative estimation of probability of appearance of negative processes and the phenomena reducing environment quality, and quantitative estimation of possible damage from their appearance in case of refusal to make a decision on WWTP reconstruction. The results of the calculations and studies have used in the investment program of the enterprise for the next five years.

References

1. Methodological Recommendations on Efficiency Assessment of Investment Projects [Metodicheskie rekomendatsii po otsenke effektivnosti investitsionnykh proektov], 3rd edn, 2004. Institute of Modern Analysis, Russian Academy of Sciences. Central Institute of Economics and Mathematics, Russian Academy of Sciences), Moscow
2. Behrens W, Hawranek PM (1991) Manual for the preparation of industrial feasibility studies. UNIDO, Vienna
3. Akulinjin AI (2020) FEED—stadia of project. <https://finswin.com/projects/osnovnye/feed.html>. Accessed 30.12.2021
4. AACE, Inc. (2005) AACE International Recommended Practice No. 18R-97. Cost estimate classification system—as applied in engineering, procurement, and construction for the process industries. TCM Framework: 7.3—Cost Estimating and Budgeting. https://www.costengineering.eu/Downloads/articles/AACE_CLASSIFICATION_SYSTEM.pdf. Accessed 30.12.2022
5. Polkovnikov AV, Dubovik MF (2013) Upravlenie proektami. Polnyy kurs MBA (Project management. Full MBA course). Olimp-Biznes, Moscow
6. Rowe WD (1977) An anatomy of risk. Wiley, N.Y.
7. Makhutov NA et al (2013) Risk analysis and obespechenie zashchishchennosti kriticheskikh vazhnykh ob“ektov neftegazokhimicheskogo kompleksa: ucheb.posobie (Risk Analysis and Security of Critical Facilities in the Oil and Gas Chemical Complex). Tyumen State University
8. Permyakov VN et al (2022) Forecast damage risks of gas pipeline operation in areas with permafrost. *J. Environ Protect Oil Gas Sector* 4(307):21–25. [https://doi.org/10.33285/2411-7013-2022-4\(307\)-21-25](https://doi.org/10.33285/2411-7013-2022-4(307)-21-25)
9. Koutsoukis NS (2010) Risk management standards: towards a contemporary, organization-wide management approach. *J Bus Pol Econ* 3(1):47–64
10. Moeller R (2011) COSO enterprise risk management: establishing effective governance, risk, and compliance processes. Wiley
11. Hutchins G (2018) ISO 31000:2018. enterprise risk management: CERM academy series on enterprise risk management. Quality + engineering
12. ISO 31000 (2009) Risk management—principles and guidelines
13. ISO 14001 (2015) Environmental management systems. Requirements with guidance for use
14. Mochalova LA (2008) Ekologicheskii menedzhment kak instrument obespecheniya ustoychivogo razvitiya promyshlennogo predpriyatiya (Environmental management as a tool for sustainable development of an industrial enterprise). Ekaterinburg
15. Gusev AA (2004) Sovremennye ekonomicheskie problemy prirodopol’zovaniya (Current economic problems of environmental management). International Relations, Moscow
16. Korneeva VM, Pupentsova SV (2020) Sovremennye metody upravleniya risky na predpriyatiyakh (Modern enterprise risk management methods). *J Prob Socio-Econo Development in Siberia* 2(40):33–38. <https://doi.org/10.18324/2224-1833-2020-2-33-38>
17. Responsible energy: a sustainability report. Rosneft (2021) https://www.rosneft.ru/upload/site1/document_file/Rosneft_CSR2021_RUS.pdf. Accessed 24.12.2022
18. Group Sustainability Report LUKOYL (2021) Responsible energy producer. <https://lukoil.ru/FileSystem/9/592424.pdf>. Accessed 29.05.2022
19. Gazprom (2021) The future is ours. Group Sustainability Report. <https://sustainability.gazpromreport.ru/fileadmin/f/2021/sustainability-report-ru-2021.pdf>. Accessed 29.05.2022
20. ESG and green finance. Report (2022) Expert and analytical platform: infrastructure and finance for sustainable development INFRAGREEN. https://infragreen.ru/frontend/images/PDF/INFRAGREEN_Green_finance_ESG_in_Russia_2018-2022-cut.pdf. Accessed 29.01.2023

21. The consequences of a fuel spill in Norilsk (2020) https://www.rbc.ru/photoreport/03/06/2020/5ed7b4ac9a794710786cc0d1?from=article_body. Accessed 20.01.2022.
22. Otsenka vozdeystviya na okruzhdayushchuyu sredu pri obosnovanii investitsiy v stroitel'stve (Environmental impact assessment in construction investment justification. Practical manual for SP-11-101-95) Moscow
23. Khoroshavin AV, Kholodov AS (2018) Podkhody k otsenke ostroychivogo razvitiya organizatsiy. Razrabotka i aprobatsiya ekologo-ekonomicheskikh pokazateley ustoychivogo razvitiya dlya neftegazovykh predpriyatiy (Approaches to assessing the sustainable development of organisations. Development and testing of environmental and economic indicators of sustainable development for oil and gas enterprises). *J Environ Econ* 6:24–41
24. Telin NV et al (2009) Metodologiya stabilizatsionnoy obrabotki vody v sisteme oborotnogo vodosnabzhenia (Methodology of stabilization water treatment in the recycling water supply system of metallurgical enterprises) *Bulletin of Cherepovets State University. Indust Therm Pow Eng* 1(20):95–98
25. Balabin-Irmenin Y et al (2011) The use of antinakupins in low-parameter power engineering. *Heat supply News*, Moscow
26. Vurdova NG, Yur'ev Y (2022) Investitsionnyy proekt sozdaniya zamknytykh vodooborotnykh tsiklov na promyshlennom predpriyatii (Investment project for closed water cycles in an industrial plant). *J Izv. Higher Education Institutions. Investment. Construction. Real Estate* 12, 4(43):529–538. <https://doi.org/10.21285/2227-2917-2022-4-529-538>
27. Velizhanskaya SS (2019) Puti povysheniya effektivnosti proizvodstva (Ways to improve production efficiency). *J Plan Econ Aff* 7(103):37–48. https://www.profiz.ru/peo/7_2019/effektivnost_proizvodstva. Accessed 02.05.2023
28. Frankevich Z, Gagarina AY (2018) Analysis of risks investitsionnogo proekta i metody ih otsenki (Analysis of investment project risks and methods of their assessment). *Mining Info Anal Bull* 3:183–192. <https://doi.org/10.25018/0236-1493-2018-3-0-183-192>



Evaluation of the Effectiveness of the Occupational Health and Safety Management System Using Fuzzy Logic Methods (Harrington Desirability Function)

A. Yu Semeykin^(✉), E. V. Klimova, O. N. Tomarovschenko, V. A. Petrova,
and I. A. Kochetkova

Belgorod State Technological University Named After V.G. Shukhov, 46, Kostyukov Str.,
Belgorod 308012, Russia
semeykin.ay@bstu.ru

Abstract. The paper presents a methodology for evaluation the effectiveness of an occupational safety management system using fuzzy logic methods—calculating the Harrington desirability function. This function is used to describe criteria and constraints in solving multi-criteria problems and allows you to establish a correspondence between linguistic assessments of the desirability of the values of the evaluation indicator (expert assessment) and numerical preference intervals. The use of Harrington’s desirability function makes it possible to bring all evaluation indicators to unified values and compare particular indicators measured on different scales (numerical, verbal, etc.). This makes it possible to adapt this assessment methodology to the conditions of various organizations and implement it into expert decision support systems for decision makers in the field of ensuring occupational health and safety at enterprises. An example of calculating the Harrington desirability function for the performance indicators of the labor protection management system for a light industry enterprise is shown. The above methodology can be used to introduce the rating of departments of large organizations in terms of the effectiveness of the occupational health and safety management system.

Keywords: Harrington function · Occupational risk · Decision support system · Occupational health and safety system · Fuzzy logic · Effectiveness criteria

1 Introduction

The reduction of injuries at work remains an urgent problem both in Russia and in the world as a whole, given the complex of economic problems that have recently begun to influence the attitude of employers to this problem.

Injury prevention should be based on a multi-criteria analysis, which should consider a large number of factors, such as [1–4]: personnel composition of the enterprise

(factors related to personnel—gender, age, work experience, work experience in the specialty, qualifications, competence, personal qualities (leadership, motivation, attitude to work, indicators of personnel reliability), etc.); working conditions at the workplace (factors related to the workplace—the nature of the work performed, the conditions of the labor process, the presence of harmful or dangerous factors, the performance of high-risk work); features of the occupational health and safety management system at the enterprise (factors related to safety management at the enterprise—the presence of an occupational health and safety management system, which includes the company's policy in the field of occupational health and safety, goals, clearly described procedures for achieving goals, clear processes for ensuring the functioning of the occupational health and safety management system).

At the same time, each parameter of the analysis, which is used for a comprehensive assessment of the effectiveness of occupational safety management, has its own meaning and dimension. In this regard, a methodological problem arises, which consists in the need to establish priority between the criteria for the transition to a generalized evaluation indicator. This problem is typical for many interdisciplinary branches of science—medicine, ecology, sociology, etc. [5–8].

In safety management, scoring systems for assessing risks and various indicators related to occupational safety are often used. Methods of scoring risk assessment, methods of expert assessments, matrix methods are known. For risk assessment, the Elmerly method is also known, based on the calculation of the number of positive and negative ratings [9]. However, the problem with these methods is that many operations, including calculating averages and determining generalized indicators, are inapplicable to point estimates related to a scale of ranks of different values by their nature.

At the same time, in our opinion, it is necessary to develop methods for evaluating the effectiveness of occupational safety management system based on multi-criteria analysis using fuzzy logic methods.

In the works of Belgorod State Technological University named after V. G. Shukhov, expert decision support systems were developed for the management of occupational risks and occupational safety [10, 11]. This work is aimed at improving the decision-making system in the field of occupational safety related to the evaluation of the effectiveness of this system.

2 Materials and Methods

The main problem of assessing the effectiveness of occupational safety management is the disparity of particular criteria, the need to simultaneously take into account both quantitative and qualitative indicators, which is associated with the presence of various types of uncertainties [12, 13].

Often, when it is necessary to choose from among alternatives, measurements are used using special verbal-numerical scales. Such scales are used in cases where the assessments are subjective. These scales are called psychophysical and allow you to formalize the expert's system of preferences. Psychophysical scales are set by functions of a special kind—desirability functions and establish a correspondence between the natural values of indicators in physical scales and psychological parameters—subjective assessments of the “value” of these values.

The most well-known and frequently used is the Harrington desirability function [14]. The introduction of the desirability scale makes it possible to reduce the original multi-criteria decision-making problem with different-dimensional criteria to a multi-criteria problem with criteria measured in the same scale.

The function proposed by E. S. Harrington in 1963 to describe criteria and constraints in solving multi-criteria problems allows us to establish a correspondence between linguistic estimates of the desirability of the values of the evaluation indicator and numerical preference intervals [12]. The intervals take values that increase continuously from 0 to 1 when the corresponding quality parameter changes from the least to the most desirable values. The specific type of desirability functions is set by the decision-maker, based on his subjective ideas. Then, by convolution of partial desirability functions, a global process quality criterion is calculated, the maximization of which is the optimum [15]. The Harrington desirability function has the following advantages [15–17]:

- is quantitative;
- is expressed as a single number, i.e. it is a single;
- is unambiguous, i.e. a given set of values of particular evaluation parameters corresponds to one value of the function;
- versatile and can be used in various fields;
- comprehensively characterizes the object, i.e. meets the requirement of completeness;
- provides an easy way to convert metrics using a single graph for all criteria;
- “neutral” in generalization, only personal preferences affect the final result when constructing the desirability scale;
- is adequate. The adequacy of a particular and generalized desirability function should be understood as their equivalence to the measured values of optimization parameters in the sense that all computational actions defined on a set of optimization parameter values can be performed with them.

The evaluation process consists of the following steps:

1. Determination of the list of particular evaluation parameters, i.e. criteria by which the object will be evaluated (quantitative, qualitative). For example, among the group of evaluation parameters may be the number of security violations per person.
2. Setting the limit of acceptable values for all numerical evaluation indicators. The most convenient is when there are clear restrictions set, for example, in instructional documents, standards, norms and rules. For example, as the values of individual indicators, it is possible to take normalized indicators in the field of occupational safety—the number of accidents, the number of employees who committed a violation. However, acceptable values of individual parameters may not be available due to the innovative nature of the study or the lack of data. Then the limitations for such indicators are established by expert means based on the experience and intuition of the experimenter, i.e., the assessment is subjective.

When setting the limit of permissible values of numerical evaluation parameters, it should be borne in mind that restrictions can be set one-sided or two-sided. Unilateral restrictions are established if the improvement of the desirability function occurs only with a unidirectional change in the indicator (decrease or increase). Unilateral restrictions

are denoted as $y_i \leq y_{max}$ or $y_i \geq y_{min}$, bilateral restrictions are denoted as $y_{min} \leq y_i \leq y_{max}$.

3. Selection of the desirability scale. To obtain a desirability scale, it is convenient to use the developed Table 1 of correspondences between preference relations in empirical and numerical (psychological) systems [14, 15]. The scale should be of the same type for all combined parameters (responses). However, the standard values on the desirability scale are not strictly mandatory.

Table 1 Numerical intervals of the Harrington scale

Linguistic assessment	Intervals of desirability function values
Very good	1.00–0.80
Good	0.80–0.63
Satisfactorily	0.63–0.37
Badly	0.37–0.20
Very badly	0.20–0.00

In accordance with the Harrington scale, the values of the desirability function d_i vary in the range from 0 to 1. The value of the i -th private parameter d_i , translated into a dimensionless desirability scale, is called the private desirability ($i = 1, 2, 3 \dots n$ is the current parameter number, n is the number of private parameters). In this case, the value $d_i = 1$ corresponds to the most desired value of the i -th parameter. This level is often unknown, but sometimes precisely defined [18]. For example, the complete absence of accidents at work, the complete absence of jobs with an unacceptable level of risk or dangerous working conditions—the maximum possible level of group parameters.

$d_i = 1-0,8$ —acceptable and excellent level;

$d_i = 0,8-0,6$ —acceptable and good level;

$d_i = 0,6-0,37$ —acceptable and sufficient level;

$d_i = 0,37-0$ —unacceptable level;

$d_i = 0$ corresponds to an unacceptable value of the i -th optimization indicator.

The value $d_i = 0.37$ is usually used as the limit of acceptable values. The choice of marks on the desirability scale of 0.37 and 0.63 is explained by the convenience of calculation, since $0.37 \approx 1/e$, and $0.63 \approx 1-1/e$ [15]. The lower bound of each range of values is included in the corresponding interval. The specific value of each interval is taken by the decision-maker at its discretion and remains unchanged when evaluating two or more sites.

4. Determination of the desirability level in accordance with the Harrington scale for each parameter of the y_i assessment. With a unilateral restriction of $y_i \geq y_{min}$ or $y_i \leq y_{max}$ (i.e., lower or upper limit), the mark on the desirability scale $d_i = 0.37$ corresponds to the value of y_{min} or y_{max} . The choice of this point is due to the fact that it is the inflection point of the curve, which in turn creates certain convenience in calculations. The same is true for the desirability value corresponding to 0.63. Choosing this

curve is not the only possibility. However, it arose as a result of observations of real solutions of experimenters and has such useful properties as continuity, monotony, smoothness. If a parameter change is possible in the direction of maximum and minimum from the optimal value, then the restriction is two-sided. In this case, the mark $d_i = 0.37$ on the desirability scale corresponds to y_{min} or y_{max} [15].

The desirability function for a unilateral constraint is determined by the formula (1):

$$d = e^{-e^{-y'}} \quad (1)$$

where e is the exponent notation; y' —is the encoded value of a particular parameter y , i.e., its value on a conditional scale.

For a bilateral constraint, the desirability function has the form of formula (2):

$$d = e^{-e^{-|y'|^n}} \quad (2)$$

where n is the exponent, which can vary from 0 to ∞ .

If the desirability function is determined by the formula (2), then the value of the parameter y' can be determined by the formula (3):

$$y' = \frac{(2y - (y_{max} + y_{min}))}{(y_{max} - y_{min})} \quad (3)$$

The exponent of the degree n can be determined by the formula (4), having previously assigned a certain value of the parameter y desirability d (better than the level “good” or “very good” on the desirability scale).

$$n = \frac{\ln \ln \frac{1}{d}}{\ln |y'|} \quad (4)$$

For each numerical evaluation parameter for which a bilateral constraint is set, the type of desirability function is determined in accordance with formula (2).

If a unilateral constraint is set and a function defined by formula (1) is used, then the value of y' can be determined graphically (by constructing a nomogram) or analytically. The graphical method is simpler and avoids intermediate transformations, but the analytical method allows you to get more accurate values, but requires additional calculations, which is not difficult when using computer technology.

Graph of the Harrington desirability function with unilateral restriction and is shown in Fig. 1. The curve of the desirability function demonstrates that in the regions of desirability close to 0 or 1, its “sensitivity” is much lower than in the middle zone of the graph.

There may be a situation when restrictions (unilateral or bilateral) take on a single meaning. Such a case may be, for example, a strict restriction of certain personnel or social parameters. Then inside the limits $d_i = 1$, and outside the limits $d_i = 0$. With a unilateral constraint, the desirability function will take the form (5):

$$\begin{aligned} d_i &= 0, \text{ if } y_i < y_{min} \\ d_i &= 1, \text{ if } y_i \geq y_{min} \end{aligned} \quad (5)$$

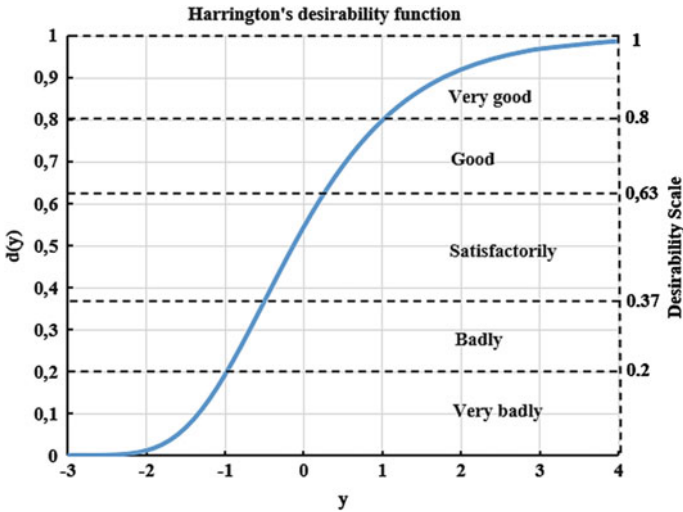


Fig. 1 Harrington desirability function on the desirability scale

With a bilateral constraint, we get the system (6):

$$\begin{aligned}
 d_i &= 0, \text{ if } y_i < y_{min} \text{ and } y_i > y_{max} \\
 d_i &= 1, \text{ if } y_{min} \leq y_i \leq y_{max}
 \end{aligned}
 \tag{6}$$

To determine the encoded value of the parameter y' , the following analytical methods can be used [15]:

- according to the translation mechanisms selected for each parameter of the form $y' = a \cdot y + b$;
- by simplified analytical dependencies determined by formulas (7) and (8):

$$y'_i = \frac{y - y_{min}}{y_{max}}
 \tag{7}$$

$$y'_i = \frac{y - y_{min}}{y_{min}}
 \tag{8}$$

where y_{max} , y_{min} are the upper and lower limits of the unilateral constraint on the i -th parameter; y'_i is the value of the i -th parameter, translated into the desirability scale.

5. Convolution of partial desirability functions d_i into a generalized criterion D (generalized desirability function), defined as the geometric mean of partial desirability by formula (9):

$$D = \sqrt[n]{d_1 \cdot d_2 \cdot d_3 \cdot \dots \cdot d_i \cdot \dots \cdot d_n}
 \tag{9}$$

The same preference scale is used for the generalized indicator as for the optimization parameters. Formula (9) makes it possible to decide on an unacceptable level of safety

(the effectiveness of the occupational safety management system) if at least one particular desirability $d_i = 0$. In this case, the generalized function will also be zero. At the same time, the generalized function $D = 1$ only if all the particular desirability $d_i = 1$.

At the same time, it should be noted that the disadvantage is that in it all responses are recognized as equilibrium, although in practice this is far from the case.

3 Results and Discussion

For assessment of the effectiveness of occupational safety management system, a light industry enterprise was selected.

The performance indicators of the occupational safety management system presented in Table 2 were selected as the initial data for the analysis [18, 19]. The indicators were grouped into 5 blocks. Each block included private indicators related to this block.

Each possible indicator from the block, in turn, can be evaluated by several indicators. For example, the group of indicators X10 "Preventive and regulatory measures" (block "Planning of OT measures") is characterized by the following indicators:

- the proportion of workplaces where an occupational risk assessment has been carried out and documented (X10.1);
- the proportion of workplaces where risk management measures have been taken based on the assessment carried out (X10.2);
- the specific number of employees employed in workplaces employed in workplaces with acceptable and optimal conditions (X10.3);
- the share of jobs with an average level of risk (X10.4);
- the share of jobs with a high level of risk that require increased attention (X10.5);
- the share of jobs with an unacceptable level of risk that require urgent measures (X10.6);
- the proportion of workplaces where the risk level is reduced due to the use of collective protection means (X10.7);
- the proportion of reduction in the use of PPE due to the use of other risk management measures (X10.8);
- the average time from hazard/risk identification to the implementation of measures to manage the corresponding risk (X10.9).

In the same way, calculated indicators for the remaining blocks were compiled.

The calculation of private performance indicators was carried out according to the formula:

$$x_i = \frac{k_i}{n}. \quad (10)$$

where k_i is the corresponding quantitative indicator; n is the maximum value of the indicator (for example, the total number of workplaces, employees, recorded violations, etc.)

At the next stage, the partial utility functions for each indicator were calculated, considering the weighting coefficients according to the formula (1). For a light industry

Table 2 Performance indicators of the occupational safety and health (OSH) management system

Group code	The group of performance indicators	Indicator
X1	OSH policy	The developed policy of the organization in the field of OSH
X2		Participation of employees and their representatives
X3		Availability of goals in the field of OSH
X4	Organization and functioning of the OSH management system	Distribution of responsibilities
X5		Competence and training of employees
X6		Documentation of the OSH management system
X7		Efficiency of the information exchange system
X8	Planning of OSH activities	The quality of the initial data for planning
X9		Planning, development and application of OHS management system
X10		Preventive and regulatory measures
X11		Change Management
X12		Emergency prevention
X13		Material and technical support of the OSH management system
X14		Contract work
X15	Evaluation and control	Monitoring and evaluation of performance
X16		Investigation of accidents, deterioration of health
X17		Verification and audit
X18		Analysis of the effectiveness of the OSH management system
X19	Actions to improve the OSH management system	Preventive and corrective actions
X20		Continuous improvement

enterprise, an analysis of the effectiveness of the occupational health and safety management system was performed by the factor “Preventive and regulatory measures”. The calculation results are presented in Table 3.

Comparing the obtained value of the Harrington desirability function with the scale given in Table 1 and Fig. 1, we can see that the value of the generalized Harrington criterion for the enterprise under consideration corresponds to the linguistic assessment of the effectiveness of the occupational safety management system is “good”.

Table 3 The results of the calculation of the Harrington function for evaluating the effectiveness of the occupational safety management system

Group code	The group of performance indicators	Code of indicator	Encoded value y'	d —function (desirability function)	Generalized desirability function D
X10	Preventive and regulatory measures	X10.1	1,49,994	0,692,201	0,718,530,614
		X10.2	1,49,994	0,692,201	
		X10.3	0,676,507	0,330,353	
		X10.4	3,532,019	0,976,057	
		X10.5	4,936,544	0,996,309	
		X10.6	–	–	
		X10.7	1,49,994	0,692,201	
		X10.8	1,49,994	0,692,201	
		X10.9	1,49,994	0,692,201	

4 Conclusion

The paper presents a methodology for evaluating the effectiveness of the occupational safety management system using fuzzy logic methods—calculating the Harrington desirability function. This technique makes it possible to bring all private evaluation indicators to unified values, which makes it possible to compare indicators measured in various scales (numerical, verbal, linguistic, etc.). This makes it possible to adapt this assessment methodology to the conditions of various organizations and implement it into expert decision support systems for decision makers in the field of occupational safety at enterprises. An example of using the Harrington desirability function to evaluate the effectiveness of the OHS management system is shown.

Acknowledgements. The work was realized in the framework of the Program "Priority 2030" on the base of the Belgorod State Technological University named after V.G. Shukhov. The work was realized using equipment of High Technology Center at the Belgorod State Technological University named after V.G. Shukhov.

References

1. Klimova EV, Semeykin AY, Nosatova EA (2018) Improvement of processes of professional risk assessment and management in occupational health and safety system. IOP Conf Ser: Mater Sci Eng 451:012198. <https://doi.org/10.1088/1757-899X/451/1/012198>
2. Sugak EB (2018) Occupational risks management as a basis of industrial injuries and occupational disease prevention system. IOP Conf Ser: Mater Sci Eng 365:062038. <https://doi.org/10.1088/1757-899X/365/6/062038>

3. Podgórski D (2015) Measuring operational performance of OSH management system—a demonstration of AHP-based selection of leading key performance indicators. *Saf Sci* 73:144–166. <https://doi.org/10.1016/j.ssci.2014.11.018>
4. Delatour G, Laclemece P, Calcei D et al (2014) Safety performance indicators: a questioning diversity. *Chem Eng Trans* 36:55–60. <https://doi.org/10.3303/CET1436010>
5. Dubnitskiy V, Kobylin A, Kobylin O et al (2023) Calculation of Harrington function (desirability function) values under interval determination of its arguments. *Adv Info Syst* 7(1):71–81
6. Terskaya LA, Slesarchuk IA (2020) Harrington desirability function for multi-attribute outdoor space quality assessment. *IOP Conf Ser: Mater Sci Eng* 753(8):082030. <https://doi.org/10.1088/1757-899X/753/8/082030>
7. Tazmeev BK, Tsybulevsky VV, Tazmeeva RN et al (2022) Application of the Harrington function in substantiating the choice of the best equipment for plasma processing of materials. *J Phys: Conf Ser* 2270(1):012013. <https://doi.org/10.1088/1742-6596/2270/1/012013>
8. Voitenko L, Voitenko A (2017) Integrated assessment of irrigation water quality based on Harrington's desirability function. *Int J Agric Environ Food Sci* 1:55–58. <https://doi.org/10.31015/jaefs.17007>
9. Laitinen H, Rasa LP, Räsänen T (1999) Elmerly observation method for predicting the accident rate and the absence due to sick leaves. *Am J Indust Med Suppl* 1:86–88. [https://doi.org/10.1002/\(SICI\)1097-0274\(199909\)36:1+3.0.CO;2-Z](https://doi.org/10.1002/(SICI)1097-0274(199909)36:1+3.0.CO;2-Z)
10. Semeykin AY, Kochetkova IA, Klimova EV et al (2019) Expert information-analytical decision support system for professional risk management based on the database of real cases of industrial injuries *IOP Conf Ser: Earth Environ Sci* 224:012011. <https://doi.org/10.1088/1755-1315/224/1/012011>
11. Semeykin AY, Kochetkova IA, Klimova EV et al (2019) Decision-making process modeling for occupational safety management system based on a fuzzy analysis of production incidents. *J Phys: Conf Ser* 1333:072021. <https://doi.org/10.1088/1742-6596/1333/7/072021>
12. Nikulin AN, Dolzhikov IS, Klimova IV et al (2021) Assessment of the effectiveness and efficiency of the occupational health and safety management system at a mining enterprise. *Occup Safe Indust* 1:66–72. <https://doi.org/10.24000/0409-2961-2021-1-66-72>
13. Nikulin A, Nikulina AY (2017) Assessment of occupational health and safety effectiveness at a mining company. *Ecol, Environ Conserv* 23(1):351–355
14. Harrington J (1965) The desirability function. *Ind Qual Cont* 21(10):494–498
15. Trautmann H, Weihs C (2006) On the distribution of the desirability index using Harrington's desirability function. *Metrika* 63(2):207–213. <https://doi.org/10.1007/s00184-005-0012-0>
16. Trautmann H (2004) The desirability index as an instrument for multivariate process control. Technical Report, Universität Dortmund, SFB 475 Komplexitätsreduktion in Multivariaten Datenstrukturen. <https://doi.org/10.17877/DE290R-15023>
17. Kim KJ, Lin DKJ (2000) Simultaneous optimization of multiple responses by maximizing exponential desirability functions. *J R Stat Soc: Ser C: Appl Stat* 49(3):311–325. <https://doi.org/10.1111/1467-9876.00194>
18. Reiman T, Pietikäinen E (2012) Leading indicators of system safety—monitoring and driving the organizational safety potential. *Saf Sci* 50(10):1993–2000. <https://doi.org/10.1016/j.ssci.2011.07.015>
19. Marhavidas PK, Pliaki F, Koulouriotis DE (2022) International management system standards related to occupational safety and health: an updated literature survey. *Sustain* 14(20):13282. <https://doi.org/10.3390/su142013282>



Prospects for the Use of Drilling Sludge from the Oil Fields of the Southern Federal District as Raw Materials for the Production of Ceramic Building Bricks

V. S. Romanyuk^(✉), T. A. Bondareva, V. M. Kurdashov, N. A. Vilbitskaya, and A. A. Yakovenko

Platov South-Russian State Polytechnic University (NPI), 132, Prosveshcheniya St.,
Novocherkassk 346428, Russia
lera_romanyuk_1999@mail.ru

Abstract. The construction industry is one of the main leading sectors of the economy in the country. Among them, materials from clay raw materials have been widely used. One of these materials is ceramic building bricks. Due to the depletion of reserves of clay deposits, which is the main material in the raw material mixture for the production of ceramic building materials, further search for solutions necessary for the development of resource-saving technologies is relevant. Another urgent problem today is the disposal of man-made waste. One of the types of such waste is drilling sludge formed during drilling of oil wells. The relevance of the research lies in the need to develop new modern technologies and methods for the production of ceramic building bricks, using drilling sludge from oil fields of the Southern Federal District (SFD) in the raw material composition. This is due to the rapid growth in the volume of non-recyclable drilling waste in the sludge accumulators of oil-producing stations, and the depletion of reserves of natural clay raw materials used in the ceramic industry. The research is aimed at the disposal and reuse of drilling mud, which will create a reserve of affordable competitive raw materials for the production of ceramic bricks.

Keywords: Ceramic building bricks · Drilling mud · Clay · Resource-saving technology · Man-made waste · Clay raw materials · Recycling

1 Introduction

Currently, the restoration of the natural process of the ecological system of our planet is one of the most important tasks that requires an immediate search for all possible solutions. Taking into account the important factor that the ecology of the environment suffers most from mass pollution of various ecospheres, the launch of its restorative cleansing effect will not be able to take place without the participation of humanity.

One of the sources of pollution of the ecosystem is the reserves of drilling mud–drilled rock, which contains the remains of drilling mud, drilling wastewater and fluid

layers of wells. Over the past decades, the volume indicators of drilling mud deposits have been increasing. In this regard, the ecological state of the world suffers from the negative impact of man-made waste. The oil industry, although not the most polluted production, but its waste has a negative impact on the environment. From 2009 to the present, it has been noticed that the volume of formed drilling sludge has increased tenfold, since its processing is not carried out naturally. Also, the increase in the volume of non-processed drilling sludge is due to the fact that the number of wells created for oil production has increased [1, 2].

According to official data for 2023, Russia is among the three leaders in oil and gas production. The amount of drilling mud formed in a year reaches several million tons. The development of hydrocarbon deposits in the SFD is carried out by 49 enterprises, the largest of which are Gazprom Open Joint Stock Company, Rosneft Open Joint Stock Company, LUKOIL Open Joint stock Company and their subsidiaries. 310 oil and gas fields have been discovered on the territory of the district, 270 of them are purely oil. The Krasnodar Territory, Volgograd Region and Stavropol Territory are the leaders in terms of the number of deposits, which account for more than 75% of recoverable reserves [3–5].

The main oil fields in the SFD are:

- (1) Bezdnoye (Republic of Adygea);
- (2) Beshkul'skoye (Astrakhan region);
- (3) Stavropol oil and gas field (Stavropol Territory);
- (4) Morozovskoye (Krasnodar Territory);
- (5) Slavyanskoye (Krasnodar Territory);
- (6) Vostochno-Chumakovskoye (Krasnodar Territory).

It is quite difficult to get rid of a large amount of man-made waste completely. As a result, drilling sludge accumulates for years and has a detrimental effect on the ecosystem of our country. It is necessary to contribute to the reduction of accumulated waste of this type or even their complete disposal.

In addition to the global problem associated with the increase in deposits of drilling mud, there is another equally important one—the depletion of reserves of deposits of clay raw materials used in the production of ceramic building materials. In the Russian market, these products are in great demand, as they have a long service life. One of these materials is ceramic building bricks—the most common and widely used in the construction of external walls and load-bearing partitions. Due to the fact that clay deposits are being exhausted, the search for solutions to this problem, aimed at developing new resource-saving technologies, becomes in demand [6, 7]. Making changes in the technology of ceramic brick production, namely in the raw material composition of products, is one of the ways to solve. Since 2016, the Russian Federation has been implementing a Strategy for the Development of the Building Materials industry, in which support for manufacturers of building materials involved in the disposal of industrial waste is fixed at the state level.

Thus, the introduction of drilling mud as a raw material component in the production of ceramic building bricks is a promising area of research that requires special attention.

2 Experimental Part

The object of the study was selected drilling sludge from two oil fields of the SFD (Slavyansky and Morozovsky fields of Krasnodar Krai). To determine the possibility of using the studied drilling mud as a raw material component in the production of ceramic building bricks, a comparative analysis of drilling mud with clay extracted on the territory of the SFD (Vladimirovsky deposit of the Rostov region) was carried out. The physicochemical and technological properties of the materials under consideration were investigated. All studies were carried out in the laboratory "Recycling of fuel energy waste" on the basis of the Platov South-Russian State Polytechnic University (NPI).

Studies of the chemical composition of the studied raw materials were carried out by X-ray spectral fluorescence analysis (XRF) on a sequential vacuum spectrometer of the PW2400 model by melting samples with a mixture of lithium borates. Mass loss during calcination was determined according to the methodology of the Scientific Council on Analytical Research Methods using secondary ion mass spectrometry 418-X at a temperature of 1050 °C [8]. During the determination of the chemical composition of drilling mud and clay, the following data were obtained, presented in Tables 1, 2, and 3.

Table 1 Chemical composition of drilling mud from the Morozovskoye oil field (Krasnodar Territory)

Material	Content, mass %												
	Na ₂ O	MgO	Al ₂ O ₃	SiO ₂	K ₂ O	CaO	TiO ₂	Fe ₂ O ₃	SO ₃	Cl	BaO	Other	L.O.I
Drilling waste	1.15	1.17	10.26	62.14	1.48	4.35	0.54	3.82	2.07	0.25	1.83	1.67	9.27

Table 2 Chemical composition of drilling mud from the Slavyanskoye oil field (Krasnodar Territory)

Material	Content, mass %												
	Na ₂ O	MgO	Al ₂ O ₃	SiO ₂	K ₂ O	CaO	TiO ₂	Fe ₂ O ₃	MnO	P ₂ O ₅	BaSO ₄	L.O.I	
Drilling waste	1.45	0.78	5.33	22.36	0.89	4.37	0.26	3.14	0.105	0.1	49.8	9.85	

Table 3 Chemical composition of clay of the Vladimirovsky deposit of the Rostov region

Material	Content, mass %										
	SiO ₂	Al ₂ O ₃	Fe ₂ O ₃	CaO	MgO	TiO ₂	P ₂ O ₅	K ₂ O	Na ₂ O	SO ₃	L.O.I
Clay	63.20	20.45	3.26	1.37	0.48	0.90	0.06	2.05	0.61	0.04	7.37

As can be seen from Tables 1 and 2, chemical analysis confirms the predominant content of the main mineral-forming elements in drilling mud, such as SiO₂ and Al₂O₃.

It is also worth noting that in the drilling sludge from the Slavyansk deposit, the content of these elements is 2–3 times less than in the sludge from the Morozovsk deposit. Silicon and aluminum oxides reduce the temperature coefficient of linear expansion (TCLE) of the clay material, at low values of which the heat resistance of the raw material increases. This indicates that the drilling sludge from the Slavyansk deposit has better heat resistance, which allows the material not to crack with sudden and repeated temperature changes.

From Table 3, one can notice a significant content of the main oxides SiO_2 (63,20%) and Al_2O_3 (20,45%). The clay of the Vladimirovsky deposit consists mainly of kaolinite (37,8%) and a small amount (10,6%) of hydrosilicate. It includes a package of montmorillonite (9,6%) with impurities of sericite (7,7%) and quartz grains (26,4%) between the packages of hydrosilicates. The clay under study has a cellular microstructure with a feldspar content (pelitized) of 5,9%.

According to the results of a comparative analysis of the chemical compositions of drilling mud and clay, it was found that the presence of the main clay-forming oxides in drilling mud allows them to be used as a raw material component in the production of ceramic building bricks. The studied type of technogenic waste is similar in composition and properties to the clay raw materials used in the production technology of construction ceramics.

As can be seen from the chemical composition (Tables 1 and 2), heavy metal oxides are present in drilling slurries from the Morozovskoye and Slavyanskoye oil fields, the content of which is within acceptable limits in accordance with SanPiN 2.6.1.2523 “Radiation safety standards (NRB-99/2009)” (no more than 2.0 wt.%) [9].

Sources of heavy metals in nature are natural (weathering of rocks and minerals, volcanic activity and others) and man-made (mining and processing of minerals, motor transport and others). Natural radionuclides and harmful bacteria are present in drilling mud. In this regard, radiological and sanitary-epidemiological studies were conducted. Radiological studies of drilling slurries were carried out using the MULTIRAD spectrometric complex with PROGRESS software. The results of radiological studies of drilling waste from the Morozovsk and Slavyansk oil fields are presented in Table 4.

According to the obtained radiological research data from Table 4, it can be seen that the studied drilling slurries belong to the I class of building materials, depending on their specific effective activity, which indicates the possibility of their use in all types of construction, in particular in the production of ceramic building bricks.

A set of sanitary and epidemiological measures is necessary before using raw materials. The main stage is disinfection, which is a set of measures aimed at destroying harmful bacteria found in drilling mud (cocci chains, cylindrical sticks, spiral-curved spirilli). To check for the presence of harmful bacteria, samples of drilling sludge were sent to the branch of the Center for Hygiene and Epidemiology in the Rostov Region in Novocherkassk. The studies were conducted in accordance with MU 2.1.7.730-99 “Hygienic assessment of the soil quality of populated areas” [10].

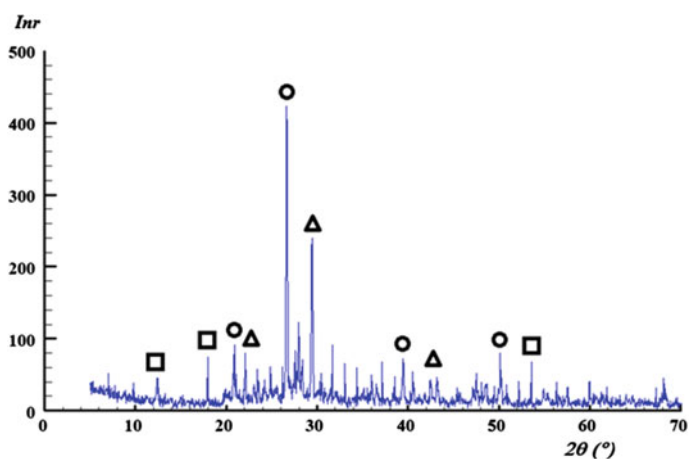
During the research, it was found that no harmful bacteria (pathogens of botulism, tetanus, gangrene and anthrax bacillus) were detected. Only spiral-curved spirillae and cocci chains were recognized, which, when heated to 100–120 °C, disintegrate with

Table 4 The results of radiological studies of drilling waste from the Slavyanskoye and Morozovskoye oil fields

Name of the material under study	Defined indicators	Research results; units of measurement; confidence probability	The value of the permissible level; units of measurement	ND on the research method
Drilling mud from the Slavyansk deposit	Effective specific activity of natural radionuclides Ra-226, Th-232, K-40	(62 ± 10) Bk/kg; P = 0,95	No more than 370 Bk/kg (1st class)	GOST 30,108-94 "MICMII GNMC "VNIIFTRI" dated 22.12.2003
Drilling mud from the Morozovsk deposit		(89 ± 14) Bk/kg; P = 0.95		

the formation of a small amount of alphasellulose. For final disinfection, the studied drilling slurries should be dried within 24 h at a temperature of 120–150 °C.

Next, the phase composition of drilling mud was studied, which was determined using powder X-ray diffraction analysis (PRD). The samples were crushed and examined using an ARL X' TRA (Thermo Fisher Scientific) X-ray powder diffractometer, which is part of the Center for Collective use of "Nanotechnology" of the Platov South-Russian State Polytechnic University (NPI). Interpretation of the obtained data was carried out using the ICDD database (The International Center for Diffraction Data) [3–5]. The results of determining the phase composition of drilling mud from the Morozovskoye oil field are shown in Fig. 1.

**Fig. 1** X-ray of drilling waste from the Morozovskoye oil field (○—quartz; □—sodalite; Δ—kaolinite)

As can be seen from Fig. 1, the main phase in the studied drilling mud is β -quartz (β - SiO_2), which is in an amount of about 25–30%. Other phases are kaolinite ($\text{Al}_2\text{O}_3 \cdot 2\text{SiO}_2 \cdot 2\text{H}_2\text{O}$) and sodalite ($3\text{Na}_2\text{O} \cdot 3\text{Al}_2\text{O}_3 \cdot 6\text{SiO}_2 \cdot 2\text{NaCl}$).

The results of determining the phase composition of drilling mud from the Slavyanskoye oil field are shown in Fig. 2.

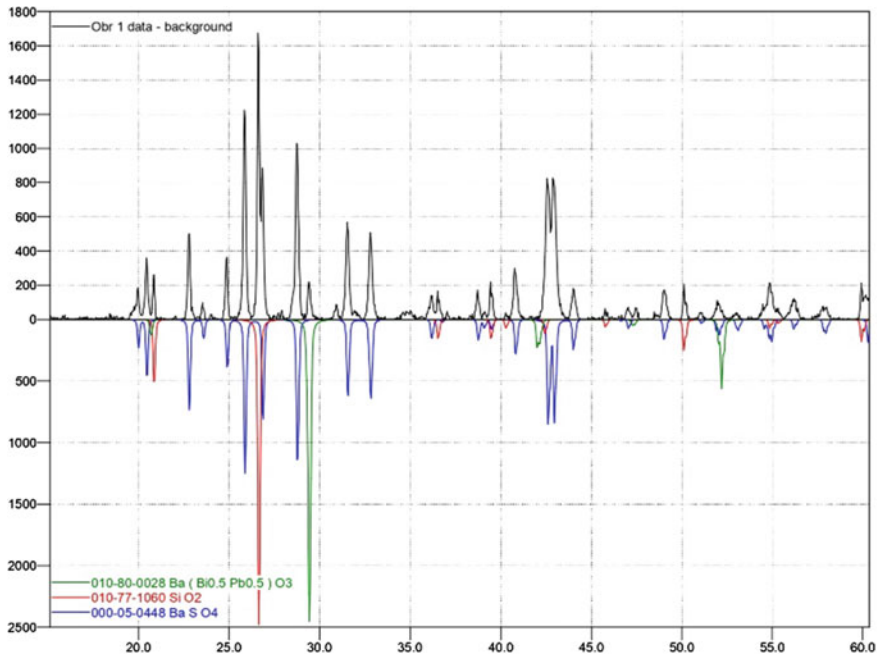


Fig. 2 X-ray of drilling mud from the Slavyanskoye oil field

According to the research results (Fig. 2), the main phase in this drilling mud is α -quartz (α - SiO_2), which is in an amount of about 30–35%.

The presence of the main phases of α -quartz and β -quartz in the composition of the studied drilling mud indicates the possibility of their use as raw materials in the production of ceramic building bricks.

The plasticity of the material in the production of ceramic bricks is one of the most important characteristics. Determination of the plasticity of the studied raw materials was carried out on the Vasiliev device and in accordance with GOST 5180-2015 [11]. For this purpose, the moisture content of the material in the state of the upper limit of plasticity was found by the standard weight method. The determination of the lower limit of plasticity was made at the boundary of rolling, at which the bundles crumble into separate, non-connecting parts. The value of the plasticity number was found as the average of the two definitions. The results of determining the plasticity of the studied drilling slurries from the Slavyanskoye and Morozovskoye oil and clay deposits of the Vladimirovskoye field are shown in Table 5.

Table 5 Plasticity of the studied drilling slurries from the Slavyanskoye and Morozovskoye oil and clay deposits of the Vladimirovskoye field

Material	Upper limit of plasticity W_m , %	Lower limit of plasticity W_p , %	Plasticity number P , %
Drilling mud from the Slavyansk deposit	28.32	19.29	9.03
Drilling mud from the Morozovskoye deposit	50.30	29.62	20.68
Clay of the Vladimirovskoye deposit	49.42	25.00	24.42

Table 5 shows that the number of plasticity of drilling mud from the Slavyanskoye and Morozovskoye oil and clay deposits of the Vladimirovskoye field is 9,03%, 20,68% and 24,42% respectively. Consequently, drilling mud from the Slavyansk deposit is a moderate plastic material, drilling mud from the Morozovsky deposit and clay from the Vladimirovsky deposit belong to the class of medium–plastic, according to the classification depending on the number of plasticity of clay materials according to GOST 9169-2021 [12]. Thus, it can be concluded that the more plastic the material, the wider its humidity range, at which plasticity manifests itself. Since the drilling slurries under study have a molding ability, their use in the production of building ceramic bricks is permissible.

The most promising direction that can combine the two stages of conversion of drilling mud into raw materials for the production of building ceramic bricks with the production of finished products is the combination of chemical and thermal methods. In this regard, prototypes were molded using the studied drilling slurries and clay in the raw material mixture, and the firing properties of the feedstock were also checked.

Drilling mud from the Slavyanskoye and Morozovskoye oil fields and clay from the Vladimirovskoye field, pre-dried to a residual humidity of 4–6%, with further grinding and sieving on a 008 sieve, was used to obtain prototypes. 4 series of samples were formed (two of which using drilling mud from the Slavyanskoye oil field and two with drilling mud from the Morozovskoye oil field) with a percentage of clay/drilling mud equal to 50/50% and 40/60%, followed by drying and firing at a temperature of 1000° C. During the firing process, the temperature rose at a rate of 2° / min and at the final temperature there was an exposure for 1 h. Cooling is natural, lasting at least 10 h (Figs. 3, 4, 5, and 6). During the firing process, the process of burning out of the organic components of the drilling mud was observed in the heating temperature range of 500–600 °C, which indicates the utilization of waste in the technological process of ceramic brick production [13].

After firing, each sample was carefully examined, noting at the same time the location of the samples in the furnace; the color and uniformity of its distribution over the shard; cracks; shape change due to various shrinkage, which may occur due to uneven

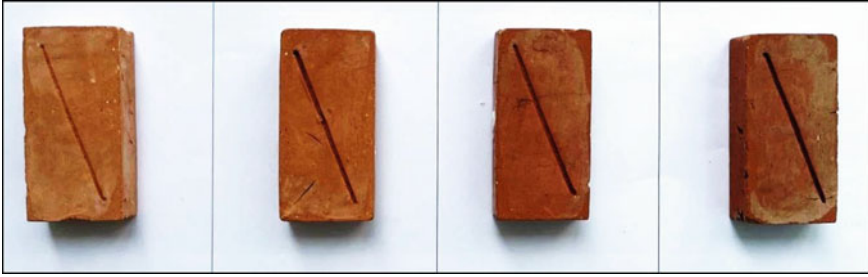


Fig. 3 Series number 1 of fired samples using drilling mud from the Slavyanskoye oil field in the raw material composition

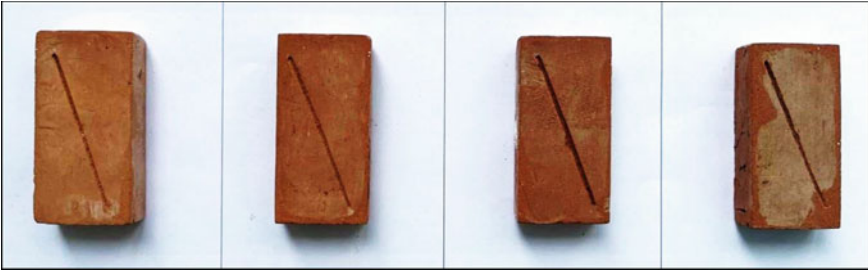


Fig. 4 Series number 2 of fired samples using drilling mud from the Slavyanskoye oil field in the raw material composition

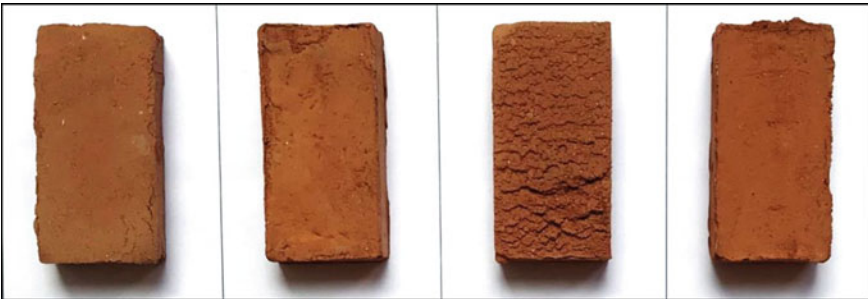


Fig. 5 Series number 1 of fired samples using drilling mud from the Morozovskoye oil field in the raw material composition

temperature distribution in the furnace; deformation or melting of samples associated with burnout.

During the post-firing visual examination of the samples, if we consider each sample of the series, it was revealed that the tiles of the same composition and the same firing temperature regime at first glance do not differ much from each other, but if we consider each sample separately, we can notice changes in visual characteristics: the color varies from light brown to brown and depends on the mode drying and arrangement of tiles

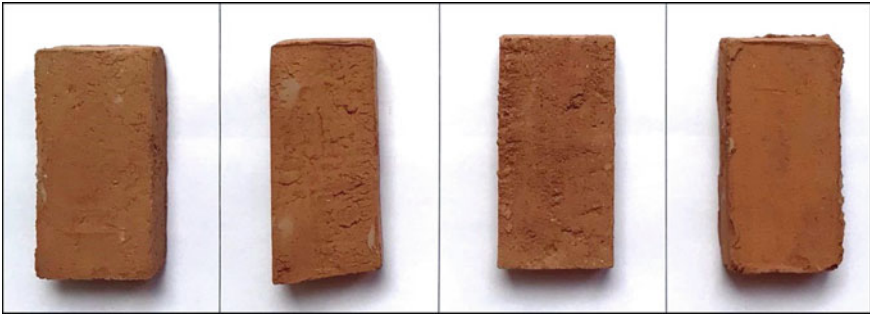


Fig. 6 Series number 2 of fired samples using drilling mud from the Morozovskoye oil field in the raw material composition

in the kiln during firing; on some samples, efflorescences are observed on the surface, as well as shiny and yellow inclusions are present on these samples, which indicates the content of various impurities in the sludge and clay; the presence of a small number of cracks; there is a slight deformation and melting of the samples. All samples have a dense well-baked shard.

If we compare two series of samples using the same drilling mud, but with different percentages of it in the mass, we can observe a slight difference in color, which indicates a different chemical composition of raw materials and different firing temperature conditions. The color of the studied samples is also affected by the content of Fe_2O_3 and TiO_2 . The presence of a large amount of these oxides in the raw material mixture gives the material a characteristic red-brown color [14–16].

In the drilling mud from the Morozovskoye oil field, the content of $\text{TiO}_2 = 0,54\%$, and $\text{Fe}_2\text{O}_3 = 3,82\%$. In the drilling sludge from the Slavyanskoye oil field, the content of $\text{TiO}_2 = 0,26\%$, and $\text{Fe}_2\text{O}_3 = 3,14\%$. In the clay of the Vladimirovskoye deposit, the content of these oxides is $0,90\%$ and $3,26\%$, respectively. Thus, it can be concluded that the higher the content of coloring oxides in the ceramic mixture, the richer and darker the color.

With an increase in the firing temperature and the content of drilling mud in the raw mixture, the fire shrinkage of the samples decreases. Since clay is refractory, and the value of its fire shrinkage is in the range from 2 to 8%, when drilling mud is added, the fire shrinkage indicators decrease, which indicates an intensification of the sintering process. Thus, the criterion for the suitability of clay materials for the manufacture of ceramic building bricks is the absence of swelling of the material during firing in the temperature range of $950\text{--}1100\text{ }^\circ\text{C}$.

3 Conclusion

The use of man-made waste, in particular drilling sludge from oil fields, in a raw mixture of ceramic building materials allows to obtain an environmental effect as a result of the neutralization of oil sludge and the economy of the main clay raw materials used in the production technology of ceramic building materials.

During the tests carried out, it was revealed that partial substitution of clay raw materials for drilling mud of the SFD in the production of ceramic building bricks is permissible. At the same time, this building material retains its basic properties and can be used in construction according to GOST 530-2018 [17]. The proposed technology will contribute to the utilization of drilling waste from oil-producing stations and subsequently reduce the volume of man-made non-recyclable waste in nature, as well as preserve natural reserves of clay raw materials.

Acknowledgements. The work was carried out within the framework of the strategic project «Scientific and Innovative cluster “Contact R&D Center”» The development program of SRSPU (NPI) in the implementation of the strategic academic leadership program “Priority-2030”.

References

1. Yatsenko EA, Tretyak AA, Chumakov AA, Smoliy VA (2022) Research of the possibility of using glass and sodium hydroxide for synthesis of aluminum silicate propants based on drill sludges. *Key Eng Mater* 910:678–683
2. Yatsenko EA, Goltsman BM, Chumakov AA, Vilbitskaya NA, Li W (2021) Research on the synthesis of propants applied for oil production by the method of hydraulic facing. *Mater Sci Forum* 1037:181–188
3. Klimova LV, Smoliy VA, Romanyuk VS (2022) The use of drilling waste in the production of ceramic building materials. *IOP Conference Series: Earth Environ Sci* 1061
4. Romanyuk VS, Klimova LV, Kurdashov VM, Izvarin AI, Yatsenko VS (2022) Prospects for the use of painted ceramic facing materials using man-made waste. *Lecture Notes in Civil Engineering*
5. Tretyak AA, Yatsenko EA, Onofrienko SA, Karelskaya EV (2021) Identification of drilling wastes and their use. *Bulletin of the Tomsk Polytechnic University, Georesource Engineering*
6. Kuvykin NA, Bubnov AG, Grinevich VI (2004) Hazardous industrial waste (p 148). Ivanovo State Chemical-Technological Unit
7. Pichugin EA (2013) Assessment of the impact of drilling waste on the environment. *Young Scient* 9:122–124
8. Al'myashev VI, Gusarov VV (1999) Thermal methods of analysis: textbook allowance. SPbGTU (LETI), St. Petersburg, p 40
9. SanPiN 2.6.1.2523 (2010) Radiation safety standards (NRB-99/2009). Standartinform, Moscow, p 222
10. MU 2.1.7.730-99 (1999) Hygienic requirements for the quality of soil in populated areas. Department of Sanitary and Epidemiological Supervision of the Ministry of Health of the Russian Federation, Moscow, p 20
11. Interstate standard GOST 5180-2015 (2015) Soils. Methods for laboratory determination of physical characteristics. Interstate Council for Standardization, Metrology and Certification (IGU). Standartinform, Moscow
12. Interstate standard GOST 9169-2021 (2021) Clay raw materials for the ceramic industry. Classification. Interstate Council for Standardization, Metrology and Certification (IGU). Standartinform, Moscow
13. Pashchenko AA (1986) Physical chemistry of silicates: a textbook for universities. Ed. Higher school, Moscow, p 367
14. Gorshkov BS, Saveliev VG, Fedorov NF (1988) Physical chemistry of silicates and other refractory compounds: textbook. Higher school, Moscow, p 400

15. Deneko Y (2014) About the problem of drilling waste processing. *Oil Gas Siberia* 1(14):29–30
16. Maksimovich VG, Bukov NN (2013) Neutralization of oil sludge and cleaning oil pipelines of oil deposits in the Krasnodar Territory. In: *Materials of the XI International Seminar on Magnetic Resonance (spectroscopy, tomography and ecology)*, Rostov-on-Don, p 120
17. Interstate standard GOST 530-2018 (2018) Brick and ceramic stone. General specifications. Interstate Council for Standardization, Metrology and Certification (IGU), Standartinform, Moscow



Study of the Effect of Zirconium Dioxide on the Physical and Mechanical Properties of Foamed Geopolymer Materials for Construction Purposes Based on Coal Combustion Waste at Arctic Thermal Power Plants

B. M. Goltsman, V. A. Smoliiy, Yu. V. Novikov^(✉), V. S. Yatsenko, and D. A. Golovko

Platov South-Russian State Polytechnic University (NPI), 132, Prosveshcheniya St.,
Novocherkassk 346428, Russia
novikovtnv@yandex.ru

Abstract. The possibility of obtaining foamed geopolymers—building heat-insulating materials based on coal combustion waste at thermal power plants of Severodvinskaya CHPP-1 and Apatitskaya CHPP was considered. A complex of studies of the considered waste was carried out, its chemical (oxide) composition, X-ray phase composition, and microstructural structure were determined. The mechanisms of pore formation during the synthesis of geopolymers are considered, and the most optimal pore former is chosen. The influence of the addition of zirconium dioxide on the strength characteristics of the samples has been established. The density and porous structure of the obtained geopolymer materials based on coal generation waste are analyzed, and the strength characteristics of the samples are also investigated.

Keywords: Geopolymer · Coal combustion waste · Solid fuel energy · Coal energy · Thermal insulation materials · Building materials · Foaming agents · Zirconium dioxide

1 Introduction

One of the main goals of improving resource-saving technologies is to find new ways to utilize and process man-made waste. The most acute problem is the processing of waste generated by burning coal at thermal power plants. It is known that according to the International Energy Agency (IEA), the share of coal energy in 2020 amounted to a third of the total generated electricity. This shows that coal generation is the largest source of electricity. In 2021, coal-fired energy reached record levels, with an increase in emissions not only of gases such as carbon dioxide, carbon monoxide, nitrogen oxides, sulfur oxides, but also of a number of solid mineral products of coal combustion, such

as ash, slag and ash and slag mixtures (ASM) [1]. It is well known that at the moment in the world the total volume of accumulation of waste from coal combustion every year is 1 billion tons [2].

Annually, coal-fired power plants of the Russian Federation generate more than 22 million tons of coal combustion waste (CCW), which is its mineral part, mainly consisting of fly ash and slag [3]. According to existing estimates, the total amount of waste from coal combustion at ash dumps reaches 1.8 billion tons, occupying an area of over 20 thousand square meters [4]. The volume of processing waste from coal combustion is low and amounts to only 10–12% [5]. In this regard, it is necessary to search for modern methods of processing waste from coal generation.

In the Arctic zone of the Russian Federation, the share of coal-fired thermal power plants is at least 20%, and therefore for this region the issue of processing CCW is the most urgent [6]. One of the promising methods for processing CCW is to obtain new materials based on them—geopolymers, which are hydraulic binders of alkaline activation [7]. Their structure is represented by three-dimensional glass-crystalline aluminosilicates, which consist of aluminum-oxygen and silicon-oxygen tetrahedra connected by oxygen into rings and chains. Also, the use of CCW for the production of geopolymers is due to the presence in them of a high proportion of the vitreous aluminosilicate phase and their dispersion, and has a positive effect on the performance properties of the finished material [8]. At the same time, the introduction of CCW into alkaline activation binders makes it possible to reduce their radiation impact on the environment [9]. Based on economic considerations, it is advisable to synthesize geopolymers at temperatures below 100 °C and give them a cellular structure, which makes it possible to obtain lightweight materials with a density of less than 1000 kg/m³. The cellular structure of the geopolymer is obtained by introducing into their composition special gas-generating additives—foaming agents, which react with the raw components of the geopolymer, or decompose under external influence with the formation of a gas phase that foams the liquid raw mixture capable of maintaining the formed shape and is converted into solid foam when drying out.

Geopolymer materials are durable, environmentally friendly, resistant to aggressive environments. It is known [10–12] about the high frost resistance of geopolymers—they are able to withstand about 150 cycles of thawing—freezing. This property of these materials may subsequently allow the use of geopolymers for road construction in harsh climatic conditions with negative temperatures. However, despite their advantages, geopolymers are of limited use, mainly due to insufficient information about the effect of the used aluminosilicate raw materials and production parameters on the properties of the geopolymer, and, accordingly, its operational characteristics, which in some cases leads to the complication of predicting the properties of the material.

The process of geopolymerization proceeds in a strongly alkaline environment, for which alkaline activators are used, which are a mixture of solutions of liquid glass and strong alkali. It is known [13] that the process of geopolymerization includes the following stages: dissolution of silicon and aluminum oxides in sodium hydroxide with the formation of silicates and aluminates; destruction of polymer structures in CCW with

the formation of monomers; setting and compaction as a result of the polymerization of monomers. The general formula of geopolymers can be represented by Eq. (1):



where M is an alkali metal atom, z is 1, 2, or 3, and n is the degree of polycondensation or polymerization [14–17]. Thus, the origin of aluminosilicate raw materials and the strong alkali solutions used affect the composition and properties of the resulting geopolymer.

Since geopolymer materials for road construction must meet high mechanical properties, the urgent task is to find ways to increase their strength characteristics.

It is known that in order to improve the properties of geopolymer, special inorganic and organic additives are introduced into them, which can be in a solid or liquid state, have a different granulometric composition, be nanopowders, etc. Previously, the authors tested the effect of cullet additives and quartz sand on foamed geopolymer materials. It was established [18] that the addition of cullet tends to increase the strength properties of geopolymer materials, the strength of the material more than doubles. Quartz sand also positively affects the strength of the studied geopolymer samples, however, to a lesser extent, increasing the strength of the material by 1.8 times. In this case, cullet had a better effect on the properties of the final material, apparently due to the fact that it is an amorphous material, similar in structure to coal waste, which is also amorphous. In addition, tests were carried out on the effect on the properties of geopolymer materials of such inorganic substances as CaO, MgO, ZnO, TiO₂, Al₂O₃, SiC etc. [19–23].

It has been established [24] that the inclusion of a small amount of zirconium dioxide into the composition of geopolymers significantly increases their ultimate strength, which is due to the formation of zirconium dioxide bonds with three-dimensional polysilicate chains, which leads to a decrease in the mobility of sodium ions. It is also known [25] that zirconium dioxide does not take part in geopolymerization processes, but acts as a filler, penetrating between the polysilicate structure and forming a strong microstructure, which, consequently, increases the strength of the geopolymer, while if zirconium dioxide content exceeds 10%, deceleration occurs. the process of geopolymerization, and, consequently, negatively affects the ultimate strength of the geopolymer material.

The authors of [24] studied the effect of adding zirconium dioxide on the strength characteristics of a geopolymer based on fly ash. The addition of zirconium dioxide in an amount of 3% made it possible to increase the strength of the sample by 30%.

Studies have also been carried out on the effect of the mineral zircon (ZrSiO₄) on the properties of dense geopolymer materials based on metakaolin. The authors of [25] found that the presence of zircon in an amount of 10 g per 100 g of metakaolin led to an improvement in the microstructure of the geopolymer. The authors suggest that the zircon was embedded between the polysilicate chains, forming a rigid structure of the material, and thereby increasing its compressive strength to 74 MPa. However, the above studies are devoted to the effect of zirconium dioxide and the mineral zircon on the properties of dense geopolymer materials (geopolymer concrete). Studies on the effect of these components on the properties of foamed geopolymers with a cellular structure have not been found, and therefore this study is particularly relevant.

2 Experimental Part

To carry out the study, 2 series of compositions were developed; The oxide composition of the studied CCW s is presented in Table 1.

Table 1 Oxide composition of the studied coal combustion wastes

CCW	Chemical composition ^a [wt. %]										
	SiO ₂	Al ₂ O ₃	Fe ₂ O ₃	CaO	MgO	SO ₃	TiO ₂	K ₂ O	Na ₂ O	P ₂ O ₅	LOI
Apatity CHP	52.39	22.15	7.73	3.59	2.63	0.37	1.05	1.94	0.78	0.36	6.05
Severodvinsk CHP-1	60.75	17.67	5.93	2.07	2.71	0.32	0.82	2.29	3.54	0.21	2.29

^a represented oxides, the content of which is higher than 0.1 wt. %

The true density of CCW was determined by the pycnometric method; for waste from Severodvinsk CHP-1 it is 2034 kg/m³, for waste from Apatity CHP it is 1832 kg/m³.

Study of the microstructure of waste from coal combustion at Severodvinsk CHP-1 and Apatity CHP, electron microscopy of the material was carried out. Figure 1 shows the microstructure of the studied CCW.

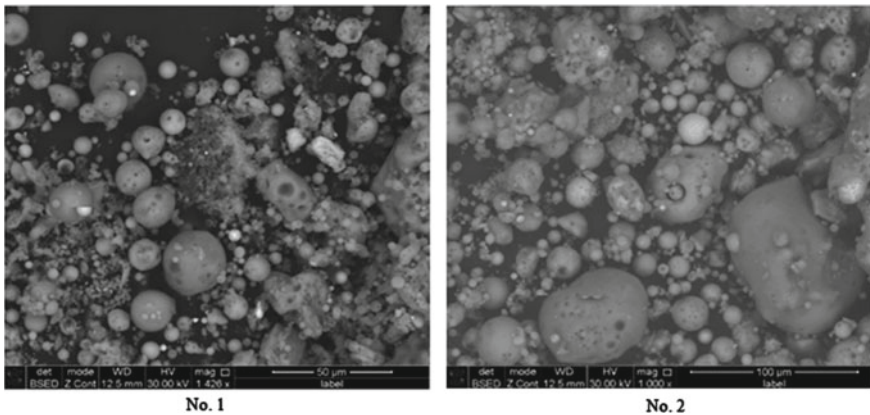


Fig. 1 Microscopic images of the studied wastes from coal combustion: No. 1—microstructure of the wastes of the Apatity CHP; No. 2—microstructure of the waste of Severodvinsk CHP-1

Figure 1 shows that the microstructure of the considered materials is represented by spherical particles with a size of 1–100 microns. These particles are hollow aluminosilicate microspheres, which are glass–ceramic balls formed during the combustion of coal fuel in power plant boilers. The outer coating of these microscopic spheres is expressed by a vitreous substance with a smooth non-porous surface. The internal space of aluminosilicate microspheres is filled with gases formed during coal combustion, such as carbon oxides, nitrous gases, etc. [26].

Microscopic images make it possible to see that in the studied coal combustion waste there is a variety of morphological properties of hollow aluminosilicate microspheres. So it can be seen that there are rather large aggregates of imperfect shape, 50–90 microns in size. Along with them, there are smaller aluminosilicate microspheres with a smooth surface and an ideal spherical shape, 5–20 μm in size.

To study the phase composition of CCW at the Apatitskaya CHPP and Severodvinsk CHPP-1, a qualitative X-ray phase analysis of these materials was carried out on an ARLX'TRA diffractometer (Thermo Fisher Scientific, Waltham, Massachusetts, USA). In the analysis, the Bragg–Brentano method was applied, which consists in reflecting a focused beam of X-rays [27]. The results of X-ray phase analysis of waste are shown in Fig. 2.

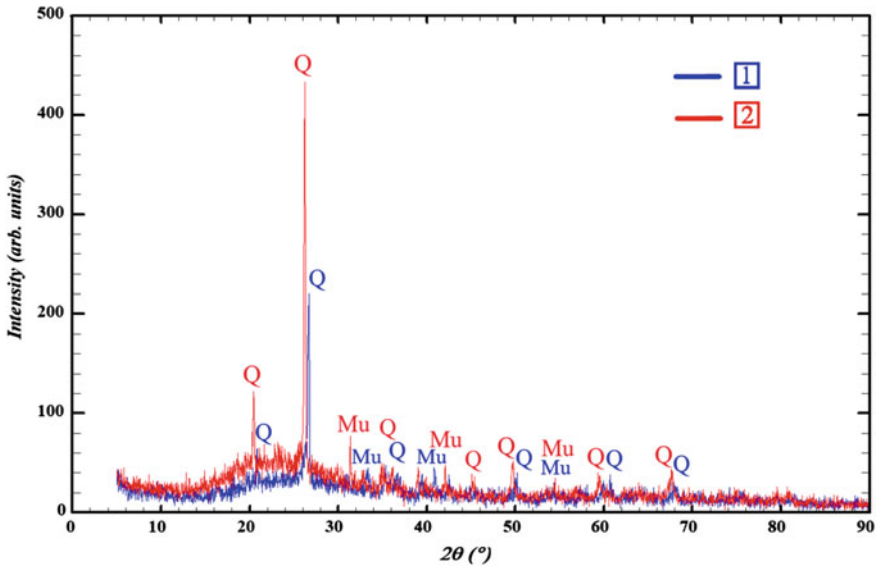


Fig. 2 X-ray pattern of the investigated coal combustion wastes: 1—wastes of the Apatity CHP; 2—waste from Severodvinsk CHP-1. Q—high quartz, Mu—mullite

The interpretation of the data obtained in the course of X-ray phase analysis was carried out using the Crystallographica Search-Match Version 3 software package of the ICDD PDF 2 database (International Center for Diffraction Data).

Figure 2 shows that in the studied CCW, the crystalline phase is expressed by the presence of high quartz and mullite. It is also seen that the materials contain mainly an amorphous phase, expressed as a halo. Thus, the studied waste is an amorphous material containing high quartz and mullite crystals dissolved in it.

Radiological studies of CCW were carried out using the MULTIRAD spectrometric complex with the PROGRESS software. These studies are aimed at establishing the content of radioactive isotopes such as K-40, Ra-226 and Th-232.

Radiological studies of CCW from Apatitskaya CHPP and Severodvinskaya CHPP-1 showed that their effective specific activity is no more than 370 Bq/kg, which confirms

their relation to the first class of building materials. Based on this, the samples of the investigated waste can be used in all types of construction.

Waste from coal combustion, which is the main precursor for obtaining geopolymers, was dried at a temperature of 105 °C for 24 h, ground and sifted through a sieve with a mesh size of 250 μm. In accordance with Table 2, mixing was carried out and an alkali activator solution was obtained: a 12 M aqueous solution of caustic soda was prepared, a 44% aqueous solution of sodium silicates of variable composition (silicate glue) was added to it, and the mixture was continuously stirred for 10 min. The resulting alkaline activator solution was mixed with previously prepared precursors—CCW, as well as the necessary amount of water necessary to obtain a homogeneous geopolymer paste, and stirred for 20 min. Aluminum powder for paint and varnish purposes and a 30% aqueous solution of hydrogen peroxide, as well as a hardening additive, zirconium dioxide, were used as blowing agents. In addition, a foam stabilizer—surfactant—sodium salt of stearic acid was introduced into the composition. It affects the interfilm fluid flow, stopping it, which positively affects the stability of the system's foam frame. The resulting geopolymer mixture was poured into cylindrical molds 40 × 40 mm in size. After 24 h, the samples were removed from the molds and dried for 14 days. Further, the physical and mechanical characteristics of the finished samples, namely the density and compressive strength, were investigated. Samples of a similar composition were also obtained, but without the introduction of zirconium dioxide, in order to establish the effect of the latter on the strength characteristics of geopolymers by comparing the strength of the samples.

Table 2 Raw material composition of geopolymers based on the studied wastes of coal combustion

No.	The content of the component [wt. %]						
	CCW	NaOH	Silicate glue	Al powder (over 100%)	H ₂ O ₂ 30% (over 100%)	Sodium stearate (over 100%)	ZrO ₂ (over 100%)
<i>Severodvinsk CHP-1</i>							
1.1	73	2	25	–	2	1	3
1.2	73	2	25	2	–	1	3
<i>Apatity CHP</i>							
2.1	73	2	25	–	2	1	3
2.2	73	2	25	2	–	1	3

The charge composition of geopolymers is presented in Table 2.

3 Results and Discussions

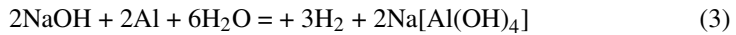
During the experiment, the mechanisms that occur when blowing agents are introduced into the geopolymer mixture were studied, their structure formation was studied, their density and compressive strength were determined.

The mechanism of foaming of a geopolymer suspension with hydrogen peroxide consists in the catalytic decomposition of H_2O_2 to form water and oxygen gas according to Eq. (2):



Catalysts for the decomposition of hydrogen peroxide are metal oxides contained in ash and slag.

The mechanism of foaming of a geopolymer suspension with aluminum powder consists in the interaction of aluminum with sodium hydroxide—a component of an alkaline activator and the formation of a complex sodium aluminate and hydrogen gas according to Eq. (3):



The structure of the obtained samples containing zirconium dioxide is shown in Fig. 3.

The study of samples of the obtained materials for ultimate compressive strength was carried out using a test press TP-1-350 “Universal”. The experimentally obtained physical and mechanical properties of geopolymer samples are shown in Table 3.

From Table 3 it follows that the density of the obtained materials is lower compared to the true density of the studied CCW, which are used as precursors. Hydrogen peroxide showed great pore-forming activity, however, when it is used, the pore size varies in a wide range, for sample 1.2 the pore diameter is from 1 to 4 mm, for sample 2.2—from 1.0 to 3.0 mm. This factor may adversely affect the operational properties of the geopolymer, and therefore, it is preferable to use aluminum powder as a powder-forming additive, since the pores in its use have a uniform distribution, a regular spherical shape, in the sample 1.1 the pore diameter is from 0.9 to 2.1 mm, in the sample 2.1—from 1.0 to 2.0 mm.

Tests for ultimate compressive strength of samples 1.1 and 1.2 based on CCW from Severodvinsk CHP-1 showed that zirconium dioxide has a positive effect on the strength of the material. The strength of sample 1.1 increased by 4.2 times, the strength of sample 1.2 increased by 4.5 times compared to a sample not containing zirconium dioxide. The strength characteristics of samples based on CCW from the Apatity CHP showed the worst results. Despite the fact that the strength of sample 2.1 increased by 4.6 times, and the strength of sample 2.2 increased by 4.5 times, it is not sufficient to operate these samples. This is mainly due to the raw materials used—samples of geopolymers from the combustion waste of the Apatity CHP are unstable, which, apparently, is associated with an insufficiently high content of silicon oxide in the initial composition of the waste.

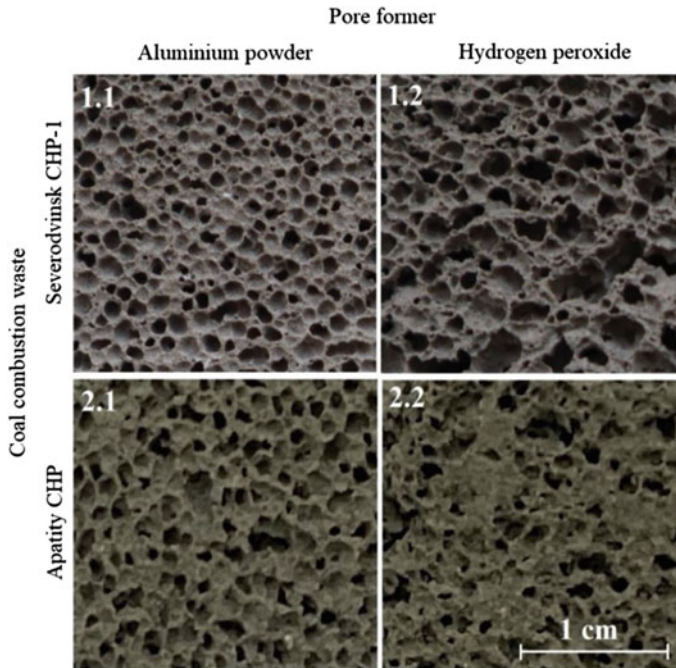


Fig. 3 Structure of geopolymer samples obtained on the basis of the studied coal combustion wastes

Table 3 Physico-mechanical parameters obtained from samples of geopolymers based on the studied wastes of coal combustion

Sample No	Sample density [kg/m ³]	Strength of sample containing ZrO ₂ [MPa]	Strength of the sample free of ZrO ₂ [MPa]
1.1	518	2.86	0.68
1.2	497	2.75	0.61
2.1	522	1.58	0.34
2.2	481	1.39	0.31

4 Conclusion

Thus, the effect of adding zirconium dioxide on the strength properties of foamed geopolymer materials based on coal combustion wastes from Severodvinsk CHP-1 and Apatity CHP, located in the harsh Arctic climatic conditions of the Russian Federation, was experimentally studied:

1. A scientific and technical review of existing studies in the field of the influence of zirconium dioxide on the strength characteristics of geopolymers was carried out. It was found that zirconium dioxide, as well as the mineral zircon, has a positive effect

- on the strength of geopolymer concretes, however, studies aimed at the effect of this component on the properties of foamed geopolymers have not been found.
2. The chemical and phase analysis of the investigated wastes of coal combustion—ash and slag mixtures of Apatitskaya CHP and Severodvinsk CHP-1 was studied. It was revealed that they are aluminosilicate amorphous material with a small amount of crystalline phase in the form of quartz and mullite. Thus, these materials are suitable for the production of geopolymers.
 3. Microscopic analysis of the studied waste showed that their microstructure is represented by hollow aluminosilicate microspheres of various diameters—from 10 to 100 microns.
 4. A series of samples containing the addition of 3% zirconium dioxide has been developed. In order to be able to compare the final properties of the material, a series of samples was also developed that did not contain this additive.
 5. It has been established that a 3% addition of zirconium dioxide made it possible to increase the strength of the studied samples by more than 4 times, which confirms its positive effect on the physical and mechanical properties of foamed geopolymer materials.

Acknowledgements. The work was carried out at SRSPU (NPI) with the financial support of the Russian Science Foundation, Agreement No. 21-19-00203 “Effective temperature-curing eco-geopolymers for road construction in the Arctic zone of the Russian Federation based on solid fuel combustion wastes at local thermal power plants” (headed by E.A. Yatsenko).

References

1. Report on the functioning of the UES of Russia in 2020 (2021) https://www.so-ups.ru/fileadmin/files/company/reports/disclosure/2021/ups_rep2020.pdf. Accessed 21 Jan 2021
2. The Ministry of Energy of the Russian Federation “round table” on the topic “Legislative regulation of the use of ash and slag waste of coal-fired CHP”. <https://minenergo.gov.ru/node/14014>. Accessed 18 Feb 2019
3. On the state and protection of the environment of the Russian Federation in 2020 (2021) State report. Ministry of Natural Resources of Russia; Moscow State University named after M.V. Lomonosov, Moscow, 1000 p
4. State Report (2019) On the state and protection of the environment of the Russian Federation in 2018. Ministry of Natural Resources of Russia. NPP “Cadastre”, Moscow, 844 p
5. Yatsenko EA, Smolii VA, Goltsman BM, Kosarev AS (2012) Investigation of the macro- and microstructure of foam glass based on slag waste from thermal power plants. *Izvestia of higher educational institutions. North Caucasian Region. Tech Sci* 6:127–130
6. Duxson P, Fernandez-Jimenez PJJ et al (2007) Geopolymer technology: the current state of the art. *J Mater Sci* 42:2917–2933
7. Ahmed MF, Nuruddin MF, Shafiq N (2011) Compressive strength and workability characteristics of low-calcium fly ash-based self-compacting geopolymer concrete. *Intern J Civil Environ Eng* 3:72–78
8. Provis JL, Van Deventer JSJ (2009) *Geopolymers structure, processing, properties and industrial applications*. Woodhead Publishing
9. Steinerova M (2011) Mechanical properties of geopolymer mortars in relation to their porous structure. *Ceramics–Silikáty* 55:362–372

10. Škvára F, Jílek T, Kopecký L (2005) Geopolymer materials based on fly ash. *Ceramics–Silikáty* 49:195–204
11. Davidovits J (2002) 30 Years of successes and failures in geopolymer applications. Market trends and potential breakthroughs. In: *Geopolymer 2002 Conference*, October 28–29, Melbourne, Australia
12. Davidovits J, Geopolymers (1991) Inorganic polymeric new materials. *J Thermal Anal Calor* 37:1633–1656
13. Xu H, Van Deventer JSJ (2000) The geopolymerisation of aluminosilicate minerals. *Int J Miner Process* 59:247–266
14. Li C, Sun H, Li L (2010) A review: the comparison between alkali-activated slag (Si + Ca) and metakaolin (Si + Al) cements. *Cement Concr* 40:1341–1349
15. Provis JL, van Deventer JSJ (2009) *Geopolymers*, Woodhead Publishing Limited
16. Yatsenko EA et al (2023) Influence of various coal energy wastes and foaming agents on foamed geopolymer materials. *Synthesis/Mat* 16:264
17. Yatsenko EA et al (2023) Influence of modifying additives on the structure and properties of porous geopolymer building materials based on solid fuel combustion waste of arctic thermal power plants. In: *Proceedings of the 6th International Conference on Construction, Architecture and Technosphere Safety: ICCATS 2022*. Springer International Publishing, Cham, pp 534–543
18. Yatsenko EA, Goltsman BM, Trofimov SV, Kurdashov VM, Novikov YV, Smolii VA, Ryabova AV, Klimova LV (2022) Improving the properties of porous geopolymers based on TPP ash and slag waste by adjusting their chemical composition. *Materials* 15:2587
19. Zawrah MF, Abdel-Kader H, Elbaly NE (2012) Fabrication of Al₂O₃–20 vol.% Al nanocomposite powders using high energy milling and their sinterability. *Mater Res Bull* 47:655–661
20. Wahsh MMS, Khattab RM, Zawrah MF (2013) Sintering and technological properties of alumina/zirconia/nano-TiO₂ ceramic composites. *Mater Res Bull* 48:1411–1414
21. Abdel-Gawwad HA, Abd El-Aleem S (2015) Effect of reactive magnesium oxide on properties of alkali activated slag geopolymer cement pastes. *Ceramics–Silikáty* 59:37–47
22. Ma B et al (2022) The influence of calcium hydroxide on the performance of MK-based geopolymer. *Constr Build Mater* 291:27224
23. Okoye FN, Prakash S, Singh NB (2017) Durability of fly ash based geopolymer concrete in the presence of silica fume. *J Clean Prod* 149:1062–1067
24. Phair JW, Van Deventer JSJ, Smith JD (2008) The mechanism of polysialation in the incorporation of zirconia into fly ash based geopolymers. *Ind Eng Chem Res* 39:2925–2934
25. Zawrah MF, Farag RS, Kohail MH (2018) Improvement of physical and mechanical properties of geopolymer through addition of zircon. *Mater Chem Phys* 217:90–97
26. Yang T et al (2018) Effect of fly ash microsphere on the rheology and microstructure of alkali-activated fly ash/slag pastes. *Cem Concr Res* 109:198–207
27. Yatsenko EA, Smolii VA, Klimova LV, Goltsman BM, Ryabova AV, Golovko DA, Chumakov AA (2022) Solid fuel combustion wastes at CHPP in the Arctic Zone of the Russian Federation: utility in eco-geopolymer technology. *Glass Ceram* 78:374–377



Evaluation of the Physical and Performance Properties of Porous Polymers Depending on the Curing Mode

E. A. Yatsenko, S. V. Trofimov^(✉), A. A. Chumakov, S. A. Vilbitsky,
and N. S. Goltsman

Platov South-Russian State Polytechnic University (NPI), 132, Prosveshcheniya St.,
Novocherkassk 346428, Russia
23zarj23@mail.ru

Abstract. During the work, an analytical review was carried out, including the study of the harmful effects of ash and slag dumps and the experience of their use during disposal. The definition of geopolymers has been compiled, as well as the ways of their application in various construction industry areas. Coal generation waste provided by Severodvinsk CHPP-1 was studied for its chemical composition and content of natural radionuclides, and on the basis of this, a class of radiological hazard of materials was assigned. A composition for the synthesis of porous geopolymer materials has been developed, including aluminosilicate raw materials, an alkaline activator and a foaming agent. Coal generation waste was used as aluminosilicate raw material; alkaline activator—a mixture of caustic soda solution and liquid sodium glass; aluminium powder was used as a blowing agent. As a curing mode, low-temperature curing is used—at room temperature, in an oven, as well as microwave radiation in a microwave oven. The effect of temperature-time regimes on the final macrostructure and technical and operational properties of the synthesized porous geopolymers has been studied.

Keywords: Recycling · Curing mode · Ash and slag waste · Coal generation waste · Porous geopolymer · Microwave radiation · Aluminosilicate

1 Introduction

At the moment, positions on correcting environmental problems in Russia and the world as a whole are receiving more attention. As one of the rather important problems that has a negative effect, one can single out the accumulation of coal generation waste in landfills, which is formed due to the combustion of solid fuels at thermal power plants. To ensure the stable and reliable operation of the ash and slag removal system and reduce the financial costs for its construction and operation, the site for waste dumps is designed cleanly next to the territory of the thermal power plant and residential development, which means the possible occurrence of negative consequences on the environment and public health in general. In accordance with the “European List of Waste Codes”, as well

as the “Federal Classification Catalog of Waste of the Russian Federation”, solid fuel waste belongs to hazard class 5, which means that they are practically harmless. But, ash dumps can carry a potential hazard in environmental pollution through dusting of ash from the surface of ash and slag, as well as leaching of heavy elements and various erosion products into the soil by melt or rain streams. The combination of all this can lead to deterioration of the surface layer of the atmosphere and pollution of water and soil [1, 2].

Currently, according to the report of the Joint Stock Company “System Operator of the Unified Energy System” in the Russian Federation, by January 1, 2022, the number of thermal power plants reached 66.14% of all electricity generating stations in the state, of which 24% use coal for operation. At the moment, approximately 2 billion tons of coal generation waste has accumulated in Russia, occupying more than 230 km², and the accumulation trend is rising by 20–25 million tons annually. The remaining ash and slag wastes are sent for temporary storage, to ash dumps [3–6].

In foreign countries, the issue of processing man-made raw materials has more extensive solutions. In most European countries, coal generation waste is used as additives to Portland cement and concrete, the volume of processing of which is much higher than in Russia and is more than 90% [7]. This is achieved through legislative measures in these countries, a high tax on the lease of land for ash dumps and, in addition, the use of various incentives for the use of secondary raw materials in production. In turn, in India, coal generation waste is sent to ash dumps only in a small volume, within 30%, while the rest is sent to the production of various building materials: ceramic bricks; tiles; concrete [8]. In various states of America, coal generation waste in volumes close to 60% are used as a partial replacement for natural raw materials in the cement industry, or in the construction of protective structures and dams. Taking into account all of the above, we can conclude that the search for new ways to dispose of coal generation waste, taking into account the geographical needs and legislation of the country, is a very urgent task.

It can be noted that at the moment, geopolymer materials are an innovative way to dispose of ash and slag waste, due to their unique composition and properties by type: high chemical resistance, high temperature stability, significant mechanical properties, as well as low energy consumption in their production [9–11]. Geopolymers binders are obtained by mixing man-made aluminosilicate secondary products and wastes, either natural or synthetic minerals, such as coal generation waste (including fly ash and slag), metakaolin, perlite, cullet, clay and rice husk ash, with aqueous solutions containing chemically active substances, called geopolymers [12–15]. Currently, such geopolymers are used only in the pilot industry. Nevertheless, the growth of the prospect of industrial production of geopolymers exists under conditions when there are sources of industrial waste that are not involved in any way. Therefore, on the basis of the above aluminosilicate raw materials, it is possible to obtain both geopolymer concretes and highly porous materials that can be used as membranes and membrane substrates, adsorbents and filters, catalysts, and sound and heat insulating materials [16–18].

The term “geopolymer” was proposed by the French scientist D. Davidovits. In the 1970s, throughout France, cases of ignition of finishing materials, furniture and appliances, which were made from polymer materials based on organic compounds, became more frequent. As a result of massive fires causing damage to property, the

environment was polluted due to the release of toxic substances during combustion. Then a workaround was found, consisting in replacing the used polymeric materials with aluminosilicate polymers, that is, a geopolymers [19].

At the initial stages of work on the technology of geopolymers, they were obtained on the basis of heat-treated kaolin, the polymerization of which was carried out in solutions of sodium hydroxide or liquid glass. Due to their higher cost, they have not been replaced by polymers, but they have found a wide range of applications. Further, in the course of scientific research, it was found that industrial wastes, such as ash from thermal power plants, slags and sludge, can be used in the production of geopolymers. The cost of new materials has decreased significantly and has risen in line with the cost of conventional polymers, which made it possible to consider geopolymers as an alternative option [20, 21].

The use of geopolymer materials in construction is due to the fact that they provide resistance to high temperatures, which is achieved due to the three-dimensional structure of the geopolymer network, which allows water molecules bound both physically and chemically to evaporate without problems. Also, the structure of the geopolymer provides water resistance, that is, water molecules do not penetrate the geopolymer matrix, so structures using geopolymer concrete do not require additional protection from water. In this regard, geopolymer materials have good frost resistance. Another unique property of such materials is resistance to aggressive environments, that is, the material has absolute chemical resistance. Consequently, the cost of construction using geopolymer materials will be many times less [22].

The creation of heat-insulating materials from porous geopolymers is very relevant when creating frost-protective layers of roads and asphalt concrete pavement, in particular in places with a climate close to extreme conditions, for example, in Norway or the Arctic zone of the Russian Federation. One of the very painful conditions that are present during the installation of roads in permafrost conditions is considered to be “frost heaving”, that is, defect formation on the road surface when unevenly distributed capillary moisture freezes in the soil layer. Theoretically, porous geopolymers will help solve this problem in harsh climatic conditions by creating moisture drainage deep into the soil, thereby increasing its stability.

It is known that overall porosity and pore size distribution are the most important factors influencing the mechanical properties of porous geopolymers. Therefore, it is so important to study the influence of the temperature-time regime of synthesis on their structure and properties, because with the correct structural design, porous geopolymers can become universal and Eco-conscious materials with a low footprint carbon throughout the entire product life cycle.

2 Experimental Part

2.1 Materials, Sample Synthesis and Methods

To solve the problem, as the main aluminosilicate raw materials, we used coal-fired waste from the Severodvinsk CHPP-1, located in the city of Severodvinsk, Arkhangelsk Region, Russia.

The technology for the synthesis of porous geopolymer materials is shown in Fig. 1. Dried and crushed coal waste was sieved through a sieve with a mesh size of $250\ \mu\text{m}$ [23]. The alkaline activator of aluminosilicate components was prepared in a separate container by preparing a 12 M NaOH solution and mixing it with sodium liquid glass (silicate modulus = 2, water content 56%) manufactured by SilEx, Russia. The alkali used was a chemically pure (main component content of at least 99%) powder NaOH produced by LenReaktiv, Russia. After that, the resulting alkaline activator was poured into a pre-weighed sample of coal generation waste and sent for further mixing to the MSL-1S drum mill manufactured by PromStroyMash LLC, Russia. The mixing of the components was carried out at 120 rpm for 300 s. At the end of mixing, a spherical finely dispersed aluminium powder with a purity of at least 99% and a specific surface area of $140\ \text{m}^2/\text{g}$ produced by Metall Energo Holding, Russia was introduced into the suspension as a foaming agent. After that, the suspension was additionally stirred for 30 s, since a further increase in the mixing time adversely affects the foaming due to the volatilization of gas bubbles and the onset of the reaction of aluminium powder with an alkaline component [24, 25].

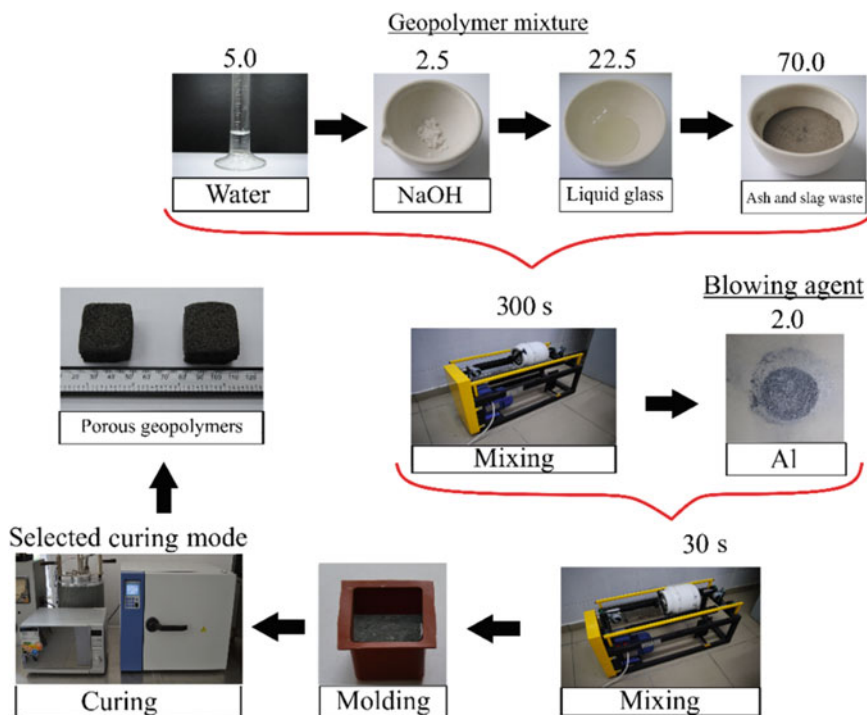


Fig. 1 Porous geopolymer synthesis technology

Upon completion of mixing, the resulting geopolymer suspension is poured into silicone cubic molds with an edge of 3 cm for further curing in a two-stage mode. The first stage is the same for all samples—curing takes place within 24 h at room temperature

($25 \pm 2^\circ\text{C}$) and relative humidity of $65 \pm 5\%$ in the room without direct sunlight on the samples. The second stage was carried out with further placement of the samples in an drying oven (LOIP LF 25/350-VS2, Joint-Stock Company “Laboratory Equipment and Devices”, Russia) at temperatures of 60, 70, 80 and 90°C and holding for 8 h. Also for comparison, as additional modes, the results of curing geopolymer materials in a room without direct sunlight on samples at room temperature ($25 \pm 2^\circ\text{C}$) for 14 days (RT) and using microwave radiation (M) in a Midea C4E AM720C4E-S microwave oven (Midea Group Co., Ltd, China) are given. For 5 min, the sample was exposed to microwave radiation with a power of 700 W at a frequency of 2500 MHz.

At present, microwave radiation is widely used as an innovative method for accelerating heating and increasing the intensity of chemical reactions. This is due to the fact that microwaves are able to quickly penetrate almost any material and release energy, which leads to volumetric heating of the entire material. It also simplifies process control. Microwaves can be especially useful for making geopolymer foams because they have low thermal conductivity, and microwaves can improve heat transfer.

To study the technical-operating and physicochemical properties of the synthesized porous geopolymer materials, the following methods and characteristics were chosen: chemical oxide composition, qualitative X-ray phase analysis, bulk density, kg/m^3 , ultimate compressive strength, MPa, and thermal conductivity, $\text{W}/(\text{m}\cdot\text{K})$. Previously, the authors described the measurement techniques used and the formulas in the article [26].

3 Results and Discussions

Like any other raw materials used for various construction industries, coal-fired generation wastes must be examined for the content of natural radionuclides, since it is known that when solid fuels are burned in CHP boilers, they are concentrated and accumulated. The specific activity of radionuclides of radium (226), thorium (232) and potassium (40) in the studied waste is $157 \pm 19 \text{ Bq/kg}$, which does not exceed the limit values of 370 Bq/kg . This content does not impose restrictions on the area of use of the studied wastes [24].

The chemical oxide composition of the used aluminosilicate raw materials in the form of waste from coal generation and synthesized porous geopolymer materials is presented in Table 1.

Table 1 Chemical composition of coal generation waste and synthesized porous geopolymer materials, wt.%

Material	SiO ₂	Al ₂ O ₃	Fe ₂ O ₃	MgO	Na ₂ O	K ₂ O	CaO	TiO ₂	MnO	P ₂ O ₅	SO ₃	Loss on calcination
Coal generation waste	61.55	17.91	6.01	2.74	3.61	2.32	2.11	0.83	0.07	0.21	0.32	2.32
Porous geopolymer	62.00	14.50	4.45	1.91	6.99	2.07	2.03	0.67	0.05	0.19	0.08	5.04

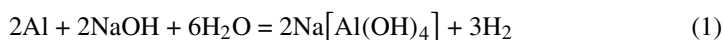
As can be seen from the data obtained, the chemical composition of the synthesized porous geopolymer material differs slightly from the raw material used. There was an increase in the content of silicon dioxide and sodium oxide, in other cases, a decrease in the mass content of oxides can be observed. This is probably due to the fact that the added components, namely, the alkaline activator, partially dissolve oxides, as a result of which they pass into an amorphous structure in the form of a glass phase. An increase in the content of sodium oxide from 3.6% to 7% is also associated with the addition of sodium liquid glass and sodium hydroxide. In both cases, the content of calcium and magnesium oxides does not exceed 5%, which classifies both materials as acidic. "Loss on calcination" in the waste of coal generation are probably represented by "underburnt (unburned fuel)", and in the synthesized porous geopolymer also underburnt and hydroxocomplex $\text{Na}[\text{Al}(\text{OH})_4]$, which has a decomposition temperature of 800 °C.

The component composition used for the synthesis of porous geopolymer is presented in Table 2. As mentioned earlier, to research the effect of the temperature–time regime of synthesis on the physicochemical properties and structure of porous geopolymers, 6 modes of two-stage curing were selected: 24 h at room temperature $25 \pm 2^\circ\text{C}$ followed by 8 h in a drying cabinet temperature of 60 ± 1 , 70 ± 1 , 80 ± 1 and $90 \pm 1^\circ\text{C}$. Also added for comparison is indoor curing at room temperature ($25 \pm 2^\circ\text{C}$) without direct sunlight on the samples for 14 days (RT) and in a microwave oven using 700W microwave (M) at 2500 MHz.

Table 2 Component composition of the raw mixture, wt.%

Ash and slag waste	Alkali [NaOH]	Water [H ₂ O]	Liquid glass	Aluminium powder, over 100
70.0	2.5	5.0	22.5	2.0

The use of aluminium powder as a blowing agent theoretically should increase the strength of the synthesized sample due to the formation of a hydroxocomplex, in contrast to the use of hydrogen peroxide [27]. The foaming mechanism during its use consists in interaction with an alkaline solution, in which hydrogen is released and the $\text{Na}[\text{Al}(\text{OH})_4]$ hydroxocomplex is formed, which can be represented by reaction 1:



X-ray phase analysis has been carried out to identify phases or crystalline peaks of minerals present in porous geopolymers. As mentioned earlier, 6 different low temperature conditions were used in the present study, however only 1 composition. Based on this, the authors carried out an x-ray phase analysis of 3 temperature–time modes: RT, 80 °C and M. The obtained x-ray patterns during merged do not differ from each other, since there were no high-temperature heat treatment modes and a change in the component composition, which can affect phase composition. Therefore, in Fig. 2 shows 1 typical X-ray diffraction pattern of the porous geopolymers of composition (80).

According to the data obtained, it should be noted that the X-ray diffraction pattern is characterized by the presence of an amorphous aluminosilicate glass phase, which

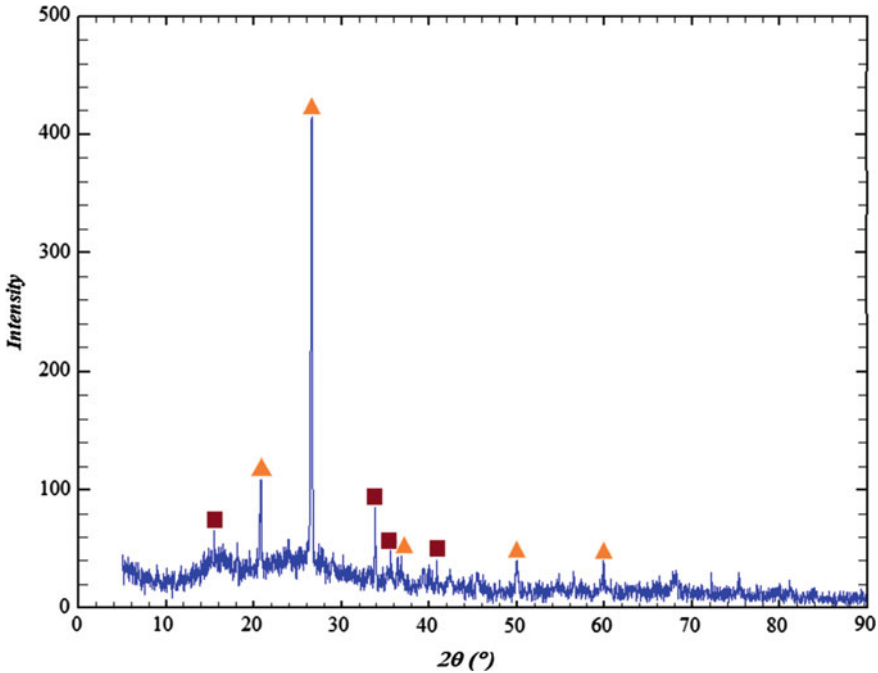


Fig. 2 Results of X-ray analysis porous geopolymer (80 °C): Δ —quartz (SiO_2), \square —mullite

confirms the presence of a “halo” at shooting angles of 18–34° (2θ). It is formed as a result of solidification of slag in water and the subsequent sharp decrease in its temperature, as a result of which the aluminosilicate melt does not have time to crystallize and an amorphous glass phase is formed. It should also be noted that the presence of an amorphous structure increases the reactivity of the raw material. Porous geopolymers are composed of the same crystalline phases in the form of quartz (ICCD PDF# 82-0512) and mullite, at the sensitivity limit of the instrument (ICCD PDF# 15-0776).

Based on the component composition of the raw mixture and the presented technology, porous geopolymer materials were obtained with the following external structure and physicochemical properties, shown in Fig. 3 and in Table 3.

As can be seen from the data obtained, a change in the curing temperature has an insignificant effect on the density of the geopolymers: rise in temperature for every 10 °C reduces the density of the samples by an average of 2.5%. The density difference between 60 and 90 °C is 8%. Curing of porous geopolymers at room temperature 25 ± 2 for 14 days also has no significant effect on the density of the samples—it is at the level of 60–70 °C. However, using microwave as the curing mode increases the average density by 19% compared to the RT composition. Since thermal conductivity depends almost linearly on density and porosity, a similar development of this indicator can be observed.

A completely different trend can be observed when studying the ultimate compressive strength of synthesized samples. An increase in temperature has a significant effect on

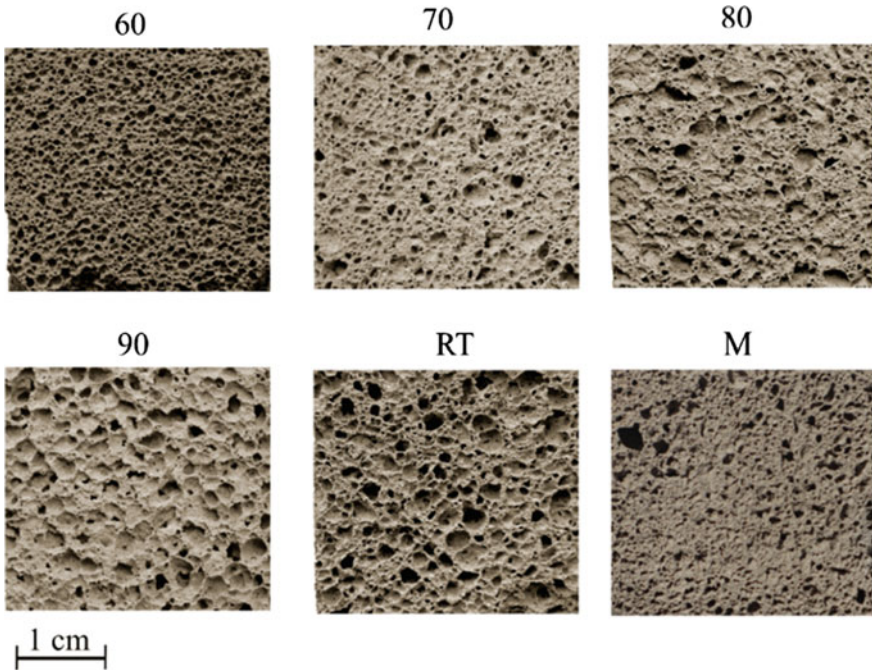


Fig. 3 Structure of porous geopolymers

Table 3 Average characteristics of porous geopolymers

Curing mode, °C	Density, ρ , [kg/m ³]	Strength, R , [MPa]	Thermal Conductivity, [W/(m·K)]
60	332 ± 2	1.02 ± 0.04	0.0754 ± 0.0006
70	325 ± 14	0.89 ± 0.05	0.0745 ± 0.0006
80	316 ± 15	0.76 ± 0.02	0.0719 ± 0.0009
90	306 ± 12	0.73 ± 0.05	0.0699 ± 0.0007
RT	328 ± 12	0.58 ± 0.01	0.0749 ± 0.0011
M	391 ± 16	1.31 ± 0.05	0.0875 ± 0.0016

strength characteristics: so increasing it by 10 °C, from 60 to 70 °C, reduces strength by 13%, from 70 to 80 °C by 15%, from 80 to 90 °C by 4%, which ultimately leads to a 30% deterioration in strength characteristics. Samples with curing mode RT show the worst strength of 0.58 MPa. The use of microwave radiation, on the contrary, significantly increases the ultimate compressive strength: relative to the RT composition, there was an increase in strength by 126%, which is an excellent result. If we compare microwave radiation with thermal conditions (60 °C), we can see a not so grandiose, but very noticeable increase in tensile strength by 28%, which is also a good result.

The obtained dynamics of strength reduction is probably associated with the following factors: with an increase in temperature, the intensity of water evaporation increases and, as a result, macropores increase in size. This contributes to a decrease in the thickness of the inter pore partitions, which ultimately affects the density and ultimate strength of the samples.

Also, due to the increase in the rate of the geopolymerization reaction and the rapid release of water from the samples, the solid/liquid phase ratio changes, which has a huge impact on the viscosity and rheology of the reaction mixture. Due to the rapid increase in viscosity and, as a result, a decrease in the reactivity of the geopolymer mixture, the geopolymerization reaction does not have time to complete before the samples are cured, which has a negative effect on the ultimate strength of porous geopolymers.

With regard to exposure by microwave radiation, presumably, it also allows to increase the temperature of the geopolymer raw material mixture in the shortest possible time, which leads to the adhesion reaction of aluminosilicate groups and the creation of an impermeable film. Further heating above 100 °C results in the formation of steam, which expands the film, causing swelling and pore formation. This continues until the aluminosilicate groups form a rigid brittle bond consisting of sialates. Probably, with further heating for more than 5 min, the pore size increases, which affects the final properties of the obtained samples.

4 Conclusion

Analyzing the above, we can summarize the following results:

1. Despite the maximum density among all temperature–time modes, with the component composition used, the mode using microwave radiation is the most optimal. In this case, the obtained density is $391 \pm 16 \text{ kg/m}^3$, and the compressive strength is $1.31 \pm 0.05 \text{ MPa}$.
2. Among the low-temperature conditions using a drying oven, the best is the curing of porous geopolymers with exposure for 24 h at room temperature, followed by placement in an oven for 8 h at a temperature of 60 °C. In this case, the obtained density is $332 \pm 2 \text{ kg/m}^3$, and the ultimate compressive strength is $1.02 \pm 0.04 \text{ MPa}$.
3. When the curing temperature rises from 60 to 90 °C, the density decreases by 8% from 332 to 306 kg/m^3 , and the compressive strength from 1.02 to 0.73 MPa, which is 30%. The most significant factor influencing the decrease in density and strength is an increase in the size of macropores and a decrease in the thickness of inter pore partitions due to more intensive water evaporation. Also, the ratio of solid and liquid phases, which slows down or accelerates the rate of the geopolymerization reaction, which is individual for each chemical composition of the raw material and the component composition of the geopolymer mixture, has a huge impact on the properties obtained.

Acknowledgements. The research was supported by Russian Science Foundation (project No. 21-19-00203), "Efficient temperature-solidifiable eco-geopolymers for road construction in the Arctic zone of the Russian Federation based on waste from the local thermal power plants solid fuel

combustion" (supervisor Yatsenko E.A.), in the framework of the 2021 competition "Conducting fundamental scientific research and exploratory scientific research by separate scientific groups".


References

1. Cherentsova AA, Olesik SM (2013) Evaluation of ash waste as a source of pollution and a source of secondary raw materials. *Mining Info Anal Bull (Scient Tech J)* S3:230–243
2. Guidance on classification of waste according to EWC-Stat categories. <https://ec.europa.eu/eurostat/documents/342366/351806/Guidance-on-EWCStat-categories-2010.pdf/0e7cd3fc-c05c-47a7-818f-1c2421e55604>. Accessed 11 June 2023
3. State report "On the state and protection of the environment of the Russian Federation in 2020" https://www.mnr.gov.ru/docs/gosudarstvennye_doklady/gosudarstvennyy_doklad_o_sostoyanii_i_ob_okhrane_okruzhayushchey_sredy_rossiyskoy_federatsii_v_2020/?special_version=Y. Accessed 11 June 2023
4. Khagleev EP (2017) Ash and slag dumps of annual regulation, differentiated flows of ash and slag from coal thermal power plants. *News of High Educ Insitu, Energy Prob* 19:21–32
5. Thang VL, Nguyen ZT, Samchenko SV (2019) Addition of additives of ash and slag waste to the properties of sulfoaluminate Portland cement. *Vestnik MGSU* 14:991–1003
6. Ivashina MA, Krivoborodov YuR (2017) The use of industrial waste in the technology of sulfoaluminate clinker. *Adv Chem Chem Tech* 31:22–24
7. Jin S et al (2021) Comparison and summary of relevant standards for comprehensive utilization of fly ash at home and abroad. *IOP Conf Ser: Earth Environ Sci* 621(1):012006
8. Yousuf A et al (2020) Fly ash: production and utilization in India-an overview. *J Mater Environ Sci.* 11(6):911–921
9. Novais RM, Buruberri LH, Ascensão G et al (2016) Porous biomass fly ash-based geopolymers with tailored thermal conductivity. *J Clean Prod* 119:99–107
10. Hlaváček P, Šmilauer V, Škvára F et al (2015) Inorganic foams made from alkali-activated fly ash: mechanical. *Chem Phys Prop, J Eur Ceram Soc* 35(2):703–709
11. Hemra K, Aungkavattana P (2016) Effect of cordierite addition on compressive strength and thermal stability of metakaolin based geopolymer. *Adv Powder Technol* 27(3):1021–1026
12. Cyr M, Idir R, Poinot T (2012) Properties of inorganic polymer (geopolymer) mortars made of glass cullet. *J Mater Sci* 47(6):2782–2797
13. Vaou V, Panias D (2010) Thermal insulating foamy geopolymers from perlite. *Miner Eng* 23(14):114–1151
14. Badanoiu AI, Al Saadi THA, Stoleriu S et al (2015) Preparation and characterization of foamed geopolymers from waste glass and red mud. *Constr Build Mater* 84:284–293
15. He J, Jie Y, Zhang J et al (2013) Synthesis and characterization of red mud and rice husk ash-based geopolymer composites. *Cem Concr Compos* 37:108–118
16. Bai C, Colombo P (2017) High-porosity geopolymer membrane supports by peroxide route with the addition of egg white as surfactant. *Ceram Int* 43(2):2267–2273
17. Minelli M, Medri V, Papa E et al (2016) Geopolymers as solid adsorbent for CO₂ capture. *Chem Eng Sci* 148:267–274
18. Alzeer MIM, MacKenzie KJD, Keyzers RA (2016) Porous aluminosilicate inorganic polymers (geopolymers): a new class of environmentally benign heterogeneous solid acid catalysts. *Appl Catal A: Gen* 524:173–181
19. Davidovits J (2002) 30 years of successes and failures in geopolymer applications. In: *Market Trends and Potential Breakthroughs. Geopolymer Conference, October 28–29. Melbourne, Australia*

20. Davidovits J (2011) Geopolymer chemistry and applications, 3rd edn. Institute Geopolymer, France, Saint-Quentin, 614 p
21. Davidovits J (1989) Geopolymers and geopolymeric materials. *J Therm Anal* 35:429–441
22. Alfred J (2013) Engineering properties of a proprietary premixed geopolymer concrete. In: *Proceeding Concrete Institute of Australia Biennial Conference, Understanding Concrete*, Gold Coast, Australia
23. Yatsenko EA, Goltsman BM, Klimova LV, Yatsenko LA (2020) Peculiarities of foam glass synthesis from natural silica-containing raw materials. *J Therm Anal Calorim* 142(1):119–127
24. Yatsenko EA, Goltsman BM, Trofimov SV et al (2022) Improving the properties of porous geopolymers based on TPP ash and slag waste by adjusting their chemical composition. *Materials* 15:2587
25. Lynch JLV et al (2018) Preparation, characterization, and determination of mechanical and thermal stability of natural zeolite-based foamed geopolymers. *Constr Build Mater* 172:448–456
26. Yatsenko EA, Goltsman BM, Trofimov SV, Novikov YV, Smoliy VA, Ryabova AV, Klimova LV (2023) Influence of various coal energy wastes and foaming agents on foamed geopolymer materials' synthesis. *Mat* 16:264. <https://doi.org/10.3390/ma16010264>
27. Yatsenko EA, Ryabova AV, Vilbitskaya NA et al (2021) Ecogeopolymers based on ash and slag waste from thermal power plants—Promising materials for the construction of roads in the Arctic zone of the Russian Federation. *Glass Ceram* 12:32–37



Conceptual Foundations of Methodology in the Creation and Development of a Class of Natural-Technical Systems

E. D. KHetsuriani^{1,3}, V. L. Bondarenko², O. A. Surzhko¹, T. E. KHetsuriani¹,
and A. A. Asatryan¹

¹ Platov South-Russian State Polytechnic University (NPI), 132, St. Prosvescheniya,
Novocherkassk 346428, Russia
goodga@mail.ru

² Novocherkassk Engineering and Land Reclamation Institute Named After A.K. Kortunov of
Don State Agrarian University, 111, Pushkinskaya Str, Novocherkassk 346428, Russia

³ Don State Technical University (DSTU), 1, Gagarin Sqr., Rostov-on-Don 344003, Russia

Abstract. The purpose of the research is the scientific substantiation of the conceptual foundations of the methodology for the creation and development of a class of natural-technical systems (NTS) as part of a natural component in the form of a “Natural environment” (“NE”) in the spatial limits of a river basin geosystem, where quantitative and qualitative indicators of water runoff (surface, underground), “Technogenic component” are formed in the form of various types of hydraulic structures (HS) and related buildings, referred to as the “Object of activity” (“OA”) and the social component—the “Population” (“P”) living in the zones of influence of “OA”, which in the systemic understanding are interconnected, interacting and interrelating (III) in the processes of using water resources in various technological schemes of water consumption and water use of economic and other activities. The relevance of research on the creation and development of the methodology of the NTS class “NE-OA-P” is determined by the need to study the processes of formation of orderliness between natural, man-made and social components and integrity as a management mechanism to ensure the preservation of development, and through development—ensuring the preservation of the dominant role of the whole, as part of the system, which becomes achievable by creating a methodology for assessing the impact of the technogenic component “OA” with its elements on the natural “NE” and social “P” components in the space and time of the river basin geosystem.

Keywords: System · System approach · System analysis · Component · Element · Structure · Integrity

1 Introduction

In the creation and development of the NTS class “NE-OA-P”, related to the use of water resources in almost all branches of modern economic and other activities, it determines both theoretical and practical significance [1].

The theoretical significance of a relatively new class of systems is determined by the fact that due attention is not paid to the study of this type of systems in the scientific domestic and foreign literature and practice, although the problem of “Water” as a renewable resource in its significance ranks second among the most important problems—“Energy” and “Food” in the global system “Nature—Society—Man”. The problem of “Ecology” in importance and among the 10 most important problems is in fourth place after the three main problems.

The practical significance of the methodology for the creation and development of the NTS class “NE-OA-P” is conditioned by modern environmental requirements to ensure environmental safety in the zones of influence of “OA”, which determines the need for an objective assessment of the impact of the functioning of “OA” during construction and operation on the processes of vital activity in the plant and animal world in natural environments, the social sphere of the resident “P” and the emerging changes in the dynamics of the movement of flows of matter, energy and information (MEI) within the river hydrographic network and the upper layers of the lithosphere. It should be noted that in this formulation of the solution of environmental requirements in the environmental impact assessment (EIA) procedure, “OA” in the form of a complex of hydraulic structures (CHS) was first performed during the construction and operation of the Zelenchuk HPP-HPSP (2005–2015).

According to its functional purpose, located within the catchment area of the river hydrographic network, it carries out intra-basin regulation and inter-basin redistribution of water flow between tributaries of the main riverbed, for example, the Upper Kuban, by constructing reservoir waterworks, taking estimated water flow rates ($Q \text{ m}^3/\text{s}$) from the water body and transporting them to specific water consumers (systems irrigation, drinking water supply of cities and settlements) and water users (hydroelectric power plants, hydraulic pumped storage power stations, thermal power plants, state district power stations, nuclear power plants, industrial enterprises, etc.) [2–4].

The changes introduced into the natural processes of the movement of MEI flows in the considered space and time of the river basin geosystem affect almost all processes of vital activity in the plant and animal world of the natural component “NE” and the hydrological channel-forming processes included in it on the river hydrographic network, which have a special impact on the vital activity of the animal world in the riverbeds of the river network and, in particular, in particular, ichthyofauna (fish species, crayfish, etc.), as well as on the life processes of the social component—the resident “P” in the zones of influence of the technogenic component “OA” in accordance with modern environmental requirements [5, 6] cause the need to assess the impact of “OA” on the natural “NE” and social “P” components in the composition of the NTS “NE-OA-P” [7, 8].

2 Materials and Methods

The methodology in the creation and development of the NTS class “NE-OA-P” acts in the form of prescriptions and regulatory requirements, which fix the content and sequence of evaluation of the processes of the man-made component in the form of “OA” with the natural component “NE” in the spatial limits of the river basin geosystem, which

includes surface atmospheric layers (up to 10 km.), where water precipitation (rain, snow) is formed; the catchment area of the river hydrographic network, where surface water runoff is formed; the upper layers of the lithosphere, where underground water runoff is formed, entering the river network; soil cover with underlying rocks; diversity of flora and fauna on the earth's surface of the catchment area territories and in the aquatic environment of the river network (flora and fauna); social component as a resident of "P" in the zones of influence of "OA" (Fig. 1) [9–11].

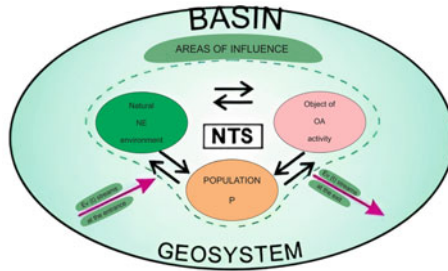


Fig. 1 Diagram of the model of interaction of components in the NTS “NE-OA-P” in the spatial limits of the river basin geosystem

The methodology of the study of the processes of III components as part of the considered NTS class “NE-OA-P” in the general array of scientific knowledge has two bases as its source. Firstly, the scientific cognition of the NTS class “NE-OA-P” masters very complex objects of economic and other activities related to the use of water resources, which leads to an increase in the level of abstraction on physical and mathematical models of research, as a result of this, the question of the means of research and the principles of the approach to the III processes of the components of the NTS “NE-OA-P” become one of the central ones and occupy a relatively independent place in the system of cognitive activity, for example, to ensure environmental safety [12, 13] in the use of water resources in economic and other activities. Secondly, engaging in scientific research on various issues related to the hydrological processes of the formation of water runoff (surface, underground) in the space and time of the river basin geosystem, its partial use in technological processes of economic and other activities, assessing the level of influence of “OA” on the processes of vital activity in the plant and animal world as in “NE”, and a resident “P” in the zones of influence of “OA” [14–16].

In the methodology of the creation and development of the NTS class “NE-OA-P”, system concepts are important, reflecting the essential properties, connections and relationships of natural, man-made and social components in their contradiction and development. So, the concept is a thought (or a system of thoughts) that generalizes and distinguishes the elements that are part of the components of the considered class of NTS class “NE-OA-P” by a certain common and collectively pacific feature for them [15, 16]. The concept finds its real mental being in the deployment of definitions in judgments as part of a certain methodology, and in the case under consideration, this is the methodology for the creation and development of the NTS class “NE-OA-P” on the use of water resources. In the creation and development of this methodology, basic and

important concepts have been formulated for practical use, which are the methodological and theoretical basis for the study of important issues on the creation and development of the NTS class “NE-OA-P”, which is relatively young [17–19].

One of the features of the formation of scientific thinking in the methodology of the creation and development of the NTS class “NE-OA-P” are fundamental basic concepts as a universal measure of the forms of motion and interaction of matter—Energy and its “shadow” Entropy, time and the Arrow of time, system and system approach, whole and integrity, system analysis, development and a number of important concepts—irreversibility, complexity, structure, element, dissipation, bifurcation and fluctuation, self-organization, environmental hazard and environmental safety, ecological acceptability and ecological unacceptability, the dominant role of the whole, natural and man-made components, coevolution [15–19].

3 System Concepts

The “System approach” and “System analysis” in the creation and development of the fundamentals of the methodology of the NTS class “NE-OA-P” is based on the central concept of “System” and it should be noted that the primacy in the use of this concept can be traced to Aristotle. The use of system concepts with an awareness of the system and the surrounding world in scientific and economic activities began to be widely used after the publication of N. Wiener’s scientific work entitled “Cybernetics” in 1948 (Fig. 2).

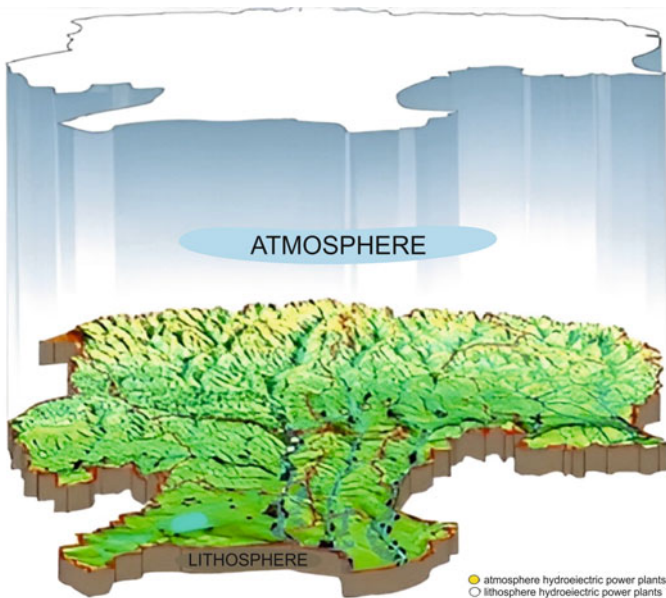


Fig. 2 Spatial scheme of the basin geosystem of the Upper Kuban

The fundamentals of the methodology for the creation and development of the NTS class “NE-OA-P” is based on system principles—the integrity, structurality, interdependence of the system on the state of the spatial limits of the river basin geosystem, where quantitative and qualitative indicators of water resources are formed, some of which are used for technological processes of economic and other activities and the hierarchy of the system, where each component of the NTS “NE-OA-P” can be considered as a sub-system. In the classification assessment, NTS “NE-OA-P” are considered as dynamic systems that change their state in time and space where water resources are formed [17].

By the nature of the III components in the composition of the NTS “NE-OA-P” and the elements included in them (flora and fauna in the catchment area of the river network, soil cover with underlying rocks, river ichthyofauna, protective devices against ingress into technological systems of juvenile fish, entrained sediments, etc.) in space and time of the river basin geosystem are open and nonequilibrium with respect to the basin geosystems higher in the hierarchical series, within which the input and output of flows of matter, energy and information is constantly taking place [18].

4 Results

The use of water resources in the branches of economic and other activities in the scientific and methodological understanding of this process is conditioned by the dialogue with the natural environment (“NE”) in the space and time of the river basin geosystem. But what makes this dialogue possible. Cognition of the ongoing III processes of the technogenic component “OA” in the form of CHS placed on the catchment area of the river network with a natural component (“NE”) and its constituent elements and social component, a resident “P” creates a difference between the past before the construction of “OA” and the future during the operation of “OA”, that is, restoration is taking place—an integral attribute in the methodology of creating a NTS “NE-OA-P” on the use of water resources in economic and other activities [19].

In his work “The Open Universe” Karl Popper notes that any phenomenon is caused by certain previous phenomena and therefore any phenomenon can be explained or predicted... “On the other hand, common sense suggests a free choice between alternative possibilities to act”. The dilemma of determinism—causality is closely related to the meaning of time. Is the future set or in the process of being built? There is a deep dilemma in this question, since time is the fundamental dimension of all living and inanimate things. At the fundamental level, when studying the processes of III components in the NTS “NE-OA-P”, the past and future play various roles [19], which determines the concept of “Arrow of Time”, which determines the paradox of time, which indicates the direction of irreversibility of the phenomena occurring on the river network when using water resources in technological processes, each of which illustrates the constructive role of the Arrow of Time. Irreversibility, as it is established, in the use of water resources leads to coherence (consistency in time) to new phenomena, effects covering almost the entire hydrographic river network of the basin geosystem where water resources are formed. Irreversible processes have a direction in time, for example, due to viscosity, the fluid flow stops over time. Reversible processes are the lot of idealization. In order for the pendulum to oscillate reversibly in time, it is necessary to neglect friction [20].

The distinction between reversible and irreversible processes entered through the concept of entropy associated with the second principle of thermodynamics, which was defined by R. Yu Clausius in 1865. Irreversible processes produce entropy, and reversible processes leave entropy constant. According to the proposed formulation of R. Yu Clausius: “The energy of the world is constant, and the entropy of the world is increasing” became the first formulation of the evolutionary picture of the world based on the existence of irreversible processes [20]. In the considered spatial limits of the river basin geosystem, where quantitative and qualitative indicators of water resources are formed, a certain estimated part of which will be used in various technological systems of water use and water consumption, for which intra-basin regulation and redistribution of water runoff are carried out, causing irreversible processes in the natural (“NE”) and social (“P”) components in interaction with the technogenic component “OA” as part of the NTS “NE-OA-P” [21].

The irreversibility of processes in the formation of water resources, both at the level of the global system of the Earth’s biosphere and at the local level of the river basin geosystem occurs due to solar energy flows (radiation), which occurs as a result of irreversible nuclear processes occurring in the Sun. In the spatial limits of river basin geosystems, irreversibility is caused by the processes of formation of water runoff (surface, underground) in the spatial limits of the river basin geosystem and its partial use in various technological systems of water consumption and water use by intra-basin regulation and inter-basin redistribution with the creation of reservoir waterworks, the use of various types of hydraulic structures, associated buildings, irrigation systems, drinking and technical water supply, etc. [21].

It is important to note the constructive role of irreversibility in the methodology of creation and development of the NTS class “NE-OA-P”, since the systems under consideration are characterized as nonequilibrium, in which nonequilibrium leads to special forms of coherence in the processes between natural “NE”, social “P” and technogenic “OA” components. Objective examples can be the “OA” operating for many decades in the form of reservoir waterworks providing water consumption and water use systems of industrial and agricultural enterprises, water transport, etc. [22].

Whatever the past, there are two types of processes in the present: time-reversible processes, for example, the movement of the Moon, and irreversible processes in which the asymmetry of the past and the future is obvious, which is reflected in the evolutionary nature of the Universe and the fundamental laws of physics [22].

The concept of complexity is one of the concepts that are an integral part of the problems they generate. For the NTS class “NE-OA-P” this is the ability to carry out intra-basin regulation or inter-basin redistribution of water runoff through the construction of reservoir hydroelectric units and the corresponding CHS. The concept of complexity for the NTS class “NE-OA-P” is also conditioned by the fact that the regulation or redistribution of water flow within the river basin geosystem largely affects the evolutionary processes in the natural component “NE” [21, 22].

In the methodology of cognition of the complex in the considered NTS class “NE-OA-P” of the real “NE”, unstable processes are observed in the movement of MEI flows in the vital activity of biota, various types of instability and fluctuations that cause the diversity, richness of forms and structures that we encounter when creating and operating

“OA” in part of the NTS “NE-OA-P”. The concepts of complexity, coherence, and orderliness for the NTS class “NE-OA-P” are fundamental. Coherence in the considered NTS class “NE-OA-P” is a constant relationship in time between the elements of the natural component (“NE”), the technogenic component (“OA”) and the needs of the social component (“P”) in water resources taken from the water bodies of the river hydrographic network.

In the modern climate system of the Earth, an important role is assigned to water resources, which occupy about 70% of the Earth’s surface by the World Ocean (361 million km²), and land occupies 149 million km². The rivers of the land carry the flow of about 45.8 thousand km³, and 44.7 thousand km³ is discharged into the World Ocean, 1.1 km³ is lost during transportation through river networks. The inflow of underground runoff from the land continents into the World Ocean is about 47 thousand km³. In methodological terms, it is important to note that all the Water in the Solar System originates from a giant primary “cloud” consisting of gas and dust, which shrank sharply 4 billion years ago, forming the Solar System (journal “In the World of Sciences” No. 6 pp. 46–47, 2015).

In the methodology of the NTS class “NE-OA-P” one of the basic concepts is integrity, which determines the dominant role of the whole over the parts—natural “NE”, technogenic “OA” and social “P” components and their elements, and it is necessary to take into account this technical relationship with concepts such as integrity, structure, element in the construction and operation of “OA” as part of the NTS class “NE-OA-P” [22]. System principles—integrity (irreducibility of the properties of the system to the sum of the properties of its constituent elements in the components and irreducibility of the last properties of the whole); dependence of each element, its properties and the relationship of the system on its place, function, etc. within the whole); structures (the possibility of describing the system, the conditionality of the behavior of the system by the behavior of its components and the interdependence of the system and the environment in the zones of influence of the “OA” (the system forms and manifests its properties in the process of interaction with the environment in the spatial limits of the basin geosystem, where water resources are formed). The multiplicity of the description of the considered NTS class “NE-OA-P” necessitates the construction of various models, for example, a change in the channel hydrograph in sections of the riverbed, etc.

The system integrity in the NTS class “NE-OA-P”, as established by studies on the example of operating “OA” within the river basin geosystems of the Kuban, Terek and Lower Don rivers, is determined by a number of system functional indicators:

- self-organization processes;
- openness to the environment of the spatial limits of the river basin geosystem;
- the growth of opportunities to influence the external environment;
- reflection of objective reality in the functioning of the “OA” as part of the NTS “NE-OA-P”
- demand for the use of water resources in the branches of economic and other activities;
- a steady trend in the possibility of ensuring the growth of useful capacity (P) in the created and operating NTS “NE-OA-P”;
- a steady tendency to decrease the growth rate of power losses in the system (G);
- a potential opportunity to increase efficiency in the functioning of the “OA” as part of the NTS “NE-OA-P”;

- ensuring a steady trend towards increasing the efficiency of the use of natural resources and reducing the growth rate of energy consumption.

Reflection of the objective reality of the operating NTS “NE-OA-P” is manifested in the processes of III between natural (“NE”), technogenic “OA” and social (“P”) components as part of the class of systems under consideration.

The demand for “OA” as part of the NTS class “NE-OA-P” is determined, on the one hand, by the ecological acceptability of the technogenic component and its elements to the natural component (“NE”) in the zones of its influence, and on the other hand, by the vital need of the social component (“P”) [23].

The ecological acceptability of “OA” as part of the NTS class “NE-OA-P” is determined by constructive perfection, for example, protection from ingress into technological systems of water consumption of ichthyofauna (fish species, etc.) and the ability to self-organization processes in the processes of transformation in the natural component (“NE”) under the influence of “OA” [23].

The ecological acceptability of “OA” contributes to the dominance of natural transformation processes in the natural component (“NE”) and, as a consequence, to a decrease in the growth rate of the entropy level in the space and time of the zones of influence of “OA”. The assessment of the level of ecological acceptability of the “OA” as part of the NTS “NE-OA-P” is determined on the basis of the results of the system integrated environmental monitoring (SIEM) in the periods. Construction and operation of “OA” [22, 23]. The natural component is formed by the processes of global moisture turnover, the technogenic component is determined by the functional orientation of the “OA” as part of the NTS “NE-OA-P”, for example, water consumption of water supply systems, irrigation or water use of technical water supply systems of hydroelectric power plants, hydraulic pumped storage power stations, state district power stations, nuclear power plants, etc. [23].

In the processes of functioning of the technogenic component “OA” in the natural (“NE”) and social (“P”) components, certain changes inevitably occur in the movements of the MEI flows, which determine the processes of vital activity in the biota and the living population (“P”). The changes introduced in the space and time of the river basin geosystem determine the processes of self-organization between the “OA”, natural (“NE”) and social (“P”) components that ensure the sustainable functioning of the NTS “NE-OA-P”.

For the NTS class “NE-OA-P”, there are three types of self-organization processes:

- self-origin of an organization or the emergence of a certain set of integral objects of a certain hierarchical level, a new integral system with its own specific patterns;
- the processes by which the system maintains a certain level of organization when the external and internal conditions of its functioning change;
- the third type of self-organization processes is associated with the improvement and development of the system, when the accumulated experience in self-organization processes is used.

In a generalized sense, self-organization in the III processes between components and their constituent elements in the NTS class “NE-OA-P” should be understood as a natural process in which the organization of a complex dynamic system in space and

time of a river basin geosystem is created, reproduced and improved. The term self-organizing system was introduced by the English scientist W.R. Ashby (1947). For the NTS class “NE-OA-P”, the processes of self-organization to a greater extent correspond to the third type, in which “OA” is used as much as possible, both in highly active and in active and weakly active zones of influence.

Long-term experience of monitoring studies of operating “OA” as part of the NTS “NE-OA-P”, in which there is a steady trend of self-adaptation of the elements of “OA” to the elements of natural “NE” and social “P” components, which is provided by structural transformations in natural environments. Consequently, an important conclusion can be drawn that the processes of self-organization in the zones of influence of “OA” can be considered as a universal model of transformations that contributes to ensuring natural and man-made integrity, in which natural processes play a dominant role.

Based on the results of studies operating within the river basin geosystems of the Kuban, Terek and Lower Don and the created NTS “NE-OA-P”, in the basin of the Upper Kuban—Zelenchuk HPP-HPSP and downstream of the Kuban Upper-Krasnogorsk HPP-1 and HPP-2, an important conclusion can be drawn, that self-organization in the NTS class “NE-OA-P” is carried out by purposeful processes, in the course of which there is a transformation in the ordering, complication of existing and formation of new III between the natural “NE” component, with biotic and abiotic elements included in it, and technogenic “OA” and social “P” components in response to a change in the “NE” state under the influence of “OA” in space and time of the river basin geosystem. The study of self-organization processes in the created and operating NTS “NE-OA-P” will allow more objectively and reasonably perform an environmental impact assessment (EIA) of “OA” during the period of engineering and environmental surveys at the design, construction and subsequent operation stage [23].

The methodology of the NTS class “NE-OA-P”, as established by research, is based on system concepts and principles, which, according to functional use, are divided into fundamental ones—energy, entropy, time, Arrow of time, system approach, integrity, development, a number of important ones—irreversibility, reversibility, complexity, structure, self-organization, environmental hazard, ecological acceptability, environmental safety, environmental condition, the dominant role of the whole, natural and man-made components.

The methodology of classification assessment considers the NTS class “NE-OA-P” as a dynamic system that changes its state in space and time, where quantitative and qualitative indicators of water resources are formed.

References

1. Bondarenko VL, Ylyasov AI, Khetsuriani ED, Semenova EA, Larin DS, Khetsuriani TE (2020) Environmental safety conditions and factors in zones of influence of water facilities. In the Collection. materials science and engineering, series construction materials and technologies of binders, concrete and building ceramics. Novochoerkassk, p 129–138
2. Badalyan LH, Kurdyukov VN, Ovcharenko AM (2014) The current state of research in the field of integrated assessment of the safety of the ecosystem of the city under the influence of motor transport. *Rat Use Cons Aquatic Biol Res*, Novochoerkassk, 142–151

3. Bondarenko VL, Gutenev VV, Privalenko VV, Polyakov ES (2007) Environmental impact assessment (EIA) in the design of the Zelenchuk hydroelectric power plant water management complex. *Theo Appl Ecol* 1:47–54
4. Bondarenko VL, Klimenko OV, Semenova EA, Nikolaenko DA (2016) Environmental safety in construction. Engineering and environmental surveys in the complex of surveys for the construction of water facilities: monograph of Bondarenko V.L. Novochoerkassk, pp 227–243
5. Bondarenko VL, Privalenko VV, Kuvalkin AV (2009) Solving environmental problems in the design of hydraulic structures (on the example of the basin geosystem of the Upper Kuban). Monograph of the Publishing House of the SSC RAS, Rostov-on-Don, pp 306–319
6. Bondarenko VL, Semenova EA, Aliferov AV, Klimenko NV (2016) Natural and technical systems in the use of water resources: territories of basin geosystems. Monograph of the South Russian State Polytechnic University (NPI) named after M. I. Platov, Novochoerkassk, pp 204–215
7. Bondarenko VL, Skibin GM, Azarov VN, Semenova EA, Privalenko VV (2016) Environmental safety in environmental management, water use and construction: assessment of the ecological state of basin geosystems. Monograph of the South Russian State Polytechnic University (NPI) named after M. I. Platov, Novochoerkassk, pp 419–425
8. Budyko MI, Drozdov OA (1950) About moisture turnover in a limited land area. Questions of hydrometeorological efficiency of protective afforestation, Moscow, pp 248–264
9. Vernadsky VI (1988) Philosophical thoughts of a naturalist. Publishing house “Science”, Moscow, pp 520–582
10. Ged RD (1990) Energy for planet earth. *In the World Sci* 11:7–16
11. Denisov OV, Zimenko VA, Kohanov YuB (2014) Assessment of the level of ecosystem safety by forecasting bioecological parameters based on an integral safety indicator. *Rational Use Conserv Aquatic Biol Res*, Saint-Petersburg, pp 301–316
12. Kovalchuk MV, Naraykin OS (2011) Designer for the future. *In the World of Science* 9:24–31
13. Kuznetsov OL, Kuznetsov PG, Bolshakov BE (2000) The nature—society—man system: sustainable development. State Scientific Center of the Russian Federation Research Institute of Geosystems, Dubna, pp 410–426
14. Losev KS (2001) Ecological problems and prospects of sustainable development of Russia in the XXI century. Moscow, pp 400–411
15. Moiseev NN (1992) Man and the Noosphere. Moscow, pp 439–458
16. Nikolis G, Prigozhin I (1990) Cognition of the complex. Moscow, pp 425–437
17. Nikolis G, Prigozhin I (1979) Self-organization in nonequilibrium systems. Moscow, pp 440–449
18. Prigozhin I, Stengers I (1986) Order from chaos. Moscow, pp 256–261
19. Rumyantsev IS, Kromer R (2003) The use of engineering biology methods in the practice of hydrotechnical and environmental construction. Moscow, pp 259–276
20. Tyurina TA, Basilaia MA (2014) Technology and its role in the environmental crisis. *Rational Use Conserv Aquatic Biol Res*. Rostov-on-Don, pp 163–171
21. Schmal AG (2005) Methodology for creating a national environmental safety system. *Ecological Bulletin of Russia*, Moscow, pp 57–59
22. Ashby WS (1969) General theory of systems as a new scientific discipline. *Research on the General Theory of Systems*, Moscow, pp 184–190
23. Bertalanffy L (1969) General Theory of systems—a critical review. *Research on the General Theory of System*, New York, pp 231–265



Study of Primary Graphite Separation Products for the Creation of Petroleum Product Sorbents on Their Basis

N. Orekhova^{1,2}(✉), N. Fadeeva¹, E. Musatkina¹, and L. Isaeva¹

¹ Nosov Magnitogorsk State Technical University, 38, Lenin Avenue, Magnitogorsk 455000, Russia

n_orekhova@mail.ru

² Research Institute of Comprehensive Exploitation of Mineral Resources of the Russian Academy of Sciences, 4, Kryukovskiy Tupik, Moscow 111020, Russia

Abstract. Today Russia is experiencing a serious Shortage of natural Graphite. At the same time, little attention is paid to the waste product of iron and steel production—kish graphite. This waste contains a significant amount of harmful impurities and cannot be returned to the metallurgical cycle. Its either incinerated or buried and harmful to the environment. With the support of a grant from the Russian Science Foundation, research is being conducted to develop technologies for recycling graphitized dust from various sections of metallurgical processing to produce marketable products. One type of commercial products can become Sorbents of oil products. The sorption capacity of technogenic graphitized dusts and products of their enrichment has been studied. The intercalation Method for preparing graphite for bloating was selected. The possibility of obtaining thermally expanded graphite with magnetic properties has been studied. The need to preserve magnetic properties imposes restrictions on the method of intercalation and heat treatment. At the presented stage of works it was theoretically substantiated and experimentally proved the principle possibility of obtaining a Sorbent with magnetic properties from the iron–graphite concentrate from metallurgical Waste with a bulk weight less than 70 mg/cm^3 capable of retaining more than 15 g of common oil products per gram sorbent. The expansion coefficient at a thermal shock temperature of $450 \text{ }^\circ\text{C}$ was 32.

Keywords: Enrichment · Iron-graphite dust · Thermal expanded graphite · Sorbent · Oil products · Research

1 Introduction

Over the past year, the total volume of oil exported by sea from our country has increased by 30–50%. Shipment increased both at the Baltic and Black Sea marinas, and from the Pacific ports [1]. As a result of these there will also be an increase in multi-scale oil spills in the oceans. Spills of oil and oil products also occur on land, at almost all stages of the product life cycle: production, transportation, processing, storage and use.

To eliminate the consequences of oil and oil products spills, mechanical and sorption methods are mainly used. However, when the thickness of the oil film is less than 1–2 mm, as well as at a shallow depth of the reservoir, the use of mechanical means becomes impossible [2]. Under such conditions, special oil-sorbing materials are most effective; therefore, restorative measures include the use of sorbents. Analysis of research papers [3–5] showed that recently there have been many studies on the prospects of using thermally expanded graphite (TEG) as such a sorbent. Based on thermally expanded graphite, which is given magnetic properties or due to the introduction of highly dispersed ferromagnetic particles [6–8], or due to the formation of magnetic clusters on their surface by physicochemical methods [9], magnetically active sorbents are obtained, which, having a high sorption capacity of conventional sorbents [10], allow the removal of oil pollution from the surface of water and land using a magnetic field. TEG is obtained by thermal shock treatment of oxidized flake graphites of natural or artificial origin [11, 12].

Today Russia is experiencing a serious shortage of graphite. The most scarce is coarse-flake graphite. The raw material base of flake crystalline graphite in our country is based only in two regions—the Chelyabinsk and the Jewish Autonomous Regions [13]. The country also produces artificial graphite from carbon raw materials, mainly coke. The annual demand for crystalline graphite is only about 1/3 covered by the company’s own raw material base.

At the same time, in our country, little attention is paid to the processing of metallurgical graphite-containing dusts, which, in fact, are a renewable raw material for quiche graphite. Kish graphite, a precipitate of excess carbon formed when molten iron is cooled, is one of the by-products associated with smelting. According to the World Steel Association (WSA, World Steel Association), steel production in Russia in 2022 amounted to 71.5 million tons [14]. According to a marketing research of the pig iron market (TK Solutions Company), in 2022, Russian enterprises produced 51.6 thousand tons of mirror and pig iron. Recalculation to average indicators of the specific emission of graphitized dust per ton of pig iron makes it possible to estimate the annual amount of graphitized dust formed at 20 thousand tons.

The purpose of the study is to study the possibility of obtaining magnetic and non-magnetic thermally expanded graphite from technogenic graphitized dusts and products of their enrichment for use as a Sorbent for oil products.

2 Problem Statement

Production of expanded graphite proceeds according to the following scheme (Fig. 1.)

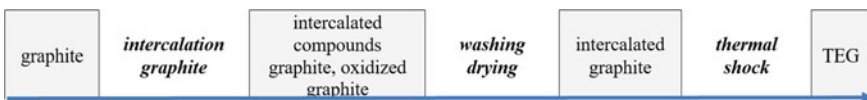


Fig. 1 Main stages of obtaining of expanded graphite

Our research group is carrying out studies on the development of processing technology for graphitized dusts in the areas of production, transportation and processing of pig iron at Magnitogorsk Iron and Steel Works [13, 15]. Graphite flakes included in iron-graphite dust of the blast-furnace shop are characterized by contamination of their surface and interlayer space by spherical particles of iron oxides. This imparts magnetic properties to almost all sample particles. Magnetic removal of iron-containing impurities is therefore ineffective. Selective separation of graphite from graphitized blast furnace dust is possible using flotation after selective disintegration of spelt particles. But even in this case a part of flakes from the concentrate shows magnetic properties. It is of interest to study the possibility of obtaining thermal expanded graphite with magnetic properties from blast-furnace kish graphite. This requires selecting the method of intercalation and subsequent bloating of graphite without significant reduction in the amount and loss of magnetic properties of iron-oxygen compounds. The possibility of obtaining such a product from dispersed iron-graphite waste back in 2016 was stated by the authors of article [16], but the product itself with magnetic properties has not been obtained.

It is of interest to study the possibility of obtaining non-magnetic thermo expanded graphite with high sorption capacity in relation to petroleum products on the basis of sintering products. This requires the selection of intercalation method that promotes simultaneous iron leaching and subsequent swelling of graphite with the highest expansion coefficient.

3 Research Methods

Iron-graphite sinter was sampled in the metallurgical production shops of the Magnitogorsk Iron and Steel Works. The samples are dispersed black material with different maximum coarseness depending on the place of sampling and a small amount of solidified metal spatter. The naked eye can detect the presence of coarse scaly graphite in the samples.

Microscopic study of fractions was carried out on Mineral C7 SIAMS Photolab in reflected light. Particle size distribution in terms of specific surface area was performed by laser diffraction (PRO-7000, Seishin Kigyo Co., Ltd.). The mass fraction of carbon was determined using a CS-144DR sulfur and carbon analyzer by burning the sample in an oxygen atmosphere to CO_2 . The content of magnetic particles of different magnetic susceptibility was determined using a hand magnet ($H = 42.8 \text{ kA/m}$) and a permanent magnet of ERGA N30 ($H = 725 \text{ kA/m}$). The flotation separation was carried out according to the scheme (Fig. 2).

The sorption capacity of magnetic and non-magnetic separation products of spelt, flotation concentrates was determined under static conditions. Preliminarily prepared and suspended samples of dust on a grid or held on the surface of a magnet were immersed in a model system simulating a spill of oil products on the water surface with a fixed thickness of NP layer of 5 mm. The amount of sorbed NP was determined by the weight method. The material with the weight of 0.3 g was in contact with oil product during the set period of time, after saturation the excess of NP was drained and the sorbent powder was weighed on electronic scales. The contact time was 3 min. The residual concentration of oil product in water was determined by volumetric method.

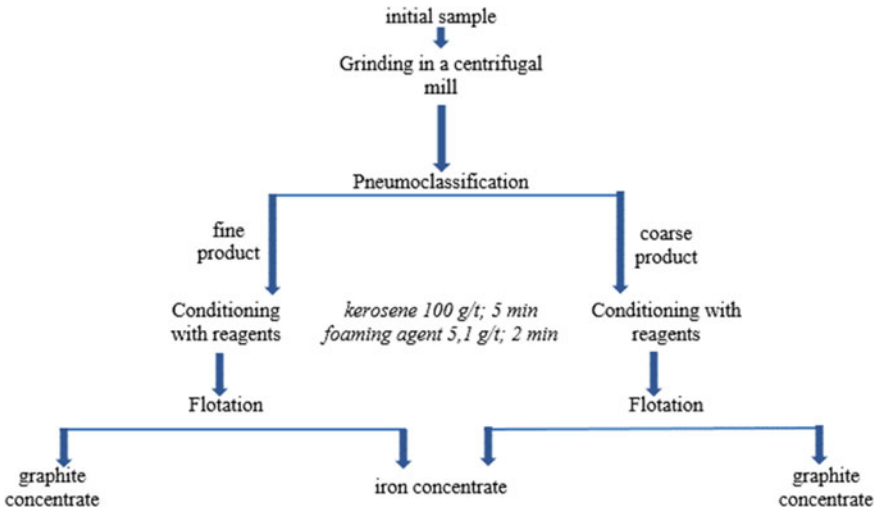


Fig. 2 Scheme of flotation enrichment of iron-graphite dust

The sorption capacity (g/g) was calculated by the formula:

$$E = \frac{(m_1 - m_2)}{m_1} \quad (1)$$

where m_1 —mass of the graphite sample, g; m_2 —mass of the graphite sample with the absorbed NP. Depending on the temperature of thermal shock, the magnetic properties of TEG were preserved or disappeared. The thermal expansion coefficient was calculated by the formula:

$$K_v = \frac{V}{m} \quad (2)$$

where K_v is the coefficient of volume thermal expansion, cm^3/g ; V is the volume of TEG graphite, cm^3 ; m is the mass of the original sample, g. The intercalation of graphite concentrates was carried out with a combination of oxidizing agents ($\text{H}_2\text{SO}_4 + \text{HNO}_3$, $\text{H}_2\text{SO}_4 + \text{K}_2\text{Cr}_2\text{O}_7$). The duration of treatment was chosen taking into account the fact that the oxidation of various graphite's in concentrated sulfuric and nitric acids, as well as their mixtures, occurs at a much lower rate than in a chromium mixture [17] and recommendations on the duration of oxidation in sources [16, 18]. Thermal shock was carried out in a muffle furnace heated to a predetermined temperature.

The following schemes were used in the study (Fig. 3):

4 Results and Discussion

A detailed study of the chemical and phase composition of sinter samples from different areas showed that iron–graphite dust of the blast furnace shop (BF) has the lowest carbon content of 10.17%. Samples from the oxygen converter shop (OC) and electric

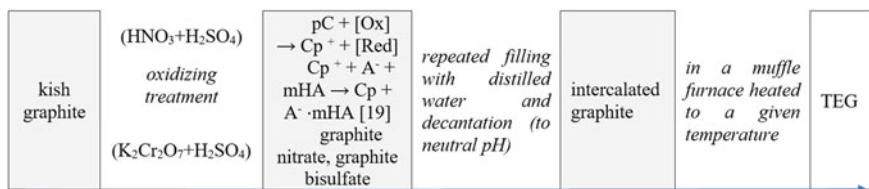


Fig. 3 Methodology for obtaining thermally expanded graphite in research

steel smelting shop (ES) are rich, the mass fraction of carbon in them is more than 30%. Dusts contain impurities, such as sulfur, phosphorus and zinc, which are harmful for their recycling in metallurgical processing. The iron–graphite dust of the blast-furnace shop is characterized by a high iron content and an order of magnitude higher content of impurities. A distinctive feature of the iron–graphite bed of the blast-furnace shop is the low value of weight loss during ignition—10.4%, in contrast to the sand of the oxygen-converter and electric steel-smelting shops, in which the value of weight loss during ignition was 31.0–30.3%. According to granulometric and magnetic analyses, the particle size classes of the initial blast furnace dust are dominated by -0.071 mm (44%) and -0.315 – 0.25 mm (23%). The thin classes, which account for 45% of the sinter, are almost entirely magnetic, due to the association of graphite flakes (Fig. 4) with rounded iron-oxygen formations, which are found both on the surface of the flakes (Fig. 4b) and in the interlayer space. (Fig. 4c).

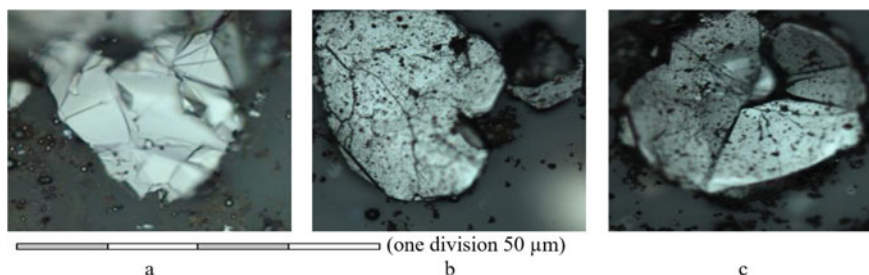


Fig. 4 Graphite particles under an optical microscope: **a** particle with a clean mirror surface; **b** particle with a surface sprinkled with spherical iron-oxygen formations; **c** particle with a spherical iron-oxygen phase embedded in the interlayer space

The content of the magnetic fraction in pellets OC of and ES are 60.01% and 33.9%, respectively.

According to X-ray quantitative phase analysis (XQPA), it was established that the main mineral components of iron–graphite dust are graphite, magnetite, hematite and quartz. The types and parameters of the elementary cells of the graphite crystal lattices that prevail in samples of graphitized dust from different areas are determined. The presence of a centrally symmetric hexagonal, asymmetric hexagonal and rhombic system was revealed. The proportion of rhombic graphite increases in the series electric steelmaking dust—oxygen-converter dust—blast-furnace shop dust.

First, the sorption activity of the products obtained by separation of blast furnace dust on a magnetic analyser was studied. The results of studying the sorption activity of non-magnetic products of magnetic dust separation showed that for the sorption value a more significant factor than the increase in the mass fraction of carbon in the product is a decrease in the particle size of products (Fig. 5) by the example of blast furnace sinter. The sorption capacity of the studied products was in the range 0.6–1.3 g/g.

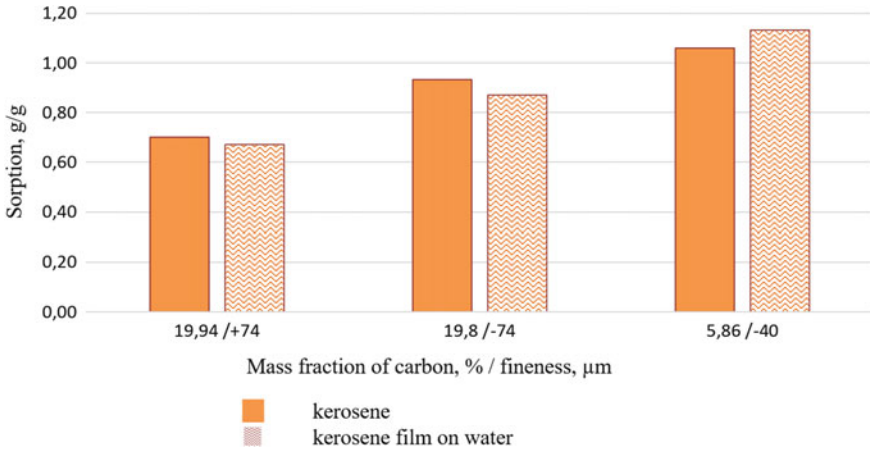


Fig. 5 Influence of the mass fraction of carbon and particle size of graphite of the non-magnetic product of the separation of graphitized dust of a blast-furnace shop on the sorption of kerosene

For a magnetic product of magnetic separation carried out with different magnetic field strength at the current strength of 0.5–2 A, it was noted that the change of sorption capacity of the magnetic product does not correlate with the mass fraction of carbon in it. In our opinion, this is a consequence of the fact that the magnetic susceptibility of the product, without affecting the sorption itself, affects the compactness of the stacking of particles on the surface of the magnet and the access of the petroleum product to the sorbent particle.

The sorption capacity of the graphite flotation concentrates was then studied. As a result of combination of centrifugal-impact grinding, air classification and flotation, graphite concentrates with mass fraction of carbon (%): 74.94 and 80.5 respectively were obtained from dusts of oxygen-converter and electric steelmaking conversion processes. Improvement of quality of graphite concentrates of blast-furnace sintering up to carbon content 22.7% with increase of reactivity of graphite particles provides dry milling with mechanical activation in centrifugal-impact mill. The results of the study on the enrichment of graphite dust of the Magnitogorsk Iron and Steel Works are described in detail by the authors of the article in the publications [20, 21].

The obtained flotation concentrates are lined up in the series BF (0.6 g/g), OC (1.3 g/g), ES (1.4 g/g) according to the increase of sorption capacity relative to kerosene. Gasoline sorption is lower for all studied concentrates by an average of 22%.

Comparison of the sorption capacity of flotation concentrates obtained from light and heavy products of pneumoclassification showed that with an almost equal mass

fraction of carbon in concentrates and a close content of particles less than 74 μm , 95.3 and 98.9%, a concentrate from a light product sorbs kerosene and gasoline by 12–18% worse than a concentrate from a heavy product. The study of the specific surface area of the concentrates showed that it is 3.2 times higher for the light product concentrate (0.317 m^2/g). It is likely that the lower sorption capacity of the higher specific surface area flotation concentrate is due to the larger amount of collector absorbed during flotation. Intercalation and subsequent heat treatment of the concentrates clean the surface of the particles from the previously fixed collector.

In further experiments, concentrates obtained by flotation of the heavy pneumoclassification fraction were used.

The concentrate obtained from blast furnace dust was intercalated with sulphuric acid with addition of nitric acid. After intercalation of the almost completely magnetic flotation concentrate a weight loss of 28% was observed. That is, when preparation of kish-graphite by intercalation to obtain TEG there is a chemical enrichment of the material due to dissolution of iron-oxygen compounds. The content of the magnetic fraction (hand magnet ($H = 42.8 \text{ kA/m}$) after intercalation was 70.4%. The magnetic fraction content at 500 °C and 700 °C thermoshock was 66.9% and 3.5% respectively. At thermoshock over 600 °C the magnetic properties of kish graphite almost disappear.

The expansion coefficient of intercalated concentrate obtained from blast-furnace graphite at 500 °C was low, which is explained by its low mass fraction of carbon. The expansion coefficient was 2.4–2.6 cm^3/g with an increase in sorption of kerosene by a factor of 3–3.5. After thermal shock of 700 °C $K_v = 2.8\text{--}3.2 \text{ cm}^3/\text{g}$ the sorption of kerosene was 3.1 g/g.

For intercalation of flotation concentrate obtained from OC dust the method described in source [16] was chosen. The concentrate was mixed with potassium bichromate, poured with sulfuric acid in a mass ratio of 1 to 2 and after 10 min of intensive stirring was washed by decantation to neutral pH. Thermal bloating was carried out at 200 and 450 °C. After placing the intercalated graphite in a thin, uniform layer on a metal plate heated to a predetermined temperature in the muffle, the graphite was kept in the furnace until the visible evaporation was complete. Under the microscope investigated TEGs were worm-shaped curved pellets (Fig. 6a). The metal on the surface of the pellets is represented by thin inclusions of different shapes. The appearance of irregularly shaped iron oxide particles is probably a consequence of uneven dissolution of the iron spheres during acid treatment.

The results obtained are presented in Table 1.

The sorption of thermally expanded graphite increased 8.6 times compared to the original flotation concentrate. Despite the low temperature of thermal shock to preserve the magnetic properties of the sorbent, not more than 600 °C (recommended in [16] is 1000 °C), the resulting material easily adheres to the water surface in the oil product layer, creates a thin layer of the sorbent, and after saturation is quickly and completely collected. magnet N30.

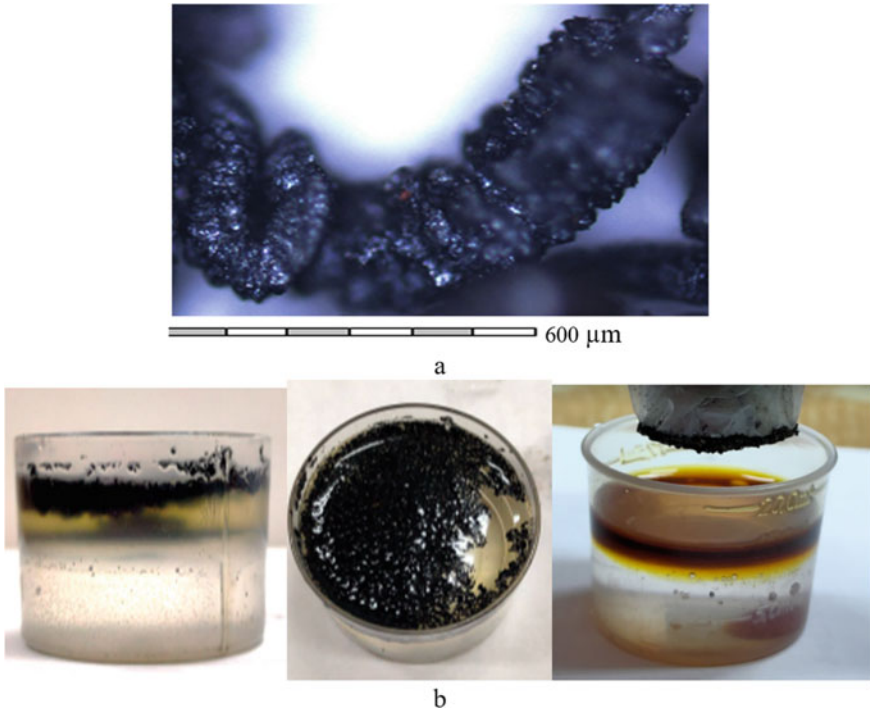


Fig. 6 Results of experiments on obtaining TEG: **a** graphite particles under an optical microscope; **b** floating TEG particles in the oil film and particle collection by magnet

5 Conclusion

In the near future the number of oil and petroleum product spills is predicted to increase, and consequently the surface area of the hydro- and pedosphere polluted by petroleum products will also grow.

The most promising and popular sorbents for elimination of hydrosphere and soil pollution by oil products are thermally expanded graphites. Sorbents with magnetic properties are convenient to use due to easy separation of the saturated sorbent from the environment to be cleaned.

The raw materials for production of magnetically active sorbents can be graphitized metallurgical dust, which contains coarse scaly graphite associated with iron oxide spherules (kish-graphite).

Concentrates obtained from graphitized dust from BOF and EAF shops by the beneficiation schemes including crushing, pneumatic classification, magnetic separation and flotation are magnetic and have a high carbon content (more than 70%).

The principle possibility of obtaining thermally expanded graphite with magnetic properties from the concentration concentrate of iron-graphite shot of metallurgical processing is shown, which can be used as a sorbent for collecting oil products from the surface of the reservoir. A sorbent with magnetic properties and a bulk weight of less than 70 mg/cm^3 , capable of retaining more than 15 g per gram of sorbent of conventional

Table 1 Results of experiments on obtaining TEG

Indicator	Experiment	
	1	2
Gain after intercalation, %	12	
Temperature of thermal shock, °C	200	450
K_V , cm ³ /g	14	32
Bulk weight, mg/cm ³	72.56	31.25
<i>Content of magnetic fraction, %</i>		
42,8 kA/m	7	0,5
725 kA/m	99	98
<i>Sorption, g/g</i>		
Gasoline	11	19
Kerosene	11.2	18.5
Machine oil	10.6	16

petroleum products, has been obtained. The expansion coefficient at a thermal shock temperature of 450 °C was 32.

Acknowledgements. The work was carried out with the financial support of the Russian Science Foundation for Basic Scientific Research and exploratory scientific research No. 22-27-20068 dated 25.03.2022

References

1. Makeev N (2023) Marine oil exports from Russia broke records/MK.ru. <https://www.mk.ru/economics/2023/01/26/.txt>. Accessed 29 May 2023
2. Vorobiev YuL, Akimov VA, Sokolov Yu (2005) Prevention and liquidation of emergency spills of oil and oil products. “In-octavo”, Moscow
3. Temirkhanov BA, Temerdashev ZA, Sultygova ZK (2015) Application of thermally expanded graphite in the technology of rehabilitation of aquatic ecosystems polluted with oil. J Oil Gas Tech 3(98):37
4. Voytash AA et al (2020) Purification of water from oil products with a sorbent based on thermally expanded graphite for irrigation of agricultural land. J Scientific Agron J 3(110):4–8
5. Sultygova ZK, Temirkhanov BA, Archakova RD (2021) Study of the properties of thermally expanded graphite for the rehabilitation of oil-contaminated water ecosystems. J Ecology Industry of Russia 7(25):37–41
6. Process of cleaning oil spills and the like (1993) Pat. 5215407 USA
7. Höhne R et al (2008) The influence of iron, fluorine and boron implantation on the magnetic properties of graphite. J Magn Magn Mater 320(6):966–977
8. Petrova LA et al (1985) Method of obtaining a carbon ferromagnetic sorbent. RF Patent no. SU 1148834:04

9. Gorshenev VN, Bibikov SB, Spector VN (2001) Modifying of materials by counter diffusion of reagent. mater. J Chem Phys 8898:1–6
10. Gorshenyov VN, Dontsov AE, Yakovleva MA (2021) Sorption materials controlled by an external magnetic field for the purification of aqueous media from contamination. J Chemical Safety Sci 5(2):78–95
11. Nawaz S et al (2021) Mitigation of environmentally hazardous pollutants by magnetically responsive composite materials. J Chemosphere 276:130241
12. Sorokina NE, Avdeev VV, Tikhomirov AS et al (2010) Composite nanomaterials based on intercalated graphite. Publishing House of Moscow State University, Moscow
13. Fadeeva NV, Orekhova NN, Gorlova OE (2019) Experience of processing graphite-containing dust of metallurgical production. J Ferrous Metallurgy, Bull Scient, Tech Econ Info 5(75):632–640
14. Zainullin E, Steel does not bend under sanctions. <https://www.kommersant.ru/doc/https://russiasnews.com/steel-does-not-bend-under-sanctions/>. Accessed 29 May 2023
15. Orekhova NN, Fadeeva NV, Kolodezhnaya EV, Efimova Y (2022) Study of the influence of the method of disintegration of graphite sinter on its disperse composition, particle shape and flotation indices. J Obogashchenie Rud 6:45–52. <https://doi.org/10.17580/or.2022.06.08>
16. Maslov VA et al (2016) Study of the oxidation of dispersed iron-graphite waste in order to obtain compounds intercalated graphite. J Vestnik Priazovsky State Technical University. Series: Technical Sciences 32:48–53
17. Fokin MN, Emelyanov YuV (1981) Protective coatings in the chemical industry. Chemistry, Moscow
18. Shornikova ON et al (2009) Sposob polichenya intercalirovannogo grafita. RF Patent no. 20091365 09 mai 2009
19. Illarionov IE et al (2018) Studies of physical and chemical properties of foundry graphite undergoing chemical and chemical-mechanical activation. Theory and Technology of Metallurgical Production 3(26):31–41
20. Fadeeva NV et al (2022) Study on the physical and chemical regularities of the kish graphite flotation process. J Bulletin Magnitogorsk State Tech Univ G.I. Nosova 4(20):37–46
21. Fadeeva NV, Orekhova NN, Kolodezhnaya EV (2022) The study of enrichment of graphite sinter by flotation method. Materials Plaksin readings, 4–7 October. Publishing House DFU, Vladivostok, pp 385–388



Methodology for Predicting Work on the Maintenance and Repair of Urban Facilities Using Machine Learning

L. Adamtsevich^(✉) and A. Adamtsevich

National Research Moscow State University of Civil Engineering, 129337 Moscow, Russian Federation

AdamtsevichLA@mgsu.ru

Abstract. This research work is devoted to the development of a methodology for predicting work on the maintenance and repair of urban facilities using machine learning. The initial data was collected from various sources of appeals for buildings in Moscow. Data processing was carried out, a dataset with new attribute fields was formed, an exploratory data analysis was carried out, where the main task was to identify data dependencies. The results of the study made it possible to form a hypothesis about the relationship that certain types of repairs can statistically reduce the number of incidents recorded by various sources. Hypothesis testing was carried out using cohort data analysis and A/B testing. Next was the stage of developing ML models to predict the level of importance of performing various types of repairs at a particular facility in terms of reducing the number of incidents at this facility and directly predicting repairs for facilities. After testing the hypothesis and validating the model on an example, a methodology was developed for predicting work on the maintenance and repair of urban facilities.

Keywords: Machine learning · ML · Industry 4.0 · Urban facilities · Predictive analytics · New technology

1 Introduction

With the aim of sustainable urban development, there is a need to review the process of creating built-up space, in which it is necessary to abandon linear systems and strive to ensure a continuous process of transformation and redistribution of materials.

It is obvious that the creation of new buildings and structures is possible, considering the main trends in the field of secondary use of materials, the use of modern digital technologies of Industry 4.0. However, most of the capital construction projects are at the operational stage, which leads to the need to reduce tensions in a circular economy and develop approaches to the use of Industry 4.0 technologies in relation to existing facilities.

To identify promising areas of research in the chosen area, a sample of relevant publications presented in the international Scopus database was collected.

The sample was formed by keywords “Construction 4.0” and “Machine learning” for the last 5 years from 2017 to 2022. The distribution of publications by year is shown in Fig. 1a, the distribution of publications by country (top 10 countries) is shown in Fig. 1b.

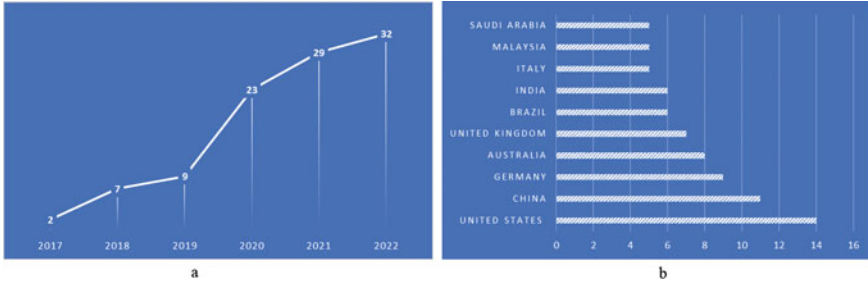


Fig. 1 a The distribution of publications by year, b the distribution of publications by country (top 10 countries)

A total of 102 publications were collected in the sample. To identify the main trends in the development of research in this area, a cluster map has been created.

Figure 2 shows the relationship of the keywords of the collected sample. The minimum number of matching keywords in selected publications was set to 5. The threshold value corresponded to 5 words out of 377. For each of 377 keywords, the program calculated the frequency of simultaneous links with other keywords used in publications. The keywords with the highest frequency and relevant to the research topic were selected.

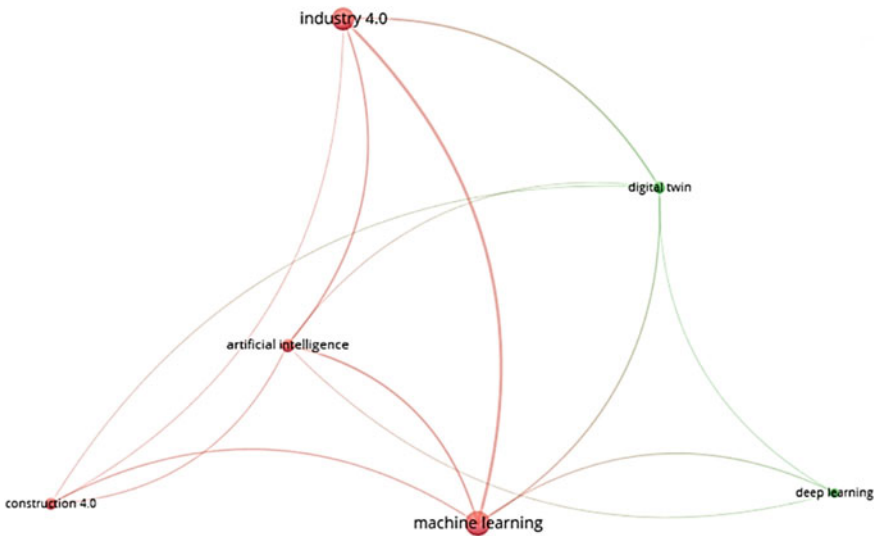


Fig. 2 The cluster map of the relationship of keywords in the sample

As can be seen from the Fig. 2, the relationship can be traced with technologies such as digital twins, in addition, attention is paid to deep learning and artificial intelligence.

Most of the publications are reviews [1–7]. For example, the article [1] presents a comprehensive scientometric study assessing the current state of AI research in architecture, design and construction. The review [2] summarizes research on the use of MoCap technologies in industry research. The paper [3] provides an overview of current applications based on artificial intelligence, machine learning and deep learning in architectural design and visualization of objects.

Several works contain new solutions for using machine learning methods, blockchain and other Industry 4.0 technologies. For example, the study [8] designs federated learning with blockchain assisted image classification model for clustered UAV networks on IIoT environment.

The study [9] presents Implications of ML integrated technologies for construction progress detection under Industry 4.0. The theoretical framework was designed for the ML integrated project progress detection technologies according to the literature outcomes.

The work [10] aims to use ML algorithms to process a dataset of industrial machine components event logs failure. The approach aims to use the conditional probability relations generated by the Bayesian Networks and the ranking of criteria relevance for the design of an attribute relevance analysis decision-making model within the scope of industrial maintenance to prioritize which components of a specific machine are more susceptible to failures. Predictive maintenance planning for Industry 4.0 using Machine Learning for Sustainable Manufacturing is presented in [11].

This work is devoted to the development of a methodology based on machine learning for predicting the maintenance and repair of urban facilities to extend their life and ensure safe operation or make a decision on their dismantling, saving material resources, in accordance with the requirements of the circular economy.

2 Materials and Methods

The initial data was collected from various sources of appeals for apartment buildings in Moscow. The appeals concerned the issues of replacing elevator equipment, repairing in-house engineering drainage systems, repairing in-house engineering heating systems, repairing in-house engineering power supply systems, window blocks, garbage chutes, repairing in-house cold and hot water supply systems, repairing entrances and basements, repairing facades and roofs, etc. This led to the fact that it became necessary to process the data and form a single data set, create new attribute fields. Next, direct work with the data and exploratory data analysis were carried out. At this stage, the main task was to identify dependencies in the data. The results of the study made it possible to form a hypothesis about the relationship that certain types of repairs can statistically significantly reduce the number of incidents recorded by various sources. Hypothesis testing was carried out using cohort data analysis and A / B testing, i.e. division of data on the basis before/after the key event, the formation of cohorts depending on the types of events and/or sources.

Next was the stage of developing machine learning (ML) models to predict the level of importance of performing various types of repairs at a particular facility in terms

of reducing the number of incidents at this facility and directly predicting repairs for facilities.

After testing the hypothesis and validating the model on a specific example, a methodology for predicting work on the maintenance and repair of urban facilities using machine learning was compiled.

Thus, the flowchart of the study is shown in Fig. 3.

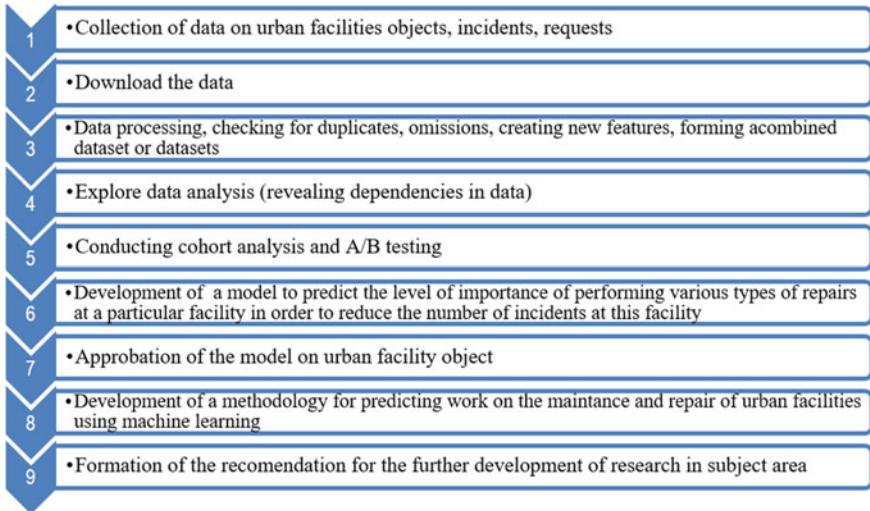


Fig. 3 The algorithm of the presented study

3 Results

Exploratory analysis showed an imbalance of classes on many categorical grounds. The seasonality of calls by source can also be highlighted.

To form a labeled dataset for machine learning, the objects from the sample were divided into cohorts according to the types of repairs and sources of calls. The cohorts were used to run a series of A/B tests to improve hypotheses about the equality of the means of dependent paired samples and to determine the relationship between the fact that repairs were performed and the change in the number of recorded incidents for each source.

The dynamics of changes in registered incidents by various sources for the repair of facades and roofs are shown in Figs. 4 and 5. These graphs are built according to the initial data.

As a result, a labeled data set was obtained for repaired objects, where the target attribute value of 1 corresponded to objects for which, after repair, there was a statistically significant decrease in the number of calls for a given source, and 0 for objects where this did not occur.

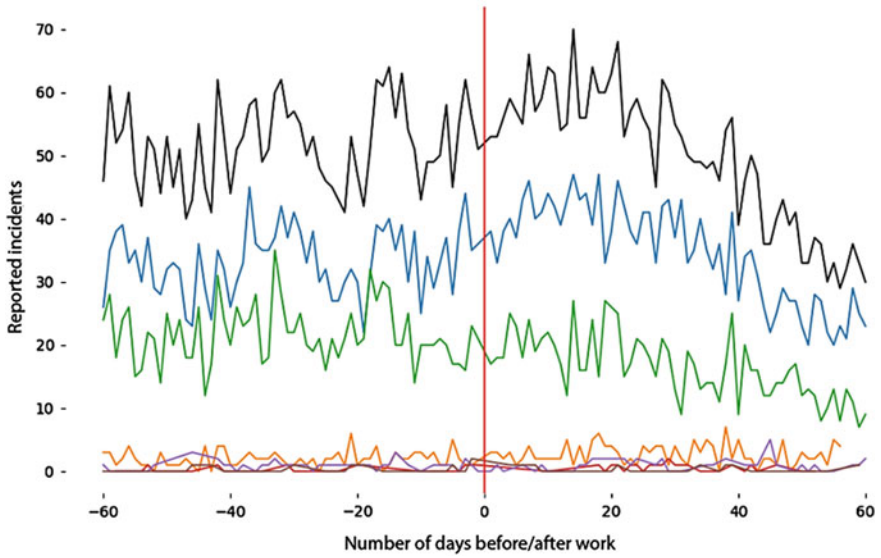


Fig. 4 The dynamics of changes in registered incidents by various sources for the repair of facades

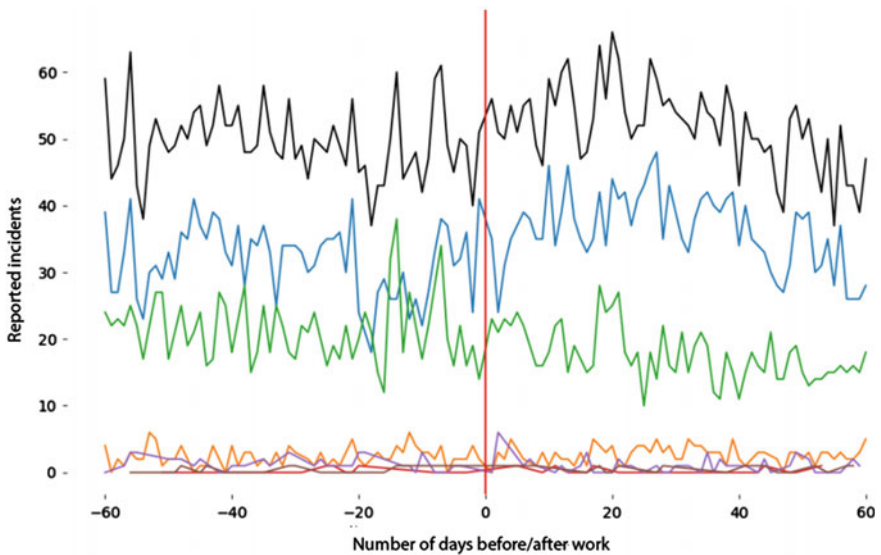


Fig. 5 The dynamics of changes in registered incidents by various sources for the repair of roofs

For each selected type of repair, 3600 `LGBMClassifier()` gradient boosting models were trained with different hyperparameter settings in order to obtain the best solution. We performed hyperparameter optimization with `GridSearchCV` to maximize the `f1_score` metric.

As a result, models were obtained that effectively predict a decrease in the number of incidents by two sources by predicting the feasibility of repairing roofs and facades (Fig. 6).

TRAIN					TRAIN				
	precision	recall	f1-score	support		precision	recall	f1-score	support
0	0.75	0.55	0.63	33	0	0.91	0.40	0.56	25
1	0.78	0.90	0.83	58	1	0.83	0.99	0.90	72
accuracy			0.77	91	accuracy			0.84	97
macro avg	0.76	0.72	0.73	91	macro avg	0.87	0.69	0.73	97
weighted avg	0.77	0.77	0.76	91	weighted avg	0.85	0.84	0.81	97

TEST					TEST				
	precision	recall	f1-score	support		precision	recall	f1-score	support
0	0.73	0.47	0.57	17	0	0.86	0.32	0.46	19
1	0.68	0.86	0.76	22	1	0.63	0.96	0.76	23
accuracy			0.69	39	accuracy			0.67	42
macro avg	0.70	0.67	0.67	39	macro avg	0.74	0.64	0.61	42
weighted avg	0.70	0.69	0.68	39	weighted avg	0.73	0.67	0.62	42

a

b

Fig. 6 a Parameters of the model predicting a decrease in the number of calls due to roof repairs b parameters of the model predicting a decrease in the number of calls due to facades repairs

Figure 6a shows the parameters of the model that predicts a decrease in the number of calls due to roof repairs, Fig. 6b—due to facade repairs.

Thus, we have reduced the problem solved using ML to a binary classification to identify those objects, the repair of which will lead to a statistically significant reduction in the number of incidents.

The “before” parameter represents the number of incidents according to the source identified at the previous stage for a specific type of repair work:

- 60 days before the actual repair date on the Train training set;
- 60 days before the date of prediction on the test sample Test.

The importance of the features of the model that predicts the feasibility of repairing the roof is shown in Fig. 7, and in Fig. 8 for the model predicting the feasibility of repairing facades.

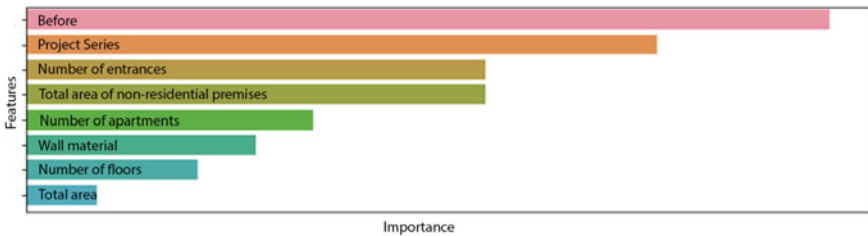


Fig. 7 The importance of the features of the model that predicts the feasibility of roof repairs

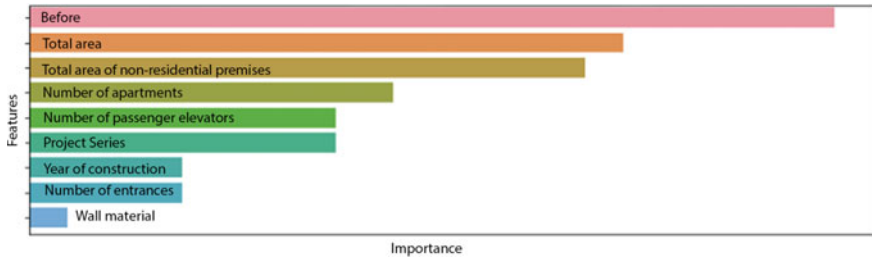


Fig. 8 The importance of the features of the model predicting the expediency of facade repairs

For all objects for which a prediction of the need for both types of repairs was obtained, it is proposed to enter such a parameter as “major repairs”, if both objects have a high probability of repairing both the roof and the facade at the same time.

Figure 9 shows the results of using the model to predict the feasibility of various types of repairs for a specific object. The obtained data according to the model correspond to the planned ones.

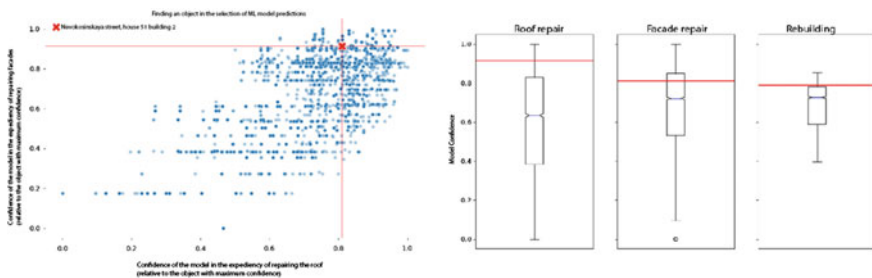


Fig. 9 The results of using the model to predict the feasibility of types of repairs at the facility

In accordance with the study, a generalized block diagram of the methodology for predicting work on the maintenance and repair of urban facilities using machine learning was formed, which is shown in Fig. 10.

4 Conclusions

The study made it possible to establish that in the initial data on objects there are several fields for which there is almost no data. Events for individual sources account for more than 90% of all registered, and for individual sources there is a seasonality in requests.

While performing cohort and statistical analyzes, it was found that a number of events in terms of performing repairs at the facility leads to statistically significant differences between the number of events before and after according to different sources. However, only 4 types of repairs led not just to a change, but to a statistically significant reduction in the number of incidents. It was these types of repairs that were decided to be included in the shortlist of areas for creating ML solutions.

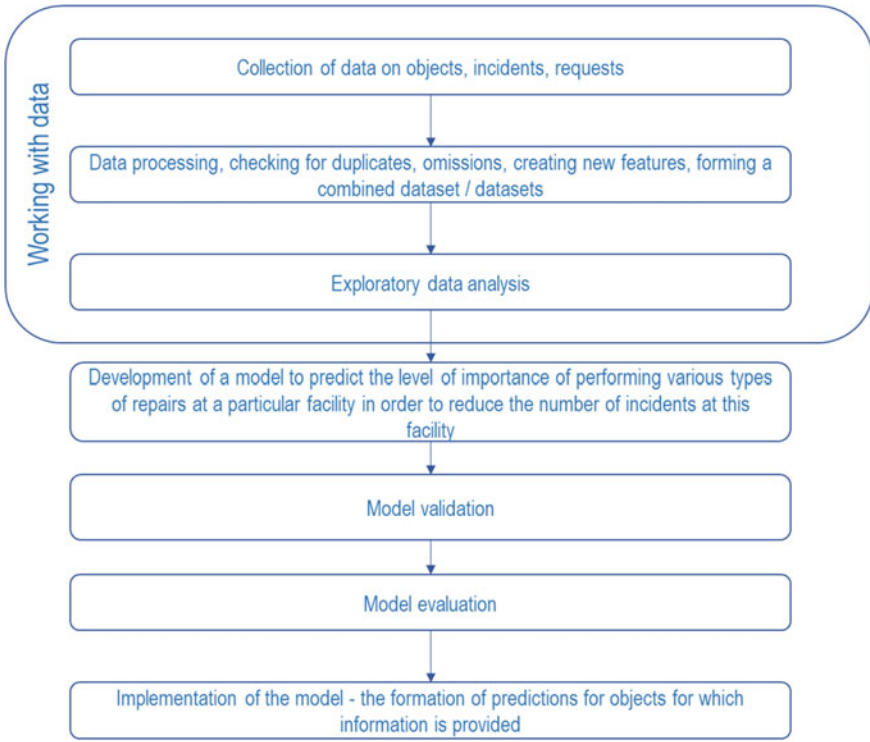


Fig. 10 Enlarged block diagram of the methodology for predicting work on the maintenance and repair of urban facilities using machine learning

Machine learning was applied to solve a binary classification problem. As a target feature, the share of reduction in the number of incidents for a specific source after the repair was chosen. When forming a training sample for objects where the number of incidents within 60 days after repair decreased relative to the number of incidents within 60 days before repair, the target attribute was set equal to 1. Otherwise, 0.

For each type of repair, 3600 `LGBMClassifier()` gradient boosting models were trained with different hyperparameter settings in order to obtain the best solution. The `f1_score` metric was used as the target metric for choosing the optimal solution. During the training, it was found that it was impossible to obtain solutions that meet the target requirements for predicting the need to repair in-house engineering systems of cold and hot water supply due to insufficient data in the training sample. In this connection, these models were not included in the final ensemble of solutions.

As a result of the project, models were obtained to predict the need for roof and facade repairs. In order to provide the ability to rank objects in order of importance, the `predict_proba()` method of the model was used for predictions, and not the `predict()` method.

For all objects for which the prediction of the need for both types of repairs was received, the parameter of the need for major repairs was also introduced, if both objects

have a high level of probability of repairing both the roof and the facade at the same time.

As a further development of the study, it seems appropriate to train the model on a deeper sample.

References

1. Darko A, Chan APC, Adabre MA, Edwards DJ, Hosseini MR, Ameyaw EE (2020) Artificial intelligence in the AEC industry: scientometric analysis and visualization of research activities. *Autom Constr* 112:103081. <https://doi.org/10.1016/j.autcon.2020.103081>
2. Menolotto M, Komaris D-S, Tedesco S, O'flynn B, Walsh M (2020) Motion capture technology in industrial applications: a systematic review. *Sensors (Switzerland)* 20(19):5687. <https://doi.org/10.3390/s20195687>
3. Baduge SK, Thilakarathna S, Perera JS, Arashpour M, Sharafi P, Teodosio B, Shringi A, Mendis P (2022) Artificial intelligence and smart vision for building and construction 4.0: Machine and deep learning methods and applications. *Auto Const* 141:10440. <https://doi.org/10.1016/j.autcon.2022.104440>
4. Wu C, Li X, Guo Y, Wang J, Ren Z, Wang M, Yang Z (2022) Natural language processing for smart construction: current status and future directions. *Autom Constr* 134:104059. <https://doi.org/10.1016/j.autcon.2021.104059>
5. Azeem M, Haleem A, Javaid M (2021) Symbiotic Relationship between machine learning and industry 4.0: a review. *J Indust Integration Manage*, 2130002. <https://doi.org/10.1142/S2424862221300027>
6. Wang K, Guo F, Zhang C, Hao J, Schaefer D (2022) Digital technology in architecture, engineering, and construction (AEC) industry: research trends and practical status toward construction 4.0. *Construction Research Congress 2022: Project Management and Delivery, Controls, and Design and Materials—Selected Papers from Construction Research Congress 3-C*:983–992. <https://doi.org/10.1061/9780784483978.100>
7. Kukushkin K, Ryabov Y, Borovkov A (2022) Digital twins: a systematic literature review based on data analysis and topic modeling. *Data* 7(12):173. <https://doi.org/10.3390/data7120173>
8. Abunadi I, Althobaiti MM, Al-Wesabi FN, Hilal AM, Medani M, Hamza MA, Rizwanullah M, Zamani AS (2022) Federated learning with blockchain assisted image classification for clustered UAV networks. *Computers, Mat Contin* 72(1):1195–1212. <https://doi.org/10.32604/cmc.2022.025473>
9. Qureshi AH, Alaloul WS, Manzoor B, Musarat MA, Saad S, Ammad S (2020) Implications of machine learning integrated technologies for construction progress detection under industry 4.0 (IR 4.0). In: 2020 2nd International Sustainability and Resilience Conference: Technology and Innovation in Building Designs, 9319974. <https://doi.org/10.1109/IEEECONF51154.2020.9319974>
10. Lima E, Gorski E, Loures EFR, Portela Santos EA, Deschamps F (2019) Applying machine learning to AHP multicriteria decision making method to assets prioritization in the context of industrial maintenance 4.0. *IFAC-PapersOnLine* 52(13):2152–2157. <https://doi.org/10.1016/j.ifacol.2019.11.524>
11. Abidi M, Mohammed MK, Alkhalefah H (2022) Predictive maintenance planning for industry 4.0 using machine learning for sustainable manufacturing. *Sustainability (Switzerland)* 14(6):3387. <https://doi.org/10.3390/su14063387>



The Carbon Dioxide Capture Potential of Ash and Slag from Waste Incineration Plants

K. A. Vorobyev^{1,2(✉)}, I. V. Shadrunkova¹, and T. V. Chekushina^{1,3}

¹ Peoples' Friendship, University of Russia Named After Patrice Lumumba (RUDN University), 6, Miklukho-Maklaya Str., Moscow 117198, Russia
kirill.vorobyev@stud.thga.de

² Technische Hochschule Georg Agricola, 45, Herner Str., 44787 Bochum, Germany

³ Institute of Comprehensive Exploitation of Mineral Resources, Russian Academy of Sciences, 4, Kryukovskiy Tupik, Moscow 111020, Russia

Abstract. This article explores the potential of using slag from waste incineration plants to capture carbon dioxide (CO₂) in gaseous environments. The study investigates the efficacy of slag as an absorbent for CO₂ in gas streams. It examines the purification process, CO₂ absorption capacity, activation techniques, and CO₂ release mechanisms. The findings suggest that slag has significant potential as a CO₂ capture material, offering a promising solution for reducing greenhouse gas emissions from waste incineration plants. The research contributes to the development of effective strategies for mitigating climate change by utilizing waste materials for carbon capture and storage. Additionally, the article discusses various methods of enhancing the CO₂ capture capability of slag, such as optimizing particle size, modifying the surface properties, and adding activating agents. The authors present experimental results indicating the improved CO₂ adsorption capacity of treated slag samples compared to untreated ones. Furthermore, the study investigates the CO₂ release mechanisms during the regeneration of the slag material. It examines factors affecting the release efficiency, such as temperature, gas flow rate, and regeneration time. The findings demonstrate the feasibility of using slag as a cyclic sorbent, with the ability to release and capture CO₂ repeatedly. This article provides valuable insights into the possibilities of CO₂ capture using slag from waste incineration plants in gas environments. The research contributes to the ongoing efforts in developing effective strategies for mitigating climate change and advancing the field of carbon capture and storage.

Keywords: Carbon dioxide capture · Slag · Waste incineration plants · Gas environments · CO₂ absorption · Activation techniques · Greenhouse gas emissions

1 Introduction

The issue of anthropogenic impact on the environment is one of the most pressing global challenges. Specifically, the issue of carbon emissions and their impact on climate change is attracting increasing attention. Innovative and efficient solutions are required to reduce carbon emissions [1–10].

The increasing global concern over climate change and the urgent need to reduce greenhouse gas emissions has prompted a search for effective solutions to mitigate the release of carbon dioxide (CO₂) into the atmosphere. One such solution is the capture and storage of CO₂, which involves capturing and storing CO₂ emissions from industrial processes before they are released into the atmosphere. In recent years, there has been growing interest in exploring the carbon dioxide capture potential of ash and slag generated from waste incineration plants.

Waste incineration plants are widely used as a method for managing and disposing of municipal solid waste. These facilities burn waste at high temperatures, resulting in the production of ash and slag, which are by-products of the combustion process. Traditionally, these by-products have been considered as waste and often disposed of in landfills. However, recent studies have shown that ash and slag have the potential to capture and store CO₂, making them valuable resources for reducing greenhouse gas emissions.

Ash and slag from waste incineration plants contain high levels of calcium oxide (CaO) and other alkaline compounds, which exhibit a high affinity for CO₂. When exposed to CO₂, these compounds undergo a chemical reaction called carbonation, where CO₂ is chemically bonded and sequestered in the form of calcium carbonate (CaCO₃). This reaction is similar to the natural process by which limestone is formed.

The carbonation of ash and slag can occur via two different routes: direct carbonation and indirect carbonation. In direct carbonation, CO₂ is directly injected into the ash and slag, allowing for a more rapid carbonation process. Indirect carbonation, on the other hand, involves the exposure of ash and slag to ambient air, where CO₂ is naturally absorbed over time. Both routes have been explored in various research studies, each with its own advantages and challenges.

The potential benefits of utilizing ash and slag for CO₂ capture include not only the reduction of greenhouse gas emissions but also the utilization of waste materials that would otherwise be landfilled. This approach offers a more sustainable alternative to conventional waste management practices and has the potential to contribute to a circular economy. Additionally, the carbonated ash and slag can potentially be used as a building material or as a replacement for traditional cement, further reducing carbon emissions in the construction industry.

The carbon dioxide capture potential of ash and slag from waste incineration plants presents a compelling opportunity to address the pressing challenge of reducing CO₂ emissions. By harnessing the chemical properties of these waste materials, it is possible to sequester CO₂ and simultaneously contribute to more sustainable waste management practices. Further research and development in this area are needed to optimize carbonation processes, explore potential applications for carbonated ash and slag, and overcome any technical and logistical challenges.

One potential source for reducing carbon emissions is slag from waste incineration plants. Slag generated during the incineration process contains a significant amount of carbon and can be utilized for capturing carbon dioxide from gas environments. Therefore, there is a need to explore the possibilities of using slag from waste incineration plants as a medium for carbon capture and emissions reduction [11].

The main aim of this article is to study the rate of carbon dioxide capture by slag in gas environments and determine the feasibility and effectiveness of using slag for reducing carbon emissions. To achieve this objective, a laboratory setup was proposed, which enables experiments with various slag samples and gas environments [12–17].

The article provides a comprehensive review of existing studies on the use of slag from waste incineration plants for emissions reduction. It also describes the laboratory setup and experimental methodology. The development of the laboratory setup is significant for both the scientific community and practical applications. The proposed methods and solutions can be utilized in industries to reduce carbon emissions and improve the environmental conditions. Moreover, this research provides novel scientific data and contributes to the advancement of the field of carbon capture.

2 Theoretical Review

The use of slag generated from the incineration of municipal solid waste (MSW) in waste incineration plants is one of the primary methods for waste disposal and energy production. During the incineration process, slag is formed as the residue of burned waste and contains various components, including carbon. Utilizing slag from waste incineration plants for reducing carbon emissions presents an environmentally sound approach to waste management [18–25].

Carbon, present in slag, is an effective substance for capturing carbon dioxide (CO₂) from gas environments. Since carbon dioxide is the main contributor to global warming, reducing its emissions is an important goal in mitigating climate change [26–29].

In July 2022, amendments were made to the Federal Law “On Waste Production and Consumption,” and separate legislative acts were enacted. The main changes pertained to the terminology:

- secondary resources—waste or parts thereof that can be reused for manufacturing goods, performing work, providing services, or generating energy, and obtained through separate collection, gathering, or processing of waste or formed during production processes;
- secondary raw materials—products derived directly from secondary resources (without processing) or in accordance with the technological processes, methods, and techniques provided by Russian standardization documents, which can be used in manufacturing other products and/or in other economic activities.

In 2021, the average fee for waste removal per cubic meter of waste in Russia was 500 rubles. A family of four would pay 400 rubles per month for MSW removal. Waste removal is carried out by private regional operators, and tariff determination for waste removal is conducted by executive bodies of the subjects.

“Ekotechprom” State Unitary Enterprise (SUE) is a waste processing and disposal enterprise established in accordance with the Government Resolution of Moscow No. 604 dated June 29, 1993. It is the largest and the first in Russia to perform a full range of sanitary cleaning operations for MSW. “Ekotechprom” SUE engages in collection, transportation, selective sorting, and thermal treatment of municipal solid waste, as well as biological and medical waste. It also provides information and advisory services

in the waste management sphere. The problem of MSW disposal was identified by the Moscow Government as a priority in the city's economic development due to the increasing population and, consequently, the volume of household waste.

"Ekotechprom" SUE expands through the construction and reconstruction of waste treatment facilities in Moscow. In 2008, the enterprises "Spectrans," "MiSAT," "Specav-tobaza," "Kotlyakovo," and "Rudnevo" transported over 550 thousand tons of waste. The largest waste sorting facility in Russia, "Kotlyakovo," which has been operating since 2005, processed over 380 thousand tons of waste in 2008. Thermal treatment of waste with energy recovery is intensively developing in Moscow due to a shortage of land for landfills, and the first waste incineration plant was commissioned in Moscow in 1975.

Currently, Moscow is home to Waste Incineration Plant No. 4, which was commissioned in 2003 on the territory of the "Rudnevo" industrial zone in the Eastern Administrative District. The plant's capacity for receiving MSW is 250 thousand tons per year. The six stages of waste gas purification and the gas cleaning system installed at the plant comply with European standards for thermal treatment and flue gas cleaning. While waste landfilling in the Moscow region remains the main method of disposal, thermal treatment continues to rapidly develop in the city due to the need to meet environmental requirements and restrictions on landfill placement in urban areas.

"Ekotechprom" SUE ensures the environmental safety of all its facilities, including waste incineration plants, through its own ecologists and city services. Operating waste incineration plants helps reduce the number of waste collection trucks, fuel consumption, and road congestion while freeing up land in the Moscow region for other purposes. Waste transfer stations (WTS) are used to reduce the cost of city cleaning, with the first WTS built in 1995 in the Northern Administrative District. The volume of waste transported to landfills through the WTS network was 1.2 million tons in 2008. "Ekotechprom" SUE also operates a veterinary-sanitary plant, which safely treats biological and medical waste at two landfills. Incineration plants, like the ones in Moscow, are typical for thermal treatment of MSW, and their main task is to ensure environmental safety during waste treatment and the generation of thermal and electrical energy.

These incineration plants, including the one located within "Ekotechprom" SUE, are integral components of the MSW management system. They help reduce waste volume, lower the risk of environmental pollution, significantly decrease the need for waste collection trucks, and improve resource efficiency. Additionally, such plants can operate on autonomous sources of energy, reducing dependence on centralized power supply and minimizing the risk of accidents and power outages during periods of high demand. All of this is important for ensuring environmental safety and maintaining cleanliness in the urban environment.

However, it should be noted that certain environmental organizations and residents express dissatisfaction and concerns regarding the use of waste incineration plants, citing potential negative consequences for the environment and human health. Therefore, it is essential to continue monitoring and improving plant operation technologies to minimize negative effects and ensure maximum safety.

Each year, a plan for environmental protection measures is developed, which includes construction, repair, and modernization of equipment to ensure uninterrupted and reliable

landfill operation and compliance with environmental legislation. Currently, a transitional period is underway for the new waste management system, which includes source separation of waste, prohibition of landfilling waste suitable for recycling, and other measures. To implement these measures, corresponding changes are made to legislation at the federal and regional levels, and target-oriented development programs and territorial waste management schemes are being developed.

However, it is necessary to consider that transition to the new waste management system is a complex and lengthy process that requires significant changes in infrastructure and citizen behavior. It is important to conduct extensive public awareness campaigns on proper waste separation and the consequences of improperly disposing waste [30].

One of the primary methods for carbon dioxide capture is its physical or chemical interaction with carbon-containing materials. Slag from waste incineration plants, which contains a significant amount of carbon, can serve as such materials for CO₂ capture from various gas environments.

To conduct a study on the rate of carbon dioxide capture by slag in gas environments, a laboratory setup was proposed (Fig. 1). The main components of the setup include a sealed chamber, a carbon dioxide cylinder, a reducer, a flexible hose, a chemical gas analyzer, a domestic fan, slag samples, a bowl with saturated salt solution, and a low-speed fan system. The control panel of the automatic gas analyzer OKA-T-CO₂ allows for monitoring the process of carbon dioxide capture during the experiment.

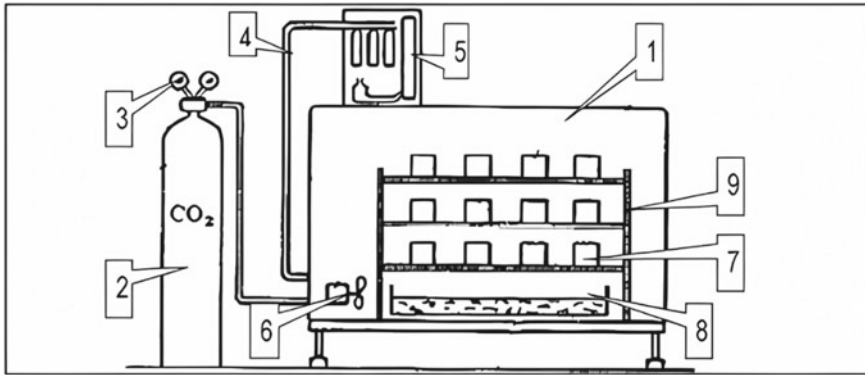


Fig. 1 Schematic diagram of the laboratory setup for studying the rate of carbon dioxide capture by slag in gas environments: 1—sealed chamber; 2—CO₂ cylinder; 3—reducer; 4—flexible hose; 5—chemical gas analyzer; 6—domestic fan; 7—samples; 8—bowl with saturated salt solution; 9—rack; 10—U-tube; 11—control panel of the automatic gas analyzer OKA-T-CO₂; 12—sensor of the automatic gas analyzer installed inside the chamber; 13—low-speed fan system; 14—grid for sample placement

This laboratory setup is designed to determine the rate of carbon dioxide capture by slag in various gaseous environments. The gas mixture from the CO₂ cylinder (2) is delivered to the reducer (3), which allows for pressure control and maintenance. The mixture then flows through a flexible hose (4) into a sealed chamber (1) where slag samples (7) are placed.

To ensure uniform distribution of the gas mixture within the chamber, a domestic fan (6) is employed, while a system of low-speed fans (13) is used to maintain continuous air circulation. A grid (14) within the chamber is provided for the placement of slag samples.

For monitoring carbon dioxide content, a chemical gas analyzer (5) is utilized. The control panel of the automatic gas analyzer OKA-T-CO₂ (11) enables adjustment and monitoring of the analyzer's operation. An automatic gas analyzer sensor (12) is installed inside the chamber to measure the carbon dioxide content in the gaseous environment.

The bowl (8) filled with a saturated solution of table salt serves to create a specific concentration of water vapor in the chamber, simulating more realistic conditions.

After conducting the experiment and obtaining the results, an analysis of the rate of carbon dioxide capture by slag in gas environments will be performed. Based on the data obtained, conclusions can be drawn regarding the potential of using slag from waste incineration plants as a medium for reducing carbon emissions and contributing to the development of efficient waste disposal methods and CO₂ emission reduction.

The presented theoretical review provides a better understanding of the physicochemical basis of the carbon dioxide capture process by slag and its potential for reducing carbon emissions in gas environments.

3 Research Methodology

The research methodology will consist of three main stages:

1. Preparation of the laboratory setup [31]: This stage is necessary to ensure the proper functioning and safe operation of all components, as well as to create optimal conditions for conducting experimental research. It includes the installation, verification, and calibration of equipment and ensuring safety in the laboratory area. The specific steps include:
 - setting up the sealed chamber on a rack;
 - connecting the reducer to the CO₂ cylinder;
 - connecting the flexible hose from the reducer to the chamber for gas supply;
 - installing the chemical gas analyzer and automatic gas analyzer sensor inside the chamber;
 - placing slag samples on the grid inside the chamber.
2. Conducting the experiment: This stage is necessary to obtain specific data and information that will allow for testing hypotheses, confirming or refuting assumptions, and obtaining objective results and conclusions based on observations and measurements. It enables the testing and refinement of scientific theories, the development of new methods and technologies, and the enrichment of the research basis for further studies and the advancement of scientific fields. The specific steps include:
 - filling the bowl with saturated salt solution;
 - activating the control panel of the automatic gas analyzer OKA-T-CO₂;
 - activating the low-speed fan system to ensure gas mixing inside the chamber;
 - passing gas through the flexible hose into the chamber for a specified period;

- starting the chemical gas analyzer to monitor the concentration of CO₂ in the chamber during the experiment;
 - recording data on the rate and efficiency of carbon dioxide capture by slag in gas environments.
3. Analysis and processing of results: This stage is essential for identifying patterns, relationships, and conclusions based on the data obtained from the experiment or research. It involves statistical analysis of the data, visualization of the results, interpreting their significance, and explaining the phenomena observed. This allows for formulating conclusions and making scientific inferences. The specific steps include:
- processing and analyzing data obtained from the chemical gas analyzer;
 - determining the rate of carbon dioxide capture by slag in gas environments;
 - comparing results for different slag samples and experimental conditions;
 - calculating the efficiency of CO₂ capture by slag based on the data obtained;
 - performing statistical analysis and interpreting the results.

4 Experimental Research

Experimental research on this topic has several objectives: it allows us to investigate the effectiveness of waste incineration slag in capturing and retaining carbon. This is important for assessing the potential use of such slag as a low-carbon material or for reducing emissions into the atmosphere. Additionally, it enables us to evaluate the impact of various factors (e.g., slag composition, exposure conditions, and temperature) on the efficiency of carbon capture [32–34]. This information can be used to optimize the process and determine the optimal conditions for utilizing slag to reduce carbon emissions. The experimental research will consist of six main stages:

1. Preparation of slag samples: this is necessary for analysis and testing to study their composition, properties, and potential use. The specific steps include:
 - collecting slag samples from waste incineration plants;
 - cleaning and sorting the samples;
 - crushing the slag to the required particle size.
2. Preparation of the chamber and samples: This stage is necessary to ensure the proper experimental conditions and obtain reliable results. It involves equipment setup, sample placement, and creating a controlled environment for their investigation. The specific steps include:
 - preparing the sealed chamber for the experiment;
 - installing the grid inside the chamber for placing the slag samples;
 - placing a bowl with saturated salt solution inside the chamber.
3. Sample placement and beginning of the experiment: This stage is necessary to start collecting data and conducting the research, allowing for testing hypotheses, obtaining measurement results and observations, and gathering information for achieving the research goals and drawing conclusions. The specific steps include:
 - placing the slag samples on the grid inside the chamber;

- activating the low-speed fan system to ensure gas mixing inside the chamber;
 - obtaining baseline data from the chemical gas analyzer to determine the initial concentration of carbon dioxide in the chamber;
 - starting the system and initiating the supply of carbon dioxide into the chamber through the flexible hose.
4. Monitoring of carbon dioxide capture: This is necessary to assess the efficiency and effectiveness of the systems and technologies used to reduce carbon emissions and ensure compliance with regulations and standards for carbon emissions into the environment. The specific steps include:
- regularly measuring the concentration of carbon dioxide in the chamber using a chemical gas analyzer;
 - recording data on the rate of carbon dioxide capture by slag in gas environments over a specified period.
5. Completion of the experiment: This stage is necessary for analyzing the data obtained, drawing conclusions, evaluating the achievement of research goals, preparing a final report, and disseminating research results. The specific steps include:
- stopping the supply of carbon dioxide into the chamber;
 - recording the final data from the chemical gas analyzer to determine the final concentration of carbon dioxide in the chamber;
 - disassembling the slag samples and cleaning the laboratory setup.
6. Analysis and processing of results: This is essential for extracting meaningful information from the data obtained, identifying patterns, determining statistical significance, testing hypotheses, and formulating conclusions to understand and interpret the research results. The specific steps include:
- processing and analyzing the data on the rate of carbon dioxide capture by slag in gas environments.
 - comparing results for different slag samples and experimental conditions.
 - calculating the efficiency of CO₂ capture by slag based on the data obtained.
 - performing statistical analysis and interpreting the results.

The current methodology does not account for possible control experiments and the consideration of various factors such as CO₂ concentration, pressure, temperature, and experiment duration on the capture process. A detailed research methodology should be developed considering specific requirements and research goals, as well as potential external factors that may influence the experiment's results.

5 Conclusion

The present study proposes an investigation into the potential use of waste incineration slag for carbon reduction. The objective of the research is to study the rate of carbon dioxide capture by slag in gas environments and determine their potential for reducing carbon emissions.

Through the development of a laboratory setup, it is possible to conduct experiments to examine the rate of carbon dioxide capture by different slag samples.

Based on the analysis of the data obtained, the following conclusions can be confirmed:

- waste incineration slag has the ability to capture carbon dioxide from gas environments;
- different slag samples exhibit varying rates of carbon dioxide capture, highlighting the importance of selecting an optimal slag composition for maximum capture efficiency;
- specific experimental conditions such as CO₂ concentration, pressure, temperature, and duration can influence the rate of carbon dioxide capture.

The research methodology will yield reliable results that have practical and scientific significance. The potential application of waste incineration slag as a medium for carbon capture can contribute to carbon emission reduction and environmental improvement.

Further investigations in the field of using waste incineration slag for carbon reduction can be directed towards:

- optimizing the composition of slag to enhance its carbon dioxide capture efficiency;
- examining the influence of various factors on the capture process, such as CO₂ concentration, pressure, temperature, and experiment duration;
- scaling up the research to an industrial level to validate the applicability of the obtained results and develop carbon capture technologies;
- expanding the economic and environmental analysis to evaluate the effectiveness and viability of using waste incineration slag in industrial processes.

The results of the presented study open up new perspectives for utilizing waste incineration slag for carbon capture and emission reduction. This can contribute to sustainable industrial development and promote environmental sustainability in the context of climate change mitigation.

References

1. Bazhin VY (2016) Changes in thermal plasticity of low grade coals during selective extraction of metals. *J Mining Inst* 220:578–581. <https://doi.org/10.18454/PMI.2016.4.578>
2. Bocharov VL, Kramarev PN, Strogonova LN (2005) Geoecological aspects of the forecast of environmental changes in the areas of dumpsites for the disposal of ash and slag waste from power plants. *Vestnik Voronezhskogo gosudarstvennogo universiteta. Seriya: Geologiya* 1:233–239
3. Borowski G, Smirnov Y, Ivanov A, Danilov A (2020) Effectiveness of carboxymethyl cellulose solutions for dust suppression in the mining industry. *Int J Coal Prep Util.* <https://doi.org/10.1080/19392699.2020.1841177>
4. Bykova MV, Alekseenko AV, Pashkevich MA, Drebenstedt C (2021) Thermal desorption treatment of petroleum hydrocarbon-contaminated soils of Tundra, Taiga, and forest steppe landscapes. *Environ Geochem Health* 43:2331–2346. <https://doi.org/10.1007/s10653-020-00802-0>
5. Chekushina TV, Vorobyev KA (2022) Kataliticheskaya pererabotka dioksida uglidora v sinteticheskoe toplivo (Catalytic Conversion of Carbon Dioxide into Synthetic Fuels. Monograph). Sputnik+, Moscow, p 120

6. Chukaeva M, Zaytseva T, Matveeva V, Sverchkov I (2021) Purification of Oil-Contaminated Wastewater with a Modified Natural Adsorbent. *Ecol Eng Environ Technol* 22(2):46–51. <https://doi.org/10.12912/27197050/133331>
7. Dmitrienko MA, Nyashina GS, Strizhak PA (2017) Environmental indicators of the combustion of prospective coal water slurry containing petrochemicals. *J Hazard Mater* 338:148–159. <https://doi.org/10.1016/j.jhazmat.2017.05.031>
8. Ermakova LA, Mochalov SP, Kalashnikov SN, Permyakov AA (2012) Mechanism of coal-water fuel drops combustion in the swirl burner of an automated energy generating complex. *Vestnik Kemerovskogo gosudarstvennogo universiteta* 4(52):164–169
9. Gendler SG, Fazylov IR (2020) Methods of regulation air temperature in the Russian oil mains. *Topical Issues of Rational Use of Natural Resources*. St. Petersburg, pp 16–21
10. Glushkov DO, Lyrshchikov SY, Shevyrev SA, Strizhak PA (2016) Burning properties of slurry based on coal and oil processing waste. *Energy Fuels* 30(4):3441–3450. <https://doi.org/10.1021/acs.energyfuels.5b02881>
11. Ibrahim NM, Ismail KN, Chea Mat R, Peng PJ (2018) Effect of pre-treated incineration bottom ash as sand replacement material to compressive strength of foamed concrete. *AIP Conf Proc* 2030:020203. <https://doi.org/10.1063/1.5066844>
12. Ivanov AV, Smirnov YuD, Chupin SA (2021) Development of the concept of an innovative laboratory installation for the study of dust-forming surfaces. *J Mining Inst* 251:757–766. <https://doi.org/10.31897/PMI.2021.5.15>
13. Kairakbaev AK, Abdrakhimov VZ, Abdrakhimova ES (2019) The use of ash material of East Kazakhstan in the production of porous aggregate on the basis of liquid-glass composition. *Ugol* 1:70–73. <https://doi.org/10.18796/0041-5790-2019-1-70-73>
14. Kharko P, Matveeva V (2021) Bottom sediments in a river under acid and alkaline wastewater discharge. *Ecol Eng Environ Technol* 22:35–41. <https://doi.org/10.12912/27197050/134870>
15. Kim B, Prezzi M, Salgado R (2005) Geotechnical properties of fly and bottom ash mixtures for use in highway embankments. *J Geotech Geoenviron Eng* 131:914–924. [https://doi.org/10.1061/\(ASCE\)1090-0241\(2005\)131:7\(914\)](https://doi.org/10.1061/(ASCE)1090-0241(2005)131:7(914))
16. Li J, Zhang X, Yang W, Blasiak W (2013) Effects of flue gas internal recirculation on NO_x and SO_x emissions in a co-firing boiler. *Int J Clean Coal Energy* 2(2):13–21. <https://doi.org/10.4236/ijcce.2013.22002>
17. Marinin MA, Dolzhikov VV, Isheyskiy VA (2019) Improving the efficiency of drilling and blasting operations for high water cut conditions. *J Min Sci* 55(5):783–788. <https://doi.org/10.4028/www.scientific.net/KEM.836.124>
18. Matveeva VA, Isakov AE, Sverchkov IP (2019) The reduction of negative impact on environment in the area of coal processing enterprises. *Innovation-based development of the mineral resources sector: challenges and prospects*. In: 11th Conference of the Russian-German raw materials, Vol 1, pp 431–436
19. Murko VI, Senchurova YuA, Fedyayev VI, Karpenok VI (2013) Research on the technology of combustion of suspension coal fuel in a vortex chamber. *Vestnik Kuzbasskogo gosudarstvennogo tekhnicheskogo universiteta* 2:103–105
20. Nyashina GS (2018) Study of ways to reduce the impact of thermal power plants on the environment when burning suspension fuels from coal waste and biomass: Avtoref. dis. ... kand. tekhn. nauk. Tomsk: Natsionalnyi issledovatel'skii Tomskii politekhnicheskii universitet, p 22
21. Ogunro VO, Inyang HI, Hooper F et al (2004) Control of bottom ash aggregate in superpave bituminous mixes. *J Mater Civ Eng* 16:604–613. [https://doi.org/10.1061/\(ASCE\)0899-1561\(2004\)16:6\(604\)](https://doi.org/10.1061/(ASCE)0899-1561(2004)16:6(604))
22. Ovchinnikov RV (2013) The modified slags of thermal power plants an effective component of the mixed knitting. *Izvestiya vysshikh uchebnykh zavedeniy. Severo-Kavkazskiy region. Tekhnicheskkiye nauki* 2:70–74

23. Park J-H, Lee Y-J, Jin M-H et al (2017) Enhancement of slurryability and heating value of coal water slurry (CWS) by torrefaction treatment of low rank coal (LRC). *Fuel* 203:607–617. <https://doi.org/10.1016/j.fuel.2017.03.016>
24. Qiao XC, Ng BR, Tyrer M et al (2008) Production of lightweight concrete using incinerator bottom ash. *Constr Build Mater* 22:473–480. <https://doi.org/10.1016/j.conbuildmat.2006.11.013>
25. Salavatov TS, Bayramova ASK, Vorobyev KA (2021) Ispol'zovanie dioksida uglidora v kachestve khimicheskogo syr'ya (utilization of carbon dioxide as chemical feedstock). *Vestnik evraziiskoi nauki (Eurasian Sci Bull)* 13(2):2
26. Sarapulova GI (2018) Environmental geochemical assessment of technogenic soils. *J Mining Inst* 234:658–662. <https://doi.org/10.25515/PMI.2018.6.658>
27. Shulginov N, Kucherov Y, Fedorov Y (2015) National regulation and standards development for Russian power system operation and control. In: *International ETG Congress; Die Energiewende—Blueprints for the new energy age*, Bonn, Germany, N 7388537
28. Smolii VA, Kosarev AS, Yatsenko EA, Goltsman BM (2018) Physical and chemical features of the production of cellular glass materials based on cullet and ash and slag wastes of thermal power engineering. *Izvestiya vysshikh uchebnykh zavedenii. Severo-Kavkazskii region. Tekhnicheskie nauki* 3:112–118. <https://doi.org/10.17213/0321-2653-2018-3-112-118>
29. Sorokin AP, Avdeiko GP, Alekseev AV et al (2001) The strategy of the development of fuel and energy potential i the Russian Far East economic region up to 2020. *Dalnauka, Vladivostok*, pp 15–23
30. Vorobiev AE, Vorobyev KA, Zhang L, Kozhogulova GK (2023) Metodologiya i laboratornye metody issledovaniya fiziko-khimicheskikh svoistv nanochastits (Methodology and laboratory methods for studying the physicochemical properties of nanoparticles). In: *Educational and methodical complex for the discipline “methods of studying minerals, ores, and rocks”*. Sputnik+, Moscow, p 36
31. Vorobyev AE, Zhang L, Vorobyev KA (2022) Effektivnost' nanokatalizatorov pri pererabotke uglevodorodov (Efficiency of nanocatalysts in hydrocarbon processing. monograph). Sputnik+, Moscow, p 180
32. Vorobyev KA, Shcherba VA (2021) Dioksid uglidora kak khimicheskoe syr'ye (Carbon dioxide as chemical feedstock). In: *Geografiya: razvitie nauki i obrazovaniya. Sbornik statei po materialam ezhegodnoi mezhdunarodnoi nauchno-prakticheskoi konferentsii LXXIV Gertsensovskie chteniya (Geography: development of science and education. Collection of articles from the annual international scientific-practical conference LXXIV Gertsen readings)*. St. Petersburg, pp 149–157
33. Vorobyev KA, Yushkova VD, Ivanova EM (2023) Metody mineral'noi karbonizatsii i utilizatsii dioksida uglidora na territorii Rossiiskoi Federatsii (Methods of mineral carbonization and carbon dioxide utilization in the Russian Federation. Monograph). Sputnik+, Moscow, p 34
34. Xue Z, Gong Y, Guo Q et al (2019) Visualization study on breakup modes of coal water slurry in an impinging entrained-flow gasifier. *Fuel* 244:40–47. <https://doi.org/10.1016/j.fuel.2019.01.186>



Penicillin Antibiotics and Their Phytotoxicity

S. S. Timofeeva^(✉) and O. V. Tyukalova

Irkutsk National Research Technical University, 83, Lermontova St, Irkutsk 664074, Russia
timofeeva@istu.edu

Abstract. The aim of this work is to evaluate the phytotoxic properties of a veterinary antibiotic. The article presents the results of a study that investigated the phytotoxicity of bicillin-3, one of the most commonly used antibiotics in agriculture when raising farm animals, which enters the soil in high concentrations with manure when applied to the fields as fertilizer. We have carried out tests by germinating seeds of watercress, industrial hemp, sowing rice, as well as on the growth reactions of an aquatic plant *Elodea canadensis*. It has been established that bicillin-3 is toxic for watercress in the concentration range from 0.5 to 100 mg/l, and has low toxicity for rice and hemp. At high concentrations, we have noted stimulation of the growth of cannabis roots. It has been concluded that it is possible to use hemp as an accumulator plant for phytoremediation of soils contaminated with antibiotics. The possibility of bicillin-3 elimination from the aquatic environment with the help of Canadian pondweed has been studied. The value of the phytoremediation potential of Canadian pondweed to bicillin-3 depends on the concentration of the antibiotic and ranges from 0.10 to 1.80 mg/g of the live weight of the aquatic plant. It has been shown that it is possible to use Canadian pondweed for the elimination of bicillin-3 from the aquatic environment.

Keywords: Antibiotics · Pollution · Ecotoxicity · Phytotesting

1 Introduction

Around the world, antibiotics are now widely used to treat people, animals, livestock and aquaculture for infectious diseases. After application, residual amounts of antibiotics with solid and liquid wastes end up in the natural environment and create potential environmental risks directly for humans, animals, and components of biocenoses. Increasing demand for animal protein stimulates the use of intensive forms in agriculture, which leads to the accumulation of antibiotics in animal products and ultimately to antibiotic resistance [1]. According to the WHO, antibiotic resistance is a very serious problem, since antibiotic-resistant microorganisms can be easily transmitted through food chains, widely spread in the environment through animal waste, cause complex incurable long-term infections in humans and economic losses in healthcare [2, 3].

The annual production of antibiotics in the world is growing, their consumption already makes up 200 thousand tons per year [4]. Only for a fifteen-year period (2000–2015), 76 countries of the world consumed up to 42 billion daily doses [5]. Along with

developed countries (USA, France, Italy), there is a steady upward trend in antibiotic consumption in India, China, and Pakistan, and by 2030, global antibiotic consumption will double [5].

Due to the low cost of drugs in medical practice and veterinary medicine, fluoroquinolones, cephalosporins, macrolides, and penicillins are widely used in the USA and EU countries [6]. The latter are a group of antibiotics of natural and semi-synthetic origin, containing 6-aminopenicillanic acid, consisting of thiazolidine ring and P-lactam ring.

The action of penicillins is based on their ability to inhibit the synthesis of peptidoglycan in microorganisms, while this substance is not present in animal organisms. A group of natural and semi-synthetic penicillins is used in the treatment of diseases of the genitourinary, respiratory, digestive systems of animals, as well as in surgical interventions.

The volume of import and consumption of veterinary penicillin preparations for productive animals in Russia in 2017 amounted to 12.1 million US dollars. At that point 60 veterinary drugs were traded on the market, among which aminopenicillins (amoxicillin, ampicillin) held a significant share. They differ from natural antibiotics in their lower potency, but they are not inferior to them in the breadth of the antibacterial activity spectrum and the duration of the drug effect [7].

An analysis of the ways antibiotics enter the environment has shown that the main contribution to the pollution process is made by the natural physiological processes of humans and animals—excretion, since only 10% of the antibiotics introduced into the body are used in the treatment process, the remaining 90% are excreted unchanged [2, 8]. In addition, antibiotics enter the environment with sewage from hospitals, veterinary clinics, as well as with melt and storm water from manure storage areas, cattle yards, poultry plants, and farms. Due to the processes of ecological metabolism, they are redistributed between natural environments, filtered into groundwater, accumulated in livestock and crop products. All these processes are beyond control and pose a serious environmental threat [8].

Solid municipal waste thrown into landfills from households is difficult to account for sources of contamination with penicillins and other antibiotics as there is no collection system for unused expired drugs. Getting to the MSW landfills, they dissolve and with drainage runoff enter the sources of drinking water supply [8].

Antibiotic pollution in the environment includes: food chains, bioaccumulation and biomagnification from irrigation of crops with wastewater from wastewater treatment plants and the application of manure as fertilizer.

Antibiotic residues, in addition to the risk of developing microbial resistance, can be absorbed by plants, thereby interfering with physiological processes and causing potential ecotoxicological effects [9]. Numerous tests for chronic and acute toxicity revealed the effect of antibiotics on photosynthesis and mitochondria. In addition, antimicrobial agents can slow down germination or reduce biomass, which negatively affects the yield of agricultural land [3].

When studying phytotoxic properties on a wide range of cultivated and wild plants, it was found that wild plants were more sensitive to antibiotics than agricultural crops [10]. When assessing the effect of 5 main veterinary antibiotics on seed germination

and root elongation in lettuce, tomatoes, carrots and cucumbers, these compounds were shown to inhibit root elongation. Lettuce was the most sensitive to antibiotics and was recommended for use as a marker of antibiotic contamination [11].

When testing antibiotics on germinating seeds of yellow lupine, peas, lentils, soybeans, adzuki beans and alfalfa, it was found that yellow lupine can be used as a soil pollution marker [12]. Screening studies of 10 antibiotics on lettuce (*Lactuca sativa*), alfalfa (*Medicago sativa*) and carrot (*Daucus carota*) revealed a wide range of antibiotic phytotoxicity from 3.9 $\mu\text{g/l}$ to $> 10,000 \mu\text{g/l}$, with chlortetracycline and levofloxacin being the most toxic and sulfamethoxazole for carrots [13].

The need for phytotesting on plants of agricultural interest is primarily due to the presence of antibiotics in soils and waters used for irrigation. Reviews [14, 15] present the results of a study of their effect on the primary (photosynthesis, respiration, nitrogen assimilation) and oxidative metabolism of plants, as well as on the processes of germination and rooting.

Despite numerous studies on the phytotoxicity of antibiotics, there is still no clear understanding of the physiological changes observed in plants caused by exposure to antibiotics used in veterinary medicine in each specific region.

2 Materials and Methods

The aim of this work is to evaluate the phytotoxic properties of one of the most commonly used antibiotics in medical practice, including veterinary medicine, bicillin-3.

We used bicillin-3 obtained from a pharmacy chain. Bicillin-3 is a combined antibacterial drug of the penicillin group. It is classified as a penicillin of natural origin. The drug is produced in the form of a powder for injection, since it has low efficiency when administered enterally. Bicillin-3 is characterized by an effect on anaerobic microorganisms, cocci and gram-positive bacteria [16].

The phytotoxicity of bicillin-3 was tested by the growth of plant roots in accordance with [17], as well as by the growth reaction of Canadian pondweed [18].

As test organisms, we used the seeds of industrial hemp *Cannabis sativa* L. 1753, which is planned to be planted on the lands of the Irkutsk Region, watercress *Lepidium sativum* L. 1753 known as a marker of antibiotic contamination, and rice *Oryza sativa* L. 1753 as a potential component of plant microbial elements.

All used utensils, filter paper, test solutions, water were sterilized in an autoclave before testing. Before testing, plant seeds were soaked in a 3% hydrogen peroxide solution for 10 min and washed with running water.

The testing procedure was performed according to the following algorithm: 30 seeds were evenly distributed on filter paper in Petri dishes with a diameter of 10 cm; 5 ml of the test solution or sterile water for control was poured into each dish; exposed for 3 days at room temperature; then the number of germinated seeds and the length of the roots were counted (Fig. 1).

In accordance with the recommendations of the methodology, if, compared with the control, the seeds in the test water did not germinate at all, or if the length of the roots as a percentage of the control is below 70%, then the test water will be unsuitable for irrigation. The threshold of 70% is justified by the fact that the soil, due to its sorption capacity,



Fig. 1 Procedure of testing on cannabis seeds

reduces the inhibitory effect of the water under study. When the length of the roots in the experiment is over 120% of the control, it is assumed that the water has stimulating properties.

The results were statistically processed using the computer program Microsoft Excel 2016 with the probability of an error-free forecast ≥ 0 .

Testing on the aquatic plant *Elodea canadensis* was carried out according to the following scheme: the plants were selected in the Angara River, the apical part of the shoots 5 cm long was selected, 500 ml of the test bicillin-3 solution was mixed in flasks and exposed in the laboratory at room temperature. After 3–7 days, the length of the shoots was measured and the growth in % of the control was estimated (Fig. 2).



Fig. 2 Phytotesting procedure for growth reactions of the aquatic plant *Elodea canadensis*

The study of the elimination of bicillin-3 from the aquatic environment was carried out as follows: 5 g the aquatic plant *Elodea canadensis* were thoroughly washed and placed in flasks containing 500 ml of antibiotic solutions of various concentrations. After 1, 3, 5 and 7 days the solution was filtered and the concentration of bicillin-3 was evaluated by UV absorption at 290 nm. Quantification was performed using a *Shimadzu*

UV-1800 spectrophotometer. The antibiotic concentration was determined according to the calibration curve.

3 Results and Discussion

Figure 3a, b and c shows the germination of hemp, rice and watercress roots

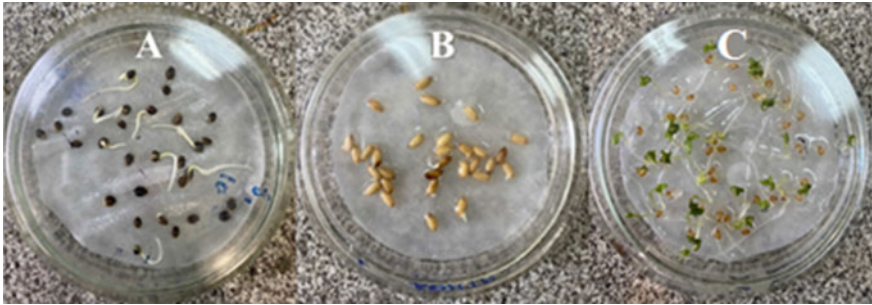


Fig. 3 Sprouted seeds of hemp (a), rice (b) and watercress (c)

It was experimentally established that in watercress seeds a significant decrease ($p < 0.05$ – 0.01) in germination energy ranged from 12.6 to 60.6 abs. %, laboratory germinating capacity—from 14.2 to 59.8 abs. % at bicillin-3 concentrations ranging from 0.5 to 100 mg/l. The greatest toxic effect of the tested concentrations was registered at concentrations of 25–100 mg/l.

In hemp seeds, the decrease in seed germination energy was less than in the control by 29.3–76.5 abs. %, and germinating capacity—by 24.3–82.6%. The greatest toxic effect in the range of studied concentrations was observed at a concentration of 100 mg/l.

In experiments with rice, it was found that a significant decrease ($p < 0.05$ – 0.01) in germination energy ranged from 19.3 to 68.8 abs. %, laboratory germinating capacity—from 25.1 to 72.8 abs. % compared to the control group.

The results of phytotesting of hemp, rice and watercress by the length of the roots are shown in Fig. 4.

The data obtained let us conclude that bicillin-3 is toxic for watercress in the concentration range from 0.5 to 100 mg/l, and has low toxicity for rice and hemp. At high concentrations, we have noted stimulation of the growth of the roots.

When evaluating the effect on the growth reactions of the aquatic plant *Elodea Canadensis* M., 1803 (Fig. 5), it was found that, in the range of the studied concentrations from 5 to 100 mg/l, the growth of *Elodea* shoots was inhibited under the conditions of a chronic experiment.

To study the possibility of the effect of aquatic plants on the dissolved antibiotic, we considered the change in the concentration of bicillin-3 in water with the aquatic plant *Elodea canadensis* depending on the concentration of the antibiotic (10, 30, and 50 mg/l).

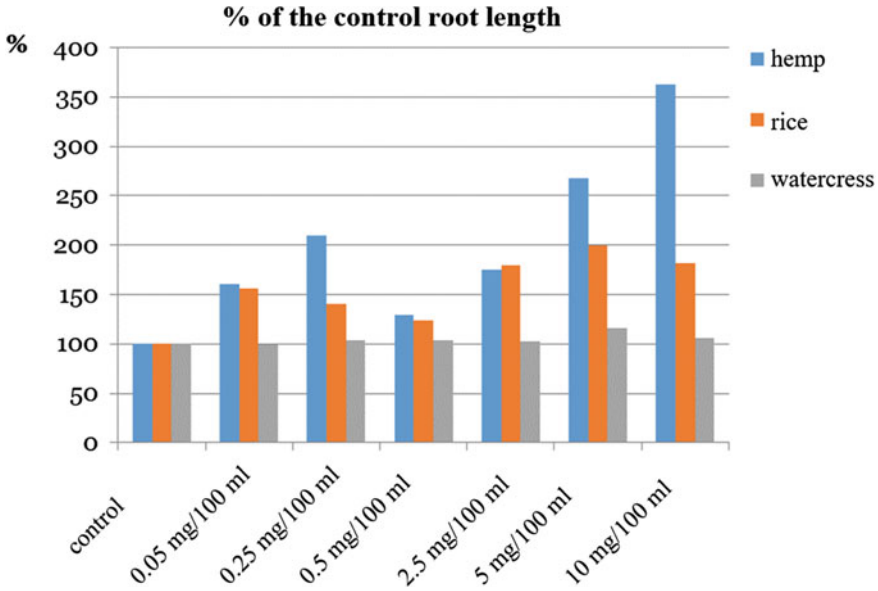


Fig. 4 Growth of roots of tested plants depending on the concentration of bicillin-3

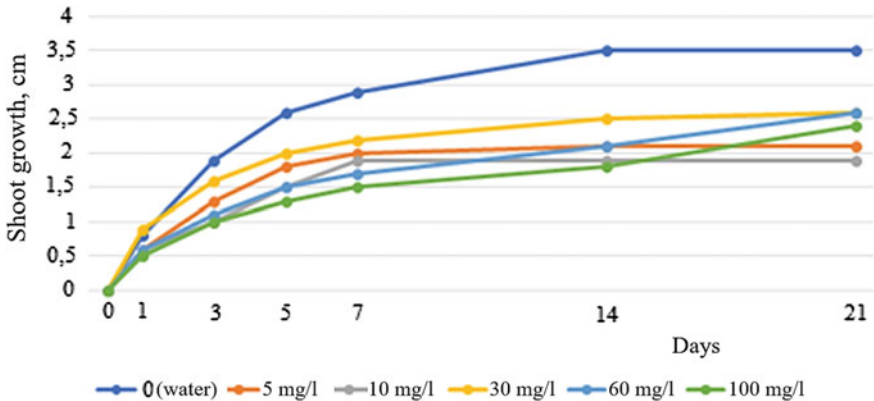


Fig. 5 Growth of the aquatic plant *Elodea canadensis* in solutions of bicillin (compiled by the authors)

Bicillin-3 has an intense UV absorption band at 290 nm (Fig. 6a). Figure 6b shows a calibration graph specifying the dependence of the optical density of UV absorption on the concentration of bicillin-3 at 290 nm.

The decrease in UV absorption in the region of 290 nm makes it possible to assess the degree of elimination of the antibiotic from water. Elimination is understood as the whole set of processes leading to a decrease in the content of bicillin-3 in an external solution including both absorption by plants and metabolism under the action of enzyme systems of plants and microorganisms.

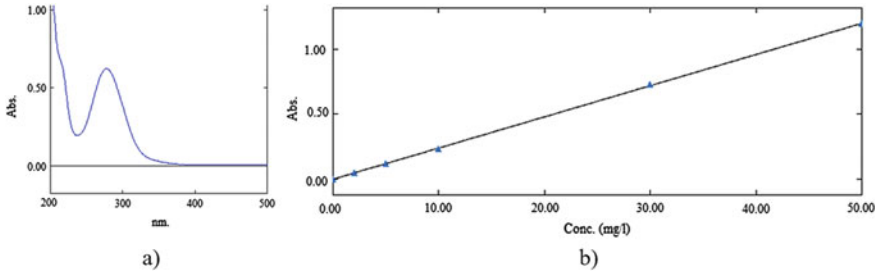


Fig. 6 a) UV absorption band of bicillin-3; b) calibration curve for the quantitative determination of bicillin-3

Figure 7 shows that within 1–7 days there is a decrease in the concentration of bicillin-3 in the aquatic environment. The amount of elimination depends on the concentration of the antibiotic. The decrease in the concentration of bicillin-3 for 7 days is 15.4, 23.7 and 36.0% for solutions containing 10, 30 and 50 mg/l of the antibiotic, respectively.

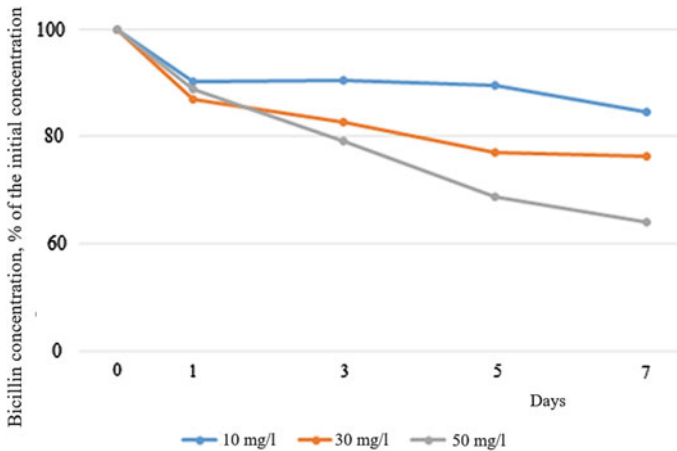


Fig. 7 Changes in the concentration of bicillin-3 in aqueous solutions with the aquatic plant *Elodea canadensis* depending on the initial concentration

We estimated the value of the phytoremediation potential of the aquatic plant *Elodea canadensis* with respect to bicillin-3 (Table 1) at exposures of 3 and 7 days. It has been established that it depends on the initial concentration and varies in the range from 0.1 to 1.8 mg/g of fresh plant weight. The phytoremediation potential increases as the antibiotic concentration increases.

Having compared the results of our own studies with the literature data [19] on the extraction of anti-inflammatory drugs *Scirpus validus* and *Typha angustifolia*, we can conclude that the efficiency of extraction of bicillin-3 by these plants is commensurate

Table 1 Phytoremediation potential of aquatic plants to bicillin-3, mg/g fresh weight (compiled by the authors)

Exposure time	Initial concentration of bicillin-3, mg/l		
	10	30	50
3 days	0.10	0.46	1.05
7 days	0.15	0.71	1.80

with Canadian pondweed and reaches 11–60%. This allows us to consider phytoremediation as one of the inexpensive solutions for removing antibiotics from the aquatic environment. It is necessary to continue research on the creation of flexible phytoengineering systems for cleaning environmental objects from veterinary antibiotics.

4 Conclusion

When studying the phytotoxicity of bicillin-3 solutions, we observed a significant ($p < 0.05$ – 0.01) inhibition of the vital functions of the tested plants, such as germination energy and seed germination root length at high bicillin-3 concentrations of 50–100 mg/l. Watercress was the most sensitive. Hemp and rice were resistant to bicillin-3, and at high concentrations, root growth was stimulated. Probably, bicillin-3 can accumulate in hemp plants and it can be used for phytoremediation of soils contaminated with antibiotics. The aquatic plant *Elodea canadensis* can be used in phytoremediation facilities.

Acknowledgements. The work was supported by a grant from the Academic Council of INRTU 18RAS/2020 “Man-made risks of the Baikal Region”.

References

1. Ayusheeva AV, Timofeeva SS (2021) Penicillin in the environment and technologies for ecological rehabilitation of contaminated territories. *Technosphere Safety in the XXI century. Materials of the XI All-Russian Scientific and Practical Conference of Undergraduates, Postgraduates and Young Scientists (Irkutsk, December 1–3, 2021): collection of research papers*—Irkutsk: Publishing house of Irkutsk National Research Technical University, pp 255–260. https://www.istu.edu/upload/iblock/ea2/sb_21.pdf
2. Timofeeva SS, Shupletsova ID (2020) Prediction of environmental risks of micro-pollutants in the Baikal region. *XXI century Technos Saf* 5(3):269–283. <https://doi.org/10.21285/2500-1582-2020-3-269-283>
3. Cycoń M (2019) Antibiotics in the soil environment—degradation and their impact on microbial activity and diversity *Front Microbiol* 10(58):71
4. Joakim Larsson DG (2014) Antibiotics in the environment. *PMC Labs* 119:108–112
5. Gelband H (2015) State of the world’s antibiotics center for disease dynamics. *Econ Policy* 5(1):84
6. Klein E (2018) Global increase and geographic convergence in antibiotic consumption between 2000 and 2015. *Proc Natl Acad Sci USA* 115(63):79

7. The market of veterinary drugs based on penicillins in Russia. <https://www.tsenovik.ru/articles/veterinariya/rynok-veterinarykh-preparatov-na-osnove-penitsillinov-v-rossii>
8. Timofeeva SS, Gudilova OS (2021) Antibiotics in the environment: status and issues. *XXI century Technos Safety* 6(3):251–265 <https://doi.org/10.21285/2500-1582-2021-3-251-265>
9. Wang M (2017) Stepwise impact of urban wastewater treatment on the bacterial community structure, antibiotic contents, and prevalence of antimicrobial resistance. *Environ Pollut* 2:1578–1585
10. Manyi-Loh C, Mamphweli S, Meyer E, Okoh A (2018) Antibiotic use in agriculture and its consequential resistance in environmental sources: potential public health implications. *Mol* 23(4):795. <https://doi.org/10.3390/molecules23040795>
11. Carballo M, Rodríguez A, Torre de la A (2022) Phytotoxic effects of antibiotics on terrestrial crop plants and wild plants: a systematic review. *Arch Environ Contam Toxicol* 82(1):48–61 <https://doi.org/10.1007/s00244-021-00893-5>
12. Pan M, Chu LM (2016) Phytotoxicity of veterinary antibiotics to seed germination and root elongation of crops. *Ecotoxicol Environ Saf* 126:228–237. <https://doi.org/10.1016/j.ecoenv.2015.12.027>
13. Piotrowicz-Cieślak AI, Adomas B, Nałecz-Jawecki G, Michalczyk DJ (2010) Phytotoxicity of sulfamethazine soil pollutant to six legume plant species. *J Toxicol Environ Health A* 73(17–18):1220–1229. <https://doi.org/10.1080/15287394.2010.492006>
14. Hillis DG, Fletcher J, Solomon KR, Sibley PK (2011) Effects of ten antibiotics on seed germination and root elongation in three plant species. *Arch Environ Contam Toxicol* 60(2):220–232. <https://doi.org/10.1007/s00244-010-9624-0>
15. Rocha DC, Silva da RC, Tavares DS, Morais Calado de SL, Gomes MP (2021) Veterinary antibiotics and plant physiology: an overview. *Sci Total Environ* 767:144902. <https://doi.org/10.1016/j.scitotenv.2020.144902>
16. Edin M (1958) Environmental penicillin and penicillin-resistant staphylococcus aureus. *The Lancet* 27:489–493
17. GOST R ISO 22030-2009 (2009) Soil quality. Biological methods. Chronic phytotoxicity in relation to higher plants
18. Timofeeva SS, Morozova OV (2014) Phytotesting of the reagent technology for the prevention of river jams. *Fund Res* 3–1:39–45; <https://fundamental-research.ru/ru/article/view?id=33581>
19. Fletcher J, Willby N, Oliver DM, Quilliam RS (2020) Chapter 7 Phytoremediation using aquatic plants. https://www.researchgate.net/publication/340047038_Phytoremediation_Using_AquaticPlants



Using Constructed Wetlands to Clean Wastewater from Various Sources

O. A. Samodolova¹(✉), A. P. Samodolov¹, D. V. Ulrikh^{1,2}, and M. N. Bryukhov^{1,2}

¹ South Ural State University, 76 Lenin Prospekt, Chelyabinsk 454080, Russia
Samodolova@mail.ru

² Saint Petersburg State University of Architecture and Civil Engineering, 4, 2Nd
Krasnoarmeiskaya Str, St Petersburg 190005, Russia

Abstract. Biological wastewater treatment systems have been used for many years. Constructed wetlands are one such system. Constructed wetlands are a modern bio-engineered system which can remove many forms of pollutants from wastewater from various sources. Thanks to the varied forms and configurations of such systems, they harmoniously blend in to existing landscapes and do not disturb elements of harmony in the environment. The goal of this work is to review existing publications and research into the use of constructed wetlands in various regions to remove a wide range of pollutants from wastewater. It was determined that constructed wetlands are effective in treating urban surface runoff, industrial wastewater, and agricultural wastewater. Wetlands can effectively remove many pollutants: heavy metals (iron, copper, nickel, zinc, boron), biological contaminants, food industry waste, glycol, hydrocarbons, mineral nitrogen compounds, chlorine, radionuclides, and more. Constructed wetlands can serve as an inexpensive and easy-to-maintain solution for wastewater treatment which does not require the use of chemical or energy-intensive processes, can ensure the output of wastewater of the required quality while performing decorative and aesthetic functions, and improve the microclimate and condition of recreational areas and parks.

Keywords: Constructed wetlands · Wetlands · Wastewater · Biological wastewater treatment

1 Introduction

Constructed wetlands are modern bio-engineering systems which have been used for many years for informal wastewater treatment. There is archaeological evidence of the use of prototypes of modern wetlands in China in 2000 BC. In 1950, at the Max Planck Institute, German professor and hydrobotanist Kathe Seidel began to study the properties of wetlands used to remove a certain volume of pollutants. Later, she was joined by Reinhold Kickuth from the University of Goettingen, but the researchers subsequently began to study this issue separately, as rivals.

In 1953, Kathe Seidel put forth Max-Planck institute–process cleaning systems, consisting of four or five stages of purification, each of which consisted of several consecutive and parallel ponds. In the mid-1960s, Reinhold Kickuth presented the root zone method. An artificial (constructed) wetland based on the root zone method was built in Othfresen (Germany) in 1974. Irrigation fields first appeared in CIS territories in Odessa (1887), then in Kiev (1894), and the Lyublinsk irrigation fields appeared in Moscow in 1898. Currently there are more than 2500 operational constructed wetlands across the world [1].

There are four types of constructed wetlands: surface, horizontal, vertical infiltration, and mixed. Each type has its advantages and disadvantages; the dominating form of pollutant in a given area determines which of these wetlands will be chosen. Figure 1 shows horizontal and vertical constructed wetlands.

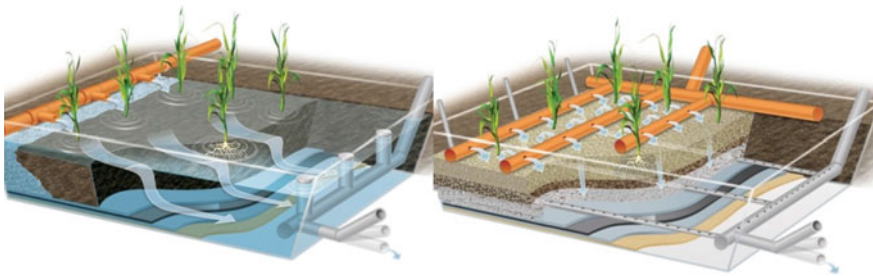


Fig. 1 Horizontal (left) and vertical flow (right) constructed wetlands [2]

The various types of constructed wetlands allows for them to be effectively integrated into various conditions. Modern systems can be placed in confined spaces without losing efficiency of wastewater treatment. For example, cone-shaped infiltration constructed wetlands have been installed on 113 m², while treating wastewater with the same efficiency as horizontal constructed wetlands taking up 309 m² of territory [3].

The form and configuration of the system depends on various conditions and should be chosen with respect to the climactic, topographic, geological, and hydrological characteristics of the territory and the ecological characteristics of the flora [4].

In the further evolution of these systems, various useful models were created to improve performance [5].

The experience of building constructed wetlands in various cold-weather countries, including the West (Sweden, Finland, Norway, Canada) and Russia has shown that these systems do not lose efficiency even in the winter; there is an insignificant decrease in the activity of the systems [6].

The main advantages of constructed wetlands is their low energy use, high level of purification, environmental friendliness, and ability to accumulate various types of pollutants [7].

2 International Use Cases

A large number of these systems have been built across the world. The technology has been widely used in Europe, Asia, and America. They are used to treat wastewater containing pollutants from various sources: urban surface runoff and industrial and agricultural runoff.

Constructed wetlands are widely used to treat wastewater in urban territories.

In 1998, a system was implemented to treat village wastewater in the municipality of Roussillon in the south of France. The reed beds completely blend in to the valley, which is visited by many tourists. The wastewater treatment system has a capacity of 1320 people in the peak summer season and 550 people in the off-season [8].

In 2011, a project was implemented in Chinchá, Peru to build a two-stage wetland system to treat the domestic wastewater of 55 residents and staff of the Hogar de Ancianos Sta. Ana y San Joaquín y Asociación Ayuda Me Perú Retirement Home [9]. Constructed wetlands have also been successfully applied to treat wastewater in Provincial domain Huizingen, Belgium. The wetland is designed to treat domestic wastewater from a toilet building which serves up to 30 people. The treated wastewater flows into a basin with a reverse osmosis unit, where drinking water is produced from the wastewater and supplies a small fountain. The rest is discharged into a pond [10].

In Cuba, water treated by constructed wetlands is used for utilities (including flushing toilets); in Israel, treated wastewater is used for desert landscaping [11].

In addition to municipal wastewater treatment, these systems are widely used for wastewater treatment in various industrial applications.

In the Jebel Ali Free Zone, Dubai, UAE, at the seafood processing plant of Kulimer Seafood Ltd., a constructed wetland has been implemented to treat wastewater from fish and shellfish cleaning in a wetland planted with papyrus. This wastewater is reused after ozonation at the plant [12].

At the end of 2010, IRIDRA designed a wetland in Val delle Rose (Cecchi Val delle Rose, Grosseto, Italy) to provide a new winery with a treatment system. A similar system had already been successfully used for wastewater treatment at another winery operated by the same client (Casa Vitivinicola Cecchi & F.). Monitoring of this installation allowed for the operations to be optimized, both in terms of the treatment and purification and the owner's wishes for improved maintenance [13].

Constructed wetlands are widely used in the food industry to treat runoff of various origins. De Moerenaar is an artisanal cheese factory near the west coast of Belgium which produces a variety of local cheeses. Wastewater from the cheese factory and the dairy farm that supplies the milk is treated in an aerated wetland of 240 m² [14].

In 2017, a 1650 m² two-stage aerated wetland was put into operation to treat wastewater at Frupeco (Fruit Peeling Company) in Lendelde, Belgium, which processes various types of fruit for fruit salads and packaged fruit for restaurants and grocery stores [15].

Dufftown Distillery, owned by Diageo (Scotland, UK), produces 4 million liters of whisky per year. The distillery produces wastewater containing significant amounts of copper, which is leached from the distillation cubes during distillation and treatment. An 800 m² horizontal reed treatment system was designed and constructed to remove soluble copper from the distillery wastewater [16].

Wetlands can be used to solve airport wastewater problems. The Mayfield Wastewater Treatment Plant was commissioned in 2001 and designed to treat runoff from the southern catchment area of Heathrow Airport, London, UK. The runoff is contaminated with glycols from de-icing. Treatment of glycol contaminated runoff is a challenge faced by every airport in winter in cold climate areas [17].

Constructed wetlands have proven themselves effective for the treatment of very specific wastewater. For example, the treatment of wastewater from a firefighting training center at an international airport (Teeside Airport in County Durham, UK) [18].

Wetlands are capable of providing efficient treatment of urban surface runoff: from parking lots (shopping centers, city facilities, etc.), from gas stations, and from sidewalks. The IKEA warehouse in Peterborough (Peterborough, UK) works as a distribution center for IKEA outlets in the region. The warehouse itself is of considerable size and forms a significant catchment for rainfall. The runoff from the warehouse generated during rainfall requires treatment before being returned to the environment [19].

The city of Genk, Belgium has an effective constructed wetland that treats runoff from a 1-hectare sidewalk and water from street washing [20].

A constructed wetland is an environmentally-sound technology to prevent the eutrophication of water bodies as a result of anthropogenic activity. This technology can launch the biological self-cleaning of water bodies. This includes preventing the massive, uncontrolled spread of phytoplankton and restoring the oxygen regime. Including flowers in the wetlands achieves decorative and aesthetic goals while improving the microclimate and the condition of recreation areas and parks [21].

A number of modern studies aim to utilize constructed wetlands to restore recreational resources. In this case, constructed wetlands are used as a regeneration area—they support the efficient clarification and treatment of water; contribute to the restoration of the ecosystem of the recreational area; and minimize costs, as no additional equipment is required [22]. Due to the production and release of wastewater from many nearby enterprises, thermal power station TETs-1 at Lake Kaban (Kazan, Republic of Tatarstan) became unsuitable for lounging and bathing. A project developed by the Russian-Chinese consortium Turenscape + MAP architects, a cascade phyto-purification system entitled “Elastic Band. An Immortal Legend of Kazan”, was chosen to treat water at the site. A unified concept was created for the development of the embankments of the Kaban lake system: the Upper, Middle, and Lower lakes, starting from the channel adjacent to Bulak and up to the site where the Sabantui of the Privolzhsky district is located. It has been proposed to supplement the lake embankments with floating gardens (constructed wetlands). The Lower Lake Kaban phyto-purification facilities are located across several tiers. Water is supplied to the facilities through a 15-m channel. Wastewater, having passed through a system of water cascades with planted plants, is purified before entering Lake Kaban [23].

Zero emissions are a common goal for sustainable development, especially for industrial production. Tertiary treatment of constructed wetlands may be a suitable solution to close the loop. The constructed wetlands at Changshu Advanced Materials Industrial Park, Haiyu City, Jiangsu Province, China, are not just for water reclamation. They serve as a landing pad for people seeking nature and endangered species in an industrialized area. Created as a beautiful park, the wetland provides recreation while also serving as a

buffer strip between chemical plants and urban areas. The Wetlands Visitor Center, with its rooftop and water level terraces, offers a stunning new view [24].

One of the most serious environmental hazards that must be addressed is the generation of wastewater by mining and mineral processing. In addition to wastewater generated directly from smelting and refining, existing pollutants also contaminate groundwater. Abandoned mines also pose a threat—water passes freely through the tunnels and accumulates existing pollution. Studies conducted by a number of Russian institutes clearly demonstrate the effectiveness of these facilities in removing pollutants from wastewater, including iron (common reed planted in an area irrigated with polluted wastewater accumulates 4 times more iron at the end of the growing season than reed not irrigated with the same water) [25, 26].

Quarry wastewater is very often contaminated by mineral nitrogen compounds, which are produced by blasting using nitrogen compounds. A study conducted on a retention pond collecting mine waters from the vast territory of the Kirovogorsky quarry of AO OLCON (mining and processing plant in Olenegorsk, Murmansk region) resulted in the development of an innovative technology for mining wastewater treatment. After implementing floating wetlands, ammonium nitrogen content in the water at the outlet of the sedimentation tank decreased from 3.7 times (July) to 2.1 times (October); nitrite nitrogen content throughout the experiment was below the threshold [27, 28].

A group of researchers performed laboratory experiments and developed a new method of constructing floating constructed wetlands which can extract radionuclides (cesium-137 with activity of 1.5 kBq/l.) from wastewater [7]. There are publications proving that higher aquatic plants are able to extract uranium, radium, and thorium from wastewater [1].

Properly selected remediation agents can achieve the extraction of various heavy metals from wastewater, including copper, nickel, iron, zinc, and boron ions [1, 4]. In addition, experiments on increasing the level of purification have been carried out [29].

In 2021, Zhitnitsa Kryma APH and the Biopositive Construction and Resource Conservation engineering center of V. I. Vernadsky Crimean Federal University presented the Constructed Wetlands project, which includes an environmentally-friendly and cost-effective technology for wastewater treatment. This system can return about 100 million m³ of water which has entered the sewerage system (no less than three volumes of Simferopol reservoir). After treatment, the water will meet the requirements of the State Sanitary and Epidemiological Rules and Hygienic Standards of the Russian Federation [11].

Water scarcity from arid and semi-arid regions forces researchers to look for alternative means of extracting and utilizing water. One excellent alternative is to use treated municipal wastewater for irrigation. From 1991 to 1995, several experiments on macrophytes and artificial wetlands were conducted in the laboratory of the ECOSERVICE Scientific Consulting Center in Tashkent, Uzbekistan. A riverbed and floating constructed wetland with macrophytes were designed and built. These systems proved to be highly effective in removing pollution within a few days after installation. A bioengineered infiltration structure (BIC) with macrophytes was installed in 2000 in Karakalpakstan, located in the semi-arid northwest of Uzbekistan to provide drinking water to small communities. Concentrations of total nitrogen, phosphorus, and organic matter were

reduced 10–100 times. Chemical analyses showed that 22–38% of organic pollutants were removed in the BIC pond and the remaining 62–78% were removed in the filtration zone via the biological activity of macrophytes and biocenosis. Floating structures were used in the drainage channel to prevent soil erosion and improve water quality [30].

In Turkmenistan, researchers conducted experiments on using wetlands to treat lake Altyn Asyr and its drainage reservoirs at the Ecological Biotechnology R&D center of the Oguz Khan Engineering and Technical Institute. In their studies, wastewater was passed through a 100 m long wetland. As a result, chlorine ions were reduced by 2 times and the concentration of bicarbonate ions was reduced to 25 mg/l, which allows treated water to be used to grow fodder plants and create forest areas in the Karakums [27].

3 Conclusion

The literature analysis has shown that constructed wetlands are a modern highly effective biological system which can be used to treat wastewater from various sources. For effective operation, the correct species, form, and variety of native plants must be chosen.

References

1. Kireeva IY (2020) The role of macrophytes in the constructed wetlands system. In Innovative development of regions: the potential of science and modern education: proceedings of the III national scientific and practical conference, pp 17–21
2. Treatment Wetlands—Constructed Wetlands. <https://www.globalwettech.com/about-constructed-wetlands.html>. Accessed 22 June 2023
3. Krasnogorskaya NN (2018) Comparative analysis of different forms of constructed wetlands for wastewater treatment of urban areas. In: XVIII Proceedings of the international research conference on chemistry and engineering ecology, Kazan, pp 289–292
4. Ridiger AV (2018) Removing heavy metal ions from wastewater using aquatic plants in bioengineered systems. *Construct Wetlands* 2:102–105
5. Mishta VP (2016) Utility Mesh box container to form constructed wetland walls in a wastewater treatment system. Russian Federation Patent 2015150465/05, appl. 24.11.2015: published 10.06.2016
6. Masloboev VA (2017) Methods to reduce the concentration of sulfates in the wastewater of mining enterprises. *Bull Kola Sci Centre RAS* 9:99–115
7. Mikheev AN (2015) New means of designing constructed wetlands to remove radionuclides from water bodies. *Modern Trends Develop Sci Technol* 8–4:107–113
8. Roussillon. <https://www.globalwettech.com/references/ref-municipal/item/63-roussillon.html>. Accessed 22 June 2023
9. Peru, Chinchá, Treatment of domestic effluent of 55 residents and employees of a nursing home. <https://www.globalwettech.com/references/ref-municipal/item/59-4-peru-chinchá-treatment-of-domestic-effluent-of-55-residents-and-employees-of-a-nursing-home.html>. Accessed 22 June 2023
10. Provincial domain Huizingen, Belgium. <https://www.globalwettech.com/references/ref-municipal/item/10-huizingen.html> FTP site. Accessed 22 June 2023
11. Lisichkin VA (2021) Bioplato in Crimea—the solution to an old problem. *Constr Econ* 4(70):46–52

12. Culimer seafood processing Dubai. <https://www.globalwettech.com/references/ref-industrial/item/7-culimer.html>. Accessed 22 June 2023
13. Cecchi Val delle Rose—Winery. <https://www.globalwettech.com/references/ref-agriculture/item/36-cecchi-val-delle-rose.html>. Accessed 22 June 2023
14. De Moerenaar. <https://www.globalwettech.com/references/ref-industrial/item/116-de-moerenaar.html>. Accessed 23 June 2023
15. Frupeco. <https://www.globalwettech.com/references/ref-industrial/item/99-changshu-ip-wetland.html>. Accessed 23 June 2023
16. Dufftown. <https://www.globalwettech.com/references/ref-industrial/item/46-dufftown.html>. Accessed 23 June 2023
17. Mayfield. <https://www.globalwettech.com/references/ref-industrial/item/45-mayfield.html>. Accessed 22 June 2023
18. Teeside Airport. <https://www.globalwettech.com/references/ref-industrial/item/38-teeside-airport.html>. Accessed 22 June 2023
19. Peterborough. <https://www.globalwettech.com/references/ref-industrial/item/41-peterborough.html>. Accessed 23 June 2023
20. Warsco Genk. <https://www.globalwettech.com/references/ref-industrial/item/54-warsco-constructed-wetland-genk-belgium.html>. Accessed 23 June 2023
21. Goncharova EN (2018) Preventing the eutrophication of water bodies with the help of floating constructed wetlands. Innovative means of solving urgent problems of nature management and environmental protection. In: International scientific and technical conference, Alushta, pp 46–50
22. Gayanova KR (2022) Constructed wetlands in recreational areas Mavlyutovskie readings. In: Proceedings of the XVI Russian youth scientific conference in 6 volumes, Vol 4, Ufa, pp 156–158
23. Urmitova N, Nizamova A (2021). Use of higher aquatic vegetation for post-treatment of wastewater. E3S Web Conf 274:08005
24. Changshu Industrial Park Tertiary Treatment Wetland. <https://www.globalwettech.com/references/ref-industrial/item/99-changshu-ip-wetland.html>. Accessed 23 June 2023
25. Yagodkin FI (2017) Theoretical studies for the use of “bioplateau” for defferization of water treatment. South Russia Ecol Develop 12–2:147–158
26. Dunbabin JS (1992) Potential use of constructed wetlands for treatment of industrial wastewaters containing metals. Sci Total Environ 111:151–168
27. Yuldashov B (2023) The role of drainage system plants in drainage purification. <https://doi.org/10.5281/zenodo.7783123>
28. Yevdokimova GA (2015) Floating bioplateau for treatment of waste quarry waters from mineral nitrogen compounds at the arctic conditions. Ecol Indust Russia 19–9:35–41
29. Dolganova OA (2017) Developing wastewater treatment technologies for constructed wetlands systems. World Mod Sci 3–43:14–17
30. Kattakulov F (2017) Advantages and disadvantages of irrigation: focus on semi-arid regions. In: The holistic approach to environment, pp 29–38



Digital Platform for Construction of Environmental and Economic Water Resource Maps

A. I. Semyachkov, Yu. O. Slavikovskaya, and V. A. Pochechun^(✉)

Institute of Economics of the Ural Branch of the Russian Academy of Sciences, 29,
Moskovskaya, Yekaterinburg 620014, Russia
viktoriyapochechun@mail.ru

Abstract. Today, for balanced environmental management, it is necessary to consider and assess the availability and condition of natural resources and the environment quality on time. To accomplish the goals specified, this paper suggests using the databases characterizing the water resource management in Ural, Siberian, and Far Eastern Federal Districts to prepare the environmental and economic maps that reflect the water resource availability, quality, and use efficiency as well as the adverse affecting factors. The maps were created on the basis of public statistics as well as the data provided by the companies using natural resources. The maps were made with the statistics collection and analysis methods to develop the indicators that reflected the intensity, efficiency, and environmental friendliness of water resource use as well as the software products like Microsoft Excel and Surfer. The research results can be used by water management and environmental protection specialists as well as federal and regional authorities to develop water management and protection programs.

Keywords: Water resources · Digital platform · Environmental and economic maps · Natural resource management · Databases

1 Introduction

Mapping as a research method and a data representation tool is extensively used in different research areas to solve a wide range of problems. The goal of environmental mapping is the analysis of the environmental situation and its dynamics, i.e., identifying spatial and temporal changes in natural factors affecting human health and ecosystem conditions.

The collected and analyzed statistics on the state of water resources and their use efficiency were used to create environmental and economic maps and establish a database for three industrial regions: the Ural, Siberian, and Far Eastern Federal Districts for a period from 1990 to 2019.

The database (dB) contains information on the natural indicators of the environmental and economic capacities of water bodies, as well as the anthropogenic impacts on them in

the federal districts mentioned. The dB can be accessed in the **XLSX and CSV** formats using such software tools as Microsoft Excel, Access; OpenOffice, and LibreOffice Scal. These formats can be used in programming environment ecosystems like Python; R (programming language).

The dB is designed to facilitate research, practice, and training. The dB can be useful for the specialists solving water management and water ecology problems, as well as responsible for environmental and water resource management in industrial regions. This information product is recognized as intellectual property following patent No. 2022620537 dated March 09, 2022.

2 Constructing Spatial Models Using Maps

Environmental and economic water resource maps were constructed using the Surfer software, which is the most relevant for this test according to the reviewed publications [1–4]. In practice, maps can be created using various methods [5, 6]. In our research, we used the Kriging method to develop the environmental and economic water resource maps.

3 The Environmental and Economic Efficiency Indicators for Water Resources Used During the Mapping

To create environmental and economic maps reflecting the consumption of water resources and the adverse impacts they experience, we used the following indicators:

- freshwater consumption in millions of m³;
- discharge of polluted drain water to surface waterbodies in millions of m³;
- the volume of recirculated and reclaimed water in millions of m³;
- costs of drain water collection and cleaning, millions of rubles;
- investments in water resource protection and rational use, millions of rubles;
- environmental and economic indicator

$$K_i = \frac{C_i}{B_i} \quad (1)$$

where K_i is the normalized environmental and economic indicator for a specific year; C_i is the natural environmental and economic indicator, e.g., the discharge of drain water in a region in millions of m³; B_i is the volume of reclaimed and recycled water, millions of m³

- efficiency of environmental and economic activities

$$E_i = \frac{C_i}{Z_i + I_i} \quad (2)$$

where E_i is the efficiency of environmental and economic activities; C_i is the natural environmental and economic indicator, the discharge of drain water to water bodies in millions of m³ for a specific year; Z_i is the costs of implementing water protection activities in millions of rubles for a specific year; I_i is the investments in the implementation of environmental protection activities, millions of rubles, for a specific year.

These indicators were provided for three industrial regions, namely the Ural, Siberian, and Far Eastern Federal Districts for the period between 1995 and 2019.

4 The Environmental and Economic Mapping of Water Resources

In this research, we used the statistics on the state of water resources and their use in the Ural, Siberian, and Far Eastern Federal Districts (from 1995 to 2019) [7–14].

We used the previously-obtained statistics and analytical data to perform the environmental mapping of water resources in the districts mentioned above with the help of the 3D surface imaging function of the Surfer software. The research results are shown in Figs. 1, 2, 3, 4, 5, 6, 7, 8, 9, 10, 11, 12, 13, 14, 15, 16, 17, 18, 19, 20, 21, 22, 23, 24 and 25.

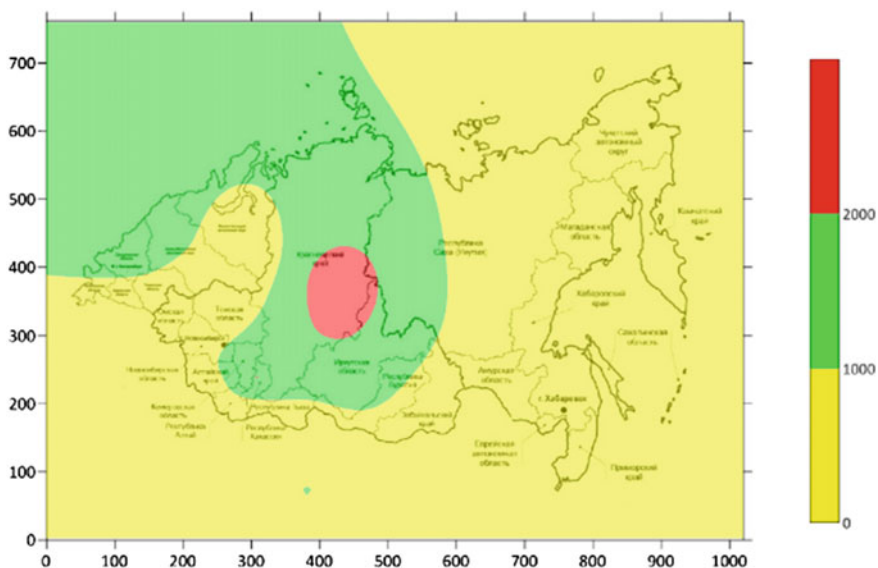


Fig. 1 The fresh water use in 1995

Figures 1, 2, 3 and 4 show the obtained map options reflecting the usage of fresh water in the Ural, Siberian, and Far Eastern Federal Districts.

The analysis of water consumption showed that, in the federal districts in question, fresh water is mainly used for production and household purposes (56.52% and 34.4%, respectively). Agriculture and irrigation only consume 1.95% of the total freshwater used. Note that the structure of freshwater use mainly depends on the industrial sector specifics and the development of freshwater recycling and reclamation systems.

The obtained maps show positive water consumption dynamics, i.e., the reduction of freshwater usage in the federal districts considered from 1995 to 2019.

As of 1995, the highest water consumption was observed in the Krasnoyarsk Krai (2671 million m³/year), and the lowest was observed in the Jewish Autonomous Oblast

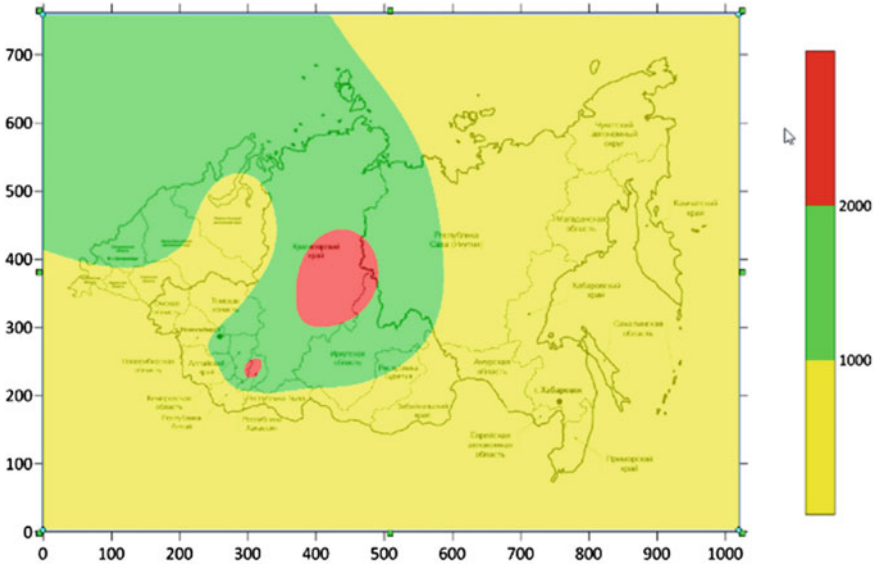


Fig. 2 The fresh water use in 2000

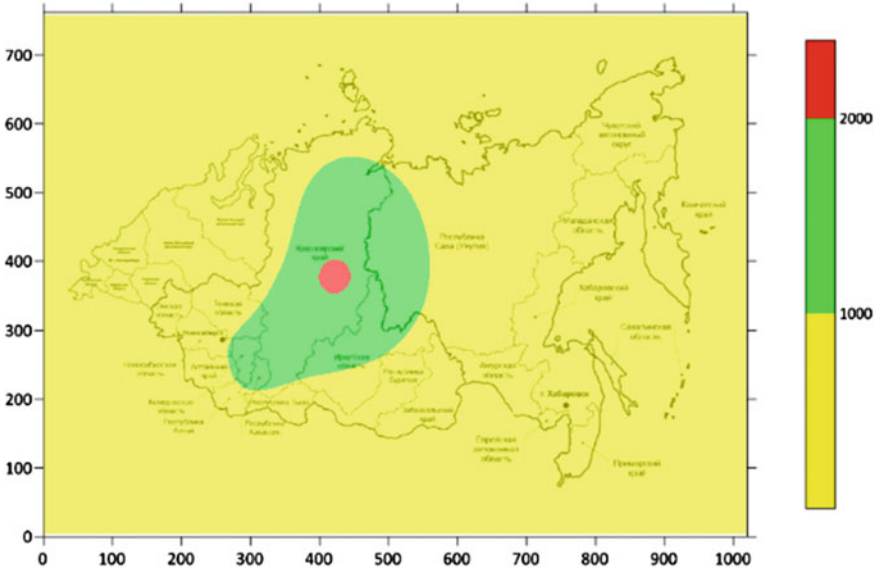


Fig. 3 The fresh water use in 2010

and the Altai Republic (23 million m³/year). These proportions remained the same between 2000 and 2019.

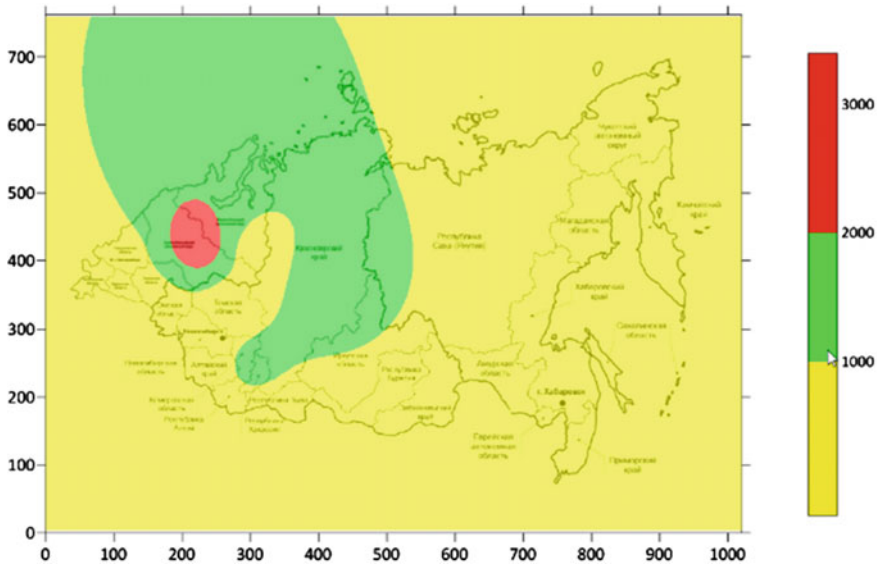


Fig. 4 The fresh water use in 2019

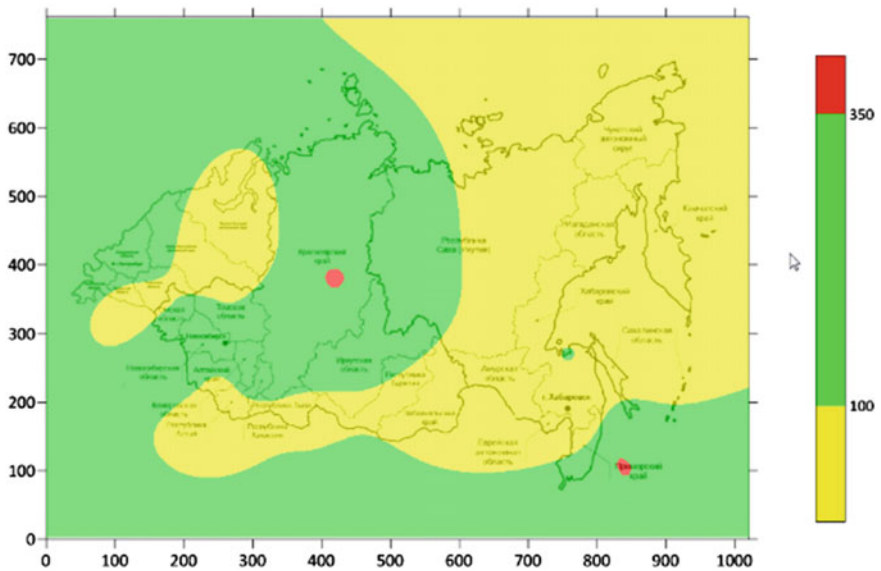


Fig. 5 The discharge of polluted drain water to surface water bodies in 1995

When reviewing the previously-obtained statistics and analytical data on freshwater usage in the Ural, Siberian, and Far Eastern Federal Districts between 1995 and 2019 in detail, we can draw the following conclusions:

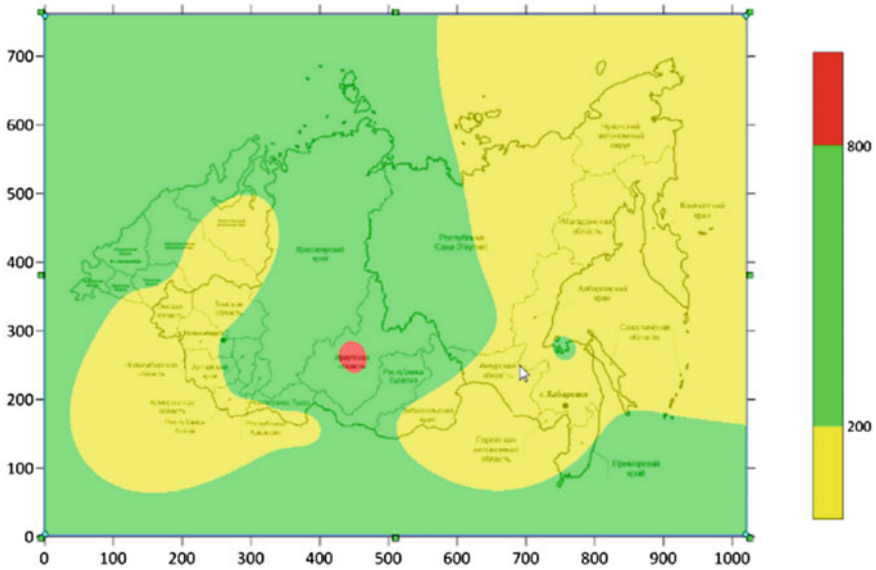


Fig. 6 The discharge of polluted drain water to surface water bodies in 2000

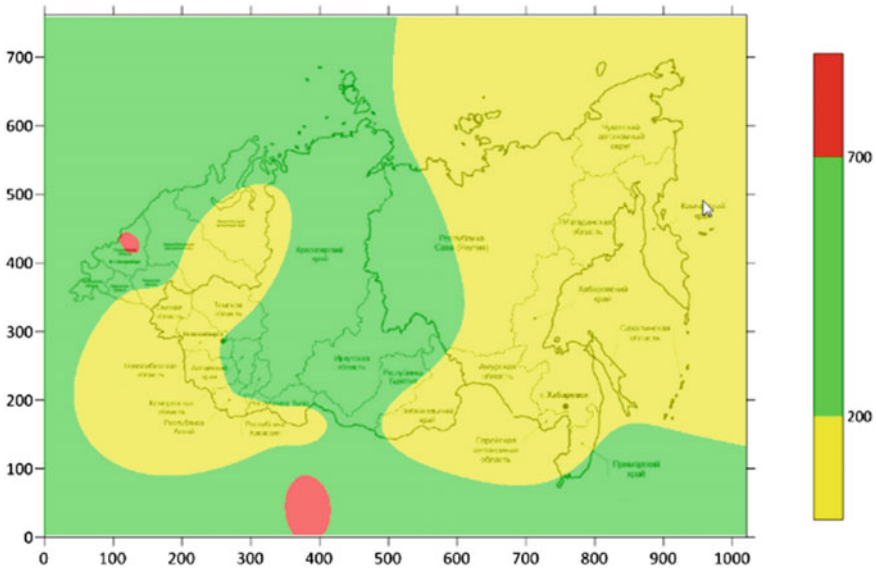


Fig. 7 The discharge of polluted drain water to surface water bodies in 2010

- In the Ural Federal District, freshwater consumption increases on average by 58.76% due to KMAO (an increase of 75.7%) and YNAO (8.98%). In Kurgan Oblast, a reduction of 70.6% is observed, while in Sverdlovsk Oblast this figure is 67%, in Tyumen Oblast—14.03%, and in Chelyabinsk Oblast—38.8%;

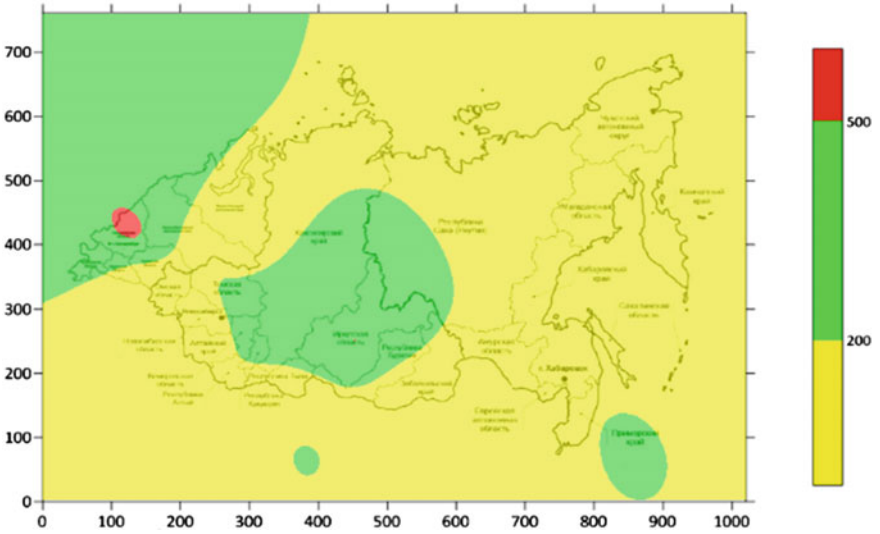


Fig. 8 The discharge of polluted drain water to surface water bodies in 2019

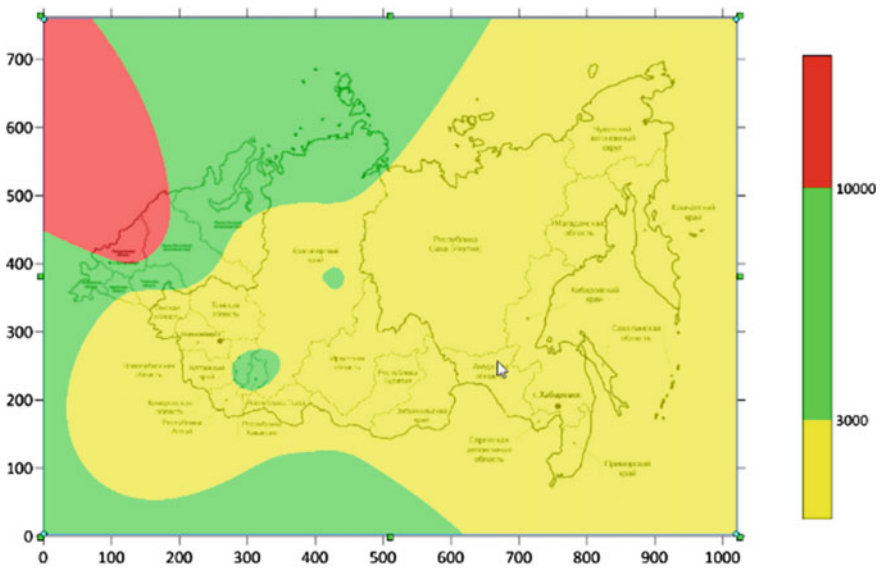


Fig. 9 The consumption rate of recycled/reclaimed water, 1995

- In the Siberian Federal District, water consumption decreased by 53% from 12,657 million m³ in 1990 to 5948 million m³ in 2019. This was achieved by reductions in the Altai Republic (77.42%), Altai Krai (64.24%), Irkutsk Oblast (63.13%), Kemerovo Oblast (43.31%), Krasnoyarsk Krai (51.81%), Novosibirsk Oblast (51.76%), and Omsk Oblast (71.01%), while Tomsk Oblast was the only

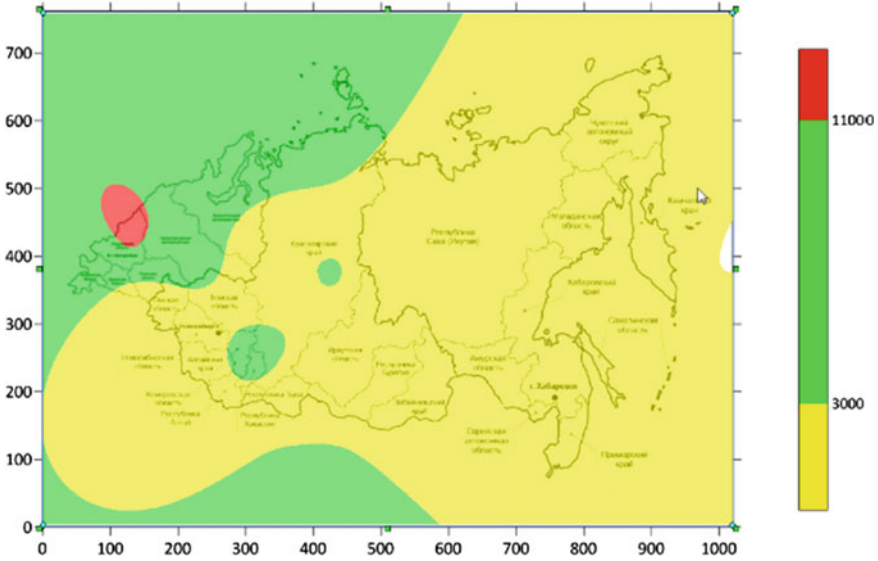


Fig. 10 The consumption rate of recycled/reclaimed water, 2000

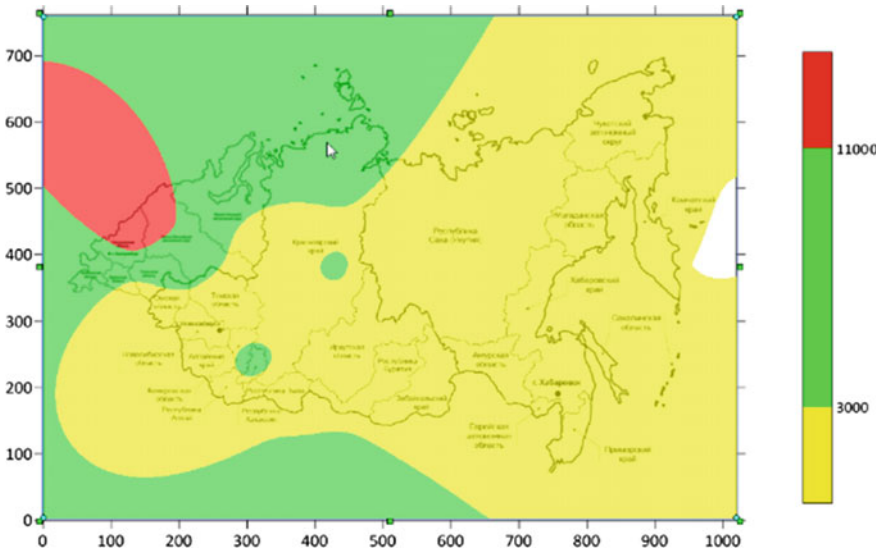


Fig. 11 The consumption rate of recycled/reclaimed water, 2010

region where water consumption increased by 84.95%. Overall, there are the following water consumption trends and patterns in the Siberian Federal District: the lowest freshwater consumption is observed in the Altai Republic (0.12% of the total water consumption volume), the Republic of Tyva (1%), and the Republic of Khakassia

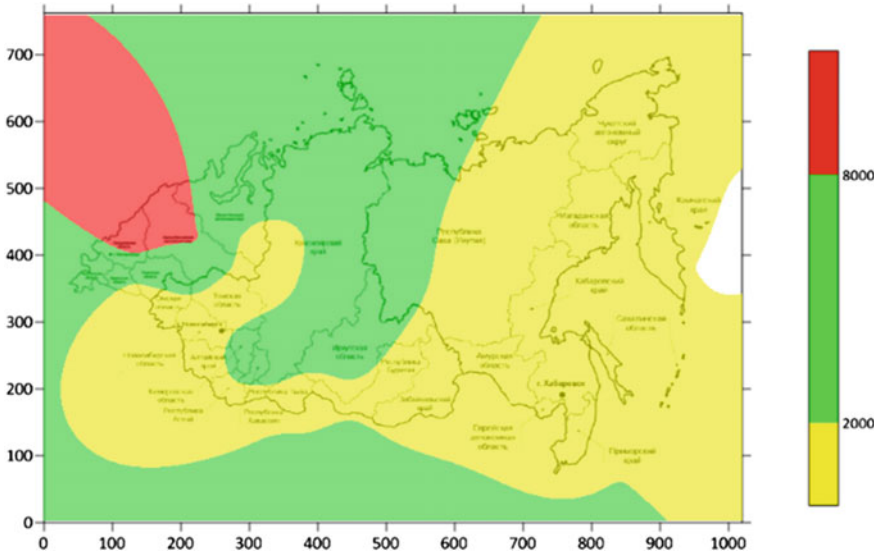


Fig. 12 The consumption rate of recycled/reclaimed water, 2019

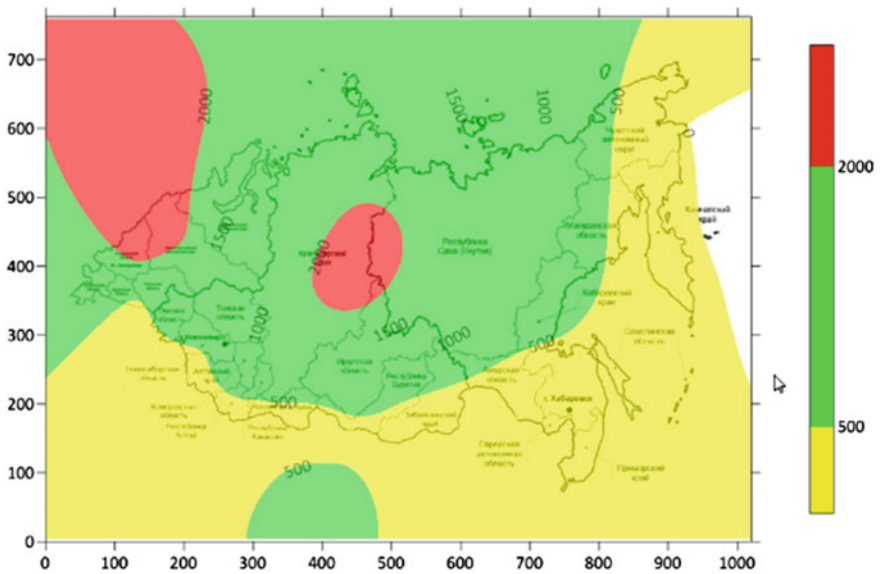


Fig. 13 Costs of drain water collection and purification in 2000

(1%); while the highest consumption can be found in Kemerovo Oblast (26%) and Krasnoyarsk Krai (32%).

- In the Far Eastern Federal District, the reduction made up 46.91%, mainly due to the Amur Oblast (58.24%), the Republic of Sakha (Yakutia) (38.62%), Kamchatka Krai

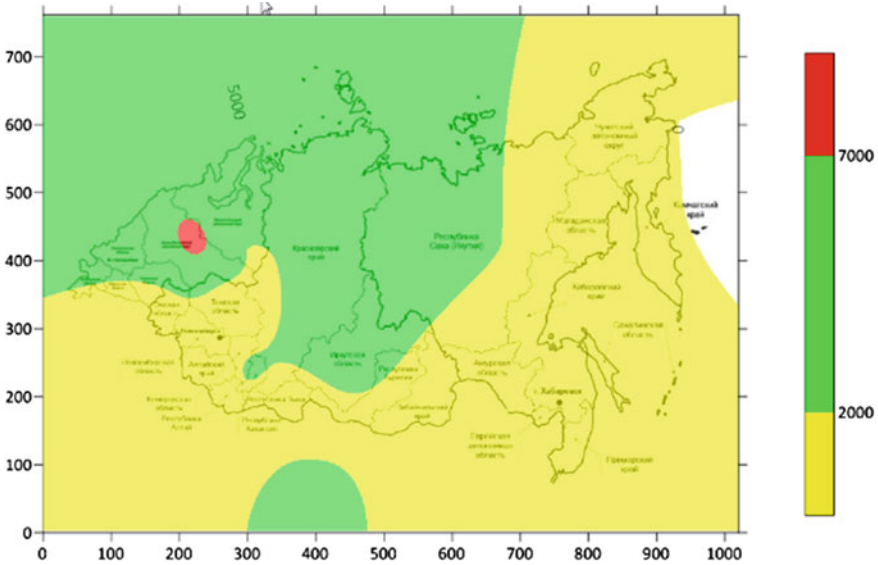


Fig. 14 Costs of drain water collection and purification in 2010

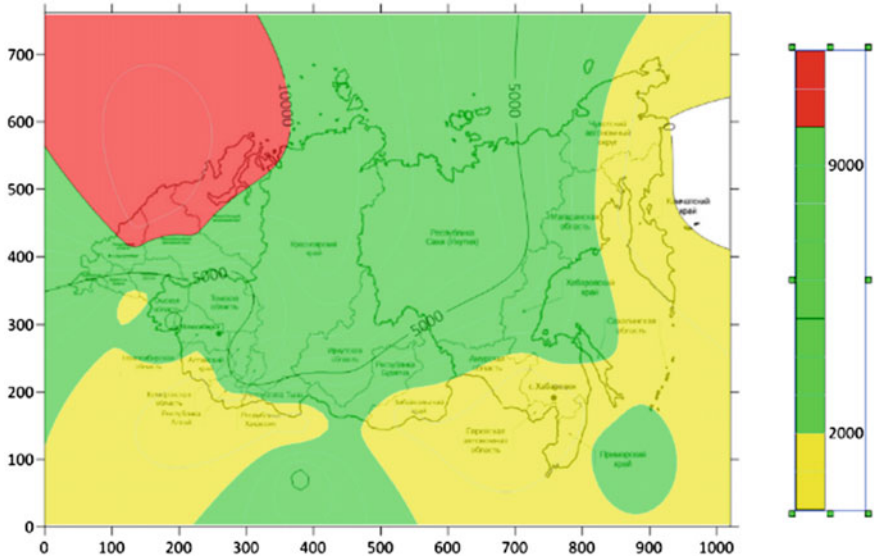


Fig. 15 Costs of drain water collection and purification in 2019

(50.67%), Primorsky Krai (56.43%), Khabarovsk Krai (74.15%), Magadan Oblast (39.57%), Sakhalin Oblast (69.31%), the Jewish Autonomous Oblast (50.00%), and Chukotka Autonomous District (70.11%), although, in some of the regions,

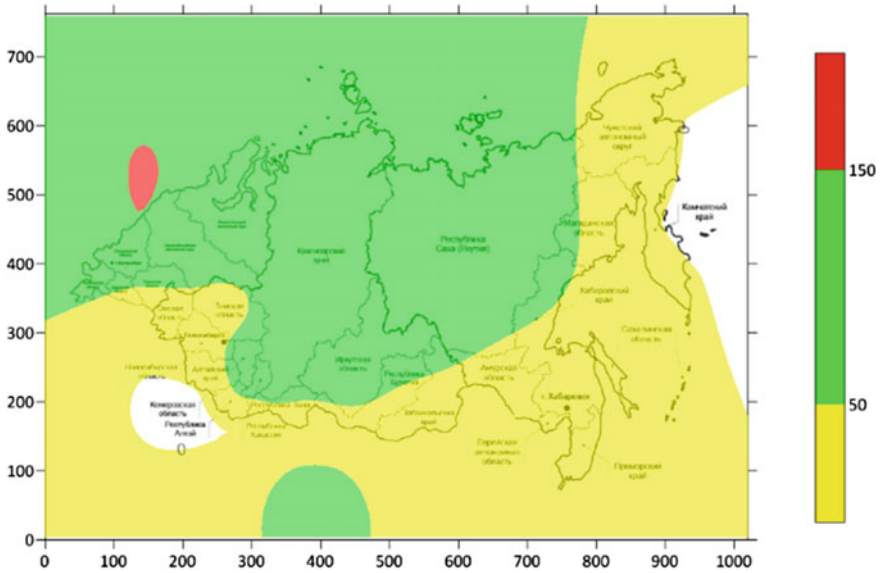


Fig. 16 Investments in water resource protection and rational usage, 1995

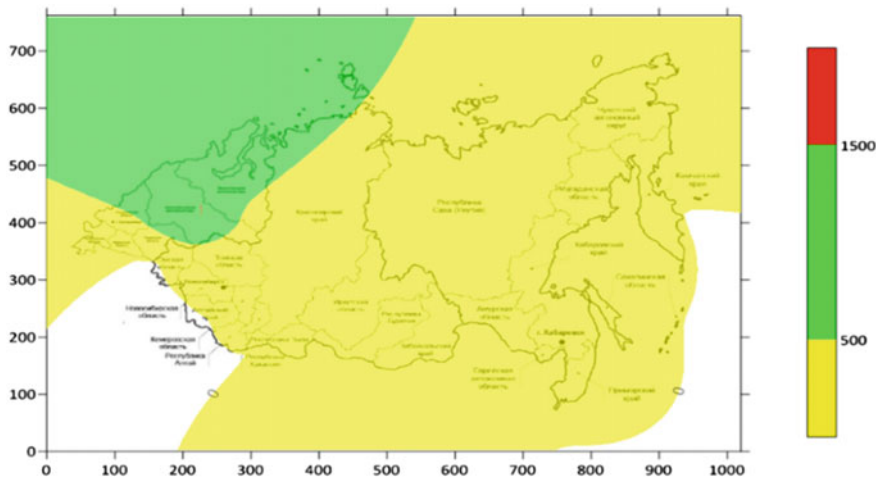


Fig. 17 Investments in water resource protection and rational usage, 2000

the water consumption increased, including the Republic of Buryatia (49.40%) and Zabaykalsky Krai (9.09%).

Figures 5, 6, 7 and 8 show the maps that reflect the discharge of polluted drain water. The results obtained are unchanged and, in some cases, feature negative trends, which can be attributed to the changes in the structure of industrial production [15]. According to Fig. 5, the highest polluted drain water discharge in 1995 was in Primorsky Krai

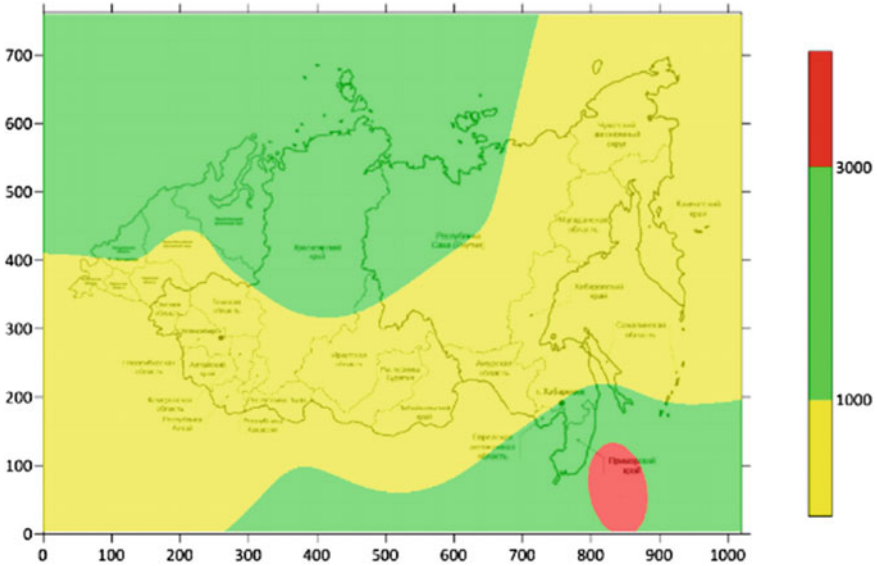


Fig. 18 Investments in water resource protection and rational usage, 2010

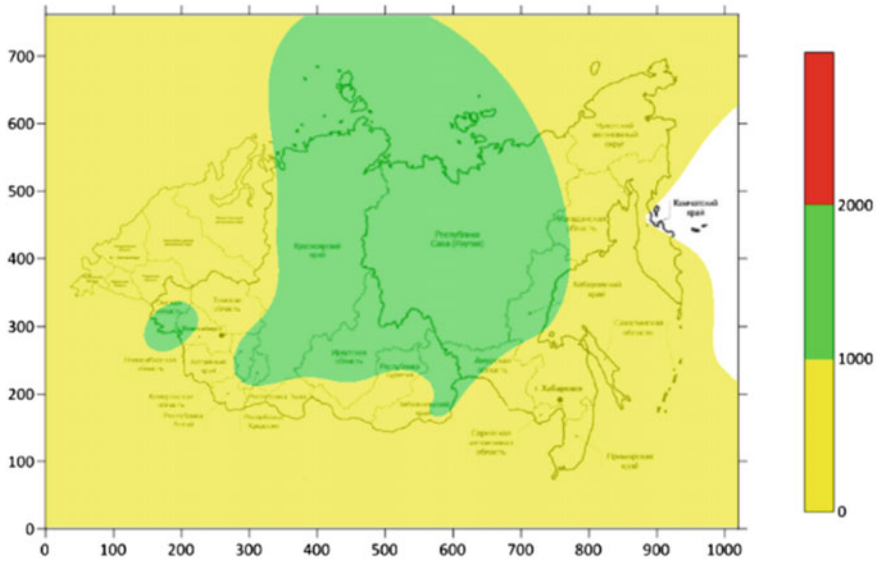


Fig. 19 Investments in water resource protection and rational usage, 2018

(369.3 million m³), and the smallest was found in KMAO—Yugra (0.4 million m³). Following Fig. 6, the trends shifted in 2000, and the highest drain water discharge was observed in Irkutsk Oblast (826 million m³), and the lowest in the Altai Republic (0.6 million m³).

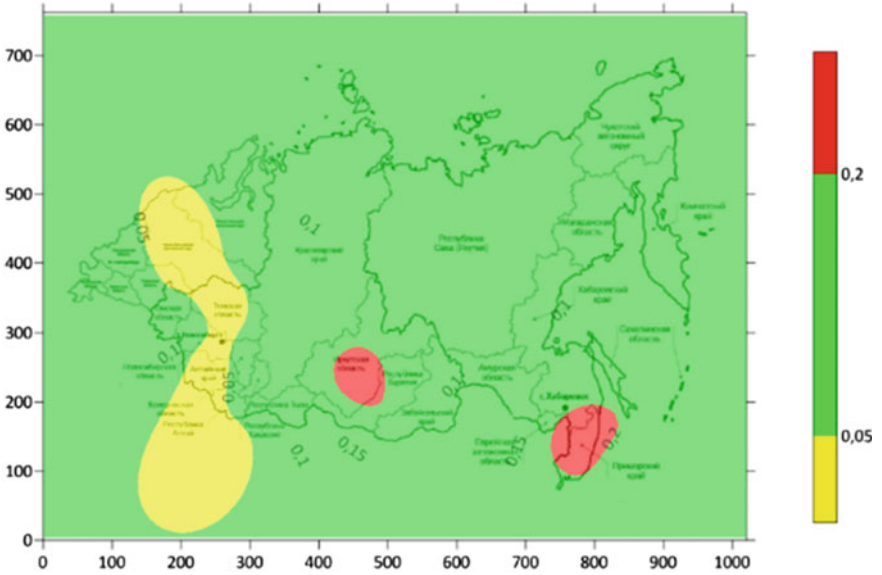


Fig. 20 Environmental and economic indicator, 2000

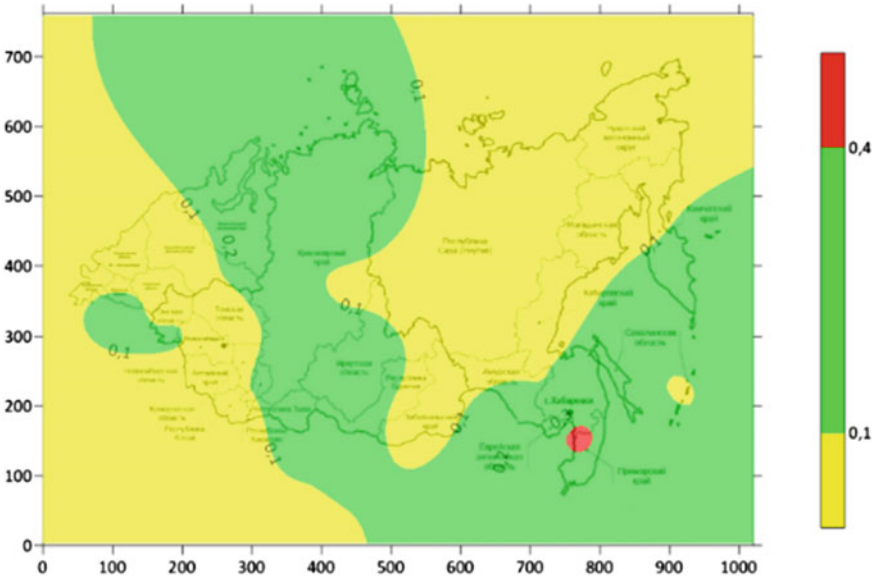


Fig. 21 Environmental and economic indicator, 2010

In 2010, the highest drain water discharge was observed in Sverdlovsk Oblast (763 million m³) and Chelyabinsk Oblast (712 million m³), while the lowest discharge

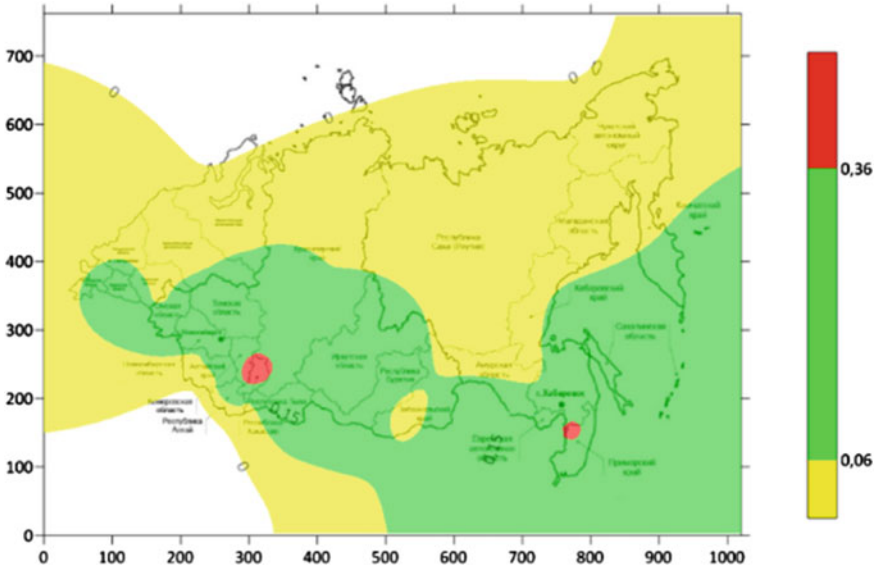


Fig. 22 Environmental and economic indicator, 2019

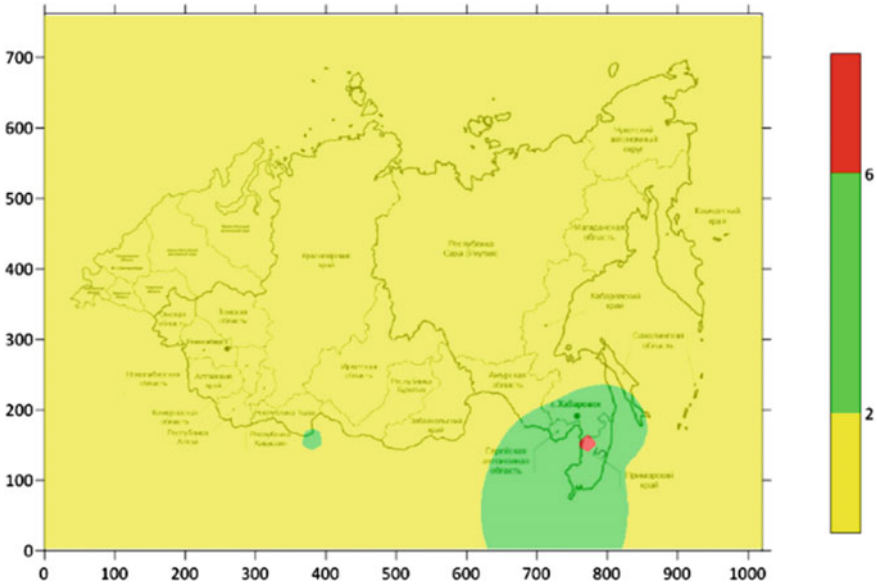


Fig. 23 The efficiency of environmental and economic activities, 2000

was still registered in the Altai Republic (0.3 million m³), Fig. 7. In 2019, the patterns from the previous period are preserved, Fig. 8.

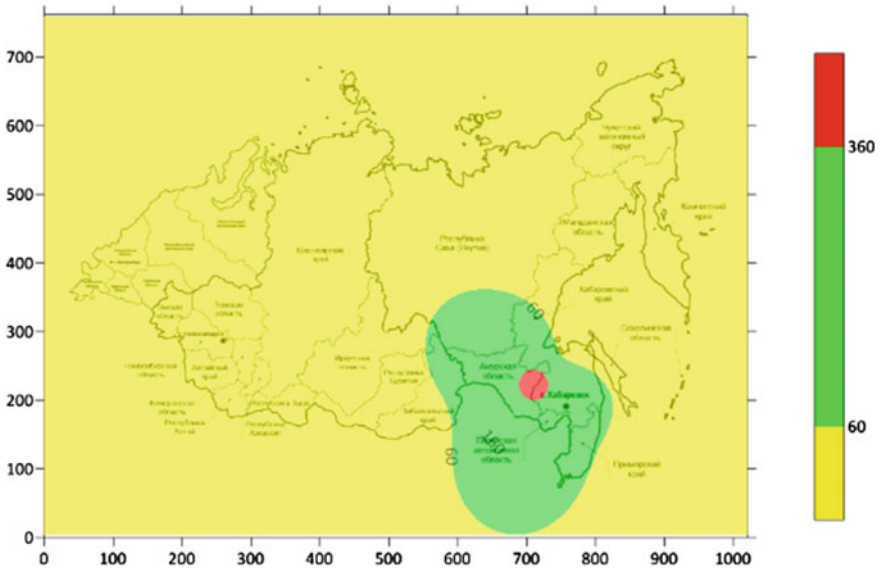


Fig. 24 The efficiency of environmental and economic activities, 2010

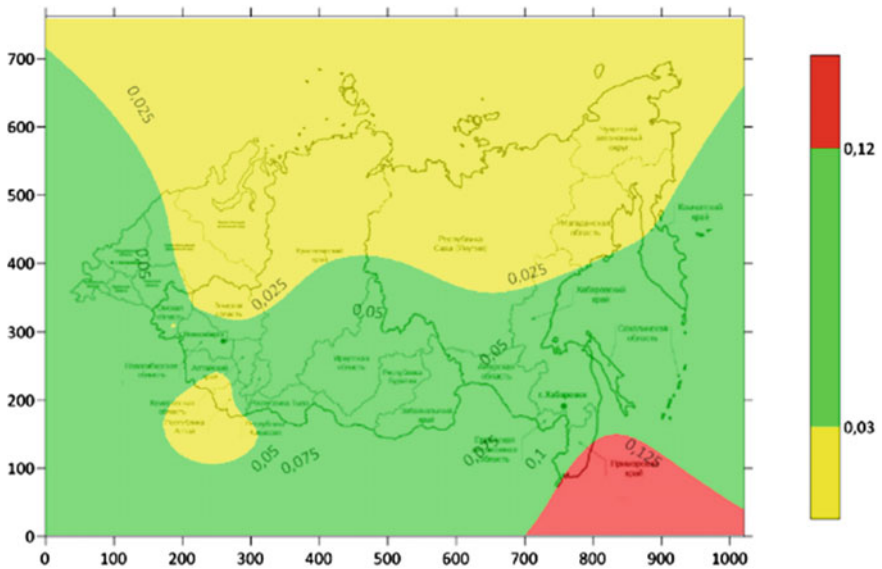


Fig. 25 The efficiency of environmental and economic activities, 2018

During the analysis, we established that the polluted drain water in almost all of the regions of the Ural Federal District in 2019 was mainly made up of insufficiently purified drain water. The shares of the Ural Federal District regions in the discharge of polluted drain water changed significantly since 1995 when they were as follows:

Sverdlovsk Oblast—74.22%, Chelyabinsk Oblast—24.94%, Tyumen Oblast—n/a, Kurgan Oblast—0.71%, YNAO—0.1%, KMAO—Yugra—0.1%. In 2018, it became as follows: Sverdlovsk Oblast—39%, Chelyabinsk Oblast—45%, Tyumen Oblast—6%, Kurgan Oblast—2%, YNAO—2%, KMAO—Yugra—6%.

The discharge of polluted water in the Ural Federal District as a whole during this period increased by 39.1%, from 1055.5 million m³ in 1990 to 1435 million m³ in 2019.

The analysis of the statistics showed that, in the Siberian Federal District, the discharge of polluted drain water decreased by 65.5%, from 4314.5 million m³ in 1995 to 1487.3 million m³ in 2019. The polluted drain water in this district was also mainly made up of insufficiently purified drain water. The largest shares of polluted drain water discharge in 2019 for the regions of the Siberian Federal District were observed in Irkutsk Oblast (35.43%), Kemerovo Oblast (23.87%), and Krasnoyarsk Krai (20.51%). The smallest shares were observed in the Altai Republic (0.02%), Altai Krai (1.14%), Novosibirsk Oblast (5.98%), Omsk Oblast (8.74%), and Tomsk Oblast (1.61%), as well as the Republic of Tyva (0.47%) and Republic of Khakassia (2.22%).

The analysis of the polluted drain water discharge data for the Far Eastern Federal District showed that there was an increase from 676 million m³ in 1995 to 744 million m³ in 2019, which makes up 10.1%. The polluted drain water in almost all of the Far Eastern Federal District regions was also mainly made up of insufficiently purified drain water. The largest polluted drain water discharge shares for the regions of the Far Eastern Federal District in 2019 were observed in Primorsky Krai (35.75%) and Khabarovsk Krai (25.54%), while the contribution of other Krai and Oblasts in the total drain water discharge is insufficient: Zabaykalsky Krai—6.99%, Republic of Buryatia—4.70%, Republic of Sakha (Yakutia)—7.66%, Kamchatka Krai—3.63%, Amur Oblast—9.01%, Magadan Oblast—1.48%, Sakhalin Oblast—3.36%, Jewish Autonomous Oblast—1.48%, and Chukotka Autonomous District—0.40%.

Consumption rates make up the next analyzed indicator. The results of mapping for the consumption of recycled and reclaimed water are shown in Figs. 9, 10, 11 and 12.

In 1995, the lowest usage rates of reclaimed/recycled water across the three federal districts were observed in the Altai Krai (1276 million m³) and the highest in Sverdlovsk Oblast (13,066 million m³), Fig. 9. In 2000, this pattern was unchanged, Fig. 10.

In 2010, the patterns are the same (Fig. 11), with the minimum in the Jewish Autonomous Oblast (6 million m³) and the maximum in Sverdlovsk Oblast (13,297 million m³). As of 2019 (Fig. 12), the patterns are preserved.

If we review the dynamics of this indicator across the districts, we can draw the following conclusions:

- The indicator decreased in the Ural Federal District by 17.46%, although some of its regions saw it increase, e.g., in Khanty-Mansi Autonomous Okrug this indicator grew by 14.17%, in Yamalo-Nenets Autonomous Okrug it grew by 228.57%, and in Tyumen Oblast, it grew by 10.1%. The reduction in Kurgan Oblast amounted to 54.17%, in Sverdlovsk Oblast—28.23%, and Chelyabinsk Oblast—19.46%. Within the total use of recycled/reclaimed water, KMAO-Yugra takes up 27.98%, and Chelyabinsk Oblast takes up 29.71%. The smallest shares belong to Kurgan Oblast (1.04%), YNAO (1.03%), and Tyumen Oblast (5.04%).

- The Siberian Federal District saw this indicator decrease by 22.42%. The per-region reductions are as follows: Altai Krai—46%, Irkutsk Oblast—32.21%, Kemerovo Oblast—15.71%, Krasnoyarsk Krai—15.63%, Novosibirsk Oblast—37.07%, Omsk Oblast—40.15%, Republic of Tyva—63.64%. The indicator increased in the Altai Republic (600%), Tomsk Oblast (56.25%), and the Republic of Khakassia (52.91%). Overall, the highest recycled/reclaimed water consumption share belongs to Kemerovo Oblast (33.05%), Krasnoyarsk Krai (19%), and Irkutsk Oblast (18.66%), while the lowest was in the Altai Republic (0.14%), Altai Krai (5.64%), Novosibirsk Oblast (5.27%), Omsk Oblast (8.45%), Tomsk Oblast (5.35%), Republic of Tyva (0.08%), and Republic of Khakassia (3.99%).
- The Far Eastern Federal District also had this indicator decreased by 24.35%. The shares of the regions are as follows: Amur Oblast—12.68%, Republic of Buryatia—4.09%, Jewish Autonomous Oblast—0.16%, Kamchatka Krai—0.14%, Primorsky Krai—24.22%, Khabarovsk Krai—19.03%, Zabaykalsky Krai—14.05%, Magadan Oblast—5.72%, Sakhalin Oblast—2.06%, Chukotka Autonomous District—1.90%, Republic of Sakha—15.96%.

The costs of drain water collection and purification are shown in Figs. 13, 14 and 15 (the data were compared using absolute values without indexation).

Territories in red are characterized by high costs. In 2000, the highest costs were observed in Sverdlovsk Oblast (2313.2 million rubles), and the lowest was found in the Jewish Autonomous Oblast (1 million rubles). In 2010, the highest environmental protection costs were observed in KMAO—Yugra (8164 million rubles), and the lowest in Chukotka Autonomous District (12 million rubles).

The trend for the costs increase is preserved in 2019 (Fig. 15). Overall, the analysis of the statistics showed the following:

- The costs tend to increase in the Ural Federal District (358.7%), with the highest growth in YNAO (496.68%), KMAO—Yugra (392.02%), Chelyabinsk Oblast (351.47%), Sverdlovsk Oblast (280.95%), and Kurgan Oblast (109.09%), while in Tyumen Oblast it is only 25.31%. In 2019, in absolute values, KMAO—Yugra had 8,904.6 million rubles or 33.05% of the total costs of the federal district, Sverdlovsk Oblast had 8812.1 million rubles or 32.71%; Chelyabinsk Oblast had 4456.02 million rubles or 16.54%, YNAO had 2984 million rubles or 11.08%, and the lowest costs were observed in Tyumen Oblast (1,233.3 million rubles or 4.58%) and Kurgan Oblast (549.7 million rubles or 2.04%).
- In the Siberian Federal District, this indicator also grew from 7183.9 million rubles in 2000 to 24,078.4 million rubles in 2019, making for an increase of 235.17%. The highest increase of this indicator within the period in question was observed in the Altai Republic (from 4.2 million rubles to 67.3 million rubles, or 1502.38%). In Irkutsk Oblast the growth made up 335.59%, from 1100 to 4791.5 million rubles; in Kemerovo Oblast—346.06%, from 1224.2 to 5460.7 million rubles; in Omsk Oblast—333.55%, from 621.7 to 2695.4 million rubles; in Tomsk Oblast—132.21%, from 602.7 to 1399.5 million rubles; in the Republic of Tyva—4864.71%, from 3.4 to 168.8 million rubles; in the Republic of Khakassia—345.13%, from 116.1 to 516.8 million rubles; in Krasnoyarsk Krai—170.59%, from 2575.6 to 6969.3 million rubles; in Altai Krai

134.52%, from 478.3 to 1121.7 million rubles; and in Novosibirsk Oblast—93.88%, from 457.7 to 887.4 million rubles.

- In the Far Eastern Federal District, the indicator also increased from 2863.2 million rubles in 2000 to 8783.14 million rubles in 2019, making for an increase of 206.76%. The highest increase of this indicator was observed in the Jewish Autonomous Oblast (7590%, from 1 to 76.9 million rubles). In Primorsky Krai, the growth made up 394.23%, from 266.8 to 1318.6 million rubles; in Amur Oblast—336.74%, from 67.5 to 294.8 million rubles; in Kamchatka Krai—714.35%, from 45.3 to 368.9 million rubles, in Khabarovsk Krai—406.76%, from 365.4 to 1851.7 million rubles; in Chukotka Autonomous District—429.03%, from 3.1 to 16.4 million rubles; in Sakhalin Oblast—282.16%, from 101.8 to 389.04 million rubles; in Magadan Oblast—185.08%, from 156.8 to 447 million rubles; in Zabaykalsky Krai—164.31%, from 196.7 to 519.9 million rubles; in the Republic of Sakha—134.52%, from 1413.5 to 3017.1 million rubles; and in the Republic of Buryatia—96.82%, from 245.3 to 482.8 million rubles.

The investments in the protection and rational usage of water resources are presented in Figs. 16, 17, 18 and 19. This indicator was at the highest in Sverdlovsk Oblast (145 million rubles), and the lowest in the Jewish Autonomous Oblast (0.5 million rubles). (1995) The trends remain the same in the subsequent periods.

The distribution of the indicator was as follows:

- Within the Ural Federal District, Kurgan Oblast takes up 3.08% of the total investments, Sverdlovsk Oblast takes up 29.68%, KMAO—1.96%, YNAO—23.29%, Tyumen Oblast—12.65%, and Chelyabinsk Oblast—29.33%.
- In the Siberian Federal District, the increase in investment amounted to 9.5 thousand times. The distribution of the indicator across the regions and autonomous units of the Siberian Federal District is as follows: Altai Republic—0.40% of the total investments, Altai Krai—2.31%, Irkutsk Oblast—19.41%, Kemerovo Oblast—24.15%, Krasnoyarsk Krai—17.94%, Novosibirsk Oblast—2.42%, Omsk Oblast—29.44%, Tomsk Oblast—3.13%, Republic of Tyva—0.02%, Republic of Khakassia—0.78%.
- In the Far Eastern Federal District, the increase in investments amounted to 266.44 times. The distribution of the indicator across the regions and autonomous units of the Far Eastern Federal District in 2018 was as follows: Amur Oblast—11.1%, Republic of Buryatia—0.23%, Jewish Autonomous Oblast—0.58%, Zabaykalsky Krai—20.73%, Kamchatka Krai—1.22%, Magadan Oblast—0.14%, Primorsky Krai—9.60%, Republic of Sakha—37.61%, Sakhalin Oblast—0.91%, Khabarovsk Krai—15.89%, Chukotka Autonomous District—2.01%.

The results of the research on the assessment of the environmental and economic indicator for water resources are shown in Figs. 20, 21 and 22. The growth of this indicator characterizes the positive changes in water protection activities, i.e., the reduction of polluted drain water discharge and the increase in water consumption through recycled/reclaimed water rather than fresh water.

According to the obtained analytics, the best conditions are found in the Jewish Autonomous Oblast (the indicator value of 0.256, mainly production companies with

low water consumption), while the minimum value (0.004) can be found in KMAO—Yugra, which is explained by the rapid increase in the amount of polluted drain water as confirmed by Figs. 5, 6, 7 and 8, and this trend is typical of the entire period in question.

The situation is gradually changing, even though for KMAO—Yugra this indicator is still low (0.007), while the minimum can be registered in Primorsky Krai (0.48), which can be attributed to the increased investment in water protection activities, according to Figs. 21 and 22, resulting in the improved efficiency of water management.

The results of the assessment of the environmental and economic efficiency of water protection activities are shown in Figs. 23, 24 and 25. This indicator reflects the efficiency of polluted drain water collection and purification costs, as well as the investments in water protection activities observed as the anthropogenic impact on water bodies increases. The growth of this indicator signifies there are some positive changes in water protection activities due to preventive actions. According to the data shown in Figs. 23, 24 and 25, the highest efficiency of water protection activities in 2000 was found in Primorsky Krai. The indicator is set at 0.146, Fig. 24. In 2010, the costs and investments were somewhat redistributed in favor of the Amur Oblast (463), while the indicator is still insignificant in KMAO—Yugra (0.005). According to Fig. 25, the indicator value for Tyumen Oblast is 0.08, which means the funding for water protection activities is insufficient. The value for the Jewish Autonomous Oblast is 6.875, which means there are significant costs and investments per unit of waterbody pollution.

Based on the data provided, we can say that, during the analyzed period, the environmental protection costs increase pro rata with the adverse impacts on water resources due to industrial production as made evident by the previous maps illustrating the listed indicators, although their value is often insufficient to mitigate the negative impacts on water resources. For instance, in the Ural Federal District, the increase in polluted drain water discharge is accompanied by an increase in the drain water collection and purification costs, as well as an increase in the water protection activity investments according to Figs. 5, 6, 7 and 8.

5 Conclusion

During the research, we performed a detailed study of water resources in three federal districts: Ural, Siberian, and Far Eastern. They are good examples of resource-rich regions with good economic prospects. The current situation with water resources was evaluated, and objective data were obtained concerning the environmental situation and its dynamics in the regions in question.

Based on the research results, a database containing information on water usage, pollution, and protection activities was established. It helped analyze the efficiency of water management over the selected period. Based on the results of this analysis, several maps were developed.

To identify reliable scientific data, we used the methods and laws of statistics, as well as the Kriging mapping method.

References

1. Yu SK (2008) Golden software surfer 8, a geoinformation system. Voronezh State University, Voronezh, p 66
2. Ivanov IA, Chekantsev VA (2008) Solving geological problems with the surfer software package: a practical exercise book for the students of applied geology. Tomsk Polytechnic University, Tomsk, p 92
3. Astakhova IA (2009) Geodesy: a university textbook. Maikop State Technological University, Maikop State Technological University, Maikop, p 68
4. Bobylev SN, Khodzhaev ASH (1997) Environmental management economics. Teis, Moscow, p 272
5. Maltsev KA, Mukharamova SS (2014) Building spatial variable models (using the surfer software package): Study guide. Kazan University, Kazan, p 103
6. Silkin KY (2008) Golden software surfer 8, a geoinformation system: university textbook. Voronezh State University, Voronezh, p 66
7. Research Report on the Methodology and Tools of Balanced Environmental Management to Mitigate Environmental and Economic Threats, Yekaterinburg, 2020, p 200
8. Report on the Environmental Situation in Khanty-Mansi Autonomous Okrug—Yugra in 2008–2019. <https://prirodnadzor.admhmao.ru/doklady-i-otchyety/>
9. The Water Registry of the Russian Federation (2017) The resources of surface and underground waters, their usage, and quality. The yearbook. OOO RPTs Ofort, Moscow, p 164
10. Report on the Environmental Situation in Tyumen Oblast in 2008, 2009–2019. https://admtyumen.ru/ogv_ru/about/ecology/eco_monitoring/more.htm?id=11552245@cmsArticle
11. Integrated report on the State of Environment in Chelyabinsk Oblast in 2008, 2009–2019. http://mineco174.ru/htmlpages/Show/protectingthepublic/2016/222Gosudarstvennyj_uchetvod
12. State report on the State and Protection of Environment in Sverdlovsk Oblast in 2008, 2009–2019. <https://mprso.midural.ru/news/show/id/405>
13. State report on the Natural Resources and Environmental Protection in Kurgan Oblast in 2008, 2009–2019. <http://www.priroda.kurganobl.ru/3434.html>
14. Report on the Environmental Situation in Yamalo-Nenets Autonomous Okrug in 2008, 2009–2019. <http://www.vossta.ru/doklad-ob-ekologicheskoy-situacii-v-yamalo-neneckom-avtonomnom-v2.html?page=5>
15. Semyachkov AI, Kuchin VV, Arkhipov MV (2021) Regional water environment analysis of the mining and metallurgy complex of the Middle Urals, in the problems of modern reservoirs and catch basins. In: The proceedings of the VIII All-Russian research and practice conference with international participation, Perm State University, Electronic details, Perm, pp 474–479. <http://www.psu.ru/files/docs/science/books/sborniki/modernproblems-of-reservoirs-and-their-catchments.pdf>. Heading from screen